



**UMCS**

**UNIWERSYTET MARII CURIE-SKŁODOWSKIEJ  
W LUBLINIE  
Szkoła Doktorska Nauk Ścisłych i Przyrodniczych**

Dziedzina: nauki ścisłe i przyrodnicze

Dyscyplina: nauki chemiczne

**Agnieszka Katarzyna Krzyszczak-Turczyn**

nr albumu: 248578

**Badania pochodnych wielopierścieniowych  
węglowodorów aromatycznych w biowęglach  
(Studies on the derivatives of polycyclic aromatic  
hydrocarbons in biochar)**

Rozprawa doktorska  
przygotowywana pod kierunkiem naukowym  
dr hab. Bożeny Czech, prof. UMCS

w Instytucie Nauk Chemicznych

**LUBLIN, 2023**



*Z całego serca pragnę podziękować mojemu promotorowi*

*Pani dr hab. Bożenie Czech, prof. UMCS*

*za nieocenione wsparcie naukowe, wielką życzliwość, opiekę merytoryczną, liczne dyskusje oraz rady udzielone w trakcie realizowania pracy.*

*Serdecznie dziękuję **Koleżankom i Kolegom** z Katedry Radiochemii i Chemii Środowiskowej UMCS za życzliwość i stworzenie wspaniałej atmosfery naukowej  
oraz*

***Koleżankom i Kolegom** z Katedry Chemii Wydziału Medycznego KUL i Katedry Biomedycyny i Badań Środowiskowych Wydziału Medycznego KUL za ogromne wsparcie.*

*Serdeczne podziękowania składam mojej **Rodzinie** za okazane*

*wsparcie oraz bezgraniczną wiarę w moją osobę.*

*Szczególnie dziękuję mojemu **Mężowi** za ogromną cierpliwość, wyrozumiałość  
i motywację w chwilach zwątpienia.*

## **Spis treści**

---

1.	Wykaz publikacji wchodzących w skład rozprawy doktorskiej .....	6
2.	Streszczenie w języku polskim .....	8
3.	Streszczenie w języku angielskim.....	10
4.	Aktualny stan wiedzy .....	12
4.1.	Wprowadzenie .....	12
4.2.	Rolniczy potencjał aplikacyjny biowęgla.....	13
4.3.	Wielopierścieniowe węglowodory aromatyczne i ich pochodne w biowęglu .	14
4.4.	Całkowita i biodostępna frakcja związków szkodliwych.....	17
4.5.	Wpływ czynników środowiskowych na właściwości biowęgla.....	18
4.6.	Toksyczność pochodnych wielopierścieniowych węglowodorów aromatycznych i ich zawartość w próbkach środowiskowych .....	19
5.	Cel badań oraz wpływ uzyskanych wyników na zrównoważony rozwój i zieloną chemię.....	22
6.	Ogólny opis metod zastosowanych w badaniach .....	26
6.1.	Charakterystyka fizykochemiczna biowęgla .....	26
6.2.	Oznaczanie frakcji całkowitej WWA i ich pochodnych .....	27
6.3.	Oznaczanie frakcji biodostępnej WWA i pochodnych.....	30
6.4.	Przeprowadzenie starzeń modelowych.....	31
7.	Wyniki badań własnych .....	34
7.1.	Wpływ surowca na charakterystykę fizykochemiczną biowęgli .....	34
7.2.	Wpływ surowca na zawartość frakcji całkowitej oraz biodostępnej WWA i pochodnych w biowęglu.....	36
7.3.	Wpływ temperatury pirolizy na charakterystykę fizykochemiczną biowęgli ..	37
7.4.	Wpływ temperatury na zawartość frakcji całkowitej oraz biodostępnej WWA i pochodnych w biowęglach .....	38
7.5.	Wpływ starzenia fizycznego oraz chemicznego na zawartość frakcji całkowitej i biodostępnej WWA i ich pochodnych.....	39
7.6.	Wpływ starzenia biologicznego oraz enzymatycznego na zawartość frakcji całkowitej i biodostępnej WWA i pochodnych .....	44
7.7.	Wpływ WWA i ich pochodnych na stres oksydacyjny u roślin .....	46

7.8. Zawartość frakcji całkowitej oraz biodostępnej WWA i pochodnych w glebach wzbogaconych biowęglem .....	47
8. Wnioski .....	51
9. Literatura .....	54
10. Życiorys naukowy .....	59
11. Dorobek naukowy .....	62
12. Wykaz pozostałych osiągnięć i aktywności naukowych .....	74
ANEKS - TEKSTY PUBLIKACJI BĘDĄCYCH PRZEDMIOTEM ROZPRAWY DOKTORSKIEJ.....	80

## **1. Wykaz publikacji wchodzących w skład rozprawy doktorskiej**

---

**D1 A. Krzyszczak, B. Czech**

*Occurrence and toxicity of polycyclic aromatic hydrocarbons derivatives in environmental matrices*

Science of the Total Environment, 2021, 788: 147738

**IF<sub>2021</sub>:** 10,757

**Punkty MEiN:** 200

**D2 A. Krzyszczak, M. Dybowski, B. Czech**

*Formation of polycyclic aromatic hydrocarbons and their derivatives in biochars: The effect of feedstock and pyrolysis conditions*

Journal of Analytical and Applied Pyrolysis, 2021, 160, 105339

**IF<sub>2021</sub>:** 6,437

**Punkty MEiN:** 100

**D3 A. Krzyszczak, M.P. Dybowski, M. Kończak, B. Czech**

*Low bioavailability of derivatives of polycyclic aromatic hydrocarbons in biochar obtained from different feedstock*

Environmental Research, 2022, 214(1), 113787

**IF<sub>2022</sub>:** 8,3

**Punkty MEiN:** 100

**D4 A. Krzyszczak, M.P. Dybowski, R. Zarzycki, R. Kobyłecki, P. Oleszczuk, B. Czech**

*Long-term physical and chemical aging of biochar affected the amount and bioavailability of PAHs and their derivatives*

Journal of Hazardous Materials, 2022, 440, 129795

**IF<sub>2022</sub>:** 13,6

**Punkty MEiN:** 200

**D5 A. Krzyszczak, M.P. Dybowski, B. Czech**

*Microorganisms and their metabolites affect the content of polycyclic aromatic hydrocarbons and their derivatives in pyrolyzed material*

Science of the Total Environment, 2023, 886, 163966

**IF<sub>2022</sub>:** 9,8

**Punkty MEiN:** 200

**Sumaryczny IF prac będących przedmiotem rozprawy doktorskiej:** 70,894

**Sumaryczna liczba punktów MEiN prac będących przedmiotem rozprawy doktorskiej:** 1100

## **2. Streszczenie w języku polskim**

---

Rozprawa doktorska pt.: „Badania pochodnych wielopierścieniowych węglowodorów aromatycznych w biowęglach” składa się z sześciu powiązanych ze sobą tematycznie artykułów opublikowanych w recenzowanych czasopismach naukowych, które posiadają wskaźnik wpływu (z ang. impact factor) oraz jednego artykułu znajdującego się na etapie recenzji w czasopiśmie Journal of Hazardous Materials.

Badania przeprowadzone w ramach pracy doktorskiej składają się z czterech głównych części. Pierwszą z nich stanowiły eksperymenty dotyczące wyjściowych, niezmodyfikowanych biowęgli, a dokładniej wpływu temperatury pirolizy, jak również zastosowanego surowca na charakterystykę fizykochemiczną spirolizowanego materiału, zawartość frakcji całkowitej oraz biodostępnej wielopierścieniowych węglowodorów aromatycznych (WWA) i ich pochodnych w biowęglach. W celu wyizolowania poszczególnych frakcji analitów wykorzystano odpowiednio: technikę przyspieszonej ekstrakcji za pomocą rozpuszczalnika oraz pasywne próbki polioksymetylenowe. Próbki analizowano metodą chromatografii gazowej sprzężonej z tandemową spektrometrią mas. Wyniki wskazują na znaczący wpływ temperatury pirolizy, jak również zastosowanego surowca na zawartość WWA i ich pochodnych oraz wybrane parametry fizykochemiczne biowęgla.

W trakcie rolniczego zastosowania, materiał węglowy ulega przemianom pod wpływem różnych czynników środowiskowych. Dlatego też druga część badań polegała na przeprowadzeniu procesów starzenia, które symulowały zmiany zachodzące podczas wzbogacenia gleby spirolizowanym materiałem w warunkach rzeczywistych. W tym celu biowęgle poddano procesom starzenia fizycznego, chemicznego, biologicznego oraz enzymatycznego, po czym wyznaczono ich podstawowe parametry fizykochemiczne, jak również oznaczono zawartości frakcji całkowitej i biodostępnej analitów. Otrzymane wyniki odniesiono do danych uzyskanych dla wyjściowych próbek. Procesy starzenia wpływały znacząco na charakterystykę fizykochemiczną biowęgli oraz całkowitą zawartość WWA i pochodnych, jak również biodostępność omawianych związków. Np. frakcja całkowita WWA, tlenowych oraz azotowych pochodnych w materiałach węglowych (otrzymanych z osadu ściekowego, BCZ500,

BCZ600, BCZ700) poddanych starzeniu fizycznemu i chemicznemu wzrosła, podczas gdy frakcja biodostępna analitów niemal we wszystkich przypadkach zmalała.

Trzecia część pracy dotyczy wyników oznaczenia aktywności przeciwitleniającej dysmutazy ponadtlenkowej (SOD), katalazy (CAT), peroksydazy (POD) i zawartości wolnego dialdehydu malonowego (MDA) oraz wyznaczeniu poziomu transkrypcji genów odpowiedzialnych za stres oksydacyjny w roślinie modelowej *Hordeum vulgare* L. wysianej na glebie wzbogaconej biowęglem. Wyniki potwierdzają, że frakcja biodostępna WWA i ich pochodnych indukuje stres oksydacyjny w jęczmieniu zwyczajnym. Wskazuje na to wzrost aktywności enzymatycznej SOD, która stanowi pierwszą linię obrony rośliny. Aktywności pozostałych przeciwitleniaczy zmalały, co świadczy o przezwyciężeniu skutków stresu oksydacyjnego przez organizm modelowy. Ponadto, roślina była zdolna do prowadzenia swojej wegetacji w tych warunkach, gdyż organizm wykazywał tolerancję na obecność frakcji biodostępnej analitów.

Czwarta część badań obejmowała weryfikację bezpieczeństwa praktycznego zastosowania biowęglą, jako dodatek do gleb poprawiający ich jakość. W tym celu przeprowadzono eksperyment wazonowy (modyfikacja gleb spirolizowanym materiałem w warunkach kontrolowanych, w laboratorium) oraz dwa eksperymenty polowe (wzbogacenie gleb biowęglem w warunkach rzeczywistych). Zgodnie z wynikami dotyczącymi doświadczenia wazonowego, zawartości analitów były niższe niż spodziewane, wynikające ze znanej zawartości WWA i pochodnych w węglowym materiale wyjściowym. Spadek zawartości omawianych związków może być związany z aktywnością mikroorganizmów glebowych, gdyż, jak zostało dowiedzione w części drugiej eksperymentów prowadzonych w ramach rozprawy doktorskiej, skutkiem przeprowadzenia starzenia biologicznego, w większości przypadków, był spadek lub brak zmian w zawartości WWA i pochodnych w spirolizowanym materiale. Wyniki dotyczące eksperymentu polowego wskazują na wzrost zawartości analitów (lub brak zmian, tj. zawartość pochodnych WWA była poniżej granicy wykrywalności w przypadku eksperymentu polowego z materiałem węglowym BCS600) w glebie zmodyfikowanej biowęglem wraz z czasem trwania wzbogacenia.

### **3. Streszczenie w języku angielskim**

---

The doctoral thesis entitled: „Studies on the derivatives of polycyclic aromatic hydrocarbons in biochar” consists of six articles, thematically related to each other, and published in peer-reviewed scientific journals with an impact factor and one article at the review stage in the Journal of Hazardous Materials.

The studies carried out as part of a doctoral dissertation, consist of four main parts. The first of them constituted the experiments concerning initial unmodified biochar, specifically the effect of pyrolysis temperature and the feedstock on the physicochemical characteristic of pyrolyzed material as well as the content of total and bioavailable fraction of polycyclic aromatic hydrocarbons (PAHs) and their derivatives in biochar. The analyte fractions were isolated through pressurized liquid extraction and polyoxymethylene passive samplers, respectively. The samples were analyzed via gas chromatography coupled with tandem mass spectrometry. The results indicated that the pyrolysis temperature and the feedstock affected the content of analytes as well as the selected physicochemical parameters of biochar.

During the agricultural application of biochar, various environmental factors affect the material. Thus, the second part of the studies included the aging processes which simulated the changes occurring during the soil enrichment with pyrolyzed material in real environment conditions. The biochars were aged physically, chemically, biologically, and enzymatically. Then the main physicochemical parameters as well as the content of the total and bioavailable fraction of analytes were determined. The results were compared to the data obtained for initial biochar. The aging affected significantly the physicochemical characteristics of pyrolyzed material as well as the total and bioavailable fraction of PAHs and derivatives. For example, the total fraction of PAHs and their derivatives in biochar (obtained from sewage sludge, BCZ500, BCZ600, and BCZ700) aged physically and chemically increased, whereas in almost all cases, the bioavailable fraction of analyte decreased.

The third part of the experiment included the determination of the activity of the antioxidative enzymes superoxide dismutase (SOD), catalase (CAT), peroxidase (POD), the content of malondialdehyde as well as the expression of genes related to oxidative stress in the model plant. *Hordeum vulgare* L. was planted on the biochar-modified soil.

The results indicated that the bioavailable fraction of PAHs and their derivatives induced oxidative stress in barley due to the increase in the enzymatic activity of SOD (which constitutes the first line of plant defense). However, the other enzyme's antioxidant activity decreased which indicates that the effects of oxidative stress by the model organism were overcome. Moreover, the plant was able to vegetate in these conditions because the organisms tolerated the presence of a bioavailable fraction of analytes.

The fourth part included the safety verification of the practical application of biochars as a soil addition improving its properties. For this purpose, the pot experiment (the soil modification with BC in controlled conditions, in the laboratory) as well as two field experiments (soil enrichment with biochar in real conditions) were carried out. The results considering the pot studies revealed that the content of analytes was lower than it could be expected considering the known amount of analytes in initial biochars. The drop in the content of the studied compounds may be associated with soil microorganisms' activity. Thus, as it was presented in the second part of the experiment conducted as part of the doctoral dissertation, in almost all cases, the biological aging caused the decrease (or remained constant) in the content of PAHs and their derivatives in pyrolyzed material. The results of the field experiments indicated that the content of analytes in soil enriched with biochar increased (or remained the same, i.e. the content of PAHs derivatives was below the limit of detection in the case of field experiment with BCS600) with the time of application.

## **4. Aktualny stan wiedzy**

---

### **4.1. Wprowadzenie**

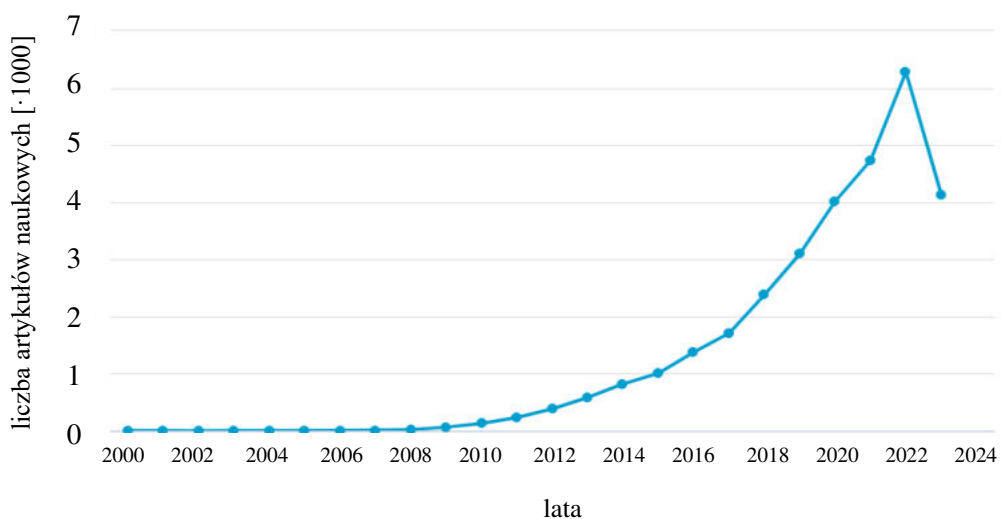
Biowęgiel (z ang. biochar, BC) jest to amorficzna i stabilna forma materiału węglowego, otrzymywana w wyniku termicznej dekompozycji biomasy w atmosferze beztlenowej lub ubogiej w tlen, czyli podczas procesu pirolizy, bądź gazyfikacji [1,2]. Materiał ten charakteryzuje się wysoką porowatością, stabilnością i niską gęstością. Jego właściwości fizykochemiczne zależą od wielu czynników, uwzględniających wstępne przygotowanie surowca (suszenie, oczyszczanie, rozdrobnienie, homogenizacja, chemiczna modyfikacja), etap procesu pirolizy (szybkość ogrzewania, najwyższa zastosowana temperatura oraz czas jej utrzymywania, ciśnienie, gaz nośny, naczynie reakcyjne - jego orientacja i wielkość, obecność lub brak katalizatora, jakość i przepływ gazu/gazów dodatkowych), jak również czynniki obejmujące obróbkę otrzymanego spirolikowanego materiału (rozdrobnienie, przemywanie specjalną procedurą, suszenie, homogenizacja, aktywacja) [3]. Jednakże temperatura pirolizy oraz rodzaj surowca wywierają największy wpływ na charakterystykę fizykochemiczną BC.

Generalnie, biowęgiel otrzymuje się w temperaturze poniżej 700°C [3]; dolnym zakresem temperaturowym może być nawet 200°C [4]. Surowcem do produkcji materiału jest szeroko rozumiana biomasa, która składa się głównie z trzech grup naturalnie występujących polimerów, tj. celulozy, hemicelulozy oraz ligniny [5]. Są to zarówno odpady drzewne [2], jak również trawa, skorupy orzechów, słoma pszeniczna, łuski ryżowe, czy rośliny słodkowodne [2,4]. Ponadto, spirolikowany materiał można otrzymać z osadów ściekowych [4], pozostałości po produkcji biogazu [6], nawozu zwierzęcego [4] oraz odpadów spożywczych [2]. Charakterystyka fizykochemiczna surowca znacznie wpływa na właściwości otrzymanego biowęgla. W zależności od zastosowanej biomasy, zmianie ulega całkowita zawartość węgla organicznego, węgla związanego, zawartość składników mineralnych oraz popiołu, wielkość powierzchni właściwej, jak również liczba i wielkość porów [2,4,7,8]. Różnice w tych parametrach są niezwykle istotne, gdyż wpływają na ogólne właściwości BC, a co za tym idzie, jego potencjalne zastosowanie. Na przykład, charakter struktur węglowych jest kluczowym czynnikiem decydującym o stabilności spirolikowanego materiału [9,10]. Natomiast

temperatura pirolizy wpływa na wielkość powierzchni właściwej biowęglą oraz jego pH [4], jak również pojemność kationowymienną, zawartość metali śladowych, węgla [7,11,12], aromatyczność, polarność, stabilność i trwałość spirolikowanego materiału [2,7]. W zależności od zastosowanej temperatury pirolizy zmienia się także dostępność zawartych w BC składników odżywczych ważnych dla roślin [13]. Biowęgiel otrzymany z odpadów pochodzących z hodowli zwierząt charakteryzuje się mniejszą powierzchnią właściwą, mniejszą zawartością węgla oraz substancji lotnych, w porównaniu do materiału pozyskanego z surowca roślinnego (biomasa drzewna oraz różnego rodzaju zboża) [8]. Jednakże jego pojemność kationowymienna, jak również wartość pH jest większa [8,14]. Wymienione wyżej znaczące różnice w podstawowych parametrach fizykochemicznych BC wynikają głównie z odmiennego składu (stosunku celulozy do ligniny) i zawartości wody w biomasie [8].

#### 4.2. Rolniczy potencjał aplikacyjny biowęglą

W ostatnich latach zainteresowanie biowęglem dynamicznie wzrasta, co potwierdza rosnąca liczba publikacji naukowych dotyczących tego tematu (Rys. 1). Wiąże się to między innymi z bardzo szerokim potencjałem aplikacyjnym BC.



Rys. 1. Wyniki wyszukiwania hasła „biochar” w tytule artykułu, streszczeniu i słowach kluczowych w bazie danych SCOPUS (dostęp dnia 06.07.2023 r.).

Spirolizowany materiał może być stosowany w wielu gałęziach przemysłu. Jednakże jednym z najważniejszych potencjalnych zastosowań jest wykorzystanie biowęglą jako dodatku do gleb poprawiającego ich jakość i żywność.

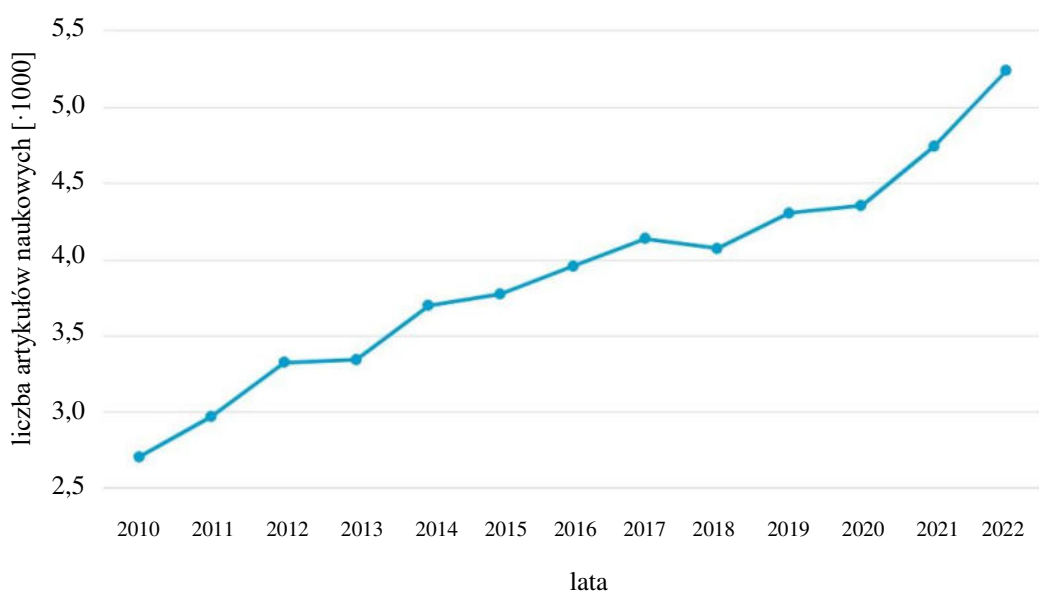
BC bierze udział w oczyszczaniu gleby poprzez immobilizację metali ciężkich, jak również katalizowanie reakcji utleniania i redukcji zanieczyszczeń organicznych, czy też nieorganicznych [16,17]. Dodatek spirolikowanego materiału polepsza plonowanie i agregację cząstek glebowych oraz zwiększa pH gleby [16,18]. Ponadto, rolnicze zastosowanie BC, jako naturalnego nawozu, skutkuje regradacją gleb, wzrostem puli dostępnych składników odżywcznych oraz ich retencji [19,20]. Praktyczne wykorzystanie biowęglą wpisuje się w gospodarkę w obiegu zamkniętym [21] oraz pozwala ograniczyć negatywny wpływ działalności ludzkiej na klimat, gdyż dodatek spirolikowanego materiału do gleb zmniejsza emisję amoniaku i ditenku węgla do atmosfery [22].

#### **4.3. Wielopierścieniowe węglowodory aromatyczne i ich pochodne w biowęglu**

Biowęgiel posiada wiele niekwestionowanych zalet, niemniej rozważając możliwości rolniczego zastosowania BC należy wziąć pod uwagę także jego wady oraz ograniczenia podczas użytkowania. Najważniejsze z nich to zwiększenie zagęszczenia gleby oraz jej zanieczyszczenie metalami ciężkimi, czy innymi toksycznymi związkami organicznymi [23], jak również zwiększenie podatności na erozję [24,25]. Szkodliwe substancje znajdujące się w otrzymanym materiale mogą pochodzić z dwóch źródeł: zarówno z surowca, jak również mogą tworzyć się podczas procesu pirolizy [25].

Wielopierścieniowe węglowodory aromatyczne (WWA) (z ang. Polycyclic Aromatic Hydrocarbons, PAHs) to stabilne, hydrofobowe związki organiczne składające się z atomów węgla i wodoru oraz z co najmniej dwóch pierścieni aromatycznych [26]. Mogą pochodzić ze źródeł naturalnych (pożary lasów), czy antropogenicznych (spalanie materii organicznej oraz paliw, procesy przemysłowe) [27], jak również tworzą się podczas wysokotemperaturowego procesu otrzymywania biowęglą [28]. WWA są toksyczne, mutagenne i kancerogenne dla organizmów żywych [29–31], a ich zawartość w BC determinowana jest głównie przez warunki pirolizy [17,32]. W związku z ich szkodliwym działaniem na organizm ludzki, zwierzęcy oraz

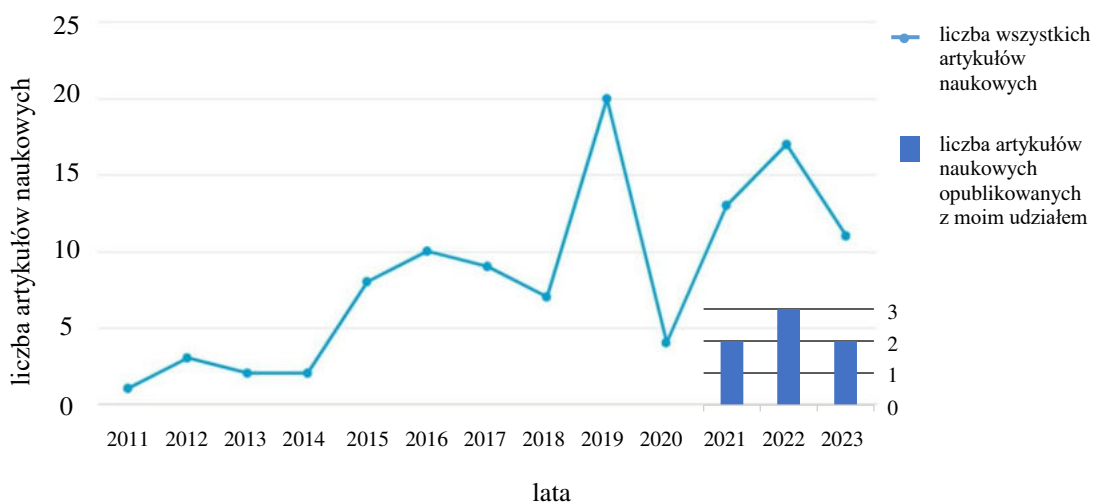
roślinny, 16 spośród wszystkich WWA zostało włączone na priorytetową listę zanieczyszczeń ustanowioną przez Agencję Ochrony Środowiska Stanów Zjednoczonych (United States Environmental Protection Agency, US EPA), dlatego ich obecność w różnego rodzaju próbkach jest intensywnie badana (Rys. 2). Natomiast dopuszczalne zawartości  $\Sigma$ WWA w biowęglach są ograniczone poprzez wartości graniczne ustanowione przez International Biochar Initiative [33] oraz European Biochar Certificate [34] (wynoszą odpowiednio 6 - 300 mg/kg suchej masy oraz 4 mg/kg suchej masy dla biowęgla podstawowego (z ang. basic) i 12 mg/kg suchej masy dla materiału wyższej jakości (z ang. premium)).



Rys. 2. Wyniki wyszukiwania haseł „polycyclic AND aromatic AND hydrocarbons” w tytule artykułu, streszczeniu i słowach kluczowych w bazie danych SCOPUS (dostęp dnia 06.07.2023 r.).

Zarówno podczas wysokotemperaturowej modyfikacji biomasy, jak również w trakcie procesów środowiskowych (w wyniku reakcji chemicznych, fizycznych oraz fotochemicznych) mogą tworzyć się tlenowe (O-WWA), azotowe (N-WWA) i siarkowe (S-WWA) pochodne WWA [12,35–37] (z ang. Polycyclic Aromatic Hydrocarbon (PAHs) derivatives). W wielu artykułach naukowych dowiedziono, że parametry pirolizy wpływają na zawartość WWA w biowęglu. Ostatnie doniesienia literaturowe potwierdzają, że podczas otrzymywania spirolizowanego materiału powstają również pochodne WWA [38]. Temat ten jest istotny, gdyż O-, S- oraz N-WWA są uważane za bardziej toksyczne od związków rodzimych [39].

Pochodne wielopierścieniowych węglowodorów aromatycznych są stabilne termicznie. Związki te różnią się od rodzimych WWA obecnością atomu tlenu (O-WWA), azotu (N-WWA) lub siarki (S-WWA) w cząsteczce. Tlenowe pochodne zawierają grupę karbonylową, tworząc ketony oraz chinony. Charakteryzują się również większą masą cząsteczkową oraz mniejszą prężnością par w porównaniu do związków rodzimych. W środowisku O-WWA powstają w wyniku fotochemicznego utleniania WWA oraz reakcji z rodnikami ( $\text{NO}_3^-$ ,  $\cdot\text{OH}$ ) lub związkami ( $\text{NO}_x$ ,  $\text{O}_3$ ) i pod wpływem światła ultrafioletowego [35]. Właściwości fizykochemiczne azotowych pochodnych zależą od liczby grup funkcyjnych w cząsteczce, jak również od masy cząsteczkowej związku. Charakteryzują się one większym współczynnikiem podziału oktanol-powietrze, współczynnikiem podziału cząstki stałe-gaz oraz mniejszym współczynnikiem podziału węgiel organiczny-woda i współczynnikiem podziału oktanol-woda w porównaniu do związków rodzimych [37], co wskazuje na większą mobilność, jak również dostępność pochodnych WWA w środowisku.



Rys. 3. Wyniki wyszukiwania haseł „polycyclic AND aromatic AND hydrocarbons AND derivatives AND biochar” w tytule artykułu, streszczeniu i słowach kluczowych w bazie danych SCOPUS (dostęp dnia 06.07.2023 r.).

Azotowe pochodne WWA można podzielić na dwie grupy, zawierające ziązki: w których grupa nitrowa przyłączona jest do pierścienia aromatycznego oraz posiadające wbudowany w pierścień aromatyczny atom azotu (z ang. azaarenes) [40]. Obecność już jednej azotowej grupy funkcyjnej powoduje obniżenie ciśnienia par, jak również rozpuszczalności związku o odpowiednio 3 i 1 rzad wielkości [41]. N-WWA są

toksyczne, mutagenne, kancerogenne i teratogenne. Ponadto, związki zawierające atom azotu w pierścieniu aromatycznym charakteryzują się większą rozpuszczalnością w wodzie w porównaniu do związków rodzimych [40], co wpływa na ich mobilność w środowisku. Biorąc pod uwagę właściwości pochodnych WWA (zarówno tlenowych, jak i azotowych) oraz ich większą szkodliwość dla organizmów żywych, istnieje ogromna potrzeba monitorowania zawartości tych związków w próbkach środowiskowych, a zainteresowanie naukowców (Rys. 3) jest uzasadnione.

#### **4.4. Całkowita i biodostępna frakcja związków szkodliwych**

Związki, zarówno toksyczne, jak i bezpieczne dla organizmów żywych, czy też o właściwościach prozdrowotnych, w różnym stopniu mogą być izolowane z badanego materiału. Zazwyczaj celem naukowca jest ekstrakcja całkowitej ilości analitu (frakcja całkowita). Często jest to trudne wyzwanie, szczególnie w przypadku próbek charakteryzujących się złożonym składem matrycy, gdyż prawidłowe oznaczenie zawartości wymaga m. in. optymalizacji procesu przygotowania próbki i ekstrakcji, usunięcia albo zmniejszenia wpływu związków interferujących lub powodujących efekty matrycowe, wzbogacenia próbki ze względu na niski zakres stężeń analitu, walidacji metody analitycznej, optymalizacji warunków aparaturowych. Jednakże, biorąc pod uwagę środowiskowy punkt widzenia, istotna jest biodostępność związków, gdyż tylko biodostępna frakcja (która zwykle nie jest równoznaczna z całkowitą ilością analitu w materiale) może wywierać efekt toksyczny na organizmy żywe [25]. Przyjmuje się, że substancje, które mogą być ekstrahowane fazą wodną z badanej próbki, są zdolne do migracji w środowisku, czyli są „biodostępne”. Oznacza to, że mają możliwość przejścia przez błony biologiczne z otoczenia, w którym żywy organizm w danej chwili się znajduje [42]. W przypadku rolniczego zastosowania biowęgla, obecność toksycznej frakcji biodostępnej może wywoływać stres oksydacyjny u roślin, a szkodliwe ziązki mogą migrować z gleb do wód gruntowych, zanieczyszczając je [23].

WWA obecne w spirolizowanym materiale charakteryzują się niewielką biodostępnością. Wynika to przede wszystkim z tego, że są one silnie związane z matrycją próbki. Między biowęglem, a aromatycznymi związkami występują silnie oddziaływanie  $\pi-\pi$  [23]. Ponadto, WWA mogą być zokludowane i uwieńczone

w strukturze spirolizowanego materiału, wówczas ich ekstrakcja może być niemożliwa [23]. Warto podkreślić, że rozpoczynając badania będące przedmiotem rozprawy doktorskiej, żadna dostępna pozycja literaturowa nie prezentowała, ani nie charakteryzowała stopnia biodostępności pochodnych WWA w BC.

#### **4.5. Wpływ czynników środowiskowych na właściwości biowęglia**

Podczas rolniczego zastosowania BC, materiał poddawany jest wielu przemianom w wyniku działania szeregu czynników środowiskowych. Całość tych procesów nazwano starzeniem biowęglia. Różnice temperatur, opady deszczu czy śniegu, aktywność mikrobiologiczna mogą prowadzić do zmiany parametrów fizykochemicznych BC, a także jego mechanicznej fragmentacji, rozpadu, uwalniania rozpuszczonej materii organicznej, rozpuszczania minerałów, jak również utleniania spirolizowanego materiału [43]. Co więcej, procesy zamrażania, rozmrażania, rozkład fotochemiczny, susze czy nadmierna wilgotność oraz utlenianie wynikające z aktywności mikroorganizmów i obecności tlenu atmosferycznego powodują zmiany w podstawowym składzie chemicznym BC, wielkości powierzchni właściwej (oraz objętości i średnicy porów), morfologii powierzchni, kwasowości, czy też aromatyczności [43]. Struktura biowęglia dodanego do gleby staje się bardziej nieregularna z widocznymi śladami rozpadu [44]. Natomiast wielkość powierzchni właściwej może zarówno wzrosnąć lub zmaleć w zależności od warunków środowiskowych. Z kolei, objętość i średnica porów zazwyczaj zmniejsza się m.in. ze względu na sorpcję związków (np. minerałów), fizyczną niedrożność spowodowaną składnikami gleby, powstanie w wyniku aktywności mikroorganizmów bakteryjnego biofilmu itd. [43].

Przemiany biowęglia wprowadzonego do gleby i procesy temu towarzyszące, zachodzące pod wpływem czynników środowiskowych, mogą być przyspieszone doświadczalnie w warunkach ściśle kontrolowanych, przeprowadzając starzenie chemiczne, fizyczne, biologiczne oraz enzymatyczne. Tego typu eksperymenty polegające na sztucznym starzeniu spirolizowanego materiału, imitują przemiany, jakie zachodziłyby podczas rolniczego zastosowania biowęglia (jako dodatek do gleb). Ponadto, skracają czas trwania eksperymentu z lat lub miesięcy do dni, a nawet godzin [43]. Co więcej, pozwalają na dokładniejsze poznanie mechanizmów procesów

zachodzących w glebie, gdyż znając wpływ poszczególnych typów starzeń (tzn. czynników środowiskowych) na parametr będący przedmiotem zainteresowania naukowca, można zweryfikować, który z nich jest dominujący i determinuje w większym stopniu daną właściwość materiału węglowego.

#### **4.6. Toksyczność pochodnych wielopierścieniowych węglowodorów aromatycznych i ich zawartość w próbkach środowiskowych**

Wzrost zainteresowania pochodnymi WWA, a w szczególności ich występowaniem w próbkach środowiskowych, przemianami, jakimi poddawane są pod wpływem różnych czynników oraz przede wszystkim toksycznością, są w pełni uzasadnione, gdyż uważa się je za bardziej szkodliwe dla organizmów żywych niż związki rodzime [39,45]. Drogi narażenia na pochodne WWA mogą być zróżnicowane. Jedną z nich jest spożycie termicznie przetworzonej żywności lub mającej kontakt z zanieczyszczoną glebą, osadami, wodami gruntowymi czy rzecznymi [31,46]. Głównym sposobem narażenia jest droga inhalacyjna [31,47] lub pozażywieniowa poprzez powietrze atmosferyczne, a dokładniej cząstki stałe zawieszone w powietrzu (z ang. Particulate Matter, PM), gdzie oznaczane zawartości pochodnych WWA są rzędu  $\text{ng}/\text{m}^3$  [48]. Drobny pył z atmosfery charakteryzuje się małą średnicą aerodynamiczną ( $\leq 2,5 \mu\text{m}$ ) i skomplikowanym składem chemicznym, w tym obecnością zanieczyszczeń oraz substancji toksycznych. Dzięki tym właściwościom, dostaje się on drogą wziewną do organizmu ludzkiego i osadza głęboko w płucach powodując szereg zaburzeń układu oddechowego [49].

W zależności od miejsca prowadzenia badań nad obecnością pochodnych WWA, stężenie związków w pyle zawieszonym w powietrzu może być niższe niż rodzimych WWA [37], jak również wartość ta może być bardzo podobna [50]. Dla przykładu, Ren i in. [50] wyznaczyli całkowite stężenia zarówno  $\Sigma 14\text{-WWA}$ , jak i  $\Sigma 7\text{O-WWA}$  w cząstках zawieszonych w powietrzu w dwóch miastach w Chinach i wynosiły one nawet  $57 \pm 20 \text{ ng}/\text{m}^3$  i  $18 \pm 23 \text{ ng}/\text{m}^3$  (rodzime WWA) oraz  $54 \pm 15 \text{ ng}/\text{m}^3$  i  $23 \pm 32 \text{ ng}/\text{m}^3$  (O-WWA). W innych próbkach środowiskowych stężenie O-WWA może być wyższe niż związków rodzimych [51]. W przypadku azotowych pochodnych WWA, większość związków o mniejszej masie cząsteczkowej znajduje się w fazie gazowej powietrza atmosferycznego, podczas gdy pochodne zawierające 4 i więcej pierścieni

aromatycznych (czyli o dużej masie cząsteczkowej) oznaczane są głównie w fazie cząstek stałych [52,53], co jest istotne z perspektywy możliwych dróg narażenia na te toksyny oraz ich toksyczności. Stąd ogromna potrzeba monitorowania nie tylko Σ16WWA, ale również ich tlenowych oraz azotowych pochodnych w różnych próbkach.

Mechanizmy toksyczności, mutagenności i kancerogenności pochodnych WWA nie są jeszcze dobrze zbadane oraz poznane. Jednakże wpływ związków na organizmy żywego jest ściśle związany z ich właściwościami fizykochemicznymi. Ponadto, ilość badań dotyczących tlenowych pochodnych WWA, w porównaniu z azotowymi pochodnymi WWA jest zdecydowanie mniejsza [31]. Może to być związane z mniejszą liczbą oraz niższym poziomem stężeń O-WWA w badanych próbkach [31]. Biorąc pod uwagę polarność oraz rozpuszczalność tlenowych WWA, wykazują one większą mobilność w porównaniu do związków rodzimych, przez co ich transport do wód gruntowych, czy powierzchniowych jest ułatwiony [51,54].

Aktualny stan badań nad toksycznością azotowych i tlenowych pochodnych WWA został przedstawiony w publikacji:

**D1 A. Krzyszczak, B. Czech, *Occurrence and toxicity of polycyclic aromatic hydrocarbons derivatives in environmental matrices*, Science of the Total Environment, 2021, 788: 147738.**

Informacje dotyczące toksyczności O-WWA są bardzo ograniczone. Lecz wiadomość jest, że zawartość tlenowych pochodnych w pyle zawieszonym w powietrzu jest ściśle związana z powstawaniem reaktywnych form tlenu (z ang. Reactive Oxygen Species, ROS) [55]. Tworzenie ROS wiąże się przede wszystkim z produkcją enzymów przeciwtleniających, która ma miejsce podczas wywołania stresu oksydacyjnego. Ponadto, efektem narażenia hodowanych ludzkich komórek nabłonkowych pęcherzyków płucnych (A549) na PM<sub>2,5</sub> zebrany w dużych przemysłowych miastach, był wzrost zawartości cytokin (czynnik martwicy nowotworów (TNF-α) i interleukiny IL6) oraz tlenku azotu, jak również spadek żywotności komórek [56].

Badania dotyczące toksyczności azotowych pochodnych WWA są bardziej obszerne. W większości z nich weryfikowane są skutki narażenia na 1-nitropiren (1-NP), który jest głównym przedstawicielem N-WWA. Występuje on w cząstkach spalin generowanych przez silnik wysokoprężny. 1-NP posiada właściwości cytotoxisyczne,

genotoksyczne i mutagenne [45,57] oraz może wywoływać stan zapalny w organizmie [58,59]. Dodatkowo indukuje on powstawanie ROS w komórkach A549 [60] oraz prowadzi do uszkodzeń DNA u szczurów i wzrostu stężenia 8-hydroksy-2'-deoksyguanozyny (8-OH-dG), która jest metabolitem rozkładu 1-NP w organizmie żywym [61]. Dlatego 8-OH-dG jest uważana za biomarker świadczący o narażeniu na spaliny samochodowe [62] oraz informujący o uszkodzeniu oksydacyjnym DNA [60]. Natomiast, 1,8-dinitropiren jest 3 razy bardziej toksyczny od benzo[a]pirenu [63].

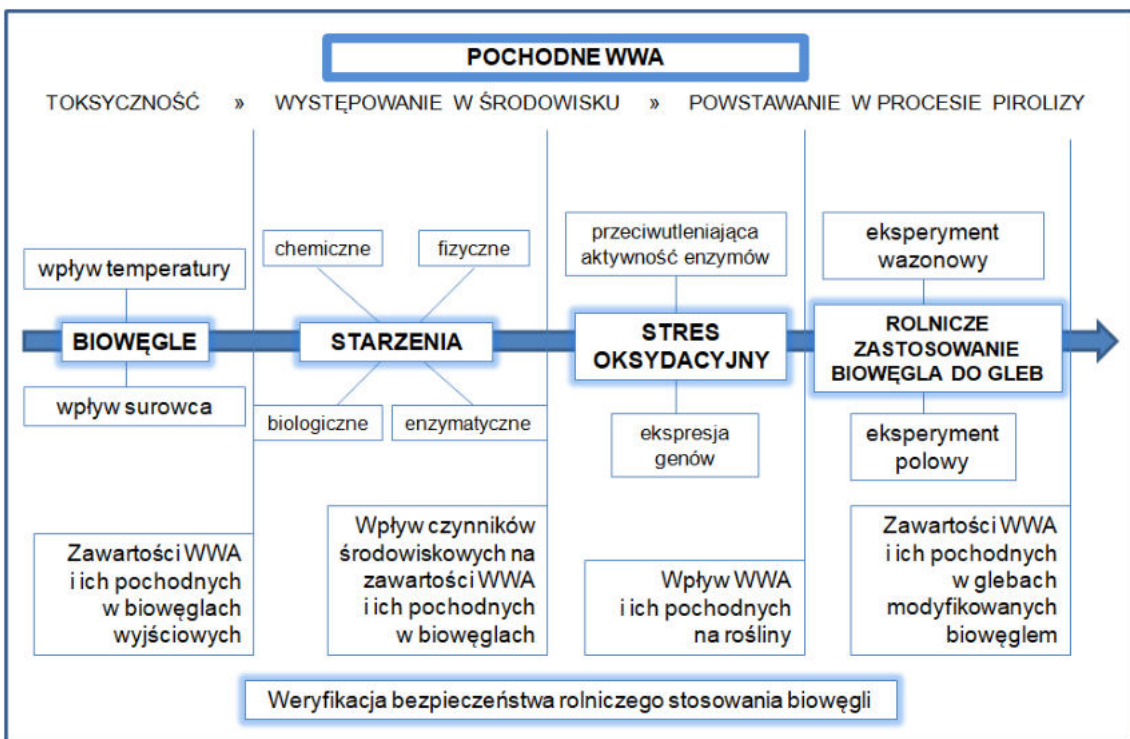
Niestety, w dostępnych danych literaturowych nadal brakuje informacji dotyczących toksyczności siarkowych pochodnych WWA. Jedynie pewne przypuszczenia zakładają podobną toksyczność i jej mechanizmy do rodzimych WWA [64]. S-WWA mogą indukować stres oksydacyjny oraz wykazywać działanie cytotoxisyczne.

Temat toksyczności pochodnych WWA wymaga jeszcze wielu uzupełnień. Na chwilę obecną, dostępne dane literaturowe wskazują na potrzebę monitorowania ich stężenia w próbkach środowiskowych (wodach, glebie, powietrzu), żywności (np. rybach) oraz przede wszystkim w produktach procesu pirolitycznego, gdyż wysokotemperaturowym beztlenowym przemianom biomasy towarzyszy powstawanie zarówno WWA, jak również ich pochodnych.

## **5. Cel badań oraz wpływ uzyskanych wyników na zrównoważony rozwój i zieloną chemię**

---

Celem badań będących podstawą rozprawy doktorskiej była weryfikacja bezpieczeństwa rolniczego zastosowania biowęglę pod kątem ilości i jakości pochodnych wielopierścieniowych węglowodorów aromatycznych obecnych w spirolikowanym materiale. W pierwszym etapie, cel ten realizowałam poprzez dokonanie przeglądu literaturowego dotyczącego charakterystyki, właściwości i zawartości pochodnych WWA w próbkach środowiskowych (publikacja **D1**). Podejrzenie większej toksyczności pochodnych WWA od związków rodzimych zainspirowało do kolejnych etapów badań, które rozpoczęły się od otrzymania i charakterystyki fizykochemicznej biowęgli, a także zbadania wpływu temperatury pirolizy (publikacja **D2**), jak również zastosowanego surowca (publikacja **D3**) na zawartość frakcji całkowitej i biodostępnej WWA oraz ich pochodnych w tym biomateriale. Kolejnym etapem było określenie zmian fizykochemicznych oraz zawartości analitów w węglowym materiale poddanym procesom starzenia fizycznego, chemicznego (publikacja **D4**), biologicznego oraz enzymatycznego (publikacja **D5**), które symulowały przemiany zachodzące podczas rolniczego zastosowania biowęglę jako dodatku do gleby. Oczywiście było również sprawdzenie reakcji wybranych roślin na wzbogacenie gleby spirolikowanym materiałem (m. in. oznaczenie enzymów stresu oksydacyjnego) (publikacja **D6**). Ostatni etap badań zakładał przeprowadzenie eksperymentów wazonowych i polowych (publikacja **D7**), polegających na wzbogaceniu gleb BC, zarówno w warunkach laboratoryjnych, kontrolowanych (doświadczenie wazonowe), jak również w otoczeniu rzeczywistym (eksperiment polowy). Wyniki przedstawiające, w jaki sposób zmieniały się zawartości WWA i ich pochodnych w zmodyfikowanych glebach w czasie (do 18 miesięcy) przedstawiono w publikacji **D7**. Przebieg badań zrealizowanych w ramach pracy doktorskiej przedstawiono na rysunku 4.

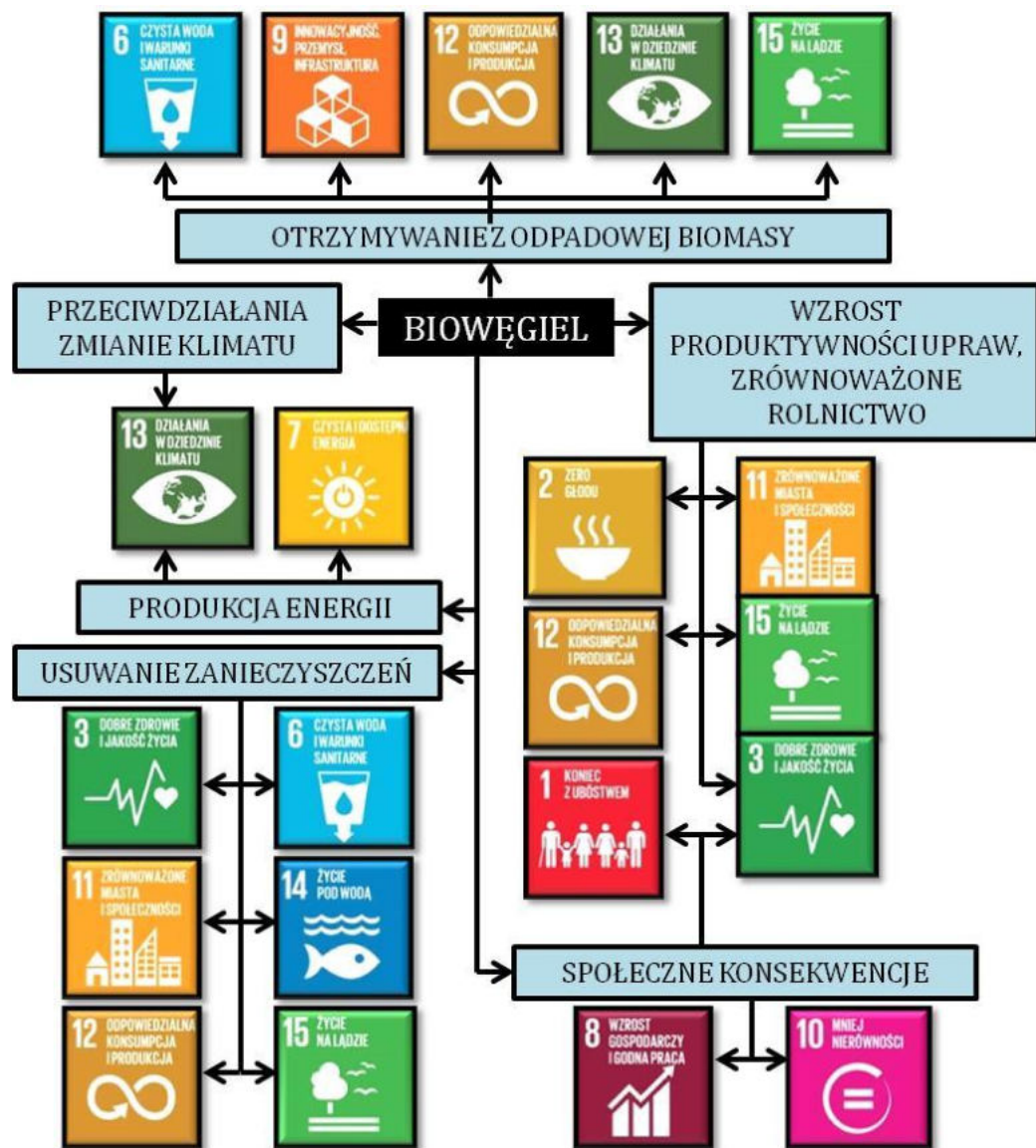


Rys. 4. Schemat przedstawiający badania przeprowadzone w ramach rozprawy doktorskiej.

Założono następujące hipotezy badawcze:

- Temperatura pirolizy wpływa na charakterystykę fizykochemiczną biowęgla, zatem powinna również rzutować na zawartość i biodostępność WWA oraz ich pochodnych w spirolikowanym materiale.
- Charakterystyka fizykochemiczna biowęgla zależy od zastosowanego surowca, zatem powinna również wpływać na zawartość i biodostępność WWA oraz ich pochodnych w spirolikowanym materiale.
- Procesy środowiskowe w różnym stopniu wywierają wpływ na podstawowe parametry fizykochemiczne BC.
- Procesy środowiskowe w różnym stopniu wywierają wpływ na ilość oraz jakość WWA i pochodnych (frakcja biodostępna i frakcja całkowita) w glebie użyźnionej biowęglem.
- Zawartości WWA oraz ich pochodnych w glebie wzbogaconej BC (w warunkach naturalnych) zmieniają się w zależności od czasu trwania wzbogacenia.

Dodatek biowęglę do gleb poprawia jej jakość, właściwości fizykochemiczne oraz strukturę. Zrównoważenie w produkcji polowej opiera się na własnej żyzności gleby, wspieranej jedynie nawozami. W przypadku zastosowania BC, wykorzystany „nawóz” jest pozyskany z materiałów odpadowych i w przeciwnieństwie do sztucznych, ogranicza wpływ rolnictwa na środowisko. W efekcie, potencjalne gospodarstwo produkuje więcej i taniej.



Rys. 5. Możliwe osiągnięcia celów zrównoważonego rozwoju poprzez otrzymywanie i zastosowanie biowęglę [65].

Dodatek biowęglę do gleb zwiększa ilość dostępnych składników pokarmowych potrzebnych roślinom, jak również powoduje wzrost retencji wodnej gleb, co jest ściśle

związane z efektywnym i optymalnym wykorzystaniem zasobów wodnych, co z kolei pozwala na zapewnienie stabilności oraz trwałości produkcji rolniczej, szczególnie w kontekście zmian klimatycznych.

Idea rolnictwa zrównoważonego obejmuje prawidłowe zarządzanie odpadami (Rys. 5). Biowęgiel można otrzymać z poprodukcyjnych odpadów rolnych i obornika, co ściśle wiąże się z ich utylizacją, wykorzystaniem, a nie składowaniem, które jest problematyczne, szkodliwe dla środowiska, wymaga odpowiednich warunków oraz nakładów finansowych, a zachodzące procesy gnilne są źródłem metanu i ditlenku węgla, które w konsekwencji są uwalniane do atmosfery. Produkcja BC z rolnych materiałów odpadowych, jak również jego praktyczne zastosowanie jako dodatek do gleb są powiązane z dążeniem do redukcji emisji gazów cieplarnianych.

Innym założeniem idei zrównoważonego rozwoju jest podejmowanie działań dla społecznej akceptacji rolnictwa. Postęp wiedzy to przede wszystkim badania naukowe, ale również połączenie wiedzy naukowej, polityki i ekonomii. Istnieje ogromne zapotrzebowanie na stworzenie systemu edukacji oraz doradztwa dotyczącego sposobu pozyskiwania, wykorzystywania biomasy, co przyczyniłoby się do wzrostu świadomości społeczeństwa. Podjęcie tych kroków wprowadziłoby w życie wiele zasad zielonej chemii, np. zapobieganie tworzeniu odpadów, efektywne wykorzystanie energii, jak również stosowanie surowców odnawialnych.

## **6. Ogólny opis metod zastosowanych w badaniach**

---

### **6.1. Charakterystyka fizykochemiczna biowęgla**

Biowęgle wykorzystywane w badaniach prowadzonych w ramach rozprawy doktorskiej zostały scharakteryzowane poprzez określenie wielkości powierzchni właściwej, porowatości, wartości pH, zawartości popiołu, zawartości C, O, N i H. Ponadto, dokonano charakterystyki powierzchni materiału (m. in. pod względem składu chemicznego, obecności grup funkcyjnych, morfologii). Poniżej wymieniono wyznaczone parametry fizykochemiczne oraz zastosowane metody:

- Wielkość powierzchni właściwej oraz porowatość.

W tym celu wykorzystano metodę niskotemperaturowej adsorpcji azotu. Próbki biowęgli odgazowano w temperaturze 200°C przez 12 godz. w warunkach podciśnieniowych, a następnie za pomocą analizatora ASAP 2420 (Micromeritics, Stany Zjednoczone) oznaczono parametry: wielkość powierzchni właściwej wyznaczona metodą BET (Brunauer-Emmett-Teller), objętość, średnica i rozkład wielkości porów.

- Wartość pH.

Do 1 g biowęgla dodano 10 mL wody destylowanej (ultra-czystej ( $< 0,08 \mu\text{S}/\text{cm}$ ), Hydrolab, Polska), a pomiar pH przeprowadzono z wykorzystaniem cyfrowego pH-metru HQ430d Benchtop Single Input (HACH, Stany Zjednoczone).

- Zawartość popiołu.

Parametr wyznaczono poprzez spalenie próbek biowęgla w temperaturze 760°C przez 6 godz. w piecu Megatherm (Polska). Następnie z ubytku masy obliczono procentową zawartość popiołu.

- Zawartość węgla, azotu, wodoru i tlenu.

Procentowe zawartości C, N i H wyznaczono z wykorzystaniem aparatu EuroEA Elemental Analyser (EuroVector, Włochy). Natomiast zawartość O obliczono matematycznie, uwzględniając dodatkowo zawartość popiołu.

- Charakterystyka powierzchniowych grup funkcyjnych.

W tym celu wykorzystano spektroskopię fotoakustyczną w podczerwieni z transformacją Fouriera (z ang. Fourier-Transform Infrared Photoacoustic Spectroscopy, FTIR-PAS) oraz spektroskopię fotoelektronów w zakresie promieniowania X (z ang. X-ray Photoelectron Spectroscopy, XPS). Pierwsza z nich posłużyła do scharakteryzowania struktury chemicznej powierzchni i analizy jakościowej grup funkcyjnych obecnych na spirolizowanym materiale. Widma próbek zostały zarejestrowane z wykorzystaniem spektrometru Bio-Rad Excalibur 3000 MX wyposażonego w detektor fotoakustyczny MTEC300 (detektor w komorze wypełnionej helem) w zakresie  $4000\text{-}400\text{ cm}^{-1}$ , przy rozdzielczości  $4\text{ cm}^{-1}$ . Natomiast do badań składu powierzchniowego materiałów techniką XPS wykorzystano spektrometr UHV Prevac (Polska). System analityczny UHV umożliwił wykonanie analiz z rozdzielczością  $<1\text{ meV}$ . Uzyskane wyniki pozwoliły na jakościowe i ilościowe określenie grup funkcyjnych występujących na powierzchni biowęglu.

- Morfologia powierzchni.

Do badań morfologii powierzchni spirolizowanego materiału wykorzystano technikę skaningowej mikroskopii elektronowej (z ang. Scanning Electron Microscopy, SEM). Wyniki zebrano przy użyciu skaningowego mikroskopu elektronowego Quanta 3D FEG (FEI, Stany Zjednoczone) z systemem spektroskopii dyspersji energii (SEM-EDS). Moduł EDS umożliwił przeskanowanie rozmieszczenia poszczególnych składników próbki na powierzchni badanych materiałów.

## 6.2. Oznaczanie frakcji całkowitej WWA i ich pochodnych

Do oznaczenia całkowitej zawartości WWA i ich tlenowych oraz azotowych pochodnych wykorzystana została technika przyspieszonej ekstrakcji za pomocą rozpuszczalnika (z ang. Pressurized Fluid Extraction, PFE, Accelerated Solvent Extraction, ASE lub Pressurized Liquid Extraction, PLE) przy użyciu aparatu Dionex 350 System (Thermo Fisher Scientific, Stany Zjednoczone). 22 mL celki ze stali nierdzewnej, poczynając od dolnej warstwy, zostały wypełnione odpowiednio: filtrem celulozowym (Thermo Fisher Scientific, Stany Zjednoczone), żellem krzemionkowym

(aktywowanym w temperaturze 300°C przez 5 godz.) (Macherey-Nagel, Niemcy) wymieszany z 0,1 g sproszkowanej miedzi (Merck, Niemcy) (dodanej w celu związania siarki) oraz 0,5 g biowęglą (lub 4 g gleby) wymieszany z 0,1 g kwasu etylenodiaminotetraoctowym (EDTA, Sigma-Aldrich, Stany Zjednoczone). Bezpośrednio przed ekstrakcją, do celek wprowadzono roztwór deuterowanych WWA (PAH Mix 9 deuterated standard (Dr Ehrenstorfer GmbH, Niemcy) – 100 ng/μL), który stanowił wzorzec wewnętrzny. Pozostałą przestrzeń wypełniono kulkami szklanymi. Ekstrakcja była przeprowadzona z wykorzystaniem heksanu (Chempur, Polska), pozostałe parametry wynosiły odpowiednio:

- temperatura 150°C,
- ilość cykli ekstrakcji: 2,
- objętość przepłukująca: 60%,
- czas ekstrakcji statycznej: 5 min,
- czas przepłukiwania: 60 s przy ciśnieniu 1 MPa za pomocą N<sub>2</sub>.

Tabela 1. Wykaz WWA i ich pochodnych oznaczanych podczas badań prowadzonych w ramach rozprawy doktorskiej.

Lp.	Nazwa związku	CAS <sup>(1)</sup>	Wzór sumaryczny	Granica wykrywalności <sup>(2)</sup> [μg/L]	Granica oznaczalności <sup>(2)</sup> [μg/L]
1	naftalen*	91-20-3	C <sub>10</sub> H <sub>8</sub>	1,01	3,36
2	1,3-di-izo-propylnaftalen	57122-16-4	C <sub>16</sub> H <sub>20</sub>	1,41	4,69
3	2-fenylnaftalen	612-94-2	C <sub>16</sub> H <sub>12</sub>	1,90	6,33
4	acenaftylen*	208-96-8	C <sub>12</sub> H <sub>8</sub>	2,10	6,99
5	acenaften*	83-32-9	C <sub>12</sub> H <sub>10</sub>	2,30	7,66
6	fluoren*	86-73-7	C <sub>13</sub> H <sub>10</sub>	1,10	3,66
7	antracen*	120-12-7	C <sub>14</sub> H <sub>10</sub>	1,30	4,33
8	fenantren*	85-01-8	C <sub>14</sub> H <sub>10</sub>	1,34	4,36
9	3-metylfenantren	832-71-3	C <sub>15</sub> H <sub>12</sub>	2,42	8,06
10	2-metylfenantren	2531-84-2	C <sub>15</sub> H <sub>12</sub>	2,42	8,06
11	9-metylfenantren	883-20-5	C <sub>15</sub> H <sub>12</sub>	3,23	10,76
12	3,6-dimetylfenantren	1576-67-6	C <sub>16</sub> H <sub>14</sub>	2,20	7,33
13	fluoranten*	206-44-0	C <sub>16</sub> H <sub>10</sub>	1,87	6,22
14	piren*	129-00-0	C <sub>16</sub> H <sub>10</sub>	1,91	6,36
15	2-metylpiren	3442-78-2	C <sub>17</sub> H <sub>12</sub>	1,92	6,39
16	4-metylpiren	3353-12-6	C <sub>17</sub> H <sub>12</sub>	1,92	6,39

17	benzo[a]fluoren	238-84-6	C <sub>17</sub> H <sub>12</sub>	1,30	4,33
18	benzo[a]antracen*	56-55-3	C <sub>18</sub> H <sub>12</sub>	1,30	4,33
19	chryzen*	218-01-9	C <sub>18</sub> H <sub>12</sub>	2,20	7,33
20	3-metylchryzen	3351-31-3	C <sub>19</sub> H <sub>14</sub>	1,02	3,40
21	5-metylchryzen	3697-24-3	C <sub>19</sub> H <sub>14</sub>	1,55	5,16
22	6-metylchryzen	1705-85-7	C <sub>19</sub> H <sub>14</sub>	1,02	3,40
23	benzo[a]fluoranten	203-33-8	C <sub>20</sub> H <sub>12</sub>	2,10	6,99
24	benzo[b]fluoranten*	205-99-2	C <sub>20</sub> H <sub>12</sub>	2,10	6,99
25	benzo[k]fluoranten*	207-08-9	C <sub>20</sub> H <sub>12</sub>	2,10	6,99
26	benzo[j]fluoranten	205-82-3	C <sub>20</sub> H <sub>12</sub>	1,39	4,63
27	benzo[a]piren*	50-32-8	C <sub>20</sub> H <sub>12</sub>	2,11	7,03
28	indenol[1,2,3-cd]piren*	193-39-5	C <sub>22</sub> H <sub>12</sub>	1,30	4,33
29	benzo[ghi]perylen*	191-24-2	C <sub>22</sub> H <sub>12</sub>	1,33	4,43
30	dibenzo[a,h]antracen*	53-70-3	C <sub>22</sub> H <sub>14</sub>	2,21	7,36
31	dibenz[a,e]piren	192-65-4	C <sub>24</sub> H <sub>14</sub>	1,89	6,29
32	dibenz[a,h]piren	189-64-0	C <sub>24</sub> H <sub>14</sub>	1,89	6,29
33	dibenz[a,i]piren	189-55-9	C <sub>24</sub> H <sub>14</sub>	1,89	6,29
34	dibenz[a,l]piren	192-65-4	C <sub>24</sub> H <sub>14</sub>	1,89	6,29
Tlenowe i azotowe pochodne WWA					
35	nitronaftalen	86-57-7	C <sub>10</sub> H <sub>7</sub> NO <sub>2</sub>	2,41	8,03
36	1-metyl-5-nitronaftalen	91137-27-8	C <sub>11</sub> H <sub>9</sub> NO <sub>2</sub>	1,21	4,03
37	1-metyl-6-nitronaftalen	105752-67-8	C <sub>11</sub> H <sub>9</sub> NO <sub>2</sub>	1,21	4,03
38	9,10-antracendion	84-65-1	C <sub>14</sub> H <sub>8</sub> O <sub>2</sub>	1,44	4,80
39	4H-cyklopenta(def)fenantren	203-64-5	C <sub>15</sub> H <sub>10</sub>	3,01	10,02
40	nitropiren	5522-43-0	C <sub>16</sub> H <sub>9</sub> NO <sub>2</sub>	1,66	5,53

<sup>(1)</sup>numer identyfikacyjny nadany przez Chemical Abstracts Service (CAS);

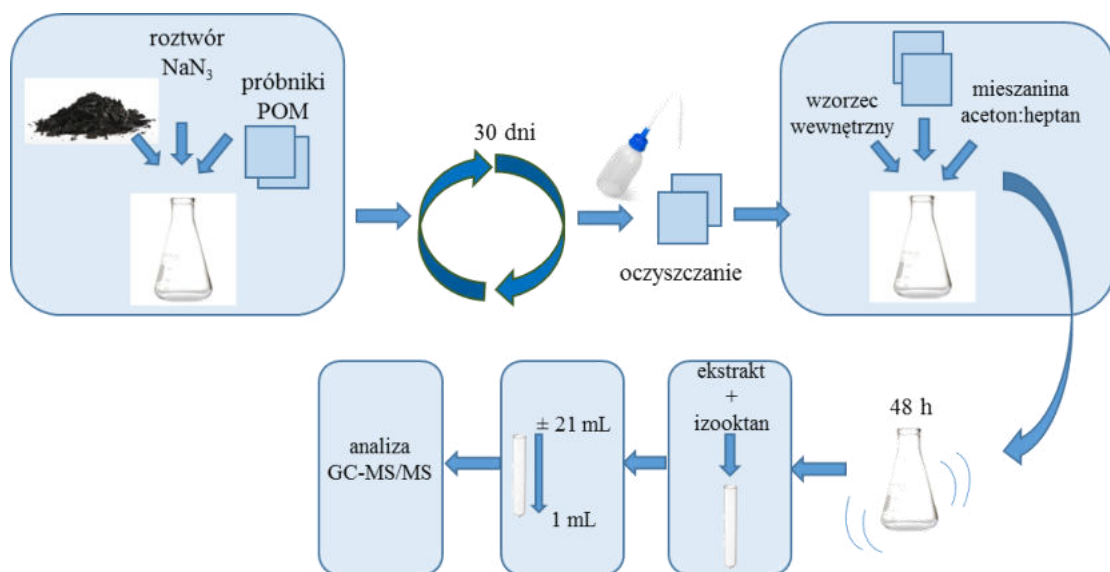
<sup>(2)</sup>wartości granic wykrywalności i oznaczalności zostały wyznaczone jako stosunek sygnału do szumu pomnożony odpowiednio przez 3 lub 10;

\*WWA z listy Agencji Ochrony Środowiska Stanów Zjednoczonych (US EPA).

Otrzymany roztwór wzbogacono 1 mL izooktanu (Chempur, Polska), odparowano w wyparce rotacyjnej RVC 2-25 CD plus (Martin Christ, Niemcy) do objętości 1 mL i analizowano metodą chromatografii gazowej sprzężonej z tandemową spektrometrią mas (GC-MS/MS) z wykorzystaniem chromatografu gazowego sprzężonego z detektorem mas typu potrójny kwadrupol (GCMS-TQ8040; Shimadzu, Kyoto, Japonia). W Tabeli 1 przedstawiono zestawienie wszystkich WWA i ich pochodnych oznaczanych ilościowo podczas badań wykonywanych w ramach rozprawy doktorskiej.

### 6.3. Oznaczanie frakcji biodostępnej WWA i pochodnych

Zawartość biodostępnej frakcji WWA i pochodnych wyznaczono z wykorzystaniem metody bazującej na zastosowaniu pasywnego próbnika polioksymetylenowego (POM). Schemat eksperymentu przedstawiono na Rys 6. Przed docelową analizą, próbniki o wymiarach 4 cm na 4 cm (około 35 g, 76 µm grubości) były kondycjonowane wg ścisłe określonej procedury, która zakładała 24-godzinne wytrząsanie w metanolu (Merck, Niemcy) (na mieszadle horyzontalnym (ELPIN 358A, Polska), a następnie w n-heptanie (POCH, Polska) (24 godz.) i wodzie destylowanej (24 godz.). Do momentu właściwego oznaczania, POMy były przechowywane w wodzie destylowanej w temperaturze 4°C.



Rys. 6. Schemat procedury oznaczania frakcji biodostępnej WWA i pochodnych w biowęglach.

Docelowa procedura obejmowała umieszczenie próbki biowęgla (1 g) w kolbie Erlenmayera (o objętości 50 mL), do której następnie dodano 40 mL wodnego roztworu azydku sodu (Chempur, Polska) (w celu zahamowania rozwoju mikroorganizmów) o stężeniu 200 mg/L oraz dwa próbniaki. Tak przygotowane, odpowiednio zabezpieczone kolby wytrząsano przez 30 dni na mieszadle obrotowym ROTAX 6.8 VELP Scientifica (Włochy) z prędkością 10 obrotów/min. Następnie próbniaki zostały wyjęte, oczyszczone wodą destylowaną, po czym poddano je ekstrakcji mieszaniną

acetonu (POCH, Polska) i heptanu (POCH, Polska) (1:4, obj.) z dodatkiem wzorca wewnętrznego (rozdział 6.2.) przez 48 godz. na mieszadle horyzontalnym. Ekstrakt wzbogacono 1 mL izooktanu, odparowano do 1 mL stosując wyparkę rotacyjną. Otrzymane próbki analizowano metodą chromatografii gazowej sprzężonej z tandemową spektrometrią mas.

Stężenie poszczególnych WWA i pochodnych na pasywnym próbniku ( $C_{POM}$  [ng/kg]) obliczono według równania (1):

$$C_{POM} = m_{WWA} / m_{2POM} \quad (1)$$

gdzie:  $m_{WWA}$  (lub  $m_{\text{pochodne WWA}}$ ) oznacza masę analitu oznaczoną techniką GC-MS/MS [ng];  $m_{2POM}$  [kg] oznacza masę dwóch wysuszonych pasywnych próbników, zastosowanych do ekstrakcji.

Natomiast stężenie frakcji biodostępnej  $C_{free}$  [ng/L] (z ang. freely dissolved) obliczono z równania (2):

$$C_{free} = C_{POM} / K_{POM} \quad (2)$$

gdzie:  $K_{POM}$  [L/kg] jest współczynnikiem podziału WWA (lub pochodnych WWA) pomiędzy próbniem i wodą wyznaczonym przez Hawthorne i in. [66]. W przypadku braku informacji o współczynniku podziału dla niektórych pochodnych WWA, do obliczeń została wykorzystana wartość odpowiadająca rodzimym WWA.

#### 6.4. Przeprowadzenie starzeń modelowych

W celu określenia wpływu czynników środowiskowych na parametry fizykochemiczne biowęglę oraz zawartości frakcji całkowitej i biodostępnej WWA, jak również ich pochodnych, przeprowadzono badania modelowe starzenia (z ang. aging). Do wykonania eksperymentu wybrano cztery rodzaje starzeń: fizyczne, chemiczne, biologiczne oraz enzymatyczne. Większość artykułów naukowych prezentuje efekt krótkotrwałego narażenia spirolizowanego materiału na czynniki środowiskowe [43], dlatego celem moich badań było określenie zmian w charakterystyce BC oraz w zawartości poszczególnych frakcji analitów w biowęglach poddanych 6-miesięcznym procesom starzenia.

### Starzenie fizyczne i chemiczne

Pierwszym etapem obydwu procesów była sterylizacja biowęglą, którą przeprowadzono poprzez dodanie wodnego roztworu azydku sodu (200 mg/L) oraz wody destylowanej na poziomie 40% pojemności wodnej BC (wyznaczonej przed docelowym eksperymentem). Przez cały okres trwania doświadczenia wartość ta była utrzymywana na zadanym poziomie (ubytki były uzupełniane wodą destylowaną). Starzenie fizyczne (z ang. Physical Aging, PA) przeprowadzono poprzez wystawienie biowęglą na działanie skoku temperatur +20°C oraz -20°C w tygodniowych interwałach. Natomiast starzenie chemiczne (z ang. Chemical Aging, CA) realizowano dwutorowo narażając spirolizowany materiał na temperaturę 60°C (CA60) oraz na 90°C (CA90). Zastosowanie tych temperatur (60°C, 90°C) pozwoliło na przyspieszenie naturalnych procesów chemicznych, jakim poddawany byłby biowęgiel w środowisku. Zgodnie z regułą van't Hoffa [67], zmiany zachodzące w BC podczas 6-miesięcznego starzenia w temperaturze 60°C lub 90°C będą odpowiadały przemianom węglowego materiału inkubowanego przez odpowiednio 8 i 64 lata w 20°C, 24 oraz 191 lat w 4°C, bądź 126 i 1010 lat w -20°C. Procesy starzeniowe prowadzono przez 6 miesięcy, po czym starzony BC suszono w temperaturze 105°C przez 4 godz.

### Starzenie biologiczne i enzymatyczne

Pierwszym etapem starzenia biologicznego (z ang. Biological Aging, BA) była ekstrakcja *inoculum* mikrobiologicznego z gleby rolnej z Podborcza, województwo lubelskie (szczegółowy opis inkubacji oraz ekstrakcji znajduje się w publikacji **D5**) oraz przygotowanie roztworu z substancjami odżywczymi (skład zaprezentowany w publikacji **D5**). Eksperyment prowadzono dwutorowo, gdyż tylko do jednego zestawu próbek dodano zarówno *inoculum* mikrobiologiczne, jak i odżywkę (próbki BAi). Drugi zestaw wzbogacono tylko roztworem ze składnikami odżywczymi (biowęgle BAn). Objętość dodawanych roztworów wynosiła 40% pojemności wodnej BC. Wartość ta była utrzymywana przez cały czas trwania eksperymentu (ubytki były uzupełniane wodą destylowaną). Procesy prowadzono przez 6 miesięcy, a starzony materiał węglowy wysuszono w temperaturze 105°C przez 4 godz.

Starzenie enzymatyczne (z ang. Enzymatic Aging, EA) przeprowadzono z wykorzystaniem enzymu peroksydazy chrzanowej (Sigma-Aldrich, Polska).

Biowęgiel (1 g) zawieszono w wodnym roztworze chlorku sodu buforowanym fosforanami (1 L, w składzie: NaCl, KCl, Na<sub>2</sub>HPO<sub>4</sub> oraz KH<sub>2</sub>PO<sub>4</sub>, Chempur, Polska) (z ang. Phosphate-Buffered Saline, PBS) o pH = 6, do którego następnie dodano 600 jednostek enzymu modelowego. Układ inkubowano przez 24 godz. na mieszadle magnetycznym (IKA, Polska) o amplitudzie 300 obrotów/min. Po czym enzym aktywowano dodatkiem nadtlenku wodoru (500 µmol/L) (Chempur, Polska) i ponownie inkubowano przez 10 dni. Zawiesinę przesączono przez filtr, a starzony biowęgiel suszono w temperaturze 105°C przez 4 godz.

## 7. Wyniki badań własnych

---

### 7.1. Wpływ surowca na charakterystykę fizykochemiczną biowęgli

Celem badań było sprawdzenie, w jaki sposób rodzaj surowca zastosowanego do otrzymania biowęglę wpływa na podstawowe parametry fizykochemiczne spirolikowanego materiału (**publikacja D2** oraz **D3**). Materiał wyjściowy wykorzystany podczas badań, będących przedmiotem rozprawy, można podzielić na trzy grupy:

- surowiec pochodzenia roślinnego (PT): i) bogaty w celulozę: wierzba (*Salix viminalis*) (BCW), słoma pszeniczna (*Triticum L.*) (BCS), słonecznik (*Helianthus annuus L.*) (BCA) oraz ii) bogaty w ligninę: odpady z drzew liściastych (BCD) oraz iglastych (BCF),
- pozostałości po produkcji biogazu (RBP) pozyskane z Biogazowni Kocergi (BCKOS), Piaski (BCPIL), Uhnin (BCUHS),
- osad ściekowy (SSL) pozyskany z Oczyszczalni Ścieków w Chełmie (CCCH), Kaliszu (BCKZ), Zamościu (BCZ) i Suwałkach (BCSI).

Tabela 2. Porównanie wybranych właściwości fizykochemicznych biowęgli.

	Wybrane podstawowe parametry fizykochemiczne biowęgli				
	zawartość popiołu [%]	zawartość C [%]	zawartość H [%]	zawartość N [%]	zawartość O [%]
najwyższa wartość	SSL	PT	PT	SSL	PT
średnia wartość	RBP	RBP	RBP	RBP	RBP
najniższa wartość	PT	SSL	SSL	PT	SSL

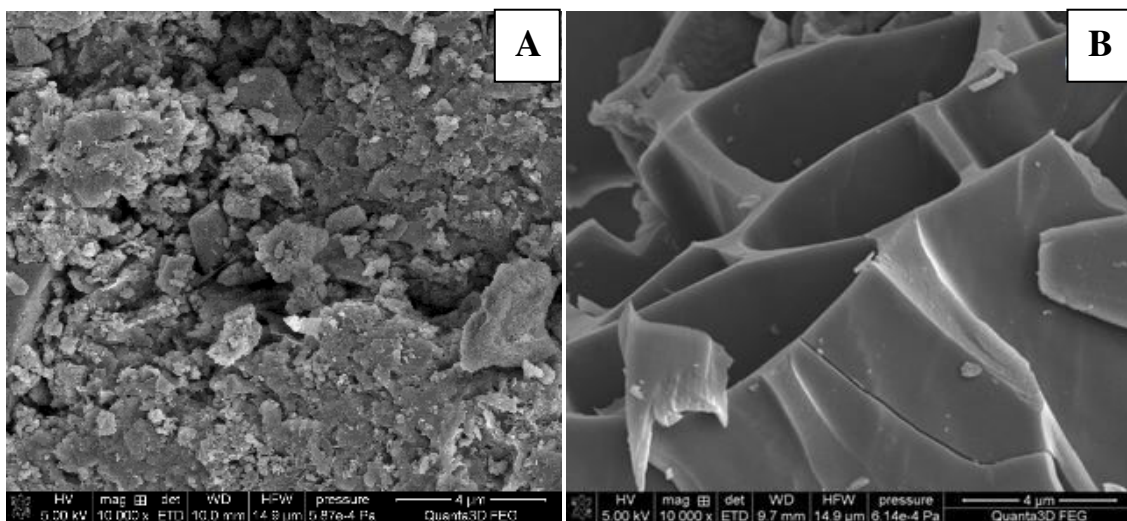
PT – surowiec pochodzenia roślinnego;

RBP – pozostałości po produkcji biogazu;

SSL – osad ściekowy.

Biorąc pod uwagę zawartość popiołu, podstawowych pierwiastków, jak również aromatyczność, polarność i hydrofobowość biowęgli, uwidocznili się wyraźny wpływ zastosowanej biomasy. Najniższe zawartości popiołu oraz azotu oznaczono w BC otrzymanych z surowca roślinnego, podczas gdy najwyższe dla materiału powstałego z osadów ściekowych (Tabela 2). Odwrotne tendencje uzyskano w przypadku zawartości pozostałych pierwiastków (C, H i O) (publikacja **D3**).

Jednakże nie dla wszystkich podstawowych parametrów fizykochemicznych biowęgli zaobserwowano wyraźną tendencję dotyczącą wybranego materiału wyjściowego. W przypadku niektórych właściwości wpływ każdej zastosowanej biomasy należy interpretować indywidualnie, gdyż przykładowo, biorąc pod uwagę wielkość powierzchni właściwej spirolizowanego materiału, największe wartości uzyskano dla BC otrzymanych z wierzby oraz dwóch osadów ściekowych (pozyskanych z Chełma i Zamościa) (publikacja **D2** i **D3**). Podobne wnioski można przedstawić biorąc pod uwagę wartości pH. Największą powierzchnię właściwą charakteryzował się materiał otrzymany z wierzby (BCW) ( $145,02\text{ m}^2/\text{g}$ ), podczas gdy wartości dla pozostałych biowęgli pozyskanych z surowców roślinnych wynosiły poniżej  $2,5\text{ m}^2/\text{g}$ . Z kolei dane otrzymane techniką XPS ukazują, że powierzchnia BCZ600, oprócz C, O, N i Ca (znajdującego się również na innych materiałach, np. BCW600), zawierała również Si, P, Al, S oraz Fe (publikacja **D3**).



Rys. 7. Zdjęcia wykonane techniką SEM biowęglów otrzymanego z osadu ściekowego (A) oraz wierzby (B) (publikacja **D2**).

Zdjęcia wykonane techniką SEM również obrazują różnice w strukturze BC. W przypadku materiałów otrzymanych z osadów ściekowych, część biowęgli nadal posiadała organizację częstek podobną do wyjściowego surowca, a inne fragmenty były pokruszone i pokryte substancjami smolistymi (Rys. 7A). Natomiast BC otrzymany z wierzyby charakteryzował się bardziej uporządkowaną strukturą, widoczne były wydłużone pory o kształcie zdeformowanych okrągów lub zniekształconych plastrów miodu, przy czym niektóre z nich były przedzielone przegrodą (publikacja D3) (Rys. 7B). Wygląd szkieletu biowęglu BCW jest ściśle powiązany z biologiczną kapilarną strukturą surowca (publikacja D2).

Wyniki przedstawione w pracach **D2** i **D3** potwierdzają hipotezę, że charakterystyka fizykochemiczna biowęglu zależy od zastosowanego surowca.

## **7.2. Wpływ surowca na zawartość frakcji całkowitej oraz biodostępnej WWA i pochodnych w biowęglu**

Zgodnie w wynikami zawartymi w publikacjach **D2** i **D3**, surowiec wypływa na zawartość analitów w spirolizowanym materiale. Podobnie jak w przypadku wartości pH, czy wielkości powierzchni właściwej, zależności dotyczące zawartości frakcji całkowitej i biodostępnej WWA oraz pochodnych nie dotyczą podziału surowców na trzy grupy (rozdział 7.1.), lecz każdy z biowęgli należy interpretować indywidualnie.

Tabela 3. Zestawienie wyników zawartych w publikacji **D3**.

Zasto- wana grupa surowców	Średnia zawartość analitów ± SD*			
	Całkowita frakcja WWA [µg/g]	Całkowita frakcja pochodnych WWA [µg/g]	Biodostępna frakcja WWA [ng/L]	Biodostępna frakcja pochodnych WWA [ng/L]
PT <sup>a</sup>	133,83 ± 46,15	9,97 ± 11,32	3,21 ± 0,89	0,43 ± 0,30
RBP <sup>b</sup>	189,71 ± 10,93	8,41 ± 6,83	20,76 ± 17,99	1,91 ± 2,38
SSL <sup>c</sup>	146,26 ± 30,91	16,79 ± 18,85	15,62 ± 16,51	0,95 ± 0,67

SD – odchylenie standardowe; a – średnia arytmetyczna z 5 rodzajów BC otrzymanych z surowców pochodzenia roślinnego; b – średnia arytmetyczna z 3 rodzajów BC otrzymanych z pozostałości po produkcji biogazu; c – średnia arytmetyczna z 4 rodzajów BC otrzymanych z osadów ściekowych.

Dane przedstawione w Tabeli 3 wskazują na duży rozrzut (wysoka wartość SD) wyników uzyskanych dla spirolizowanych materiałów otrzymanych z tej samej grupy surowców (PT, RBP lub SSL). Założenie (niepodparte wynikami badań), że wybrany biowęgiel jest bardziej bezpieczny (pod kątem rolniczego zastosowania), gdyż jest otrzymany z danej grupy biomasy, jest dużym uproszczeniem i może być błędne. Jednakże, szczególnie analizując biodostępność analitów, uwidocznioło się pewne zróżnicowanie. BC otrzymane z surowców roślinnych charakteryzowały się niższymi zawartościami frakcji biodostępnej zarówno WWA, jak i ich tlenowych oraz azotowych pochodnych.

Procentowe zawartości poszczególnych grup WWA zróżnicowanych pod względem liczby pierścieni aromatycznych zależą od zastosowanego surowca. Na przykład zawartości frakcji biodostępnej 2-pierścieniowych WWA w biowęglach otrzymanych ze słomy, wierzby oraz odpadów z drzew liściastych były poniżej granicy wykrywalności, podczas gdy w materiale z odpadów z drzew iglastych, związki zawierające dwa pierścienie aromatyczne w cząsteczce stanowiły ponad 50% wszystkich oznaczonych ilościowo WWA. Wyniki przedstawione w publikacjach **D2**, **D3** potwierdzają hipotezę, że zawartość frakcji całkowitej oraz biodostępnej WWA i ich pochodnych w biowęglach zależy od zastosowanego surowca.

### 7.3. Wpływ temperatury pirolizy na charakterystykę fizykochemiczną biowęgli

Celem kolejnych badań był określenie wpływu temperatury procesu pirolizy na podstawową charakterystykę fizykochemiczną biowęgli (publikacja **D2**). Spirolizowane materiały otrzymano w temperaturach 500°C, 600°C oraz 700°C. Jako surowce wybrano zarówno osady ściekowe (BCKZ i BCCH), jak również biomasę roślinną (BCW oraz BCS). Wyraźne zależności temperaturowe otrzymano dla:

- wartości pH (niemal we wszystkich przypadkach wzrost temperatury powodował wzrost pH biowęgla);
- zawartości popiołu (zwiększenie temperatury pirolizy skutkowało spadkiem zawartości popiołu dla BC otrzymanych z biomasy roślinnej i wzrostem dla spirolizowanych osadów ściekowych);

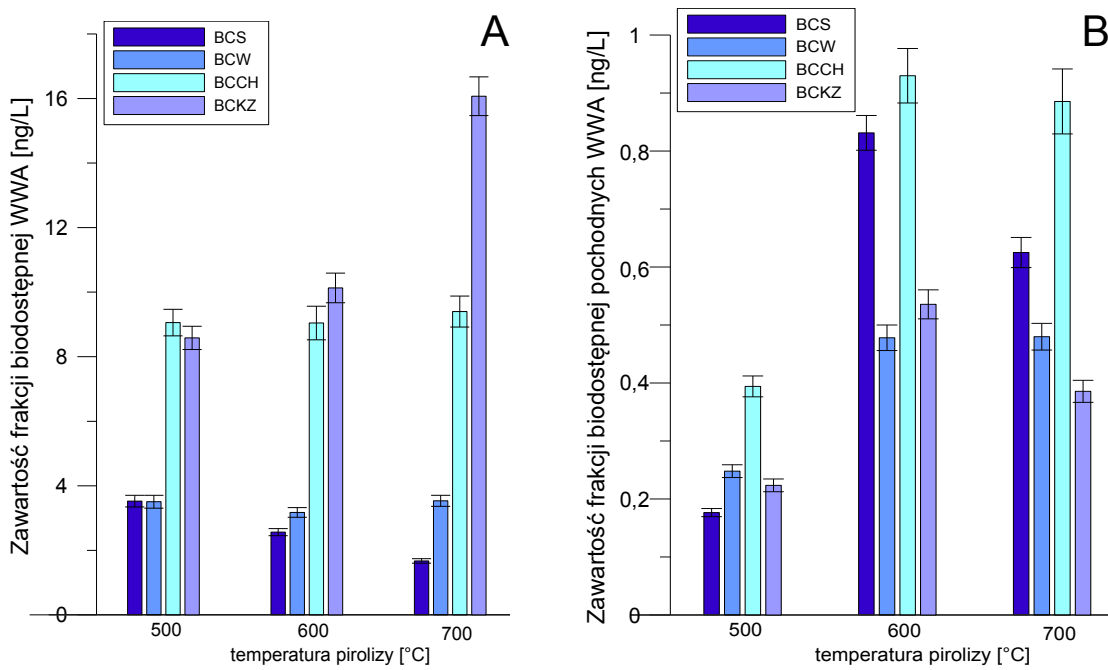
- zawartości azotu, wodoru i aromatyczności (wzrost temperatury powodował spadek wartości dla wszystkich węglowych materiałów);
- zawartości tlenu i polarności (niemal we wszystkich przypadkach wzrost temperatury powodował spadek wartości danych parametrów, z wyjątkiem BCS, dla którego tendencja była odwrotna).

Wielkość powierzchni właściwej materiałów nie była wyraźnie determinowana przez zastosowaną temperaturę pirolizy. Natomiast biowęgle otrzymane w temperaturze 600°C wyróżniały się spośród innych największą zawartością węgla.

Bazując na uzyskanych danych wynioskowano, że temperatura pirolizy znacząco wpływa na podstawową charakterystykę fizykochemiczną biowęgli. Dlatego chcąc otrzymać materiały węglowe zaprojektowane do konkretnych celów oraz charakteryzujące się ściśle określonymi parametrami, należy skrupulatnie wybrać zarówno surowiec, jak i temperaturę pirolizy.

#### **7.4. Wpływ temperatury na zawartość frakcji całkowitej oraz biodostępnej WWA i pochodnych w biowęglach**

Zgodnie w wynikami badań zawartymi w publikacji **D2**, zastosowana temperatura pirolizy wpływa na zawartość frakcji biodostępnej WWA i pochodnych w węglowych materiałach. W zależności od surowca użytego do pirolizy, wzrost temperatury procesu spowodował spadek zawartości frakcji biodostępnej WWA dla BCS, wzrost dla BCKZ, a w pozostałych przypadkach utrzymywał się na podobnym poziomie (Rys. 8A). Jednakże interpretując wyniki dotyczące frakcji biodostępnej pochodnych WWA zauważono tendencję, która zaważyła na dalszych badaniach. BC otrzymane w temperaturze 600°C (niezależnie od zastosowanego surowca) zawierały największe stężenie frakcji biodostępnej pochodnych WWA (Rys. 8B). Ta informacja, razem z podejrzeniem większej toksyczności pochodnych WWA w porównaniu ze związkami rodzimymi, zainspirowała do dalszych badań węglowych materiałów, w dużej mierze skupiając się na biowęglach otrzymanych w tej temperaturze.



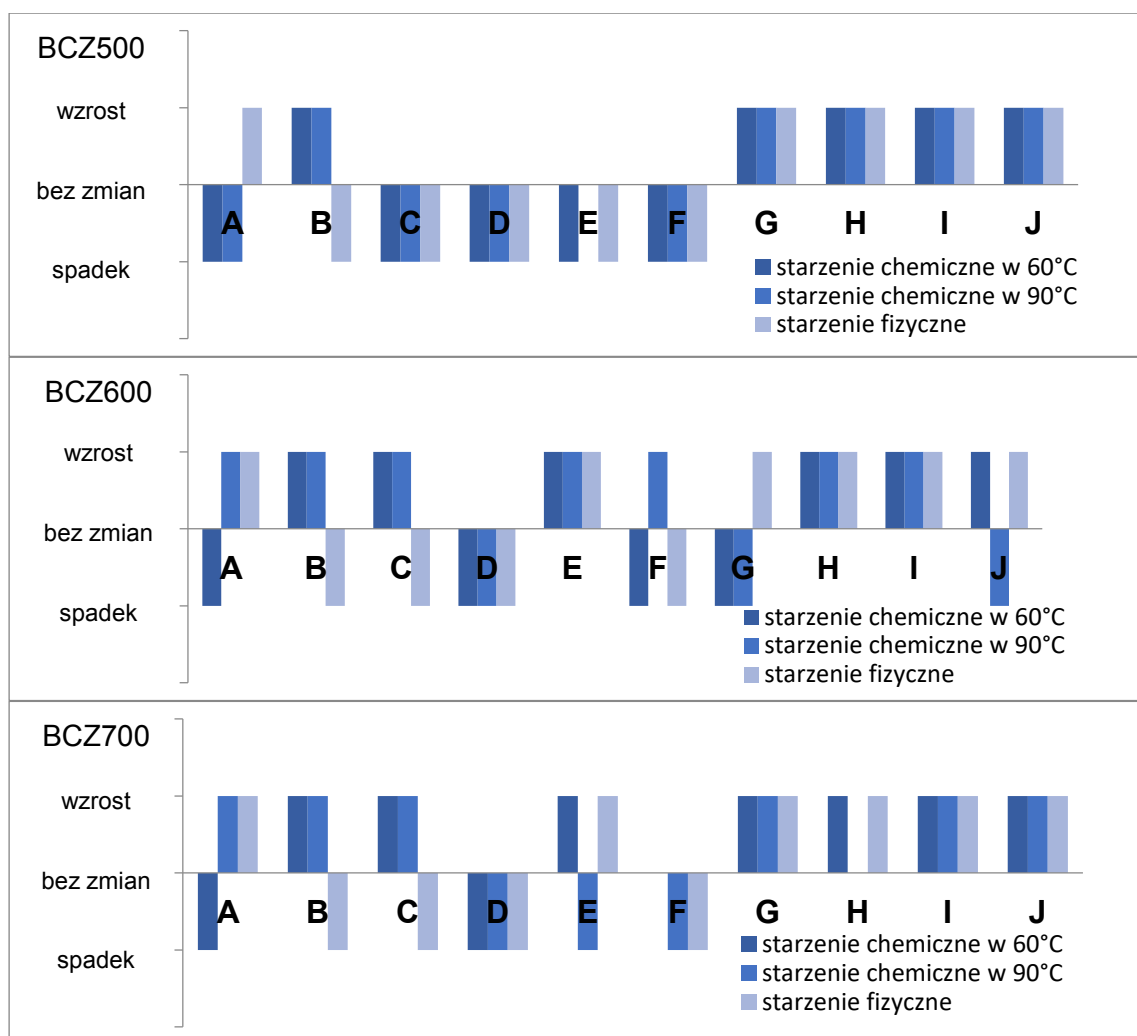
Rys. 8. Zawartość frakcji biodostępnej WWA (A) i pochodnych (B) w biowęglach (publikacja D2).

Zgodnie z wynikami zawartymi w publikacji D4, największe zawartości frakcji całkowitej WWA otrzymano dla biowęgli uzyskanych w 600°C ( $181,08 \pm 8,29 \mu\text{g/g}$  dla BCW600 i  $125,83 \pm 5,76 \mu\text{g/g}$  dla BCZ600). Z kolei największą całkowitą zawartość pochodnych WWA oznaczono ponownie dla BCZ600 ( $5,30 \pm 0,25 \mu\text{g/g}$ ). W przypadku materiałów otrzymanych z wierzby, wzrost temperatury pirolizy powodował wzrost zawartości analitów od  $1,48 \pm 0,07 \mu\text{g/g}$  (BCW500) do  $4,31 \pm 0,20 \mu\text{g/g}$  (BCW700). Spośród wszystkich badanych BC, materiały otrzymane z odpadów z drzew liściastych w temperaturze 600°C charakteryzowały się najmniejszą zawartością pochodnych WWA (wartości poniżej granicy wykrywalności) oraz jedną z najmniejszych zawartości rodzinnych WWA.

## 7.5. Wpływ starzenia fizycznego oraz chemicznego na zawartość frakcji całkowitej i biodostępnej WWA i ich pochodnych

Wyniki dotyczące wpływu starzenia fizycznego oraz chemicznego na charakterystykę fizykochemiczną BC, jak również zawartości frakcji całkowitej

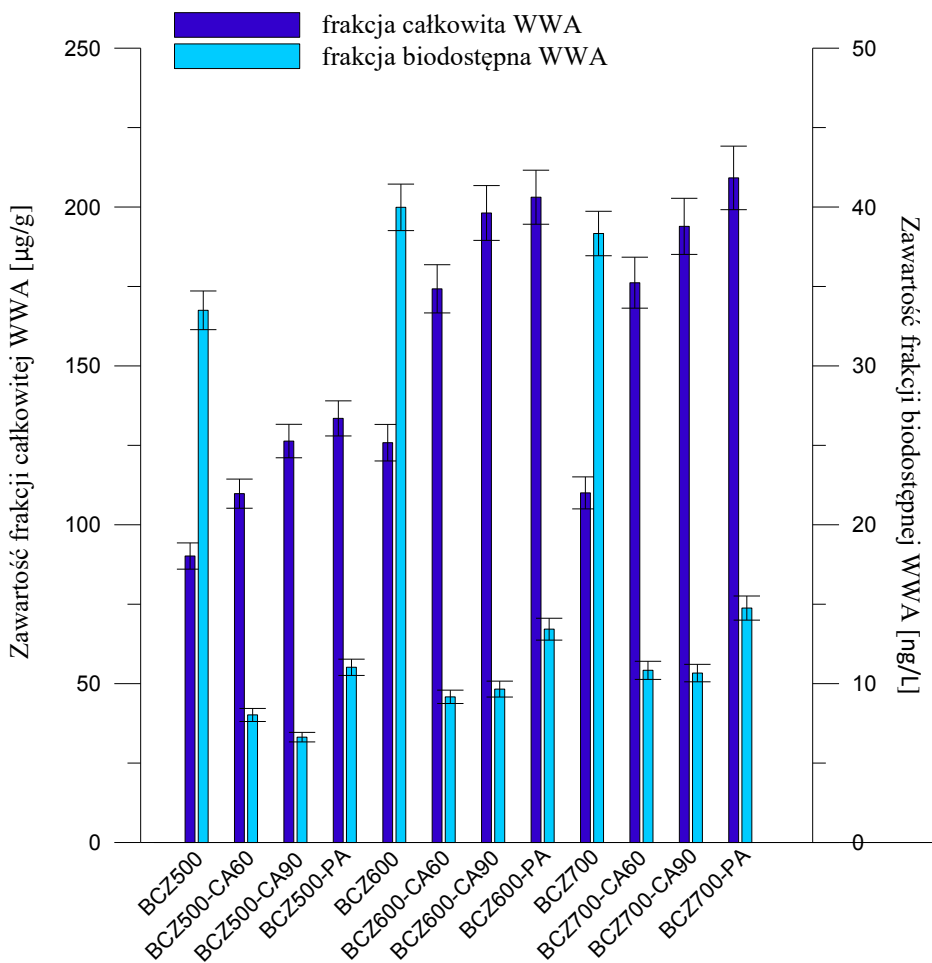
i biodostępnej WWA wraz z ich pochodnymi w spirolizowanym materiale przedstawiono w publikacji D4. Celem badań była weryfikacja zmian wybranych parametrów fizykochemicznych oraz zawartości WWA i ich pochodnych w materiale poddanym modelowym przemianom imitującym procesy, jakie zachodziłyby podczas rolniczego zastosowania biowęglę. Ponadto, BC poddano starzeniom trwającym 6 miesięcy, gdyż zgodnie z danymi literaturowymi [68], w tym okresie dochodzi do największych zmian w charakterystyce fizykochemicznej materiału, a wydłużenie tego czasu nie wpływa już tak znacząco.



Rys. 9. Zmiany parametrów fizykochemicznych biowęgli otrzymanych z osadu ściekowego (w temperaturach 500°C – BCZ500, 600°C – BCZ600 i 700°C – BCZ700), a następnie starzonych chemicznie w dwóch temperaturach oraz fizycznie. A - wielkość powierzchni właściwej; B - pH; C - zawartość popiołu; D - zawartość węgla; E - zawartość wodoru; F - zawartość azotu; G - zawartość tlenu; H - aromatyczność; I - polarność; J - hydrofilowość.

Starzenia fizyczne oraz chemiczne w dwóch temperaturach (60°C i 90°C) wpływają na parametry fizykochemiczne biowęgli otrzymanych z wierzby (BCW) oraz z osadu ściekowego (BCZ) (publikacja D4). Posługując się tylko wynikami dotyczącymi tych ostatnich (BCZ500, BCZ600 i BCZ700) (Rys. 9), można zauważyc, że starzenie chemiczne w 60°C spowodowało wzrost pH, aromatyczności, polarności oraz spadek wielkości powierzchni właściwej i zawartości węgla w spirolizowanych materiałach otrzymanych w różnych temperaturach. Zmiany pozostałych parametrów zależą od zastosowanej temperatury pirolizy (np. zawartość popiołu maleje dla BCZ500 i rośnie dla BCZ600 oraz BCZ700). Na Rys. 9 przedstawiono również zmiany parametrów spowodowane starzeniem chemicznym w 90°C oraz fizycznym. Przy czym ostatnie z nich było w mniejszym stopniu zależne od temperatury pirolizy, gdyż starzenie spowodowało wzrost wielkości powierzchni właściwej, zawartości tlenu, polarności oraz spadek pH, zawartości popiołu, węgla i azotu we wszystkich BC otrzymanych z osadu ściekowego. W wyniku procesów starzenia doszło do utleniania biowęgli, wzrostu zawartości tlenowych grup funkcyjnych oraz zróżnicowania form węglowych, a także usuwania najbardziej lotnych związków ze spirolizowanego materiału.

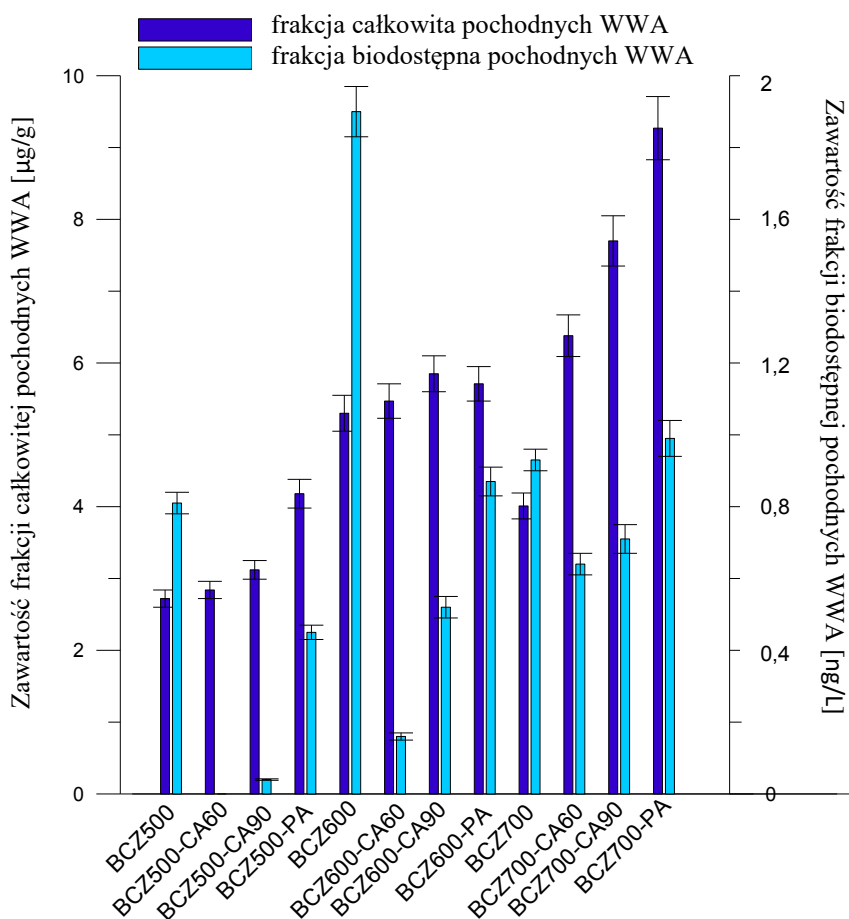
W przypadku BC otrzymanych z osadów ściekowych, zawartości frakcji całkowitej WWA i pochodnych znacząco wzrosły w wyniku starzeń chemicznych oraz fizycznego (Rys. 10 i 11). Większy wzrost obserwowano po starzeniu chemicznym w 90°C niż w 60°C, a największy po starzeniu fizycznym (niemal we wszystkich przypadkach). Zawartość analitów w biowęglach otrzymanych z surowca roślinnego również wzrosła po starzeniu fizycznym, natomiast po starzeniach chemicznych obserwowano znaczący spadek, zarówno z przypadku WWA, jak i ich pochodnych. Świadczy to o dużym wpływie wyboru surowca na końcowe parametry BC (w szczególności zawartości toksycznych związków w spirolizowanym materiale) podczas jego rolniczego zastosowania. Ponadto, procentowe zawartości poszczególnych grup WWA zróżnicowanych pod względem liczby posiadanych pierścieni aromatycznych, po przeprowadzeniu starzeń modelowych zmieniały się w różnym stopniu, gdyż np. starzenie fizyczne promowało powstawanie WWA o większej masie cząsteczkowej.



Rys. 10. Zawartości frakcji całkowitej oraz biodostępnej WWA w biowęglach przed i po starzeniach (publikacja D4).

Zawartość frakcji biodostępnej WWA w węglowych materiałach otrzymanych z osadów ściekowych znaczco spadła po przeprowadzeniu starzeń chemicznych oraz fizycznego (Rys. 10), co jest ogromną zaletą w kontekście rolniczego potencjału aplikacyjnego tego typu spirolizowanych materiałów. Natomiast w przypadku BC otrzymanych z surowca roślinnego, biodostępność analitów wzrosła nawet 4,5-krotnie. Procesy zachodzące podczas starzenia fizycznego ułatwiają uwalnianie badanych związków do środowiska. Ponadto, biowęgle otrzymane w temperaturze 600°C (BCW600) charakteryzowały się najmniejszą zawartością frakcji biodostępnej WWA, podczas gdy po starzeniach ich biodostępność była największa spośród wszystkich materiałów otrzymanych z wierzby. Podobnie jak w przypadku frakcji całkowitej, starzenie chemiczne w wyższej temperaturze (90°C), spowodowało większy wzrost zawartości frakcji biodostępnej WWA w BC niż CA w 60°C. Wyniki dotyczące biodostępności pochodnych WWA są dużo bardziej zróżnicowane. Starzenia chemiczne

doprowadziły do spadku zawartości frakcji biodostępnej pochodnych WWA w biowęglach BCZ (Rys. 11), natomiast wpływ starzenia fizycznego na zawartość analitów w węglowych materiałach zależy od zastosowanej temperatury pirolizy (zaobserwowano spadek dla BCZ500 i BCZ600, wzrost dla BCZ700).



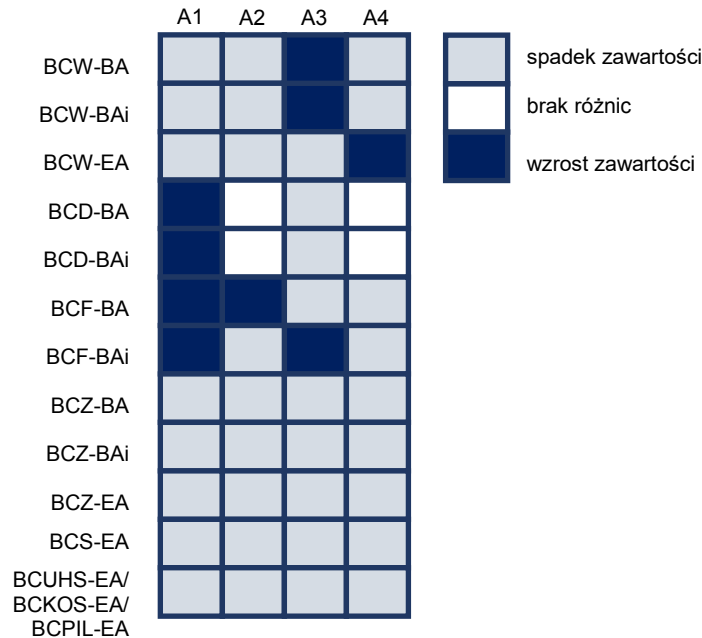
Rys. 11. Zawartości frakcji całkowitej oraz biodostępnej pochodnych WWA w biowęglach przed i po starzeniach (publikacja D4).

Obserwowane obniżenie zawartości frakcji całkowitej WWA w biowęglach otrzymanych z wierzyby spowodowane starzeniami chemicznymi i fizycznymi, przy jednocześnie znaczącym wzroście biodostępności substancji toksycznych ukazuje, jak istotne jest oznaczanie nie tylko całkowitej zawartości analitów, lecz również frakcji biodostępnej w spirolikwidowanych materiałach.

## **7.6. Wpływ starzenia biologicznego oraz enzymatycznego na zawartość frakcji całkowitej i biodostępnej WWA i pochodnych**

W publikacji **D5** przedstawiono wyniki dotyczące wpływu starzenia enzymatycznego i biologicznego na właściwości fizykochemiczne, zawartości frakcji całkowitej oraz biodostępnej WWA i ich pochodnych w biowęglach otrzymanych w temperaturze 600°C. Zaprezentowane dane dotyczą materiałów pozyskanych z surowców zawierających znaczne ilości popiołu (z ang. ash-rich materials, A-rich), ligniny (z ang. lignin-rich materials, L-rich), celulozy (z ang. cellulose-rich materials, C-rich) i pozostałości po produkcji biogazu (RBP).

Procesy starzenia znacząco wpływają na parametry fizykochemiczne biowęgli. Starzenie enzymatyczne spowodowało spadek zawartości popiołu w spirolizowanych materiałach. Ponadto we wszystkich BC otrzymanych z odpadów po produkcji biogazu zaobserwowano wzrost zawartości węgla, wodoru oraz spadek zawartości tlenu. Z kolei, w materiałach otrzymanych z surowców roślinnych wzrosła wielkość powierzchni właściwej oraz zawartość C, H, O. Natomiast starzenie biologiczne spowodowało spadek zawartości węgla i wodoru niemal we wszystkich przypadkach. Ponadto, można zaobserwować różnicę pomiędzy próbками narażonymi na działanie *inoculum* mikrobiologicznego, a wzbogaconymi jedynie roztworem substancji odżywczych. W przypadku niektórych parametrów, obecność mikroorganizmów glebowych „usuwa skutki” procesów starzenia, np. w biowęglu BCD, zawartość azotu po starzeniu z substancjami odżywczymi spadła (z 1,18% na 1,07%), podczas gdy w próbce narażonej na działanie *inoculum* mikrobiologicznego wzrosła ponad wartość początkową (1,23%). W innych przypadkach starzenie biologiczne z dodatkiem mikroorganizmów glebowych skutkuje jeszcze większym pogłębieniem zmian, np. wielkość powierzchni właściwej w biowęglu BCW spadła po starzeniu z roztworem odżywki z 145,02 m<sup>2</sup>/g do 2,96 m<sup>2</sup>/g, podczas gdy w BC starzonym z *inoculum* mikrobiologicznym wartość ta zmalała do poziomu poniżej możliwości aparaturowych Analizatora.



Rys. 12. Zmiany zawartości WWA oraz ich pochodnych w biowęglach poddanych starzeniom biologicznym i enzymatycznym (A1 – frakcja całkowita WWA, A2 – frakcja całkowita pochodnych WWA, A3 – frakcja biodostępna WWA, A4 – frakcja biodostępna pochodnych WWA).

Niemal we wszystkich przypadkach starzenie enzymatyczne spowodowało znaczący spadek zawartości frakcji całkowitej i biodostępnej WWA oraz ich pochodnych (Rys. 12). Podobną tendencję zaobserwowano w przypadku starzenia biologicznego, przy czym biowęgle starzone z roztworem substancji odżywcznych charakteryzowały się większą zawartością frakcji całkowitej WWA, niż starzone z *inoculum* mikrobiologicznym. Zmianie uległ również stosunek procentowych zawartości poszczególnych grup WWA (różnicowanych pod względem liczby pierścieni aromatycznych w cząsteczkach) w BC starzonych enzymatycznie i biologicznie. W przypadku frakcji całkowitej, BA spowodowało wzrost udziału procentowego 2-pierścieniowych związków (większy wzrost dla BC starzonych z *inoculum* mikrobiologicznym niż z samą odżywką). Natomiast EA skutkowało spadkiem zawartości procentowej związków posiadających dwa pierścienie aromatyczne. Z kolei, wzrósł udział procentowy 3-, 4- i 5-pierścieniowych WWA (dla BCW). Na podstawie uzyskanych wyników stwierdzono, że mikroorganizmy glebowe wyekstrahowane z gleby pełnią ważną rolę w procesie degradacji i modyfikacji WWA oraz ich pochodnych.

## 7.7. Wpływ WWA i ich pochodnych na stres oksydacyjny u roślin

WWA, jako związki toksyczne dla organizmów żywych, indukują powstawanie reaktywnych form tlenu, których działanie skutkuje wywołaniem stresu oksydacyjnego. Z kolei pochodne WWA są uważane za bardziej szkodliwe od związków rodzimych. Podczas otrzymywania biowęglą powstają zarówno WWA, jak i tlenowe oraz azotowe pochodne (co zostało dowiedzione w publikacjach **D2** oraz **D3**). Sprawdzenie wpływu związków toksycznych obecnych w BC na rośliny, podczas rolniczego zastosowania spirolikowanego materiału, jest niezwykle istotne i stanowi kolejny krok podczas badań będących przedmiotem rozprawy doktorskiej. Dlatego celem eksperymentu było zbadanie wpływu WWA i ich pochodnych na markery stresu oksydacyjnego u rośliny modelowej, którą był jęczmień zwyczajny *Hordeum vulgare* L (publikacja **D6**).

Badania polegały na weryfikacji wpływu różnych czynników (rodzaju gleby, surowca zastosowanego do otrzymania biowęglą oraz temperatury pirolizy) na poziom markerów stresu oksydacyjnego u jęczmienia zwyczajnego. W tym celu, trzy rodzaje gleb zostały wzbogacone węglowymi materiałami otrzymanymi z biomasy roślinnej (słoma pszeniczna, słonecznik, odpady z drzew liściastych oraz iglastych) w różnych temperaturach pirolizy. Następnie przeprowadzono eksperiment wazonowy polegający na posadzeniu wykiełkowanych nasion rośliny modelowej w specjalnych pojemnikach wypełnionych glebą wzbogaconą BC. Po 12 dniach próbki roślin zostały pobrane do dalszych badań polegających na pomiarze aktywności przeciwwietleniającej dysmutazy ponadtlenkowej (SOD), katalazy (CAT), peroksydazy (POD) i zawartości wolnego dialdehydu malonowego (MDA), co pozwoliło na monitorowanie skutków stresu oksydacyjnego wywartego na organizm testowy. Kolejnym krokiem było oznaczenie poziomu transkrypcji genów Cu/Zn-SOD, CAT, peroksydazy askorbinianowej (APX) i peroksydazy glutationowej (GPX).

Zgodnie z otrzymanymi wynikami, dodatek biowęglą powoduje wzrost aktywności dysmutazy ponadtlenkowej (wyniki dla gleby  $2,02 \pm 0,17$  U/mg białka, natomiast dla gleb wzbogaconych BC od  $2,50 \pm 0,11$  U/mg białka (dla BCA600) do  $4,18 \pm 0,26$  U/mg białka (BCS500)), co wskazuje na zwiększoną produkcję anionorodników ponadtlenkowych ( $O_2^-$ ). Jednakże, nie zarejestrowano wpływu temperatury pirolizy na aktywność SOD. Z kolei, aktywność CAT i POD malała pod wpływem dodatku BC otrzymanego ze słomy (np. CAT - wyniki dla gleby  $1259,63 \pm$

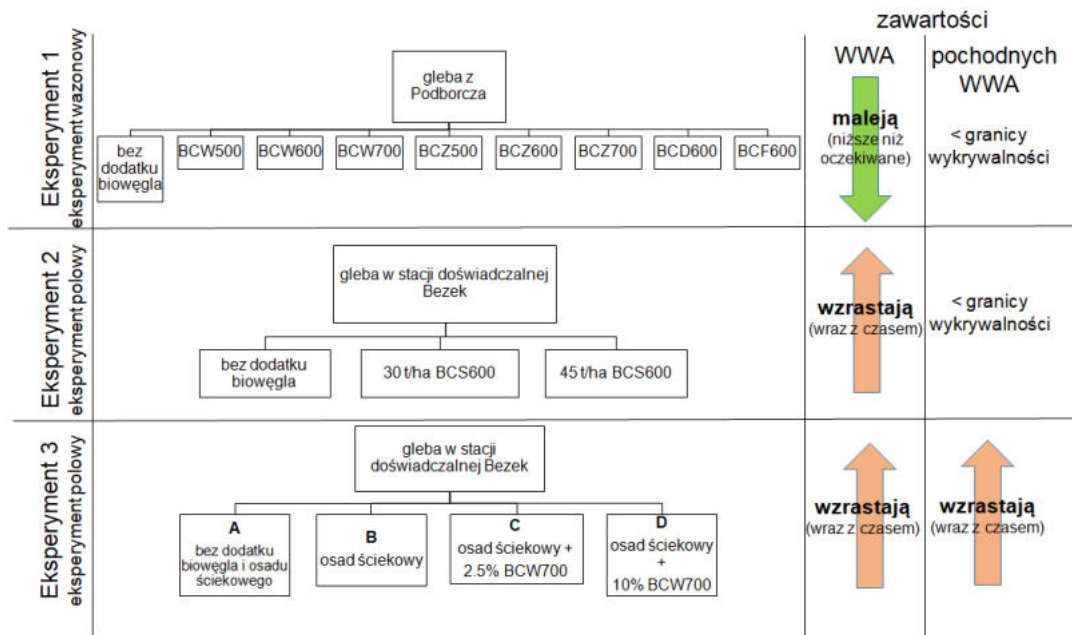
22,97 U/mg białka, natomiast dla gleb wzbogaconych BCS od  $463,38 \pm 32,65$  U/mg białka (dla BCS500) do  $566,96 \pm 18,73$  U/mg białka (BCS700)). Zawartość MDA wzrosła jedynie w przypadku BCA600, co świadczy o tym, że obecność reaktywnych form tlenowych nie skutkowała peroksydacyją lipidów.

Wyniki dotyczące ekspresji genów różniły się w zależności od wybranych biowęgli i rodzaju gleby. Relatywne poziomy transkrypcji genów dla APX, CAT i SOD malały wraz ze wzrostem temperatury pirolizy. Natomiast w przypadku BC uzyskanych z różnych surowców, graniczne wyniki dotyczące APX i SOD otrzymano dla BCF600 (odpowiednio 0,186 i 0,6) oraz BCS600 (1,355 oraz 6,713); dla CAT - BCA600 (0,161) i BCD600 (0,258) oraz dla GPX – BCS600 (0,459) i BCF600 (0,671).

Uzyskane dane jednoznacznie wskazują, że dodatek BC do gleby był związany z wystąpieniem stresu oksydacyjnego w liściach jęczmienia zwyczajnego (zwiększyły się poziom aktywności SOD). Stwierdzono wpływ temperatury pirolizy na odpowiedź transkrypcyjną rośliny modelowej. Jednymi z najważniejszych enzymatycznych zmieniających reaktywnych form tlenowych w komórkach roślinnych są CAT i APX, a ich transkrypcja była ściśle związana z obecnością frakcji biodostępnej badanych związków świadcząc o tym, że obecność WWA i jej pochodnych (ale w mniejszym stopniu) może indukować nadprodukcję  $O_2^{\bullet-}$  i  $H_2O_2$  oraz wywoływać stres oksydacyjny. Poziom transkrypcji genów SOD obniżała się wraz ze wzrostem temperatury pirolizy i zależał od zastosowanego surowca. Zgodnie z wynikami dotyczącymi tej części badań, dodatek biowęgla zawierającego biodostępna frakcję WWA i jej pochodnych jest rozwiązańem bezpiecznym dla środowiska, gdyż choć stres oksydacyjny u organizmu modelowego był wywołany, roślina zwalczyła jego skutki oraz była zdolna do dalszej wegetacji.

## **7.8. Zawartość frakcji całkowitej oraz biodostępnej WWA i pochodnych w glebach wzbogaconych biowęglem**

Celem tego etapu badań było określenie, jak zmienia się zawartość WWA i ich tlenowych, jak również azotowych pochodnych w glebie wzbogaconej biowęglem po przeprowadzeniu eksperymentu wazonowego oraz w trakcie dwóch eksperymentów polowych (publikacja D7) (Rys. 13) trwających odpowiednio około 16 i 18 miesięcy (ostatni pobór próbki).

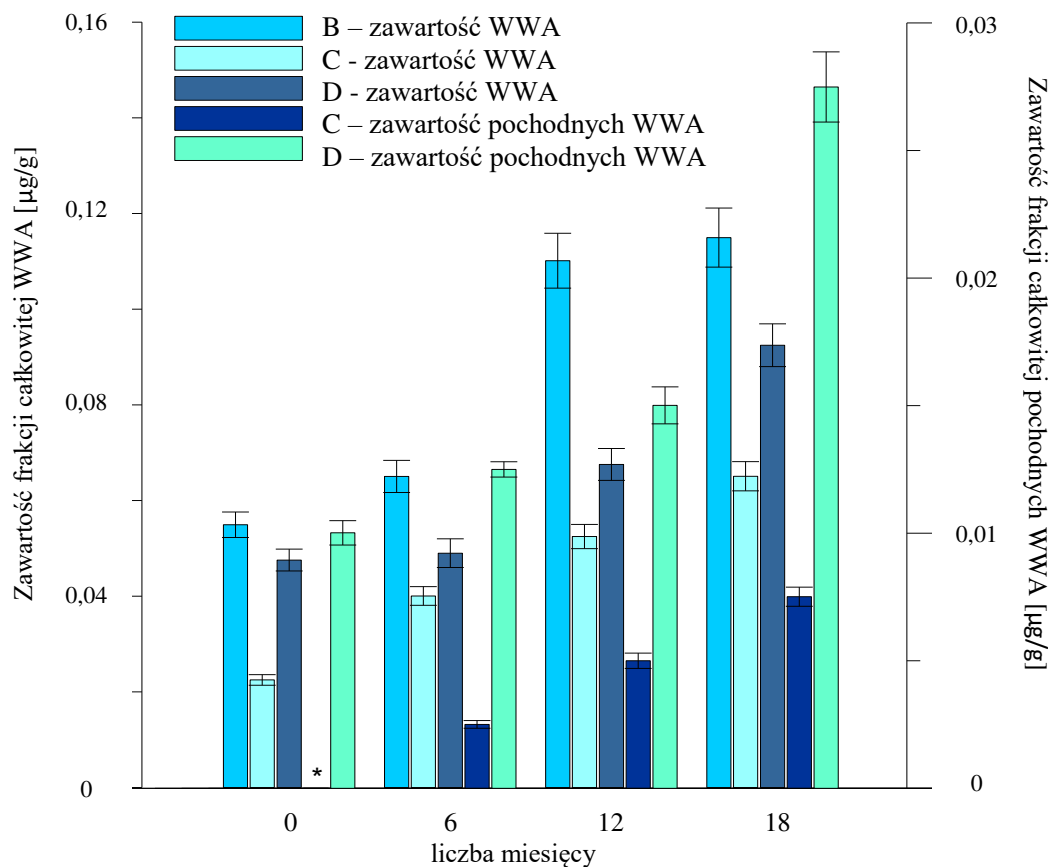


Rys. 13. Schemat eksperymentów przedstawionych w publikacji D7.

Niemal we wszystkich przypadkach, zawartości WWA w glebach wzbogaconych różnymi biowęglami (eksperyment wazonowy) były niższe niż spodziewane, biorąc pod uwagę znaną zawartość WWA w spirolizowanym materiale oraz masę dodanego BC do gleby. Lecz znaczącej zmianie uległy procentowe zawartości poszczególnych grup WWA, zróżnicowanych pod względem liczby pierścieni aromatycznych w cząsteczkach. Oprócz różnic między ilością 2-, 3- i 4-pierścieniowych związków rodzimych, zawartości WWA zawierających 5 oraz 6 pierścieni aromatycznych w cząsteczkach oraz pochodnych WWA w glebach wzbogaconych biowęglami były poniżej granicy wykrywalności. Do wyjaśnienia tych obserwacji można posłużyć się wynikami otrzymanymi po przeprowadzeniu badań modelowych (publikacja D4 i D5). Zawartości analitów w BC starzonych biologicznie i enzymatycznie znaczco zmalały. Wskazuje to na przewagę procesów zachodzących z udziałem mikroorganizmów glebowych odpowiedzialnych za obniżenie zawartości WWA oraz pochodnych.

Eksperyment 2 i 3 polegały na wzbogaceniu gleby biowęglem (lub BC i osadem ściekowym) w warunkach rzeczywistych. W celu określenia zmian zawartości WWA i pochodnych w czasie, próbki gleby były pobierane po różnych okresach wzbogacenia. W przypadku Eksperymentu 2, w wyjściowej glebie, w momencie rozpoczęcia badań, zawartości analitów były poniżej granicy wykrywalności. Natomiast, zawartości WWA rosły w czasie do wartości  $0,082 \pm 0,005 \mu\text{g/g}$  dla samej gleby oraz do  $0,112 \pm 0,006 \mu\text{g/g}$  dla gleby z dodatkiem biowęglów.

$\mu\text{g/g}$  i  $0,160 \pm 0,008$   $436 \mu\text{g/g}$  dla gleby wzbogaconej 30 t/ha i 45 t/ha biowęglą otrzymanego z wierzby (pobór próbki po 474 dniach od rozpoczęcia badania). W tym przypadku również nie oznaczono ilościowo zarówno 5- i 6-pierścieniowych WWA, jak i pochodnych.



Rys. 14. Zawartości frakcji całkowitej WWA i ich pochodnych w glebach wzbogaconych biowęglem i osadem ściekowym (\* wartości poniżej granicy wykrywalności). B, C, D – oznaczenia zgodnie z Rys. 13.

Z kolei zawartości WWA, jak również ich tlenowych oraz azotowych pochodnych w glebie wzbogaconej osadem ściekowym lub biowęglem i osadem ściekowym (Eksperyment 3) wzrastały wraz z czasem zastosowania BC w glebie (Rys. 14), a zawartości analitów w próbie kontrolnej (gleba bez dodatku biowęglą i SSL) były poniżej granicy wykrywalności przez cały okres trwania doświadczenia. W glebie wzbogaconej SSL oznaczono ilościowo tylko 2- i 3-pierścieniowe WWA (zawartości pochodnych WWA były poniżej granicy wykrywalności), podczas gdy w próbkach zmodyfikowanych biowęglem i SSL (symbol C oraz D, Rys. 13) oznaczono zarówno

związki rodzime zawierające 2, 3 i 4 pierścienie aromatyczne, jak również azotowe oraz tlenowe pochodne. Ponadto, wraz z czasem trwania eksperymentu, rosła liczba oznaczanych O- i N-WWA (w momencie rozpoczęcia doświadczenia w próbce D oznaczono ilościowo nitroacenaftalen, 9,10-antracendion, 2-metylpiren, podczas gdy po upływie 18 miesięcy wyznaczono zawartości również 1-metyl-5-nitronaftalenu, 1-metyl-6-nitronaftalenu oraz 4-metylpirenu).

## 8. Wnioski

---

- Pochodne WWA są obecne w różnych próbkach środowiskowych. Pomimo zazwyczaj niższej zawartości w porównaniu do WWA, ich udział w całkowitej toksyczności i mutagenności jest znaczny. Przegląd literaturowy wskazuje na potrzebę skupienia większej uwagi na problem zawartości pochodnych WWA w środowisku (publikacja **D1**).
- Podczas procesu pirolizy tworzą się zarówno WWA, jak i ich tlenowe oraz azotowe pochodne (publikacja **D2 i D3**).
- Temperatura pirolizy i surowiec wpływają na zawartość frakcji biodostępnej WWA w biowęglu, jak również na analizę jakościową analitów (publikacja **D2 i D3**).
- W zależności od zastosowanego surowca, wzrost temperatury pirolizy powodował zarówno spadek (np. BCS), jak i zwiększenie (np. BCKZ) zawartości frakcji biodostępnej WWA (publikacja **D2**).
- Biodostępność związków rodzimych była wyższa w materiałach otrzymanych z osadu ściekowego (3,33 – 39,98 ng/L), czy też z pozostałości po produkcji biogazu (10,36 – 41,53 ng/L), w porównaniu do BC pozyskanych z surowca roślinnego (2,21 – 4,45 ng/L) (publikacja **D3**).
- Największą zawartość frakcji biodostępnej pochodnych WWA oznaczono w biowęglach otrzymanych w temperaturze 600°C (np. wyniki dla BCS600  $0,83 \pm 0,03$  ng/L, podczas gdy dla materiałów otrzymanych ze słomy pszenicznej w temperaturze 500°C i 700°C wynosiły odpowiednio  $0,18 \pm 0,01$  ng/L i  $0,62 \pm 0,03$  ng/L). Natomiast zależność dotycząca wpływu surowca na zawartość frakcji biodostępnej pochodnych WWA była dużo bardziej złożona (publikacja **D2**).
- Temperatura pirolizy i rodzaj surowca zastosowanego do otrzymania biowęgla wpływaly na charakterystykę fizykochemiczną spirolikowanego materiału (np. wzrost temperatury powodował zwiększenie wartości pH w BCKZ, BCCH i BCW, spadek zawartości H i N oraz wiele innych (publikacja **D2**)).
- Starzenie fizyczne spowodowało wzrost zawartości frakcji całkowitej WWA i pochodnych w materiałach BCW, BCZ oraz 4,5-krotne zwiększenie biodostępności WWA w BC otrzymanych z wierzby (publikacja **D4**). Zmiany

dotyczące frakcji biodostępnej związków pochodnych są dużo bardziej złożone i brakuje wyraźnej tendencji dotyczącej wpływu temperatury pirolizy albo surowca.

- Starzenie chemiczne spowodowało znaczący spadek całkowitej zawartości WWA oraz pochodnych w materiałach otrzymanych z surowca roślinnego. Wzrosła natomiast biodostępność związków rodzimych (publikacja **D4**).
- Starzenie enzymatyczne spowodowało znaczący spadek zawartości analitów w biowęglach (publikacja **D5**). Natomiast w przypadku starzenia biologicznego, próbki narażone na działanie mikroorganizmów glebowych charakteryzowały się niższą zawartością frakcji całkowitej WWA i pochodnych w porównaniu do materiałów starzonych z roztworem substancji odżywcznych (BCZ, BCW) lub w próbkach modyfikowanych *inoculum* mikrobiologicznym zaobserwowano wyższą zawartość niż w materiałach wyjściowych, ale jednocześnie niższą, niż w BC traktowanych roztworem odżywczym (BCD, BCF) (publikacja **D5**). Zawartość frakcji biodostępnej pochodnych WWA w biowęglach znacznie spadła po przeprowadzeniu starzenia biologicznego (nawet do poziomu poniżej granicy wykrywalności).
- Dodatek BC do gleby spowodował zwiększenie poziomu aktywności SOD, co jest ściśle związane z wystąpieniem stresu oksydacyjnego w liściach jęczmienia zwyczajnego. Ponadto zmiany w transkrypcji CAT i APX były związane z obecnością frakcji biodostępnej WWA i pochodnych, świadcząc o tym, że badane anality może indukować nadprodukcję  $O_2^{\cdot-}$  i  $H_2O_2$  oraz wywoływać stres oksydacyjny (publikacja **D6**).
- Poziom transkrypcji genów SOD obniżała się wraz ze wzrostem temperatury pirolizy i zależał od surowca zastosowanego podczas otrzymywania biowęgla.
- Pomimo tego, że biowęgiel zawierający biodostępna frakcję WWA i ich pochodnych wywołał stres oksydacyjny u jęczmienia zwyczajnego, roślina modelowa zwalczyła skutki działania substancji toksycznych. Dlatego dodatek BC do gleb jest rozwiązaniem bezpiecznym dla środowiska.
- Zawartości frakcji całkowitej WWA w glebach modyfikowanych biowęglem po przeprowadzeniu eksperymentu wazonowego były niższe od spodziewanych, z kolei zawartość związków pochodnych była poniżej granicy wykrywalności.
- Wyniki dotyczące eksperymentów polowych są alarmujące, gdyż zawartości zarówno związków rodzimych, jak i ich tlenowych oraz azotowych pochodnych

rosły wraz z czasem zastosowania BC jako dodatku do gleb. Może to świadczyć o przewadze procesów towarzyszących starzeniu biologicznemu i fizycznemu, gdyż skutkiem ich przeprowadzenia był wzrost zawartości oznaczanych toksyn. Z kolei zmiany spowodowane starzeniem enzymatycznym i chemicznym (tj. spadki zawartości) są neutralizowane przez aktywność mikroorganizmów glebowych oraz nagłe skoki temperatur (publikacja D7).

## 9. Literatura

---

- [1] M. Hassan, Y. Liu, R. Naidu, S.J. Parikh, J. Du, F. Qi, I.R. Willett, *Influences of feedstock sources and pyrolysis temperature on the properties of biochar and functionality as adsorbents: A meta-analysis*, Science of The Total Environment, 2020, 744, 140714.
- [2] P. Pariyar, K. Kumari, M.K. Jain, P.S. Jadhao, *Evaluation of change in biochar properties derived from different feedstock and pyrolysis temperature for environmental and agricultural application*, Science of The Total Environment, 2020, 713, 136433.
- [3] A. Downie, A. Crosky, P. Munroe, *Physical properties of biochar*. W: J. Lehmann, S. Joseph, *Biochar for environmental management science and technology*, Earthscan, London, 2009, 13-32, Scientific Research Publishing.
- [4] L. Zhao, X. Cao, O. Mašek, A. Zimmerman, *Heterogeneity of biochar properties as a function of feedstock sources and production temperatures*, Journal of Hazardous Materials, 2013, 256–257, 1–9.
- [5] A. Sharma, V. Pareek, D. Zhang, *Biomass pyrolysis—A review of modelling, process parameters and catalytic studies*, Renewable and Sustainable Energy Reviews, 2015, 50, 1081–1096.
- [6] M. Stefaniuk, P. Oleszczuk, *Characterization of biochars produced from residues from biogas production*, Journal of Analytical and Applied Pyrolysis, 2015, 115, 157–165.
- [7] J.A. Ippolito, L. Cui, C. Kammann, N. Wrage-Mönnig, J.M. Estavillo, T. Fuertes-Mendizabal, M.L. Cayuela, G. Sigua, J. Novak, K. Spokas, N. Borchard, *Feedstock choice, pyrolysis temperature and type influence biochar characteristics: a comprehensive meta-data analysis review*, Biochar, 2020, 2, 421–438.
- [8] A. Tomczyk, Z. Sokołowska, P. Boguta, *Biochar physicochemical properties: pyrolysis temperature and feedstock kind effects*, Reviews in Environmental Science and Biotechnology, 2020, 19, 191–215.
- [9] B.T. Nguyen, J. Lehmann, W.C. Hockaday, S. Joseph, C.A. Masiello, *Temperature sensitivity of black carbon decomposition and oxidation*, Environmental Science & Technology, 2010, 44, 3324–3331.
- [10] J. Lehmann, M.C. Rillig, J. Thies, C.A. Masiello, W.C. Hockaday, D. Crowley, *Biochar effects on soil biota – A review*, Soil Biology and Biochemistry, 2011, 43, 1812–1836.
- [11] M.K. Hossain, V. Strezov, K.Y. Chan, A. Ziolkowski, P.F. Nelson, *Influence of pyrolysis temperature on production and nutrient properties of wastewater sludge biochar*, Journal of Environmental Management, 2011, 92, 223–228.
- [12] J.H. Yuan, R.K. Xu, H. Zhang, *The forms of alkalis in the biochar produced from crop residues at different temperatures*, Bioresource Technology, 2011, 102, 3488–3497.
- [13] T.T.N. Nguyen, C.Y. Xu, I. Tahmasbian, R. Che, Z. Xu, X. Zhou, H.M. Wallace, S.H. Bai, *Effects of biochar on soil available inorganic nitrogen: A review and meta-analysis*, Geoderma, 2017, 288, 79–96.
- [14] J.M. Novak, I. Lima, B. Xing, J.W. Gaskin, C. Steiner, K.C. Das, M. Ahmedna, D. Rehrhah, D.W. Watts, W.J. Busscher, H. Schomberg, *Characterization of designer*

- biochar produced at different temperatures and their effects on a loamy sand*, Annals of Environmental Science, 2009, 3.
- [15] S. Głuszek, L. Sas Paszt, B. Sumorok, R. Kozera, *Biochar-rhizosphere interactions - A review*, Polish Journal of Microbiology, 2017, 66, 151–161.
  - [16] J. Pietikäinen, O. Kiikkilä, H. Fritze, *Charcoal as a habitat for microbes and its effect on the microbial community of the underlying humus*, Oikos, 2000, 89, 231–242.
  - [17] M. Inyang, E. Dickenson, *The potential role of biochar in the removal of organic and microbial contaminants from potable and reuse water: A review*, Chemosphere, 2015, 134, 232–240.
  - [18] O. Lei, R. Zhang, *Effects of biochars derived from different feedstocks and pyrolysis temperatures on soil physical and hydraulic properties*, Journal of Soils and Sediments, 2013, 13, 1561–1572.
  - [19] K.Y. Chan, L. Van Zwieten, I. Meszaros, A. Downie, S. Joseph, *Agronomic values of greenwaste biochar as a soil amendment*, Soil Research, 2007, 45, 629.
  - [20] B. Glaser, J. Lehmann, W. Zech, *Ameliorating physical and chemical properties of highly weathered soils in the tropics with charcoal - a review*, Biology and Fertility of Soils, 2002, 35, 219–230.
  - [21] European Parliament, Circular economy: definition, importance and benefits, <https://www.europarl.europa.eu/news/en/headlines/economy/20151201STO05603/circular-economy-definition-importance-and-benefits> (dostęp dnia 07.07.2023 r.).
  - [22] I. Cabeza, T. Waterhouse, S. Sohi, J.A. Rooke, *Effect of biochar produced from different biomass sources and at different process temperatures on methane production and ammonia concentrations in vitro*, Animal Feed Science and Technology, 2018, 237, 1–7.
  - [23] S.E. Hale, J. Lehmann, D. Rutherford, A.R. Zimmerman, R.T. Bachmann, V. Shitumbanuma, A. O'Toole, K.L. Sundqvist, H.P.H. Arp, G. Cornelissen, *Quantifying the total and bioavailable polycyclic aromatic hydrocarbons and dioxins in biochars*, Environmental Science & Technology, 2012, 46, 2830–2838.
  - [24] European Commission. Joint Research Centre. Institute for Environment and Sustainability, *Biochar application to soils: a critical scientific review of effects on soil properties, processes and functions*, Publications Office, LU, 2010. <https://data.europa.eu/doi/10.2788/472> (dostęp dnia 04.05.2021 r.).
  - [25] I. Hilber, A.C. Bastos, S. Loureiro, G. Soja, A. Marsz, G. Cornelissen, T.D. Bucheli, *The different faces of biochar: contamination risk versus remediation tool*, Journal of Environmental Engineering and Landscape Management, 2017, 25, 86–104.
  - [26] B.J. Mahler, P.C.V. Metre, J.L. Crane, A.W. Watts, M. Scoggins, E.S. Williams, *Coal-tar-based pavement sealcoat and PAHs: implications for the environment, human health, and stormwater management*, Environmental Science & Technology, 2012, 46, 3039–3045.
  - [27] H. Zheng, C. Qu, J. Zhang, S.A. Talpur, Y. Ding, X. Xing, S. Qi, *Polycyclic aromatic hydrocarbons (PAHs) in agricultural soils from Ningde, China: levels, sources, and human health risk assessment*, Environmental Geochemistry and Health, 2019, 41, 907–919.
  - [28] I. Hilber, F. Blum, J. Leifeld, H.P. Schmidt, T.D. Bucheli, *Quantitative determination of PAHs in biochar: A prerequisite to ensure its quality and safe application*, Journal of Agricultural and Food Chemistry, 2012, 60, 3042–3050.
  - [29] N. Peng, Y. Li, Z. Liu, T. Liu, C. Gai, *Emission, distribution and toxicity of polycyclic aromatic hydrocarbons (PAHs) during municipal solid waste (MSW)*

- and coal co-combustion*, Science of The Total Environment, 2016, 565, 1201–1207.
- [30] R.K. Rajpara, D.R. Dudhagara, J.K. Bhatt, H.B. Gosai, B.P. Dave, *Polycyclic aromatic hydrocarbons (PAHs) at the Gulf of Kutch, Gujarat, India: Occurrence, source apportionment, and toxicity of PAHs as an emerging issue*, Marine Pollution Bulletin, 2017, 119, 231–238.
- [31] A. Krzyszczak, B. Czech, *Occurrence and toxicity of polycyclic aromatic hydrocarbons derivatives in environmental matrices*, Science of The Total Environment, 2021, 147738.
- [32] M. Kończak, P. Oleszczuk, *Application of biochar to sewage sludge reduces toxicity and improve organisms growth in sewage sludge-amended soil in long term field experiment*, Science of The Total Environment, 2018, 625, 8–15.
- [33] IBI International Biochar Initiative, *Standardized product definition and product testing guidelines for biochar that is used in soil*, Version Number: 2.1, Version Date: 23 November 2015, Document Reference Code: IBI-STD-2.1.
- [34] H.P. Schmidt, European Biochar Certificate (EBC) - guidelines version 6.1, (2015).
- [35] M. del Rosario Sienra, *Oxygenated polycyclic aromatic hydrocarbons in urban air particulate matter*, Atmospheric Environment, 2006, 40, 2374–2384.
- [36] J. Ringuet, E. Leoz-Garziandia, H. Budzinski, E. Villenave, A. Albinet, *Particle size distribution of nitrated and oxygenated polycyclic aromatic hydrocarbons (NPAHs and OPAHs) on traffic and suburban sites of a European megacity: Paris (France)*, Atmospheric Chemistry and Physics, 2012, 12, 8877–8887.
- [37] B.A.M. Bandowe, H. Meusel, R. Huang, K. Ho, J. Cao, T. Hoffmann, W. Wilcke, *PM<sub>2.5</sub>-bound oxygenated PAHs, nitro-PAHs and parent-PAHs from the atmosphere of a Chinese megacity: Seasonal variation, sources and cancer risk assessment*, Science of The Total Environment, 2014, 473–474, 77–87.
- [38] E. Weidemann, W. Buss, M. Edo, O. Mašek, S. Jansson, *Influence of pyrolysis temperature and production unit on formation of selected PAHs, oxy-PAHs, N-PACs, PCDDs, and PCDFs in biochar—a screening study*, Environmental Science and Pollution Research, 2018, 25, 3941–3942.
- [39] I. Abbas, G. Badran, A. Verdin, F. Ledoux, M. Roumié, D. Courcot, G. Garçon, *Polycyclic aromatic hydrocarbon derivatives in airborne particulate matter: sources, analysis and toxicity*, Environmental Chemistry Letters, 2018.
- [40] E.A.J. Bleeker, H.G. Van Der Geest, H.J.C. Klamer, P. De Voogt, E. Wind, M.H.S. Kraak, *Toxic and genotoxic effects of azaarenes: isomers and metabolites*, Polycyclic Aromatic Compounds, 1999, 13, 191–203.
- [41] D. Yaffe, Y. Cohen, J. Arey, A.J. Grosovsky, *Multimedia analysis of PAHs and nitro-PAH daughter products in the Los Angeles Basin*, Risk Analysis, 2001, 21, 275–294.
- [42] K.T. Semple, K.J. Doick, K.C. Jones, P. Burauel, A. Craven, H. Harms, *Defining bioavailability and bioaccessibility of contaminated soil and sediment is complicated*, Environmental Science & Technology, 2004, 38, 228A-231A.
- [43] L. Wang, D. O'Connor, J. Rinklebe, Y.S. Ok, D.C. W. Tsang, Z. Shen, D. Hou, *Biochar aging: mechanisms, physicochemical changes, assessment, and implications for field applications*, Environmental Science & Technology, 2020, 54, 14797–14814.
- [44] M.K. Rafiq, Y. Bai, R. Aziz, M.T. Rafiq, O. Mašek, R.T. Bachmann, S. Joseph, M. Shahbaz, A. Qayyum, Z. Shang, M. Danaee, R. Long, *Biochar amendment*

- improves alpine meadows growth and soil health in Tibetan plateau over a three year period*, Science of The Total Environment, 2020, 717, 135296.
- [45] A. Chatel, V. Faucet-Marquis, A. Pfohl-Leszkowicz, C. Gourlay-France, F. Vincent-Hubert, *DNA adduct formation and induction of detoxification mechanisms in Dreissena polymorpha exposed to nitro-PAHs*, Mutagenesis, 2014, 29, 457–465.
- [46] Y. Zhang, J.J. Pignatello, S. Tao, *Bioaccessibility of nitro- and oxy-PAHs in fuel soot assessed by an in vitro digestive model with absorptive sink*, Environmental Pollution, 2016, 218, 901–908.
- [47] P. Vineis, F. Forastiere, G. Hoek, M. Lipsett, *Outdoor air pollution and lung cancer: Recent epidemiologic evidence*, International Journal of Cancer, 2004, 111, 647–652.
- [48] A. Krzyszczak, M.P. Dybowski, B. Czech, *Formation of polycyclic aromatic hydrocarbons and their derivatives in biochars: The effect of feedstock and pyrolysis conditions*, Journal of Analytical and Applied Pyrolysis, 2021, 160, 105339.
- [49] Y. Song, R. Li, Y. Zhang, J. Wei, W. Chen, C.K.A. Chung, Z. Cai, *Mass spectrometry-based metabolomics reveals the mechanism of ambient fine particulate matter and its components on energy metabolic reprogramming in BEAS-2B cells*, Science of The Total Environment, 2019, 651, 3139–3150.
- [50] Y. Ren, B. Zhou, J. Tao, J. Cao, Z. Zhang, C. Wu, J. Wang, J. Li, L. Zhang, Y. Han, L. Liu, C. Cao, G. Wang, *Composition and size distribution of airborne particulate PAHs and oxygenated PAHs in two Chinese megacities*, Atmospheric Research, 2017, 183, 322–330.
- [51] M. Qiao, W. Qi, H. Liu, J. Qu, *Oxygenated polycyclic aromatic hydrocarbons in the surface water environment: Occurrence, ecotoxicity, and sources*, Environment International, 2022, 163, 107232.
- [52] A. Albinet, E. Leoz-Garziandia, H. Budzinski, E. Villenave, *Polycyclic aromatic hydrocarbons (PAHs), nitrated PAHs and oxygenated PAHs in ambient air of the Marseilles area (South of France): Concentrations and sources*, Science of The Total Environment, 2007, 384, 280–292.
- [53] H.A. Bamford, J.E. Baker, *Nitro-polycyclic aromatic hydrocarbon concentrations and sources in urban and suburban atmospheres of the Mid-Atlantic region*, Atmospheric Environment, 2003, 37, 2077–2091.
- [54] S. Lundstedt, P.A. White, C.L. Lemieux, K.D. Lynes, I.B. Lambert, L. Öberg, P. Haglund, M. Tysklind, *Sources, fate, and toxic hazards of oxygenated polycyclic aromatic hydrocarbons (PAHs) at PAH-contaminated sites*, AMBIO: A Journal of the Human Environment, 2007, 36, 475–485.
- [55] M. Sklorz, J.J. Briedé, J. Schnelle-Kreis, Y. Liu, J. Cyrys, T.M. de Kok, R. Zimmermann, *Concentration of oxygenated polycyclic aromatic hydrocarbons and oxygen free radical formation from urban particulate matter*, Journal of Toxicology and Environmental Health, Part A, 2007, 70, 1866–1869.
- [56] X. Niu, S.S.H. Ho, K.F. Ho, Y. Huang, J. Sun, Q. Wang, Y. Zhou, Z. Zhao, J. Cao, *Atmospheric levels and cytotoxicity of polycyclic aromatic hydrocarbons and oxygenated-PAHs in PM<sub>2.5</sub> in the Beijing-Tianjin-Hebei region*, Environmental Pollution, 2017, 231, 1075–1084.
- [57] D.L. Watt, C.D. Utzat, P. Hilario, A.K. Basu, *Mutagenicity of the 1-nitropyrene-DNA adduct N-(deoxyguanosin-8-yl)-1-aminopyrene in mammalian cells*, Chemical Research in Toxicology, 2007, 20, 1658–1664.

- [58] J. Øvrevik, V.M. Arlt, E. Øya, E. Nagy, S. Mollerup, D.H. Phillips, M. Låg, J.A. Holme, *Differential effects of nitro-PAHs and amino-PAHs on cytokine and chemokine responses in human bronchial epithelial BEAS-2B cells*, Toxicology and Applied Pharmacology, 2010, 242, 270–280.
- [59] E. Oya, J. Øvrevik, V.M. Arlt, E. Nagy, D.H. Phillips, J.A. Holme, *DNA damage and DNA damage response in human bronchial epithelial BEAS-2B cells following exposure to 2-nitrobenzanthrone and 3-nitrobenzanthrone: role in apoptosis*, Mutagenesis, 2011, 26, 697–708.
- [60] Y. Kim, Y. Ko, T. Kawamoto, H. Kim, *The effects of 1-nitropyrene on oxidative DNA damage and expression of DNA repair enzymes*, Journal of Occupational Health, 2005, 47, 261–266.
- [61] R. Li, L. Zhao, L. Zhang, M. Chen, C. Dong, Z. Cai, *DNA damage and repair, oxidative stress and metabolism biomarker responses in lungs of rats exposed to ambient atmospheric 1-nitropyrene*, Environmental Toxicology and Pharmacology, 2017, 54, 14–20.
- [62] A. Toriba, H. Kitaoka, R.L. Dills, S. Mizukami, K. Tanabe, N. Takeuchi, M. Ueno, T. Kameda, N. Tang, K. Hayakawa, C.D. Simpson, *Identification and quantification of 1-nitropyrene metabolites in human urine as a proposed biomarker for exposure to diesel exhaust*, Chemical Research in Toxicology, 2007, 20, 999–1007.
- [63] H. Tokiwa, Y. Ohnishi, *Mutagenicity and carcinogenicity of nitroarenes and their sources in the environment*, Critical Reviews in Toxicology, 1986, 17, 23–60.
- [64] Y. Zhang, Y. Song, Y.J. Chen, Y. Chen, Y. Lu, R. Li, C. Dong, D. Hu, Z. Cai, *Discovery of emerging sulfur-containing PAHs in PM<sub>2.5</sub>: Contamination profiles and potential health risks*, Journal of Hazardous Materials, 2021, 416, 125795.
- [65] A. Kumar, T. Bhattacharya, *Biochar: a sustainable solution*, Environment, Development and Sustainability, 2021, 23, 6642–6680.
- [66] S.B. Hawthorne, M.T.O. Jonker, S.A. van der Heijden, C.B. Grabanski, N.A. Azzolina, D.J. Miller, *Measuring picogram per liter concentrations of freely dissolved parent and alkyl PAHs (PAH-34), using passive sampling with polyoxymethylene*, Analytical Chemistry, 2011, 83, 6754–6761.
- [67] K. Dorau, S. Papenfuß, T. Mansfeldt, *Temperature-dependent oxide removal from manganese- and iron oxide-coated soil redox bars*, Journal of Soils and Sediments, 2018, 18, 680–687.
- [68] A. Siatecka, K. Różyło, Y.S. Ok, P. Oleszczuk, *Biochars ages differently depending on the feedstock used for their production: Willow- versus sewage sludge-derived biochars*, Science of The Total Environment, 2021, 789, 147458.

## **10. Życiorys naukowy**

---

W 2012 r. ukończyłam I Liceum Ogólnokształcące im. Jana Zamoyskiego w Zamościu. Studia licencjackie na kierunku „Analistyka chemiczna” prowadzone na Wydziale Chemii Uniwersytetu Marii Curie-Skłodowskiej w Lublinie zakończyłam w czerwcu 2015 r., a studia magisterskie na tym samym kierunku w czerwcu 2017 r. uzyskując tytuł zawodowy magistra. Pracę licencjacką pt. „Wpływ adenozyny na kinetykę redukcji jonów  $Zn^{2+}$  na elektrodzie rtęciowej w buforze octanowym o pH=5” oraz magisterską pt. „Badanie adsorpcji wybranych jonów na egzopolimerach immobilizowanych na nośniku stałym” realizowałam w Zakładzie Chemii Analitycznej i Analizy Instrumentalnej, Wydziału Chemii, Uniwersytetu Marii Curie-Skłodowskiej w Lublinie pod kierunkiem odpowiednio dr Doroty Sieńko oraz prof. dr. hab. Ryszarda Dobrowolskiego.

W marcu 2017 r. rozpoczęłam pracę na stanowisku referenta technicznego w Pracowni Materiałów Kompozytowych i Biomimetycznych Interdyscyplinarnego Centrum Badań Naukowych Katolickiego Uniwersytetu Lubelskiego Jana Pawła II w Lublinie, a badania realizowałam w zespole dr hab. Elżbiety A. Stefaniak, prof. KUL. W grudniu 2017 r. awansowałam na stanowisko starszego referenta technicznego, w kwietniu 2021 r. na stanowisko specjalisty badawczo-technicznego, a w styczniu 2022 r. na stanowisko starszego specjalisty badawczo-technicznego, na którym pracuję do dziś jako pracownik Katedry Chemii Instytutu Nauk Biologicznych Wydziału Medycznego KUL w Lublinie. Aktualnie jednym z realizowanych tematów jest oznaczanie związków per- i polifluoroalkilowych (z ang. Per- and Polyfluoroalkyl Substances, PFAS) oraz ich usuwanie z zanieczyszczonych wód i ścieków wykorzystując m.in. sorpcję tych związków na różnych materiałach, w tym węglowych. Przedsięwzięcie jest realizowane we współpracy z dr Iloną Sadok (Katedra Chemii, Instytut Nauk Biologicznych, KUL w Lublinie), dr hab. Bożeną Czech, prof. UMCS, zespołem prof. Minoo Naebe (Carbon Nexus, Institute for Frontier Materials, Deakin University, Australia) oraz prof. Mirabbosem Hojabberdiev (Institut für Chemie, Technische Universität Berlin, Niemcy).

W październiku 2019 r. rozpoczęłam studia III stopnia w Szkole Doktorskiej Nauk Ścisłych i Przyrodniczych UMCS w Lublinie. Prace badawcze prowadzone

w ramach rozprawy doktorskiej pt. „Badania pochodnych wielopierścieniowych węglowodorów aromatycznych w biowęglach” realizowałam w dziedzinie nauk chemicznych w Katedrze Radiochemii i Chemii Środowiskowej na Wydziale Chemii UMCS pod kierunkiem dr hab. Bożeny Czech, prof. UMCS. Równocześnie w okresie od 01.01.2020 r. do 31.03.2022 r. byłam wykonawcą w projekcie grantowym OPUS-16 finansowanym z Narodowego Centrum Nauki, nr 2018/31/B/NZ9/00317, pt. „Tworzenie się pochodnych wielopierścieniowych węglowodorów aromatycznych w biowęglach i ich biodostępność oraz trwałość podczas przyrodniczego wykorzystania biowęgla”, którego Kierownikiem była dr hab. Bożena Czech, prof. UMCS. W czerwcu 2023 roku złożyłam do Narodowego Centrum Nauki wniosek grantowy do projektu Preludium-22 pt. „Porowate mikrosfery 4-winylopirydyny usicowane komonomerami metakrylanu jako nowe sorbenty do usuwania polifenoli z matrycy próbki przed oznaczaniem mykotoksyn metodą LC-MS/MS”, w którym pełnię rolę Kierownika. Wniosek jest w trakcie rozpatrywania.

Byłam laureatką stypendium przyznanego w ramach Projektu „Od studenta do eksperta – ochrona środowiska w praktyce” (w roku akademickim 2012/2013), jak również Stypendium Rektora UMCS dla Najlepszych Studentów (w latach akademickich 2013/2014, 2014/2015, 2015/2016). W czerwcu 2015 r. otrzymałam Nagrodę Rektora UMCS dla Najlepszej Absolwentki na Wydziale Chemii UMCS. W grudniu 2021 r. dostałam nagrodę indywidualną czwartego stopnia Rektora KUL w Lublinie, w grudniu 2022 r. nagrodę zespołową Rektora KUL za pracę zawodową znacznie wykraczającą poza zakres zwykłych obowiązków służbowych, a w październiku 2022 r. list gratulacyjny od Rektora UMCS w uznaniu dorobku naukowego na rzecz UMCS w Lublinie. W latach akademickich 2021/2022 oraz 2022/2023 otrzymałam Stypendium z Własnego Funduszu Stypendialnego UMCS dla najlepszych doktorantów, a w styczniu 2023 r. stypendium z „Miejskiego programu stypendialnego dla studentów i doktorantów” na rok akademicki 2022/2023 przyznanego przez Prezydenta Miasta Lublin, Krzysztofa Żuka. Jestem współautorem 19 artykułów naukowych opublikowanych w czasopismach z listy filadelfijskiej o łącznym współczynniku IF: 136,942 (łączna liczba punktów ministerialnych: 2765), 13 rozdziałów w monografii, jak również brałam udział w licznych krajowych i międzynarodowych konferencjach naukowych, których wynikiem jest 1 wystąpienie ustne i 4 plakatowe na naukowych konferencjach międzynarodowych oraz 13 wystąpień ustnych i 36 plakatowych na naukowych konferencjach krajowych. Jedno z moich

wystąpień zostało wyróżnione I miejscem w konkursie na najlepszy poster na V Zjeździe Naukowym Polskiego Towarzystwa Biologii Medycznej „Biologia-Medycyna-Terapia” (17.09.2022, Lublin).

Oprócz aktywności naukowych, od 2019 r. jestem członkiem Rady Uczelnianej Samorządu Doktorantów UMCS, Rady Szkoły Doktorskiej Nauk Ścisłych i Przyrodniczych UMCS oraz od 04.2020 r. V-ce Przewodniczącą Rady Doktorantów Szkoły Doktorskiej Nauk Ścisłych i Przyrodniczych UMCS. Byłam również członkiem Komitetu Organizacyjnego Konferencji „Biologia-Medycyna-Terapia” oraz redaktorem Materiałów Pokonferencyjnych V Zjazdu Polskiego Towarzystwa Biologii Medycznej „Biologia-Medycyna-Terapia” (15-17.09.2022 r., Lublin) oraz wspomagałam ze strony organizacyjnej 64. Zjazd Polskiego Towarzystwa Chemicznego w Lublinie. Od marca 2020 r. do chwili obecnej jestem członkiem Polskiego Towarzystwa Chemicznego. W latach akademickich 2020/2021 oraz 2022/2023 byłam członkiem Komisji Rekrutacyjnej do Szkoły Doktorskiej Nauk Ścisłych i Przyrodniczych UMCS. Od października 2019 r. reprezentuję UMCS w kraju i na arenie międzynarodowej jako chórzystka śpiewając w Chórze Akademickim UMCS im. Jadwigi Czerwińskiej pod kierunkiem prof. dr hab. Urszuli Bobryk. Uczestniczyłam również w wielu wydarzeniach popularyzujących naukę.

## 11. Dorobek naukowy

---

### *Publikacje naukowe w czasopismach z listy filadelfijskiej*

1. R. Dobrowolski, **A. Krzyszczak**, J. Dobrzyńska, B. Podkościelna, E. Zięba, M. Czemierska, A. Jarosz-Wilkółazka, E.A. Stefaniak, *Extracellular polymeric substances immobilized on microspheres for removal of heavy metals from aqueous environment*, Biochemical Engineering Journal, 2019, 143: 202 – 211. IF<sub>2019</sub>: 3,475; punkty MEiN: 100.
2. A. Szmagara, **A. Krzyszczak**, I. Sadok, K. Karczmarz, M. Staniszewska, E.A. Stefaniak, *Determination of ellagic acid in rose matrix by spectrofluorimetry*, Journal of Food Composition and Analysis, 2019, 78: 91–100. IF<sub>2019</sub>: 3,721; punkty MEiN: 100.
3. A. Szmagara, **A. Krzyszczak**, *Monitoring of fluoride content in bottled mineral and spring waters by ion chromatography*, Journal of Geochemical Exploration, 2019, 202: 27 – 34. IF<sub>2019</sub>: 3,352; punkty MEiN: 100.
4. **A. Krzyszczak**, B. Czech, *Occurrence and toxicity of polycyclic aromatic hydrocarbons derivatives in environmental matrices*, Science of the Total Environment, 2021, 788: 147738. IF<sub>2021</sub>: 10,757; punkty MEiN: 200.
5. **A. Krzyszczak**, M. Dybowski, B. Czech, *Formation of polycyclic aromatic hydrocarbons and their derivatives in biochars: The effect of feedstock and pyrolysis conditions*, Journal of Analytical and Applied Pyrolysis, 2021, 160, 105339. IF<sub>2021</sub>: 6,437; punkty MEiN: 100.
6. K. Shirvanimoghaddam, B. Czech, S. Abdikheibari, G. Brodie, M. Kończak, **A. Krzyszczak**, A. Al-Othman, M. Naebe, *Microwave synthesis of biochar for environmental applications*, Journal of Analytical and Applied Pyrolysis, 2022, 161, 105415. IF<sub>2022</sub>: 6,0; punkty MEiN: 100.
7. **A. Krzyszczak**, M. Dybowski, I. Jośko, M. Kusiak, M. Sikora, B. Czech, *The antioxidant defense responses of Hordeum vulgare L. to polycyclic aromatic hydrocarbons and their derivatives in biochar-amended soil*, Environmental Pollution, 2022, 294, 118664. IF<sub>2022</sub>: 8,4; punkty MEiN: 100.

8. B. Czech, **A. Krzyszczak**, A. Boguszewska-Czubara, G. Opielak, I. Jośko, M. Hojamberdiev, *Revealing the toxicity of lopinavir- and ritonavir-containing water and wastewater treated by photo-induced processes to Danio rerio and Allivibrio fischeri*, Science of The Total Environment, 2022, 824, 153967. IF<sub>2022</sub>: 9,8; punkty MEiN: 200.
9. P. Sagan, I.V. Hadzaman, V.D. Popovych, R. Mroczka, **A. Krzyszczak**, M. Wiertel, D. Chocik, *Growth morphology and phase composition of hierarchically self-organized oxyspinel composite films deposited by radio frequency magnetron sputtering*, Ceramics International, 2022, 48(6). IF<sub>2022</sub>: 5,2; punkty MEiN: 100.
10. **A. Krzyszczak**, M.P. Dybowski, R. Zarzycki, R. Kobyłecki, P. Oleszczuk, B. Czech, *Long-term physical and chemical aging of biochar affected the amount and bioavailability of PAHs and their derivatives*, Journal of Hazardous Materials, 2022, 440, 129795. IF<sub>2022</sub>: 13,6; punkty MEiN: 200.
11. **A. Krzyszczak**, M.P. Dybowski, M. Kończak, B. Czech, *Low bioavailability of derivatives of polycyclic aromatic hydrocarbons in biochar obtained from different feedstock*, Environmental Research, 2022, 214(1), 113787. IF<sub>2022</sub>: 8,3; punkty MEiN: 100.
12. A. Szmagara, **A. Krzyszczak**, E.A. Stefaniak, *Determination of fluoride content in teas and herbal products popular in Poland*, Journal of Environmental Health Science and Engineering, 2022, 202, 27-34. IF<sub>2022</sub>: 3,4; punkty MEiN: 100.
13. I. Sadok, A. Szmagara, **A. Krzyszczak**, *Validated QuEChERS-based UHPLC-ESI-MS/MS method for the postharvest control of patulin (mycotoxin) contamination in red-pigmented fruits*, Food Chemistry, 2023, 400, 134066. IF<sub>2022</sub>: 8,8; punkty MEiN: 200.
14. A. Szmagara, M. Szmagara, **A. Krzyszczak**, I. Sadok, *Morphological and phytochemical characterization of Rosa sweginzowii fruit from Poland*, LWT - Food Science and Technology, 2023, 173, 114349. IF<sub>2022</sub>: 6,0; punkty MEiN: 100.
15. B. Nasri-Nasrabadi, B. Czech, R. Yadav, K. Shirvanimoghaddam, **A. Krzyszczak**, V. Unnikrishnan, M. Naebe, *Radially aligned hierarchical N-doped porous carbon beads derived from oil-sand asphaltene for long-life water filtration and wastewater treatment*, Science of The Total Environment, 2023, 863, 160896. IF<sub>2022</sub>: 9,8; punkty MEiN: 200.

16. A. Krzyszczak, M.P. Dybowski, B. Czech, *Microorganisms and their metabolites affect the content of polycyclic aromatic hydrocarbons and their derivatives in pyrolyzed material*, Science of the Total Environment, 2023, 886, 163966. IF<sub>2022</sub>: 9,8; punkty MEiN: 200.
17. I. Sadok, A. Krzyszczak-Turczyn, A. Szmagara, R. Łopucki, *Honey analysis in terms of nicotine, patulin and other mycotoxins contamination by UHPLC-ESI-MS/MS - method development and validation*, Food Research International, 2023, 172, 113184. IF<sub>2022</sub>: 8,1; punkty MEiN: 140.
18. B. Czech, B. Nasri-Nasrabadi, A. Krzyszczak-Turczyn, I. Sadok, M. Hojamberdiev, R. Yadav, K. Shirvanimoghaddam, M. Naebe, *Enhanced PFAS adsorption with N-doped porous carbon beads from oil-sand asphaltene*, Journal of Water Process Engineering, 2023, 54, 104058. IF<sub>2022</sub>: 7,0; punkty MEiN: 100.
19. M. Hojamberdiev, A.L. Larralde, R. Vargas, L.M. Madriz Ruiz, K. Yubuta, L.S. Koodlur, I. Sadok, A. Krzyszczak, P. Oleszczuk, B. Czech, *Unlocking the Effect of Zn<sup>2+</sup> on Crystal Structure, Optical Properties, and Photocatalytic Degradation of Perfluoroalkyl Substances (PFAS) of Bi<sub>2</sub>WO<sub>6</sub>*, Environmental Science: Water Research & Technology, 2023. IF<sub>2022</sub>: 5,0; punkty MEiN: 100.

### *Publikacje krajowe*

1. K. Grąż, E.A. Stefaniak, A. Szmagara, A. Krzyszczak, D. Nowak, *Charakterystyka fizykochemiczna nanocząstek srebra zsyntetyzowanych na drodze redukcji roztworem cytrynianu*, Nauka i przemysł – lubelskie spotkania studenckie, Praca zbiorowa pod red. prof. dr hab. Doroty Kołodyńskiej, 25.06.2018 r., Lublin, s. 146-149, ISBN 978-83-945225-5-1, Wydawnictwo Uniwersytetu Marii Curie-Skłodowskiej, punkty MEiN: 20.
2. B. Czech, A. Krzyszczak, *Pochodne WWA w próbkach gleb nawożonych biowęglem*, 2020, Nauka i przemysł – metody spektroskopowe w praktyce, nowe wyzwania i możliwości, Praca zbiorowa pod red. prof. dr. hab. Zbigniewa Hubickiego, str. 308-310, ISBN 978-83-227-9369-5, Wydawnictwo Uniwersytetu Marii Curie-Skłodowskiej, punkty MEiN: 20.

3. B. Czech, **A. Krzyszczak**, *Wpływ środowiskowy pochodnych WWA obecnych w różnych matrycach*, 2020, Nauka i przemysł – metody spektroskopowe w praktyce, nowe wyzwania i możliwości, Praca zbiorowa pod red. prof. dr. hab. Zbigniewa Hubickiego, str. 301-307, ISBN 978-83-227-9369-5, Wydawnictwo Uniwersytetu Marii Curie-Skłodowskiej, punkty MEiN: 20.
4. **A. Krzyszczak**, B. Czech, *Azotowe pochodne wielopierścieniowych węglowodorów aromatycznych w biowęglach*, 2020, Nauka i przemysł – lubelskie spotkania studenckie, Praca zbiorowa pod red. prof. dr hab. Doroty Kołodyńskiej, str. 146-149. ISBN 978-83-227-9370-1, Wydawnictwo Uniwersytetu Marii Curie-Skłodowskiej, punkty MEiN: 0.
5. B. Czech, **A. Krzyszczak**, *Rolnicze wykorzystanie biowęgla*, 2021, Nauka i przemysł – metody spektroskopowe w praktyce, nowe wyzwania i możliwości, Praca zbiorowa pod red. prof. dr. hab. Zbigniewa Hubickiego, str. 334-338, ISBN 978-83-227-9504-0, Wydawnictwo Uniwersytetu Marii Curie-Skłodowskiej, punkty MEiN: 20.
6. **A. Krzyszczak**, B. Czech, *Możliwości i wyzwania w oznaczaniu wielopierścieniowych węglowodorów aromatycznych w próbkach środowiskowych*, 2021, Nauka i przemysł – lubelskie spotkania studenckie, Praca zbiorowa pod red. prof. dr hab. Doroty Kołodyńskiej, str. 141-144, ISBN 978-83-227-9503-3, Wydawnictwo Uniwersytetu Marii Curie-Skłodowskiej, punkty MEiN: 20.
7. **A. Krzyszczak**, B. Czech, I. Sadok, *Aspekty analityczne ilościowego oznaczania związków per- i polifluoroalkilowych – ważnych zanieczyszczeń środowiskowych*, 2022, Nauka i przemysł – lubelskie spotkania studenckie, Praca zbiorowa pod red. prof. dr hab. Doroty Kołodyńskiej, str. 107-110, ISBN 978-83-227-9603-0, Wydawnictwo Uniwersytetu Marii Curie-Skłodowskiej, punkty MEiN: 20.
8. B. Czech, **A. Krzyszczak**, *Wpływ procesów środowiskowych na właściwości biowęgli*, 2022, Nauka i przemysł – metody spektroskopowe w praktyce, nowe wyzwania i możliwości, Praca zbiorowa pod red. prof. dr. hab. Zbigniewa Hubickiego, str. 412-415, ISBN 978-83-227-9602-3, Wydawnictwo Uniwersytetu Marii Curie-Skłodowskiej, punkty MEiN: 20.
9. **A. Krzyszczak**, B. Czech, *Surowce do produkcji biowęgla oraz ich wpływ na właściwości otrzymanego materiału*, 2021, Zagadnienia Aktualnie Poruszane

przez Młodych Naukowców, str. 12-14, ISBN 978-83-66772-02-1,  
CreativeTime, punkty MEiN: 5.

10. A. Krzyszczak, A. Sokołowski, B. Czech, *Toksyczność biowęgli – testy ekotoksykologiczne z wykorzystaniem bakterii *Allivibrio fischeri**, 2023, Nauka i przemysł – lubelskie spotkania studenckie, Praca zbiorowa pod red. prof. dr hab. Doroty Kołodyńskiej, str. 238-241, ISBN 978-83-227-9701-3, Wydawnictwo Uniwersytetu Marii Curie-Skłodowskiej, punkty MEiN: 20.
11. A. Sokołowski, A. Krzyszczak, B. Czech, *Żywłość jako źródło narażenia na estry ftalanów*, 2023, Nauka i przemysł – lubelskie spotkania studenckie, Praca zbiorowa pod red. prof. dr hab. Doroty Kołodyńskiej, str. 97-100, ISBN 978-83-227-9701-3, Wydawnictwo Uniwersytetu Marii Curie-Skłodowskiej, punkty MEiN: 20.
12. B. Czech, A. Krzyszczak, A. Sokołowski, *Biodostępność wielopierścieniowych węglowodorów aromatycznych i ich pochodnych*, 2023, Nauka i przemysł – metody spektroskopowe w praktyce, nowe wyzwania i możliwości, Praca zbiorowa pod red. prof. dr. hab. Zbigniewa Hubickiego, str. 297-300, ISBN 978-83-227-9700-6. Wydawnictwo Uniwersytetu Marii Curie-Skłodowskiej, punkty MEiN: 20.
13. B. Czech, A. Krzyszczak, A. Sokołowski, *Losy wielopierścieniowych węglowodorów aromatycznych w środowisku*, 2023, Nauka i przemysł – metody spektroskopowe w praktyce, nowe wyzwania i możliwości, Praca zbiorowa pod red. prof. dr. hab. Zbigniewa Hubickiego, str. 301-304, ISBN 978-83-227-9700-6. Wydawnictwo Uniwersytetu Marii Curie-Skłodowskiej, punkty MEiN: 20.

Łączny IF wszystkich prac: **136,942**

Łączna liczba punktów MEiN: **2765**

### ***Projekty badawcze***

1. Kierownik Wydziałowego Grantu dla Młodych Naukowców (Instytucja przyznająca: Katolicki Uniwersytet Lubelski Jana Pawła II w Lublinie), pt. „Materiały hybrydowe – synteza, charakterystyka i zastosowanie analityczne”, okres realizacji 02.2018 - 02.2019, kwota dotacji 1000,00 zł.

2. Kierownik złożonego wniosku grantowego w konkursie Preludium-21 (Narodowe Centrum Nauki) pt. „Usieciowane 4-winylopirydyną porowate mikrosfery jako nowoczesne sorbenty do doczyszczania próbek do oznaczeń mykotoksyn metodą LC-MS/MS w owocach bogatych w antocyjany”, czerwiec 2022 r. Wniosek nie zakwalifikowany do finansowania.
3. Kierownik złożonego wniosku grantowego w konkursie Preludium-22 (Narodowe Centrum Nauki) pt. „Porowate mikrosfery 4-winylopirydyny usieciowane komonomerami metakrylanu jako nowe sorbenty do usuwania polifenoli z matrycy próbki przed oznaczaniem mykotoksyn metodą LC-MS/MS”, czerwiec 2023 r. Wniosek w trakcie oceny.
4. Wykonawca w projekcie badawczym OPUS 16 nr 2018/31/B/NZ9/00317 finansowanym z NCN, pt. „Tworzenie się pochodnych wielopierścieniowych węglowodorów aromatycznych w biowęglach i ich biodostępność oraz trwałość podczas przyrodniczego wykorzystania biowęgla” (kierownik dr hab. Bożena Czech, prof. UMCS, okres zaangażowania: od stycznia 2020 r. do stycznia 2023 r.).

## ***UDZIAŁ W KONFERENCJACH NAUKOWYCH***

### ***Międzynarodowe konferencje naukowe***

#### **Wystąpienia referatowe**

1. **A. Krzyszczak**, B. Czech, *The effect of physical aging on the contents of polycyclic aromatic hydrocarbons and their derivatives in biochars*, Summer School for PhD students - Modern Research Techniques for Physicochemical Characterization of the Potential Application Systems, 18-20.05.2022 r., Lublin, Polska, str. 26, ISBN 978-83-227-9590-3.

#### **Wystąpienia plakatowe**

1. **A. Krzyszczak**, B. Czech, *The effect of chemical aging on the physicochemical characteristics of sewage sludge-derived biochars*, Summer School for PhD students - Modern Research Techniques for Physicochemical Characterization of

the Potential Application Systems, 18-20.05.2022 r., Lublin, Polska, str. 51, ISBN 978-83-227-9590-3.

2. **A. Krzyszczak**, M. Barczak, B. Czech, *Environmental hazard of biochar*, Eleventh International Symposium Effects of Surface Heterogeneity in Adsorption, Catalysis and related Phenomena, 18-22.09.2022 r., Zegrze, Polska, str. 66.
3. **A. Krzyszczak-Turczyn**, A. Sokołowski, B. Czech, *The effect of soil microorganisms on polycyclic aromatic hydrocarbons derivatives content in biochar*, 14th International Conference on Agrophysics, 11-13.09.2023 r., Lublin, Polska, str. 168, ISBN 978-83-89969-82-8.
4. **A. Krzyszczak-Turczyn**, A. Sokołowski, B. Czech, *Organic waste-derived adsorbents for environmental application*, 14th International Conference on Agrophysics, 11-13.09.2023 r., Lublin, Polska, str. 169, ISBN 978-83-89969-82-8.

### ***Krajowe konferencje naukowe***

#### ***Wystąpienia referatowe***

1. **A. Krzyszczak**, B. Czech, *Oznaczanie azotowych pochodnych wielopierścieniowych węglowodorów aromatycznych w biowęglach*, I Interdyscyplinarna Konferencja Doktorantów Nauk Biologicznych BIO-IDEA 2020, 06.07.2020 r., Lublin.
2. B. Czech, **A. Krzyszczak**, *Pochodne WWA w próbках gleb nawożonych biowęglem*, VII Ogólnopolska Konferencja „Nauka i przemysł – metody spektroskopowe w praktyce nowe wyzwania i możliwości”, 22.06.2020 r., Lublin, str. 308-310, ISBN 978-83-227-9369-5, Wydawnictwo Uniwersytetu Marii Curie-Skłodowskiej.
3. B. Czech, **A. Krzyszczak**, *Wpływ środowiskowy pochodnych WWA obecnych w różnych matrycach*”, VII Ogólnopolska Konferencja „Nauka i przemysł – metody spektroskopowe w praktyce nowe wyzwania i możliwości”, 22.06.2020 r., Lublin, str. 301-307, ISBN 978-83-227-9369-5, Wydawnictwo Uniwersytetu Marii Curie-Skłodowskiej.

4. B. Czech, **A. Krzyszczak**, *Wpływ dodatku biowęgla do gleb na rośliny*, VII Ogólnopolska Konferencja „Innowacje w Praktyce”, 20.10.2020 r., Lublin, str. 31, ISBN 978-83-943796-6-7.
5. B. Czech, **A. Krzyszczak**, *Rolnicze wykorzystanie biowęgla*, XV Ogólnopolska Konferencja „Nauka i przemysł – metody spektroskopowe w praktyce, nowe wyzwania i możliwości”, 29–30.06.2021 r., online, str. 334-338, ISBN 978-83-227-9504-0.
6. B. Czech, **A. Krzyszczak**, *Wpływ procesów środowiskowych na właściwości biowęgli*, XV Ogólnopolskie Sympozjum „Nauka i przemysł – metody spektroskopowe w praktyce, nowe wyzwania i możliwości”, 28-29.06.2022 r., Lublin, str. 412-415, ISBN 978-83-227-9602-3, Wydawnictwo Uniwersytetu Marii Curie-Skłodowskiej.
7. **A. Krzyszczak**, B. Czech, *Zmiany zawartości wielopierścieniowych węglowodorów aromatycznych i ich pochodnych w biowęglach poddanych presji środowiska*, 64. Zjazd Naukowy Polskiego Towarzystwa Chemicznego, 11-16.09.2022 r., Lublin, str. 461, ISBN 978-83-60988-35-0.
8. B. Czech, **A. Krzyszczak**, *Czarne złoto - szansa dla rolnictwa czy zagrożenie?* 64. Zjazd Naukowy Polskiego Towarzystwa Chemicznego, 11-16.09.2022 r., Lublin, str. 456, ISBN 978-83-60988-35-0.
9. **A. Krzyszczak**, A. Sokołowski, R. Kobyłecki, R. Zarzycki, B. Czech, *Pochodne WWA - występowanie i losy w środowisku*, Fizykochemia Granic Faz – Metody Instrumentalne, 16-20.04.2023 r., Lublin, str. 123.
10. **A. Krzyszczak**, A. Sokołowski, B. Czech, *Starzenie biowęgli - modelowe badania zmian zachodzących pod wpływem presji czynników środowiskowych*, Fizykochemia Granic Faz – Metody Instrumentalne, 16-20.04.2023 r., Lublin, str. 128.
11. B. Czech, **A. Krzyszczak**, A. Sokołowski, *Pochodne wielopierścieniowych węglowodorów aromatycznych w materiałach węglowych – nowy problem środowiskowy?*, X Ogólnopolska Konferencja Naukowa „Innowacje w praktyce”, 15-16.06.2023 r., Lublin, str. 31, ISBN 978-83-943796-9-8.
12. B. Czech, **A. Krzyszczak**, A. Sokołowski, *Biodostępność wielopierścieniowych węglowodorów aromatycznych i ich pochodnych*, XVI Ogólnopolskie Sympozjum „Nauka i przemysł – metody spektroskopowe w praktyce, nowe

wyzwania i możliwości”, 27-29.06.2023 r., Lublin, str. 297-300, ISBN 978-83-227-9700-6, Wydawnictwo Uniwersytetu Marii Curie-Skłodowskiej.

13. A. Krzyszczak-Turczyn, A. Sokołowski, B. Czech, *Termiczne modyfikacje osadów ściekowych oraz ich zagospodarowanie w kierunku dodatków do gleb*, 65. Zjazd Naukowy Polskiego Towarzystwa Chemicznego, 18-22.09.2023 r., Toruń, str. 64.

### Wystąpienia plakatowe

1. A. Krzyszczak, A. Szmagara, A. Stachniuk, E.A. Stefaniak, *Zastosowanie chromatografii jonowej w oznaczeniach zawartości azotanów(III) i azotanów(V) w ogórkach szklarniowych*, IV Ogólnopolska Konferencja Naukowa „Innowacje w Praktyce”, 23-24.11.2017 r., Lublin, str. 100 – 101, ISBN 978-83-943796-3-6.
2. A. Szmagara, I. Sadok, A. Krzyszczak, E.A. Stefaniak, *Zawartość antocyjanów jako parametr charakteryzujący złożoność matrycy owoców*, IV Ogólnopolska Konferencja Naukowa „Innowacje w Praktyce”, 23-24.11.2017 r., Lublin, str. 150 – 151, ISBN 978-83-943796-3-6.
3. E.A. Stefaniak, J. Ostrowski, A. Skiba, U. Ryszko, A. Krzyszczak, E. Zięba, T. Gałuszka, *Oznaczanie metali i metaloidów w miodzie i w pszczołach z hodowli miejskiej*, XXII Konferencja „Nowoczesne metody instrumentalne w analizie śladowej”, 11-12.12.2017 r., Białystok.
4. A. Szmagara, A. Krzyszczak, E.A. Stefaniak, *Zawartość fluorków w butelkowanych wodach mineralnych*, V Ogólnopolska Konferencja Naukowa „Innowacje w Praktyce”, 5-6.04.2018 r., Lublin, s. 144-145, ISBN 978-83-943796-4-3.
5. K. Grąż, E.A. Stefaniak, A. Szmagara, A. Krzyszczak, D. Nowak, *Charakterystyka fizykochemiczna nanocząstek srebra zsyntetyzowanych na drodze redukcji roztworem cytrynianu*, VI Ogólnopolskie sympozjum „Nauka i przemysł – lubelskie spotkania studenckie”, 25.06.2018 r., Lublin, s. 146-149, ISBN 978-83-945225-5-1.
6. E.A. Stefaniak, A. Buczynska, R. Kuduk, W.Z. Polak, A. Krzyszczak, M.P. Fischer, *Zastosowanie parametru  $\delta^{13}\text{C}$  do ustalenia źródła emisji sadzy (Application of  $\delta^{13}\text{C}$  for source identification of soot)*. Konwersatorium Spektrometrii Atomowej, 24-26.09.2018 r., Białystok.

7. **A. Krzyszczak**, A. Szmagara, J. Ostrowski, A. Skiba, U. Ryszko, E. Zięba, T. Gałuszka, E.A. Stefaniak, *Akumulacja metali w pszczołach z hodowli miejskiej*, VI Ogólnopolska Konferencja Naukowa „Innowacje w Praktyce”, 4-5.04.2019 r., Lublin, str. 128-129, ISBN 9788394379650.
8. A. Szmagara, **A. Krzyszczak**, I. Sadok, E.A. Stefaniak, *Oznaczanie kwasu elagowego w owocach liofilizowanych metodą spektrofluorymetryczną*, VI Ogólnopolska Konferencja Naukowa „Innowacje w Praktyce”, 4-5.04.2019 r., Lublin, str. 267-268, ISBN 9788394379650.
9. **A. Krzyszczak**, B. Czech, *Azotowe pochodne wielopierścieniowych węglowodorów aromatycznych w biowęglach*, VII Ogólnopolska Konferencja „Nauka i przemysł – lubelskie spotkania studenckie”, 22.06.2020 r., Lublin, str. 146-149. ISBN 978-83-227-9370-1, Wydawnictwo Uniwersytetu Marii Curie-Skłodowskiej.
10. **A. Krzyszczak**, B. Czech, *Wielopierścieniowe węglowodory aromatyczne i ich pochodne w próbkach gleb*, VII Ogólnopolska Konferencja „Innowacje w Praktyce”, 20.10.2020 r., Lublin, str. 65, ISBN 978-83-943796-6-7.
11. **A. Krzyszczak**, B. Czech, *Wielopierścieniowe węglowodory aromatyczne i ich pochodne w biowęglach jako problem środowiskowy*, Interdyscyplinarna Konferencja Naukowa „Green Week 2020: Nowy początek dla ludzkości i natury”, 21.10.2020r., Lublin, str. 52, ISBN 978-83-959540-0-9.
12. A. Szmagara, **A. Krzyszczak**, H. Vishniavetskaya, *Wykorzystanie metod spektrofotometrycznych do charakterystyki miodu*, Interdyscyplinarna Konferencja Naukowa „Green Week 2020: Nowy początek dla ludzkości i natury”, 21.10.2020 r., Lublin, str. 52, ISBN 978-83-959540-0-9.
13. **A. Krzyszczak**, B. Czech, *Surowce do produkcji biowęgla oraz ich wpływ na właściwości otrzymanego materiału*, Nowe trendy w badaniach naukowych, 20-22.11.2020 r., online, str. 13, ISBN 978-83-63058-99-9, Wydawca CreativeTime.
14. **A. Krzyszczak**, B. Czech, *Możliwości i wyzwania w oznaczaniu wielopierścieniowych węglowodorów aromatycznych w próbkach środowiskowych*, IX Ogólnopolskie Sympozjum „Nauka i przemysł – lubelskie spotkania studenckie”, 28.06.2021 r., online, str. 141-144, ISBN 978-83-227-9503-3.

15. **A. Krzyszczak**, B. Czech, *Wpływ temperatury procesu pirolizy na zawartość frakcji całkowitej i biodostępnej wielopierścieniowych węglowodorów aromatycznych w biowęglach*, VIII Ogólnopolska konferencja naukowa „Innowacje w praktyce”, 14.10.2021 r., online, str. 52.
16. A. Szmagara, **A. Krzyszczak**, A. Jastrzębski, *Miody: do wyboru do koloru. Porównanie spektrofotometrycznych metod oznaczania barwy miodu*, VIII Ogólnopolska konferencja naukowa „Innowacje w praktyce”, 14.10.2021 r., online, str. 63.
17. **A. Krzyszczak**, B. Czech, I. Sadok, *Aspekty analityczne ilościowego oznaczania związków per-i polifluoroalkilowych ważnych zanieczyszczeń środowiskowych*, X Ogólnopolskie Sympozjum „Nauka i przemysł – lubelskie spotkania studenckie”, 27.06.2022 r., Lublin, str. 107-110, ISBN 978-83-227-9603-0, Wydawnictwo Uniwersytetu Marii Curie-Skłodowskiej.
18. **A. Krzyszczak**, B. Czech, *Feedstock – the key parameter affecting the content of polycyclic aromatic hydrocarbons and their derivatives in biochars*, 64. Zjazd Naukowy Polskiego Towarzystwa Chemicznego, 11-16.09.2022 r., Lublin, str. 470, ISBN 978-83-60988-35-0.
19. B. Czech, **A. Krzyszczak**, *CPBE-BC: chemical, physical, biological and enzymatic ageing of biochars*, 64. Zjazd Naukowy Polskiego Towarzystwa Chemicznego”, 11-16.09.2022 r., Lublin, str. 469, ISBN 978-83-60988-35-0.
20. **A. Krzyszczak**, B. Czech, *Sorpcaja leków przeciwwirusowych na biowęglach*, V Zjazd Naukowy Polskiego Towarzystwa Biologii Medycznej „Biologia-Medycyna-Terapia”, 15-17.09.2022 r., Lublin, str. 226-227, ISBN 978-83-8288-050-2.
21. **A. Krzyszczak**, B. Czech, *Toksyczność pozostałości leków przeciwwirusowych w próbkach ścieków oczyszczonych różnymi metodami*, V Zjazd Naukowy Polskiego Towarzystwa Biologii Medycznej „Biologia-Medycyna-Terapia”, 15-17.09.2022 r., Lublin, str. 228-229, ISBN 978-83-8288-050-2.
22. **A. Krzyszczak**, A. Sokołowski, R. Kobyłecki, R. Zarzycki, B. Czech, *Wpływ mikroorganizmów glebowych i ich metabolitów na bezpieczeństwo rolniczego użytkowania biowęgla*, Fizykochemia Granic Faz – Metody Instrumentalne, 16-20.04.2023 r., Lublin, Polska, str. 131.

23. A. Krzyszczak, A. Sokołowski, B. Czech, *Zmiany właściwości fizykochemicznych biowęgli wywołane starzeniem chemicznym*, Fizykochemia Granic Faz – Metody Instrumentalne, 16-20.04.2023 r., Lublin, Polska, str. 136.
24. A. Sokołowski, A. Krzyszczak, B. Czech, *Biodostępność WWA w biowęglach otrzymanych z materiałów odpadowych*, Fizykochemia Granic Faz – Metody Instrumentalne, 16-20.04.2023 r., Lublin, Polska, str. 146.
25. A. Sokołowski, A. Krzyszczak, B. Czech, *Właściwości fizykochemiczne biowęgli otrzymanych z odpadów rolniczych*, Fizykochemia Granic Faz – Metody Instrumentalne, 16-20.04.2023 r., Lublin, Polska, str. 147.
26. B. Czech, A. Krzyszczak, A. Sokołowski, *Ekobiotesty i ich zastosowanie w ocenie bezpieczeństwa biowęgli*, X Ogólnopolska Konferencja Naukowa „Innowacje w praktyce”, 15-16.06.2023 r., Lublin, str. 57, ISBN 978-83-943796-9-8.
27. A. Krzyszczak, B. Czech, I. Sadok, *Nowe sposoby usuwania związków perfluorowanych z roztworów wodnych*, X Ogólnopolska Konferencja Naukowa „Innowacje w praktyce”, 15-16.06.2023 r., Lublin, str. 72, ISBN 978-83-943796-9-8.
28. A. Krzyszczak, A. Sokołowski, B. Czech, *Dodatek biowęglu do gleb – remedium na zubożałe gleby czy źródło zanieczyszczenia?*, X Ogólnopolska Konferencja Naukowa „Innowacje w praktyce”, 15-16.06.2023 r., Lublin, str. 73, ISBN 978-83-943796-9-8.
29. A. Sokołowski, A. Krzyszczak, B. Czech, *Toksyczność osadów pofermentacyjnego z biogazowni i ściekowego a otrzymanych z nich biowęgli*, X Ogólnopolska Konferencja Naukowa „Innowacje w praktyce”, 15-16.06.2023 r., Lublin, str. 88, ISBN 978-83-943796-9-8.
30. A. Sokołowski, A. Krzyszczak, B. Czech, *Odpady rolnicze jako surowiec do produkcji materiałów węglowych*, X Ogólnopolska Konferencja Naukowa „Innowacje w praktyce”, 15-16.06.2023 r., Lublin, str. 89, ISBN 978-83-943796-9-8.
31. A. Krzyszczak, A. Sokołowski, B. Czech, *Toksyczność biowęgli – testy ekotoksykologiczne z wykorzystaniem bakterii *Allivibrio fischeri**, XI Ogólnopolskie Sympozjum „Nauka i przemysł – lubelskie spotkania studenckie”, 26.06.2023 r., Lublin, str. 238-241, ISBN 978-83-227-9701-3.

32. A. Sokołowski, **A. Krzyszczak**, B. Czech, *Żywność jako źródło narażenia na estry ftalanów*, XI Ogólnopolskie Sympozjum „Nauka i przemysł – lubelskie spotkania studenckie”, 26.06.2023 r., Lublin, str. 97-100, ISBN 978-83-227-9701-3.
33. B. Czech, **A. Krzyszczak**, A. Sokołowski, *Losy wielopierścieniowych węglowodorów aromatycznych w środowisku*, XVI Ogólnopolskie Sympozjum „Nauka i przemysł – metody spektroskopowe w praktyce, nowe wyzwania i możliwości”, 27-29.06.2023 r., Lublin, str. 301-304, ISBN 978-83-227-9700-6, Wydawnictwo Uniwersytetu Marii Curie-Skłodowskiej.
34. **A. Krzyszczak-Turczyn**, A. Sokołowski, B. Czech, *New materials for the photodegradation of perfluoroalkyl substances*, 65. Zjazd Naukowy Polskiego Towarzystwa Chemicznego, 18-22.09.2023 r., Toruń, str. 73.
35. A. Sokołowski, **A. Krzyszczak-Turczyn**, B. Czech, *Bezpieczeństwo stosowania osadów pofermentacyjnego z biogazowni i ściekowego oraz otrzymanych z nich biowęgli*, 65. Zjazd Naukowy Polskiego Towarzystwa Chemicznego, 18-22.09.2023 r., Toruń, str. 87.
36. A. Sokołowski, **A. Krzyszczak-Turczyn**, B. Czech, *Wielopierścieniowe węglowodory aromatyczne (WWA) w biowęglach otrzymanych z odpadów roślinnych*, 65. Zjazd Naukowy Polskiego Towarzystwa Chemicznego, 18-22.09.2023 r., Toruń, str. 88.

## 12. Wykaz pozostałych osiągnięć i aktywności naukowych

---

### *Działalność popularyzująca naukę*

1. Kierownik Projektu „Co się kryje w wodach - technika chromatograficzna”, przeprowadzonego w ramach XVII edycji Lubelskiego Festiwalu Nauki pod hasłem „Nauka bez granic. Enjoy Science!”, 21.09.2021 r., Katolicki Uniwersytet Lubelski Jana Pawła II w Lublinie.
2. Współorganizator Projektu „Plastik w naszym życiu codziennym” przeprowadzonego w ramach XVII edycji Lubelskiego Festiwalu Nauki pod

hasłem „Nauka bez granic. Enjoy Science!”, 21.09.2021 r., Katolicki Uniwersytet Lubelski Jana Pawła II w Lublinie.

3. Wykonawca Projektu „Pokazy chemiczne - Laboratoryjny bar” przeprowadzonego w ramach XVII edycji Lubelskiego Festiwalu Nauki pod hasłem „Nauka bez granic. Enjoy Science!”, 22.09.2021 r., Katolicki Uniwersytet Lubelski Jana Pawła II w Lublinie.
4. Współprowadząca warsztaty dotyczące techniki miareczkowania dla młodzieży licealnej, 30.09.2021 r., Katolicki Uniwersytet Lubelski Jana Pawła II w Lublinie.
5. Wykonawca pokazów chemicznych dla dzieci z Niepublicznego Przedszkola „Kolorowe Kredki” z Lublina, 22.09.2021 r., Katolicki Uniwersytet Lubelski Jana Pawła II w Lublinie.
6. Współprowadząca pokazy chemiczne dla dzieci z Niepublicznego Przedszkola „Kolorowe Kredki” z Garbowa, 22.09.2021 r., Katolicki Uniwersytet Lubelski Jana Pawła II w Lublinie.
7. Współrowadząca warsztaty dla młodzieży ze szkoły średniej, 11.10.2021 r., Katolicki Uniwersytet Lubelski Jana Pawła II w Lublinie.
8. Współrowadząca warsztaty dla młodzieży szkolnej w ramach Nocy Biologów 2022, 14.01.2022 r., Katolicki Uniwersytet Lubelski Jana Pawła II w Lublinie.
9. Kierownik projektu pt. ”Identyfikacja (oraz analiza ilościowa) niewidzialnych składników wód – chromatografia jonowa” w ramach Nocy Biologów 2022, 14.01.2022 r., Katolicki Uniwersytet Lubelski Jana Pawła II w Lublinie.
10. Współrowadząca warsztaty dla młodzieży szkolnej pt. „Plastik plastikowi nierówny – identyfikacja tworzyw sztucznych” w ramach Nocy Biologów 2022, 14.01.2022 r., Katolicki Uniwersytet Lubelski Jana Pawła II w Lublinie.
11. Współrowadząca warsztaty i pokazy chemiczne w ramach Dni Otwartych Wydziału Nauk Ścisłych i Nauk o Zdrowiu Katolickiego Uniwersytetu Lubelskiego Jana Pawła II w Lublinie, 28.03.2022 r.
12. Współorganizator projektu „Ukwiecona polana” przeprowadzonego w ramach Pikniku Naukowego XVIII Lubelskiego Festiwalu Nauki „Ogrody Nauki”, 11.09.2022 r., Plac Teatralny w Lublinie.
13. Współrowadząca pokazy chemiczne pt. ”Kolorowe eksperymenty – nauka czy magia?” w ramach XVIII Lubelskiego Festiwalu Nauki „Ogrody Nauki”, 13.09.2022 r., Katolicki Uniwersytet Lubelski Jana Pawła II w Lublinie.

14. Organizator projektu pt. „Suchy lód kontra woda – zjawiskowa sublimacja” w ramach Nocy Biologów 2023 pod hasłem „Woda - źródło życia - teraźniejszość i przyszłość”, 13.01.2023 r., Katolicki Uniwersytet Lubelski Jana Pawła II w Lublinie.
15. Organizator projektu pt. „Lodowa kraina” w ramach Nocy Biologów 2023 pod hasłem „Woda - źródło życia - teraźniejszość i przyszłość”, 13.01.2023 r., Katolicki Uniwersytet Lubelski Jana Pawła II w Lublinie.
16. Współprowadząca pokazy chemiczne promujące Wydział Medyczny Katolickiego Uniwersytetu Lubelskiego Jana Pawła II w Lublinie w ramach wydarzenia Piknik rodzinny „Z nauką za pan brat!”, 25.06.2023 r., Zalew Zemborzycki.
17. Współrowadząca pokazy chemiczne promujące Wydział Medyczny Katolickiego Uniwersytetu Lubelskiego Jana Pawła II w Lublinie w ramach wydarzenia „Studiuj w Lublinie – Europejskiej Stolicy Młodzieży 2023”, 21.03.2023 r., Plac Litewski w Lublinie.
18. Kierownik Projektu „Oznaczanie całkowitej zawartości polifenoli w napojach” przeprowadzonego w ramach XIX edycji Lubelskiego Festiwalu Nauki pod hasłem „Nauka dla przyszłości”, 22.09.2023 r., Katolicki Uniwersytet Lubelski Jana Pawła II w Lublinie.
19. Współorganizator Projektu „Innowacyjne eksperymenty z suchym lodem” przeprowadzonego w ramach XIX edycji Lubelskiego Festiwalu Nauki pod hasłem „Nauka dla przyszłości”, 22.09.2023 r., Katolicki Uniwersytet Lubelski Jana Pawła II w Lublinie.
20. Współorganizator Projektu „Mroźne eksperymenty” przeprowadzonego w ramach XIX edycji Lubelskiego Festiwalu Nauki pod hasłem „Nauka dla przyszłości”, 22.09.2023 r., Katolicki Uniwersytet Lubelski Jana Pawła II w Lublinie.

## ***Działalność organizacyjna i reprezentacyjna***

1. Członek Rady Uczelnianej Samorządu Doktorantów UMCS w latach akademickich 2019/2020, 2020/2021, 2021/2022, 2022/2023.
2. Członek Rady Szkoły Doktorskiej Nauk Ścisłych i Przyrodniczych UMCS w latach akademickich 2019/2020, 2020/2021, 2021/2022, 2022/2023.
3. V-ce Przewodnicząca Rady Doktorantów Szkoły Doktorskiej Nauk Ścisłych i Przyrodniczych UMCS od 04.2021 r. do chwili obecnej.
4. Członek Komisji Rekrutacyjnej do Szkoły Doktorskiej Nauk Ścisłych i Przyrodniczych UMCS w latach akademickich 2020/2021, 2022/2023.
5. Członek Komitetu Organizacyjnego V Zjazdu Naukowego Polskiego Towarzystwa Biologii Medycznej „Biologia-Medycyna-Terapia”, 15-17.09.2022 r., Lublin.
6. Redaktor materiałów konferencyjnych V Zjazdu Naukowego Polskiego Towarzystwa Biologii Medycznej „Biologia-Medycyna-Terapia”, 15-17.09.2022 r., Lublin.
7. Aktywny udział w 64. Zjeździe Polskiego Towarzystwa Chemicznego polegający na obsłudze sal wykładowych (11-16.09.2022 r., Lublin).
8. Członek Polskiego Towarzystwa Chemicznego od marca 2020 roku do chwili obecnej.
9. Reprezentantka Uniwersytetu jako chórzystka w Chórze Akademickim UMCS im. Jadwigi Czerwińskiej pod kierunkiem prof. dr hab. Urszuli Bobryk, od 10.2019 r. do chwili obecnej, udział w 36 wydarzeniach:
  - „Christmas Party” Koncert kolęd w ramach projektu „UMCS Hakuna Matata” (13.12.2019 r.).
  - Koncert w Filharmonii Lubelskiej w ramach XXIV Forum im. Witolda Lutosławskiego (21.05.2021 r.).
  - Koncert dyplomowy studentów I i II stopnia Edukacji artystycznej w zakresie sztuki muzycznej w Archikatedrze św. Jana Chrzciciela i św. Jana Ewangelisty w Lublinie (25.06.2021 r.).
  - Koncert w Ochrydzie na Międzynarodowym Festiwalu „Kostoski” w Macedonii (25.07.2021 r.).

- Pokaz fontann na Placu Litewskim pn. Symfonia nauki (udział w nagraniu utworu „Symphony of Silence” Piotra Bańki) (18.09.2021 r.).
- Koncert „Siema Żaki” organizowany przez ACKiM UMCS Chatka Żaka (01.10.2021 r.).
- Otwarta próba i Koncert Chóru Akademickiego UMCS w ramach “Wolnej Chatki” w ACKiM UMCS Chatka Żaka (08.10.2021 r.).
- Koncert chóralny w kościele św. Teresy od Dzieciątka Jezus w Lublinie (17.10.2021 r.).
- Oprawa muzyczna mszy świętej z okazji inauguracji roku akademickiego 2021/2022 w Archikatedrze Lubelskiej (12.10.2021 r.).
- Oprawa muzyczna uroczystości nadania tytułu doktora honoris causa UMCS prof. Yurijowi Oganessianowi (21.10.2021 r.).
- Oprawa muzyczna uroczystej inauguracji roku akademickiego UMCS na Wydziale Prawa i Administracji UMCS (23.10.2021 r.).
- Koncert chóralny w hołdzie św. Janowi Pawłowi II w parafii Matki Bożej Częstochowskiej w Borzechowie (24.10.2021 r.).
- Występ kolędowy Chóru podczas uroczystego rozświetlenia choinki na placu Marii Curie-Skłodowskiej przez Rektora UMCS prof. dr. hab. Radosława Dobrowolskiego (06.12.2021 r.).
- Koncert “Pieśni Bardów Stanu Wojennego” z udziałem Lubelskiej Federacji Bardów w ramach 40. Rocznicy Wprowadzenia Stanu Wojennego w ACKiM UMCS Chatka Żaka (13.12.2021 r.).
- Koncert kolęd w kościele św. Teresy od Dzieciątka Jezus w Lublinie (16.01.2022 r.).
- Koncert kolęd w kościele św. Agnieszki w Lublinie (23.01.2022 r.).
- Wykonanie “Modlitwy o pokój” Norberta Blachy w języku polskim i ukraińskim z chórami z województwa lubelskiego pod Nowym Ratuszem w Lublinie (26.03.2022 r.).
- Wielki “Koncert Wdzięczności” dla TV Puls w Centrum Spotkań Kultur z emisją koncertu w telewizji ogólnokrajowej (29.04.2022 r.).
- Nagranie utworu i teledysku “Żywego Mur” z Orkiestrą Reprezentacyjną Straży Granicznej w Filharmonii Lubelskiej (30.04.2022 r.).

- Multimedialny pokaz na Placu Litewskim pt. "Symfonia Nauki" z wykonaniem utworu „Symphony of Silence” Piotra Bańki (07.05.2022 r.).
- Występ na Wieży Trynitarskiej w ramach Nocy Kultury (02.06.2022 r.).
- Multimedialny pokaz na Placu Litewskim pt. "Symfonia Nauki" z wykonaniem utworu „Symphony of Silence” Piotra Bańki (11.06.2022 r.).
- Koncert dyplomowy studentów Edukacji artystycznej w zakresie sztuki muzycznej w kościele św. Agnieszki w Lublinie (28.06.2022 r.)
- Koncert w Kościele Rektoralnym pw. Wniebowzięcia Najświętszej Maryi Panny Zwycięskiej w Lublinie (16.10.2022 r.).
- Koncert w kościele św. Teresy od Dzieciątka Jezus w Lublinie (16.10.2022 r.).
- Oprawa muzyczna Gali Sportu Akademickiego 2022 w Centrum Spotkań Kultur w Lublinie (21.10.2022 r.).
- Oprawa muzyczna konferencji “Pedagogika tolerancji. W kręgu myśli Karola Wojtyły - Jana Pawła II” w ACKiM UMCS Chatka Żaka (07.11.2022 r.).
- Narodowy Koncert Listopadowy w Filharmonii Lubelskiej (12.11.2022 r.).
- Wyjazd chóru do Niemiec (25 - 28.11.2022 r.) i koncert (26.11.2022 r.) na Międzynarodowym Festiwalu Muzycznym w Essen.
- Koncert kolęd w Archikatedrze św. Jana Chrzciciela i św. Jana Ewangelisty w Lublinie (22.01.2023 r.).
- Koncert Walentynkowy z Beata Kozidrak i Bajm w Centrum Spotkań Kultur w Lublinie (14.02. 2023 r.).
- Występ chóru na Gali Otwarcia Europejskiej Stolicy Młodzieży Lublin 2023 w Chatce Żaka (16.03.2023 r.).
- Koncert chóru na Międzynarodowej Konferencji Naukowej „Trybut dla prof. Stanisława Hałasa | 30 rocznica Pracowni Geologii Izotopowej i Geoekologii” w Oratorium Marianum Uniwersytetu Wrocławskiego (09.05.2023 r.).
- Koncert w ramach obchodów Jubileuszu 50-lecia kształcenia artystycznego w UMCS w Filharmonii Lubelskiej (12.05.2023 r.).
- Koncert dyplomowy studentów Edukacji artystycznej w zakresie sztuki muzycznej, wykonanie utworu Misa a Buenos Aires - Misatango, Martina Palmeriego (13.06.2023 r.).
- Występ chóru podczas promocji doktorskich Wydziału Filologicznego (28.06.2023 r.).

**ANEKS - TEKSTY PUBLIKACJI BĘDĄCYCH PRZEDMIOTEM ROZPRAWY  
DOKTORSKIEJ**

## **Publikacja D1**

**A. Krzyszczak, B. Czech**

*Occurrence and toxicity of polycyclic aromatic hydrocarbons derivatives in environmental  
matrices*

Science of the Total Environment, 2021, 788: 147738



## Review

## Occurrence and toxicity of polycyclic aromatic hydrocarbons derivatives in environmental matrices



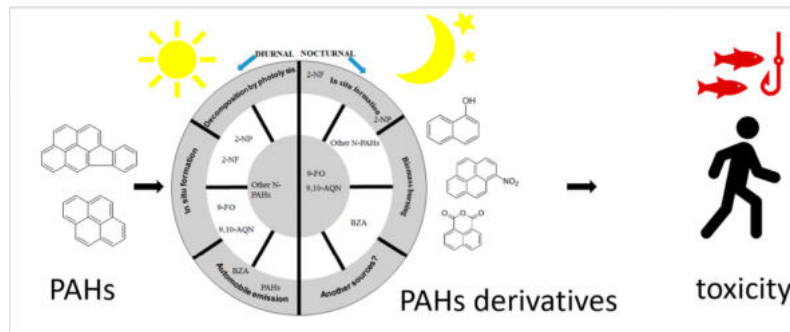
Agnieszka Krzyszczak, Bożena Czech \*

Department of Radiochemistry and Environmental Chemistry, Institute of Chemical Sciences, Faculty of Chemistry, University of Maria Curie-Skłodowska, Pl. M. Curie-Skłodowskiej 3, 20-031 Lublin, Poland

## HIGHLIGHTS

- PAHs derivatives are formed during PAHs formation and transformation.
- The presence of O, N, or S in PAHs aromatic rings increased their toxicity.
- The primary sources of PAHs derivatives are biological processes and combustion.
- Secondary resources involved photochemical, radical- and oxidants mediated reactions.
- The review describes the determination of PAHs derivatives in different matrices.

## GRAPHICAL ABSTRACT



## ARTICLE INFO

## Article history:

Received 15 April 2021

Received in revised form 8 May 2021

Accepted 9 May 2021

Available online 15 May 2021

Editor: Shuzhen Zhang

## Keywords:

PAHs  
PAHs derivatives  
Toxicity  
N-PAHs  
O-PAHs

## ABSTRACT

In the last years, there is great attention paid to the determination of polycyclic aromatic hydrocarbons (PAHs) in different environmental matrices. Extensive reviews on PAHs presence and toxicity were published recently. However, PAHs formation and transformation in the environment lead to the production of PAHs derivatives containing oxygen (O-PAHs), nitrogen (N-PAHs and azaarenes AZA) or sulfur (PASHs) in the aromatic ring. The development of new analytical methods enabled the determination of these novel contaminants. The presence of oxygen, nitrogen, or sulfur in PAHs aromatic rings increased their toxicity. The most common primary sources of PAHs derivatives are biological processes such as microbial activity (in soil, water, and wastewater treatment plants (O-PAHs)) and all processes involving combustion of fuel, coal, and biomass (O-PAHs, N-PAHs, AZA, PASHs). The secondary resources involved i) photochemical (UV light), ii) radical-mediated ( $\cdot\text{OH}$ ,  $\text{NO}_3^\bullet$ ), and iii) reactions with oxidants ( $\text{O}_3$ ,  $\text{NO}_x$ ) (O-PAHs, N-PAHs, AZA). Furthermore, N-PAHs were able to transform to their corresponding O-PAHs, while other derivatives were not. It indicated that N-PAHs are more vulnerable to photooxidation in the environment. 85% of O- and N-PAHs were detected with particle matter below 2.5  $\mu\text{m}$  suggesting their easier bioaccessibility. More than 90% of compounds with four and more aromatic cycles were present in the particle phase in the air. Although the concentrations of N-PAHs or O-PAHs may be similar to PAHs concentration or even 1000 times lower than parent PAHs, PAHs derivatives accounted for a significant portion of the total mutagenicity. The present review is describing the results of the studies on the determination of PAHs derivatives in different environmental matrices including airborne particles, sediments, soil, and organisms. The mechanisms of their formation and toxicity were assessed.

© 2021 The Author(s). Published by Elsevier B.V. This is an open access article under the CC BY license (<http://creativecommons.org/licenses/by/4.0/>).

\* Corresponding author.

E-mail address: [bczech@hektor.umcs.lublin.pl](mailto:bczech@hektor.umcs.lublin.pl) (B. Czech).

## Contents

1. Introduction . . . . .	2
1.1. PAHs derivatives in the air . . . . .	2
1.2. PAHs derivatives in soil and sediments . . . . .	4
1.3. PAHs derivatives in other matrices . . . . .	5
2. Toxicity of PAHs derivatives. . . . .	5
2.1. Toxicity of O-PAHs . . . . .	8
2.2. Toxicity of N-PAHs . . . . .	8
2.3. Toxicity of PASHs . . . . .	9
3. Conclusions and future perspectives . . . . .	9
Declaration of competing interest. . . . .	9
Acknowledgments . . . . .	9
Appendix A. Supplementary data. . . . .	9
References . . . . .	9

## 1. Introduction

In the last years, there is great attention paid to the determination of polycyclic aromatic hydrocarbons (PAHs) (Jazza et al., 2016; Khillare et al., 2020; Syed et al., 2017; Zheng et al., 2019). Due to the increased awareness about air quality (smog episodes and particulate matter's presence in the air) and its effect on human health (cancer potential), there is an increased number of studies on PAHs presence in airborne particles (Cachon et al., 2014; Dieme et al., 2012; Landkocz et al., 2017; Leclercq et al., 2016).

PAHs consist of two or more aromatic rings. They are persistent, semi-volatile compounds commonly found in the environment (Ren et al., 2017). However, both during PAHs creation and in the environment (in air, water, or soil) during various chemical, physical and photochemical reactions their derivatives containing oxygen, nitrogen, or sulfur can be observed (Table S1) (Zhang et al., 2011). Therefore various O-, OH-, N-PAHs, PASHs, or aazarenes (AZAs) can be created. N-PAHs, AZAs, O-PAHs, OH-PAHs, and PASHs belong to the group of thermally stable compounds. Generally, the more rings PAHs derivatives have, the smaller their solubility in water is (Hien et al., 2007).

Oxygenated-PAHs differ from their parent PAHs by the possessing of two or more carbonyl oxygens (ketones and quinones) attached to the aromatics rings. O-PAHs have also a higher molecular weight and lower vapor pressure than parent PAHs (Sienra, 2006). At ambient conditions, O-PAHs adsorb onto particulate matter (vapor pressure 10 Pa) (Ren et al., 2017).

O-PAHs can be formed as a result of photochemical oxidation of parent PAHs or reaction with  $\text{NO}_3^{\bullet}$ ,  $\bullet\text{OH}$ ,  $\text{NO}_x$ ,  $\text{O}_3$ , or UV-light (Sienra, 2006). 2-nitrofluoranthene (2-NF) is formed in ambient air by two different processes: concerning the daytime and nighttime, which indicates the effect of the photochemical reactions (Atkinson and Arey, 1994). 2-NF is derived from fluoranthene as a result of gas-phase reaction with  $\bullet\text{OH}$  and  $\text{NO}_3^{\bullet}$  radicals (Hien et al., 2007). The concentration of O-PAHs in ambient air was highly correlated to the airborne Reactive Oxygen Species (ROS) formation potential of PM, even more than the concentration, or particulate mass (Sklorz et al., 2007).

The physicochemical properties of N-PAHs are closely associated with the number of nitro-functional groups and molecular weight. Firstly, the presence of nitro functional group leads to an increase of the molecular weight, octanol-air partition, and particle-gas partition coefficients, and leads to a decrease of vapor pressure, water solubility, organic carbon-water partition, and octanol-water partition coefficients or Henry constants in comparison to the parent PAHs. With the increase of molecular weight of N-PAHs melting points, organic carbon-water partition coefficient, octanol-water partition coefficients, octanol-air partition coefficients, and particle-gas partition coefficients also increase. Whereas, vapor pressure, water solubility, and Henry constants decrease (Bandowe and Meusel, 2017). Some studies showed the

advantage of photochemical formation of N-PAHs which were  $\bullet\text{OH}$ -initiated reactions occurring in the atmosphere (Albinet et al., 2008).

Aazarenes are a group of heterocycles that contain a nitrogen atom in place of the carbon one in the aromatic ring. Like parent PAHs and their other derivatives, AZAs also exhibit toxic, mutagenic, carcinogenic, and teratogenic effects. They are increasingly available to organisms because of their higher solubility in water. Small amounts of AZAs occur in the environment, but they can originate from anthropogenic sources. They can be formed by incomplete combustion of fossil fuels, in industrial effluents, or during oil drilling (Bleeker et al., 1999).

There is little information on the PASHs formation mechanism. The studies of Liang et al. indicated that the majority of organosulfur in diesel fuel was PASHs (Liang et al., 2006). The only paper published recently was describing the concentration of PASHs determined in PM samples collected from two regions of China (Zhang et al., 2021). In  $\text{PM}_{2.5}$  samples, the concentration of PASHs was up to  $21.126 \text{ ng m}^{-3}$ , and the highest majority revealed dibenzothiophene and its derivatives: 4-methylbibenzothiophene, 1,4-dimethylbibenzothiophene, 4,6-dimethylbibenzothiophene (4,6-DMDBT), benzo[b]Naphtho[2,3-d]thiophene. Origin of PASHs included primary sources such as combustion of sulfur-containing fuels: coal in Taiyuan (industrial area) and gasoline and diesel oil in Guangzhou (big city with traffic) or secondary sources: photochemical reactions (in case of 2-nitrobibenzothiophene and 2,8-dinitrobibenzothiophene).

In summary, PAHs derivatives can be formed from primary and secondary sources. The most common primary sources of PAHs derivatives are biological processes such as microbial activity (in soil, water, and wastewater treatment plant (O-PAHs)) and all processes involving combustion of fuel, coal, and biomass (N-PAHs, AZAs, PASHs) (J. Wang et al., 2017). The secondary resources involved photochemical (UV light) reactions, radical-mediated reactions ( $\bullet\text{OH}$ ,  $\text{NO}_3^{\bullet}$ ), and reactions with oxidants ( $\text{O}_3$ ,  $\text{NO}_x$ ) (O-, N-PAHs, PASHs) (Barrado et al., 2012b; Walgraeve et al., 2010). Furthermore, N-PAHs were able to transform to their corresponding O-PAHs, while other derivatives were not. It indicated that N-PAHs are more vulnerable to photo-oxidation (Qiao et al., 2014).

### 1.1. PAHs derivatives in the air

Increased environmental awareness on airborne hazards has resulted in many studies on air quality and control. Researchers exhibit a growing interest in PAHs derivatives determination in the atmosphere and in the last years, a few extensive reviews on PAHs and their derivatives in the air were published (Cochran et al., 2012; Du et al., 2018).

The presence of particle matter (PM) in the air is connected both with environmental and health hazards. Detailed analysis of PM revealed that both PAHs and their derivatives can be adsorbed onto PM revealing, however, different affinity. For example, Wang et al.

(2011) demonstrated that the concentration of measured PAHs derivatives was 8% higher than their parent PAHs, but their direct-acting mutagenicity was 200% higher than indirect-acting mutagenicity of PAHs. This statement indicated that PAHs derivatives accounted for a significant portion of the total mutagenicity. Simultaneously, high bioaccessibility of PAHs derivatives was predicted since 85% of O- and N-PAHs were detected with particle matter  $<2.5\text{ }\mu\text{m}$  (Ringuet et al., 2012).

The presence of O-and N-PAHs was determined in several samples simultaneously (Fig. S1, Table S2). In almost every case the higher concentrations were obtained for O-PAHs than N-PAHs (Bandowe et al., 2014; J. Wang et al., 2017; Wei et al., 2012). The results presented in Fig. 1. show the O-PAHs and N-PAHs distribution in different sizes of particulate matter, e.g. in  $\text{PM}_{10}$  (Ringuet et al., 2012),  $\text{PM}_{2.5}$  (J. Wang et al., 2017; Wei et al., 2012) or in total suspended particles (TSP) (Souza et al., 2014). More than 50% of compounds with molecular weight less than  $202\text{ g mol}^{-1}$  can be found in the free gas phase. Whereas more than 90% of compounds with four and more aromatic cycles were present in the particle phase (Albinet et al., 2008). The majority of N-PAHs (Teixeira et al., 2011) and O-PAHs (Ren et al., 2017) were concentrated in fine ( $\text{PM}_{1.1}$ ) than coarse particles.

Generally, the lighter molecular weight N-PAHs were detected mostly in the gas phase (>50%), while higher molecular weight derivatives ( $\geq 4$  aromatics cycles) were detected in a particle phase (Albinet et al., 2007; Bamford and Baker, 2003). The concentrations of 26 measured N-PAHs were from 2 to 1000 times lower than parent PAHs (Bamford and Baker, 2003).

Generally, the percentage of PAHs derivatives in the air samples is broad and reaches 8.23% and 27.68%, when the sum of minimum values of determined N-PAHs and O-PAHs, respectively is considered. However, considering the maximum values the percentage of PAHs derivatives was lower (4.83% and 20.78%, respectively) (Fig. S2, Table S2).

The concentrations of N- and O-PAHs were strongly related with their alkyl and parent PAHs in  $\text{PM}_{2.5}$  indicating a primary combustion emission formation mechanism mass  $\text{PM}_{2.5}$  of varied depending on the time of the year. The higher concentration occurred in the cold season and this was caused by dwelling heating, beneficial meteorological factors, lower photochemical transformation, amenable gas, and particle portioning (Bandowe et al., 2014). A decrease of PAHs and O-PAHs concentrations (compared to winter in 2003 ( $\text{PM}_{2.5}$ ) and winter in 2013 ( $\text{PM}_{3.3}$ )) due to the changes in the manner in household heating (Ren et al., 2017).

The sampling place characteristic had a significant influence on O-PAHs and N-PAHs concentration (Tang et al., 2013). Different concentrations were noted in rural, suburban, or urban areas or near busy roads. Largely higher concentrations of O-PAHs and N-PAHs at the traffic sites than in suburban areas were noted (Ringuet et al., 2012). These observations were confirmed by Alves et al. (2017). The gas-phase reactions have a significant contribution to the content of 2-NF in the air. The concentration of 2-NF in PM from urban sites was higher than 1-nitropyrene (1-NP), in general. Moreover, reactions that are initiated by  $\text{NO}_3^{\bullet}$  radicals were the prevailing route for 2-NF formation in the environmental air. At the traffic site, 2-NF formation may be related to the  $\cdot\text{OH}$ -mediated reactions (Hien et al., 2007). In the studies of Albinet et al. (2008), the concentrations of parent PAHs and O-PAHs were of the same order of magnitude. However, the N-PAHs concentrations were about one or two orders of magnitude lower even in the localizations remote from pollution sources. PAHs derivatives showed significant seasonal variation and their concentrations were 2–3 orders of magnitude lower than parent PAHs. In most cases, the concentration was higher in winter than in warm months (Wei et al., 2012).

The concentration of single N- and O-PAHs derivatives in the gas and particle phase were differed significantly depending on the day or season (Albinet et al., 2007; Bamford and Baker, 2003; Hien et al., 2007). The results showed that the content of 19 N-PAHs (with the most abundant 9-nitroanthracene, 9-NA) in TSP in the samples collected in Chiang Mai (Thailand) was considerably higher in the dry season than in the wet season of 2010 (Chuesaard et al., 2014). In winter the concentration of O-PAHs was the highest, subsequently fall, spring and summer. This diversity may be caused by lower mixing height in cold months, higher emission of O-PAHs, or lower partitioning of O-PAHs into the gas phase, and higher in particle phase in winter. The concentration of perinaphthenone was the highest. O-PAHs and parent PAHs may origin from the same sources. A greater part in the formation of O-PAHs probably had primary emission than the atmospheric reactions. Higher radiative forcing has resulted in the increase in the photolysis and decrease of O-PAHs concentration in summer (Lee et al., 2018).

In the Chinese megacities air, all seven examined O-PAHs were detected in the winter months but only one of them, 9,10-anthraquinone (9,10-AQN), was detected in the summer. The most widespread O-PAHs were 6H-benzo[cd]pyrene-6-one, secondly 9,10-AQN, 9H-fluorene-9-one, and benzanthrone (BZA). But the trend was the same: in both cities, the total concentration of O-PAHs was higher in winter and smaller in summer ( $54 \pm 15$  and  $23 \pm 32\text{ ng m}^{-3}$  in winter and  $29 \pm$

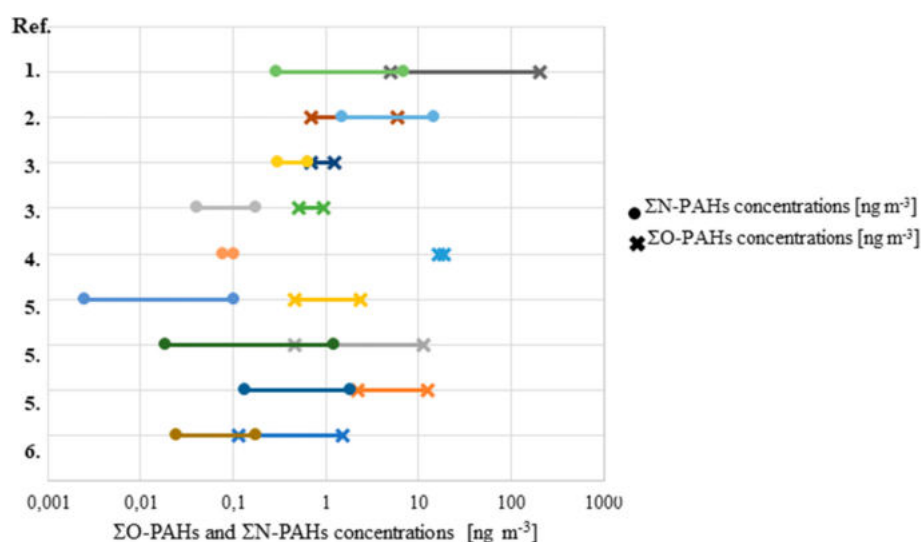


Fig. 1. The sum of O-PAHs and N-PAHs in the air samples determined simultaneously; 1-(Bandowe et al., 2014), 2-(Souza et al., 2014), 3-(Wei et al., 2012), 4-(J. Wang et al., 2017), 5-(Albinet et al., 2007), 6-(Ringuet et al., 2012).

30 and  $11 \pm 10 \text{ ng m}^{-3}$  in summer, respectively) (Ren et al., 2017). The same trend was observed for OH-PAHs (Barrado et al., 2012a, 2012b) and N-PAHs (Bandowe et al., 2014; Barrado et al., 2013; Tang et al., 2005; Valle-Hernández et al., 2010; Wada et al., 2001). These observations were further confirmed by Alves et al. (2017). But in some studies, the opposite conclusions were drawn (Reisen and Arey, 2005). The concentrations of O-PAHs and AZAs have not exhibited statistically significant differences between various seasons of the year (Alves et al., 2017).

The obtained results indicated that motor vehicles (notably diesel vehicles) were responsible for seasonal differences and concentrations of N-PAHs in the atmosphere (Marr et al., 1999; Scipioni et al., 2012). Mechanisms of the formation of N-PAHs differed considering nighttime and daytime (Fig. S3). The content of N-PAHs isomers was connected with NO<sub>x</sub> and diesel particles (Garcia et al., 2014; Ørevik et al., 2010) and 1-NP is one of the most prevalent N-PAH occurring in diesel exhaust particulate matter (Laumbach et al., 2008; Toriba et al., 2007). The occurrence of 3-nitrofluoranthene (3-NF) and 1-NP was closely associated with mobiles, diesel and gasoline exhausts (Teixeira et al., 2011; Wang et al., 2014). To assess the balance between primary emission and secondary formation of N-PAHs the concentration ratio of [(2 + 3)-NF]/[1-NP] was studied. The results indicated the predominance of gas-phase formation of N-PAHs. The highest ratio was observed during winter and early spring. Furthermore, the data from spring were significant associated with NO<sub>3</sub><sup>-</sup> concentration. These results demonstrated the correlation between nitrate chemistry, source of N-PAHs and photochemical conditions. The authors proposed some explanations. The high content of NO<sub>3</sub><sup>-</sup>, caused by oxidation of NO<sub>2</sub>, may be able to combine with PAHs and form N-PAHs simultaneously. This reaction should be initiated by •OH and/or NO<sub>3</sub>• radicals. Considering the ratio of O-PAHs or N-PAHs on parent PAHs it can be seen that the secondary origin of these compounds dominated (Tomaz et al., 2017). The increase in temperature, solar radiation and ozone levels reduced the OH-PAHs levels (Barrado et al., 2012a, 2012b).

At the rural site, Albinet et al. observed that the substantial variations of gas/particle portioning presented only one compound – 9-Phen. A higher concentration was observed in the night samples. It indicates that gaseous O-PAHs and N-PAHs were subjected to degradation by photolysis during the daytime. At night the efficiency of photolysis is much lower, therefore the content of O-PAHs and N-PAHs was higher (Albinet et al., 2007). Biomass burning may be the main source of N-PAHs at night hours. However, during the daytime, a greater part of analyzed pollutants was connected with vehicular emission (Souza et al., 2014). N-PAHs showed different diurnal and nocturnal characterization. During the night the concentration of N-PAHs was lower than in the daytime. This may be caused by the photolysis reaction. Souza proposed this mechanism as the main route of the removal N-PAHs from the environment. There was a strong correlation between the presence of parent PAHs and their nitro derivatives (Souza et al., 2014; Wang et al., 2011). This pointed to the same emission source. O-PAHs also presented distinct diurnal and nocturnal characterization (Reisen and Arey, 2005; Souza et al., 2014). These derivatives showed no association with their parent compounds, which suggested that their sources were different (Souza et al., 2014).

1-NP is an interesting compound, that is not formed as a result of photochemical oxidation in ambient conditions, but it is a constitute of diesel exhaust and is detected in the particulate phase (Toriba et al., 2007). Therefore, 1-NP is considered as a molecular marker of diesel particulate matter (Laumbach et al., 2008; Miller-Schulze et al., 2013). Several indicators for PAHs derivatives formation mechanism were described. One of them is [2-NF]/[1-NP] ratio. This value was used for indications of the gas-phase formation of N-PAHs in cold months. However, pollutants were formed by primary emission.

It was demonstrated that the part of the pollution made by coal combustion and diesel-engine vehicles to urban air particulates can be monitored by [1-NP]/[Pyrene] concentration ratio (Tang et al., 2005). Chuesaard et al. (2014) proposed the [9-NA]/[1-NP] ratio as a

new indicator for evaluating the contribution of biomass burning which was the main source of N-PAHs in the dry season. Sienna (2006) suggested that the content of O-PAHs in the atmosphere is an indicator of particulates from automobiles because methyl- and dimethylphenanthrenes presented in the PM<sub>10</sub> were emitted by vehicles. 1-Pyrenecarboxaldehyde was the most abundant O-PAHs and its concentration was not related to the season. Tomaz et al. (2017) suggested that 6H-dibenzo[b,d]pyran-6-one, diphenaldehyde and 3-nitrophenanthrene are relevant markers of PAHs oxidation processes in the surrounding air.

Considering the S-PAHs, there are very few studies about their concentration in airborne particles (Zhao et al., 2020). Liang et al. (2006) determined the organosulfur compounds in diesel particle matter. High-sulfur and low sulfur diesel fuels had 2284 and 433 ppm of sulfur, respectively. The majority of sulfur was present in the form of PASHs. The high-sulfur diesel fuel (HSDF) contained a higher concentration of individual PASHs and lighter PASHs than low-sulfur diesel fuel (LSDF). Higher concentrations of heavier PASHs (like 4,6-DMDBT) were measured in LSDF indicating that LSDF contained a larger fraction of heavier compounds than HSDF. Moreover, fuel sulfur and engine load affected total organic sulfur, PASHs concentration and distribution in diesel particulate matter. The more sulfur in fuel was, the higher total organosulfur in PM and the more PASHs with lower molecular weights in PM were. With the growing engine load, the prevailing PASHs species in diesel particle matter shifted to high molecular weight derivatives.

## 1.2. PAHs derivatives in soil and sediments

The other matrixes in which the contents of PAHs and their derivatives were also investigated, were soils. As it can be seen in Fig. 2, the contents of PAHs in studied soils were generally higher than the contents of their derivatives. Moreover, Bandowe et al. found that the concentrations of PAHs and their oxygenated derivatives were much higher in the 0–10 cm of soil than in the 10–20 cm layer (Bandowe et al., 2010). And after incubation of soil (under appropriate, strictly defined conditions) the concentration of individual compounds decreased up to 14% and 37% (for PAHs and O-PAHs, respectively) (Wilcke et al., 2014b).

The way of land using (urban, rural, forest, agriculture) had the greatest impact on the concentration of all studied PAHs and their derivatives (Table 1). The higher concentration occurred in urban soils than rural, and forest soils than agricultural. The latitudinal and longitudinal locations had also a pronounced influence. The lower concentration in plateau and tropical climates was caused by the dominance of low molecular weight compounds, the weaker industrial activity, prevalence of low-temperature combustion processes, biological sources and the scavenging effect of the tropical region (Bandowe et al., 2019). Wilcke et al. (2014b) studied changes in concentration of PAHs and O-PAHs and during the 19-week incubation of fertile soil. The initial concentration of 28 PAHs and 14 O-PAHs amounted to  $21.5 \pm 1.7$  and  $4.2 \pm 0.34 \mu\text{g g}^{-1}$ . The most abundant PAHs and O-PAHs were benzo [b + j + k]fluoranthenes, pyrene and benz[a]anthracene, and benzo [a]fluorenone, 9,10-AQN and BZA, respectively. The average concentrations of studied compounds decreased during incubations, but the differences were not statistically significant. The percentage of the initial amount of particular compounds ranged between 86% - 113% for the PAHs and was correlated significantly positively with their octanol-water partitioning coefficients. For the O-PAHs the range amounted to 63–117%, some of the compounds demonstrated the same trend as PAHs, but some of O-PAHs were net produced in the process of incubation. The authors suggested that O-PAHs were formed in soils during the microbial turnover of PAHs (Wilcke et al., 2014b).

The decreasing anthropogenic effect from North to South is associated with increasing content of low molecular weight PAHs. Low molecular weight O-PAHs were predominantly detected in the South (the influence of biological sources). The other O-PAHs detected in the North suggested association with parent compounds (Wilcke et al.,

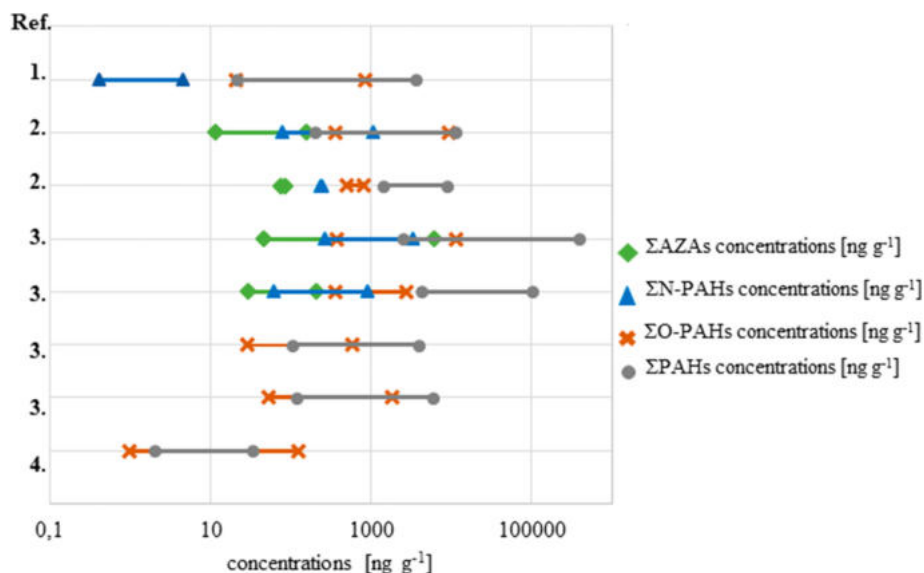


**Fig. 2.** The sum of O-PAHs, N-PAHs, AZAs and PAHs in the soil samples determined simultaneously; 1-(Wilcke et al., 2014a), 2-(Bandowe et al., 2010), 3-(Idowu et al., 2020), 4-(Cai et al., 2017).

2014a). Concentrations of PAHs and their derivatives varied for the different depths of sample collection: the content of studied pollutants was mostly higher in the 0–10 cm than in the 10–20 cm layer indicating the concentration of studied compounds in topsoil samples (Bandowe et al., 2010; Cai et al., 2017).

Lundstedt et al. (2014) conducted the first intercomparison study on the determination of PAHs, O-PAHs and nitrogen heterocyclic polycyclic aromatic compounds in soil samples to standardize the analytical methods used in the determination of these compounds in soil samples. For the O-PAHs, the results were satisfactory. The laboratories could have chosen method used in the analysis between their own and suggested reference method (pressurized liquid extraction, column fractionation with deactivated silica gel and anhydrous sodium sulfate packed in glass columns, chosen solutions: n-Hex, n-Hex/DCM and DCM, and GC-MS analysis with El-ionization and selected ion monitoring mode). The results were greatly affected by the selected internal standard. The laboratory which omitted the clean-up step obtained similar results as other laboratories, but they had a higher frequency of missing data points during analysis. It was associated with the higher complexity of the chromatograms. Another laboratory, which also resigned from the clean-up step, but applying GCxGC/TOF system had peak-integration problems.

The content of PAHs and their derivatives were also investigated in sediments (Table 1). 4-Rings PAHs were the most abundant compounds in the marine sediments from the North Sea, Chinese Bohai, European Baltic, and Yellow Seas (Wang et al., 2020). Researchers suggested that major sources of PAHs in marine sediments are coal combustion, coke plant, vehicular emission, and petroleum residues. Higher level in sediments from 44 sites in Osaka Bay, Japan, of PAHs (6.40–7800 ng g<sup>-1</sup> dw) and alkylated PAHs (13.7–1700 ng g<sup>-1</sup> dw) originating from pyrogenic or petrogenic sources occurred in the vicinities of ports, industrialized regions (Miki et al., 2014).

### 1.3. PAHs derivatives in other matrices

PAHs and their derivatives, due to their harmful effects on living organisms, should be determined in different types of matrices. Qiao et al. (2014) studied the content of 16 parent PAHs, O-PAHs, N-PAHs, and methyl-PAHs in river samples (Table 1). The concentration of O-PAHs was higher than parent PAHs, while the content of N-PAHs was below the limit of detection, most likely due to photochemical degradation in the water environment. Furthermore, N-PAHs are more vulnerable to

photo-oxidation and can transform to their corresponding O-PAHs, while the other derivatives not. The researchers suggested that O-PAHs originated from PAHs modifications. Moreover, the wastewater treatment plant has been identified as the primary source of methyl-PAHs, PAHs and O-PAHs in the rivers.

Considering the distribution of PAHs and their derivatives, the harmful effect of haze cannot be overlooked. The major role of adverse health effects of haze constitutes particle size. PAHs, O-PAHs and Cl-PAHs were concentrated in the 0.7–1.1 and 1.1–2.1 mm fractions of PM in all sampling sites. It was noted that 4–6 ring PAHs prevailed in all samples (Cao et al., 2020).

The content of PAHs and their oxygen, nitrogen, sulfur, hydroxyl, carboxyl, and methyl-derivatives was also tested in three edible marine fish (*Lutjanus argentimaculatus*, *Lethrinus microdon* and *Scomberomorus guttatus*). A higher amount of PAHs was located in fish liver than muscle with a predominance of low molecular weight compounds. Moreover, fish lipid content has an impact on PAHs level and distribution (Ranjabar Jafarabadi et al., 2019) confirming that the liver is the place of PAHs and their derivatives accumulation and detoxification. Additionally, the process of coal gasification and its products e.g. ash, tar, char, are enriched in PAHs and their derivatives: up to 56.2% of 3-ring PAHs in the char (Ütnü et al., 2020).

## 2. Toxicity of PAHs derivatives

Bioaccessibility is a significant parameter determining exposure to pollutants. In the studies on the apparent bioaccessibility (Bapp) of selected N-PAHs and O-PAHs in a composite fuel soot sample in in vitro human gastrointestinal model: third-phase absorptive sink with a silicone sheet it was observed that increase of Bapp occurred as the results of greater mass transfer of studied compounds from soot to fluid and from fluid to sheet. These processes can be affected by adding food lipids, changing bile acid concentration, or raising small intestinal pH. PAHs derivatives were characterized by the higher soot residue-fluid distribution ratio of the labile sorbed fraction after digestion and lower partition coefficients to various hydrophobic reference phases than parent compounds (Zhang et al., 2016). The aging of soot in a soil-water mixture caused a decrease in the apparent gastrointestinal bioaccessibility of PAHs and their derivatives. They also defined two reasons for reduction of Bapp by soil: aging time-independent effect corresponding to competitive sorption by the soil of labile desorbed form of soot pollutants (because digestion test), and increased soot nanoporosity and

**Table 1**  
PAHs derivatives in soil, sediments and other matrices.

Matrix	Country	(Σ) AZAs [ng g <sup>-1</sup> ]	No. of determined compounds	Σ O-PAHs [μg g <sup>-1</sup> ]	No. of determined compounds	Σ N-PAHs [ng g <sup>-1</sup> ]	No. of determined compounds	Σ16PAHs [μg g <sup>-1</sup> ]	Σ All PAHs [μg g <sup>-1</sup> ]	No. of all PAHs	Method	Extraction	Ref
Soil	Qinghai Lake Basin, Xi'an, Chao Lake Basin and Zhanjiang, China	5.7 ± 3.7	4	0.108 ± 0.0667	15	3.2 ± 3.4	11	0.206 ± 0.215	0.352 ± 0.283	29	GC-MS, SIM	Pressurized liquid extraction with organic solvent, purification and fractionation by column chromatography	(Bandow et al., 2019)
	Berne, Switzerland	LD	LD	4.2 ± 0.34	14	LD	LD	18.5 ± 1.5	22.0 ± 1.7	28	GC-MS, EI	Pressurized liquid extraction with DCM (first cycle) and CH <sub>3</sub> COCH <sub>3</sub> /DCM/CF <sub>3</sub> COOH (250:125:1 v/v/v) (second cycle), evaporation, purification and fractionation on a SG column	(Wilcke et al., 2014b)
	Umeå, Sweden	4988 ± 4282	4	164.45 ± 69.89	10	LD	LD	1767.54 ± 557.76	LD	LD	GC-MS, EI, SIM	Pressurized liquid extraction with n-Hex/Ace (1:1, v/v), fractionation using open SG column with ASS, elution with n-hex, n-Hex/DCM and DCM	(Lundstedt et al., 2014)
	Argentina	ND - 0.97, mean 0.24	4	0.001–0.124, mean 17	15	LD	LD	LD	0.0020–0.0326	27	GC-MS	Pressurized liquid extraction with DCM (first cycle) and CH <sub>3</sub> COCH <sub>3</sub> /DCM/CF <sub>3</sub> COOH (250:125:1 v/v/v) (second cycle), filtration through SS, evaporation, addition of Hex, fractionation onto a SG, addition of toluene, evaporation to 0.5 mL	(Wilcke et al., 2014a)
	Angren industrial region, Uzbekistan, topsoil	LD	LD	0.054–1.848	12	LD	LD	0.078–4.23	0.118–5.913	31	GC-MS	Pressurized liquid extraction with DCM (first cycle) and CH <sub>3</sub> COCH <sub>3</sub> /DCM/CF <sub>3</sub> COOH (250:125:1 v/v/v) (second cycle), filtration through SS, fractionation onto a SG, elution of PAHs/alkyl-PAHs with Hex/DCM (5:1 v/v), elution of O-PAHs with DCM and Ace	(Bandow et al., 2010)
	Angren industrial region, Uzbekistan, subsoil	LD	LD	0.029–0.595		LD	LD	0.07–3.18	0.104–3.852				
	Australia, recreational area	28.9–211.2	5	0.357–2.790	7	60.3–890.1	3	LD	4.314–100.931	13	GC-MS	Pressurized liquid extraction with Hex: Ace (3:1, v/v), filtration through SS, evaporation, fractionation onto a SG + alumina, elution of PAHs with Hex/DCM (5:1 v/v), elution of polar PAHs with DCM and Ace	(Idowu et al., 2020)
	Australia, industrial area	46.7–6190.9		0.377–11.536		269.9–3293.1			2.508–392.932				
	Australia, smoking area	74.1–83.1		0.503–0.804		230.46–245.55			1.395–8.741				
	Australia, residential area	11.6–153.2		0.354–9.185		79.4–1043.4			0.2013–11.176				
	Yangtze River Delta, eastern China	LD	LD	0.021–0.834, mean 0.0363	4	0.4–4.6, mean 0.6	4	0.010–3.059, mean 0.267	0.021–3.563, mean 0.310	27	GC-MS	Soxhlet extraction with Hex/Ace (1:1, v/v), evaporation, purification using SG/alumina columns,	(Cai et al., 2017)

		China	LD	LD	$0.009 \pm 0.008$	4	$0.000050 \pm 0.000045$	11	LD	LD	LD	GC-MS	elution with Hex/DCM mixture, evaporation to 1 mL MW extraction with Hex/Ace (1:1, v/v), concentration, purification by SG/alumina column, elution with Hex-DCM, evaporation to 1 mL	(Sun et al., 2017)
	Marine sediments	European Baltic North Seas Chinese Bohai Yellow Seas	LD	LD	LD	LD	LD	LD	LD	0.00091–5.361	18	GC-MS	UD extraction, purification through SG column, concentration	(Wang et al., 2020)
	Sediments	Jiuxiang River of Nanjing, China	LD	LD	$0.0718\text{--}0.259$	9	$2.53\text{--}45.4$	14	$0.162\text{--}0.309$	LD	LD	GC-EI-SIM for PAHs, GC-NICI-SRM for N-PAHs, GC-EI-SRM for the O-PAHs	Pressurized liquid extraction with Hex/Ace (1:1, v/v), concentration, SPE, elution by n-Hex; DCM (1:1, v/v), evaporation dissolution in n-Hex	(Han et al., 2019)
	Rivers	Wenyu River, North Canal, and Yongdingxin River	LD	LD	Dissolved phase: 0.06–0.19; particulate phase 0.41–17.98	4	Nd	LD	Dissolved phase: 0.16–1.20 µg/L; particulate phase: 1.56–79.38 µg g <sup>-1</sup>	LD	LD	GC-MS, EI, SIM	Dissolved phase: reversed SPE, elution in DCM and Hex. Particulate phase: pressurized liquid extraction with DCM/Ace (1:1, v/v). Both: purification with SG/alumina cartridges, concentration to 0.5 mL	(Qiao et al., 2014)
7	Haze	Beijing Zhengzhou Xinxiang	LD	LD	0.0272 0.0775 0.0307	4	LD LD	LD	LD LD	0.0981 0.0779 0.041	15	SI	UD extraction with DCM/Ace (1:1, v/v), evaporation to 2 mL, purification by SPE, elution of PAHs by n-Hex/DCM (4:1, v/v) and O-PAHs by DCM, evaporation, dissolution in n-Hex, filtration through 0.45 µm PTFE filters	(Cao et al., 2020)
	Fish <i>Lutjanus argentimaculatus</i> -muscle	Kharg Island, Iran	LD	LD	$0.0716 \pm 0.0167$	9	$51.48 \pm 14.36$	10	$0.398 \pm 0.0722$	$0.942\text{--}1.160$ , mean $1.004 \pm 0.126$	39	GC-MS	PAHs: saponification, the addition of n-Hex, rinsing with MeOH/water (4:1), concentration, purification with 5% H <sub>2</sub> O deactivated SG column, elution with DCM/n-Hex (1:3, v/v), concentration.	(Ranjbar Jafarabadi et al., 2019)
	Fish <i>Lutjanus argentimaculatus</i> -liver				$0.0965 \pm 0.0155$		$72.57 \pm 12.02$		$0.535 \pm 0.04792$	$1.204\text{--}1.511$ , mean $1.390 \pm 0.177$			Polar PAHs: SPE with DCM, concentration, purification with silica SPE cartridge, elution with DCM-Hex, concentration	
	Fish <i>Lethrinus microdon</i> -muscle				$0.0572 \pm 0.00797$		$38.76 \pm 6.93$		$0.371 \pm 0.0566$	$0.729\text{--}0.967$ , mean $0.891 \pm 0.137$				
	Fish <i>Lethrinus microdon</i> -liver				$0.0716 \pm 0.0066$		$53.75 \pm 10.73$		$0.471 \pm 0.06235$	$1.002\text{--}1.354$ , mean $1.121 \pm 0.203$				
	Fish <i>Scomberomorus guttatus</i> -muscle				$0.0487 \pm 0.0074$		$21.68 \pm 5.21$		$0.319 \pm 0.0543$	$0.634\text{--}0.859$ , mean $0.726 \pm 0.130$				
	Fish <i>Scomberomorus guttatus</i> -liver				$0.0503 \pm 0.0077$		$40.67 \pm 8.75$		$0.383 \pm 0.0722$	$0.796\text{--}1.135$ , mean $0.954 \pm 0.196$				

Ace-acetone; ACN – acetonitrile; (A)SG – (anhydrous) silica gel; (A)SS – (anhydrous) sodium sulfate; BSTFA – N, O-bis-(trimethylsilyl) trifluoroacetamide; CLD – chemiluminescence detector; DCM – dichloromethane; ECD – electron capture detector; ECNI – Electron capture negative ion; EI/SIM, electron ionization; FLD – fluorescence detector; Hex – hexane; HFBA – heptafluorobutyric anhydride; LD- Lack of data; MW- microwave; Nd- not detected; NICI – Negative ion chemical ionization; NS- nitrogen stream; Q-ToF-MS - mass quadrupole time-of-flight mass spectrometry; SIM – single ion monitoring; TSP – total suspended particles; UD- ultrasonic.

area, because of releasing soluble substances from the soot throughout the aging process (Zhang et al., 2018).

It is generally recognized that PAHs derivatives are regarded as more toxic than parent PAHs (Chatel et al., 2014). However, the toxicity of different PAHs derivatives depends on their chemical character and number and character of substituents. It is reported that about 75–90% of cancer cases of humans are predominantly caused by PAHs (Ütnü et al., 2020) but the other results do not confirm that statement. Considering the IARC grouping (Group 1: carcinogenic to humans (e.g. coal-tar, tobacco smoke); Group 2A: probably carcinogenic to humans (e.g. benzo[a]pyrene B[a]P, benzo[a]anthracene B[a]A); Group 2B: possibly carcinogenic to humans (e.g. benzo[b]fluoranthene B[b]F, B[f]F, B[k]F, dibenzo[a,h] anthracene DB[a,h]A, DB[a,j]A, dibenzo[a,e]pyrene DB[a,e]P, DB[a,h]P, DB[a,f]P, 1-NP, 4-NP, 1,6-dinitropyrene 1,6-DNP, 1,8-DNP, 6-nitrochrysene, 2-nitrofluorene). It can be seen that none of PAHs and their derivatives are classified as carcinogenic to humans. The excess lifetime cancer risk values for industrial soils and residential soils ( $8.2 \cdot 10^{-7}$  to  $2.3 \cdot 10^{-6}$ , respectively) indicate negligible cancer risks (Idowu et al., 2020).

## 2.1. Toxicity of O-PAHs

Determination of the physical-chemical properties of O-PAHs is important due to their influence on the environment and the human body. This topic has not been explored in detail yet. There are far fewer studies about O-PAHs toxicity compared to N-PAHs. It may be connected with the fact that the number of O-PAHs determined is usually lower than N-PAHs (Fig. S1). However, these derivatives must be taken into consideration during risk assessment because they represent an abundant group of pollutants (Walgraeve et al., 2010). It was confirmed that O-PAHs are toxic for living organisms, but the mechanism of mutagenicity and carcinogenicity are not yet well understood. Moreover, Lundstedt et al. demonstrated that O-PAHs have higher mobility than parent PAHs due to their polarity. These pollutants can be more easily conveyed to the groundwater or surface water (Lundstedt et al., 2007).

The most toxic to zebrafish embryos (*Danio rerio*) exposed on 38 O-PAHs were O-PAHs containing adjacent diones on 6-carbon moieties or terminal, para-diones on multi-ring structure, whereas 5-carbon moieties with adjacent diones were least toxic. The results showed that selected O-PAHs had different aryl hydrocarbon receptor (AHR) dependency stressing the role of oxidative stress in the toxicity mechanism (Knecht et al., 2013). B[a]A or benzantraquinone in zebrafish bodies caused damage to protein biosynthesis, mitochondrial and cardiac function, neural and vascular development (Elie et al., 2015).

The concentration of O-PAHs in ambient particulate matter is highly correlated to ROS formation (Sklorz et al., 2007) causing oxidative stress and triggering of anti-oxidative enzymes. A549 (Alveolar epithelial cells) test cells were subjected to PM<sub>2.5</sub> extracts collected in winter 2015 in four cities: Beijing, Tianjin, Shijiazhuang, and Hengshui, China. The results showed an increase in the content of two cytokines (tumor necrosis factor alpha (TNF- $\alpha$ ) and interleukin 6 (IL-6)), a decline in cell viability, and heightened production of nitric oxide (Niu et al., 2017). A549 exposed at the air-liquid interface to diesel exhaust containing N- and O-PAHs and their parent counterparts, CO, CO<sub>2</sub>, NO<sub>x</sub>, etc. for 24 h were revealing increased oxidative stress, the cell viability, and pro-inflammatory response – the content of IL-8 decreased (Kooter et al., 2013). The low molecular weight PAHs such as 9H-fluorene-9-one can inhibit the transcription of TNF- $\alpha$ , IL-1b, and IL-6 and caused an increase in ROS generation (C. Wang et al., 2017).

Inhalation or non-dietary ingestion of O-PAHs are the main routes for exposure for humans. This group of compounds has proved to be more soluble and more mobile in the environment compared to their parent counterparts. For this reason, toxicity studies of O-PAHs must be expanded, because now they are limited.

## 2.2. Toxicity of N-PAHs

N-PAHs are widespread in the environment toxic, carcinogenic, and mutagenic pollutants. The main route of exposure to N-PAHs to human beings is the respiratory tract (Vineis et al., 2004). Fine particle matter is characterized by considerably greater direct mutagenicity per unit mass than coarse particles. The *Salmonella* mutagenicity assay results revealed that the reduction of air pollution by nitro compounds is necessary to improve preventive measures (Traversi et al., 2011).

Several studies demonstrated that 1-NP possessed cytotoxic and genotoxic properties (Chatel et al., 2014) and mutagenic activity (Watt et al., 2007). The results on freshwater mussel *Dreissena polymorpha* exposed to the higher concentration of 1-NP affected AHR and HSP70 genes in digestive glands. Moreover, P-glycoprotein (Pgp) mRNA levels were increased in both tissues. What is most interesting, studied organisms were able to partially detoxify 1-NP, because of the low amount of DNA adducts that were recorded after 5 days of exposure to the high concentration of 1-NP (Chatel et al., 2014).

7 N-PAHs used for feeding marbled flounder *Pleuronectes yokohamae* for 7 days revealed the tendency to cumulate in the fish body after exposure but the level of N-PAHs was not as high as added to diet indicating for the possible transformation in the fish body (Bacolod et al., 2013).

Inhaled particles originated from vehicle exhaust can cause a systematic effect on oxidative stress, inflammation, and endothelial activation (Park and Park, 2009). 1-NP is a component of diesel exhaust particles and may lead to inflammatory diseases (Øvrevik et al., 2010; Oya et al., 2011). 1-NP induced the generation of ROS in a cultured human lung epithelial cell line (A549 cell) (Kim et al., 2005). 1-NP formed π-π and hydrogen bonds with AHR, simultaneously weakening the cytokine level and causing CYP1A1 transcription. The inflammatory state caused by PAHs and their derivatives turned out to be related to cytotoxic potency. When low molecular weight PAHs bonded without activating AHR, they caused mild inflammation (C. Wang et al., 2017).

1-NP is metabolized in the same manner both in humans and in animals: after nitroreduction and N-acetylation, the compounds were hydroxylated in the liver and hydroxylated metabolites were excreted with urine. Therefore the metabolites OHNAAPs (hydroxy-N-acetyl-1-aminopyrenes) and OHNPs (hydroxy-1-nitropyrenes) such as 8-hydroxy-2'-deoxyguanosine (8-OH-dG) may be used as biomarkers for evaluating the impact of exposure to automobile exhaust (Toriba et al., 2007). 1-NP triggered DNA damage and 8-OH-dG formation and inhibited the DNA repair capacity in rat lungs (Li et al., 2017). I was noticed that there was an association between PM<sub>2.5</sub> levels and the concentration of oxidative damage marker 8-OHdG in urine and organic carbon influenced inflammation marker - IL-6 levels (Neophytou et al., 2013). However, 3-nitrobenzanthrone (3-NBA) was more toxic than 1-NP or B[a]P. Moreover, this compound triggered the accumulation of cells in the S-phase and the typical apoptotic cell death. The presence of 3-NBA caused a DNA damage response as a result of phosphorylation of ataxia-telangiectasia mutated, checkpoint kinase (Chk) 2/Chk1, H2AX, and p53 (Oya et al., 2011). Cytokine/chemokine gene expression pattern differs between 1-NP, 3-NF, and their amino analogs. The response caused by 1-NP/3-NF was dominated by effects on IL-8 and TNF- $\alpha$  expression, while response induced by 1-AP/-3-AF was dominated by C-C motif chemokine ligand 5 (CCL5) and CXCL10 (IP-10) expression. 3-NBA triggered DNA damage because it accumulated in cells in S-phase. In conclusion, selected compounds induced different effects on cytokine/chemokine expression, cell cycle alterations, DNA damage, and cytotoxicity (Øvrevik et al., 2010). Genotoxicity was developed based on significantly higher frequencies of micronuclei and other nuclear abnormalities formed in erythrocytes (Bacolod et al., 2013).

In the *Drosophila melanogaster* somatic mutation and recombination test, 1-nitronaphthalene (1-Nnap), 1,5-dinitronaphthalene, 2-NF, and 9-NA caused an increase in the frequency of homologous

recombination (HR) in proliferative somatic cells that may lead to loss of heterozygosity (Dihl et al., 2008). PAHs and N-PAHs in tests on all-trans retinoic acid (ATRA)-mediated activity (*in vivo*) have hindered retinoid signaling indicating indirect teratogenicity (Beníšek et al., 2008). The results showed that some PAHs derivatives may affect the embryonic development and differentiation process by disrupting ATRA signaling and changing octamer-4 levels (Beníšek et al., 2011).

The carcinogenicity of 3-NBA and their metabolites: 3-aminobenzanthrone (3-ABA), 3-acetylaminobenzanthrone (3-Ac-ABA) and *N*-acetyl-*N*-hydroxy-3-aminobenzanthrone (*N*-Ac-*N*-OH-ABA) in the human B lymphoblastoid cell line MCL-5 was examined. The lower concentrations of 3-NBA and *N*-Ac-*N*-OH-ABA were, the more active these compounds were. *N*-Ac-*N*-OH-ABA caused the highest DNA binding, subsequently 3-NBA, 3-ABA, and 3-Ac-ABA. The obtained results showed that 3-NBA and its metabolites may cause DNA damage in human MCL-5 cells. These compounds may have genotoxic potential to humans and also caused the clastogenic effect, and triggered lung tumors in rats (Arlt et al., 2004a; Kawanishi et al., 2013; Lamy et al., 2004; Nagy et al., 2005a, 2005b; Phousongphouang et al., 2000). The results showed that 3-NBA is an extremely potent mutagen for the mouse because it caused chromosomal aberrations in blood reticulocytes, micronucleus formation, and DNA-binding mainly at guanine residues (Arlt et al., 2004b). Although, the effect of studied compounds (1-Nnap or 1-NP) on fish reproduction seems to be insignificant due to low environmental concentrations, exclusive of genomic effects on embryos (Onduka et al., 2015).

Miller-Schulze et al. (2016) proposed a novel indicator for the determination of exposure to diesel exhaust: the content of two metabolites of 1-NP in urine: 6-hydroxy-1-NP and 8-hydroxy-1-NP. They noticed that there was a positive association between 1-NP and 8-OHNP in urine. Besides, 1-NP can be metabolized to 1-NP eliminated with urine. The metabolites of N-PAHs: 1- and 2-aminonaphthalene and 1-aminopyrene can be used as biomarkers of exposure to automobile exhaust, too (Laumbach et al., 2008; Neophytou et al., 2014).

International Agency for Research on Cancer divided N-PAHs into several groups. Neither of the nitro derivatives was classified as carcinogenic or probably not carcinogenic to humans. 1-Nnap, 2-Nnap, 7-nitrobenz[a]anthracene, 2-NP, 3-nitroperylene, 6-nitrobenzo[a]pyrene were not classified as carcinogenic to humans. Different N-PAHs were probably or possibly carcinogenic (Bandowe and Meusel, 2017). 1-NP is classified as possibly carcinogenic to humans (Park and Park, 2009).

### 2.3. Toxicity of PASHs

There is a lack of information on PASHs toxicity. Some predictions include that due to the similarity of PASHs structures to parent PAHs, their cell toxicities should be comparable (Zhang et al., 2021). It has been proven recently that the main mechanism of PASHs toxicity includes PASH-induced reactive oxygen species (ROS) production (oxidative stress) and cell toxicity (*in human bronchial epithelial cells (BEAS2B cells)*). As in the case of other PAHs derivatives, PASHs may reveal similar or increased toxicity in comparison to pyrene and B[a]P.

## 3. Conclusions and future perspectives

The presence of PAHs and their possible transformations lead to the formation of PAHs derivatives. The present review is describing the results of the studies on the determination of PAHs derivatives in different environmental matrices including airborne particles, sediments, soil, and organisms. The greatest problem nowadays is the variety of the applied analytical techniques. The different sampling methodologies and data from various analytic techniques make the direct comparison difficult. It still does not exist any suitable legislation about the concentration of PAHs derivatives in airborne particles or soils. Although the concentrations of N-PAHs, O-PAHs, or PASHs may be similar to PAHs concentration or even 1000 times lower than parent PAHs, PAHs

derivatives accounted for a significant portion of the toxicity. ROS formation is the main mechanism of PAHs derivatives-induced toxicity, however, the other mechanisms include cell toxicity (O-PAHs, PASHs), inflammation (O-PAHs, N-PAHs), mutagenicity (N-PAHs), genotoxicity (N-PAHs), teratogenicity (N-PAHs), or carcinogenicity (N-PAHs). Most of the toxicity data include the effects of single compounds at non-environmentally relevant concentrations and the effect of real sample components is omitted. Due to the similar structure of PAHs derivatives to their parent PAHs, their interaction with the human body should be similar. The number of studies about the influence of PAHs derivatives on human life is still not enough. But due to its potential toxic and mutagenic character, the determination of the presence, bioavailability, and toxicity of PAHs derivatives in environmental matrices is of key importance.

### Declaration of competing interest

The authors declare that they have no known competing financial interests or personal relationships that could have appeared to influence the work reported in this paper.

### Acknowledgments

This work was supported by grant 2018/31/B/NZ9/00317 from the National Science Centre, Poland.

### Appendix A. Supplementary data.

Supplementary data to this article can be found online at <https://doi.org/10.1016/j.scitotenv.2021.147738>.

### References

- Albinet, A., Leoz-Garziandia, E., Budzinski, H., Villenave, E., 2007. Polycyclic aromatic hydrocarbons (PAHs), nitrated PAHs and oxygenated PAHs in ambient air of the Marcellus area (South of France): concentrations and sources. *Sci. Total Environ.* 384, 280–292. <https://doi.org/10.1016/j.scitotenv.2007.04.028>.
- Albinet, A., Leoz-Garziandia, E., Budzinski, H., Villenave, E., Jaffrezo, J.-L., 2008. Nitrated and oxygenated derivatives of polycyclic aromatic hydrocarbons in the ambient air of two French alpine valleysPart 1: concentrations, sources and gas/particle partitioning. *Atmos. Environ.* 42, 43–54. <https://doi.org/10.1016/j.atmosenv.2007.10.009>.
- Alves, C.A., Vicente, A.M., Custólio, D., Cerqueira, M., Nunes, T., Pio, C., Lucarelli, F., Calzolai, G., Nava, S., Diapouli, E., Eleftheriadis, K., Querol, X., Musa Bandowe, B.A., 2017. Polycyclic aromatic hydrocarbons and their derivatives (nitro-PAHs, oxygenated PAHs, and azaarenes) in PM 2.5 from Southern European cities. *Sci. Total Environ.* 595, 494–504. <https://doi.org/10.1016/j.scitotenv.2017.03.256>.
- Arlt, V.M., Cole, K.J., Phillips, D.H., 2004a. Activation of 3-nitrobenzanthrone and its metabolites to DNA-damaging species in human B lymphoblastoid MCL-5 cells. *Mutagenesis* 19, 149–156. <https://doi.org/10.1093/mutage/geh008>.
- Arlt, V.M., Zhan, L., Schmeiser, H.H., Honma, M., Hayashi, M., Phillips, D.H., Suzuki, T., 2004b. DNA adducts and mutagenic specificity of the ubiquitous environmental pollutant 3-nitrobenzanthrone in Muta Mouse. *Environ. Mol. Mutagen.* 43, 186–195. <https://doi.org/10.1002/em.20014>.
- Atkinson, R., Arey, J., 1994. Atmospheric chemistry of gas-phase polycyclic aromatic hydrocarbons: formation of atmospheric mutagens. *Environ. Health Perspect.* 102, 117–126.
- Bacolod, E.T., Uno, S., Tanaka, H., Koyama, J., 2013. Micronuclei and other nuclear abnormalities induction in erythrocytes of marbled flounder, *Pleuronectes yokohamae*, exposed to dietary nitrated polycyclic aromatic hydrocarbons. *Jpn. J. Environ. Toxicol.* 16, 79–89. <https://doi.org/10.11403/jset.16.79>.
- Bamford, H.A., Baker, J.E., 2003. Nitro-polycyclic aromatic hydrocarbon concentrations and sources in urban and suburban atmospheres of the Mid-Atlantic region. *Atmos. Environ.* 37, 2077–2091. [https://doi.org/10.1016/S1352-2310\(03\)00102-X](https://doi.org/10.1016/S1352-2310(03)00102-X).
- Bandowe, B.A.M., Meusel, H., 2017. Nitrated polycyclic aromatic hydrocarbons (nitro-PAHs) in the environment – a review. *Sci. Total Environ.* 581–582, 237–257. <https://doi.org/10.1016/j.scitotenv.2016.12.115>.
- Bandowe, B.A.M., Shukurov, N., Kersten, M., Wilcke, W., 2010. Polycyclic aromatic hydrocarbons (PAHs) and their oxygen-containing derivatives (OPAHs) in soils from the Angren industrial area, Uzbekistan. *Environ. Pollut.* 158, 2888–2899. <https://doi.org/10.1016/j.envpol.2010.06.012>.
- Bandowe, B.A.M., Meusel, H., Huang, R., Ho, K., Cao, J., Hoffmann, T., Wilcke, W., 2014. PM2.5-bound oxygenated PAHs, nitro-PAHs and parent-PAHs from the atmosphere of a Chinese megacity: seasonal variation, sources and cancer risk assessment. *Sci. Total Environ.* 473–474, 77–87. <https://doi.org/10.1016/j.scitotenv.2013.11.108>.
- Bandowe, B.A.M., Wei, C., Han, Y., Cao, J., Zhan, C., Wilcke, W., 2019. Polycyclic aromatic compounds (PAHs, oxygenated PAHs, nitrated PAHs and azaarenes) in soils from

- China and their relationship with geographic location, land use and soil carbon fractions. *Sci. Total Environ.* 690, 1268–1276. <https://doi.org/10.1016/j.scitotenv.2019.07.022>.
- Barrado, A.I., García, S., Barrado, E., Pérez, R.M., 2012a. PM2.5-bound PAHs and hydroxy-PAHs in atmospheric aerosol samples: correlations with season and with physical and chemical factors. *Atmos. Environ.* 49, 224–232. <https://doi.org/10.1016/j.atmosenv.2011.11.056>.
- Barrado, A.I., García, S., Castrillejo, Y., Perez, R.M., 2012b. Hydroxy-PAH levels in atmospheric PM10 aerosol samples correlated with season, physical factors and chemical indicators of pollution. *Atmos. Pollut. Res.* 3, 81–87. <https://doi.org/10.5094/APR.2012.007>.
- Barrado, A.I., García, S., Castrillejo, Y., Barrado, E., 2013. Exploratory data analysis of PAH, nitro-PAH and hydroxy-PAH concentrations in atmospheric PM10-bound aerosol particles. Correlations with physical and chemical factors. *Atmos. Environ.* 67, 385–393. <https://doi.org/10.1016/j.atmosenv.2012.10.030>.
- Beníšek, M., Bláha, L., Hilscherová, K., 2008. Interference of PAHs and their N-heterocyclic analogs with signaling of retinoids in vitro. *Toxicol. in Vitro* 22, 1909–1917. <https://doi.org/10.1016/j.tiv.2008.09.009>.
- Beníšek, M., Kubincová, P., Bláha, L., Hilscherová, K., 2011. The effects of PAHs and N-PAHs on retinoid signaling and Oct-4 expression in vitro. *Toxicol. Lett.* 200, 169–175. <https://doi.org/10.1016/j.toxlet.2010.11.011>.
- Bleeker, E.A.J., Van Der Geest, H.G., Klamer, H.J.C., De Voogt, P., Wind, E., Kraak, M.H.S., 1999. Toxic and genotoxic effects of azaarenes: isomers and metabolites. *Polycycl. Aromat. Compd.* 13, 191–203. <https://doi.org/10.1080/10406639908020563>.
- Cachon, B.F., Firmin, S., Verdin, A., Ayi-Fanou, L., Billet, S., Cazier, F., Martin, P.J., Aissi, F., Courcot, D., Sanni, A., Shirali, P., 2014. Proinflammatory effects and oxidative stress within human bronchial epithelial cells exposed to atmospheric particulate matter (PM2.5 and PM>2.5) collected from Cotonou, Benin. *Environ. Pollut.* 185, 340–351. <https://doi.org/10.1016/j.envpol.2013.10.026>.
- Cai, C., Li, J., Wu, D., Wang, X., Tsang, D.C.W., Li, X., Sun, J., Zhu, L., Shen, H., Tao, S., Liu, W., 2017. Spatial distribution, emission source and health risk of parent PAHs and derivatives in surface soils from the Yangtze River Delta, eastern China. *Chemosphere* 178, 301–308. <https://doi.org/10.1016/j.chemosphere.2017.03.057>.
- Cao, Z., Wang, M., Shi, S., Zhao, Y., Chen, X., Li, C., Li, Y., Wang, H., Bao, L., Cui, X., 2020. Size-distribution-based assessment of human inhalation and dermal exposure to airborne parent, oxygenated and chlorinated PAHs during a regional heavy haze episode. *Environ. Pollut.* 263, 114661. <https://doi.org/10.1016/j.envpol.2020.114661>.
- Chatel, A., Faucet-Marquis, V., Pfohl-Leszkowicz, A., Gourlay-France, C., Vincent-Hubert, F., 2014. DNA adduct formation and induction of detoxification mechanisms in Dreissena polymorpha exposed to nitro-PAHs. *Mutagenesis* 29, 457–465. <https://doi.org/10.1093/mutage/geu040>.
- Chuesaard, T., Chetiyankornkul, T., Kameda, T., Hayakawa, K., Toriba, A., 2014. Influence of biomass burning on the levels of atmospheric polycyclic aromatic hydrocarbons and their nitro derivatives in Chiang Mai, Thailand. *Aerosol Air Qual. Res.* 14, 1247–1257. <https://doi.org/10.4209/aaqr.2013.05.0161>.
- Cochrane, R.E., Dongari, N., Jeong, H., Beránek, J., Haddadi, S., Shipp, J., Kubátová, A., 2012. Determination of polycyclic aromatic hydrocarbons and their oxy-, nitro-, and hydroxy-oxidation products. *Anal. Chim. Acta* 740, 93–103. <https://doi.org/10.1016/j.aca.2012.05.050>.
- Dieme, D., Cabral-Ndior, M., Garçon, G., Verdin, A., Bille, S., Cazier, F., Courcot, D., Diouf, A., Shirali, P., 2012. Relationship between physicochemical characterization and toxicity of fine particulate matter (PM2.5) collected in Dakar city (Senegal). *Environ. Res.* 113, 1–13. <https://doi.org/10.1016/j.envres.2011.11.009>.
- Dihl, R.R., Bereta, M.S., do Amaral, V.S., Lehmann, M., Reguly, M.L., de Andrade, H.H.R., 2008. Nitropolycyclic aromatic hydrocarbons are inducers of mitotic homologous recombination in the wing-spot test of *Drosophila melanogaster*. *Food Chem. Toxicol.* 46, 2344–2348. <https://doi.org/10.1016/j.fct.2008.03.014>.
- Du, W., Chen, Y., Shen, G., Wang, W., Zhusuo, S., Huang, Y., Pan, X., Tao, S., 2018. Winter air pollution by and inhalation exposure to nitrated and oxygenated PAHs in rural Shanxi, north China. *Atmos. Environ.* 187, 210–217. <https://doi.org/10.1016/j.atmosenv.2018.06.004>.
- Elie, M.R., Choi, J., Nkrumah-Elie, Y.M., Gonnerman, G.D., Stevens, J.F., Tanguay, R.L., 2015. Metabolomic analysis to define and compare the effects of PAHs and oxygenated PAHs in developing zebrafish. *Environ. Res.* 140, 502–510. <https://doi.org/10.1016/j.envres.2015.05.009>.
- Garcia, K.O., Teixeira, E.C., Agudelo-Castañeda, D.M., Braga, M., Alabarse, P.G., Wiegand, F., Kautzmann, R.M., Silva, L.F.O., 2014. Assessment of nitro-polycyclic aromatic hydrocarbons in PM1 near an area of heavy-duty traffic. *Sci. Total Environ.* 479–480, 57–65. <https://doi.org/10.1016/j.scitotenv.2014.01.126>.
- Han, M., Kong, J., Yuan, J., He, H., Hu, J., Yang, S., Li, S., Zhang, L., Sun, C., 2019. Method development for simultaneous analyses of polycyclic aromatic hydrocarbons and their nitro-, oxy-, hydroxy- derivatives in sediments. *Talanta* 205, 120128. <https://doi.org/10.1016/j.talanta.2019.120128>.
- Hien, T.T., Thanh, L.T., Kameda, T., Takenaka, N., Bandow, H., 2007. Nitro-polycyclic aromatic hydrocarbons and polycyclic aromatic hydrocarbons in particulate matter in an urban area of a tropical region: Ho Chi Minh City, Vietnam. *Atmos. Environ.* 41, 7715–7725. <https://doi.org/10.1016/j.atmosenv.2007.06.020>.
- Idowu, O., Semple, K.T., Ramadass, K., O'Connor, W., Hansbro, P., Thavamani, P., 2020. Analysis of polycyclic aromatic hydrocarbons (PAHs) and their polar derivatives in soils of an industrial heritage city of Australia. *Sci. Total Environ.* 699, 134303. <https://doi.org/10.1016/j.scitotenv.2019.134303>.
- Jaza, S., Al-Adhub, A., Al-Saad, H., 2016. Polycyclic Aromatic Hydrocarbons (PAHs) in water of Al-Kahlaa River in Missan Province, Iraq. *ILMU KELAUTAN Indones. J. Mar. Sci.* 21, 1–8. <https://doi.org/10.14710/ikijms.21.1.1-8>.
- Kawanishi, M., Fujikawa, Y., Ishii, H., Nishida, H., Higashigaki, Y., Kanno, T., Matsuda, T., Takamura-Enya, T., Yagi, T., 2013. Adduct formation and repair, and translesion DNA synthesis across the adducts in human cells exposed to 3-nitrobenzanthrone. *Mutat. Res. Genet. Environ. Mutagen.* 753, 93–100. <https://doi.org/10.1016/j.mrgentox.2013.03.005>.
- Khililare, P.S., Sattawan, V.K., Jyethi, D.S., 2020. Profile of polycyclic aromatic hydrocarbons in digested sewage sludge. *Environ. Technol.* 41, 842–851. <https://doi.org/10.1080/09593330.2018.1512654>.
- Kim, Y., Ko, Y., Kawamoto, T., Kim, H., 2005. The effects of 1-nitropyrene on oxidative DNA damage and expression of DNA repair enzymes. *J. Occup. Health* 47, 261–266. <https://doi.org/10.1539/joh.47.261>.
- Knecht, A.L., Goodale, B.C., Truong, L., Simonich, M.T., Swanson, A.J., Matzke, M.M., Anderson, K.A., Waters, K.M., Tanguay, R.L., 2013. Comparative developmental toxicity of environmentally relevant oxygenated PAHs. *Toxicol. Appl. Pharmacol.* 271, 266–275. <https://doi.org/10.1016/j.taap.2013.05.006>.
- Kooter, I.M., Alblas, M.J., Jedynska, A.D., Steenhof, M., Houtzager, M.M.G., Ras, M. van, 2013. Alveolar epithelial cells (A549) exposed at the air–liquid interface to diesel exhaust: first study in TNO's powertrain test center. *Toxicol. in Vitro* 27, 2342–2349. <https://doi.org/10.1016/j.tiv.2013.10.007>.
- Lamy, E., Kassie, F., Gminski, R., Schmeiser, H.H., Mersch-Sundermann, V., 2004. 3-Nitrobenzanthrone (3-NBA) induced micronucleus formation and DNA damage in human hepatoma (HepG2) cells. *Toxicol. Lett.* 146, 103–109. <https://doi.org/10.1016/j.toxlet.2003.07.001>.
- Landkocz, Y., Ledoux, F., André, V., Cazier, F., Genevray, P., Dewaele, D., Martin, P.J., Lepers, C., Verdin, A., Courcot, L., Boushina, S., Sichel, F., Gualtieri, M., Shirali, P., Courcot, D., Bille, S., 2017. Fine and ultrafine atmospheric particulate matter at a multi-influenced urban site: physicochemical characterization, mutagenicity and cytotoxicity. *Environ. Pollut.* 221, 130–140. <https://doi.org/10.1016/j.envpol.2016.11.054>.
- Laumbach, R., Tong, J., Zhang, L., Ohman-Strickland, P., Stern, A., Fiedler, N., Kipen, H., Kelly-McNeil, K., Lioy, P., Zhang, J., 2008. Quantification of 1-nitropyrene in human urine after a controlled exposure to diesel exhaust. *J. Environ. Monit.* 11, 153–159. <https://doi.org/10.1039/B810039>.
- Leclercq, B., Happillon, M., Anthierieu, S., Hardy, E.M., Alleman, L.Y., Grova, N., Perdrix, E., Appenzeller, B.M., Lo Guidice, J.-M., Coddeville, P., Garçon, G., 2016. Differential responses of healthy and chronic obstructive pulmonary diseased human bronchial epithelial cells repeatedly exposed to air pollution-derived PM4. *Environ. Pollut.* 218, 1074–1088. <https://doi.org/10.1016/j.envpol.2016.08.059>.
- Lee, H.H., Choi, N.R., Lim, H.B., Yi, S.M., Kim, Y.P., Lee, J.Y., 2018. Characteristics of oxygenated PAHs in PM 10 at Seoul, Korea. *Atmos. Environ.* 9, 112–118. <https://doi.org/10.1016/j.apr.2017.07.007>.
- Li, R., Zhao, L., Zhang, L., Chen, M., Dong, C., Cai, Z., 2017. DNA damage and repair, oxidative stress and metabolism biomarker responses in lungs of rats exposed to ambient atmospheric 1-nitropyrene. *Environ. Toxicol. Pharmacol.* 54, 14–20. <https://doi.org/10.1016/j.etap.2017.06.009>.
- Liang, F., Lu, M., Birch, M.E., Keener, T.C., Liu, Z., 2006. Determination of polycyclic aromatic sulfur heterocycles in diesel particulate matter and diesel fuel by gas chromatography with atomic emission detection. *J. Chromatogr. A* 1114, 145–153. <https://doi.org/10.1016/j.chroma.2006.02.096>.
- Lundstedt, S., White, P.A., Lemieux, C.L., Lynes, K.D., Lambert, I.B., Öberg, L., Haglund, P., Tykkilä, M., 2007. Sources, fate, and toxic hazards of oxygenated polycyclic aromatic hydrocarbons (PAHs) at PAH-contaminated sites. *AMBIO* 36, 475–485. [https://doi.org/10.1579/0044-7447\(2007\)36\[475:SFATHO\]2.0.CO;2](https://doi.org/10.1579/0044-7447(2007)36[475:SFATHO]2.0.CO;2).
- Lundstedt, S., Bandowe, B.A.M., Wilcke, W., Boll, E., Christensen, J.H., Vila, J., Grifoll, M., Faure, P., Biache, C., Lorgeoux, C., Larsson, M., Frech Igurm, K., Ivarsson, P., Ricci, M., 2014. First intercomparison study on the analysis of oxygenated polycyclic aromatic hydrocarbons (oxy-PAHs) and nitrogen heterocyclic polycyclic aromatic compounds (N-PACs) in contaminated soil. *TrAC Trends Anal. Chem.* 57, 83–92. <https://doi.org/10.1016/j.trac.2014.01.007>.
- Marr, L.C., Kirchstetter, T.W., Harley, R.A., Miguel, A.H., Hering, S.V., Hammond, S.K., 1999. Characterization of polycyclic aromatic hydrocarbons in motor vehicle fuels and exhaust emissions. *Environ. Sci. Technol.* 33, 3091–3099. <https://doi.org/10.1021/es981227l>.
- Miki, S., Uno, S., Ito, K., Koyama, J., Tanaka, H., 2014. Distributions of polycyclic aromatic hydrocarbons and alkylated polycyclic aromatic hydrocarbons in Osaka Bay, Japan. *Mar. Pollut. Bull.* 85, 558–565. <https://doi.org/10.1016/j.marpolbul.2014.04.004>.
- Miller-Schulze, J.P., Paulsen, M., Kameda, T., Toriba, A., Tang, N., Tamura, K., Dong, L., Zhang, X., Hayakawa, K., Yost, M.G., Simpson, C.D., 2013. Evaluation of urinary metabolites of 1-nitropyrene as biomarkers for exposure to diesel exhaust in taxi drivers of Shenyang, China. *J. Expo. Sci. Environ. Epidemiol.* 23, 170–175. <https://doi.org/10.1038/jes.2012.40>.
- Miller-Schulze, J.P., Paulsen, M., Kameda, T., Toriba, A., Hayakawa, K., Cassidy, B., Naehler, L., Villalobos, M.A., Simpson, C.D., 2016. Nitro-PAH exposures of occupationally-exposed traffic workers and associated urinary 1-nitropyrene metabolite concentrations. *J. Environ. Sci.* 49, 213–221. <https://doi.org/10.1016/j.jes.2016.06.007>.
- Nagy, E., Johansson, C., Zeisig, M., Möller, L., 2005a. Oxidative stress and DNA damage caused by the urban air pollutant 3-NBA and its isomer 2-NBA in human lung cells analyzed with three independent methods. *J. Chromatogr. B Anal. Antioxid. Biomark. Oxidative Stress* 827, 94–103. <https://doi.org/10.1016/j.jchromb.2005.03.014>.
- Nagy, E., Zeisig, M., Kawamura, K., Hisamatsu, Y., Sugeta, A., Adachi, S., Möller, L., 2005b. DNA adduct and tumor formations in rats after intratracheal administration of the urban air pollutant 3-nitrobenzanthrone. *Carcinogenesis* 26, 1821–1828. <https://doi.org/10.1093/carcin/bgi141>.
- Neophytou, A.M., Hart, J.E., Cavallari, J.M., Smith, T.J., Dockery, D.W., Coull, B.A., Garshick, E., Laden, F., 2013. Traffic-related exposures and biomarkers of systemic inflammation, endothelial activation and oxidative stress: a panel study in the US trucking industry. *Environ. Health* 12, 105. <https://doi.org/10.1186/1476-069X-12-105>.

- Neophytou, A., Hart, J., Chang, Y., Zhang, J., Smith, T., Garshick, E., Laden, F., 2014. Short-term traffic-related exposures and biomarkers of nitro-PAH exposure and oxidative DNA damage. *Toxicics* 2, 377–390. <https://doi.org/10.3390/toxics2030377>.
- Niu, X., Ho, S.S.H., Ho, K.F., Huang, Y., Sun, J., Wang, Q., Zhou, Y., Zhao, Z., Cao, J., 2017. Atmospheric levels and cytotoxicity of polycyclic aromatic hydrocarbons and oxygenated-PAHs in PM2.5 in the Beijing-Tianjin-Hebei region. *Environ. Pollut.* 231, 1075–1084. <https://doi.org/10.1016/j.envpol.2017.08.099>.
- Onoduka, T., Ojima, D., Ito, K., Mochida, K., Koyama, J., Fujii, K., 2015. Reproductive toxicity of 1-nitronaphthalene and 1-nitropyrene exposure in the mummichog, Fundulus heteroclitus. *Ecotoxicology* 24, 648–656. <https://doi.org/10.1007/s10646-014-1412-6>.
- Øvrevik, J., Arlt, V.M., Øya, E., Nagy, E., Mollerup, S., Phillips, D.H., Låg, M., Holme, J.A., 2010. Differential effects of nitro-PAHs and amino-PAHs on cytokine and chemokine responses in human bronchial epithelial BEAS-2B cells. *Toxicol. Appl. Pharmacol.* 242, 270–280. <https://doi.org/10.1016/j.taap.2009.10.017>.
- Øya, E., Øvrevik, J., Arlt, V.M., Nagy, E., Phillips, D.H., Holme, J.A., 2011. DNA damage and DNA damage response in human bronchial epithelial BEAS-2B cells following exposure to 2-nitrobenzanthrone and 3-nitrobenzanthrone: role in apoptosis. *Mutagenesis* 26, 697–708. <https://doi.org/10.1093/mutage/ger035>.
- Park, E.-J., Park, K., 2009. Induction of pro-inflammatory signals by 1-nitropyrene in cultured BEAS-2B cells. *Toxicol. Lett.* 184, 126–133. <https://doi.org/10.1016/j.toxlet.2008.10.028>.
- Phousongphouang, P.T., Grosovsky, A.J., Eastmond, D.A., Covarrubias, M., Arey, J., 2000. The genotoxicity of 3-nitrobenzanthrone and the nitropyrene lactones in human lymphoblasts. *Mutat. Res. Genet. Toxicol. Environ. Mutagen.* 472, 93–103. [https://doi.org/10.1016/S1383-5718\(00\)00135-2](https://doi.org/10.1016/S1383-5718(00)00135-2).
- Qiao, M., Qi, W., Liu, H., Qu, J., 2014. Oxygenated, nitrated, methyl and parent polycyclic aromatic hydrocarbons in rivers of Haihe River System, China: occurrence, possible formation, and source and fate in a water-shortage area. *Sci. Total Environ.* 481, 178–185. <https://doi.org/10.1016/j.scitotenv.2014.02.050>.
- Ranjbar Jafarabadi, A., Riyahi Bakhtiari, A., Yaghoobi, Z., Kong Yap, C., Maisano, M., Cappello, T., 2019. Distributions and compositional patterns of polycyclic aromatic hydrocarbons (PAHs) and their derivatives in three edible fishes from Kharg coral Island, Persian Gulf, Iran. *Chemosphere* 215, 835–845. <https://doi.org/10.1016/j.chemosphere.2018.10.092>.
- Reisen, F., Arey, J., 2005. Atmospheric reactions influence seasonal PAH and nitro-PAH concentrations in the Los Angeles Basin. *Environ. Sci. Technol.* 39, 64–73. <https://doi.org/10.1021/es035454l>.
- Ren, Y., Zhou, B., Tao, J., Cao, J., Zhang, Z., Wu, C., Wang, J., Li, J., Zhang, L., Han, Y., Liu, L., Cao, C., Wang, G., 2017. Composition and size distribution of airborne particulate PAHs and oxygenated PAHs in two Chinese megacities. *Atmos. Res.* 183, 322–330. <https://doi.org/10.1016/j.atmosres.2016.09.015>.
- Ringuet, J., Leoz-Garziandie, E., Budzinski, H., Villenave, E., Albinet, A., 2012. Particle size distribution of nitrated and oxygenated polycyclic aromatic hydrocarbons (NPAHs and OPAHs) on traffic and suburban sites of a European megacity: Paris (France). *Atmos. Chem. Phys.* 12, 8877–8887.
- Scipioni, C., Villanueva, F., Pozo, K., Mabilia, R., 2012. Preliminary characterization of polycyclic aromatic hydrocarbons, nitrated polycyclic aromatic hydrocarbons and polychlorinated dibenzo-*p*-dioxins and furans in atmospheric PM10 of an urban and a remote area of Chile. *Environ. Technol.* 33, 809–820. <https://doi.org/10.1080/09593330.2011.597433>.
- Sienra, M.M. del R., 2006. Oxygenated polycyclic aromatic hydrocarbons in urban air particulate matter. *Atmos. Environ.* 40, 2374–2384. <https://doi.org/10.1016/j.atmosenv.2005.12.009>.
- Sklorz, M., Briedé, J.-J., Schnelle-Kreis, J., Liu, Y., Cyrys, J., de Kok, T.M., Zimmermann, R., 2007. Concentration of oxygenated polycyclic aromatic hydrocarbons and oxygen free radical formation from urban particulate matter. *J. Toxic. Environ. Health A* 70, 1866–1869. <https://doi.org/10.1080/15287390701457654>.
- Souza, K.F., Carvalho, L.R.F., Allen, A.G., Cardoso, A.A., 2014. Diurnal and nocturnal measurements of PAH, nitro-PAH, and oxy-PAH compounds in atmospheric particulate matter of a sugar cane burning region. *Atmos. Environ.* 83, 193–201. <https://doi.org/10.1016/j.atmosenv.2013.11.007>.
- Sun, Z., Zhu, Y., Zhuo, S., Liu, W., Zeng, E.Y., Wang, X., Xing, B., Tao, S., 2017. Occurrence of nitro- and oxy-PAHs in agricultural soils in eastern China and excess lifetime cancer risks from human exposure through soil ingestion. *Environ. Int.* 108, 261–270. <https://doi.org/10.1016/j.envint.2017.09.001>.
- Syed, J.H., Iqbal, M., Zhong, G., Katsoyiannis, A., Yadav, I.C., Li, J., Zhang, G., 2017. Polycyclic aromatic hydrocarbons (PAHs) in Chinese forest soils: profile composition, spatial variations and source apportionment. *Sci. Rep.* 7, 2692. <https://doi.org/10.1038/s41598-017-02999-0>.
- Tang, N., Hattori, T., Taga, R., Igarashi, K., Yang, X., Tamura, K., Kakimoto, H., Mishukov, V.F., Toriba, A., Kizu, R., Hayakawa, K., 2005. Polycyclic aromatic hydrocarbons and nitropolycyclic aromatic hydrocarbons in urban air particulates and their relationship to emission sources in the Pan-Japan Sea countries. *Atmos. Environ.* 39, 5817–5826. <https://doi.org/10.1016/j.atmosenv.2005.06.018>.
- Tang, J., Zhu, W., Kookana, R., Katayama, A., 2013. Characteristics of biochar and its application in remediation of contaminated soil. *J. Biosci. Bioeng.* 116, 653–659. <https://doi.org/10.1016/j.jbiobio.2013.05.035>.
- Teixeira, E.C., Garcia, K.O., Meimcke, L., Leal, K.A., 2011. Study of nitro-polycyclic aromatic hydrocarbons in fine and coarse atmospheric particles. *Atmos. Res.* 101, 631–639. <https://doi.org/10.1016/j.atmosres.2011.04.010>.
- Tomaz, S., Jaffrezou, J.-L., Favez, O., Perraudin, E., Villenave, E., Albinet, A., 2017. Sources and atmospheric chemistry of oxy- and nitro-PAHs in the ambient air of Grenoble (France). *Atmos. Environ.* 161, 144–154. <https://doi.org/10.1016/j.atmosenv.2017.04.042>.
- Toriba, A., Kitaoka, H., Dills, R.L., Mizukami, S., Tanabe, K., Takeuchi, N., Ueno, M., Kameda, T., Tang, N., Hayakawa, K., Simpson, C.D., 2007. Identification and quantification of 1-nitropyrene metabolites in human urine as a proposed biomarker for exposure to diesel exhaust. *Chem. Res. Toxicol.* 20, 999–1007. <https://doi.org/10.1021/tx700015q>.
- Traversi, D., Schilirò, T., Degan, R., Pignata, C., Alessandria, L., Gilli, G., 2011. Involvement of nitro-compounds in the mutagenicity of urban PM2.5 and PM10 in Turin. *Mutat. Res. Genet. Toxicol. Environ. Mutagen.* 726, 54–59. <https://doi.org/10.1016/j.mrgentox.2011.09.002>.
- Ütnü, Y.E., Okutan, H., Aydin, A.A., 2020. Polycyclic aromatic hydrocarbon (PAH) content of Malkara lignite and its ex-situ underground coal gasification (UCG) char residues. *Fuel* 275, 117949. <https://doi.org/10.1016/j.fuel.2020.117949>.
- Valle-Hernández, B.L., Mugica-Álvarez, V., Salinas-Talavera, E., Amador-Muñoz, O., Murillo-Tovar, M.A., Villalobos-Pietrini, R., De Vizcaya-Ruiz, A., 2010. Temporal variation of nitro-polycyclic aromatic hydrocarbons in PM10 and PM2.5 collected in Northern Mexico City. *Sci. Total Environ.* 408, 5429–5438. <https://doi.org/10.1016/j.scitotenv.2010.07.065>.
- Vineis, P., Forastiere, F., Hoek, G., Lipsett, M., 2004. Outdoor air pollution and lung cancer: recent epidemiologic evidence. *Int. J. Cancer* 111, 647–652. <https://doi.org/10.1002/ijc.20292>.
- Wada, M., Kido, H., Kishikawa, N., Tou, T., Tanaka, M., Tsubokura, J., Shironita, M., Matsui, M., Kuroda, N., Nakashima, K., 2001. Assessment of air pollution in Nagasaki city: determination of polycyclic aromatic hydrocarbons and their nitrated derivatives, and some metals. *Environ. Pollut.* 115, 139–147. [https://doi.org/10.1016/S0269-7491\(01\)00093-8](https://doi.org/10.1016/S0269-7491(01)00093-8).
- Walgraeve, C., Demeestere, K., Dewulf, J., Zimmermann, R., Van Langenhove, H., 2010. Oxygenated polycyclic aromatic hydrocarbons in atmospheric particulate matter: molecular characterization and occurrence. *Atmos. Environ.* 44, 1831–1846. <https://doi.org/10.1016/j.atmosenv.2009.12.004>.
- Wang, W., Jariyasopit, N., Schrlau, J., Jia, Y., Tao, S., Yu, T.-W., Dashwood, R.H., Zhang, W., Wang, X., Simonich, S.L.M., 2011. Concentration and photochemistry of PAHs, NPAHs, and OPAHs and toxicity of PM<sub>2.5</sub> during the Beijing Olympic Games. *Environ. Sci. Technol.* 45, 6887–6895. <https://doi.org/10.1021/es201443z>.
- Wang, W., Jing, L., Zhan, J., Wang, B., Zhang, D.P., Zhang, H.W., Wang, D.Q., Yang, Y., Zhao, J., Sun, Y.F., Bi, X.H., Wang, X.T., Feng, J.L., 2014. Nitrated polycyclic aromatic hydrocarbon pollution during the Shanghai World Expo 2010. *Atmos. Environ.* 89, 242–248. <https://doi.org/10.1016/j.atmosenv.2014.02.031>.
- Wang, C., Yang, J., Zhu, L., Yan, L., Lu, D., Zhang, Q., Zhao, M., Li, Z., 2017a. Never deem lightly the “less harmful” low-molecular-weight PAH, NPAH, and OPAH – disturbance of the immune response at real environmental levels. *Chemosphere* 168, 568–577. <https://doi.org/10.1016/j.chemosphere.2016.11.024>.
- Wang, J., Xu, H., Guinot, B., Li, L., Ho, S.S.H., Liu, S., Li, X., Cao, J., 2017b. Concentrations, sources and health effects of parent, oxygenated- and nitrated- polycyclic aromatic hydrocarbons (PAHs) in middle-school school air in Xi'an, China. *Atmos. Res.* 192, 1–10. <https://doi.org/10.1016/j.atmosres.2017.03.006>.
- Wang, P., Mi, W., Xie, Z., Tang, J., Apel, C., Joerss, H., Ebinghaus, R., Zhang, Q., 2020. Overall comparison and source identification of PAHs in the sediments of European Baltic and North Seas, Chinese Bohai and Yellow Seas. *Sci. Total Environ.* 737, 139535. <https://doi.org/10.1016/j.scitotenv.2020.139535>.
- Watt, D.L., Utzat, C.D., Hilario, P., Basu, A.K., 2007. Mutagenicity of the 1-Nitropyrene-DNA Adduct *N*-(Deoxyguanosin-8-yl)-1-aminopyrene in mammalian cells. *Chem. Res. Toxicol.* 20, 1658–1664. <https://doi.org/10.1021/tx700131e>.
- Wei, S., Huang, B., Liu, M., Bi, X., Ren, Z., Sheng, G., Fu, J., 2012. Characterization of PM2.5-bound nitrated and oxygenated PAHs in two industrial sites of South China. *Atmos. Res.* 109–110, 76–83. <https://doi.org/10.1016/j.atmosres.2012.01.009>.
- Wilcke, W., Bandowe, B.A.M., Lueso, M.G., Ruppenthal, M., del Valle, H., Oelmann, Y., 2014a. Polycyclic aromatic hydrocarbons (PAHs) and their polar derivatives (oxygenated PAHs, azaarenes) in soils along a climosequence in Argentina. *Sci. Total Environ.* 473–474, 317–325. <https://doi.org/10.1016/j.scitotenv.2013.12.037>.
- Wilcke, W., Kiesewetter, M., Musa Bandowe, B.A., 2014b. Microbial formation and degradation of oxygen-containing polycyclic aromatic hydrocarbons (OPAHs) in soil during short-term incubation. *Environ. Pollut.* 184, 385–390. <https://doi.org/10.1016/j.envpol.2013.09.020>.
- Zhang, Y., Yang, B., Gan, J., Liu, C., Shu, X., Shu, J., 2011. Nitration of particle-associated PAHs and their derivatives (nitro-, oxy-, and hydroxy-PAHs) with NO<sub>3</sub> radicals. *Atmos. Environ.* 45, 2515–2521. <https://doi.org/10.1016/j.atmosenv.2011.02.034>.
- Zhang, Y., Pignatello, J.J., Tao, S., 2016. Bioaccessibility of nitro- and oxy-PAHs in fuel soot assessed by an in vitro digestive model with absorptive sink. *Environ. Pollut.* 218, 901–908. <https://doi.org/10.1016/j.envpol.2016.08.021>.
- Zhang, Y., Pignatello, J.J., Tao, S., 2018. Bioaccessibility of PAHs and PAH derivatives in a fuel soot assessed by an in vitro digestive model with absorptive sink: effects of aging the soot in a soil-water mixture. *Sci. Total Environ.* 615, 169–176. <https://doi.org/10.1016/j.scitotenv.2017.09.227>.
- Zhang, Y., Song, Y., Chen, Y.-J., Chen, Y., Lu, Y., Li, R., Dong, C., Hu, D., Cai, Z., 2021. Discovery of emerging sulfur-containing PAHs in PM2.5: contamination profiles and potential health risks. *J. Hazard. Mater.* 416, 125795. <https://doi.org/10.1016/j.jhazmat.2021.125795>.
- Zhao, J., Zhang, Y., Chang, J., Peng, S., Hong, N., Hu, J., Lv, J., Wang, T., Mao, H., 2020. Emission characteristics and temporal variation of PAHs and their derivatives from an ocean-going cargo vessel. *Chemosphere* 249, 126194. <https://doi.org/10.1016/j.chemosphere.2020.126194>.
- Zheng, H., Qu, C., Zhang, J., Talpur, S.A., Ding, Y., Xing, X., Qi, S., 2019. Polycyclic aromatic hydrocarbons (PAHs) in agricultural soils from Ningde, China: levels, sources, and human health risk assessment. *Environ. Geochem. Health* 41, 907–919. <https://doi.org/10.1007/s10653-018-0188-7>.

**Occurrence and toxicity of polycyclic aromatic hydrocarbons derivatives in  
environmental matrices**

Agnieszka Krzyszczak<sup>1</sup>, Bożena Czech<sup>1\*</sup>

<sup>1</sup>Department of Radiochemistry and Environmental Chemistry, Institute of Chemical Sciences, Faculty of Chemistry, Pl. M. Curie-Sklodowskiej 3, 20-031 Lublin, Poland

\*corresponding author: bczech@hektor.umcs.lublin.pl (B. Czech)

Journal: Science of the Total Environment

Number of figures: 3

Number of tables: 2

Number of pages: 21

## 1. Introduction

Table S1. PAHs derivatives (Abbas et al., 2018; Bleeker et al., 1999; Liang et al., 2006).

N-PAHs				
Compounds name	Abbreviations	Molecular mass	Molecular formula	Number of rings
1-Nitronaphthalene	1-Nnap	173.171	C <sub>10</sub> H <sub>7</sub> NO <sub>2</sub>	2
2-Nitronaphthalene	2-Nnap	173.171	C <sub>10</sub> H <sub>7</sub> NO <sub>2</sub>	2
1-Methyl-4-nitronaphthalene	1M4Nnap	187.19	C <sub>11</sub> H <sub>9</sub> NO <sub>2</sub>	2
2-Methyl-4-nitronaphthalene	2M4Nnap	187.19	C <sub>11</sub> H <sub>9</sub> NO <sub>2</sub>	2
1-Methyl-6-nitronaphthalene	1M6Nnap	187.19	C <sub>11</sub> H <sub>9</sub> NO <sub>2</sub>	2
2-Nitrobiphenyl	2-NBP	199.2	C <sub>12</sub> H <sub>9</sub> NO <sub>2</sub>	2
3-Nitrobiphenyl	3-NBP	199.2	C <sub>12</sub> H <sub>9</sub> NO <sub>2</sub>	2
4-Nitrobiphenyl	4-NBP	199.2	C <sub>12</sub> H <sub>9</sub> NO <sub>2</sub>	2
5-Nitroacenaphthene	5-Nace	199.21	C <sub>12</sub> H <sub>9</sub> NO <sub>2</sub>	3
2-Nitrofluorene	2-Nfluo	211.22	C <sub>13</sub> H <sub>9</sub> NO <sub>2</sub>	3
3-Nitrodibenzofuran	3-NBF	213.19	C <sub>12</sub> H <sub>7</sub> NO <sub>3</sub>	3
1,5-Dinitronaphthalene	1,5-DNnap	218.17	C <sub>10</sub> H <sub>6</sub> N <sub>2</sub> O <sub>4</sub>	2
1-Nitrophenanthrene	1-Nphen	223.23	C <sub>14</sub> H <sub>9</sub> NO <sub>2</sub>	3
3-Nitrophenanthrene	3-Nphen	223.23	C <sub>14</sub> H <sub>9</sub> NO <sub>2</sub>	3
4-Nitrophenanthrene	4-Nphen	223.23	C <sub>14</sub> H <sub>9</sub> NO <sub>2</sub>	3
9-Nitrophenanthrene	9-Nphen	223.23	C <sub>14</sub> H <sub>9</sub> NO <sub>2</sub>	3
2-Nitroanthracene	2-NA	223.23	C <sub>14</sub> H <sub>9</sub> NO <sub>2</sub>	3
9-Nitroanthracene	9-NA	223.23	C <sub>14</sub> H <sub>9</sub> NO <sub>2</sub>	3
2-Nitrodibenzothiophene	2-NDB	229.26	C <sub>12</sub> H <sub>7</sub> NO <sub>2</sub> S	3
1-Nitrofluoranthene	1-NF	247.25	C <sub>16</sub> H <sub>9</sub> NO <sub>2</sub>	4
2-Nitrofluoranthene	2-NF	247.25	C <sub>16</sub> H <sub>9</sub> NO <sub>2</sub>	4
3-Nitrofluoranthene	3-NF	247.253	C <sub>16</sub> H <sub>9</sub> NO <sub>2</sub>	4
2+3-Nitrofluoranthene (2-nitrofluoranthene+3-nitrofluoranthene)	2+3NFL			
7-Nitrofluoranthene	7-NF	247.25	C <sub>16</sub> H <sub>9</sub> NO <sub>2</sub>	4
8-Nitrofluoranthene	8-NF	247.25	C <sub>16</sub> H <sub>9</sub> NO <sub>2</sub>	4
1-Nitropyrene	1-NP	247.253	C <sub>16</sub> H <sub>9</sub> NO <sub>2</sub>	4
2-Nitropyrene	2-NP	247.26	C <sub>16</sub> H <sub>9</sub> NO <sub>2</sub>	4
4-Nitropyrene	4-NP	247.26	C <sub>16</sub> H <sub>9</sub> NO <sub>2</sub>	4
2,7-Dinitrofluorene	2,7-DNfluo	256.21	C <sub>13</sub> H <sub>8</sub> N <sub>2</sub> O <sub>4</sub>	3
1,3,8-Trinitronaphthalene	1,3,8-TNap	263.17	C <sub>10</sub> H <sub>5</sub> N <sub>3</sub> O <sub>6</sub>	2
6-Nitrochrysene	6-Nchr	273.291	C <sub>18</sub> H <sub>11</sub> NO <sub>2</sub>	4
7-Nitrobenz[a]anthracene	7-NB[a]A	273.3	C <sub>18</sub> H <sub>11</sub> NO <sub>2</sub>	4
2,8-Dinitrodibenzothiophene	2,8-DNDB	274.25	C <sub>12</sub> H <sub>6</sub> N <sub>2</sub> O <sub>4</sub> S	3
2-Nitrobenzanthrone	2-NBA	275.26	C <sub>17</sub> H <sub>9</sub> NO <sub>3</sub>	4
3-Nitrobenzanthrone	3-NBA	275.26	C <sub>17</sub> H <sub>9</sub> NO <sub>3</sub>	4
3,9-Dinitrofluoranthene	3,9-DNflt	292.25	C <sub>16</sub> H <sub>8</sub> N <sub>2</sub> O <sub>4</sub>	4
1,3-Dinitropyrene	1,3-DNP	292.25	C <sub>16</sub> H <sub>8</sub> N <sub>2</sub> O <sub>4</sub>	4
1,6-Dinitropyrene	1,6-DNP	292.25	C <sub>16</sub> H <sub>8</sub> N <sub>2</sub> O <sub>4</sub>	4
1,8-Dinitropyrene	1,8-DNP	292.25	C <sub>16</sub> H <sub>8</sub> N <sub>2</sub> O <sub>4</sub>	4
3-Nitrobenzo[a]pyrene	3-NB[a]P	297.3	C <sub>20</sub> H <sub>11</sub> NO <sub>2</sub>	5
6-Nitrobenzo[a]pyrene	6-NB[a]P	297.3	C <sub>20</sub> H <sub>11</sub> NO <sub>2</sub>	5
1-Nitrobenzo[e]pyrene	1-NB[e]P	297.3	C <sub>20</sub> H <sub>11</sub> NO <sub>2</sub>	5
3-Nitrobenzo[e]pyrene	3-NB[e]P	297.3	C <sub>20</sub> H <sub>11</sub> NO <sub>2</sub>	5

3-Nitroperylene	3-NPE	297.3	C <sub>20</sub> H <sub>11</sub> NO <sub>2</sub>	5
7-Nitrobenz(a,h)anthracene	7-NDBA	323.3	C <sub>22</sub> H <sub>13</sub> NO <sub>2</sub>	5
1,3,6-Trinitropyrene	1,3,6-TNP	337.25	C <sub>16</sub> H <sub>7</sub> N <sub>3</sub> O <sub>6</sub>	4
3,6-Dinitrobenzo[ <i>a</i> ]pyrene	3,6-DNB[ <i>a</i> ]P	342.31	C <sub>20</sub> H <sub>10</sub> N <sub>2</sub> O <sub>4</sub>	5
<b>AZAs</b>				
Quinoline	Q	129.16	C <sub>9</sub> H <sub>7</sub> N	2
Phenanthridine	-	179.217	C <sub>13</sub> H <sub>9</sub> N	3
Benzo[f]quinoline	BfQ	179.22	C <sub>13</sub> H <sub>9</sub> N	3
Benzo[h]quinoline	BhQ	179.22	C <sub>13</sub> H <sub>9</sub> N	3
Acridine	-	179.13	C <sub>13</sub> H <sub>9</sub> N	3
1,7-Phenanthroline	1,7-Pthr	180.2	C <sub>12</sub> H <sub>8</sub> N <sub>2</sub>	3
9(1OH)-Acridone	-	195.22	C <sub>13</sub> H <sub>9</sub> NO	3
6(5H)-Phenanthridinon	-	195.22	C <sub>13</sub> H <sub>9</sub> NO	3
Benz[u]acridine	BuA	229.27	C <sub>17</sub> H <sub>11</sub> N	4
Benz[c]acridine	BcA	229.27	C <sub>17</sub> H <sub>11</sub> N	4
<b>O-PAHs and carbonyl OPAHs</b>				
Name				
Benzofuran	BF	118.13	CH <sub>6</sub> O	2
1-Indanone/2,3-Dihydroinden-1-one	1-IND	132.162	C <sub>9</sub> H <sub>8</sub> O	2
1-Naphthaldehyde/Naphthalene-1-carbaldehyde/1-Naphthalenecarboxaldehyde/1-Formylnaphthalene	1-Naph	156.18	C <sub>11</sub> H <sub>8</sub> O	2
1,4-Naphthoquinone/Naphthalene-1,4-dione	1,4-NQ	158.15	C <sub>10</sub> H <sub>6</sub> O <sub>2</sub>	2
1,2-Naphthoquinone/ o-Naphthoquinone	1,2-NQ	158.156	C <sub>10</sub> H <sub>6</sub> O <sub>2</sub>	2
9H-Fluorene-9-one/Fluoren-9-one/9-Fluorenone/9-Oxofluorene	9-FO	180.206	C <sub>13</sub> H <sub>8</sub> O	3
Perinaphthenone/ Phenalen-1-one	Pnaph	180.2	C <sub>13</sub> H <sub>8</sub> O	3
1,2-Acenaphthoquinone/Acenaphthylene-1,2-dione	1,2-ACNQ	182.178	C <sub>12</sub> H <sub>6</sub> O <sub>2</sub>	3
Benzophenone/ Diphenylmethanone	Bphe	182.222	C <sub>13</sub> H <sub>10</sub> O	2
2-Biphenylcarboxaldehyde/2-Phenylbenzaldehyde/Biphenyl-2-carbaldehyde	2-BPCA	182.22	C <sub>13</sub> H <sub>10</sub> O	2
2-Fluorenecarboxaldehyde/9H-Fluorene-2-carbaldehyde/Fluorene-2-carbaldehyde	2-FOCA	194.23	C <sub>14</sub> H <sub>10</sub> O	3
Anthrone/ 10H-Anthracen-9-one	Anth	194.233	C <sub>14</sub> H <sub>10</sub> O	3
6H-Dibenzo[b,d]pyran-6-one/ Benzo[c]chromen-6-one/ 3,4-Benzocoumarin	DB[bd]P	196.2	C <sub>13</sub> H <sub>8</sub> O <sub>2</sub>	3
Xanthone/ 9H-Xanthen-9-one	XN	196.205	C <sub>13</sub> H <sub>8</sub> O <sub>2</sub>	3
1,8-Naphthalic anhydride	1,8-NANY	198.177	C <sub>12</sub> H <sub>6</sub> O <sub>3</sub>	3
1,2-Naphthalic anhydride/Naphtho[1,2-c]furan-1,3-dione/Benzo[e][2]benzofuran-1,3-dione/1,2-Naphthalenedicarboxylic anhydride	1,2-NANY	198.17	C <sub>12</sub> H <sub>6</sub> O <sub>3</sub>	3
Cyclopenta[def]phenanthrene-4-one	CpPHEone	204.22	C <sub>15</sub> H <sub>8</sub> O	4
9-Phenanthrenecarboxaldehyde/Phenanthrene-9-carbaldehyde/9-Formylphenanthrene	9-Phen	206.24	C <sub>15</sub> H <sub>10</sub> O	3
Phenantherenequinone/ Phenanthrene-9,10-dione/ Phenanthraquinone	9,10-PQ	208.216	C <sub>14</sub> H <sub>8</sub> O <sub>2</sub>	3
9,10-Anthaquinone/Anthraquinone/9,10-Anthracenedione	9,10-AQN	208.216	C <sub>14</sub> H <sub>8</sub> O <sub>2</sub>	3
1,4-Anthaquinone/Anthracene-1,4-dione/	1,4-AQN	208.21	C <sub>14</sub> H <sub>8</sub> O <sub>2</sub>	3
Diphenaldehyde/ Biphenyl-2,2'-dicarboxaldehyde/ Diphenic dialdehyde	DPA	210.23	C <sub>14</sub> H <sub>10</sub> O <sub>2</sub>	2
2-Methyl-9,10-anthaquinone/2-	2-MAQN	222.24	C <sub>15</sub> H <sub>10</sub> O <sub>2</sub>	3

Methylantraquinone				
Benzanthrone/ 7H-Benz[de]anthracen-7-one/ 7H-Benzo[de]anthracen-7-one/ Benzanthrenone	BZA	230.266	C <sub>17</sub> H <sub>10</sub> O	4
7H-Benzo[c]fluoren-7-one/ Benzo[c]fluoren-7-one/ Allochrysoketone	7-B[c]FO	230.26	C <sub>17</sub> H <sub>10</sub> O	4
1-Pyrene carboxaldehyde/Pyrene-1-carbaldehyde/1-Formylpyrene	1-PYRCA	230.26	C <sub>17</sub> H <sub>10</sub> O	4
Benzo[a]fluorenone/ 11H-Benzo[a]fluoren-11-one/ 11H-Benzo[a]fluorene-11-one	B[a]Fone	230.26	C <sub>17</sub> H <sub>10</sub> O	4
Benzo[b]fluorenone/ Benzo[h]fluoren-1-one	B[b]Fone	230.26	C <sub>17</sub> H <sub>10</sub> O	4
2,3-Dimethylantraquinone/2,3-Dimethylanthracene-9,10-dione	2,3-DMAQN	236.26	C <sub>16</sub> H <sub>12</sub> O <sub>2</sub>	3
Cyclopenta(cd)pyren-3(4H)-one	CpPyr	242.3	C <sub>18</sub> H <sub>10</sub> O	5
6H-Benzo[cd]pyrene-6-one	BPYRone	254.3	C <sub>19</sub> H <sub>10</sub> O	5
Benz[a]anthracene-7,12-Dione/ 1,2-Benzantraquinone/ Tetraphene-7,12-dione/ Benzantraquinone	BaAQ	258.27	C <sub>18</sub> H <sub>10</sub> O <sub>2</sub>	4
1,4-Chrysenequione/Chrysene-1,4-dione/Chrysene-1,4-quinone	1,4-CQ	258.3	C <sub>18</sub> H <sub>10</sub> O <sub>2</sub>	4
5,12-Naphthacenequione/Tetracene-5,12-dione/5,12-Naphthacenedione/Naphthacenequinone	5,12-NAQ	258.3	C <sub>18</sub> H <sub>10</sub> O <sub>2</sub>	4
<b>OH-PAHs</b>				
1-Naphthol	1-N	144.173	C <sub>10</sub> H <sub>8</sub> O	2
2-Hydroxybiphenyl	2-HBF	170.211	C <sub>12</sub> H <sub>10</sub> O	2
2-Hydroxyphenanthrene	2-Hph	194.233	C <sub>14</sub> H <sub>10</sub> O	3
2-Hydroxy-9-fluorenone	2-H-9-F	196.205	C <sub>13</sub> H <sub>8</sub> O <sub>2</sub>	3
1-Hydroxypyrene	1-HP	218.255	C <sub>16</sub> H <sub>10</sub> O	4
1-Hydroxypyrene	1-HP	218.25	C <sub>16</sub> H <sub>10</sub> O	4
6-Hydroxychrysene	6-Hchr	244.294	C <sub>18</sub> H <sub>12</sub> O	4
3-Hydroxybenzo[a]pyrene	3-HB[α]P	268.315	C <sub>20</sub> H <sub>12</sub> O	5
<b>PASHs</b>				
Thiophene	T	84	C <sub>4</sub> H <sub>4</sub> S	1
2-Methylthiophene	2-MT	98	C <sub>5</sub> H <sub>6</sub> S	1
3-Methylthiophene	3-MT	98	C <sub>5</sub> H <sub>6</sub> S	1
2,3-Dimethylthiophene	2,3-DMT	112	C <sub>6</sub> H <sub>8</sub> S	1
2,5-Dimethylthiophene	2,5-DMT	112	C <sub>6</sub> H <sub>8</sub> S	1
2-Ethylthiophene	2-ET	112	C <sub>6</sub> H <sub>8</sub> S	1
2-Propylthiophene	2-PT	126	C <sub>7</sub> H <sub>10</sub> S	1
Benzothiophene	BT	134.196	C <sub>8</sub> H <sub>6</sub> S	2
2-Methylbenzothiophene	2-MBT	148	C <sub>9</sub> H <sub>8</sub> S	2
3-Methylbenzothiophene	3-MBT	148	C <sub>9</sub> H <sub>8</sub> S	2
5-Methylbenzothiophene	5-MBT	148	C <sub>9</sub> H <sub>8</sub> S	2
3,5-Dimethylbenzothiophene	3,5-DMBT	162	C <sub>10</sub> H <sub>10</sub> S	2
2,3,5-Trimethylbenzothiophene	2,3,5-TMBT	162	C <sub>11</sub> H <sub>12</sub> S	2
2,3,7-Trimethylbenzothiophene	2,3,7-TMBT	162	C <sub>11</sub> H <sub>12</sub> S	2
2,3,4,7-Tetramethylbenzothiophene	2,3,4,7-TTMBT	176	C <sub>12</sub> H <sub>14</sub> S	2
Dibenzothiophene	DBT	184.25	C <sub>12</sub> H <sub>8</sub> S	3
4-Methyl dibenzothiophene	4-MDBT	198	C <sub>13</sub> H <sub>10</sub> S	3
Phenanthro[4,5-bcd]thiophene	Ph45T	208	C <sub>14</sub> H <sub>8</sub> S	4
4,6-Dimethyl dibenzothiophene	4,6-DMDBT	212	C <sub>14</sub> H <sub>12</sub> S	3

2,4,6-Trimethyldibenzothiophene	2,4,6-TMDBT	226	C <sub>15</sub> H <sub>14</sub> S	3
2-nitrodibenzothiophene	2-NDBT	229.26	C <sub>12</sub> H <sub>7</sub> NO <sub>2</sub> S	3
2,8-dinitrodibenzothiophene	2,8-DNDBT	274.25	C <sub>12</sub> H <sub>6</sub> N <sub>2</sub> O <sub>4</sub> S	3
Benzo[ <i>b</i> ]Naphtho[1,2- <i>d</i> ]Thiophene	[1,2]BNT	234.32	C <sub>16</sub> H <sub>10</sub> S	4
Benzo[ <i>b</i> ]Naphtho[2,1-d]Thiophene	[2,1]BNT	234.32	C <sub>16</sub> H <sub>10</sub> S	4
Benzo[ <i>b</i> ]Naphtho[2,3- <i>d</i> ]Thiophene	[2,3]BNT	234.32	C <sub>16</sub> H <sub>10</sub> S	4
Phenanthro[3,4-b]thiophene	Ph34T	234	C <sub>16</sub> H <sub>10</sub> S	4
Benzo[ <i>b</i> ]phenanthro[9,10-d]thiophene	BPh9,10T	284	C <sub>20</sub> H <sub>12</sub> S	5
Diacenaphthothiophene	DiAT	332	C <sub>24</sub> H <sub>12</sub> S	7

## 1.2. PAHs derivatives in the air

Table S2. PAHs and their derivatives in the particulate matter in air samples.

O-PAHs	Location	Season, year	Phase	Sampling site [above ground level]	Mean total value with SD and range [ng m <sup>-3</sup> ]	Min-max of individual O-PAHs [ng m <sup>-3</sup> ]	Method, detection	Extraction	No. of determ ined compo unds	Ref.
9-FO, 9,10-AQN, BZA, BaAQ, 1,4-CQ, 5,12-NAQ, BPYRone	Xi'an, China	Winter, 2013	TSP	[10 m]	54 ± 15 (35-70)	0.8-21	GC-MS EI	extraction with DCM/MeOH, concentration to dryness and derivatization with BSTFA	7	(Ren et al., 2017)
		Summer, 2013	TSP		29 ± 30 (5.4-79)	Nd-29				
	Guangzhou, China	Winter, 2013	TSP	[50 m]	23 ± 32 (2.7-80)	0.5-10				
		Summer, 2013	TSP		11 ± 10 (2.8-29)	Nd-11				
1,4-NQ, 9-FO, Pnaph, 9,10-AQN, CpPHEone, B[a]Fone, B[b]Fone, BZA, BaAQ, CpPyr, BPYRone	Augsburg, Germany	Summer, 2005	PM <sub>2.5</sub>	LD	LD	0.01- 0.39	GC-MS	Extraction with DCM	11	(Sklorz et al., 2007)
9,10-AQN, Anth, 2-FOCA, 9-FO, 9-Phen, 1-PYRCA, BaAQ, Bphe, XN, 5,12-NAQ, 2-MAQN, 1,4-NQ	Providencia, Chile	Winter, 2000	PM <sub>10</sub>	LD	12.3±8.6	0.14-4.66	GC-MS SIM	Soxhlet extraction with DCM, evaporation, fractionation using glass column chromatography with ASG in Hex, elution with mixtures: n-Hex, n-Hex:DCM 6:4; DCM; Ace 30% / n-Hex (v/v), evaporation to 1 Ml	12	(Sienra, 2006)
	Providencia, Chile	Spring, 2000	PM <sub>10</sub>	LD	6.0±5.3	0-3.58				
	Las Condes, Chile	Winter, 2000	PM <sub>10</sub>	LD	6.1±3.2	0.03-2.66				
	Las Condes, Chile	Spring, 2000	PM <sub>10</sub>	LD	4.3±3.6	0.02-2.6				
1-Naph, 9-FO, 9-Phen, 9,10-AQN, 1,4-AQN, B[a]Fone, B[b]Fone, BZA, BaAQ	Palaiseau, France	Summer, 2009	PM <sub>10</sub>	Suburban site	0.113-1.5	Nd-0.0557	GC/NICI-MS	Pressurized solvent extraction using DCM, purification using alumina and silica SPE (solid-phase extraction), dissolved in isoctane	9	(Ringuet et al., 2012)
	Paris, France			Traffic site		0.0051- 0.6598				
1-Naph, 9-FO, 9-Phen, 9,10-AQN, B[a]Fone, B[b]Fone, BZA, BaAQ	Chamomix Valley, France	Winter, 2002-2003	PM <sub>10+</sub> gas phase	LD	1.14-679.76	0.01-11.23	GC-NICI-MS, SIM	pressurized liquid extraction with DCM, evaporation under NS, adjustment DCM	8	(Albinet et al., 2008)
		Summer, 2003			3.34-587.22	Nd-3.53				
	Maurienne Valley France	Winter 2002-2003			9.02-673	0.16-4.10				
		Summer 2003			0.58-547.04	0.00-0.96				
1-Naph, 9-FO, 9-Phen, 9,10-AQN, B[a]Fone, B[b]Fone, BZA, B[a]AQ	Marseille, France	July 2004	Gas+particel phases	Urban	2.225-12.607	0-6.908	GC-NICI-MS, SIM	pressurised liquid extraction with DCM, evaporation under NS, adjustment with DCM	8	(Albinet et al., 2007)
				Suburban	0.466-11.436	0.01-5.275				
				Rural	0.458-2.397	0-1.249				
9-FO, AQN, BaAQ	Xi'an, China	8-22.03. 2012	PM <sub>2.5</sub>	Indoor and outdoor	19.1-16.4	2.0-12.8	GC-MS	UD extraction with DCM and MeOH (3:1, v:v), SS addition, evaporation under NS	3	(Wang et al., 2017)
9-FO, 9,10-AQN, CpPHEone,	South China	5, 16.08.2009	PM <sub>2.5</sub>	Industrial [15]	0.519-0.930	0.0056-0.447	GC-MS	UD extraction with DCM, filtration,	6	(Wei et al.,

BZA BaAQ, BPYRone		24.01. and 4.02.2010		m]	0.695-1.246	0.0194-0.493	ECNI/SIM	concentration and separation by silica-alumina column, dry, dissolved with n-Hex		2012, p. 5)
1,4-NQ, 9-FO, XN Pnaph 9,10-AQN BaAQ, 5,12-NAQ	Seoul, South Korea	09.2006-08.2007	PM <sub>10</sub>	[17 m]	1.47 – 8.70	Nd-2.88	GC-MS	ultrasonic extraction with DCM and MeOH (3:1, v:v), evaporation under NS to the appropriate volume	7	(Lee et al., 2018)
9-FO, 9,10-AQN, 2-MAQN, BZA, BaAQ	Beijing, China	07-10.2008	PM <sub>2,5</sub>	[25 m]	Data in SI	Data in SI	GC-MS ECNI	pressurized liquid extraction with DCM, purified using silica columns, elution with DCM	5	(Wang et al., 2011)
9-FO, 9,10-AQN, BZA	Araraquara, Brazil	05- 06.2010	TSP	subtropical rural region [3 m]	0.69-6.0	Nd-4.1	GC-MS SIM	Soxhlet extraction with DCM, fractionation on a silica column with Hex and DCM	3	(Souza et al., 2014)
1,4-NQ, 1,2-NQ, 9,10-PQ, 1,4-CQ, 1,2-ACNQ, 2-MAQN, 2,3-DMAQN, BaAQ, 9,10-AQN, 5,12-NAQ	Fresno, USA	1 year,	TSP	residential area [20 m]	2.36-387	Nd-4.5	GC-MS SIM	UD extraction with DCM, heating (Zn, acetyl acetate), the addition of water and pentane, centrifugation, removing of organic fraction, evaporation to dryness, redissolving in DCM	11	(Chung et al., 2006)
9,10-AQN, BZA, BaAQ, 1,8-NANY, Pnaph	Gwangju, Korea	26.03-4.05.2001	PM <sub>2,5</sub>	[20 m]	5.4-4.3	0.2-27.2	GC-MS	UD extraction with DCM and MeOH, evaporation, derivatization, methylation	5	(Park et al., 2006)
1,4-NQ, 1-Naph, 9-FO, 9,10-AQN, 1,8-NANY, 9-Phen, B[a]Fone, BZA, 1-PYRCA, BaAQ	Beijing, China	winter	PM <sub>2,5</sub>	[8 m]	1.8-95.5	0.007-36.4	GC-Q-ToF-MS	pressurized liquid extraction with ACN, evaporation under NS to 6 mL, purification on SPE silica normal-phase cartridge, evaporation to 1 mL	10	(Elzein et al., 2019)
1-IND, 1,4-NQ, 1-Naph, 2-BPCA, 9-FO, 1,2-ACNQ, 9,10-AQN, CpPHEone, 1,8-NANY, 2-MAQN, B[a]Fone, BZA, BaAQ, 5,12-NAQ, BPYRone	Xi'an, China	05.07.2008 to 08.08.2009	PM <sub>2,5</sub>	[10 m]	5-208	LD	GC-MS	pressurized liquid extraction with DCM, drying on Na <sub>2</sub> SO <sub>4</sub> , evaporation to 0.5 mL	15	(Bandowe et al., 2014)
9,10-AQN, 1,2-ACNQ, 1,8-NANY, BZA	Tokyo, Japan	12, 16, 18.02.2009	PM <sub>10</sub>	LD	0.62-3.12	LD	GC-MS SIM	UD extraction with DCM, filtration, evaporation under NS, purification by SPE, evaporation under NS	4	(Kojima et al., 2010)
9,10-ACQ, 9-FO, BF, B[a]Fone, 7-B[c]FO, 1,2-NANY	Incheon, Korea	06.2009 – 05.2010	PM <sub>2,5</sub>	LD	0.15-2.36	Nd-1.32	GC-MS	UD extraction with DCM, UD extraction with hexane, mixing both extracts, evaporation under NS	6	(Choi et al., 2012)
9-FO, BaAQ, 9,10-ACQ, 2-MAQN	Queensway Road Tunnel, Birmingham, U.K	09.2012	PM <sub>10</sub>	LD	LD	0-7.1	GC-NICI-MS	1' UD extraction with DCM, evaporation under NS, purification (chromatography column filled with glass wool and ASS), evaporation, redissolution in Hex, SPE-elution with DCM/Hex mix	4	(Keyte et al., 2016)
	Parc des Princes	06.2013				0-0.2				

	Tunnel, Paris, France	LD				0.1-1.1		2' extraction with ACN (vortex), centrifugation, evaporation under NS, redissolution in DCM,		
	Birmingham, U.K									
1-1-Naph, 9-FO, 9,10-AQN, BA, BaAQ, 9-Phen, 1,4-AQN, B[a]Fone	Chamonix and Maurienne valleys, France	Winter 2002– 2003 and summer 2003	PM	rural	LD	Nd-9.93	GC-MS/NICI	pressurized liquid extraction with DCM	9	(Albinet et al., 2006)
OH-PAHs	Location	Season, year	Phase	Sampling site	Mean total value with SD and range [ng m <sup>-3</sup> ]	Min-max of individual OH-PAHs [ng/m <sup>-3</sup> ]	Method, detection	Extraction	Num ber of deter mine d com poun ds	Ref.
2-Hph, 1-HP	Madrid suburban, Spain	Summer 2008	PM <sub>2.5</sub>	suburban	LD	3.6-80.3	HPLC-FL	low-temperature UD extraction with MeOH, filtration, evaporation under NS, adjustment of MeOH	2	(Barrado et al., 2012a)
1-HP, 2-Hph	Madrid suburban, Spain	02.2008- 02.2009			LD	5.4-207.0				
N-PAHs	Location	Season, year	Phase	Sampling site	Mean total value with SD and range [ng m <sup>-3</sup> ]	Min-max of individual N- PAHs [ng m <sup>-3</sup> ]	Method, detection	Extraction	No. of deter mine d com poun ds	Ref.
1-Nnap, 2-Nnap, 2-Nfluo, 9-NA, 9- Nphen, 3-Nphen, 2+3NFL, 4-NP, 1- NP 2-NP, 7-NB[a]A, 6-Nchr, 1,3- DNP, 1,6-DNP, 1,8-DNP, 6- NB[a]P	Marseilles, France	Summer, 2004	PM <sub>10+gas</sub> phase	Urban area	0.135-1.86	Nd-493.6	GC-NICI-MS SIM	pressurized liquid extraction with DCM evaporation under NS, adjustment with DCM	17	(Albinet et al., 2007)
				Suburban	0.0186-1.233	Nd-600.5				
				Rural	0.0025-0.104	Nd-38.7				
1-Nnap, 2-Nnap, 2-NBP, 3-NBP, 5- Nace, 2-Nfluo, 9-NA, 3-Nphen, 4- Nphen, 9-Nphen, 1-NF, 2-NF 3-NF, 7-NF, 8-NF, 1-NP, 2-NP, 4-	Baltimore and Ford Meade, the USA	Summer, 2001	Gas and particle phase	Urban and suburban	0.077-0.414	<0.1-99 and <0.1-28	GC-MS	Soxhlet extraction with DCM and petroleum, evaporation, transfer to Hex, elution through an aminopropyl SPE cartridge using 20% DCM in Hex,	26	(Bamford and Baker, 2003)
		Winter, 2001			0.179-0.525	<0.1-64 and				

NP, 7-NB[a]A, 6-Nchr, 6-NB[a]P, 1-NB[e]P, 3-NB[e]P, 1,3-DNP, 1,6-DNP, 1,8-DNP					<0.1-49		reduction to 0.5 mL			
1-Nnap, 2-Nfluo, 3-NF, 1-NP, 6-Nchr	Rio Grande do Sul, Brazil	2006-2008	PM <sub>2.5</sub>	LD	2.81	420-770	GC-ECD	Soxhlet extraction with DCM, separation/preconcentration of the extract by a cleanup procedure using SG column (N-PAHs were eluted in the third fraction by DCM and N-PAHs were fluorinated through reactions with HFBA	5	(Teixeira et al., 2011)
			PM <sub>2.5-10</sub>	LD	2.34	220-980				
1-Nnaph, 2-Nnaph, 2-Nfluo, 9-NA, 9-Nphen, 3-Nphen, 2+3-NFL, 1- NP, 2-NP, 4-NP, 7-NB[a]A, 6-NChr, 1,3-DNP, 1,6-DNP, 1,8-DNP, 1-NB[a]P, 3-NB[a]P, 6-NB[a]P	Palaiseau, France	Summer 2009	PM <sub>10</sub>	Suburban site	0.025-0.175	Nd-11.7	GC-NICI-MS	Pressurized solvent extraction using DCM, purification using alumina and silica SPE, dissolved in isoctane	18	(Ringuet et al., 2012)
	Paris, France			Traffic site		Nd-72.6				
1-Nnap, 2-Nfluo, 9-Nphen, 3-NF, 1-NP, 2,7-DNfluo, 6-Nchr, 1,8-DNP	Xi'an, China	8-22.03. 2012	PM <sub>2.5</sub>	Outdoor/ indoor [8 m]	0.1039 and 0.0785	2.4 – 57.7	GC-MS	UD extraction with DCM and MeOH (3:1, v:v), SS addition, evaporation under NS to the appropriate volume	8	(Wang et al., 2017)
1-Nnap, 2-Nfluo, 9-NA, 9-Nphen, 3-Nphen, 2+3NFL, 4-NP, 1-NP, 2-NP, 7-NB[a]A, 6-Nchr, 6-NB[a]P	South China	5, 16. 08. 2009	PM <sub>2.5</sub>	Industrial [15 m]	0.0409-0.175	0.07-73.2	GC-MS EI/SIM, ECNI/SIM	UD extraction with DCM, filtration, concentration and separation by silica-alumina column, dry, dissolved with n-Hex	12	(Wei et al., 2012, p. 5)
		24.01. and 4.02. 2010			0.302-0.645	0.15-278				
1-Nnap, 2-Nnap, 2-Nfluo, 9-NA, 9-Nphen, 3-Nphen, 2+3NFL, 4-NP, 1-NP, 2-NP, 7-NB[a]A, 6-Nchr, 1,6-DNP, 1,8DNP, 1,3-DNP, 6-NB[a]P	Chamonix valley, France	Winter, 2002	PM <sub>10+gas phase</sub>	LD	LD	Nd-659.5	GC-NICI-MS SIM	pressurized liquid extraction with DCM, evaporation under NS, adjustment with DCM	16	(Albinet et al., 2008)
		Summer, 2003			LD	Nd-55.5				
	Maurienne valley, France	Winter, 2002			LD	0.1-327.6				
		Summer, 2003			LD	Nd-63.1				
2-Nnap,2-Nnap, 2-Nfluo, 9-NA, 9-Nphen, 2-NF, 3-NF, 2-NP, 1-NP, 7-NB[a]A, 6-Nchr	São Paulo State, Brazil	05- 06.2010	TSP	subtropical rural region [3 m]	1.5-15	Nd-6000	GC-MS SIM	Soxhlet extraction with DCM, fractionation on a silica column (Hex and DCM as a mobile phase)	11	(Souza et al., 2014)
1-NP, 2-NF	Ho Chi Minh City, Vietnam	01.2005 and 03.2006	PM	Urban area (tropical region) [10 and 1.2 m]	LD	8.1-191	HPLC -CLD	UD extraction with benzene/ethanol (3/1, v/v), filtration, purification with NaOH, H <sub>2</sub> SO <sub>4</sub> , distilled water. evaporation under NS, dissolved in MeOH	2	(Hien et al., 2007)
2-NF, 2-NP, 1-NP	Athens, Greece	1996	TSP	residential areas, not exposed directly to traffic	0.05-0.47	10-210	GC-MS SIM	Soxhlet extraction with DCM-ACN 5:1, evaporation under NS, redissolution in toluene, separation by column chromatography, elution with n-Hex and DCM	3	(Marino et al., 2000)
1,6-DNP, 1,8-DNP, 1,3-DNP, 1-NP	Nagasaki, Japan	07.1997-06.1998	PM0.3	LD	910 (230-4100)	0.00404-2.87	HPLC –CLD	Extraction with Hex, filtration, washing with NaOH, H <sub>2</sub> SO <sub>4</sub> and water	4	(Wada et al., 2001)

1-Nnap, 2-Nnap, 2M4Nnap, 1M4Nnap, 1M6Nnap, 3-NBP, 9- NA, Nphen, 2NF, 1-NP, 2-NP	Los Angeles, Riverside, USA	01.2003 08.2002	TSP+gas phase	LD	LD	3-214 0.2-354	GC-MS NICI and SIM	Soxhlet extraction with DCM, evaporation, fractionation by normal- phase HPLC	11	(Reisen and Arey, 2005)
1,3-DNP, 1,6-DNP, 1,8-DNP, 1-NP	Shenyang, China	2001	TSP	Winter	738±80 <sup>a</sup>	3.2-723 <sup>a</sup>	HPLC-CLD	UD extraction with benzene/ethanol (3:1, v/v), filtration, wash with NaOH, $H_2SO_4$ and water, evaporation to dryness, dissolution in ethanol and reflux in the presence of sodium hydrosulphide. Extraction with benzene, evaporation of the benzene phase, redissolution in ACN containing ascorbic acid.	4	(Tang et al., 2005)
	Vladivostok, Russia	1999			394±317 <sup>a</sup>	1.8-385 <sup>a</sup>				
	Seoul, South Korea	2002			716±158 <sup>a</sup>	3.6-703 <sup>a</sup>				
	Kitakyushu, Japan,	1997			58±38 <sup>a</sup>	0.3-55 <sup>a</sup>				
	Kanazawa, Japan	1999			234±231 <sup>a</sup>	1.3-228 <sup>a</sup>				
	Tokyo, Japan	1997			690±253 <sup>a</sup>	2.3-680 <sup>a</sup>				
	Sapporo, Japan	1997			1114±45 <sup>a</sup>	3.9-1100 <sup>a</sup>				
	Shenyang, China	2001		Summer	122±101 <sup>a</sup>	0.9-117 <sup>a</sup>				
	Vladivostok, Russia	1999			70±79 <sup>a</sup>	0.8-67 <sup>a</sup>				
	Seoul, South Korea	2002			LD	LD				
	Kitakyushu, Japan	1997			25±9.7 <sup>a</sup>	0.5-23 <sup>a</sup>				
	Kanazawa, Japan	1999			105±116 <sup>a</sup>	0.7-102 <sup>a</sup>				
	Tokyo, Japan	1997			183±50 <sup>a</sup>	0.8-180 <sup>a</sup>				
	Sapporo, Japan	1997			515±147 <sup>a</sup>	1.2-510 <sup>a</sup>				
2-Nfluo, 9-NA, 9-Nphen, 1-Nphen, 3-Nphen, 2-NA, 2-NF, 4-NP, 1-NP, 2-NP, 7-NB[a]A, 6-Nchr, 3-NBA, 6-NB[a]P, 3-NPE, 7-NDGA	São Paulo, Brazil	08.2002 07.2003	PM <sub>10</sub>	[20 m]	0.090 (0.191- 0.458)	Nd-158	HRGC-MS (EI/SIM)	Soxhlet extraction with DCM, fractionation by HPLC, elution with isooctane (wasted) and DCM (collected)	16	(de Castro Vasconcellos et al., 2008)
	Araraquara, Brasil	08.2002 07.2003			0.479 (0.146- 1.229)	Nd-246				
	Piracicaba, Brasil	07.2003		[4 m]	0.112 (0.220- 0.362)	Nd-127				
	Paulínia, Brasil	07.2003			0.364 (0.604- 1.239)	Nd-407				
		08.2002		LD	0.175 (0.530- 1.274)	Nd-773				
				[0]	0.080 (0.241- 0.337)	Nd-123				

1-Nnap, 2-Nnap, 2-Nfluo, 9-NA, 1-NP, 2-NF, 3-NF	Oued Smar, Algeria	08.2002 to 02.2003	PM <sub>10</sub>	LD	0.093-0.264	Nd-141	GC-MS, SIM	Soxhlet extraction with DCM-Ace (4:1), evaporation, fractionation through column chromatography, elution with DCM	7	(Ladji et al., 2007)
2-Nnap, 2-Nfluo, 2-NF, 3-NF, 1-NP, 2-NP	Athens, Greece	11.2003, 01-02.2004	coarse (2.4 µm 10 µm) and fine particles (< 2.4µm)	LD	LD	0.338-2.103	GC-ECD	Soxhlet extraction with DCM, evaporation, redissolution in min volume of DCM, silica solid-phase extraction, elution with n-Hex, evaporation, redissolution in MeOH, the addition of CuCl <sub>2</sub> , NaBH <sub>4</sub> and water, extraction with benzene, evaporation. Addition of HFBA, heating, the addition of aqueous ammonia solution.	6	(Tsakas et al., 2010)
9-NA, 9-Nphen, 3-Nphen, 2-NF, 3-NF, 1-NP, 7-NB[a]A, 6-Nchr	Northern Mexico City	04.2006-02.2007	PM <sub>10</sub>	LD	0.111-0.819	LD	GC-MS, NICI	UD extraction with methylene chloride, evaporation under NS, filtration, fractionation using cyanopropylsilyl, evaporation	8	(Valle-Hernández et al., 2010)
			PM <sub>2.5</sub>		0.058-0.383					
9-NA, 9-Nphen, 3-Nphen, 2-NF, 3-NF, 7-NB[a]A, 6-Nchr, 3-NBA, 6-NB[a]P, 1-NB[e]P, 3-NB[a]P	Mexico Valley	2006	PM <sub>2.5</sub>	[3 - 12 m]	<25	0-60	GC-MS	UD extraction with methylene chloride, evaporation under NS		(Amador-Muñoz et al., 2011)
1-Nnap, 2-Nnap, 2-NBP, 3-NBP, 4-NBP, 3-NBF, 5-Nace, 2-Nfluo, 9-NA, 9-Nphen, 2-NDB, 3-Nphen, 2-NA, 2-NF, 3-NF, 1-NP, 2-NP, 7-NB[a]A, 2,8-DNDB, 6-Nchr, 3-NBA, 1,3-DNP, 1,6-DNP, 1,8-DNP, 6-NB[a]P	Beijing, China	07-10.2008	PM <sub>2.5</sub>	[25 m]	4.6±2.3	Data in SI	GC-MS, ECNI	pressurized liquid extraction with DCM, purified using silica columns, elution with DCM	25	(Wang et al., 2011)
1-Nnap, 2-Nfluo, 9-NA, 2-NF, 3-NF, 1-NP, 2-NP	Concepcion, Coyhaique, Chile	03-04.2007	PM <sub>10</sub>	LD	0.00078-0.0299	Nd -29.8	GC-MS SIM	Soxhlet extraction with toluene, evaporation, fractionation on a column packed with alumina, elution with DCM, concentration under NS	7	(Scipioni et al., 2012)
Nnap, 3-Nphen, 9-Nphen, 1-NP, 3-NF	Madrid, Spain	02.2008 - 02.2009	PM <sub>10</sub>	semiurban area	0.132 (0.112-0.162)	0.1-917.2	LC-FLD	microwave extraction with DCM, filtration, evaporation, addition of ACN, evaporation, addition of MeOH, NaBH <sub>4</sub> , CuCl <sub>2</sub> , UD extraction, water addition, liquid-liquid extraction with DCM, evaporation, addition of ACN	5	(Barrado et al., 2013)
1-Nnap, 2-NBP, 5-Nace, 2-Nfluo, 9-NA, 9-Nphen, 3-NF, 1-NP, 2,7-DNfluo, 6-Nchr	Xi'an, China	5.07.2008 – 8.08.2009	PM <sub>2.5</sub>	[10 m]	0.3-7	LD	GC-MS	pressurized liquid extraction with DCM, extract were dried on SS, evaporation to 0.5 mL	10	(Bandowe et al., 2014)

2-NF, 2- and 9-NA, 1-, 2-, and 4-NP, 2-NTP, 2- and 3-NFR; 3- NPer, 1,3- and 1,6-DNP, 1,8- DNP), 1- NFR, 6- NC, 7-NB[a]A, 6-NB[a]P, 1- NPer, 9-NPh	Chiang Mai, Thailand	02-04; 0.8-09.2010	TSP	[32 m]	0.007-0.72	$24.7 \pm 12.3$ to $523.5 \pm 197.4$	HPLC-CLD	a clean-up column, reduced in reduction column to their amino derivatives	19	(Chuesaard et al., 2014)
1-Nnap, 2-Nfluo, 3-NF, 1-NP, 6-Nchr	Porto Alegre, Brasil	08.2011 – 08.2012	PM <sub>1</sub>	LD	LD	> 47.0	GC-ECD	Soxhlet extraction with DCM, clean-up procedure using a SG column, derivatization- with HFBA	5	(Garcia et al., 2014)
1-Nnap, 2-Nnap, 2-Nfluo, 9-NA, 1-NF, 2-NF, 3-NF, 1-NP, 2-NP, 4-NP, 7-NB[a]A, 6-Nchr	Queensway Road Tunnel, Birmingham, U.K	09.2012	PM <sub>10</sub>	LD	LD	2000-1918000	GC-NICI-MS	1' UD extraction with DCM, evaporation under NS, purification (chromatography column filled with glass wool and ASS), evaporation, redissolution in Hex, SPE-elution with DCM/Hex mix 2' extraction with ACN (vortex), centrifugation, evaporation under NS, redissolution in DCM	12	(Keyte et al., 2016)
	Parc des Princes Tunnel, Paris, France	06.2013				Nd-287000				
	Birmingham, U.K	LD				Nd-135000				
2-NFO, 1- Nnap, 6- Nchr, 9-NA, 2-NP, 4-NP, 1,8-DNP, 2- Nnap, 2-NFO, 3-NF, 9-Nphe, 3-Nphe, 1-NP, 7-NB[a]A, 1,3-DNP, 1,6-DNP, 6-NB[a]P	Chamonix and Maurienne valleys, France	Winter 2002–2003 and the Summer 2003	PM	rural	LD	0- 626.5	GC-MS/NICI	pressurized liquid extraction with DCM, SPE, elution with <i>n</i> -pentane, <i>n</i> -pentane/DCM (65/35, v/v), drying in Ar, dissolution in DCM	16	(Albinet et al., 2006)
PASHs	Location	Season, year	Phase	Sampling site	Mean total value with SD and range [ng m <sup>-3</sup> ]	Min-max of individual N-PAHs [ng m <sup>-3</sup> ]	Method, detection	Extraction	No. of determined compounds	Ref.
DBT, 4-MDBT, 2-/3-MDBT, 1-MDBT, 4,6-DMDBT, 2,8-DMDBT, 1,4-DMDBT, TBT, 2-NDBT, [1,2-d]BNT, [2,3-d]BNT, 7-M[2,3-d]T, 2,8-DNDBT	Guangzhou and Taiyuan, China	May, 2017 and April, 2018 (12 months)	PM <sub>2.5</sub>	urban	0.0808-2.796	0.0044-21.126	GC-MS/MS APCI	UD, SG column	13	(Zhang et al., 2021)

<sup>a</sup> – fmol m<sup>-3</sup>; Ace-acetone; ACN – acetonitrile; (A)SG – (anhydrous) silica gel; (A)SS- (anhydrous) sodium sulfate; BSTFA - N, O-bis-(trimethylsilyl) trifluoroacetamide; CLD - chemiluminescence detector; DCM – dichloromethane; ECD – electron capture detector; ECNI - Electron capture negative ion; EI/SIM, electron ionization; FLD - fluorescence detector; Hex – hexane; HFBA- heptafluorobutyric anhydride; LD- Lack of data; Nd- not detected; NICI - Negative ion chemical ionization; NS- nitrogen stream; Q-ToF-MS - mass quadrupole time-of-flight mass spectrometry; SIM – single ion monitoring; TSP – total suspended particles; UD- ultrasonic

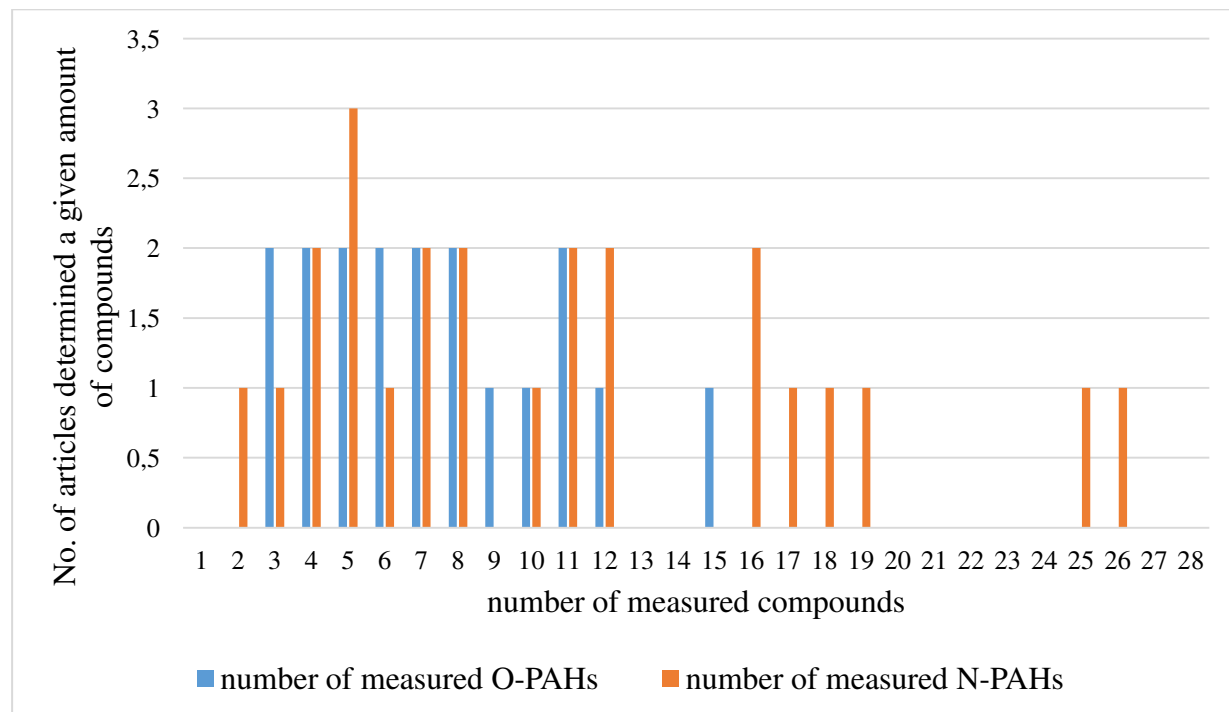


Fig. S1. The number of PAHs derivatives determined in the air samples.

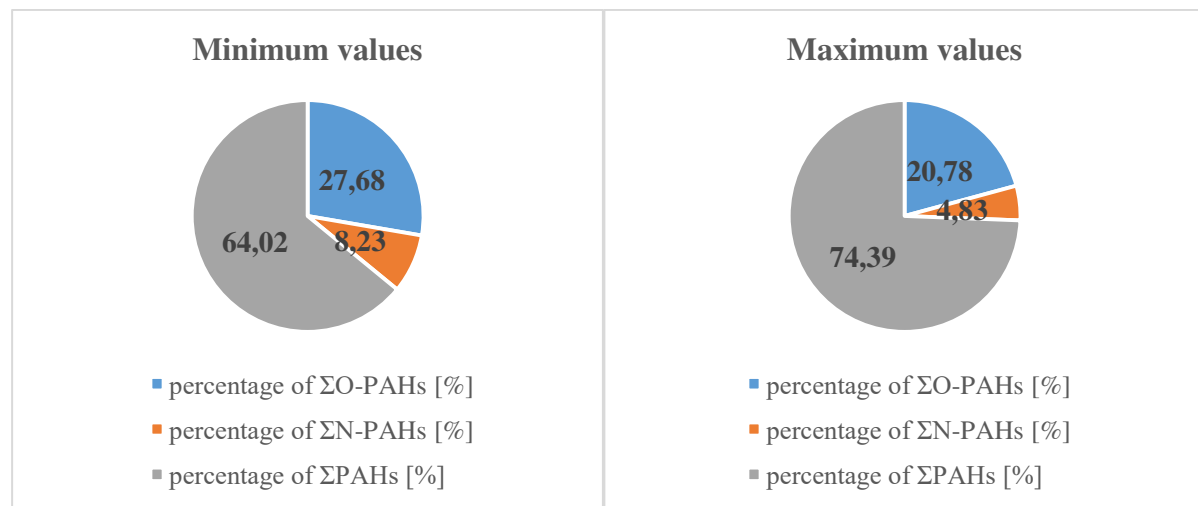


Fig. S2. The percentage (min and max) of O-PAHs, N-PAHs and PAHs in the air samples based on (Albinet et al., 2007; Bandowe et al., 2014; Souza et al., 2014; Wang et al., 2017)

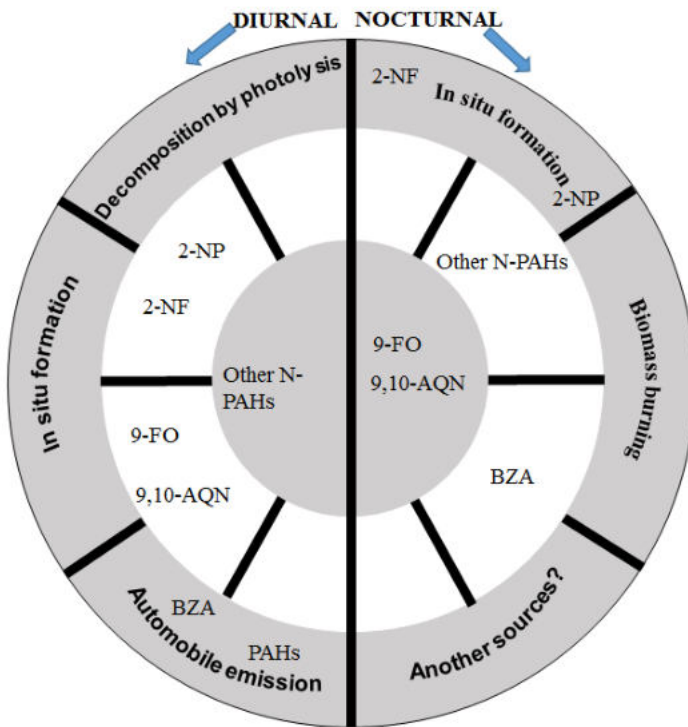


Fig. S3. The variations of N-PAHs formation during day and night, based on (Souza et al., 2014).

## References

- Abbas, I., Badran, G., Verdin, A., Ledoux, F., Roumié, M., Courcot, D., Garçon, G., 2018. Polycyclic aromatic hydrocarbon derivatives in airborne particulate matter: sources, analysis and toxicity. *Environmental Chemistry Letters* 16, 439–475. <https://doi.org/10.1007/s10311-017-0697-0>
- Albinet, A., Leoz-Garziandia, E., Budzinski, H., Villenave, E., 2007. Polycyclic aromatic hydrocarbons (PAHs), nitrated PAHs and oxygenated PAHs in ambient air of the Marseilles area (South of France): Concentrations and sources. *Science of The Total Environment* 384, 280–292. <https://doi.org/10.1016/j.scitotenv.2007.04.028>
- Albinet, A., Leoz-Garziandia, E., Budzinski, H., Villenave, E., 2006. Simultaneous analysis of oxygenated and nitrated polycyclic aromatic hydrocarbons on standard reference material 1649a (urban dust) and on natural ambient air samples by gas

- chromatography–mass spectrometry with negative ion chemical ionisation. *Journal of Chromatography A* 1121, 106–113. <https://doi.org/10.1016/j.chroma.2006.04.043>
- Albinet, A., Leoz-Garziandia, E., Budzinski, H., Villenave, E., Jaffrezo, J.-L., 2008. Nitrated and oxygenated derivatives of polycyclic aromatic hydrocarbons in the ambient air of two French alpine valleysPart 1: Concentrations, sources and gas/particle partitioning. *Atmospheric Environment* 42, 43–54. <https://doi.org/10.1016/j.atmosenv.2007.10.009>
- Amador-Muñoz, O., Villalobos-Pietrini, R., Miranda, J., Vera-Avila, L.E., 2011. Organic compounds of PM<sub>2.5</sub> in Mexico Valley: Spatial and temporal patterns, behavior and sources. *Science of The Total Environment* 409, 1453–1465.  
<https://doi.org/10.1016/j.scitotenv.2010.11.026>
- Bamford, H.A., Baker, J.E., 2003. Nitro-polycyclic aromatic hydrocarbon concentrations and sources in urban and suburban atmospheres of the Mid-Atlantic region. *Atmospheric Environment* 37, 2077–2091. [https://doi.org/10.1016/S1352-2310\(03\)00102-X](https://doi.org/10.1016/S1352-2310(03)00102-X)
- Bandowe, B.A.M., Meusel, H., Huang, R., Ho, K., Cao, J., Hoffmann, T., Wilcke, W., 2014. PM<sub>2.5</sub>-bound oxygenated PAHs, nitro-PAHs and parent-PAHs from the atmosphere of a Chinese megacity: Seasonal variation, sources and cancer risk assessment. *Science of The Total Environment* 473–474, 77–87.  
<https://doi.org/10.1016/j.scitotenv.2013.11.108>
- Barrado, A.I., García, S., Barrado, E., Pérez, R.M., 2012a. PM<sub>2.5</sub>-bound PAHs and hydroxy-PAHs in atmospheric aerosol samples: Correlations with season and with physical and chemical factors. *Atmospheric Environment* 49, 224–232.  
<https://doi.org/10.1016/j.atmosenv.2011.11.056>
- Barrado, A.I., García, S., Castrillejo, Y., Barrado, E., 2013. Exploratory data analysis of PAH, nitro-PAH and hydroxy-PAH concentrations in atmospheric PM<sub>10</sub>-bound aerosol

particles. Correlations with physical and chemical factors. *Atmospheric Environment* 67, 385–393. <https://doi.org/10.1016/j.atmosenv.2012.10.030>

Barrado, A.I., Garcia, S., Castrillejo, Y., Perez, R.M., 2012b. Hydroxy-PAH levels in atmospheric PM10 aerosol samples correlated with season, physical factors and chemical indicators of pollution. *Atmospheric Pollution Research* 3, 81–87.  
<https://doi.org/10.5094/APR.2012.007>

Bleeker, E.A.J., Van Der Geest, H.G., Klamer, H.J.C., De Voogt, P., Wind, E., Kraak, M.H.S., 1999. Toxic and Genotoxic Effects of Azaarenes: Isomers and Metabolites. *Polycyclic Aromatic Compounds* 13, 191–203.  
<https://doi.org/10.1080/10406639908020563>

Choi, J.-K., Heo, J.-B., Ban, S.-J., Yi, S.-M., Zoh, K.-D., 2012. Chemical characteristics of PM2.5 aerosol in Incheon, Korea. *Atmospheric Environment* 60, 583–592.  
<https://doi.org/10.1016/j.atmosenv.2012.06.078>

Chuesaard, T., Chetiyankornkul, T., Kameda, T., Hayakawa, K., Toriba, A., 2014. Influence of biomass burning on the levels of atmospheric polycyclic aromatic hydrocarbons and their nitro derivatives in Chiang Mai, Thailand. *Aerosol Air Qual. Res.* 14, 1247–1257. <https://doi.org/10.4209/aaqr.2013.05.0161>

Chung, M.Y., Lazaro, R.A., Lim, D., Jackson, J., Lyon, J., Rendulic, D., Hasson, A.S., 2006. Aerosol-borne quinones and Reactive Oxygen Species generation by particulate matter extracts. *Environ. Sci. Technol.* 40, 4880–4886.  
<https://doi.org/10.1021/es0515957>

de Castro Vasconcellos, P., Sanchez-Ccoyllo, O., Balducci, C., Mabilia, R., Cecinato, A., 2008. Occurrence and Concentration Levels of Nitro-PAH in the Air of Three Brazilian Cities Experiencing Different Emission Impacts. *Water Air Soil Pollut* 190, 87–94. <https://doi.org/10.1007/s11270-007-9582-y>

- Elzein, A., Dunmore, R.E., Ward, M.W., Hamilton, J.F., Lewis, A.C., 2019. Variability of polycyclic aromatic hydrocarbons and their oxidative derivatives in wintertime Beijing, China. *Atmospheric Chemistry and Physics* 19, 8741–8758.  
<https://doi.org/10.5194/acp-19-8741-2019>
- Garcia, K.O., Teixeira, E.C., Agudelo-Castañeda, D.M., Braga, M., Alabarse, P.G., Wiegand, F., Kautzmann, R.M., Silva, L.F.O., 2014. Assessment of nitro-polycyclic aromatic hydrocarbons in PM<sub>1</sub> near an area of heavy-duty traffic. *Science of The Total Environment* 479–480, 57–65. <https://doi.org/10.1016/j.scitotenv.2014.01.126>
- Hien, T.T., Thanh, L.T., Kameda, T., Takenaka, N., Bandow, H., 2007. Nitro-polycyclic aromatic hydrocarbons and polycyclic aromatic hydrocarbons in particulate matter in an urban area of a tropical region: Ho Chi Minh City, Vietnam. *Atmospheric Environment* 41, 7715–7725. <https://doi.org/10.1016/j.atmosenv.2007.06.020>
- Keyte, I.J., Albinet, A., Harrison, R.M., 2016. On-road traffic emissions of polycyclic aromatic hydrocarbons and their oxy- and nitro- derivative compounds measured in road tunnel environments. *Science of The Total Environment* 566–567, 1131–1142.  
<https://doi.org/10.1016/j.scitotenv.2016.05.152>
- Kojima, Y., Inazu, K., Hisamatsu, Y., Okochi, H., Baba, T., Nagoya, T., 2010. Comparison of PAHs, nitro-PAHs and oxy-PAHs associated with airborne particulate matter at roadside and urban background sites in downtown Tokyo, Japan. *GPOL* 30, 321–333.  
<https://doi.org/10.1080/10406638.2010.525164>
- Ladji, R., Noureddine, Y., Cecinato, A., Meklati, B., 2007. Seasonal variation of particulate organic compounds in atmospheric PM<sub>10</sub> in the biggest municipal waste landfill of Algeria. *Atmospheric Research* 86, 249–260.  
<https://doi.org/10.1016/j.atmosres.2007.06.002>

- Lee, H.H., Choi, N.R., Lim, H.B., Yi, S.M., Kim, Y.P., Lee, J.Y., 2018. Characteristics of oxygenated PAHs in PM 10 at Seoul, Korea. *Atmospheric Pollution Research* 9, 112–118. <https://doi.org/10.1016/j.apr.2017.07.007>
- Liang, F., Lu, M., Birch, M.E., Keener, T.C., Liu, Z., 2006. Determination of polycyclic aromatic sulfur heterocycles in diesel particulate matter and diesel fuel by gas chromatography with atomic emission detection. *Journal of Chromatography A* 1114, 145–153. <https://doi.org/10.1016/j.chroma.2006.02.096>
- Marino, F., Cecinato, A., Siskos, P.A., 2000. Nitro-PAH in ambient particulate matter in the atmosphere of Athens. *Chemosphere* 40, 533–537. [https://doi.org/10.1016/S0045-6535\(99\)00308-2](https://doi.org/10.1016/S0045-6535(99)00308-2)
- Park, S.S., Bae, M.-S., Schauer, J.J., Kim, Y.J., Yong Cho, S., Jai Kim, S., 2006. Molecular composition of PM2.5 organic aerosol measured at an urban site of Korea during the ACE-Asia campaign. *Atmospheric Environment* 40, 4182–4198.  
<https://doi.org/10.1016/j.atmosenv.2006.02.012>
- Reisen, F., Arey, J., 2005. Atmospheric Reactions Influence Seasonal PAH and Nitro-PAH Concentrations in the Los Angeles Basin. *Environ. Sci. Technol.* 39, 64–73.  
<https://doi.org/10.1021/es035454l>
- Ren, Y., Zhou, B., Tao, J., Cao, J., Zhang, Z., Wu, C., Wang, J., Li, J., Zhang, L., Han, Y., Liu, L., Cao, C., Wang, G., 2017. Composition and size distribution of airborne particulate PAHs and oxygenated PAHs in two Chinese megacities. *Atmospheric Research* 183, 322–330. <https://doi.org/10.1016/j.atmosres.2016.09.015>
- Ringuet, J., Leoz-Garziandia, E., Budzinski, H., Villenave, E., Albinet, A., 2012. Particle size distribution of nitrated and oxygenated polycyclic aromatic hydrocarbons (NPAHs and OPAHs) on traffic and suburban sites of a European megacity: Paris (France).

Atmospheric Chemistry and Physics 12, 8877–8887. <https://scihub.tw/https://doi.org/10.5194/acp-12-8877-2012>

Scipioni, C., Villanueva, F., Pozo, K., Mabilia, R., 2012. Preliminary characterization of polycyclic aromatic hydrocarbons, nitrated polycyclic aromatic hydrocarbons and polychlorinated dibenzo-*p*-dioxins and furans in atmospheric PM10 of an urban and a remote area of Chile. Environmental Technology 33, 809–820.  
<https://doi.org/10.1080/09593330.2011.597433>

Sienra, M.M. del R., 2006. Oxygenated polycyclic aromatic hydrocarbons in urban air particulate matter. Atmospheric Environment 40, 2374–2384.  
<https://doi.org/10.1016/j.atmosenv.2005.12.009>

Sklorz, M., Briedé, J.-J., Schnelle-Kreis, J., Liu, Y., Cyrys, J., de Kok, T.M., Zimmermann, R., 2007. Concentration of Oxygenated Polycyclic Aromatic Hydrocarbons and Oxygen Free Radical Formation from Urban Particulate Matter. Journal of Toxicology and Environmental Health, Part A 70, 1866–1869.

<https://doi.org/10.1080/15287390701457654>

Souza, K.F., Carvalho, L.R.F., Allen, A.G., Cardoso, A.A., 2014. Diurnal and nocturnal measurements of PAH, nitro-PAH, and oxy-PAH compounds in atmospheric particulate matter of a sugar cane burning region. Atmospheric Environment 83, 193–201. <https://doi.org/10.1016/j.atmosenv.2013.11.007>

Tang, N., Hattori, T., Taga, R., Igarashi, K., Yang, X., Tamura, K., Kakimoto, H., Mishukov, V.F., Toriba, A., Kizu, R., Hayakawa, K., 2005. Polycyclic aromatic hydrocarbons and nitropolycyclic aromatic hydrocarbons in urban air particulates and their relationship to emission sources in the Pan–Japan Sea countries. Atmospheric Environment 39, 5817–5826. <https://doi.org/10.1016/j.atmosenv.2005.06.018>

- Teixeira, E.C., Garcia, K.O., Meincke, L., Leal, K.A., 2011. Study of nitro-polycyclic aromatic hydrocarbons in fine and coarse atmospheric particles. *Atmospheric Research* 101, 631–639. <https://doi.org/10.1016/j.atmosres.2011.04.010>
- Tsakas, M.P., Sitaras, I.E., Siskos, P.A., 2010. Nitro polycyclic aromatic hydrocarbons in atmospheric particulate matter of Athens, Greece. *Chemistry and Ecology* 26, 251–261. <https://doi.org/10.1080/02757540.2010.495061>
- Valle-Hernández, B.L., Mugica-Álvarez, V., Salinas-Talavera, E., Amador-Muñoz, O., Murillo-Tovar, M.A., Villalobos-Pietrini, R., De Vizcaya-Ruiz, A., 2010. Temporal variation of nitro-polycyclic aromatic hydrocarbons in PM10 and PM2.5 collected in Northern Mexico City. *Science of The Total Environment* 408, 5429–5438. <https://doi.org/10.1016/j.scitotenv.2010.07.065>
- Wada, M., Kido, H., Kishikawa, N., Tou, T., Tanaka, M., Tsubokura, J., Shironita, M., Matsui, M., Kuroda, N., Nakashima, K., 2001. Assessment of air pollution in Nagasaki city: determination of polycyclic aromatic hydrocarbons and their nitrated derivatives, and some metals. *Environmental Pollution* 115, 139–147. [https://doi.org/10.1016/S0269-7491\(01\)00093-8](https://doi.org/10.1016/S0269-7491(01)00093-8)
- Wang, J., Xu, H., Guinot, B., Li, L., Ho, S.S.H., Liu, S., Li, X., Cao, J., 2017. Concentrations, sources and health effects of parent, oxygenated- and nitrated- polycyclic aromatic hydrocarbons (PAHs) in middle-school air in Xi'an, China. *Atmospheric Research* 192, 1–10. <https://doi.org/10.1016/j.atmosres.2017.03.006>
- Wang, W., Jariyasopit, N., Schrlau, J., Jia, Y., Tao, S., Yu, T.-W., Dashwood, R.H., Zhang, W., Wang, X., Simonich, S.L.M., 2011. Concentration and Photochemistry of PAHs, NPAHs, and OPAHs and Toxicity of PM<sub>2.5</sub> during the Beijing Olympic Games. *Environ. Sci. Technol.* 45, 6887–6895. <https://doi.org/10.1021/es201443z>

Wei, S., Huang, B., Liu, M., Bi, X., Ren, Z., Sheng, G., Fu, J., 2012. Characterization of PM<sub>2.5</sub>-bound nitrated and oxygenated PAHs in two industrial sites of South China. Atmospheric Research 109–110, 76–83.  
<https://doi.org/10.1016/j.atmosres.2012.01.009>

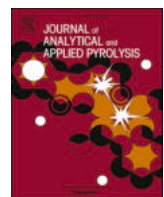
Zhang, Y., Song, Y., Chen, Y.-J., Chen, Y., Lu, Y., Li, R., Dong, C., Hu, D., Cai, Z., 2021. Discovery of emerging sulfur-containing PAHs in PM<sub>2.5</sub>: Contamination profiles and potential health risks. Journal of Hazardous Materials 416, 125795.  
<https://doi.org/10.1016/j.jhazmat.2021.125795>

## **Publikacja D2**

**A. Krzyszczak, M. Dybowski, B. Czech**

*Formation of polycyclic aromatic hydrocarbons and their derivatives in biochars: The effect  
of feedstock and pyrolysis conditions*

Journal of Analytical and Applied Pyrolysis, 2021, 160, 105339



## Formation of polycyclic aromatic hydrocarbons and their derivatives in biochars: The effect of feedstock and pyrolysis conditions

Agnieszka Krzyszczak <sup>a</sup>, Michał P. Dybowski <sup>b</sup>, Bożena Czech <sup>a,\*</sup>

<sup>a</sup> Department of Radiochemistry and Environmental Chemistry, Institute of Chemical Sciences, Faculty of Chemistry, Maria Curie-Skłodowska University in Lublin, Pl. M. Curie-Skłodowskiej 3, 20-031 Lublin, Poland

<sup>b</sup> Department of Chromatography, Institute of Chemical Sciences, Faculty of Chemistry, Maria Curie Skłodowska University in Lublin, Pl. M. Curie-Skłodowskiej 3, 20-031 Lublin, Poland

### ARTICLE INFO

#### Keywords:

PAHs  
PAHs derivatives  
Biochar  
Sewage sludge  
Temperature  
Feedstock

### ABSTRACT

During pyrolysis and several environmental processes, polycyclic aromatic hydrocarbons (PAHs) are altered and O/N/S-derivatives may be formed. The thermal utilization of sewage sludge (SSL) and bio-wastes (e.g. plant materials) towards biochars (BC) may be connected with the formation of both PAHs and their derivatives, known toxic compounds. Their toxicity depends on bioavailability. In the presented studies the effect of pyrolysis temperature on PAHs and their derivatives formation was investigated. The results clearly indicated that temperature (500, 600, and 700 °C) and feedstock (sewage sludges, wheat straw, willow) affected both the amount and type of bioavailable PAHs in biochars. The total content of bioavailable PAHs in SSL-derived BC was higher than in plant-derived BC and ranged from 8.58 to 16.07 ng L<sup>-1</sup> for BC obtained from SSL, 1.67–3.53 ng L<sup>-1</sup> for straw-derived biochars, and 3.17–3.53 ng L<sup>-1</sup> for willow-derived biochars. The percentage of quantified PAHs derivatives in SSL-derived BC was up to 10.3 %. Plant-derived BC were enriched in PAHs derivatives (1-methyl-5-nitronaphthalene, 1-methyl-6-nitronaphthalene, 4H-cyclopenta(def)phenanthrene, and nitropyrene). The increase of the pyrolysis temperature caused an increase in the percentage of PAHs derivatives from 5 % to 37.4 % (500–700 °C) for straw-derived BC whereas decrease to 15 % for willow-derived BC. The presence of toxic compounds such: 1-methyl-5-nitronaphthalene, 1-methyl-6-nitronaphthalene, nitropyrene in plant-derived BC, and B[a]P, nitronaphthalene, 9,10-anthracenedione in SSL-derived BC may significantly limit their agricultural applications.

### 1. Introduction

Polycyclic aromatic hydrocarbons (PAHs) belong to a group of persistent hydrophobic organic pollutants originating from natural sources (forest fires, volcanic eruptions) or anthropogenic activities (combustion of organic matters, fossil fuels, industrial processes) [1]. They are also produced during the incomplete combustion of biomass [2]. PAHs consist of two elements: hydrogen and carbon, and at least two linked carbon rings. Their toxicity, mutagenicity, and carcinogenicity to living organisms were confirmed [3,4]. During PAHs creation and even in the environment (e.g. in air, water, or soil), PAHs derivatives containing heteroatoms embedded in structure can be formed [5]. The presence of oxygen-, nitrogen-, or sulphur-containing PAHs derivatives noted as O-PAHs, N-PAHs or aazarenes (AZAs), and PASHs, respectively, was determined [6]. PAHs concentration in airborne particulate matter

(PM) was strictly connected with the presence of their derivatives. Moreover, some of the studies suggested that the overwhelming majority of PAHs and their derivatives occurring in atmospheric aerosols can be associated with PM having an aerodynamic diameter lower than 2.5 µm [6]. The concentrations of studied compounds were in the range of ng m<sup>-3</sup>, for example, the lowest concentration of Σhydroxyl + carboxyl-O-PAHs and ΣN-PAHs was determined at 0.2–13 and 0.3–7 ng m<sup>-3</sup>, respectively, whereas the concentrations of Σcarboxyl-O-PAHs and Σalkyl + parent-PAHs, 5–22 ng m<sup>-3</sup> and 7–387 ng m<sup>-3</sup>, respectively were the highest. To illustrate the percentage of these components in the PM<sub>2.5</sub> phase, it was established that PAHs and their derivatives constituted 0.01–0.4 % of the mass of organic carbon in PM<sub>2.5</sub> and 0.002–0.06 % and the total mass of PM<sub>2.5</sub> [5]. In another study, the total suspended particle-equivalent concentrations of Σ14PAHs in two Chinese megacities amounted up to 57 ± 20 ng m<sup>-3</sup> and 18 ± 23 ng m<sup>-3</sup>, while, the

\* Corresponding author.

E-mail address: [bczech@hektor.umcs.lublin.pl](mailto:bczech@hektor.umcs.lublin.pl) (B. Czech).

concentration of  $\Sigma$ 7O-PAHs valued  $54 \pm 15 \text{ ng m}^{-3}$  and  $23 \pm 32 \text{ ng m}^{-3}$ , respectively [7]. It indicated that the concentrations of O-PAHs can be similar to the concentration of PAHs implying that there is a need to estimate the environmental pollution not only by PAHs but also by their derivatives.

Sewage sludge (SSL) is regarded as one of the most important sources of secondary pollution in the water environment [8] and SSL is generated from the treatment of industrial and urban wastewater. SSL contains various toxic and hazardous pollutants including PAHs [9]. The SSL can be additionally polluted by polychlorinated biphenyls, pesticides, dioxins, furans, heavy metals [8]. The concentration of PAHs in SSL varies.  $\Sigma$ PAHs in SSL from two different wastewater treatment plants (North and West of Poland) were  $621.33 \mu\text{g kg}^{-1}$  of dry weight (d.w.) and  $2433.40 \mu\text{g kg}^{-1}$  d.w [10]. The higher average content of  $\Sigma$ 16PAHs was noted in the studies of Khillare et al. [11] - up to  $20.67 \pm 4.14 \text{ mg kg}^{-1}$  d.w. According to the studies of Moreda et al. [12] the total PAHs concentration in SSL can range even from  $128 \text{ mg kg}^{-1}$  to  $482 \text{ mg kg}^{-1}$  with the methylated hydrocarbons as the most abundant PAHs originated from petroliferous sources. The by-products of dried SSL gasification such as ash, charcoal, or liquid-tar were characterized by higher concentrations of contaminants including PAHs [10]. This may indicate that PAHs and their derivatives can be formed in other materials subjected to high temperatures. The disposal of SSL is a significant environmental concern [11]. The presence of numerous toxic substances limits options for its direct utilization, even though the application of anaerobic digestion or aerobic composting in sludge treatment plants results in receiving material containing a large amount of residual organic material and nutrients (e.g. N, P, K) [8] but contamination with metals or pathogens should be also considered. Lately, some studies have described SSL as feedstock biochar production [13].

Biochar (BC) is amorphous and stable material derived from thermochemical conversion (gasification or pyrolysis) of broadly understood biomass in the absence or reduced content of free oxygen [14]. BC is a porous, persistent, and low-density carbonaceous material revealing highly heterogeneous properties and can be obtained from a different type of feedstock, e.g. agricultural wastes, wood, dairy manure, microalgae, SSL [15]. The feedstock for BC is mainly composed of cellulose, hemicellulose, and lignin [14]. The type of feedstock affects the pH value, surface area, ash content, and fixed carbon value [16]. Increased pyrolysis temperature induced an increase of cation exchange capacity, polarity, mass, and energy yield, degree of aromaticity, and carbon content whereas the content of oxygen and hydrogen was decreased [16, 17].

During the last decades, the application of BC in environmental protection and soil remediation has gained interest. BC is widely used in agriculture due to the acceleration of the degradation of organic pollutants, stimulation of bacterial growth [18], and increase of soil water capacity [19]. BC plays an important role in the remediation, revegetation, and restoration of contaminated soils [20]. However, PAHs can be formed during BC preparation [21]. For this reason, International Biochar Initiative (IBI) and the European Biochar Certificate (EBC) established a range of permitted level for the sum of the 16 US Environmental Protection Agency's (EPA) PAHs in biochar being  $6\text{--}300 \text{ mg kg}^{-1}$  d.w. and  $4\text{--}12 \text{ mg kg}^{-1}$  d.w., respectively [22].

PAHs derivatives are formed during various chemical, physical and photochemical reactions including incomplete combustion. As pyrolysis conditions affected the amount of PAHs there is a great possibility, that during feedstock pyrolysis some PAHs derivatives will be created [23]. Therefore various O-, OH-, N-PAHs, PASHs, or AZAs can be created. Great attention to the PAHs derivative's presence in various materials should be paid due to the fact that they are considered more toxic than pristine PAHs [24]. For example, 1,8-dinitropyrene is found to be three times more toxic than benz[a]pyrene (B[a]P) [25]. PAHs derivatives can cause oxidative stress [26], which is one of the physiopathological signalling indicators of toxic exposures. 1-nitropyrene induced the generation of 8-hydroxy-2'-deoxyguanosine (8-OHdG) - a biomarker of

oxidative DNA damage [27]. There are significantly fewer studies on O-PAHs toxicity than N-PAHs and the toxicity mechanisms are not fully understood yet. But even at low concentration of O-PAHs these compounds revealed high toxicity [28] causing oxidative stress [29] and cell damage due to their mutagenicity, cytotoxicity, and genotoxicity [30].

PAHs have a very small bioavailability due to the strong binding to the material.  $\pi\text{--}\pi$  interactions between biochar and planar aromatic PAHs are privileged. Moreover, some PAHs can be occluded and trapped within the biochar structure being unavailable or even nonextractable [31]. As the environmental hazard of chemicals depends on their bioavailability, the presence of the bioavailable fraction of PAHs and their derivatives in biochar should be estimated.

To the best of our knowledge, there is little information about the influence of pyrolysis conditions (temperature, feedstock) on the content of bioavailable PAHs derivatives in biochars produced from biowastes. It is extremely important because during pyrolysis PAHs and their derivatives can be formed and they remain on the surface of biochars [21]. For this reason, they may pose a threat to human health and natural environment. It is necessary to evaluate the risk of biochar application before it will be widely used. The aim of this study was 1) to determine quantitatively and qualitatively the content of bioavailable PAHs and their derivatives in biochars originated from different types of feedstock (agricultural wastes: straw and willow, two different sewage sludges) and pyrolyzed at different temperatures ( $500^\circ\text{C}$ ,  $600^\circ\text{C}$ , and  $700^\circ\text{C}$ ), 2) to assess the effect of the pyrolysis temperature on PAHs derivatives formation.

## 2. Materials and methods

### 2.1. Feedstock preparation

Willow (*Salix viminalis*) was cultivated at a farm localized in the southeastern part of Poland. After the harvest, plants were air-dried for a few weeks. The *Salix viminalis* stalks were cut into smaller fragments ( $<5 \text{ cm}$ ) and grounded (TESTCHEM, Poland). SSLs were obtained from municipal wastewater treatment plants localized in Poland: Kalisz ( $51^\circ45'45''\text{N } 18^\circ05'23''\text{E}$ , population 99,106, population density  $1427,6 \text{ people/km}^2$ ) and Chełm ( $50^\circ20'04''\text{N } 23^\circ29'49''\text{E}$ , population 61,588, population density  $1745,7 \text{ people/km}^2$ ). Dried wheat straw (*Triticum L.*) was also used for the preparation of biochar. Materials were dried, crushed, sieved to obtain grains below  $2 \text{ mm}$ , and homogenized.

### 2.2. Biochar preparation

Pyrolysis of selected materials was carried out in a furnace (Czylok, Poland). Biochars were obtained via slow pyrolysis at  $500$ ,  $600$ , and  $700^\circ\text{C}$  (the heating rates: first step  $10^\circ\text{C min}^{-1}$ , second step  $3^\circ\text{C min}^{-1}$  (during the last  $30^\circ\text{C}$ ); the resident time: 3 h). To achieve an oxygen-free atmosphere, the constant flow of nitrogen ( $\text{N}_2$ ) ( $630 \text{ cm}^3/\text{min}^{-1}$ ) was kept and monitored by the mass flow controller (BETA-ERG, Poland). Obtained biochars were passed through a  $2 \text{ mm}$  sieve and homogenized. They were also washed out using distilled water in the ratio of 1:10 for 24 h. Then, biochars were dried at  $40^\circ\text{C}$  overnight. The obtained biochars were labelled considering their feedstock: sewage sludge from Chełm (BCCH), SSL from Kalisz (BCKZ), willow (BCW), straw (BCS), and pyrolysis temperature:  $500$ ,  $600$ , and  $700^\circ\text{C}$  (Table S1).

### 2.3. Freely dissolved ( $C_{\text{free}}$ ) PAHs and their derivatives determination in biochars

The determination of bioaccessibility of PAHs and their derivatives was carried out by the protocol described in Oleszczuk et al. [32] and Hale et al. [31]. Before the sample preparation procedure, 76-mm thick polyoxymethylene (POM) passive samplers ( $4 \text{ cm} \times 4 \text{ cm}$  and about  $0.35 \text{ g}$  each) were cleaned and submerged in methanol, shaken for 24 h on a shaking machine (ELPIN 358A, Poland). Subsequently, methanol was

substituted with n-heptane and Millipore water (in each solvent POM samplers were shaken for 24). Next, sheets were rinsed with Millipore water, placed in a glass bottle with water, and stored at 4 °C. Biochar (1 g) dried at 40 °C for 24 h were placed in 50 mL Erlenmeyer flasks with glass lids. 40 mL of sodium azide (200 mg/L) dissolved in water was added for the elimination of any possible effect of residual microorganisms. POM samplers were added to Erlenmeyer flasks (all carried out in triplicates) and vials were tightly sealed to prevent leakage. Flasks were rolled on a rotary shaker ROTAX 6.8 VELP Scientifica (Italy) for 1 month at 10 RCF. After this period, POM samplers were cleaned with distilled water. The remaining visible impurities were removed using a tissue. Treated POM samplers were placed in a 50 mL dry Erlenmeyer flask. Then, they were extracted in 20 mL of 20/80 acetone/heptane (v/v) with the addition of 20 µL of deuterated PAHs (naphthalene, pyrene, and phenanthrene with a concentration of 10 ng µL<sup>-1</sup>) and shaken in horizontal shaking machine ELPIN 358A (Poland) for 48 h. After this time 1 mL of iso-octane was added and obtained solvent was concentrated to about 1 mL using rotary vacuum concentrator RVC 2–25 CD plus (Martin Christ, Germany). Then, GC-MS/MS analysis was carried out. The concentration of PAHs and their derivatives on POM passive samplers ( $C_{POM}$ ) was calculated according to the Eq. (1):

$$C_{POM} (\text{ng kg}^{-1}) = \frac{m_{PAH} (\text{ng})}{m_{2POM} (\text{kg})} \quad (1)$$

where  $m_{PAH}$  (ng) (or  $m_{PAH}$  derivatives) is the mass of PAHs (or PAHs derivatives) determined by GC-MS/MS and  $m_{2POM}$  (kg) is the mass of two used POM passive samplers.

$C_{free}$  concentrations were calculated using POM-water partitioning coefficients ( $K_{POM}$ ) known from previous studies [33]. In the case of some PAHs derivatives  $K_{POM}$  was adopted considering parent PAHs due to the lack of the available data in literature: nitronaphthalene, 1-methyl-5-nitronaphthalene, 1-methyl-6-nitronaphthalene, nitropyrene, 2-phenylnaphthalene [34], benzo[a]fluorene, and benzo[a]fluoranthene [35].  $K_{POM}$  constitutes an individual value to each compound. Freely dissolved ( $C_{free}$ ) PAHs and derivatives were measured according to Eq. (2):

$$C_{free} (\text{ng L}^{-1}) = \frac{K_{POM-w} (\text{L kg}^{-1})}{C_{POM} (\text{ng kg}^{-1})} \quad (2)$$

where  $C_{free}$  (ng L<sup>-1</sup>) is the bioavailable pollutant concentration,  $K_{POM-w}$  (L kg<sup>-1</sup>) is the POM-water partitioning coefficient and  $C_{POM}$  (ng kg<sup>-1</sup>) is the measured POM concentration.

The physicochemical analysis of biochar, detailed information on GC-MS/MS measurements, chemical characteristics of analyzed compounds (Table S2) and the qualitative and quantitative parameters of PAHs and O/N-PAHs analysis (Table S3) were presented in Supporting Information.

#### 2.4. Statistical analysis

The statistical analysis was carried out and the data were compared using the general ANOVA function assuming that the population is distributed normally. If a significant interaction was identified, the means were separated using a Tukey test. Moreover, the results were processed using a statistical program Statgraphics Plus 3.0 for Windows® software. The two-way ANOVA was performed. The influence of pyrolysis temperature and type of feedstock on the concentrations of analytes (dependent variables) were calculated by a two-factorial analysis of variance (ANOVA). The differences between mean values with  $p < 0.05$  were considered statistically significant.

### 3. Results

#### 3.1. Biochar characteristics

The physicochemical characteristic of studied BCs was presented in Table 1 and Fig. 1. SSL-derived BC differed depending on the applied SSL. BCCH were characterized by the higher  $S_{BET}$  surface area, higher pH, carbon and hydrogen content (in most cases), and polarity (expressed as (O + N)/C ratio) than BCKZ and the increase of the pyrolysis temperature increased  $S_{BET}$ , pH, but lowered H, N, O content, and hydrophobicity (O/C ratio).

The biochars derived from willow were characterized by higher  $S_{BET}$ , with the highest value of 145.02 m<sup>2</sup> g<sup>-1</sup> obtained for BCW600. BCS and BCW contained higher C and H content and lower ash content than SSL-derived BC. The pyrolysis temperature affected in BCCH the ash content (positive correlation,  $p < 0.02$ ), H content, and related parameter of aromatic (H/C) (negative correlation,  $p < 0.1$ ), whereas BCKZ characteristic considering surface functional groups (O content, hydrophobicity, and polarity ratios) was lowered ( $p < 0.02$ ). Such correlations were not observed for BCW. When the pyrolysis temperature rises, ash contents increased BCs obtained from sewage sludges, while in BCS and BCW decreased (Fig. 1A). Moreover, the C content increased only in BCS, while in other samples the highest values were obtained for biochar produced in 600 °C. H and N contents decreased in all BC, and O contents decreased in SSL-derived BC and willow-derived BC. The thermal-induced dehydration, decarboxylation reactions, and breakage of weak bonds in the feedstock structure can be the reasons for these changes [40]. In the case of biochars' aromaticity, two levels of H/C values are important. If the H/C value is below 0.3 or greater than 0.7, the studied materials have a highly condensed structure or a non-condensed structure [41]. In our case, almost all biochars were characterized by H/C values below 0.3 (excluding BCKZ50 and BCS500: 0.400 and 0.401, respectively) confirming a high degree of aromatisation and carbonisation of studied materials [17] and there were no materials with non-condensed structure. The lower the H/C value was obtained, the more easily stable aromatic ring systems were created [42]. Moreover, when the pyrolysis temperature rises, the ratio H/C decrease in all samples, while (O + N)/C and O/C decreased in SSL-derived biochars and BCW, and increased only in BCS samples. These observations may indicate different mechanisms and temperature-depending transformations affecting polarity and hydrophobicity of obtained materials. All biochar showed an alkaline character (pH 7.08–12.4). In SSL-derived biochars, pH increased with increasing pyrolysis temperature. It may be due to the reduction of the amount of the organic functional groups (such as –COOH and –OH), and the carbonates (i.e. CaCO<sub>3</sub>) and inorganic alkalis (i.e. K, Na, Ca) formation [43].

The surface characteristics of studied biochars were also carried out. Due to the smaller content of PAHs and their derivatives, and thus increased application potential, willow-derived biochar was selected to present the results. In the FT-IR spectra of BCW600 (Fig. 1B) the presence of sharp peaks at 3443 cm<sup>-1</sup>, 1632 cm<sup>-1</sup>, 1384 cm<sup>-1</sup>, 1115 cm<sup>-1</sup>, and 668 cm<sup>-1</sup> was noted. Their presence confirmed the surface functionalities of NH stretching vibrations of free NH, or intramolecular H bonds (3450–3600 cm<sup>-1</sup>), C=C or C=O stretching vibrations (1632 cm<sup>-1</sup>), derived from aromatic rings (lignin), and aromatized and carbonized material from carbohydrate ring dehydration and cyclization during pyrolysis [44]. Additionally, C—H bending vibrations of the CH<sub>3</sub> group (1384 cm<sup>-1</sup>), C—C or C—OH stretching vibrations (1115 cm<sup>-1</sup>), and C—H wagging vibration 668 cm<sup>-1</sup> were noted in the spectra. The data are concise with XPS results (Fig. 1C). The band at 284.7 eV; 286.2 eV and 288.2 eV were indicating the presence of surface C=C, C—H; C—OH, C—O—C, and O—C=C, respectively constituting 96.67 % of surface carbon. Most of the oxygen (>50 % at.) was in the form of O\*—(C=O)—C (533.52 eV) and the rest (~46 %) as O=C—N (531.93 eV). Nitrogen was present predominantly as N—(C=O)—O— (400.76 eV) and C=N—C (398.8 eV).

**Table 1**

The physicochemical characteristics of studied biochar [20,36–39].

sample	S <sub>BET</sub>	pH	Ash content <sup>a</sup> [%]	C <sup>b</sup> [%]	H <sup>b</sup> [%]	N <sup>b</sup> [%]	O <sup>c</sup> [%]	H/C	(O + N)/C	O/C
BCCH500	69.70	9.40	64.10	26.30	0.99	3.26	5.38	0.038	0.329	0.205
BCCH600	75.50	12.10	67.60	26.50	0.60	2.93	2.41	0.023	0.202	0.091
BCCH700	89.20	12.40	71.40	24.50	0.29	2.10	1.71	0.012	0.156	0.070
BCKZ500	16.30	7.08	68.09	23.16	0.77	3.57	4.42	0.400	0.280	0.140
BCKZ600	9.00	11.45	70.27	23.72	0.44	3.29	2.29	0.220	0.190	0.070
BCKZ700	29.90	12.38	74.28	22.84	0.33	2.25	0.30	0.170	0.090	0.010
BCS500	24.32	10.26	21.85	65.79	2.20	1.43	8.73	0.401	0.118	0.100
BCS600	2.47	10.37	19.59	66.14	1.66	1.26	11.36	0.300	0.145	0.129
BCS700	0.37	10.26	14.73	68.39	1.20	1.22	14.48	0.210	0.174	0.159
BCW500	119.5	10.18	8.18	75.18	2.52	2.47	11.65	0.034	0.188	0.155
BCW600	145.0	10.45	7.09	82.77	2.24	1.68	9.53	0.027	0.135	0.115
BCW700	13.23	11.39	5.64	82.38	1.46	1.67	8.85	0.018	0.128	0.107

O/C, (N + O)/C, H/C = molar ratios.

S<sub>BET</sub> – specific surface area of adsorbents [ $\text{m}^2/\text{g}$ ].<sup>a</sup> ash content measured by weight loss after 6 h in 750 °C.<sup>b</sup> C (carbon), H (hydrogen) and N (nitrogen) content measured using CHN analyser (Perkin-Elmer 2400).<sup>c</sup> O (oxygen) content calculated by subtracting ash, C, H and N content from total mass of the sample.

The surface morphology of BCW600 was presented in Fig. 1D. The surface of BCW600 was cracked and some surface pores were present. Pore forms varied, but generally, they had a shape of elongated curves, circles, or deformed honeycombs. In some cases, these circles were separated with bulkheads. The pores may be classified as macropores (pores size is greater than 50 nm). The pores appear next to each other and the SEM image shows that they were running diagonally from the top-bottom to the top right. The carbonaceous skeleton which was a porous structure of BC is most likely associated with the biological capillary structure of feedstock. The presence of macropores ensured more adsorption sites [45].

Fig. 2A and B shows some relations between the content of ash, carbon, hydrogen, oxygen and nitrogen, and the concentrations of PAHs and their derivatives obtained in the studied biochars. Two main tendencies were observed. Increased PAHs and their derivatives concentration was noted over biochars with increased ash content and N content in biochar. The results clearly stress the role of inorganic compounds of ash in catalyzing of PAHs formation. Increased O%, C% and H % content reduced aromatics formation, therefore neither aromaticity, nor hydrophilicity of biochar surface itself, regulate PAHs and their derivatives formation.

### 3.2. The bioavailable PAHs and their derivatives in BC

#### 3.2.1. Bioavailable pristine PAHs

Concentrations of bioavailable PAHs are generally dependent on the applied feedstock, pyrolysis temperature, and pyrolysis time [31]. The presented results clearly indicated that feedstock affected both the amount and type of bioavailable PAHs in BC. Generally, the content of total bioavailable PAHs in SSL-derived BC was higher and ranged from 8.58 to 16.07 ng L<sup>-1</sup> for BCKZ, 9.04–9.40 ng L<sup>-1</sup> for BCCH than in plant-derived BC: 1.67–3.53 ng L<sup>-1</sup> for BCS, and 3.17–3.53 ng L<sup>-1</sup> for BCW (Table S4, Fig. 3) what may affect their agricultural application. SSL-derived biochar may pose higher ecotoxicological effect due to bioavailable PAHs presence than biochar obtained from plant wastes.

The total content of bioavailable PAHs in BCCH obtained at the lowest applied pyrolysis temperature (500 °C) amounted to 9.06 ± 0.41 ng L<sup>-1</sup> and the most abundant were 3 ring PAHs (64.2 %), among which acenaphthene represented almost 75.5 % (Fig. 4). BCCH500 was also enriched in 2-ring PAH (only one compound- naphthalene- 35.02 %), 4-ring (0.66 %), and a small amount of 5-ring (0.099 %) and 6-ring PAHs (0.0086 %). Among the total content of bioavailable PAHs, C<sub>free</sub> of Σ16PAHs (the concentration of the sum of 16 EPA PAHs) amounted to 9.00 ± 0.41 ng L<sup>-1</sup>. BCCH obtained at a higher temperature (600 °C) contained a slightly lower concentration of bioavailable PAHs. C<sub>free</sub> of ΣPAHs and C<sub>free</sub> of Σ16PAHs amounted to 9.04 ± 0.52 ng L<sup>-1</sup> and 8.92 ±

0.52 ng L<sup>-1</sup>, respectively. An increase in pyrolysis temperature of BCCH resulted in a changed PAHs profile in BCCH600. The application of higher temperature caused a change in the proportion of the percentage of PAHs due to its different number of rings. In this case, 2-ring PAH-naphthalene- was predominant (51.84 % of all PAHs and 100 % of 2-ring PAHs), whereas compounds with 3 aromatic rings represented marginally less value (46.76 %) with an acenaphthene as the most abundant (over 55 %). However, the presence of 4,5 and 6-ring PAHs was also confirmed (1.3 %; 0.066 %, and 0.0089 %, respectively).

The higher applied pyrolysis temperature, in the case of BCCH, caused the higher C<sub>free</sub> of ΣPAHs and C<sub>free</sub> of Σ16PAHs (9.40 ± 0.48 ng L<sup>-1</sup> and 9.23 ± 0.47 ng L<sup>-1</sup>, respectively). Naphthalene as the sole representative of 2-ring PAHs constituted 58.42 % of all bioavailable PAHs. 3-ring PAHs were also noted and constituted a substantial part of all PAHs (40.38 %) with prevailing values of acenaphthylene and acenaphthene (50.8 % and 40.0 %, respectively). Some of the 4, 5, and 6-ring PAHs were quantified and they accounted for 1.12 %, 0.080 % and 0.0063 % of all PAHs). Among 5-ring PAHs, the presence of B[a]P was also confirmed in all samples (BCCH500, BCCH600, and BCCH700). B[a]P is considered as an indicator of pollution and as one of the most carcinogenic PAHs [46]. The presence of B[a]P in bioavailable fractions requires great attention before use in agriculture. Generally, the higher temperature was applied, the higher content of naphthalene and the lower content of 3-ring PAHs were detected.

In BCKZ biochars, the application of different pyrolysis temperatures did not change the PAHs profile. BCKZ obtained in 500 °C was characterized by the lowest content of C<sub>free</sub> of ΣPAHs and Σ16PAHs (8.58 ± 0.36 ng L<sup>-1</sup> and 4.23 ± 0.20 ng L<sup>-1</sup>) among all BCKZ samples. 73.33 % of all PAHs constituted 2 ring compounds with a 2-phenylnaphthalene (68 %) and naphthalene (32 %) being predominant. 3-ring PAHs were represented by only acenaphthene, fluorene, and 3-methylphenanthrene that constituted 25.86 % of the sum of all bioavailable PAHs. Higher pyrolysis temperature of BCKZ caused the increase of C<sub>free</sub> of ΣPAHs and Σ16PAHs but the relations between PAHs divided into groups differing in a number of aromatic rings did not change. BCKZ obtained in 600 °C and 700 °C contained increasing concentrations of PAH<sub>free</sub> (bioavailable PAHs) (10.13 ± 0.46 ng L<sup>-1</sup> and 16.07 ± 0.60 ng L<sup>-1</sup> of C<sub>free</sub> of ΣPAHs and 7.60 ± 0.34 ng L<sup>-1</sup> and 8.94 ± 0.40 ng L<sup>-1</sup> of Σ16PAH<sub>free</sub>, respectively). 2-ring PAHs (naphthalene and 2-phenylnaphthalene) were predominant in BCKZ600 (73.26 %) and BCKZ700 (75.75 %) with a percentage of naphthalene 68.1 % and 43.8 %, and 2-phenylnaphthalene 31.9 % and 56.2 %, respectively. 3-ring PAHs constituted 25.94 % and 23.89 %, respectively, with predominant acenaphthene and fluorene. In all BCKZ samples small amounts of 4, 5, and 6-ring PAHs were also detected and quantified (Table S4).

Comparing two biochars derived from sewage sludges in different

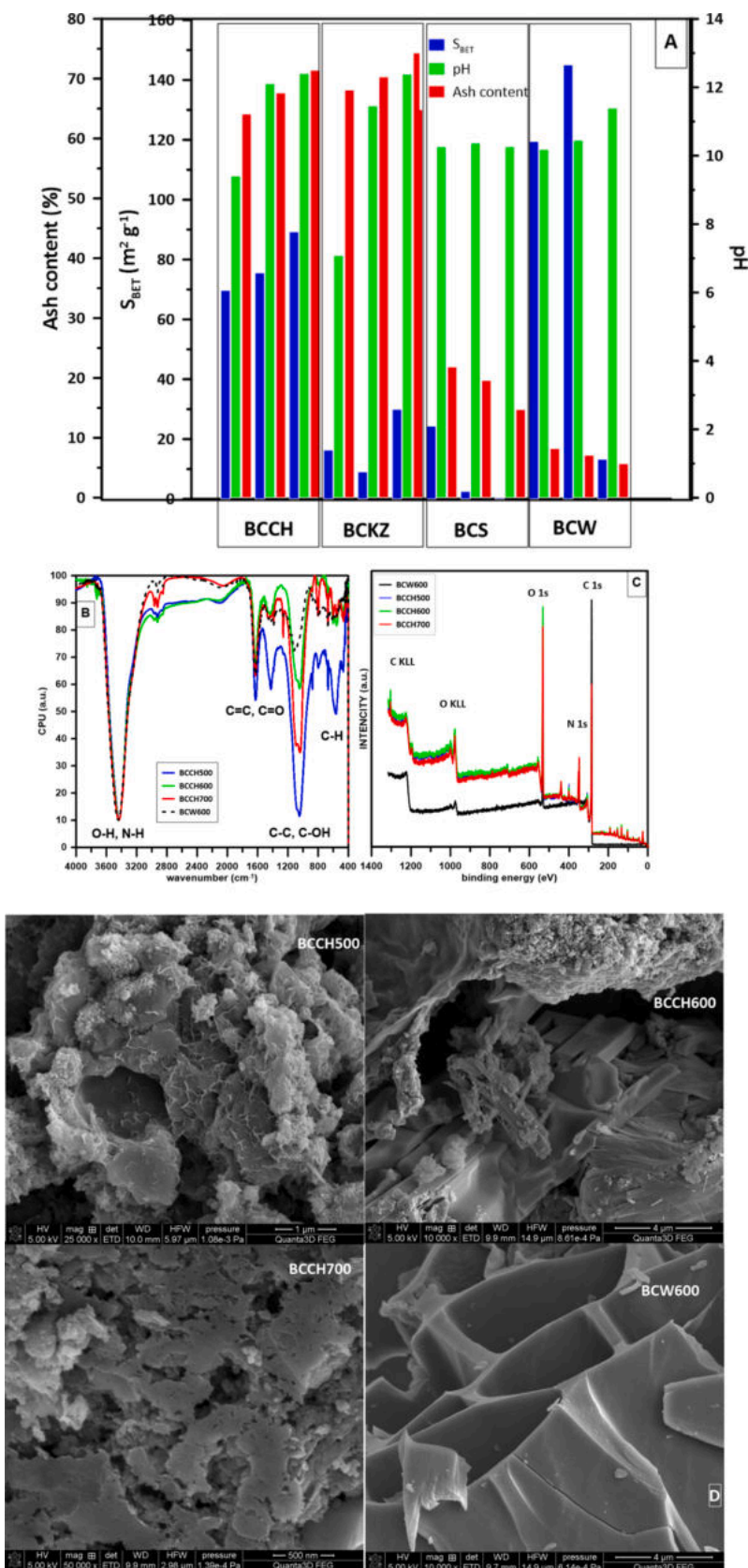


**Fig. 1.** A) comparison of main physicochemical parameters of tested biochars; B) FT-IR spectra, C) XPS spectra, D) SEM images.

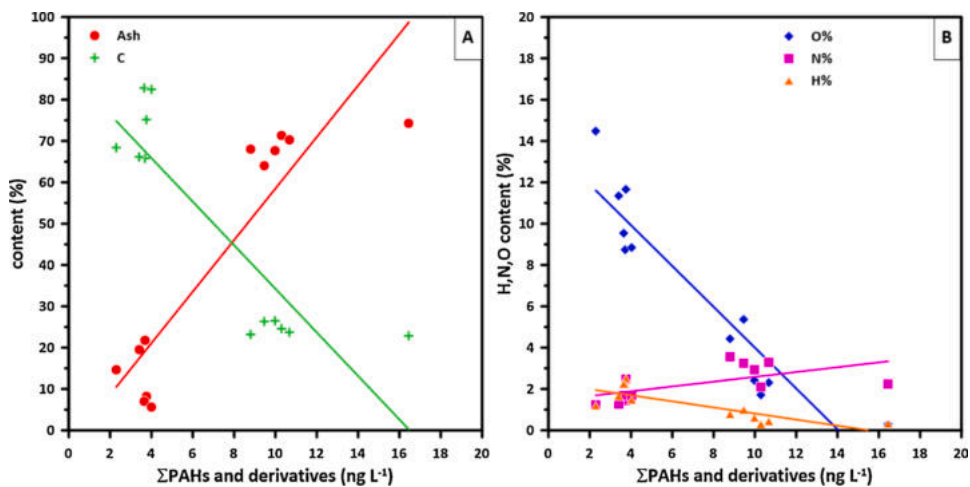


Fig. 2. The relations between the percentage contents of ash, C, H, N and O, and the concentrations of PAHs and their derivatives in tested biochars.

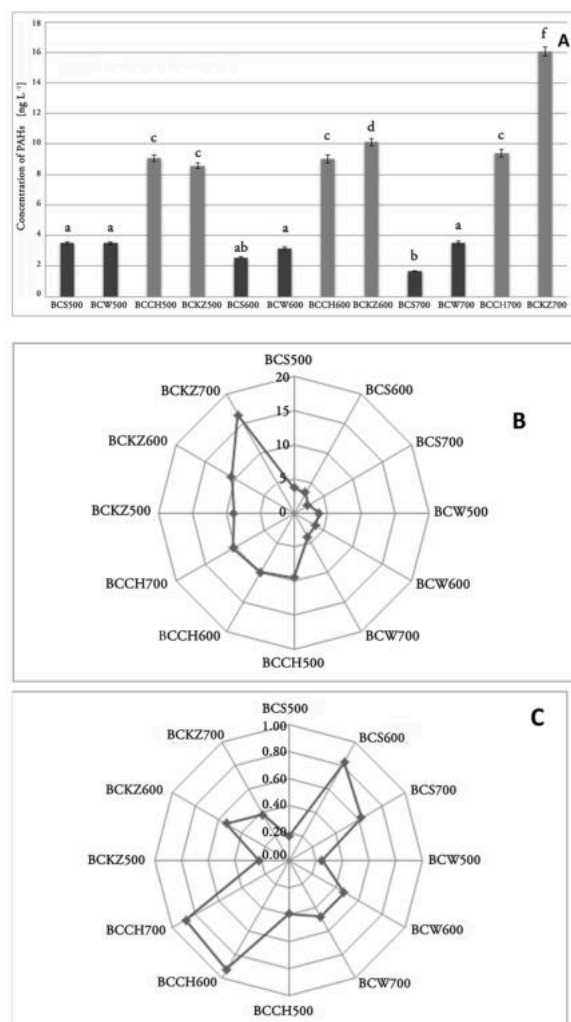


Fig. 3. ΣPAHs content in tested biochars [ $\text{ng L}^{-1}$ ], A) the effect of temperature and feedstock on the total concentration of  $\Sigma\text{PAHs}_{\text{free}}$ , B) total  $\Sigma\text{PAHs}_{\text{free}}$ , C) PAHs derivatives.

pyrolysis temperatures, BCCH samples obtained in 500, 600, and 700 °C were characterized by more stable  $\text{PAH}_{\text{free}}$  concentrations. In BCKZ samples the total concentration of  $\Sigma\text{PAHs}$  differed two times (between the lowest and the highest temperature). But in all SSL-derived samples

lighter PAHs (2 and 3-rings) were predominant. The percentage of heavier PAHs (4,5 and 6-rings) constituted less than 0.8 %, 1.4 % and 1.2 % for BCCH samples, and 0.8 %, 0.8 % and 0.36 % for BCKZ samples. Interestingly, in BCCH the concentration of  $\Sigma\text{16PAH}_{\text{free}}$  was predominant and constituted 98–99 % of  $\text{C}_{\text{free}}$  of  $\Sigma\text{PAHs}$ , whereas in BCKZ the percentage of  $\Sigma\text{16PAH}_{\text{free}}$  was lower (50 %–75 %).

In BCS samples (Table S5), increasing pyrolysis temperature caused a decrease in the total concentration of  $\Sigma\text{PAHs}$  and  $\text{C}_{\text{free}}$  of  $\Sigma\text{16PAHs}$ . Among all BCS samples, biochar obtained in 500 °C was characterized by the highest content of  $\text{PAH}_{\text{free}}$  (and simultaneously content of  $\Sigma\text{16PAH}_{\text{free}}$ ) -  $3.53 \pm 0.18 \text{ ng L}^{-1}$  (and  $3.18 \pm 0.16 \text{ ng L}^{-1}$ , respectively). In samples produced at higher temperatures, the total concentration of  $\Sigma\text{PAHs}$  and  $\Sigma\text{16PAHs}$  was:  $2.56 \pm 0.11 \text{ ng L}^{-1}$  and  $2.36 \pm 0.10 \text{ ng L}^{-1}$  in BCS600, and  $1.67 \pm 0.073 \text{ ng L}^{-1}$  and  $1.44 \pm 0.062 \text{ ng L}^{-1}$  in BCS700. The concentrations of identified 2-ring PAHs were below the limit of detection. The same situation was observed in the case of all BCW samples (Table S5). However, 3-ring PAHs were predominant in all straw-derived biochars (also in BCW samples). Among them, the most abundant were acenaphthene (52.3 %, 59.9 % and 59.9 % for BCSS500, BCS600 and BCS700, respectively) and acenaphthylene (38.9 %, 34.7 % and 31.4 %, respectively). 4-ring PAHs constituted also a significant part of all PAHs. The higher temperature of pyrolysis was applied, the higher percentage of 4 ring- $\text{PAH}_{\text{free}}$  was detected and quantified. In BCS500 PAHs with 4 aromatic rings constituted 1.10 % and among them 2-methylpyrene was predominant (61.5 %). In BCS600 and BCS700, the percentage of 4-ring PAHs increased up to 3.03 % and 6.26 %, respectively (Fig. 4). Among them, predominant compounds were 4-methylpyrene (38.3 %) and 2-methylpyrene (29.6 %) in BCS600, and 4-methylpyrene (66.3 %) for BCS700.

In willow-derived biochars obtained at 500, 600 and 700 °C,  $\text{C}_{\text{free}}$  of all quantitatively determined PAHs and  $\text{C}_{\text{free}}$  of  $\Sigma\text{16PAHs}$  changed very slightly ( $3.51 \pm 0.21 \text{ ng L}^{-1}$ ;  $3.34 \pm 0.20 \text{ ng L}^{-1}$  for BCW500,  $3.17 \pm 0.15 \text{ ng L}^{-1}$ ;  $2.92 \pm 0.14 \text{ ng L}^{-1}$  for BCW600, and  $3.53 \pm 0.17 \text{ ng L}^{-1}$ ;  $3.30 \pm 0.16 \text{ ng L}^{-1}$  for BCW700) (Table S5). In the case of BCW samples, as in BCS samples, 2-ring PAHs were also designated only qualitatively. Another similarity of willow-derived biochars to the samples obtained from straw was the predominance of 3-ring PAHs (98.41 % for BCW500; 97.78 % for BCW600 and 98.5 % for BCW700). And almost the same compounds were distinguished in percentage terms. In BCW500 (among all 3-ring PAHs), acenaphthylene amounted 47.5 %, acenaphthene 30.8 % and fluorene 18.1 %. In BCW600 and BCW700, the same compounds were distinguished but the proportions were different (acenaphthene 37.5 % and 50.6 %, fluorene 31.4 % and 35.1 %, acenaphthylene 24.6 % 11.3 %, for BCW600 and BCW700, respectively). 4, 5 and 6-ring PAHs constituted below 1.6 %, 2.3 % and 1.5 % for BCW500, BCW600 and BCW700, respectively (Fig. 4).

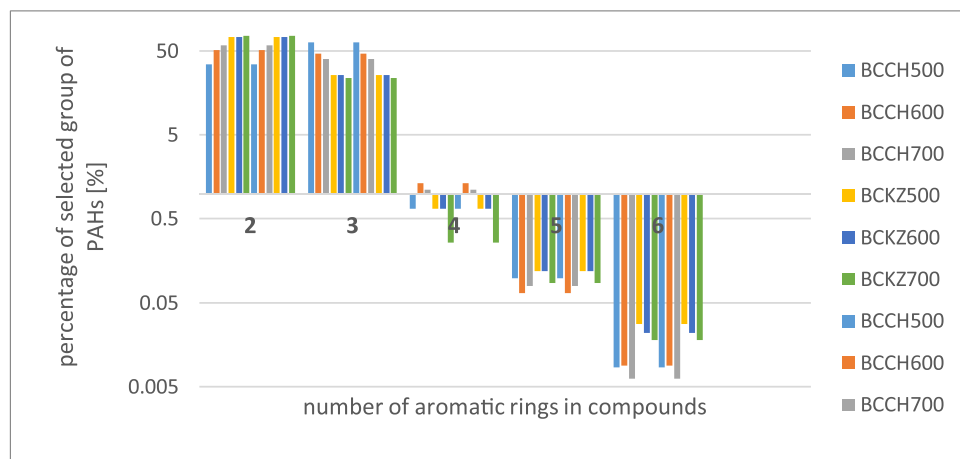


**Fig. 4.** PAHs and their derivatives in biochar samples considering the number of rings in molecules.

The applied feedstock affected both the type and the amount of PAHs and their derivatives in BC. The two factorial analysis of variance ( $p < 0.05$ ) was performed. The statistical analysis had shown the significant differences between the total concentration of bioavailable PAHs and their derivatives concentration and type of applied feedstock (ANOVA,  $p = 0.0046$ ). But on another hand, there were no significant differences between the total content of bioavailable PAHs and their derivatives concentration and applied temperature of pyrolysis (ANOVA,  $p = 0.4818$ ). An identical trend was observed in the case of total pristine PAHs concentration. The differences between the concentration of  $\Sigma$ PAHs and type of applied feedstock were significant (ANOVA,  $p = 0.0052$ ). On the contrary, there were no significant differences between the concentration of  $\Sigma$ PAHs and applied temperature of pyrolysis (ANOVA,  $p = 0.5633$ ). The performance of two factorial analyses of variance for PAHs derivatives concentration had shown the significant differences between these concentrations and pyrolysis temperature, and selected feedstock (ANOVA,  $p = 0.0035$  and  $p = 0.0250$ , respectively).

### 3.2.2. Bioavailable PAHs derivatives

As was expected, some PAHs derivatives were present in the prepared SSL-derived biochars. BCCH samples contained both N-PAHs and O-PAHs. The percentage of quantified PAHs derivatives in comparison to their parent PAHs was following 10.3 %, 9.4 %, and 2.6 % for BCCH500, BCCH600, and BCCH700; respectively indicating that the pyrolysis temperature affected the amount of created PAHs derivatives (Fig. 2b, Table S4). 1-methyl-5-nitronaphthalene and 1-methyl-6-nitronaphthalene were the 2-ring representatives of N-PAHs and they constituted 32.4 %; 16.5 % and 25.9 % of all derivatives for BCCH500, BCCH600, and BCCH700, respectively. The overwhelming majority of PAHs derivatives represented 4H-cyclopenta(def)phenanthrene (67.6 %, 83.5 % and 74.1 % respectively).

Completely different PAHs derivatives were quantified in BCKZ samples. In all samples nitronaphthalene, as a member of 2-ring PAHs derivatives, was noted and its concentration varied. Nitronaphthalene constituted 68.6 %, 62.6 % and 66.1 % of all PAHs derivatives for BCKZ500, BCKZ600, and BCKZ700, respectively (Fig. 2b). Considering O-PAHs, 3-ring PAHs derivatives were represented by 9, 10-anthracenedione (31.4 %, 37.4 % and 33.3 % for BCKZ500, BCKZ600 and BCKZ700, respectively). The percentage of PAHs derivatives in comparison to parent PAHs was 9.42 % for BCKZ500, 2.60 % for BCKZ600, and 5.29 % for BCKZ700. The data indicate that the amount and type of PAHs derivatives were connected both with the temperature of pyrolysis and applied SSL as feedstock.

In BCS samples (Table S5), PAHs derivatives, similar to those analyzed in BCCH, were quantified. In BCS500 only N-PAHs (1-methyl-

5-nitronaphthalene and 1-methyl-6-nitronaphthalene) were quantified. They constituted 100 % and 4.8 % from the sum of parent and derivatives of PAHs. In BCS600 and BCS700 additionally 4H-cyclopenta(def)phenanthrene was also quantified. In BCS600 the percentage of N-PAHs and O-PAHs amounted to 30.8 % and 69.2 %, respectively, while in BCS700 33.7 % of total PAHs were N-PAHs, and 66.3 % were O-PAHs. An increase in the pyrolysis temperature of straw was connected with an increased percentage of PAHs derivatives in comparison to their parent compounds: from 5 % in BCS500, 32.4 % BCS600 to 37.4 % in BCS700.

In BCW samples (Table S5) only 4-ring PAHs derivatives were quantified: nitropyrene and 4H-cyclopenta(def)phenanthrene. Generally, the amount of PAHs derivatives was the highest in the material obtained at a lower temperature of pyrolysis: 37.4 %. An increase in the temperature lowered the concentration of PAHs derivatives, however, the effect of temperature was not linear. In BCW600 the PAHs derivatives constituted 7.07 % and in BCW700 –PAHs derivatives were up to 15.1 %. Interestingly, 4H-cyclopenta(def)phenanthrene and nitropyrene were main PAHs derivatives noted at 97 % and 3 %, respectively. The differences in biochars obtained in the three temperatures were minor.

## 4. Discussion

The obtained results were consistent with the literature where the concentration of PAHs strongly depends on the type of feedstock [42]. Biochar obtained from wheat straw contained several times higher concentrations of PAHs than softwood-derived materials [23]. Among all PAHs and their derivatives in biochars, the majority were two- and three-ring compounds [13]. Multi-ringed species most commonly occurred in wheat straw-derived biochars. The concentration of PAH<sub>free</sub> for SSL-derived biochars in various studies differ from 44.3 to 50.5 ng L<sup>-1</sup> [13], 81 to 126 ng L<sup>-1</sup> [47]. Generally, SSL-derived biochars contained 91.1–92.2 % and 7.4–8.4 % of 2- and 3-rings compounds, respectively, as the most abundant PAHs [13]. In straw-derived biochar, C<sub>free</sub> content was low and constituted 1.74 ng L<sup>-1</sup>. The most abundant PAHs in this fraction were fluorene (39 %), phenanthrene (34 %), and anthracene (18 %) [32].

An increase in pyrolysis temperature caused a decrease in PAH<sub>free</sub> concentrations (apart from pine wood and the switch grass biochars [31]). Temperature and pressure plays also an important role in the differentiation of PAHs and their derivatives concentration. With decreasing temperature, the condensation took place and the concentration of compounds in the particle phase increased. The effect of the pressure is quite reverse [5].

The literature data indicate that basically, the higher the pyrolysis temperature was applied, the lowest the total concentrations of  $\Sigma$ PAHs

were received [13]. Devi and Saroha [48] found that the extractable PAHs concentration in paper mill sludge-derived biochar varied from  $322 \mu\text{g kg}^{-1}$  to  $16.916 \mu\text{g kg}^{-1}$ . While Yang et al. [42] investigated that contents of  $\Sigma 16\text{PAHs}$  in biochars derived from vegetable waste and pine cones ranging from 330 to  $6930 \mu\text{g kg}^{-1}$ . In both cases the significant effects of pyrolysis temperature are shown. The content of PAHs in studied biochar increased up to  $500^\circ\text{C}$  (with the maximum value at this temperature) then gradually decreased [48]. In another case, the effect of temperature can be also observed. Weidemann et al. [23] found that the higher applied HTT (the highest treatment temperature) was, the larger concentration of PAHs was. In the case of BCKZ and BCW samples, the higher temperature of pyrolysis was used, the higher concentration of bioavailable PAHs was obtained. In the other two cases, the tendency was not so clear. In the literature, it was observed that at a low-temperature mechanism ( $25$ – $300^\circ\text{C}$ ), no PAHs were detected. The contents of 2–5-ring PAHs increased in temperatures ranging  $400$ – $650^\circ\text{C}$ , whereas the contents of larger ring PAHs increased slightly. Fluorene and phenanthrene were predominant PAHs detected at  $600$  and  $650^\circ\text{C}$  [49], similarly to the results observed for BCW but not for BCS. Again, the data indicate that the type of feedstock affected the formation of bioavailable PAHs and their derivatives. On the other hand, Hale et al. [31] observed that among biochars obtained in different temperatures ( $250$ – $900^\circ\text{C}$ ) in fast pyrolysis, high temperature pyrolyzed BC (pine wood pyrolyzed at  $900^\circ\text{C}$  and  $600^\circ\text{C}$ , and in switch grass pyrolyzed at  $900^\circ\text{C}$  and  $800^\circ\text{C}$ ) were characterized by the lowest PAHs concentration. The highest amounts of PAHs were recorded within biochars produced in the  $350$ – $550^\circ\text{C}$  range. PAHs contents in biochars obtained via fast pyrolysis, slow pyrolysis, and gasification varied widely. Slow pyrolysis caused the lowest value of PAHs, while gasification—the highest. Hale et al. [31] suggested that some PAHs escaped to the gaseous phase during slow pyrolysis, whereas some condensed in biochar during fast pyrolysis. The content of solvent extractable PAHs were the greatest in biochar obtained in  $400$  and  $500^\circ\text{C}$  [50], which was, however, confirmed by our studies only in the case of BCS, whereas the amount of PAHs in BCW obtained at  $500^\circ\text{C}$  and  $700^\circ\text{C}$  was similar. The results considering SSL-derived BC were on the contrary.

Besides, the PAHs content in biochars was higher when the residence time was shorter and pyrolysis was faster [31]. PAHs with low molecular weight (MW) are formed at a temperature below  $500^\circ\text{C}$ , while compounds with high MW are created at a temperature above  $500^\circ\text{C}$  [21]. An increase in the pyrolysis temperature induced the formation of compounds with higher MW and a higher number of rings. These conclusions are consistent with the mechanisms demonstrated by Keiluweit et al. [50]. They presented two ways of PAHs formation which were distinguished by the pyrolysis temperatures. At temperatures below  $500^\circ\text{C}$  unimolecular cyclization, dehydrogenation, dealkylation and aromatization of two basic composition of biochar (lignin and cellulose), together with lipids took place. The disposal and removal of fractionabilities occurred, leaving aromatic structures. However, at the temperatures above  $500^\circ\text{C}$  PAHs are created via a free radical pathway (compounds are cracked into smaller hydrocarbon radicals) and pyro-synthesis into greater aromatic structures (combined into more stable LMW PAHs), and with the increasing of pyrolysis temperature and residence time, fuse into HMW PAHs [51]. At the temperature higher than  $950^\circ\text{C}$ , the rate of PAHs formation decreased [52] due to its dissociation into small molecule consists of hydrogen and carbon or polycondensation into coke [53]. Another Researchers suggested that the synthesis and decomposition of PAHs occurs at the same time [54]. They also presented several mechanisms of PAHs formation from which the hydrogen abstraction acetylene addition mechanisms is the most widely accepted. Acetylene and phenol are the most important precursors of PAHs, 2-ring PAHs are formed mostly from single-aromatic-ring compounds, and PAHs with more than 2 rings may create from 2- and 1-ring species. They demonstrated the reactions of PAHs formation. 1-aromatic ring species combined with acetylene and formed the intermediate product (this is typically acenaphthylene) and

by-product as hydrogen. Than 2-ring PAHs are created. This reaction is privileged because the higher reactivity of 1, 2 double bond in acenaphthylene than 3, 4 and 4, 5 aromatic bonds [54]. Apparently, in the case of our studies, the tendency is contrary. Over 97 % of all PAHs in plant-derived BC constituted 3-ring compounds. While the great majority of PAHs present in SSL-derived BC constituted 2 and 3-ring compounds. But if we take the mechanism described above as correct and occurring in the case of our biochar samples, than it can be suggested that in BCS and BCW the residence time was relevant and suitable to create 3-ring PAHs from 2-ring species. In BCCH and BCKZ these reactions were slower despite the same residence time during biochar production. Therefore the average ratio between 2-ring and 3-ring species in plant derived BC amounted 0:97, and in SSL-derived BC 61:38. The main difference stemmed from the type of feedstock. In BC obtained from plants PAHs with more than 2 rings were created more rapidly than in BC produced from sewage sludge.

Weidemann et al. [23] studied the influence of pyrolysis temperature on the formation of selected PAHs and their derivatives in biochars. The objects of the study were biochars obtained from softwood (pine and spruce) pellets, wheat straw pellets, and anaerobically digested sewage sludge. They determined 16 EPA priority PAHs, 11 O-PAHs, and 4 N-PAHs. The concentration of  $\Sigma\text{PAHs}$  varied from  $0.82$  to  $19.6 \mu\text{g g}^{-1}\text{biochar}^{-1}$ , while total O-PAHs and N-PAHs concentrations amounted  $34$ – $3100 \text{ ng g}^{-1}\text{biochar}^{-1}$  and  $0.4$ – $477 \text{ ng g}^{-1}\text{biochar}^{-1}$ , respectively. Multi-ringed species most commonly occurred in wheat straw-derived biochars. The authors tested the total fraction of PAHs and their derivatives in biochars. As some PAHs may be not bioavailable, the number of bioavailable O-PAHs and N-PAHs in our studies (6) is lower.

## 5. Conclusions

It is known that PAHs (and consequently their derivatives) are present in biochar samples. Some of them are bioavailable, so they can migrate into the environment. It is associated with the potential of biochar applications. Considerable interest is observed in the agricultural use of biochar. Biochar is regarded as fertilizer and soil conditioner. Its addition into soil improves their quality, accelerates the degradation of organic pollutants like humic substances, and improves crop productivity (applied with nitrogen fertilizer). Biochar plays an important role in the amelioration, revegetation, and restoration of contaminated soils.

The applied feedstock affected both the type and the amount of bioavailable PAHs and their derivatives in BC. Generally, in the case of SSL-derived BC, the higher temperature was applied, the higher content of naphthalene and the lower content of 3-ring PAHs were detected. 3-ring PAHs were predominant in plant-derived biochars. Interestingly, in BCCH fraction of  $\Sigma 16\text{PAH}_{\text{free}}$  was predominant and constituted 98 %–99 % of all  $C_{\text{free}}$ , whereas in BCKZ the percentage of  $\Sigma 16\text{PAH}_{\text{free}}$  was significantly lower (50 %–75 %). In BCS and BCW samples, increasing pyrolysis temperature caused a decrease in the total concentration of bioavailable  $\Sigma\text{PAHs}$  and  $\Sigma 16\text{PAHs}$ .

PAHs derivatives e.g. N-PAHs and O-PAHs were present in BC and data indicated that the amount and type of PAHs derivatives were connected both with the temperature of pyrolysis and applied feedstock. The percentage of quantified PAHs derivatives in SSL-derived BC was following 9.42 %–10.3 %, 2.60 %–9.4 % and 5.29 %–2.6 % for BC obtained at  $500^\circ\text{C}$ ,  $600^\circ\text{C}$  and  $700^\circ\text{C}$ , respectively. Plant-derived BC were enriched in PAHs derivatives as an increase of the pyrolysis temperature of straw was connected with an increased percentage of PAHs derivatives in comparison to their parent compounds from 5 % to 37.4 % ( $500$ – $700^\circ\text{C}$ ). An increase in the temperature lowered the concentration of PAHs derivatives from 37 % to 15 %; however, the effect of temperature was not linear. The presence of toxic compounds such as 1-methyl-5-nitronaphthalene, 1-methyl-6-nitronaphthalene, or nitropyrene in plant-derived BC and B[a]P and PAHs derivatives: nitronaphthalene, 9,10-anthracenedione in SSL-derived BC may significantly

affect their agricultural applications.

## CRediT authorship contribution statement

**Agnieszka Krzyszczak:** Investigation, Visualization, Writing - review & editing. **Michał P. Dybowski:** Investigation, Methodology, Visualization. **Bożena Czech:** Investigation, Methodology, Visualization, Writing - review & editing, Conceptualization, Validation, Supervision.

## Declaration of Competing Interest

The authors declare that they have no known competing financial interests or personal relationships that could have appeared to influence the work reported in this paper.

## Acknowledgements

The studies were supported by the project No. 2018/31/B/NZ9/00317 funded by the National Science Centre, Poland.

## Appendix A. Supplementary data

Supplementary material related to this article can be found, in the online version, at doi:<https://doi.org/10.1016/j.jaat.2021.105339>.

## References

- [1] H. Zheng, C. Qu, J. Zhang, S.A. Talpur, Y. Ding, X. Xing, S. Qi, Polycyclic aromatic hydrocarbons (PAHs) in agricultural soils from Ningde, China: levels, sources, and human health risk assessment, *Environ. Geochem. Health* 41 (2019) 907–919, <https://doi.org/10.1007/s10653-018-0188-7>.
- [2] W. Buss, M.C. Graham, G. MacKinnon, O. Mašek, Strategies for producing biochars with minimum PAH contamination, *J. Anal. Appl. Pyrolysis* 119 (2016) 24–30, <https://doi.org/10.1016/j.jaat.2016.04.001>.
- [3] A. Krzyszczak, B. Czech, Occurrence and toxicity of polycyclic aromatic hydrocarbon derivatives in environmental matrices, *Sci. Total Environ.* 788 (2021), 147738, <https://doi.org/10.1016/j.scitotenv.2021.147738>.
- [4] R.K. Rajpara, D.R. Dudhagara, J.K. Bhatt, H.B. Gosai, B.P. Dave, Polycyclic aromatic hydrocarbons (PAHs) at the Gulf of Kutch, Gujarat, India: occurrence, source apportionment, and toxicity of PAHs as an emerging issue, *Mar. Pollut. Bull.* 119 (2017) 231–238, <https://doi.org/10.1016/j.marpolbul.2017.04.039>.
- [5] B.A.M. Bandowé, H. Meusel, R. Huang, K. Ho, J. Cao, T. Hoffmann, W. Wilcke, PM2.5-bound oxygenated PAHs, nitro-PAHs and parent-PAHs from the atmosphere of a Chinese megacity: seasonal variation, sources and cancer risk assessment, *Sci. Total Environ.* 473–474 (2014) 77–87, <https://doi.org/10.1016/j.scitotenv.2013.11.108>.
- [6] J. Ringuet, E. Leoz-Garziandia, H. Budzinski, E. Villenave, A. Albinet, Particle size distribution of nitrated and oxygenated polycyclic aromatic hydrocarbons (NPAHs and OPAHs) on traffic and suburban sites of a European megacity: Paris (France), *Atmos. Chem. Phys.* 12 (2012) 8877–8887.
- [7] Y. Ren, B. Zhou, J. Tao, Z. Zhang, C. Wu, J. Wang, J. Li, L. Zhang, Y. Han, L. Liu, C. Cao, G. Wang, Composition and size distribution of airborne particulate PAHs and oxygenated PAHs in two Chinese megacities, *Atmos. Res.* 183 (2017) 322–330, <https://doi.org/10.1016/j.atmosres.2016.09.015>.
- [8] L. Feng, J. Luo, Y. Chen, Dilemma of sewage sludge treatment and disposal in China, *Environ. Sci. Technol.* 49 (2015) 4781–4782, <https://doi.org/10.1021/acs.est.5b01455>.
- [9] S.R. Smith, Organic contaminants in sewage sludge (biosolids) and their significance for agricultural recycling, *Philos. Trans. A Math. Phys. Eng. Sci.* 367 (2009) 4005–4041, <https://doi.org/10.1098/rsta.2009.0154>.
- [10] S. Werle, M. Dudziak, Analysis of organic and inorganic contaminants in dried sewage sludge and by-products of dried sewage sludge gasification, *Energies* 7 (2014) 462–476, <https://doi.org/10.3390/en7010462>.
- [11] P.S. Khillare, V.K. Sattawan, D.S. Jyethi, Profile of polycyclic aromatic hydrocarbons in digested sewage sludge, *Environ. Technol.* 41 (2020) 842–851, <https://doi.org/10.1080/09593330.2018.1512654>.
- [12] J.M. Moreda, A. Arranz, S. Fdez De Betono, A. Cid, J.F. Arranz, Chromatographic determination of aliphatic hydrocarbons and polycyclic aromatic hydrocarbons (PAHs) in a sewage sludge, *Sci. Total Environ.* 220 (1998) 33–43, [https://doi.org/10.1016/S0048-9697\(98\)00238-1](https://doi.org/10.1016/S0048-9697(98)00238-1).
- [13] M. Kończak, P. Oleszczuk, K. Różyło, Application of different carrying gases and ratio between sewage sludge and willow for engineered (smart) biochar production, *J. CO<sub>2</sub> Util.* 29 (2019) 20–28, <https://doi.org/10.1016/j.jcou.2018.10.019>.
- [14] M. Hassan, Y. Liu, R. Naidu, S.J. Parikh, J. Du, F. Qi, I.R. Willett, Influences of feedstock sources and pyrolysis temperature on the properties of biochar and functionality as adsorbents: a meta-analysis, *Sci. Total Environ.* 744 (2020), 140714, <https://doi.org/10.1016/j.scitotenv.2020.140714>.
- [15] J. Zhao, X.-J. Shen, X. Domene, J.-M. Alcañiz, X. Liao, C. Palet, Comparison of biochars derived from different types of feedstock and their potential for heavy metal removal in multiple-metal solutions, *Sci. Rep.* 9 (2019) 9869, <https://doi.org/10.1038/s41598-019-46234-4>.
- [16] P. Pariyar, K. Kumar, M.K. Jain, P.S. Jadhao, Evaluation of change in biochar properties derived from different feedstock and pyrolysis temperature for environmental and agricultural application, *Sci. Total Environ.* 713 (2020), 136433, <https://doi.org/10.1016/j.scitotenv.2019.136433>.
- [17] B. Chen, D. Zhou, L. Zhu, Transitional adsorption and partition of nonpolar and polar aromatic contaminants by biochars of pine needles with different pyrolytic temperatures, *Environ. Sci. Technol.* 42 (2008) 5137–5143, <https://doi.org/10.1021/es0802684>.
- [18] J. Pietikäinen, O. Kiikkilä, H. Fritz, Charcoal as habitat for microbes and its effect on the microbial community of the underlying humus, *Oikos* 89 (2000) 231–242, <https://doi.org/10.1043/j.1600-0706.2000.890203.x>.
- [19] O. Lei, R. Zhang, Effects of biochars derived from different feedstocks and pyrolysis temperatures on soil physical and hydraulic properties, *J. Soils Sediments* 13 (2013) 1561–1572, <https://doi.org/10.1007/s11368-013-0738-7>.
- [20] M. Kończak, P. Oleszczuk, Application of biochar to sewage sludge reduces toxicity and improves organisms growth in sewage sludge-amended soil in long term field experiment, *Sci. Total Environ.* 625 (2018) 8–15, <https://doi.org/10.1016/j.scitotenv.2017.12.118>.
- [21] C. Wang, Y. Wang, H.M.S.K. Herath, Polycyclic aromatic hydrocarbons (PAHs) in biochar – their formation, occurrence and analysis: a review, *Org. Geochem.* 114 (2017) 1–11, <https://doi.org/10.1016/j.orggeochem.2017.09.001>.
- [22] Hans-Peter Schmidt, European Biochar Certificate (EBC) - Guidelines Version 9.2G Vom 2, 2020, <https://doi.org/10.13140/RG.2.1.4658.7043>.
- [23] E. Weidemann, W. Buss, M. Edo, O. Mašek, S. Jansson, Influence of pyrolysis temperature and production unit on formation of selected PAHs, oxy-PAHs, N-PACs, PCDDs, and PCDFs in biochar—a screening study, *Environ. Sci. Pollut. Res.* 25 (2018) 3933–3940, <https://doi.org/10.1007/s11356-017-0612-z>.
- [24] I. Abbas, G. Badran, A. Verdin, F. Ledoux, M. Roumić, D. Courcot, G. Garçon, Polycyclic aromatic hydrocarbon derivatives in airborne particulate matter: sources, analysis and toxicity, *Environ. Chem. Lett.* 16 (2018) 439–475, <https://doi.org/10.1007/s10311-017-0697-0>.
- [25] H. Tokiwa, Y. Ohnishi, Mutagenicity and carcinogenicity of nitroarenes and their sources in the environment, *Crit. Rev. Toxicol.* 17 (1986) 23–60, <https://doi.org/10.3109/10408448609037070>.
- [26] A. Neophytou, J. Hart, Y. Chang, J. Zhang, T. Smith, E. Garshick, F. Laden, Short-term traffic-related exposures and biomarkers of nitro-PAH exposure and oxidative DNA damage, *Toxicics* 2 (2014) 377–390, <https://doi.org/10.3390/toxics2030377>.
- [27] Y.-D. Kim, Y.-J. Ko, T. Kawamoto, H. Kim, The effects of 1-nitropyrene on oxidative DNA damage and expression of DNA repair enzymes, *J. Occup. Health* 47 (2005) 261–266, <https://doi.org/10.1539/joh.47.261>.
- [28] C. Walgraeve, K. Demeestere, J. Dewulf, R. Zimmermann, H. Van Langenhove, Oxygenated polycyclic aromatic hydrocarbons in atmospheric particulate matter: molecular characterization and occurrence, *Atmos. Environ.* 44 (2010) 1831–1846, <https://doi.org/10.1016/j.atmosenv.2009.12.004>.
- [29] I.M. Kooter, M.J. Alblas, A.D. Jedynska, M. Steenhof, M.M.G. Houtzager, M. van Ras, Alveolar epithelial cells (A549) exposed at the air-liquid interface to diesel exhaust: first study in TNO's powertrain test center, *Toxicol. Vitr.* 27 (2013) 2342–2349, <https://doi.org/10.1016/j.tiv.2013.10.007>.
- [30] C. Wang, J. Yang, L. Zhu, L. Yan, D. Lu, Q. Zhang, M. Zhao, Z. Li, Never deem lightly the “less harmful” low-molecular-weight PAH, NPAH, and OPAH — disturbance of the immune response at real environmental levels, *Chemosphere* 168 (2017) 568–577, <https://doi.org/10.1016/j.chemosphere.2016.11.024>.
- [31] S.E. Hale, J. Lehmann, D. Rutherford, A.R. Zimmerman, R.T. Bachmann, V. Shitumbanuma, A. O'Toole, K.L. Sundqvist, H.P.H. Arp, G. Cornelissen, Quantifying the total and bioavailable polycyclic aromatic hydrocarbons and dioxins in biochars, *Environ. Sci. Technol.* 46 (2012) 2830–2838, <https://doi.org/10.1021/es203984k>.
- [32] P. Oleszczuk, M. Kuśmierz, P. Godlewski, P. Kraska, E. Palys, The concentration and changes in freely dissolved polycyclic aromatic hydrocarbons in biochar-amended soil, *Environ. Pollut.* 214 (2016) 748–755, <https://doi.org/10.1016/j.envpol.2016.04.064>.
- [33] S. Josefsson, H.P.H. Arp, D.B. Kleja, A. Enell, S. Lundstedt, Determination of polyoxymethylene (POM) – water partition coefficients for oxy-PAHs and PAHs, *Chemosphere* 119 (2015) 1268–1274, <https://doi.org/10.1016/j.chemosphere.2014.09.102>.
- [34] S.B. Hawthorne, M.T.O. Jonker, S.A. van der Heijden, C.B. Grabanski, N. Azzolina, D.J. Miller, Measuring picogram per liter concentrations of freely dissolved parent and alkyl PAHs (PAH-34), using passive sampling with polyoxymethylene, *Anal. Chem.* 83 (2011) 6754–6761, <https://doi.org/10.1021/ac201411v>.
- [35] Hans-Peter Schmidt, European Biochar Certificate (EBC) - Guidelines Version 6.1, 2015, <https://doi.org/10.13140/RG.2.1.4658.7043>.
- [36] A. Bogusz, P. Oleszczuk, Sequential extraction of nickel and zinc in sewage sludge- or biochar/sewage sludge-amended soil, *Sci. Total Environ.* 636 (2018) 927–935, <https://doi.org/10.1016/j.scitotenv.2018.04.072>.
- [37] M. Kończak, Y. Gao, P. Oleszczuk, Carbon dioxide as a carrier gas and biomass addition decrease the total and bioavailable polycyclic aromatic hydrocarbons in biochar produced from sewage sludge, *Chemosphere* 228 (2019) 26–34, <https://doi.org/10.1016/j.chemosphere.2019.04.029>.

- [38] P. Oleszczuk, M. Kołtowski, Changes of total and freely dissolved polycyclic aromatic hydrocarbons and toxicity of biochars treated with various aging processes, Environ. Pollut. 237 (2018) 65–73, <https://doi.org/10.1016/j.envpol.2018.01.073>.
- [39] A. Zielińska, P. Oleszczuk, B. Charmas, J. Skubiszewska-Zięba, S. Pasieczna-Patkowska, Effect of sewage sludge properties on the biochar characteristic, J. Anal. Appl. Pyrolysis 112 (2015) 201–213, <https://doi.org/10.1016/j.jaat.2015.01.025>.
- [40] J. Zhang, J. Liu, R. Liu, Effects of pyrolysis temperature and heating time on biochar obtained from the pyrolysis of straw and lignosulfonate, Bioreour. Technol. 176 (2015) 288–291, <https://doi.org/10.1016/j.biortech.2014.11.011>.
- [41] P. Cely, A.M. Tarquis, J. Paz-Ferreiro, A. Méndez, G. Gascó, Factors driving the carbon mineralization priming effect in a sandy loam soil amended with different types of biochar, Solid Earth 5 (2014) 585–594, <https://doi.org/10.5194/se-5-585-2014>.
- [42] X. Yang, W. Ng, B.S.E. Wong, G.H. Baeg, C.-H. Wang, Y.S. Ok, Characterization and ecotoxicological investigation of biochar produced via slow pyrolysis: effect of feedstock composition and pyrolysis conditions, J. Hazard. Mater. 365 (2019) 178–185, <https://doi.org/10.1016/j.jhazmat.2018.10.047>.
- [43] J.-H. Yuan, R.-K. Xu, H. Zhang, The forms of alkalis in the biochar produced from crop residues at different temperatures, Bioreour. Technol. 102 (2011) 3488–3497, <https://doi.org/10.1016/j.biortech.2010.11.018>.
- [44] C.H. Chia, B. Gong, S.D. Joseph, C.E. Marjo, P. Munroe, A.M. Rich, Imaging of mineral-enriched biochar by FTIR, Raman and SEM-EDX, Vib. Spectrosc. 62 (2012) 248–257, <https://doi.org/10.1016/j.vibspec.2012.06.006>.
- [45] J. Lehmann, J. Pereira da Silva Jr., C. Steiner, T. Nehls, W. Zech, B. Glaser, Nutrient availability and leaching in an archaeological Anthrosol and a Ferralsol of the Central Amazon basin: fertilizer, manure and charcoal amendments, Plant Soil 249 (2003) 343–357, <https://doi.org/10.1023/A:1022833116184>.
- [46] L.Q. Pan, J. Ren, J. Liu, Responses of antioxidant systems and LPO level to benzo(a)pyrene and benzo(k)fluoranthene in the haemolymph of the scallop Chlamys ferrari, Environ. Pollut. 141 (2006) 443–451, <https://doi.org/10.1016/j.envpol.2005.08.069>.
- [47] A. Zielińska, P. Oleszczuk, Effect of pyrolysis temperatures on freely dissolved polycyclic aromatic hydrocarbon (PAH) concentrations in sewage sludge-derived biochars, Chemosphere 153 (2016) 68–74, <https://doi.org/10.1016/j.chemosphere.2016.02.118>.
- [48] P. Devi, A.K. Saroha, Effect of pyrolysis temperature on polycyclic aromatic hydrocarbons toxicity and sorption behaviour of biochars prepared by pyrolysis of paper mill effluent treatment plant sludge, Bioreour. Technol. 192 (2015) 312–320, <https://doi.org/10.1016/j.biortech.2015.05.084>.
- [49] T.E. McGrath, W.G. Chan, M.R. Hajaligol, Low temperature mechanism for the formation of polycyclic aromatic hydrocarbons from the pyrolysis of cellulose, J. Anal. Appl. Pyrolysis 66 (2003) 51–70, [https://doi.org/10.1016/S0165-2370\(02\)00105-5](https://doi.org/10.1016/S0165-2370(02)00105-5).
- [50] M. Keiluweit, M. Kleber, M.A. Sparrow, B.R.T. Simoneit, F.G. Prahl, Solvent-extractable polycyclic aromatic hydrocarbons in biochar: influence of pyrolysis temperature and feedstock, Environ. Sci. Technol. 46 (2012) 9333–9341, <https://doi.org/10.1021/es302125k>.
- [51] T.D. Bucheli, I. Hilber, H.-P. Schmidt, Polycyclic aromatic hydrocarbons and polychlorinated aromatic compounds in biochar, Biochar for Environmental Management, Routledge, 2015, pp. 593–622.
- [52] Q. Dai, X. Jiang, Y. Jiang, Y. Jin, F. Wang, Y. Chi, J. Yan, Formation of PAHs during the pyrolysis of dry sewage sludge, Fuel 130 (2014) 92–99, <https://doi.org/10.1016/j.fuel.2014.04.017>.
- [53] T. McGrath, R. Sharma, M. Hajaligol, An experimental investigation into the formation of polycyclic-aromatic hydrocarbons (PAH) from pyrolysis of biomass materials, Fuel 80 (2001) 1787–1797, [https://doi.org/10.1016/S0016-2361\(01\)00062-X](https://doi.org/10.1016/S0016-2361(01)00062-X).
- [54] L. Zhao, Y. Zhao, H. Nan, F. Yang, H. Qiu, X. Xu, X. Cao, Suppressed formation of polycyclic aromatic hydrocarbons (PAHs) during pyrolytic production of Fe-enriched composite biochar, J. Hazard. Mater. 382 (2020), 121033, <https://doi.org/10.1016/j.jhazmat.2019.121033>.

**Formation of polycyclic aromatic hydrocarbons and their derivatives in biochars: the  
effect of feedstock and pyrolysis conditions**

Agnieszka Krzyszczak<sup>1</sup>, Michał P. Dybowski<sup>2</sup>, Bożena Czech<sup>1\*</sup>

<sup>1</sup>Department of Radiochemistry and Environmental Chemistry, Institute of Chemical Sciences, Faculty of Chemistry, Maria Curie-Sklodowska University in Lublin, Pl. M. Curie-Sklodowskiej 3, 20-031 Lublin, Poland

<sup>2</sup>Department of Chromatography, Institute of Chemical Sciences, Faculty of Chemistry, Maria Curie Skłodowska University in Lublin, Pl. M. Curie-Sklodowskiej 3, 20-031 Lublin, Poland

\*corresponding author: Tel.: +48 81 537 55 54; fax: +48 81 537 55 65; E-mail address:  
[bczech@hektor.umcs.lublin.pl](mailto:bczech@hektor.umcs.lublin.pl) (B. Czech)

No. of pages: 5

No. of tables: 2

No. of Figures: 0

## 2. Materials and methods

### 2.2. Biochar preparation

Table S1. The feedstock and pyrolysis temperature of tested biochars.

Feedstock	Pyrolysis temperature [°C]	Labels	Feedstock	Pyrolysis temperature [°C]	Labels
SSL Chełm	500	BCCH500	Willow	500	BCW500
	600	BCCH600		600	BCW600
	700	BCCH700		700	BCW700
SSL Kalisz	500	BCKZ500	Straw	500	BCS500
	600	BCKZ600		600	BCS600
	700	BCKZ700		700	BCS700

### 2.3. The physico-chemical properties of biochar

The pH of 1g of biochar mixed with 10 mL of deionized water was determined by a digital pH meter HQ430d Benchtop Single Input (HACH, USA). To quantified the elemental carbon (C), hydrogen (H), and nitrogen (N), biochar was milled and EuroEA Elemental Analyser was applied. ASAP 2420 (Micromeritics, USA) surface area and porosity analyzer was used for adsorption measurements and biochars were outgassed at 200°C for 12 h under vacuum. FT-IR/PAS spectra of the samples were recorded by Bio-Rad Excalibur 3000 MX spectrometer provided with photoacoustic detector MTEC300 (in the helium atmosphere in a detector) at RT over the 4000-400  $\text{cm}^{-1}$  range at the resolution of 4  $\text{cm}^{-1}$  and maximum source aperture. X-ray photoelectron spectroscopy (UHV Prevac) was used for the determination of surface functional groups of BC, whereas surface morphology was examined by scanning electron microscopy (Quanta 3D FEG, FEI).

### 2.5. GC–MS/MS measurements

Qualitative and quantitative analyses of PAHs (Table S2) were conducted using a gas chromatograph hyphenated with a triple quadruple tandem mass spectrometer detector (GCMS-TQ8040; Shimadzu, Kyoto, Japan) equipped with a ZB5-MSi fused-silica capillary column (30 m × 0.25 mm i.d., 0.25  $\mu\text{m}$  film thickness; Phenomenex, Torrance, CA, USA). Helium (grade 5.0) as a carrier gas and argon (grade 5.0) as collision gas were used. Column flow was 1.56  $\text{mL min}^{-1}$ , and 1  $\mu\text{L}$  of the sample was injected by an AOC-20i+s type

autosampler (Shimadzu). The injector was working in high-pressure mode (250.0 kPa for 1.5 min; column flow at initial temperature was 4.90 mL min<sup>-1</sup>) at the temperature of 310°C; the ion source temperature was 225°C. For qualitative purposes, the full scan mode with range 40-550 *m/z* was employed and for quantitative analyses, the SIM mode was used (Table S3).

Table S2. Chemical characteristics of analyzed compounds.

No.	Compound	CAS <sup>(1)</sup>	MW <sup>(2)</sup>	Formula
1	Naphthalene*	91-20-3	128.17	C <sub>10</sub> H <sub>8</sub>
2	Acenaphthylene*	208-96-8	152.20	C <sub>12</sub> H <sub>8</sub>
3	Acenaphthene*	83-32-9	154.20	C <sub>12</sub> H <sub>10</sub>
4	Fluorene*	86-73-7	166.22	C <sub>13</sub> H <sub>10</sub>
5	Anthracene*	120-12-7	178.23	C <sub>14</sub> H <sub>10</sub>
6	Phenanthrene*	85-01-8	178.23	C <sub>14</sub> H <sub>10</sub>
7	3-Methylphenanthrene	832-71-3	192.25	C <sub>15</sub> H <sub>12</sub>
8	2-Methylphenanthrene	2531-84-2	192.25	C <sub>15</sub> H <sub>12</sub>
9	9-Methylphenanthrene	883-20-5	192.25	C <sub>15</sub> H <sub>12</sub>
10	Fluoranthene*	206-44-0	202.25	C <sub>16</sub> H <sub>10</sub>
11	Pyrene*	129-00-0	202.25	C <sub>16</sub> H <sub>10</sub>
12	2-Phenylnaphthalene	612-94-2	204.26	C <sub>16</sub> H <sub>12</sub>
13	3,6-dimethylphenanthrene	1576-67-6	206.28	C <sub>16</sub> H <sub>14</sub>
14	Benzo[a]fluorene	238-84-6	216.27	C <sub>17</sub> H <sub>12</sub>
15	2-Methylpyrene	3442-78-2	216.28	C <sub>17</sub> H <sub>12</sub>
16	4-Methylpyrene	3353-12-6	216.28	C <sub>17</sub> H <sub>12</sub>
17	Benzo[a]anthracene*	56-55-3	228.29	C <sub>18</sub> H <sub>12</sub>
18	Chryzene*	218-01-9	228.29	C <sub>18</sub> H <sub>12</sub>
19	3-Methylchrysene	3351-31-3	242.30	C <sub>19</sub> H <sub>14</sub>
20	6-Methylchrysene	1705-85-7	242.30	C <sub>19</sub> H <sub>14</sub>
21	Benzo[a]fluoranthene	203-33-8	252.31	C <sub>20</sub> H <sub>12</sub>
22	Benzo[b]fluoranthene*	205-99-2	252.31	C <sub>20</sub> H <sub>12</sub>
23	Benzo[a]pyrene*	50-32-8	252.31	C <sub>20</sub> H <sub>12</sub>
24	Benzo[k]fluoranthene*	207-08-9	252.32	C <sub>20</sub> H <sub>12</sub>
25	Indeno[1,2,3-cd]pyrene*	193-39-5	276.33	C <sub>22</sub> H <sub>12</sub>
26	Benzo[ghi]perylene*	191-24-2	276.33	C <sub>22</sub> H <sub>12</sub>
27	Dibenzo[a,h]anthracene*	53-70-3	278.10	C <sub>22</sub> H <sub>14</sub>

N- and O-PAHs

28	Nitronaphthalene	86-57-7	173.16	C <sub>10</sub> H <sub>7</sub> NO <sub>2</sub>
29	1-Methyl-5-nitronaphthalene	91137-27-8	187.19	C <sub>11</sub> H <sub>9</sub> NO <sub>2</sub>
30	1-Methyl-6-nitronaphthalene	105752-67-8	187.19	C <sub>11</sub> H <sub>9</sub> NO <sub>2</sub>
31	9,10-Anthracenedione	84-65-1	208.21	C <sub>14</sub> H <sub>8</sub> O <sub>2</sub>
32	4H-cyclopenta(def)phenanthrene	203-64-5	190.24	C <sub>15</sub> H <sub>10</sub>
33	Nitropyrene	5522-43-0	247.25	C <sub>16</sub> H <sub>9</sub> NO <sub>2</sub>

<sup>(1)</sup>numerical identifier assigned by the Chemical Abstracts Service (CAS)

<sup>(2)</sup>MW-molecular weight

\* PAHs belonging to 16PAHs which have been classified by the United States Environmental Protection Agency (USEPA) as priority pollutants [1]

Table S3. The qualitative and quantitative parameters of PAHs and O/N-PAHs analysis.

No .	Compound	Quantification ion (m/z)	Confirmation ion (m/z)	LOD* [µg L <sup>-1</sup> ]	LOQ** [µg L <sup>-1</sup> ]
1	Naphthalene	128	102	1.01	3.36
2	Acenaphthylene	152	76	2.10	6.99
3	Acenaphthene	153	76	2.30	7.66
4	Fluorene	166	82	1.10	3.66
5	Anthracene	178	89	1.30	4.33
6	Phenanthrene	178	89	1.34	4.36
7	3-Methylphenanthrene	192	165	2.42	8.06
8	2-Methylphenanthrene	192	165	2.42	8.06
9	9-Methylphenanthrene	192	96	3.23	10.76
10	Fluoranthene	202	101	1.87	6.22
11	Pyrene	202	101	1.91	6.36
12	2-Phenylnaphthalene	204	101	1.90	6.33
13	3,6-dimethylphenanthrene	206	191	2.20	7.33
14	Benzo[a]fluorene	216	107	1.30	4.33
15	2-Methylpyrene	216	108	1.92	6.39
16	4-Methylpyrene	216	108	1.92	6.39
17	Benzo[a]anthracene	228	114	1.30	4.33
18	Chryzene	228	113	2.20	7.33
19	3-Methylchrysene	242	121	1.02	3.40
20	6-Methylchrysene	242	119	1.02	3.40
21	Benzo[a]fluoranthene	252	126	2.10	6.99
22	Benzo[b]fluoranthene	252	126	2.10	6.99

23	Benzo[a]pyrene	252	126	2.11	7.03
24	Benzo[k]fluoranthene	252	126	2.10	6.99
25	Indeno[1,2,3-cd]pyrene	276	138	1.30	4.33
26	Benzo[ghi]perylene	276	138	1.33	4.43
27	Dibenzo[a,h]anthracene	278	139	2.21	7.36
N- and O-PAHs					
28	Nitronaphthalene	173	127	2.41	8.03
29	1-Methyl-5-nitronaphthalene	187	115	1.21	4.03
30	1-Methyl-6-nitronaphthalene	187	115	1.21	4.03
31	9,10-Anthracenedione	208	180	1.44	4.80
32	4H-cyclopenta(def)phenanthrene	190	94	3.01	10.02
33	Nitropyrene	247	201	1.66	5.53

\*-LOD – limit of detection; \*\*-LOQ – limit of quantitation; LOD and LOQ were not calculated via K<sub>POM</sub>

Table S4. PAHs and their derivatives in SSL-derived BC samples (n=3; n-number of replicates).

No.	Compound	Sample description					
		BCCH500	BCCH600	BCCH700	BCKZ500	BCKZ600	BCKZ700
		Analyte concentration [ng L <sup>-1</sup> ]					
1	Naphthalene	3.17 ± 0.15	4.69 ± 0.22	5.49 ± 0.27	2.02 ± 0.09	5.05 ± 0.23	5.33 ± 0.25
2	Acenaphthylene	1.43 ± 0.06	1.54 ± 0.10	1.90 ± 0.12	< LOD	< LOD	< LOD
3	Acenaphthene	4.39 ± 0.20	2.34 ± 0.18	1.49 ± 0.07	1.22 ± 0.06	1.21 ± 0.06	1.98 ± 0.09
4	Fluorene	< LOD	< LOD	< LOD	0.98 ± 0.05	1.31 ± 0.05	1.61 ± 0.06
5	Anthracene	< LOD	0.35 ± 0.03	0.34 ± 0.02	< LOD	< LOD	< LOD
6	Phenanthrene	< LOD	< LOD				
7	3-Methylphenanthrene	< LOD	< LOD	< LOD	0.028 ± 1.3 · 10 <sup>-3</sup>	0.11 ± 5.2 · 10 <sup>-3</sup>	0.24 ± 0.01
8	2-Methylphenanthrene	< LOD	< LOD				
9	9-Methylphenanthrene	< LOD	< LOD				
10	Fluoranthene	< LOD	< LOD				
11	Pyrene	< LOD	< LOD				
12	2-Phenylnaphthalene	< LOD	< LOD	< LOD	4.27 ± 0.16	2.37 ± 0.11	6.84 ± 0.19
13	3,6-dimethylphenanthrene	< LOD	< LOD	0.063 ± 3.7 · 10 <sup>-3</sup>	< LOD	< LOD	< LOD
14	Benzo[a]fluorene	9.2 · 10 <sup>-3</sup> ± 4.1 · 10 <sup>-4</sup>	8.1 · 10 <sup>-3</sup> ± 3.8 · 10 <sup>-4</sup>	8.0 · 10 <sup>-3</sup> ± 3.7 · 10 <sup>-4</sup>	9.2 · 10 <sup>-3</sup> ± 4.3 · 10 <sup>-4</sup>	9.7 · 10 <sup>-3</sup> ± 4.5 · 10 <sup>-5</sup>	0.011 ± 5.0 · 10 <sup>-4</sup>
15	2-Methylpyrene	< LOD	0.028 ± 1.2 · 10 <sup>-3</sup>	< LOD	0.027 ± 1.5 · 10 <sup>-3</sup>	0.029 ± 1.3 · 10 <sup>-3</sup>	0.018 ± 8.2 · 10 <sup>-4</sup>

16	4-Methylpyrene	$0.041 \pm 2.1 \cdot 10^{-3}$	$0.071 \pm 3.2 \cdot 10^{-3}$	$0.093 \pm 4.0 \cdot 10^{-3}$	< LOD	< LOD	< LOD
17	Benzo[a]anthracene	< LOD	< LOD	< LOD	$8.9 \cdot 10^{-3} \pm 4.1 \cdot 10^{-4}$	$0.011 \pm 5.1 \cdot 10^{-4}$	$2.8 \cdot 10^{-3} \pm 1.3 \cdot 10^{-4}$
18	Chrysene	< LOD	< LOD	< LOD	$2.9 \cdot 10^{-3} \pm 1.4 \cdot 10^{-4}$	$9.6 \cdot 10^{-3} \pm 4.4 \cdot 10^{-4}$	$4.5 \cdot 10^{-3} \pm 2.2 \cdot 10^{-4}$
19	3-Methylchrysene	< LOD					
20	6-Methylchrysene	$9.1 \cdot 10^{-3} \pm 4.2 \cdot 10^{-4}$	$0.013 \pm 5.0 \cdot 10^{-4}$	$4.1 \cdot 10^{-3} \pm 2.0 \cdot 10^{-4}$	$8.4 \cdot 10^{-3} \pm 3.9 \cdot 10^{-4}$	$7.8 \cdot 10^{-3} \pm 3.7 \cdot 10^{-4}$	$4.8 \cdot 10^{-3} \pm 2.4 \cdot 10^{-4}$
21	Benzo[a]fluoranthene	< LOD	< LOD	< LOD	$3.7 \cdot 10^{-3} \pm 1.9 \cdot 10^{-4}$	$4.7 \cdot 10^{-3} \pm 2.5 \cdot 10^{-4}$	$6.0 \cdot 10^{-3} \pm 2.7 \cdot 10^{-4}$
22	Benzo[b]fluoranthene	< LOD	< LOD	< LOD	$4.8 \cdot 10^{-3} \pm 2.2 \cdot 10^{-4}$	$5.6 \cdot 10^{-3} \pm 2.6 \cdot 10^{-4}$	$7.0 \cdot 10^{-3} \pm 3.3 \cdot 10^{-4}$
23	Benzo[a]pyrene	$9.0 \cdot 10^{-3} \pm 3.9 \cdot 10^{-4}$	$6.0 \cdot 10^{-3} \pm 2.0 \cdot 10^{-4}$	$7.5 \cdot 10^{-3} \pm 3.5 \cdot 10^{-4}$	< LOD	< LOD	< LOD
24	Benzo[k]fluoranthene	< LOD					
25	Indene[1,2,3-cd]pyrene	$1.8 \cdot 10^{-4} \pm 8.1 \cdot 10^{-6}$	$1.9 \cdot 10^{-4} \pm 8.0 \cdot 10^{-6}$	$1.8 \cdot 10^{-4} \pm 8.2 \cdot 10^{-6}$	$5.7 \cdot 10^{-4} \pm 3.0 \cdot 10^{-5}$	$6.5 \cdot 10^{-4} \pm 3.3 \cdot 10^{-5}$	$8.2 \cdot 10^{-4} \pm 4.6 \cdot 10^{-5}$
26	Benzo[ghi]perylene	$6.0 \cdot 10^{-4} \pm 2.4 \cdot 10^{-5}$	$6.1 \cdot 10^{-4} \pm 2.4 \cdot 10^{-5}$	$4.1 \cdot 10^{-4} \pm 1.9 \cdot 10^{-5}$	$1.8 \cdot 10^{-3} \pm 8.9 \cdot 10^{-5}$	$1.6 \cdot 10^{-3} \pm 7.3 \cdot 10^{-5}$	$2.0 \cdot 10^{-3} \pm 3.4 \cdot 10^{-5}$
27	Dibenzo[a,h]anthracene	< LOD	< LOD	< LOD	$2.0 \cdot 10^{-3} \pm 9.3 \cdot 10^{-5}$	$1.7 \cdot 10^{-3} \pm 7.8 \cdot 10^{-5}$	$9.5 \cdot 10^{-4} \pm 4.4 \cdot 10^{-5}$

#### N- and O-PAHs

28	Nitronaphthalene	< LOD	< LOD	< LOD	$0.15 \pm 7.7 \cdot 10^{-3}$	$0.335 \pm 0.015$	$0.255 \pm 0.013$
29	1-Methyl-5-nitronaphthalene	$0.057 \pm 2.8 \cdot 10^{-3}$	$0.083 \pm 2.8 \cdot 10^{-3}$	$0.129 \pm 5.7 \cdot 10^{-3}$	< LOD	< LOD	< LOD
30	1-Methyl-6-nitronaphthalene	$0.071 \pm 2.8 \cdot 10^{-3}$	$0.070 \pm 4.2 \cdot 10^{-3}$	$0.100 \pm 2.9 \cdot 10^{-3}$	< LOD	< LOD	< LOD
31	9,10-Anthracenedione	< LOD	< LOD	< LOD	$0.070 \pm 3.5 \cdot 10^{-3}$	$0.20 \pm 9.4 \cdot 10^{-3}$	$0.13 \pm 5.8 \cdot 10^{-3}$
32	4H-cyclopenta(def)phenanthrene	$0.27 \pm 0.01$	$0.78 \pm 0.04$	$0.66 \pm 0.05$	< LOD	< LOD	< LOD

33	Nitropyrene	< LOD	$2.3 \cdot 10^{-3} \pm 1.5 \cdot 10^{-5}$				
----	-------------	-------	-------	-------	-------	-------	---

Table S5. PAHs and their derivatives in plant-derived BC samples (n=3; n-number of replicates).

No.	Compound	Sample description					
		BCS500	BCS600	BCS700	BCW500	BCW600	BCW700
1	Naphthalene	< LOD	< LOD	< LOD	< LOD	< LOD	< LOD
2	Acenaphthylene	$1.36 \pm 0.07$	$0.86 \pm 0.04$	$0.49 \pm 0.02$	$1.64 \pm 0.12$	$0.77 \pm 0.04$	$0.38 \pm 0.02$
3	Acenaphthene	$1.82 \pm 0.09$	$1.49 \pm 0.07$	$0.94 \pm 0.04$	$1.06 \pm 0.05$	$1.16 \pm 0.05$	$1.72 \pm 0.08$
4	Fluorene	< LOD	< LOD	< LOD	$0.62 \pm 0.03$	$0.97 \pm 0.05$	$1.19 \pm 0.06$
5	Anthracene	< LOD	< LOD	< LOD	< LOD	< LOD	< LOD
6	Phenanthrene	< LOD	< LOD	< LOD	< LOD	< LOD	< LOD
7	3-Methylphenanthrene	$0.31 \pm 0.02$	$0.134 \pm 0.006$	$0.136 \pm 0.006$	$0.12 \pm 5.0 \cdot 10^{-3}$	$0.17 \pm 7.4 \cdot 10^{-3}$	$9.9 \cdot 10^{-2} \pm 4.5 \cdot 10^{-3}$
8	2-Methylphenanthrene	< LOD	< LOD	< LOD	< LOD	$0.03 \pm 1.2 \cdot 10^{-3}$	< LOD
9	9-Methylphenanthrene	< LOD	< LOD	< LOD	< LOD	< LOD	< LOD
10	Fluoranthene	< LOD	< LOD	< LOD	< LOD	< LOD	< LOD
11	Pyrene	< LOD	< LOD	< LOD	< LOD	< LOD	< LOD
12	2-PhenylNaphthalene	< LOD	< LOD	< LOD	< LOD	< LOD	< LOD

13	3,6-dimethylphenanthrene	< LOD	$0.086 \pm 4.0 \cdot 10^{-3}$				
14	Benzo[a]fluorene	$5.2 \cdot 10^{-3} \pm 2.4 \cdot 10^{-4}$	$6.1 \cdot 10^{-3} \pm 3.1 \cdot 10^{-4}$	$0.012 \pm 5.6 \cdot 10^{-4}$	$6.2 \cdot 10^{-3} \pm 2.1 \cdot 10^{-4}$	$9.7 \cdot 10^{-3} \pm 4.6 \cdot 10^{-4}$	$7.6 \cdot 10^{-3} \pm 2.5 \cdot 10^{-4}$
15	2-Methylpyrene	$0.024 \pm 0.001$	$0.023 \pm 0.001$	< LOD	$0.024 \pm 7.6 \cdot 10^{-4}$	$0.027 \pm 1.3 \cdot 10^{-3}$	$0.023 \pm 7.3 \cdot 10^{-4}$
16	4-Methylpyrene	< LOD	$0.030 \pm 0.002$	$0.078 \pm 0.003$	< LOD	< LOD	< LOD
17	Benzo[a]anthracene	$0.0062 \pm 2.9 \cdot 10^{-4}$	$7.3 \cdot 10^{-3} \pm 3.4 \cdot 10^{-4}$	$9.9 \cdot 10^{-3} \pm 4.6 \cdot 10^{-4}$	< LOD	< LOD	< LOD
18	Chrysene	< LOD	< LOD	< LOD	$6.5 \cdot 10^{-3} \pm 3.0 \cdot 10^{-4}$	$5.6 \cdot 10^{-3} \pm 2.6 \cdot 10^{-4}$	< LOD
19	3-Methylchrysene	< LOD	$3.9 \cdot 10^{-3} \pm 1.9 \cdot 10^{-4}$	$1.7 \cdot 10^{-3} \pm 8.1 \cdot 10^{-5}$	$4.3 \cdot 10^{-3} \pm 1.9 \cdot 10^{-4}$	$4.8 \cdot 10^{-3} \pm 1.9 \cdot 10^{-4}$	$5.2 \cdot 10^{-3} \pm 2.5 \cdot 10^{-4}$
20	6-Methylchrysene	$0.0036 \pm 1.6 \cdot 10^{-4}$	$7.6 \cdot 10^{-3} \pm 1.9 \cdot 10^{-4}$	$3.2 \cdot 10^{-3} \pm 2.1 \cdot 10^{-4}$	$7.6 \cdot 10^{-3} \pm 2.8 \cdot 10^{-4}$	$8.9 \cdot 10^{-3} \pm 4.1 \cdot 10^{-4}$	$4.3 \cdot 10^{-3} \pm 1.9 \cdot 10^{-4}$
21	Benzo[a]fluoranthene	$4.9 \cdot 10^{-4} \pm 1.3 \cdot 10^{-5}$	$1.5 \cdot 10^{-3} \pm 9.8 \cdot 10^{-5}$	$8.4 \cdot 10^{-4} \pm 4.6 \cdot 10^{-5}$	$3.9 \cdot 10^{-3} \pm 1.8 \cdot 10^{-4}$	$6.8 \cdot 10^{-3} \pm 2.7 \cdot 10^{-4}$	$5.0 \cdot 10^{-3} \pm 2.4 \cdot 10^{-4}$
22	Benzo[b]fluoranthene	< LOD	< LOD	< LOD	$2.4 \cdot 10^{-3} \pm 7.0 \cdot 10^{-5}$	$2.8 \cdot 10^{-3} \pm 9.9 \cdot 10^{-5}$	$3.9 \cdot 10^{-3} \pm 1.8 \cdot 10^{-4}$
23	Benzo[a]pyrene	< LOD					
24	Benzo[k]fluoranthene	< LOD					
25	Indene[1,2,3-cd]pyrene	$0.0015 \pm 6.9 \cdot 10^{-4}$	$2.2 \cdot 10^{-3} \pm 1.0 \cdot 10^{-4}$	$6.3 \cdot 10^{-4} \pm 5.0 \cdot 10^{-5}$	< LOD	$2.2 \cdot 10^{-4} \pm 1.2 \cdot 10^{-5}$	< LOD
26	Benzo[ghi]perylene	< LOD	$1.1 \cdot 10^{-3} \pm 8.2 \cdot 10^{-5}$	$3.1 \cdot 10^{-4} \pm 2.2 \cdot 10^{-5}$	$1.0 \cdot 10^{-3} \pm 2.9 \cdot 10^{-5}$	$2.3 \cdot 10^{-3} \pm 8.0 \cdot 10^{-5}$	$1.9 \cdot 10^{-3} \pm 5.2 \cdot 10^{-5}$
27	Dibenzo[a,h]anthracene	< LOD	< LOD	< LOD	< LOD	$2.0 \cdot 10^{-3} \pm 9.1 \cdot 10^{-5}$	$1.8 \cdot 10^{-3} \pm 5.0 \cdot 10^{-5}$

#### N- and O-PAHs

28	Nitronaphthalene	< LOD	< LOD	< LOD	< LOD	< LOD	< LOD
29	1-Methyl-5-nitronaphthalene	$0.095 \pm 4.1 \cdot 10^{-3}$	$0.13 \pm 4.0 \cdot 10^{-3}$	$0.098 \pm 2.8 \cdot 10^{-3}$	< LOD	< LOD	< LOD

30	1-Methyl-6-nitronaphthalene	$0.081 \pm 2.7 \cdot 10^{-3}$	$0.12 \pm 5.4 \cdot 10^{-3}$	$0.12 \pm 4.2 \cdot 10^{-3}$	< LOD	< LOD	< LOD
31	9,10-Anthracenedione	< LOD	< LOD	< LOD	< LOD	< LOD	< LOD
32	4H-cyclopenta(def)phenanthrene	< LOD	$0.57 \pm 0.02$	$0.41 \pm 0.02$	$0.24 \pm 0.01$	$0.47 \pm 0.02$	$0.47 \pm 0.02$
33	Nitropyrene	< LOD	< LOD	< LOD	$8.2 \cdot 10^{-3} \pm 2.2 \cdot 10^{-4}$	$0.013 \pm 6.9 \cdot 10^{-4}$	$0.012 \pm 5.9 \cdot 10^{-4}$

## **References**

- [1] D. Fabbri, A.G. Rombolà, C. Torri, K.A. Spokas, Determination of polycyclic aromatic hydrocarbons in biochar and biochar amended soil, *Journal of Analytical and Applied Pyrolysis.* 103 (2013) 60–67. <https://doi.org/10.1016/j.jaap.2012.10.003>.

### **Publikacja D3**

**A. Krzyszczak, M. P. Dybowski, M. Kończak, B. Czech**

*Low bioavailability of derivatives of polycyclic aromatic hydrocarbons in biochar obtained  
from different feedstock*

Environmental Research, 2022, 214(1), 113787



## Low bioavailability of derivatives of polycyclic aromatic hydrocarbons in biochar obtained from different feedstock

Agnieszka Krzyszczak <sup>a</sup>, Michał P. Dybowski <sup>b</sup>, Magdalena Kończak <sup>c</sup>, Bożena Czech <sup>a,\*</sup>

<sup>a</sup> Department of Radiochemistry and Environmental Chemistry, Institute of Chemical Sciences, Faculty of Chemistry, Maria Curie-Skłodowska University in Lublin, Pl. M. Curie-Skłodowskiej 3, 20-031, Lublin, Poland

<sup>b</sup> Department of Chromatography, Institute of Chemical Sciences, Faculty of Chemistry, Maria Curie-Skłodowska University in Lublin, Pl. M. Curie-Skłodowskiej 3, 20-031, Lublin, Poland

<sup>c</sup> Institute of Earth and Environmental Sciences, Faculty of Earth Sciences and Spatial Management, Maria Curie-Skłodowska University, ul. Kraśnicka 2cd, 20-718, Lublin, Poland

### ARTICLE INFO

#### Keywords:

Biochar

Feedstock

Polycyclic aromatic hydrocarbons (PAHs)

PAHs derivatives

### ABSTRACT

In the last years, there is great progress in the field of studies on the thermal transformation of wastes into valuable materials such as biochar. High-temperature processes, however, are connected with the formation of polycyclic aromatic hydrocarbons (PAHs) with confirmed toxicity. However, during pyrolysis, some derivatives containing oxygen, nitrogen, or sulfur can also be formed. Their toxicity is expected to be higher than parent PAHs. However, the key parameter in the agricultural application of carbonaceous materials is PAHs' bioavailability. The aim of the presented studies was the determination of the effect of various feedstock (wheat straw (*Triticum L.*), willow (*Salix viminalis*), sunflower, residues from softwood and hardwood, sewage sludges, and residues from biogas production) on the formation of PAHs and their derivatives (O-, N-PAHs) in biochar and their bioavailability. The results indicated that the content of total and bioavailable PAHs in obtained biochar was rather low. The concentration of total PAHs in plant-derived biochar reached  $57 \pm 3 \text{ ng g}^{-1}$  -  $181 \pm 8 \text{ ng g}^{-1}$ , whereas sewage sludge-derived biochar contained from  $121 \pm 6 \text{ ng g}^{-1}$  to  $188 \pm 9 \text{ ng g}^{-1}$  of PAHs. The highest concentration of PAHs was noted in biochar obtained from residues from biochar production – up to  $202 \pm 9 \text{ ng g}^{-1}$ . The total concentration of bioavailable PAHs was lower and reached  $2-4.45 \text{ ng L}^{-1}$  for plant-derived biochar,  $3-40 \text{ ng L}^{-1}$  for sewage sludge-derived biochar. The highest content of bioavailable PAHs was noted in biochar obtained from residues from biogas production:  $9-42 \text{ ng L}^{-1}$  indicating that increased attention should be paid to using this type of biochar. Among PAHs derivatives, nitronaphthalene, 1-methyl-5-nitronaphthalene, 1-methyl-6-nitronaphthalene, 9,10-anthracenedione, 4H-cyclopenta(def)phenanthrene, nitropyrene were determined at various levels and their concentrations were from below the limit of detection (LOD) to  $28 \text{ ng L}^{-1}$  for plant-derived biochar,  $3-16 \text{ ng L}^{-1}$  for biochar obtained from residues from biogas production, and  $5-45 \text{ ng L}^{-1}$  for sewage sludge-derived biochar. The content of bioavailable PAHs derivatives was, generally, one order of magnitude lower than parent PAHs derivatives, and reached from below LOD up to almost  $1 \text{ ng L}^{-1}$  for plant-derived biochar, from  $0.5$  to  $2 \text{ ng L}^{-1}$  for biochar obtained from residues from biogas production, and from  $0.2$  to almost  $5 \text{ ng L}^{-1}$  for sewage sludge-derived biochar confirming the safety of agricultural usage of biochar.

### 1. Introduction

Biochar (BC) is a stable form of carbon material produced via the thermal decomposition of biomass under a reduced supply of oxygen or entirely without it (Pariyar et al., 2020). The applied temperatures of pyrolysis are generally below  $700 \text{ }^{\circ}\text{C}$  (Lehmann and Joseph, 2009). BC can be obtained from different types of feedstock, including wood

(Keiluweit et al., 2012; Kloss et al., 2012; Pariyar et al., 2020; Singh et al., 2010; Zhao et al., 2013), animal manure (Singh et al., 2010; Zhao et al., 2013), agricultural wastes (wheat straw (Kloss et al., 2012), grass, chlorella, peanut shell, waterweeds, shrimp hull, bone dredges (Zhao et al., 2013), poultry litter, pecan shell (Novak et al., 2009), rice husk (Pariyar et al., 2020)), biosolids (sewage sludge (Zhao et al., 2013; Zielińska et al., 2015), waste paper (Zhao et al., 2013), food waste (Pariyar et al.,

\* Corresponding author.

E-mail address: [bczech@hektor.umcs.lublin.pl](mailto:bczech@hektor.umcs.lublin.pl) (B. Czech).

2020), papermill sludge (Singh et al., 2010)) or residues from biogas production (Stefaniuk and Oleszczuk, 2015). Pyrolysis temperature and type of biomass are affecting BC properties. Simultaneously, pyrolysis conditions such as heating rate, pressure, the flow rate of auxiliary gases (air, steam, N<sub>2</sub>, CO<sub>2</sub>), the residence time, and feedstock properties are also important (Li et al., 2018; Yu et al., 2018; Zhao et al., 2013). The influence of feedstock type on BC parameters was evident in the content of total organic carbon, fixed carbon, mineral elements, and potential total C sequestration (Zhao et al., 2013). The characteristic of the surface area, pore volume, and average pore size that are connected with sorption and water holding capacity of BC depended strongly on both feedstock and pyrolysis temperature (Zhao et al., 2013). Moreover, the results from differential scanning calorimetry and Fourier-transform infrared spectroscopy pointed out that the content of unstable aliphatic compounds decreased during pyrolysis and the formation of more persistent aromatic structures was observed (Kloss et al., 2012). Table 1 shows different physicochemical properties of biochar depending on applied feedstock.

BC addition into soil has great potential and has many undeniable benefits. It causes an increase in pH, the content of C, N, and available P. BC amendment resulted in higher nutrient retention and availability which is directly connected with higher exchange capacity (Chan et al., 2007; Glaser et al., 2002). It increases also the uptake of K, Ca, Zn, and Cu but reduces the leaching of fertilizing N, Mg, and Ca (Lehmann et al., 2003). However, some negative phenomena: soil compaction, easier erosion, or soil contamination (by heavy metals, aromatic compounds) may also occur (European Commission, 2010). Simultaneously, the presence of polycyclic aromatic hydrocarbons (PAHs), formed during pyrolysis (Hilber et al., 2012) may limit biochar application into the soil (European Commission, 2010). PAHs are persistent organic aromatic compounds with two or more aromatic rings (Mahler et al., 2012). As it was suggested by Keilweit et al. (2012) PAHs can be formed via two pathways. At temperatures lower than 500 °C PAHs are produced due to carbonization and aromatization during the conversion of raw material into biochar (Bucheli et al., 2015). Whereas H<sub>2</sub>O, CO<sub>2</sub>, CH<sub>4</sub>, and H<sub>2</sub>S are removed, the low molecular weight (LMW) PAHs are created predominantly (Wang et al., 2017). However, at temperatures higher than 500 °C, PAHs are created via a free radical pathway and pyrosynthesis into greater structures (Bucheli et al., 2015). Organic compounds are cracked (for instance into ethynyl, 1,3-butadiene radicals (Wang et al., 2017)), next they are combined into thermodynamically more stable PAHs. Sullivan et al. indicated that when the temperature and the residence time increased, LMW PAHs may be transformed into high molecular weight (HMW) ones (Sullivan et al., 1989).

Some latest papers indicate that during high-temperature treatment of various materials but also in the environment (including photochemical, and microbial reactions) PAHs and their O-, N-, S-containing derivatives are formed (del Rosario Sienra, 2006; Ringuet et al., 2012; Zhang et al., 2011). PAHs derivatives belong to a group of thermally stable, organic compounds, while their water solubility is increasing with decreasing number of rings (Hien et al., 2007). O-PAHs contain at least 2 carbonyl oxygens (quinones and ketones) attached to the aromatics rings. The physicochemical characterization of N-PAHs depends on molecular weight and the number of nitro-functional groups (Bandonne and Meusel, 2017; Besis et al., 2022; Nowakowski et al., 2022). PAHs derivatives should be thoroughly studied as they are regarded to be more toxic than pristine compounds (Abbas et al., 2018). Moreover, due to the polarity, O-PAHs are more bioavailable than pristine PAHs and they can be transferred via groundwater and surface water being more toxic to living organisms (including humans) and the environment (Lundstedt et al., 2007).

The influence of the type of feedstock and pyrolysis temperatures on the physicochemical properties of BC has been widely studied (Table 1). But there are some research gaps, which have to be completed. There is still insufficient information about the formation and presence of potentially toxic and mutagenic compounds that remain or are formed in

BC during pyrolysis. From an agricultural and environmental point of view, there is still a need to monitor the physicochemical parameters and the concentration of bioavailable PAHs and their derivatives in biochars obtained from the different feedstock. In the studies of Kuśmierz et al. (2016), it was observed that PAHs in biochar-amended soil are not bioaccessible. However, there is no data on the bioaccessibility of PAHs derivatives. The aim of the presented studies was the determination the effect of various feedstock (wheat straw (*Triticum L.*), willow (*Salix viminalis*), sunflower, residues from softwood and hardwood, sewage sludges, and residues from biogas production) on the formation of PAHs and their derivatives (O-, N-PAHs) in biochar and their bioavailability.

## 2. Materials and methods

### 2.1. Feedstock and biochar preparation

For the preparation of biochars, several feedstocks were used (Table 2). The studied BC were divided into 3 groups: sewage sludge-derived BC labeled as SSL-BC, plant-derived biochar as PT-BC, and residues biogas production-derived biochar labeled as RBP-BC. BCs obtained from sunflower, and residues from softwood and hardwood were acquired from the company Fluid S.A. (Sędziszów, Poland). Pyrolysis of wheat straw, willow, sewage sludges, or residues from biogas production was carried out according to the protocol described in our previous work (Krzyszczak et al., 2021). Biochars were produced via slow pyrolysis in a furnace (Czylok, Poland) at 600 °C, with the heating rates: at the first step 10 °C min<sup>-1</sup>, and the second step 3 °C min<sup>-1</sup>, applied the resident time: 3 h. The pyrolysis process was carried out in an oxygen-free atmosphere, where the flow of nitrogen (N<sub>2</sub>) was constant (630 cm<sup>3</sup> min<sup>-1</sup>) and was monitored by the mass flow controller (BETA-ERG, Poland). Obtained biochars were grounded down to particles of about 2 mm and homogenized. Next, they were washed out using distilled water (1:10, biochar: water) continuously for 24 h and dried at 40 °C for 6 h. Before analysis BC samples were stored at room temperature in the absence of light.

### 2.2. The physicochemical properties of biochar

The physicochemical properties of BC e.g. pH, and ash content, were performed by standard methods described in Supplementary Information (SI). The other analyses and procedures: C, H, N, content, surface area and porosity, surface characteristics by FT-IR, XPS spectroscopy, and SEM-EDS were detailed in SI.

### 2.3. The total content of PAHs and their derivatives determination in biochar

Pressurized liquid extraction (PLE) was applied to extract the total content of PAHs and derivatives. The stainless steel cells were packed as follows: the first layer with silica gel and copper, and the second, biochar mixed with ethylenediaminetetraacetic acid. The internal standard (IS) was added and the cells were completed with glass beads. Then, PLE was performed with hexane at 150 °C. After extraction iso-octane was added to an extract and obtained solution was concentrated. Then, GC-MS/MS (gas chromatography with tandem mass spectrometry) analysis was carried out. Further details are described in SI.

### 2.4. Freely dissolved (C<sub>free</sub>) PAH and their derivatives determination in biochars

The qualitative and quantitative determinations of the bioaccessibility of PAHs and their derivatives were carried out by the protocol described in Oleszczuk et al. (2016) and Hale et al. (2012). The procedure involved the use of 76-mm thick polyoxymethylene (POM) passive samplers. Dried biochar, POM samplers, and the aqueous

**Table 1**

The physicochemical properties of biochar depending on applied feedstock.

property	The temperature of pyrolysis [°C]	Biochar with the lowest value (and this value)	Biochars are characterized by the values among the lowest and the highest (in ascending order)	Biochar with the highest value (and this value)	Ref.
Total carbon [%]	500	bone dregs 24.2	waterweeds, wastewater sludge, chlorella, pig manure, cow manure, shrimp hull, waste paper, grass, wheat straw, peanut shell	sawdust 75.8	Zhao et al. (2013)
Total carbon [g kg <sup>-1</sup> ]	400	cow manure (non-activ <sup>a</sup> ) $175.0 \pm 1.5$	poultry litter (non-activ <sup>a</sup> ), <i>E. saligna</i> leaves (activ <sup>a</sup> ), <i>E. saligna</i> wood (activ <sup>a</sup> )	<i>E. saligna</i> wood (non-activ <sup>a</sup> ) $697.4 \pm 4.3$	Singh et al. (2010)
	550	cow manure (activ <sup>a</sup> ) $165.3 \pm 2.5$	paper sludge (activ <sup>a</sup> ), poultry litter (activ <sup>a</sup> ), <i>E. saligna</i> leaves (activ <sup>a</sup> ), <i>E. saligna</i> wood (activ <sup>a</sup> )	<i>E. saligna</i> wood (non-activ <sup>a</sup> ) $836.1 \pm 7.6$	
pH	500	16.9 wastewater sludge 8.82	bone dregs, waste paper, grass, wheat straw, cow manure, shrimp hull, waterweeds, pig manure, peanut shell, sawdust	chlorella 10.8	Zhao et al. (2013)
	400	Spruce 6.9	Poplar	straw 9.1	Kloss et al. (2012)
	460	straw/spruce 8.7	–	poplar 9.2	
	525	spruce 8.6	Poplar	straw 9.2	
	350	sawdust $5.75 \pm 0.02$	paper sludge, poultry litter	rice husk $6.41 \pm 0.07$	Pariyar et al. (2020)
	450	sawdust $6.31 \pm 0.04$	paper sludge, rice husk, food waste	poultry litter $9.54 \pm 0.01$	
	550	sawdust $6.66 \pm 0.08$	rice husk, paper sludge, food waste	poultry litter $9.99 \pm 0.06$	
	650	sawdust $6.84 \pm 0.03$	rice husk, poultry litter,	paper sludge $10.31 \pm 0.02$	
	400	<i>E. saligna</i> wood (non-activ <sup>a</sup> ) $6.93 \pm 0.02$	<i>E. saligna</i> wood (activ <sup>a</sup> ), cow manure (non-activ <sup>a</sup> ), <i>E. saligna</i> leaves (activ <sup>a</sup> )	poultry litter (non-activ <sup>a</sup> ) $9.20 \pm 0.02$	Singh et al. (2010)
	550	<i>E. saligna</i> wood (non-activ <sup>a</sup> ) $8.82 \pm 0.01$	cow manure (activ <sup>a</sup> ), paper sludge (activ <sup>a</sup> ), <i>E. saligna</i> wood (activ <sup>a</sup> ), <i>E. saligna</i> leaves (activ <sup>a</sup> )	poultry litter (activ <sup>a</sup> ) $10.26 \pm 0.01$	
Electrical conductivity (EC) [mS m <sup>-1</sup> ]	400	spruce 42	Poplar	straw 108	Kloss et al. (2012)
	460	poplar 70	Spruce	straw 492	
	525	spruce 71	Poplar	straw 443	
	350	rice husk $0.44 \pm 0.05$	sawdust, paper sludge	poultry litter $9.31 \pm 0.04$	Pariyar et al. (2020)
	450	rice husk $0.76 \pm 0.02$	paper sludge, sawdust, poultry litter	food waste $12.29 \pm 0.09$	
	550	rice husk $0.99 \pm 0.03$	paper sludge, sawdust, poultry litter	food waste $20.06 \pm 0.10$	
	650	rice husk $1.40 \pm 0.03$	paper sludge, sawdust	poultry litter $12.73 \pm 0.01$	
Ash content [%]	500	sawdust 9.94	peanut shell, wheat straw, grass, pig manure, chlorella, waste paper, shrimp hull, wastewater sludge, waterweeds, cow manure	bone dregs 77.6	Zhao et al. (2013)
	400	spruce 1.9	Poplar	straw 9.7	Kloss et al. (2012)
	460	Spruce 3.0	Poplar	straw 12.0	
	525	spruce 4.7	Poplar	straw 12.7	
cation exchange capacity (CEC) [cmol kg <sup>-1</sup> ]	500	sawdust 41.7	peanut shell, pig manure, grass, bone dregs, wheat straw, cow manure, wastewater sludge, shrimp hull, waterweeds, waste paper	chlorella 562	Zhao et al. (2013)
	350	rice husk 41.36	paper sludge, sawdust	poultry litter 67.23	Pariyar et al. (2020)
	450	food waste 22.10	rice husk, paper sludge, sawdust	poultry litter 53.47	
	550	food waste 17.35	rice husk, sawdust, paper sludge	poultry litter 51.45	
	650	rice husk 6.69	sawdust, paper sludge	poultry litter 49.73	
cation exchange capacity (CEC) [mmol kg <sup>-1</sup> ]	400	spruce $73.5 \pm 2.9$	Poplar	straw $161.6 \pm 15.6$	Kloss et al. (2012)
	460	Spruce $54.7 \pm 6.0$	Straw	poplar $128.3 \pm 17.7$	
	525	Spruce $52.2 \pm 1.4$	Straw	Poplar $107.6 \pm 7.6$	

(continued on next page)

**Table 1 (continued)**

property	The temperature of pyrolysis [°C]	Biochar with the lowest value (and this value)	Biochars are characterized by the values among the lowest and the highest (in ascending order)	Biochar with the highest value (and this value)	Ref.
BET-N <sub>2</sub> surface area (SA) [ $\text{m}^2 \text{ g}^{-1}$ ]	500	Chlorella 2.78	Grass, waterweeds, shrimp hull, cow manure, wheat straw, peanut shell, pig manure, wastewater sludge, bone dredges, waste paper	Sawdust 203	Zhao et al. (2013)
	400	spruce $1.8 \pm 0.1$	Poplar	Straw $4.8 \pm 0.5$	Kloss et al. (2012)
	460	straw $2.8 \pm 1.8$	Poplar	spruce $14.2 \pm 2.2$	
	525	Straw $14.2 \pm 4.0$	Spruce	Poplar $55.7 \pm 19.5$	
	350	poultry litter $1.75 \pm 0.02$	Paper sludge, sawdust	Rice husk $11.61 \pm 0.31$	Pariyar et al. (2020)
	450	Food waste $0.17 \pm 0.04$	Poultry litter, paper sludge, rice husk	sawdust $179.77 \pm 2.35$	
	550	Food waste $2.07 \pm 0.06$	Poultry litter, paper sludge, rice husk	sawdust $431.91 \pm 5.46$	
	650	Poultry litter $25.33 \pm 0.38$	Paper sludge, rice husk	sawdust $443.79 \pm 0.98$	

<sup>a</sup> activ-activated (biochar with stream activation); non-activ-non-activated (biochar without stream activation).

**Table 2**  
Applied feedstock and obtained biochars.

	Feedstock	Location/supplier	Biochar label
PT-BC	Wheat straw ( <i>Triticum L.</i> )	Mostostal Sp. z o.o. (Wrocław, Poland)	PT-S
	Willow ( <i>Salix viminalis</i> )	The southeastern part of Poland	PT-W
	Sunflower	Fluid S.A. (Sędziszów, Poland)	PT-A
	Residues from hardwood	Fluid S.A. (Sędziszów, Poland)	PT-D
	Residues from softwood	Fluid S.A. (Sędziszów, Poland)	PT-F
RBP-BC	Residues from biogas production (RBP)	Uhnin (51°58'33"N, 23°03'33"E, Poland) Kocergi (51°63'33"N, 22°88'33"E, Poland) Piaski (51°61'07"N, 22°55'00"E, Poland)	RBP-UH RBP-KO RBP-PI
	Sewage sludge (SSL)		SSL-CH
	Kalisz (51°45'45"N, 18°05'23"E, Poland) Suwałki (54°06'04"N, 22°55'57"E, Poland) Zamość (50°43'14"N, 23°15'31"E, Poland)		SSL-KZ SSL-SI SSL-Z

solution of sodium azide were placed in Erlenmeyer flasks. Then, they were rolled for one month on a rotary shaker ROTAX 6.8 VELP Scientifica (Italy) at 10 RCF. After this period, POM samplers were cleaned with distilled water and extracted with an acetone/heptane (20/80, v/v) mixture with the addition of IS. Finally, obtained extract was concentrated and GC-MS/MS analysis was carried out. Further details are described in SI.

## 2.5. GC-MS/MS measurement

Qualitative and quantitative analyses of PAHs and derivatives were conducted using a gas chromatograph hyphenated with a triple quadrupole tandem mass spectrometer detector (GCMS-TQ8040; Shimadzu, Kyoto, Japan) equipped with a ZB5-MSi fused-silica capillary column (30 m × 0.25 mm i.d., 0.25 µm film thickness; Phenomenex, Torrance, CA, USA). Helium (grade 5.0) as carrier gas and argon (grade 5.0) as collision gas were used. Column flow was 1.56 mL min<sup>-1</sup>, and 1 µL of the sample was injected by an AOC-20i + s type autosampler (Shimadzu). The injector was working in high-pressure mode (250.0 kPa

for 1.5 min; column flow at initial temperature was 4.90 mL min<sup>-1</sup>) at the temperature of 310 °C; the ion source temperature was 225 °C. For qualitative purposes, the full scan mode with a range of 40–550 m/z was employed and for quantitative analyses, the SIM mode was used.

## 3. Results and discussion

### 3.1. Biochar characteristic

The applied feedstock affects the physicochemical properties of tested materials (Fig. 1 and Table 3). Although, some similarities in biochars obtained from different raw materials can be also observed. The BCs were characterized by broad values of surface area ( $S_{\text{BET}}$ ). The lowest  $S_{\text{BET}}$  ( $<1 \text{ m}^2 \text{ g}^{-1}$ ) was noted for PT-A and PT-F, e.g. plant-derived BC. Simultaneously, the highest  $S_{\text{BET}}$  ( $>70 \text{ m}^2 \text{ g}^{-1}$ ) was noted for PT-W, SSL-CH, and SSL-Z, plant- and sewage sludge-derived BC. It was observed that BC with a higher surface area was characterized by a higher content of C<sub>free</sub> PAHs (Supplementary Information), which may be associated with a greater amount of potential active sites capable of binding PAHs (Zielińska and Oleszczuk, 2016). PT-BC were characterized by broad pH values: from 7.45 (PT-F) to 10.45 (PT-W). SSL-BC may be divided into two groups: slightly basic (SSL-Z, SSL-SI) and basic (SSL-CH, SSL-KZ), whereas RBP-BC were more basic (pH 10.80–12.60).

Ash content (Table 3) in SSL-BC, and RBP-BC was higher than in PT-BC. The content of carbon in BC was combined with applied feedstock. In general, in SSL-BC, up to 30% of C% was noted, whereas in RBP-BC the content of C% reached 35–67%. PT-BC were enriched in C%: 61–83% (Table 3, Figure S2A). SSL-BC revealed the highest N% content (2.24–3.76%) and lowest (2.29–8.84%) O% content. In general, the highest aromaticity (H/C ratio) was noted for RBP-BC. PT-BC were characterized by higher polarity and hydrophilicity ((O + N)/C and O/C ratios, respectively) except BCSW600 which was more aromatic (higher H/C ratio) (Table 3, Supplementary Information). In general, SSL-KZ revealed the highest ash content and the lowest C%, H%, O%, and polarity. EDS mapping confirmed the presence of Ca (10.74 wt%), Si (4.96 wt%), Mg (0.72 wt%), P (3.51 wt%), Fe (2.35 wt%), and traces of K, S, Ti, and Na on SSL-Z surface.

The surface of BC was tested by spectroscopic methods. FT-IR spectra, presented in Fig. 1A, revealed the presence of the characteristic peaks at 4000–3300 cm<sup>-1</sup> indicating the presence of stretching O–H and N–H structures on the BC surface. Aryl and vinyl functionalities (sp<sup>2</sup> vibrations) were also noted (3100–3000 cm<sup>-1</sup>). The presence of peaks in the 2500–2000 cm<sup>-1</sup> region indicated the stretching of C≡C and C≡N, whereas at 1500–1680 cm<sup>-1</sup>: C=C (stretching). The presence of carbonyls was also evidenced (2000–1700 cm<sup>-1</sup>) (Chia et al., 2012). The

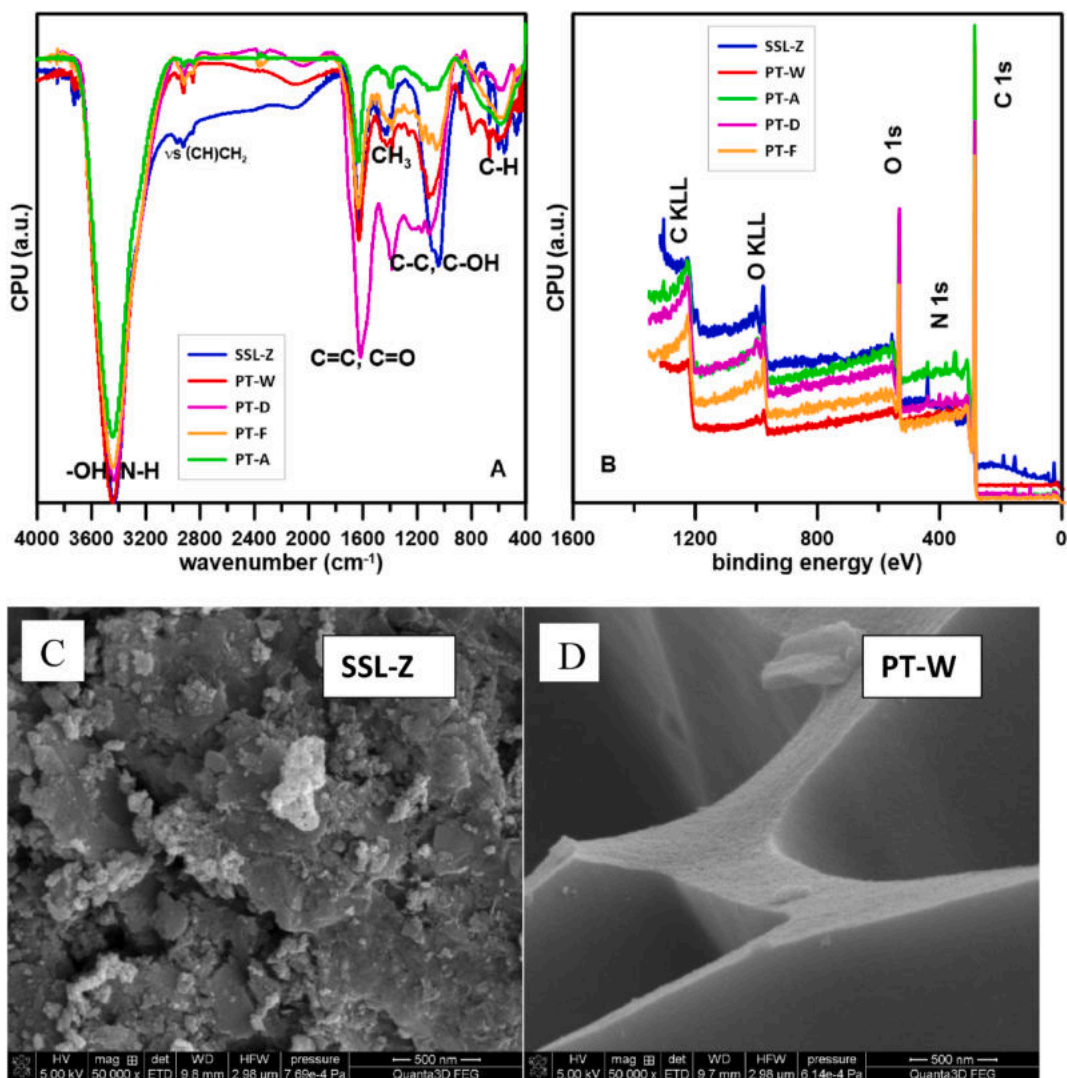


Fig. 1. Physicochemical characteristics of tested biochars: A) FT-IR spectra of tested materials, B) XPS survey, C) SEM images of SSL-Z and PT-W.

**Table 3**  
Physicochemical properties of tested biochar.

BC	S <sub>BET</sub>	pH	Ash content [%]	C [%]	H [%]	N [%]	O [%]	H/C	(O + N)/C	O/C
PT-S	2.47	10.37	19.59	66.14	1.66	1.26	11.36	0.300	0.145	0.129
PT-W	145.02	10.45	7.09	82.77	2.24	1.68	9.53	0.027	0.135	0.115
PT-A	0.494	9.89	4.42	81.29	1.58	1.03	11.61	0.019	0.155	0.143
PT-D	1.149	8.03	10.77	61.50	3.11	1.18	23.41	0.051	0.400	0.381
PT-F	0.749	7.45	3.90	77.54	3.93	0.24	22.18	0.051	0.289	0.286
RBP-UH	6.80	11.20	35.40	51.25	1.27	1.97	10.11	0.300	0.180	0.150
RBP-KO	1.20	10.80	15.00	66.86	1.67	2.09	14.37	0.300	0.190	0.160
RBP-PI	1.80	12.60	44.30	34.95	1.06	2.10	17.57	0.360	0.430	0.380
SSL-CH	75.50	12.10	67.60	26.50	0.60	2.93	2.41	0.023	0.202	0.091
SSL-KZ	9.00	11.45	70.27	23.72	0.44	3.29	2.29	0.220	0.190	0.070
SSL-Z	79.56	7.79	63.58	24.45	0.86	2.24	8.84	0.035	0.453	0.362
SSL-SI	19.20	8.05	63.86	27.68	0.82	3.76	3.89	0.360	0.220	0.110

results were confirmed by XPS (the survey was presented in Fig. 1B). XPS analysis revealed that the surface of tested BC was heterogeneous with several functionalities. The general survey indicated the presence of C, O, N and Ca mainly (91.84, 6.79, 0.78, 0.59 at.%) in PT-W, whereas the BZC600 surface beside C (52.5 at.%), O (28.15 at.%), N (2.69 at.%), Ca (5 at.%), was composed of Si (5.04 at.% peak at 102.7 eV), P (3.06 at.%, 133.2eV), Al (2.16 at.% 74.7 eV), S (0.89 at.% 168.7eV) and Fe (0.49 at.%, 713.2eV). Closer analysis, however, revealed that the predominant

fraction of carbon (from 78 in SSL to 91 at.%) were C–C and C–H groups (peak of C 1s at 284.7eV) however, some groups C–OH, C–O–C (286.2 eV), C=O (287.6 eV), O–C=O (288.2 eV) in plant-derived BC or O=C=O (288.7 eV) in SSL derived BC were noted (Okpalugo et al., 2005). Oxygen (from 36 at.% in SSL-Z to 46 at.% in PT-W) as O=C–N (531.93 or 531.44 eV), O<sup>+</sup>–(C=O)–C (533.52 eV in PT-W) or O–(C=O<sup>\*</sup>)–C (532.92 eV SSL-Z). Nitrogen was present as C=N–C (398.25–398.8 eV), N–(C=O)–O<sup>–</sup> (400.39–400.76 eV) however

ammonium salt-derived peak was also noted (peak at 402.48–403.4 eV) (Morant et al., 2006).

SEM images presented in Fig. 1C and D indicated the porous structure of BC. SSL-Z and PT-W revealed a highly porous structure. In SSL-Z, the plate-like layer construction of sewage sludge was still observed after pyrolysis. However, some plates are cracked and covered by tar agglomerates, and fragmentation is observed (Zhang et al., 2015). In PT-W pores were long and well defined suggesting that the original porous structure of the willow had become distorted during BC production (Hardie et al., 2014). In general, during pyrolysis voids were created within the biochar matrix.

### 3.2. The total content of PAHs and their derivatives in BC

The first step of the studies was the determination of the total concentration of PAHs and their derivatives in BC samples. The applied temperature (600 °C) was selected due to the results published in a previous article (Krzyszczak et al., 2021) confirming that biochar obtained at 600 °C was characterized by the highest concentration of bioavailable fraction of PAHs derivatives. The presence of PAHs and their derivatives in the currently tested BC was presented in Table 4, Supplementary Information.

#### 3.2.1. Pristine PAHs

The effect of feedstock on the total concentration of PAHs in biochar was not noticed. In PT-BC the total content of PAHs (and Σ16PAHs, appointed by US EPA) varied between  $57.36 \pm 2.63 \mu\text{g g}^{-1}$  (PT-D) and  $181.08 \pm 8.29 \mu\text{g g}^{-1}$  (PT-W) ( $20.76 \pm 0.95 \mu\text{g g}^{-1}$  (PT-D) and  $171.36 \pm 7.85 \mu\text{g g}^{-1}$  (PT-W)) (Fig. 2A). In PT-S, PT-W, and PT-A the majority of PAHs (50.91%, 36.81%, and 52.09%, respectively) were 3-ring species followed by 2-rings compounds (PT-W – 44.36%) or 4-ring compounds (PT-S (41.54%) and PT-A (37.66%)). The most abundant PAHs in tested biochars were: 3-methylphenanthrene (PT-S), naphthalene (PT-W), and acenaphthylene (PT-A). Moreover, in all PT-BC, the second-biggest concentration was determined for acenaphthene. PT-D and PT-F differ from those described above because 4-ring species were the most abundant (53.69% and 37.69%) followed by 3-rings PAHs (32.86% and 36.59%), and 2-ring (8.90% PT-D) or 5-ring compounds (18.56% PT-F). The highest content was determined for benzo[a]fluorene and 6-methylchrysene (PT-D), or fluorene and 3,6-dimethylphenanthrene (PT-F).

RBP-BC contained a higher PAHs concentration than PT-BC. The total content of PAHs (and Σ16PAHs) varied between  $180.18 \pm 8.25 \mu\text{g g}^{-1}$  (RBP-KO) and  $201.64 \pm 9.23 \mu\text{g g}^{-1}$  (RBP-UH) ( $162.65 \pm 7.45 \mu\text{g g}^{-1}$  (RBP-PI) and  $184.93 \pm 8.47 \mu\text{g g}^{-1}$  (RBP-UH)) (Fig. 2A). In RBP-KO and RBP-PI the most abundant were 3-ring PAHs (62.76% and 63.70%), 4-ring (19.03% and 21.15%), 2-ring (7.74% and 6.76%), 5-ring (7.65% and 5.83%), and 6-ring (2.82% and 2.56%) with anthracene as the most abundant compound. Naphthalene and chrysene were the most prevalent compounds in RBP-UH described biochar. The total content of PAHs

(and Σ16PAHs) in SSL-BC varied from  $120.70 \pm 5.53 \mu\text{g g}^{-1}$  (SSL-CH) and  $188.47 \pm 8.63 \mu\text{g g}^{-1}$  (SSL-KZ) ( $77.70 \pm 3.56 \mu\text{g g}^{-1}$  (SSL-CH) and  $107.16 \pm 4.91 \mu\text{g g}^{-1}$  (SSL-Z)) (Fig. 2A). The profile of PAHs (the distribution of a particular group of PAHs) differs in SSL-BC. In SSL-SI the highest concentrations were obtained for benzo[a]antracene and benzo [b]fluoranthene. In SSL-CH and SSL-KZ the most prevalent were acenaphthene, naphthalene (SSL-CH), 2-phenylnaphthalene, fluorene (SSL-KZ), and naphthalene, acenaphthylene (SSL-Z).

#### 3.2.2. PAHs derivatives

During the experiment, some O- and N-PAHs were quantified in all biochars. Their quality and quantity depended on applied feedstocks. All tested BC differ in the amount of determined PAHs derivatives (Fig. 2B). In PT-D (hardwood) there were no PAHs derivatives quantitatively determined. In PT-S and PT-A, the presence of N- and O-PAHs was confirmed. Straw-derived biochar contained 1-methyl-5-nitronaphthalene, 1-methyl-6-nitronaphthalene (cumulatively 14.77%), and 4H-cyclopenta(def)phenanthrene (85.23%), whereas sunflower-derived BC contained nitroacenaphthene (17.28%) and 4H-cyclopenta(def)phenanthrene (82.72%). In PT-W only the concentration of nitroacenaphthene ( $1.92 \pm 0.09 \mu\text{g g}^{-1}$ ) was quantitatively determined, whilst in PT-F and RBP-PI, only O-PAHs were found. In other RBP-BC N-and O-PAHs were determined: nitroacenaphthene (28.47%,  $1.60 \pm 0.07 \mu\text{g g}^{-1}$ ) in RBP-UH, 9,10-anthracenedione (71.53%,  $4.02 \pm 0.18 \mu\text{g g}^{-1}$ ) in RBP-UH and (43.27%,  $1.48 \pm 0.07 \mu\text{g g}^{-1}$ ) in RBP-KO, and nitropyrene (56.73%,  $1.94 \pm 0.09 \mu\text{g g}^{-1}$ ) in RBP-KO. In SSL-Z only N-PAHs were determined (1-methyl-5-nitronaphthalene and 1-methyl-6-nitronaphthalene). In other SSL-BC O- and N-PAHs were quantified, however, the concentrations of some compounds were below the limit of detection. Among various N-PAHs, nitropyrene is one of the most prevalent N-PAHs occurring in diesel exhaust particulate matter being (Laumbach et al., 2008) revealing toxic, genotoxic, mutagenic, and inflammatory properties due to the reactive oxygen species (Traversi et al., 2011). 1-nitropyrene was classified as possibly carcinogenic to humans (Krzyszczak and Czech, 2021).

Significantly more researchers pay attention to the total fraction of PAHs in biochar. The studies on PAHs derivatives in biochar are scarce (Krzyszczak et al., 2021). Keiluweit et al. (2012) found that the highest content of PAHs and their methylated derivatives were determined in grass-derived biochar obtained at 500 °C ( $30.2 \mu\text{g g}^{-1}$ ) and softwood derived BC produced at 400 °C ( $26.600 \mu\text{g g}^{-1}$ ). Materials obtained at 600 °C contained significantly lower content of analytes ( $1.040 \mu\text{g g}^{-1}$  and  $0.801 \mu\text{g g}^{-1}$ , respectively) (Keiluweit et al., 2012), which is still definitely more than in our studies. Devi and Saroha (2015) presented that biochar prepared from paper mill effluent treatment plant sludge by pyrolysis at 600 °C contained  $0.926 \mu\text{g g}^{-1}$  PAHs.

**Table 4**  
The summarized concentration of total and bioavailable fraction of PAHs and their derivatives in biochar derived from different feedstocks.

Sample description	The concentration of total PAHs $\pm$ SD [ng g $^{-1}$ ]	The concentration of total Σ16PAHs $\pm$ SD [ng L $^{-1}$ ]	The concentration of total PAHs derivatives $\pm$ SD [ng L $^{-1}$ ]	The concentration of bioavailable ΣPAHs <sub>free</sub> $\pm$ SD [ng L $^{-1}$ ]	The concentration of bioavailable Σ16PAHs $\pm$ SD [ng L $^{-1}$ ]	The concentration of bioavailable PAHs derivatives $\pm$ SD [ng L $^{-1}$ ]
PT-S	$145.21 \pm 6.65$	$56.63 \pm 2.59$	$28.40 \pm 1.30$	$2.56 \pm 0.11$	$2.36 \pm 0.10$	$0.83 \pm 0.03$
PT-W	$181.08 \pm 8.29$	$171.36 \pm 7.85$	$1.92 \pm 0.09$	$3.17 \pm 0.15$	$2.92 \pm 0.14$	$0.48 \pm 0.02$
PT-A	$151.47 \pm 6.94$	$75.01 \pm 3.43$	$7.64 \pm 0.35$	$4.45 \pm 0.24$	$4.24 \pm 0.23$	$0.51 \pm 0.02$
PT-D	$57.36 \pm 2.63$	$57.36 \pm 2.63$	0	$2.21 \pm 0.11$	$2.12 \pm 0.11$	0
PT-F	$134.01 \pm 6.14$	$75.49 \pm 3.46$	$11.89 \pm 0.54$	$3.67 \pm 0.17$	$3.53 \pm 0.17$	$0.32 \pm 0.02$
RBP-UH	$201.64 \pm 9.23$	$184.93 \pm 8.47$	$5.62 \pm 0.26$	$41.53 \pm 1.52$	$41.32 \pm 1.51$	$0.88 \pm 0.03$
RBP-KO	$180.18 \pm 8.25$	$164.06 \pm 7.51$	$3.42 \pm 0.16$	$10.36 \pm 0.38$	$9.41 \pm 0.34$	$0.22 \pm 7.8 \times 10^{-3}$
RBP-PI	$187.31 \pm 8.58$	$162.65 \pm 7.45$	$16.19 \pm 0.74$	$10.38 \pm 0.38$	$8.99 \pm 0.33$	$4.64 \pm 0.17$
SSL-CH	$120.70 \pm 5.53$	$77.70 \pm 3.56$	$44.58 \pm 2.04$	$9.04 \pm 0.52$	$8.92 \pm 0.52$	$0.93 \pm 0.05$
SSL-KZ	$188.47 \pm 8.63$	$92.87 \pm 4.25$	$4.86 \pm 0.22$	$10.13 \pm 0.46$	$7.60 \pm 0.34$	$0.54 \pm 0.02$
SSL-SI	$150.04 \pm 6.87$	$86.52 \pm 3.96$	$12.43 \pm 0.57$	$3.33 \pm 0.15$	$3.16 \pm 0.14$	$0.43 \pm 0.02$
SSL-Z	$125.83 \pm 5.76$	$107.16 \pm 4.91$	$5.30 \pm 0.24$	$39.98 \pm 1.46$	$39.71 \pm 1.45$	$1.90 \pm 0.07$

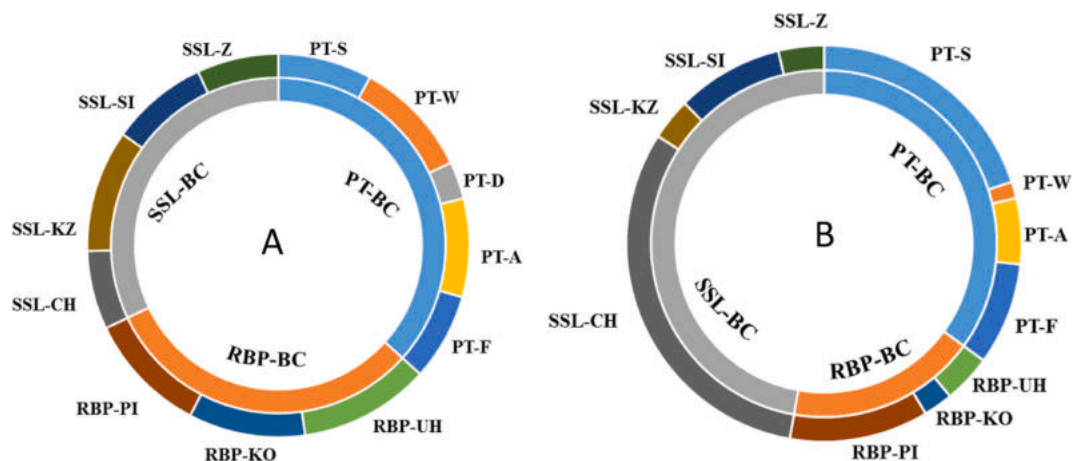


Fig. 2. The total concentration of PAHs (A) and derivatives (B) in various biochars [ $\mu\text{g g}^{-1}$ ].

### 3.3. The bioavailable PAHs and their derivatives in BC

The most important from the environmental point of view is the presence of a bioavailable fraction of PAHs and their derivatives. The presence of this fraction is connected with increased environmental hazard during BC application. The total concentration of bioavailable PAHs and their derivatives in biochars obtained from plants, sewage sludges, and RBP were measured and presented in Table 4 and Supplementary Information.

#### 3.3.1. Pristine PAHs

The results were quite similar to the total content of PAHs, and the impact of applied plants on bioavailable PAHs concentrations was negligible. The total content of bioavailable PAHs and the concentration of  $\Sigma 16$ PAHs in straw-, willow-, hardwood-, sunflower-, and softwood-derived biochar are shown in Fig. 3A and Table 4. In PT-S, PT-W, and PT-D, there were no 2-rings PAHs detected quantitatively, but in these samples (and PT-A sample) three-ring species were predominant (96.78%, 97.78%, 98.64% (and 86.10%), respectively). The most abundant PAHs in straw-derived biochar were: acenaphthene, acenaphthylene, and 3-methylphenanthrene (which constituted 58.00%, 33.54%, and 5.24% of the total PAHs concentration, respectively). But amongst the 4-ring species relatively high concentrations were quantified for 4-methylpyrene and 2-methylpyrene (38.31% and 29.64% of all four-rings PAHs, respectively). The most abundant PAHs in PT-W and

PT-D were acenaphthene, fluorene, and acenaphthylene (37.46%, 31.40%, 24.65%, and 68.56%, 15.34%, 11.17% of all 3-ring species), and in PT-A acenaphthene, acenaphthylene, and anthracene. But the most prevalent 4-ring compound was 2-methylpyrene in willow-derived BC, 6-methylchrysene in hardwood residues-derived BC, and 4-methylpyrene in sunflower-derived BC (48.57%, 57.54%, and 82.99% of all 4-ring species). PT-F sample was characterized by quite different distribution of analyte because two ring-PAH- naphthalene - was the most abundant compound (54.07%). 3-ring species constituted 44.63% of all PAHs (with the highest concentration for fluorene, acenaphthene, and acenaphthylene).

The results obtained for RBP-derived biochars were inconclusive. The total content of bioavailable PAHs in RBP-KO and RBP-PI samples ( $10.36 \pm 0.38 \text{ ng L}^{-1}$ ,  $10.38 \pm 0.38 \text{ ng L}^{-1}$ , respectively) and their percentage distribution followed a similar trend, but the data received for RBP-UH were divergent ( $41.53 \pm 1.52 \text{ ng L}^{-1}$ ). In RBP-KO and RBP-PI the most prevalent were 3-ring species (62.09% and 67.04%) (like in plant-derived biochars). In both cases, the higher concentrations were found for fluorene and anthracene (and they amounted to 43.37%, 23.27% for RBP-KO, and 60.70% and 22.26% for RBP-PI, respectively (concerning all quantified 3-ring PAHs)). The second most commonly occurred species were 2-ring PAHs. They accounted for 34.95% and 24.28% for RBP-KO and RBP-PI, respectively. In both cases, the same compounds were quantified: naphthalene, 1,3-di-iso-propynaphthalene, and 2-phenylnaphthalene, and in both cases, the first one has the

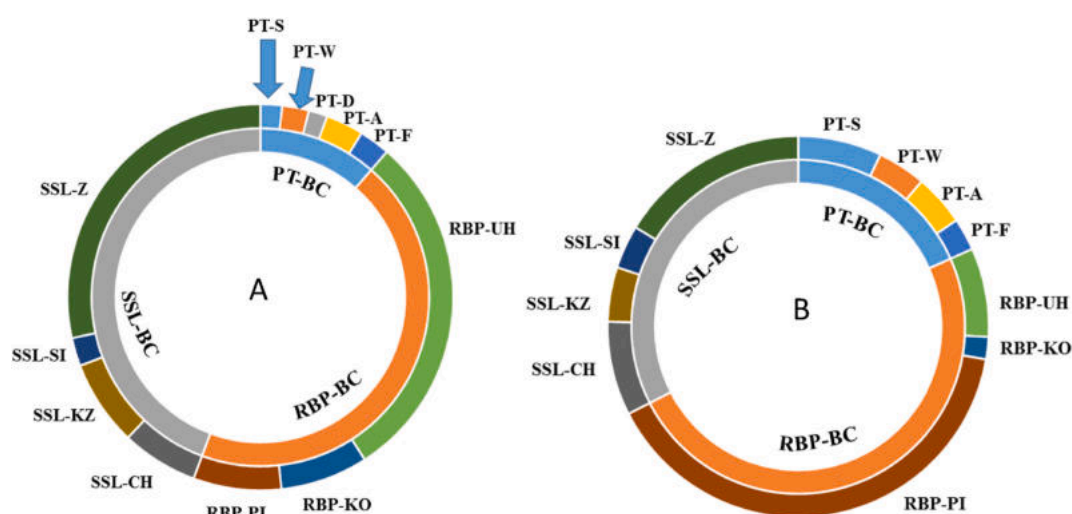


Fig. 3. The total concentration of bioavailable PAHs (A) and derivatives (B) in various biochars [ $\text{ng L}^{-1}$ ].

highest concentration ( $2.73 \pm 1.10 \text{ ng L}^{-1}$  and  $1.22 \pm 0.045 \text{ ng L}^{-1}$ , respectively). 4-, 5-, and 6-rings PAHs constituted 2.87%, 0.084%, and 0.004% for RBP-KO, 8.49%, 0.17%, and 0.012% for RBP-PI (the % of the total PAHs concentration). The results for the third RBP-derived biochar (RBP-UH) vary greatly from those described above. The total concentration of all PAHs (and the total concentration of  $\Sigma 16\text{PAHs}$ ) equated to  $41.53 \pm 1.52 \text{ ng L}^{-1}$  (and  $41.32 \pm 1.51 \text{ ng L}^{-1}$ ), which is more than four times higher than in the case of biochars obtained from the same type of feedstock (RBP-KO and RBP-PI). The 2-rings species were the most prevalent compounds, but it was because of the enormous concentration of naphthalene ( $32.88 \pm 1.20 \text{ ng L}^{-1}$ ) which constituted 79.17% of all quantified pristine PAHs. 3-rings compounds equated to 19.83% and high concentrations were observed for acenaphthene, acenaphthylene, and fluorene (46.46%, 32.85%, and 12.87% of all three rings species, respectively). 4-rings PAHs were mostly represented by pyrene and fluoranthene (40.44% and 33.10% of all 4-rings species). 5-, and 6-ring measured compounds were a minority and constituted 0.012% and  $8.2 \cdot 10^{-3}\%$  of all pristine PAHs.

The lowest concentration of bioavailable pristine PAHs (and  $\Sigma 16\text{PAHs}$ ) was determined in SSL-SI:  $3.33 \pm 0.15 \text{ ng L}^{-1}$  ( $3.16 \pm 0.14 \text{ ng L}^{-1}$ ). The concentration of identified 2-ring PAHs was below the limit of detection and 3-ring species constituted 95.78% of all determined PAHs. The concentration of acenaphthene was the highest, then acenaphthylene, fluorene, and 3-methylphenanthrene (51.57%, 22.10%, 18.94%, and 3.17%, respectively). 4-, 5-, and 6-rings PAHs represented only 4.22% of all bioavailable PAHs. SSL-CH and SSL-KZ were characterized by quite similar results: and the total concentration of bioavailable pristine PAHs (and  $\Sigma 16\text{PAHs}$ ) varied from  $9.04 \pm 0.52 \text{ ng L}^{-1}$  to  $10.13 \pm 0.46 \text{ ng L}^{-1}$  ( $8.92 \pm 0.52 \text{ ng L}^{-1}$  and  $7.60 \pm 0.34 \text{ ng L}^{-1}$ ) for SSL-CH and SSL-KZ, respectively. In both cases, the majority were 2-ring PAHs. But in the SSL-CH sample, among 2-ring species, only naphthalene was determined quantitatively and constituted 51.84% of all PAHs. In SSL-KZ, naphthalene, and 2-phenylnaphthalene represented 73.26% of all PAHs (i.e. 2-ring PAHs). 3-ring species also represented a significant part of the total concentration of bioavailable compounds in SSL-CH and SSL-KZ (46.76% and 25.94%). In SSL-CH the highest concentration was determined for acenaphthene (55.42% of all 3-ring species), while acenaphthylene and anthracene were detected at lower concentrations. In SSL-KZ, 3-rings PAHs were represented by fluorene, acenaphthene, and 3-methylphenanthrene, which constituted 49.84%, 45.97%, and 4.19%, respectively. 4-, 5-, and 6-ring species had a small contribution to the total concentration's of bioavailable PAHs, and cumulatively accounted for 1.40% for SSL-CH and 0.80% for SSL-KZ. In SSL-Z, the concentration of bioavailable PAHs with the number of rings greater or equal to 4 was also a minority and constituted 0.68% of all PAHs. But this biochar is distinguished by the highest total concentration of bioavailable PAHs (and  $\Sigma 16\text{PAHs}$ ), which amounted to  $39.98 \pm 1.46 \text{ ng L}^{-1}$  ( $39.71 \pm 1.45 \text{ ng L}^{-1}$ ). Moreover, 89.56% of them constituted 2-ring species. In addition, 99.55% of 2-ring PAHs were represented by naphthalene. PAHs with 3 aromatic rings equated to 9.77%, in which acenaphthylene, acenaphthene, and fluorene were the most abundant.

### 3.3.2. PAHs derivatives

During the experiment, some O- and N-PAHs were quantified in all biochars. Their quality and quantity depend on applied feedstocks. For all biochars, the total concentrations of PAHs derivatives are shown in Table 4 and Fig. 3B. In PT-BC the quantified PAHs derivatives constituted 24.41% (PT-S), 13.19% (PT-W), 10.30% (PT-A), and 8.02% (PT-F) of all quantified PAHs and their derivatives. In biochar obtained from hardwood residues, the concentration of derivatives was below the limit of detection. 4-rings PAHs derivatives were predominant, which is the reversed situation in comparison to pristine compounds. In PT-S, 4H-cyclopenta(def)phenanthrene, (the only representative of O-PAHs) constituted 69.20% of all derivatives, whereas 30.80% represented N-PAHs: 1-methyl-5-nitronaphthalene and 1-methyl-6-nitronaphthalene.

In PT-W only 4-rings species were quantified, from which 97.29% accounted for 4H-cyclopenta(def)phenanthrene. In PT-A and PT-F only 9,10-anthracenedione, 4H-cyclopenta(def)phenanthrene, and nitronaphthalene were quantitatively determined.

In RBP-BC, various PAH derivatives were also found. Unlike pristine PAHs, the highest concentration of the total PAHs derivatives was determined for RBP-PI ( $4.64 \pm 0.17 \text{ ng L}^{-1}$ ) which constituted 30.89% of all pristine PAHs and derivatives. In RBP-UH and RBP-KO significantly lower concentrations were noted ( $0.88 \pm 0.03 \text{ ng L}^{-1}$  and  $0.22 \pm 0.008 \text{ ng L}^{-1}$ , respectively) and constituted 2.08% and 2.05% of all compounds. In RBP-PI, 2-rings N-PAHs (nitronaphthalene, 1-methyl-5-nitronaphthalene, 1-methyl-6-nitronaphthalene) were the most abundant and equated to 99.24% of all derivatives. Moreover, their percentages were quite comparable (and amounted to 33.44%, and 35.74%, and 30.82%, respectively). The rest of all derivatives (0.76%) constituted nitropyrene. In the case of RBP-PI, there were no O-PAHs quantified. In RBP-UH, the most abundant was 9,10-anthracenedione (60.98% of all derivatives), followed by nitronaphthalene (38.54%) and 4H-cyclopenta(def)phenanthrene (0.48%). In RBP-KO only two compounds were determined, i.e. 9,10-anthracenedione (77.36%) and nitropyrene (22.64%).

$1.90 \pm 0.07 \text{ ng L}^{-1}$  of PAHs derivatives were determined in SSL-Z which constituted 4.54% of all quantified compounds. Next, in descending order were SSL-CH ( $0.93 \pm 0.05 \text{ ng L}^{-1}$ ), SSL-KZ ( $0.54 \pm 0.02 \text{ ng L}^{-1}$ ), and SSL-SI ( $0.43 \pm 0.02 \text{ ng L}^{-1}$ ), and they equated to 9.32%, 5.02%, and 11.35% of all PAHs and their derivatives. In all SS-BC, N- and O-PAHs were determined. In SSL-Z and SSL-CH, N-PAHs (1-methyl-5-nitronaphthalene and 1-methyl-6-nitronaphthalene) constituted 89.81% and 16.45% of all derivatives. The representative of O-PAHs was 9,10-anthracenedione (in SSL-Z) and 4H-cyclopenta(def)phenanthrene (in SSL-CH). In SSL-KZ, nitronaphthalene and 9,10-anthracenedione constituted 62.59% and 37.41% of all derivatives. However, 4H-cyclopenta(def)phenanthrene, 9,10-anthracenedione, and nitropyrene were the only PAH derivatives determined quantitatively in SSL-SI.

Our results clearly indicated that the quality and quantity of bioavailable PAHs and their derivatives in biochars differ considering applied feedstock (Hale et al., 2012; Koltowski and Oleszczuk, 2015; Oleszczuk et al., 2013; Weidemann et al., 2018). Considering the concentrations of bioavailable PAHs and their derivatives, the comparison of our data with the results obtained by other Researchers is quite difficult because the studies about strictly this topic are very limited. Only several groups of scientists deal with the bioavailability of PAHs and derivatives. Hale et al. (2012) in their study presented the concentrations of bioavailable PAHs but also total PAHs in biochars obtained from various feedstocks in a wide range of temperatures (250 °C–900 °C). The lowest concentration was detected for pine-derived biochar ( $0.17 \pm 0.04 \text{ ng L}^{-1}$ ) and the highest for food waste-derived BC ( $10.0 \pm 1.1 \text{ ng L}^{-1}$ ) (Hale et al., 2012). For BC obtained from wheat straw at 450 °C, the concentration of  $\Sigma 13\text{PAHs}$  amounted to  $2.633 \pm 0.5498 \text{ ng L}^{-1}$  which is very similar to our results. In the case of hardwood-derived BC, the data presented by Hale et al. (2012) ( $1.904 \pm 0.2439 \text{ ng L}^{-1}$  for hardwood-derived BC obtained at 450°C–500 °C, and  $0.281 \pm 0.1537 \text{ ng L}^{-1}$  for laurel oak-derived BC obtained at 650 °C) were lower than ours. Only a few biochars from Hale's studies were obtained at 600 °C (BC produced from digested dairy manure, food waste, paper mill waste, pinewood ( $0.831 \pm 0.231 \text{ ng L}^{-1}$ ), and switchgrass ( $0.750 \pm 0.151 \text{ ng L}^{-1}$ )) (Hale et al., 2012). And the last two results were lower than the concentrations of bioavailable PAHs obtained in our studies (for plant-derived biochars).

Weidemann et al. (2018) found that the concentration of PAHs<sub>free</sub> in wheat straw-derived biochars was nearly seven times higher than produced from softwood. Moreover, BC produced from straw was characterized by a higher content of 4-, 5-, and 6-rings PAHs than those obtained from sewage sludge, pine, or spruce (Weidemann et al., 2018). As in our results, the concentrations of PAHs derivatives in studied

biochar were lower than pristine PAHs. Kończak et al. (2019) showed that the concentration of Σ16PAHs<sub>free</sub> in SS-derived biochars amounted to 44.3–50.5 ng L<sup>-1</sup>, while in another study the concentrations of the same compounds were 81–126 ng L<sup>-1</sup> (Zielinska and Oleszczuk, 2016). As in our results, 2- and 3-ring compounds were predominant and accounted for more than 90% and approximately 8% (Kończak et al., 2019). The water solubility of PAHs derivatives is increasing when the number of rings decreases (Hien et al., 2007). In our results in all cases, there were no 5- and 6-rings PAHs derivatives detected. It can be caused by the properties of this group of compounds. Considering possible interactions of PAHs, and probably their derivatives, and biochar surface it was estimated (de Jesus et al., 2017) that π-π interactions among similar groups are the main driving force for adsorption of PAHs onto BC surface. However, physical adsorption and hydrophobic interactions cannot be excluded.

To associate the physicochemical parameters with PAHs and their derivatives concentrations and to verify some dependences the r-Pearson test and One-Way Anova, (Statgraphics Plus) were performed. The number of degrees of freedom was 10, and the statistical significance level was 0.1. Statistical analysis revealed only a few important correlations. PAHs total content in all tested materials was only connected with the pH of obtained materials ( $p < 0.05$ ). The increase of the surface area of tested biochar induced the increase of the content of 2-rings pristine PAHs ( $p < 0.02$ ) and 3-rings PAHs derivatives ( $p < 0.05$ ). An increase in pH has induced the formation of 3-rings PAHs ( $p < 0.05$ ). An increase in BC aromaticity increased the bioavailability of 4-rings pristine PAHs. The highest impact in the amount of determined PAHs revealed 3-ring PAHs, whereas in PAHs derivatives – 4-rings compounds ( $p < 0.05$ ). A strong correlation was noted between the amount of bioavailable PAHs and PAHs derivatives and 2-rings compounds ( $p < 0.01$ ). One factorial analysis of variance ( $p < 0.05$ ) was performed and data revealed that the applied feedstock affected both the quality and quantity of PAHs derivatives (0.6778) in BC.

#### 4. Conclusions

During pyrolysis, PAHs and PAH derivatives are formed in biochar. The highest total concentration of PAHs was determined in biochar obtained from residues from biogas production (up to 201.64 µg g<sup>-1</sup>), followed by sewage sludge-derived and plant-derived-BC. The bioavailable fraction of PAHs in BC was low: 2%–5% (PT-BC), 5–21% (SSL-BC) and 2–31% (RBP-BC). N-, O-PAHs constituted up to 2–10% of all quantified PAHs in RBP-BC, 20% - in PT-BC, and 2–37% in SSL-BC with bioavailability reaching 3–25% (PT-BC), 2–29% (RBP-BC), and 2–36% (SSL-BC) indicating that the lower environmental hazard of plant-derived BC.

#### Author credit statement

Agnieszka Krzyszczak: Investigation, Writing- Reviewing and Editing, Michał P. Dybowski: Investigation, Methodology, Formal analysis, Validation; Magdalena Kończak: Investigation; Bozena Czech: Investigation, Methodology, Visualization, Writing- Reviewing and Editing, Conceptualization, Validation, Supervision

#### Declaration of competing interest

The authors declare the following financial interests/personal relationships which may be considered as potential competing interests: Bozena Czech reports financial support was provided by National Science Centre Poland.

#### Acknowledgments

The studies were supported by project No. 2018/31/B/NZ9/00317 funded by the National Science Centre, Poland.

#### Appendix A. Supplementary data

Supplementary data to this article can be found online at <https://doi.org/10.1016/j.envres.2022.113787>.

#### References

- Abbas, I., Badran, G., Verdin, A., Ledoux, F., Roumié, M., Courcot, D., Garçon, G., 2018. Polycyclic aromatic hydrocarbon derivatives in airborne particulate matter: sources, analysis and toxicity. Environ. Chem. Lett. 16, 439–475. <https://doi.org/10.1007/s10311-017-0697-0>.
- Bandowe, B.A.M., Meusel, H., 2017. Nitrated polycyclic aromatic hydrocarbons (nitro-PAHs) in the environment – a review. Sci. Total Environ. 581–582, 237–257. <https://doi.org/10.1016/j.scitotenv.2016.12.115>.
- Besis, A., Gallou, D., Avgenikou, A., Serafeim, E., Samara, C., 2022. Size-dependent in vitro inhalation bioaccessibility of PAHs and O/N PAHs - implications to inhalation risk assessment. Environ. Pollut. 301, 119045 <https://doi.org/10.1016/j.envpol.2022.119045>.
- Bucheli, T., Hilber, Isabel, Schmidt, H.P., 2015. Polycyclic aromatic hydrocarbons and polychlorinated aromatic compounds in biochar. In: Biochar for Environmental Management. Routledge, pp. 593–622.
- Chan, K.Y., Van Zwieten, L., Meszaros, I., Downie, A., Joseph, S., 2007. Agronomic values of greenwaste biochar as a soil amendment. Soil Res. 45, 629. <https://doi.org/10.1071/SR07109>.
- Chia, C.H., Gong, B., Joseph, S.D., Marjo, C.E., Munroe, P., Rich, A.M., 2012. Imaging of mineral-enriched biochar by FTIR, Raman and SEM-EDX. Vib. Spectrosc. 62, 248–257. <https://doi.org/10.1016/j.vibspec.2012.06.006>.
- de Jesus, J.H.F., da Cunha, G., Cardoso, E.M.C., Mangrich, A.S., Romão, L.P.C., 2017. Evaluation of waste biomasses and their biochars for removal of polycyclic aromatic hydrocarbons. J. Environ. Manag. 200, 186–195. <https://doi.org/10.1016/j.jenvman.2017.05.084>.
- del Rosario Sierra, M.M., 2006. Oxygenated polycyclic aromatic hydrocarbons in urban air particulate matter. Atmos. Environ. 40, 2374–2384. <https://doi.org/10.1016/j.atmosenv.2005.12.009>.
- Devi, P., Saroha, A.K., 2015. Effect of pyrolysis temperature on polycyclic aromatic hydrocarbons toxicity and sorption behaviour of biochars prepared by pyrolysis of paper mill effluent treatment plant sludge. Bioresour. Technol. 192, 312–320. <https://doi.org/10.1016/j.biortech.2015.05.084>.
- European Commission. Joint Research Centre. Institute for Environment and Sustainability, 2010. Biochar Application to Soils: a Critical Scientific Review of Effects on Soil Properties, Processes and Functions. Publications Office, LU.
- Glaser, B., Lehmann, J., Zech, W., 2002. Ameliorating physical and chemical properties of highly weathered soils in the tropics with charcoal - a review. Biol. Fertil. Soils 35, 219–230. <https://doi.org/10.1007/s00374-002-0466-4>.
- Hale, S.E., Lehmann, J., Rutherford, D., Zimmerman, A.R., Bachmann, R.T., Shitumbanuma, V., O'Toole, A., Sundqvist, K.L., Arp, H.P.H., Cornelissen, G., 2012. Quantifying the total and bioavailable polycyclic aromatic hydrocarbons and dioxins in biochars. Environ. Sci. Technol. 46, 2830–2838. <https://doi.org/10.1021/es303984k>.
- Hardie, M., Clothier, B., Bound, S., Oliver, G., Close, D., 2014. Does biochar influence soil physical properties and soil water availability? Plant Soil 376, 347–361. <https://doi.org/10.1007/s11104-013-1980-x>.
- Hien, T.T., Thanh, L.T., Kameda, T., Takenaka, N., Bandow, H., 2007. Nitro-polycyclic aromatic hydrocarbons and polycyclic aromatic hydrocarbons in particulate matter in an urban area of a tropical region: Ho Chi Minh City, Vietnam. Atmos. Environ. 41, 7715–7725. <https://doi.org/10.1016/j.atmosenv.2007.06.020>.
- Hilber, I., Blum, F., Leifeld, J., Schmidt, H.-P., Bucheli, T.D., 2012. Quantitative determination of PAHs in biochar: a prerequisite to ensure its quality and safe application. J. Agric. Food Chem. 60, 3042–3050. <https://doi.org/10.1021/jf205278v>.
- Keiluweit, M., Kleber, M., Sparrow, M.A., Simoneit, B.R.T., Prahl, F.G., 2012. Solvent-extractable polycyclic aromatic hydrocarbons in biochar: influence of pyrolysis temperature and feedstock. Environ. Sci. Technol. 46, 9333–9341. <https://doi.org/10.1021/es302125k>.
- Kloss, S., Zehtner, F., Dellantonio, A., Hamid, R., Ottner, F., Liedtke, V., Schwanninger, M., Gerzabek, M.H., Soja, G., 2012. Characterization of slow pyrolysis biochars: effects of feedstocks and pyrolysis temperature on biochar properties. J. Environ. Qual. 41, 990–1000. <https://doi.org/10.2134/jeq2011.0070>.
- Koltowski, M., Oleszczuk, P., 2015. Toxicity of biochars after polycyclic aromatic hydrocarbons removal by thermal treatment. Ecol. Eng. 75, 79–85. <https://doi.org/10.1016/j.ecoleng.2014.11.004>.
- Kończak, M., Gao, Y., Oleszczuk, P., 2019. Carbon dioxide as a carrier gas and biomass addition decrease the total and bioavailable polycyclic aromatic hydrocarbons in biochar produced from sewage sludge. Chemosphere 228, 26–34. <https://doi.org/10.1016/j.chemosphere.2019.04.029>.
- Krzyszczak, A., Czech, B., 2021. Occurrence and toxicity of polycyclic aromatic hydrocarbons derivatives in environmental matrices. Sci. Total Environ. 788, 147738 <https://doi.org/10.1016/j.scitotenv.2021.147738>.
- Krzyszczak, A., Dybowski, M.P., Czech, B., 2021. Formation of polycyclic aromatic hydrocarbons and their derivatives in biochars: the effect of feedstock and pyrolysis conditions. J. Anal. Appl. Pyrol. 160, 105339 <https://doi.org/10.1016/j.jaap.2021.105339>.

- Kuśmierz, M., Oleszczuk, P., Kraska, P., Patys, E., Andruszczak, S., 2016. Persistence of polycyclic aromatic hydrocarbons (PAHs) in biochar-amended soil. *Chemosphere* 146, 272–279. <https://doi.org/10.1016/j.chemosphere.2015.12.010>.
- Laumbach, R., Tong, J., Zhang, L., Ohman-Strickland, P., Stern, A., Fiedler, N., Kipen, H., Kelly-McNeil, K., Lioy, P., Zhang, J., 2008. Quantification of 1-aminopyrene in human urine after a controlled exposure to diesel exhaust. *J. Environ. Monit.* 11, 153–159. <https://doi.org/10.1039/B810039J>.
- Lehmann, J., Joseph, S., 2009. An introduction. In: *Biochar for Environmental Management*, Routledge, second ed.
- Lehmann, J., Pereira da Silva, J., Steiner, C., Nehls, T., Zech, W., Glaser, B., 2003. Nutrient availability and leaching in an archaeological Anthrosol and a Ferralsol of the Central Amazon basin: fertilizer, manure and charcoal amendments. *Plant Soil* 249, 343–357. <https://doi.org/10.1023/A:1022833116184>.
- Li, S., Barreto, V., Li, R., Chen, G., Hsieh, Y.P., 2018. Nitrogen retention of biochar derived from different feedstocks at variable pyrolysis temperatures. *J. Anal. Appl. Pyrol.* 133, 136–146. <https://doi.org/10.1016/j.jaap.2018.04.010>.
- Lundstedt, S., White, P.A., Lemieux, C.L., Lynes, K.D., Lambert, I.B., Öberg, L., Haglund, P., Tysklind, M., 2007. Sources, fate, and toxic hazards of oxygenated polycyclic aromatic hydrocarbons (PAHs) at PAH-contaminated sites. *AMBIOT A J. Hum. Environ.* 36, 475–485. [https://doi.org/10.1579/0044-7447\(2007\)36\[475:SFATHO\]2.0.CO;2](https://doi.org/10.1579/0044-7447(2007)36[475:SFATHO]2.0.CO;2).
- Mahler, B.J., Metre, P.C.V., Crane, J.L., Watts, A.W., Scoggins, M., Williams, E.S., 2012. Coal-tar-based pavement sealcoat and PAHs: implications for the environment, human health, and stormwater management. *Environ. Sci. Technol.* 46, 3039–3045. <https://doi.org/10.1021/es203699x>.
- Morant, C., Andreu, J., Prieto, P., Mendiola, D., Sanz, J.M., Elizalde, E., 2006. XPS characterization of nitrogen-doped carbon nanotubes. *phys. stat. sol.* 203, 1069–1075. <https://doi.org/10.1002/pssa.200566110>.
- Novak, J.M., Lima, I., Xing, B., Gaskin, J.W., Steiner, C., Das, K.C., Ahmedna, M., Rehrha, D., Watts, D.W., Busscher, W.J., Schomberg, H., 2009. Characterization of designer biochar produced at different temperatures and their effects on a Loamy sand. *Annals of Environmental Science* 3.
- Nowakowski, M., Rykowska, I., Wolski, R., Andrzejewski, P., 2022. Polycyclic aromatic hydrocarbons (PAHs) and their derivatives (O-PAHs, N-PAHs, OH-PAHs): determination in suspended particulate matter (SPM) – a review. *Environ. Process.* 9, 2. <https://doi.org/10.1007/s40710-021-00555-7>.
- Okpalugo, T.I.T., Papakonstantinou, P., Murphy, H., McLaughlin, J., Brown, N.M.D., 2005. High resolution XPS characterization of chemical functionalised MWNTs and SWCNTs. *Carbon* 43, 153–161. <https://doi.org/10.1016/j.carbon.2004.08.033>.
- Oleszczuk, P., Joško, I., Kuśmierz, M., 2013. Biochar properties regarding to contaminants content and ecotoxicological assessment. *J. Hazard Mater.* 260, 375–382. <https://doi.org/10.1016/j.jhazmat.2013.05.044>.
- Oleszczuk, P., Kuśmierz, M., Godlewska, P., Kraska, P., Patys, E., 2016. The concentration and changes in freely dissolved polycyclic aromatic hydrocarbons in biochar-amended soil. *Environ. Pollut.* 214, 748–755. <https://doi.org/10.1016/j.envpol.2016.04.064>.
- Pariyar, P., Kumari, K., Jain, M.K., Jadho, P.S., 2020. Evaluation of change in biochar properties derived from different feedstock and pyrolysis temperature for environmental and agricultural application. *Sci. Total Environ.* 713, 136433 <https://doi.org/10.1016/j.scitotenv.2019.136433>.
- Ringuet, J., Leoz-Garziandia, E., Budzinski, H., Villenave, E., Albinet, A., 2012. Particle size distribution of nitrated and oxygenated polycyclic aromatic hydrocarbons (NPAHs and OPAHs) on traffic and suburban sites of a European megacity: Paris (France). *Atmos. Chem. Phys.* 12, 8877–8887. <https://doi.org/10.5194/acp-12-8877-2012>.
- Singh, B., Singh, B.P., Cowie, A.L., 2010. Characterisation and evaluation of biochars for their application as a soil amendment. *Soil Res.* 48, 516. <https://doi.org/10.1071/SR10058>.
- Stefaniuk, M., Oleszczuk, P., 2015. Characterization of biochars produced from residues from biogas production. *J. Anal. Appl. Pyrol.* 115, 157–165. <https://doi.org/10.1016/j.jaap.2015.07.011>.
- Sullivan, R.F., Boduszynski, M.M., Fetzer, J.C., 1989. Molecular transformations in hydrotreating and hydrocracking. *Energy Fuels* 3, 603–612. <https://doi.org/10.1021/ef00017a013>.
- Traversi, D., Schilirò, T., Degan, R., Pignata, C., Alessandria, L., Gilli, G., 2011. Involvement of nitro-compounds in the mutagenicity of urban Pm2.5 and Pm10 in Turin. *Mutat. Res., Genet. Toxicol. Environ. Mutagen.* 726, 54–59. <https://doi.org/10.1016/j.mrgentox.2011.09.002>.
- Wang, C., Wang, Y., Herath, H.M.S.K., 2017. Polycyclic aromatic hydrocarbons (PAHs) in biochar – their formation, occurrence and analysis: a review. *Org. Geochem.* 114, 1–11. <https://doi.org/10.1016/j.orggeochem.2017.09.001>.
- Weidemann, E., Buss, W., Edo, M., Mašek, O., Jansson, S., 2018. Correction to: influence of pyrolysis temperature and production unit on formation of selected PAHs, oxy-PAHs, N-PACs, PCDDs, and PCDFs in biochar—screening study. *Environ. Sci. Pollut. Control Ser.* 25, 3941–3942. <https://doi.org/10.1007/s11356-017-0804-6>.
- Yu, Z., Chen, L., Pan, S., Li, Y., Kuzyakov, Y., Xu, J., Brookes, P.C., Luo, Y., 2018. Feedstock determines biochar-induced soil priming effects by stimulating the activity of specific microorganisms. *Eur. J. Soil Sci.* 69, 521–534. <https://doi.org/10.1111/ejss.12542>.
- Zhang, J., Lü, F., Zhang, H., Shao, L., Chen, D., He, P., 2015. Multiscale visualization of the structural and characteristic changes of sewage sludge biochar oriented towards potential agronomic and environmental implication. *Sci. Rep.* 5, 9406. <https://doi.org/10.1038/srep09406>.
- Zhang, Y., Yang, B., Gan, J., Liu, C., Shu, X., Shu, J., 2011. Nitration of particle-associated PAHs and their derivatives (nitro-, oxy-, and hydroxy-PAHs) with NO<sub>3</sub> radicals. *Atmos. Environ.* 45, 2515–2521. <https://doi.org/10.1016/j.atmosenv.2011.02.034>.
- Zhao, L., Cao, X., Mašek, O., Zimmerman, A., 2013. Heterogeneity of biochar properties as a function of feedstock sources and production temperatures. *J. Hazard Mater.* 256–257, 1–9. <https://doi.org/10.1016/j.jhazmat.2013.04.015>.
- Zielinska, A., Oleszczuk, P., 2016. Effect of pyrolysis temperatures on freely dissolved polycyclic aromatic hydrocarbon (PAH) concentrations in sewage sludge-derived biochars. *Chemosphere* 153, 68–74. <https://doi.org/10.1016/j.chemosphere.2016.02.118>.
- Zielinska, A., Oleszczuk, P., Charmas, B., Skubiszewska-Zięba, J., Pasieczna-Patkowska, S., 2015. Effect of sewage sludge properties on the biochar characteristic. *J. Anal. Appl. Pyrol.* 112, 201–213. <https://doi.org/10.1016/j.jaap.2015.01.025>.

**Low bioavailability of derivatives of polycyclic aromatic hydrocarbons in biochar  
obtained from different feedstock**

Agnieszka Krzyszczak<sup>1</sup>, Michał P. Dybowski<sup>2</sup>, Magdalena Kończak<sup>3</sup>, Bożena Czech<sup>1\*</sup>

<sup>1</sup>Department of Radiochemistry and Environmental Chemistry, Institute of Chemical Sciences, Faculty of Chemistry, Maria Curie-Sklodowska University in Lublin, Pl. M. Curie-Sklodowskiej 3, 20-031 Lublin, Poland

<sup>2</sup>Department of Chromatography, Institute of Chemical Sciences, Faculty of Chemistry, Maria Curie Skłodowska University in Lublin, Pl. M. Curie-Sklodowskiej 3, 20-031 Lublin, Poland

<sup>3</sup>Institute of Earth and Environmental Sciences, Faculty of Earth Sciences and Spatial Management, Maria Curie-Sklodowska University, ul. Kraśnicka 2cd, 20-718 Lublin, Poland

\*corresponding author: Tel.: +48 81 537 55 54; fax: +48 81 537 55 65; E-mail address:  
[bczech@hektor.umcs.lublin.pl](mailto:bczech@hektor.umcs.lublin.pl) (B. Czech)

Journal: Environmental Research

Number of pages: 19

Number of Figures: 2

Number of Tables: 7

## **2. Materials and methods**

### **2.1. The physico-chemical properties of biochar**

To determine the pH of biochars, 1.0 g of material mixed with 10 mL of deionized water was used and a digital pH meter HQ430d Benchtop Single Input (HACH, USA) was applied. To quantify the elemental carbon (C), hydrogen (H), and nitrogen (N), biochar was milled and EuroEA Elemental Analyser was used. ASAP 2420 (Micromeritics, USA) surface area and porosity analyzer were used for adsorption measurements and biochars were outgassed at 200°C for 12 h under vacuum. FT-IR/PAS spectra of the samples were recorded by Bio-Rad Excalibur 3000 MX spectrometer provided with photoacoustic detector MTEC300 (in the helium atmosphere in a detector) at RT over the 4000-400  $\text{cm}^{-1}$  range at the resolution of 4  $\text{cm}^{-1}$  and maximum source aperture. X-ray photoelectron spectroscopy, XPS (UHV Prevac), was used for the determination of surface functional groups of BC, whereas surface morphology was examined by scanning electron microscopy (Quanta 3D FEG, FEI) with an Energy Dispersive Spectroscopy system (SEM-EDS).

### **2.2. Freely dissolved (C<sub>free</sub>) PAH and their derivatives determination in biochars**

The qualitative and quantitative determination of the bioaccessibility of PAHs and their derivatives were carried out by the protocol described in Oleszczuk et al. (Oleszczuk et al., 2016) and Hale et al. (Hale et al., 2012) presented in Fig S1.

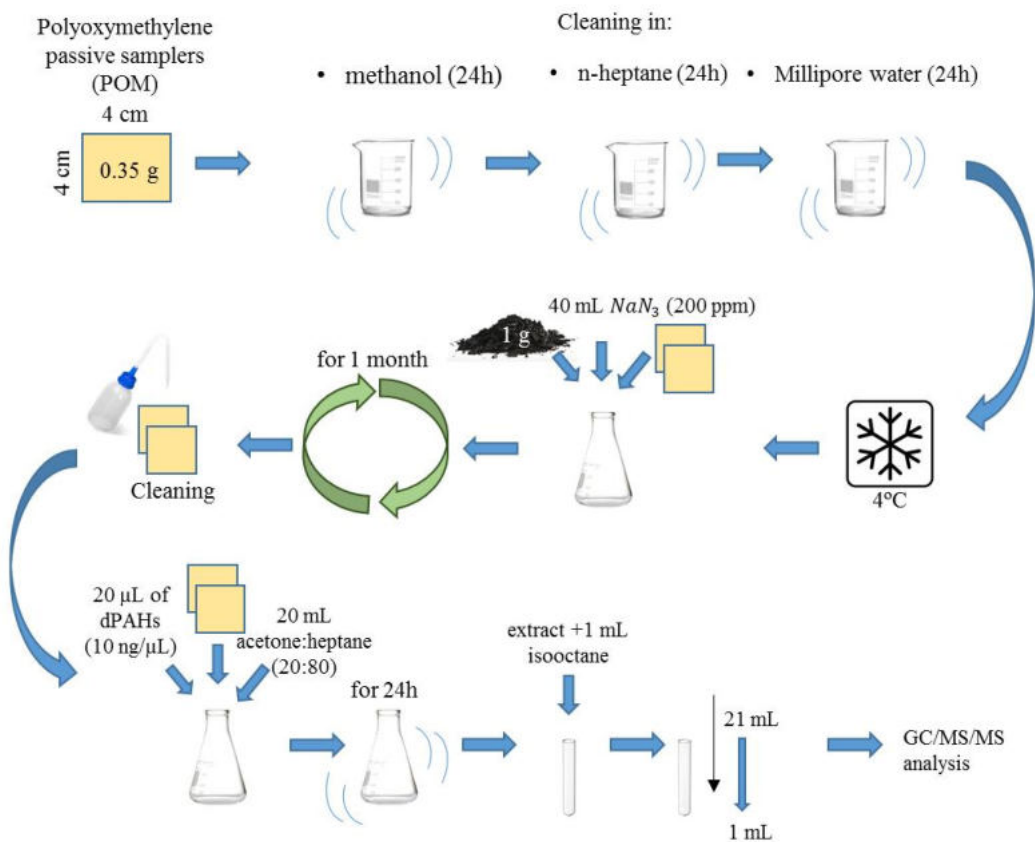


Fig. S1. Scheme of the determination of the bioavailable fraction of PAHs and their derivatives.

Before the sample preparation step, 76-mm thick polyoxymethylene (POM) passive samplers (4cm x 4cm, about 0.35 g each) were cleaned with methanol through shaking for 24 hours on a shaking machine (ELPIN 358A, Poland). Afterward, methanol was substituted with n-heptane and Millipore water, and the same procedure was applied. Cleaned POMs were stored in a glass bottle with Millipore water at 4°C until the extraction of the bioavailable fraction of PAHs and their derivatives were carried out. 1g of dried biochar was placed in 50 mL Erlenmeyer flasks with glass lids. Then, POM samplers and 40 mL of sodium azide (200 mg/L) dissolved in water were added for the elimination of any possible effect of residual microorganisms. Vials were tightly sealed to prevent leakage. Each sample was prepared in triplicate. Flasks were rolled for one month on a rotary shaker ROTAX 6.8 VELP Scientifica (Italy) at 10 RCF. After this period, POM samplers were cleaned with distilled water, placed in a 50 mL Erlenmeyer flask, and extracted with an acetone/heptane (20/80, v/v) mixture with the addition of internal standard. Subsequently, iso-octane was

added to the extract, and the obtained solvent was concentrated on a rotary vacuum concentrator RVC 2-25 CD plus (Martin Christ, Germany). Then, GC-MS/MS analysis was carried out. The concentration of PAHs and their derivatives on POM passive samplers ( $C_{POM}$ ) was calculated according to the equation (1):

$$C_{POM} = \frac{m_{PAH}}{m_{2POM}}$$

where  $m_{PAH}$  (ng) (or  $m_{PAH}$  derivatives) - the mass of PAHs (or PAHs derivatives) determined by GC-MS/MS and  $m_{2POM}$  (kg) - the mass of two used POM passive samplers.

$C_{free}$  concentrations were calculated using POM-water partitioning coefficients ( $K_{POM}$ ) known from previous studies (Hawthorne et al., 2011; Josefsson et al., 2015). In the case of certain PAHs derivatives,  $K_{POM}$  was adopted considering parent PAHs due to the lack of the available data in the literature (Hans-Peter Schmidt, 2015; Hawthorne et al., 2011). Freely dissolved ( $C_{free}$ ) PAHs and derivatives were measured according to equation (2):

$$C_{free} = \frac{K_{POM-w}}{C_{POM}}$$

where  $C_{free}$  (ng L<sup>-1</sup>) is the bioavailable pollutant concentration,  $K_{POM-w}$  (L kg<sup>-1</sup>) is the POM-water partitioning coefficient and  $C_{POM}$  (ng kg<sup>-1</sup>) is the measured POM concentration.

### 2.3. The total content of PAHs and their derivatives determination in biochar

PAHs and their derivatives were extracted via pressurized liquid extraction (PLE) using Dionex 350 system (Thermo Fisher Scientific) equipped with a 22 mL stainless steel cell. The first layer with silica gel (activated at 300°C, 5h) and copper, and the second, i.e. 0.5g of each biochar mixed with 0.1g ethylenediaminetetraacetic acid (EDTA), were loaded into the cell. The IS were added and the cells were completed by glass beads. Then, PLE was performed with hexane at 150°C using 2 extraction cycles and a flush volume at 60%. The static time was set at 5 min and the purge time was the 60s 1 MPa with N<sub>2</sub>. After extraction 1 mL of iso-octane was added to an extract and obtained solvent was concentrated to about 1 mL using a rotary vacuum concentrator RVC 2-25 CD plus (Martin Christ, Germany). Then, GC-MS/MS analysis was carried out.

### 2.4. GC-MS/MS measurement

Table S1. The qualitative and quantitative parameters of PAHs and O/N-PAHs analysis.

No.	Compound	Quantification ion ( <i>m/z</i> )	Confirmation ion ( <i>m/z</i> )	LOD* [ $\mu\text{g L}^{-1}$ ]	LOQ** [ $\mu\text{g L}^{-1}$ ]
1	Naphthalene	128	102	1.01	3.36
2	1,2-di-iso-propynaphthalene	212	124	1.44	4.79
3	2-Phenylnaphthalene	204	101	1.90	6.33
4	Acenaphthylene	152	76	2.10	6.99
5	Acenaphthene	153	76	2.30	7.66
6	Fluorene	166	82	1.10	3.66
7	Anthracene	178	89	1.30	4.33
8	Phenanthrene	178	89	1.34	4.36
9	3-Methylphenanthrene	192	165	2.42	8.06
10	2-Methylphenanthrene	192	165	2.42	8.06
11	9-Methylphenanthrene	192	96	3.23	10.76
12	3,6-dimethylphenanthrene	206	191	2.20	7.33
13	Fluoranthene	202	101	1.87	6.22
14	Pyrene	202	101	1.91	6.36
15	2-Methylpyrene	216	108	1.92	6.39
16	4-Methylpyrene	216	108	1.92	6.39
17	Benzo[a]fluorene	216	107	1.30	4.33
18	Benzo[a]anthracene	228	114	1.30	4.33
19	Chryzene	228	113	2.20	7.33
20	3-Methylchrysene	242	121	1.02	3.40
21	5-Methylchrysene	242	115	1.87	6.22
22	6-Methylchrysene	242	119	1.02	3.40
23	Benzo[a]fluoranthene	252	126	2.10	6.99
24	Benzo[b]fluoranthene	252	126	2.10	6.99
25	Benzo[k]fluoranthene	252	126	2.10	6.99
26	Benzo[j]fluoranthene	252	126	1.91	6.36
27	Benzo[a]pyrene	252	126	2.11	7.03
28	Indeno[1,2,3-cd]pyrene	276	138	1.30	4.33
29	Benzo[ghi]perylene	276	138	1.33	4.43
30	Dibenzo[a,h]anthracene	278	139	2.21	7.36
31	Dibenz[a,e]pyrene	302	151	2.04	6.79
32	Dibenz[a,h]pyrene	302	151	2.04	6.79
33	Dibenz[a,i]pyrene	302	151	2.05	6.82

34

Dibenz[a,l]pyrene

302

151

2.05

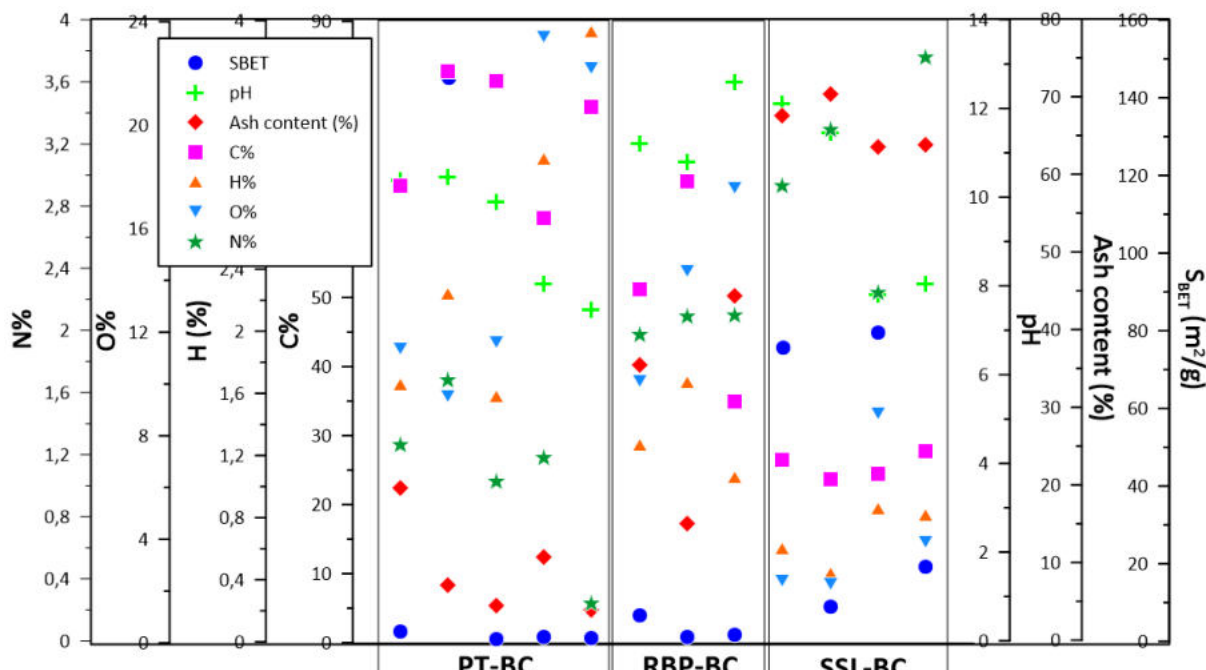
6.82

N- and O-PAHs					
35	Nitronaphthalene	173	127	2.41	8.03
36	1-Methyl-5-nitronaphthalene	187	115	1.21	4.03
37	1-Methyl-6-nitronaphthalene	187	115	1.21	4.03
38	9,10-Anthracenedione	208	180	1.44	4.80
39	4H-cyclopenta(def)phenanthrene	190	94	3.01	10.02
40	Nitropyrene	247	201	1.66	5.53

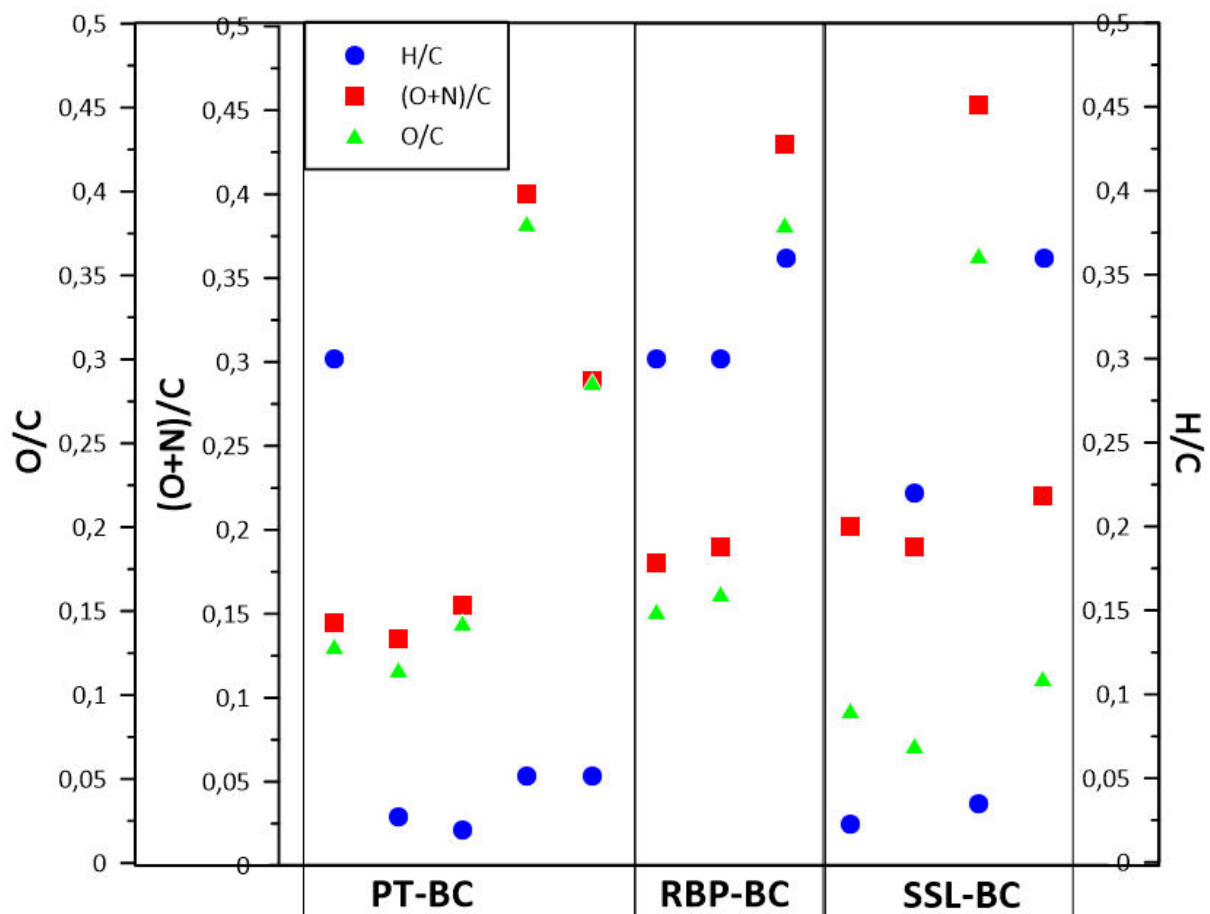
\*-LOD – limit of detection; \*\*-LOQ – limit of quantitation; LOD and LOQ were not calculated via K<sub>POM</sub>

### 3. Results and discussion

#### 3.1.Biochar physicochemical characteristics



(A)



(B)

Fig. S2. (A) Physicochemical properites of tested materials, (B) aromaticity, polairy and hydrophilicity of BC.

### 3.2.The total content of PAHs and their derivatives in BC

Table S2. The concentration of total PAHs and their derivatives in PT-BC.

No.	Compound	Sample description				
		PT-S	PT-W	PT-D	PT-A	PT-F
		Analyte concentration [ng g <sup>-1</sup> ]				
1	Naphthalene	0.24 ± 0.01	62.28 ± 2.85	< LOD	2.88 ± 0.13	9.37 ± 0.43
2	1,3-di-iso-propylnaphthalene	4.43 ± 0.20	0.88 ± 0.04	5.11 ± 0.23	0.22 ± 0.01	< LOD
3	2-Phenylnaphthalene	< LOD	< LOD	< LOD	< LOD	< LOD
4	Acenaphthylene	16.62 ± 0.72	25.12 ± 1.15	4.87 ± 0.22	29.27 ± 1.34	2.34 ± 0.11
5	Acenaphthene	18.27 ± 0.84	37.34 ± 1.71	9.31 ± 0.43	20.28 ± 0.93	6.73 ± 0.31
6	Fluorene	< LOD	0.42 ± 0.02	4.43 ± 0.20	12.30 ± 0.56	19.46 ± 0.89
7	Anthracene	1.48 ± 0.07	3.32 ± 0.15	< LOD	0.86 ± 0.04	< LOD
8	Phenanthrene	< LOD	< LOD	< LOD	< LOD	< LOD
9	3-Methylphenanthrene	27.28 ± 1.25	0.24 ± 0.01	< LOD	2.94 ± 0.14	4.88 ± 0.22
10	2-Methylphenanthrene	19.96 ± 0.50	0.22 ± 0.01	0.24 ± 0.01	0.92 ± 0.04	0.72 ± 0.03
11	9-Methylphenanthrene	< LOD	< LOD	< LOD	0.22 ± 0.01	0.22 ± 0.01
12	3,6-dimethylphenanthrene	0.32 ± 0.02	< LOD	< LOD	12.34 ± 0.57	14.91 ± 0.68
13	Fluoranthene	0.46 ± 0.02	1.98 ± 0.09	< LOD	1.38 ± 0.06	< LOD
14	Pyrene	< LOD	25.10 ± 1.15	< LOD	2.28 ± 0.10	1.24 ± 0.06
15	2-Methylpyrene	6.33 ± 0.29	0.24 ± 0.01	0.32 ± 0.02	2.28 ± 0.10	< LOD
16	4-Methylpyrene	2.30 ± 0.11	0.30 ± 0.01	0.82 ± 0.04	13.98 ± 0.64	< LOD
17	Benzo[a]fluorene	16.27 ± 0.75	6.02 ± 0.28	12.21 ± 0.56	8.88 ± 0.41	16.28 ± 0.75
18	Benzo[a]anthracene	12.04 ± 0.55	5.14 ± 0.24	< LOD	< LOD	11.47 ± 0.53
19	Chrysene	2.24 ± 0.10	0.92 ± 0.04	< LOD	< LOD	< LOD
20	3-Methylchrysene	10.02 ± 0.46	< LOD	0.82 ± 0.04	5.48 ± 0.25	6.21 ± 0.28

21	5-Methylchrysene	$8.85 \pm 0.41$	< LOD	$6.28 \pm 0.29$	$8.32 \pm 0.38$	$4.98 \pm 0.23$
22	6-Methylchrysene	$1.82 \pm 0.08$	< LOD	$10.35 \pm 0.47$	$14.52 \pm 0.67$	$10.33 \pm 0.47$
23	Benzo[a]fluoranthene	< LOD	$0.28 \pm 0.01$	$0.22 \pm 0.01$	$4.30 \pm 0.12$	$0.24 \pm 0.01$
24	Benzo[b]fluoranthene	< LOD	$0.22 \pm 0.01$	< LOD	$6.28 \pm 0.29$	< LOD
25	Benzo[k]fluoranthene	< LOD	$0.34 \pm 0.02$	< LOD	$1.22 \pm 0.06$	< LOD
26	Benzo[j]fluoranthene	< LOD	$0.12 \pm 0.01$	< LOD	$0.12 \pm 0.01$	< LOD
27	Benzo[a]pyrene	$0.38 \pm 0.02$	$7.34 \pm 0.34$	$1.94 \pm 0.09$	< LOD	$10.23 \pm 0.47$
28	Indeno[1,2,3-cd]pyrene	$4.03 \pm 0.19$	$1.10 \pm 0.05$	< LOD	< LOD	< LOD
29	Benzo[ghi]perylene	$1.88 \pm 0.09$	< LOD	< LOD	< LOD	< LOD
30	Dibenzo[a,h]anthracene	< LOD	$0.68 \pm 0.03$	< LOD	$0.24 \pm 0.01$	$14.41 \pm 0.66$
31	Dibenz[a,e]pyrene	< LOD	$1.16 \pm 0.05$	$0.22 \pm 0.01$	$0.040 \pm 0.002$	< LOD
32	Dibenz[a,h]pyrene	< LOD	$0.18 \pm 0.01$	$0.24 \pm 0.01$	< LOD	< LOD
33	Dibenz[a,i]pyrene	< LOD	$0.14 \pm 0.01$	< LOD	< LOD	< LOD
34	Dibenz[a,l]pyrene	< LOD	< LOD	< LOD	< LOD	< LOD
N- and O-PAHs						
35	Nitronaphthalene	< LOD	$1.92 \pm 0.09$	< LOD	$1.32 \pm 0.06$	< LOD
36	1-Methyl-5-nitronaphthalene	$1.88 \pm 0.09$	< LOD	< LOD	< LOD	< LOD
37	1-Methyl-6-nitronaphthalene	$2.32 \pm 0.11$	< LOD	< LOD	< LOD	< LOD
38	9,10-Anthracenedione	< LOD	< LOD	< LOD	< LOD	$0.82 \pm 0.04$
39	4H-cyclopenta(def)phenanthrene	$24.20 \pm 1.11$	< LOD	< LOD	$6.32 \pm 0.29$	$11.07 \pm 0.51$
40	Nitropyrene	< LOD	< LOD	< LOD	< LOD	< LOD

SD-standard deviation, <LOD- below the limit of detection

Table S2. The concentration of total PAHs and their derivatives in RBP-BC.

No.	Compound	Sample description		
		RBP-UH	RBP-KO	RBP-PI
		Analyte concentration [ng g <sup>-1</sup> ]		
1	Naphthalene	66.05 ± 3.02	8.83 ± 0.40	6.24 ± 0.29
2	1,3-di-iso-propylnaphthalene	< LOD	2.88 ± 0.13	6.44 ± 0.30
3	2-Phenylnaphthalene	< LOD	4.02 ± 0.18	2.30 ± 0.11
4	Acenaphthylene	16.21 ± 0.74	16.84 ± 0.77	7.93 ± 0.36
5	Acenaphthene	14.89 ± 0.68	6.31 ± 0.29	2.30 ± 0.11
6	Fluorene	3.92 ± 0.18	3.12 ± 0.14	48.84 ± 2.24
7	Anthracene	12.21 ± 0.56	82.80 ± 3.79	53.42 ± 02.45
8	Phenanthrene	< LOD	< LOD	< LOD
9	3-Methylphenanthrene	1.34 ± 0.06	< LOD	0.72 ± 0.03
10	2-Methylphenanthrene	0.68 ± 0.03	< LOD	0.88 ± 0.04
11	9-Methylphenanthrene	< LOD	2.24 ± 0.10	< LOD
12	3,6-dimethylphenanthrene	0.84 ± 0.04	< LOD	2.94 ± 0.13
13	Fluoranthene	6.38 ± 0.29	10.09 ± 0.46	32.79 ± 1.15
14	Pyrene	14.89 ± 0.68	21.90 ± 0.10	< LOD
15	2-Methylpyrene	< LOD	< LOD	< LOD
16	4-Methylpyrene	< LOD	< LOD	0.88 ± 0.04
17	Benzo[a]fluorene	8.61 ± 0.39	< LOD	< LOD
18	Benzo[a]anthracene	11.07 ± 0.51	< LOD	< LOD
19	Chrysene	27.30 ± 1.25	2.30 ± 0.11	1.94 ± 0.09
20	3-Methylchrysene	2.44 ± 0.11	< LOD	2.04 ± 0.09

21	5-Methylchrysene	$2.06 \pm 0.09$	< LOD	$1.96 \pm 0.09$
22	6-Methylchrysene	$0.74 \pm 0.03$	< LOD	< LOD
23	Benzo[a]fluoranthene	< LOD	$2.88 \pm 0.13$	$6.88 \pm 0.32$
24	Benzo[b]fluoranthene	< LOD	$1.98 \pm 0.09$	$4.04 \pm 0.19$
25	Benzo[k]fluoranthene	< LOD	$1.44 \pm 0.07$	< LOD
26	Benzo[j]fluoranthene	< LOD	$1.22 \pm 0.06$	< LOD
27	Benzo[a]pyrene	$12.03 \pm 0.55$	$6.27 \pm 0.29$	< LOD
28	Indeno[1,2,3-cd]pyrene	< LOD	< LOD	$2.32 \pm 0.11$
29	Benzo[ghi]perylene	< LOD	$1.28 \pm 0.06$	< LOD
30	Dibenzo[a,h]anthracene	< LOD	< LOD	< LOD
31	Dibenz[a,e]pyrene	< LOD	$1.44 \pm 0.07$	$1.34 \pm 0.06$
32	Dibenz[a,h]pyrene	< LOD	$0.88 \pm 0.04$	$0.62 \pm 0.03$
33	Dibenz[a,i]pyrene	< LOD	$0.76 \pm 0.04$	$0.24 \pm 0.01$
34	Dibenz[a,l]pyrene	< LOD	$0.72 \pm 0.03$	$0.28 \pm 0.01$
N- and O-PAHs				
35	Nitronaphthalene	$1.60 \pm 0.07$	< LOD	$3.24 \pm 0.15$
36	1-Methyl-5-nitronaphthalene	< LOD	< LOD	$6.88 \pm 0.32$
37	1-Methyl-6-nitronaphthalene	< LOD	< LOD	$4.16 \pm 0.19$
38	9,10-Anthracenedione	$4.02 \pm 0.18$	$1.48 \pm 0.07$	< LOD
39	4H-cyclopenta(def)phenanthrene	< LOD	< LOD	< LOD
40	Nitropyrene	< LOD	$1.94 \pm 0.09$	$1.92 \pm 0.09$

SD-standard deviation, <LOD- below the limit of detection

Table S3. The concentration of total PAHs and their derivatives in SSL-BC.

No.	Compound	Sample description			
		SSL-CH	SSL-KZ	SSL-SI	SSL-Z
		Analyte concentration ± SD [ng g <sup>-1</sup> ]			
1	Naphthalene	18.27 ± 0.84	12.23 ± 0.56	< LOD	54.80 ± 2.51
2	1,3-di-iso-propynaphthalene	< LOD	0.28 ± 0.01	< LOD	< LOD
3	2-Phenylnaphthalene	< LOD	36.27 ± 1.66	< LOD	1.26 ± 0.06
4	Acenaphthylene	25.24 ± 1.16	< LOD	8.47 ± 0.39	15.09 ± 0.69
5	Acenaphthene	17.29 ± 0.79	15.09 ± 0.69	10.27 ± 0.47	3.10 ± 0.14
6	Fluorene	0.28 ± 0.01	28.86 ± 1.32	12.23 ± 0.56	8.30 ± 0.38
7	Anthracene	10.28 ± 0.47	< LOD	< LOD	0.42 ± 0.02
8	Phenanthrene	< LOD	< LOD	< LOD	< LOD
9	3-Methylphenanthrene	< LOD	9.33 ± 0.43	8.29 ± 0.38	0.060 ± 0.003
10	2-Methylphenanthrene	< LOD	2.30 ± 0.11	2.88 ± 0.13	0.12 ± 0.01
11	9-Methylphenanthrene	< LOD	< LOD	< LOD	1.02 ± 0.05
12	3,6-dimethylphenanthrene	< LOD	< LOD	< LOD	2.42 ± 0.11
13	Fluoranthene	1.48 ± 0.07	1.42 ± 0.07	4.87 ± 0.22	< LOD
14	Pyrene	2.92 ± 0.13	1.54 ± 0.07	3.32 ± 0.15	8.30 ± 0.38
15	2-Methylpyrene	4.03 ± 0.19	5.04 ± 0.23	12.23 ± 0.56	1.10 ± 0.05
16	4-Methylpyrene	14.27 ± 0.65	< LOD	< LOD	1.96 ± 0.09
17	Benzo[a]fluorene	9.06 ± 0.42	11.09 ± 0.51	10.05 ± 0.46	0.56 ± 0.03
18	Benzo[a]anthracene	< LOD	8.45 ± 0.39	24.25 ± 1.11	1.98 ± 0.09
19	Chrysene	< LOD	5.92 ± 0.27	14.90 ± 0.68	0.24 ± 0.01
20	3-Methylchrysene	3.33 ± 0.15	1.52 ± 0.07	1.22 ± 0.06	< LOD

21	5-Methylchrysene	$8.01 \pm 0.37$	$7.05 \pm 0.32$	$7.05 \pm 0.32$	$1.92 \pm 0.09$
22	6-Methylchrysene	$4.29 \pm 0.20$	$10.21 \pm 0.47$	$0.52 \pm 0.02$	$0.66 \pm 0.03$
23	Benzo[a]fluoranthene	$0.32 \pm 0.02$	$7.53 \pm 0.35$	$7.07 \pm 0.32$	$9.72 \pm 0.45$
24	Benzo[b]fluoranthene	< LOD	$12.23 \pm 0.56$	$21.29 \pm 0.98$	$6.30 \pm 0.29$
25	Benzo[k]fluoranthene	< LOD	$1.12 \pm 0.05$	$0.92 \pm 0.04$	$2.28 \pm 0.10$
26	Benzo[j]fluoranthene	< LOD	$0.28 \pm 0.01$	< LOD	$0.26 \pm 0.01$
27	Benzo[a]pyrene	$1.64 \pm 0.08$	< LOD	< LOD	$0.52 \pm 0.02$
28	Indeno[1,2,3-cd]pyrene	< LOD	$0.88 \pm 0.04$	$0.22 \pm 0.01$	< LOD
29	Benzo[ghi]perylene	< LOD	< LOD	< LOD	< LOD
30	Dibenzo[a,h]anthracene	< LOD	$9.83 \pm 0.45$	< LOD	$2.42 \pm 0.11$
31	Dibenz[a,e]pyrene	< LOD	< LOD	< LOD	$1.04 \pm 0.05$
32	Dibenz[a,h]pyrene	< LOD	< LOD	< LOD	< LOD
33	Dibenz[a,i]pyrene	< LOD	< LOD	< LOD	< LOD
34	Dibenz[a,l]pyrene	< LOD	< LOD	< LOD	< LOD
N- and O-PAHs					
35	Nitronaphthalene	< LOD	$1.54 \pm 0.07$	< LOD	< LOD
36	1-Methyl-5-nitronaphthalene	$2.34 \pm 0.11$	< LOD	< LOD	$2.42 \pm 0.11$
37	1-Methyl-6-nitronaphthalene	$2.04 \pm 0.09$	< LOD	< LOD	$2.88 \pm 0.13$
38	9,10-Anthracenedione	< LOD	$2.04 \pm 0.09$	$0.84 \pm 0.04$	< LOD
39	4H-cyclopenta(def)phenanthrene	$40.21 \pm 1.84$	< LOD	$10.91 \pm 0.50$	< LOD
40	Nitropyrene	< LOD	$1.28 \pm 0.06$	$0.68 \pm 0.03$	< LOD

SD-standard deviation, <LOD- below the limit of detection

### 3.3.The bioavailable PAHs and their derivatives in BC

Table S4. The content of bioavailable PAHs and their derivatives in PT-BC.

No.	Compound	Sample description				
		PT-S	PT-W	PT-D	PT-A	PT-F
		Analyte concentration [ng L <sup>-1</sup> ]				
1	Naphthalene	< LOD	< LOD	< LOD	0.49 ± 0.02	1.98 ± 0.09
2	1,3-di-iso-propynaphthalene	< LOD	< LOD	< LOD	< LOD	< LOD
3	2-Phenylnaphthalene	< LOD	< LOD	< LOD	< LOD	< LOD
4	Acenaphthylene	0.86 ± 0.04	0.77 ± 0.04	0.24 ± 0.01	1.60 ± 0.11	0.15 ± 0.01
5	Acenaphthene	1.49 ± 0.07	1.16 ± 0.05	1.45 ± 0.08	1.89 ± 0.09	0.58 ± 0.03
6	Fluorene	< LOD	0.97 ± 0.05	0.33 ± 0.02	< LOD	0.79 ± 0.04
7	Anthracene	< LOD	< LOD	(10.0 ± 0.5)·10 <sup>-2</sup>	0.25 ± 0.01	< LOD
8	Phenanthrene	< LOD	< LOD	< LOD	< LOD	< LOD
9	3-Methylphenanthrene	0.130 ± 6.2·10 <sup>-3</sup>	0.170 ± 7.4·10 <sup>-3</sup>	< LOD	0.059 ± 2.7·10 <sup>-3</sup>	0.045 ± 2.1·10 <sup>-3</sup>
10	2-Methylphenanthrene	< LOD	0.030 ± 1.2·10 <sup>-3</sup>	< LOD	< LOD	< LOD
11	9-Methylphenanthrene	< LOD	< LOD	< LOD	< LOD	< LOD
12	3,6-dimethylphenanthrene	< LOD	< LOD	0.640 ± 3.4·10 <sup>-3</sup>	0.059 ± 2.7·10 <sup>-3</sup>	0.072 ± 3.3·10 <sup>-3</sup>
13	Fluoranthene	< LOD	< LOD	< LOD	< LOD	< LOD
14	Pyrene	< LOD	< LOD	< LOD	< LOD	< LOD
15	2-Methylpyrene	0.023 ± 1.1·10 <sup>-3</sup>	0.027 ± 1.3·10 <sup>-3</sup>	< LOD	< LOD	< LOD
16	4-Methylpyrene	0.030 ± 1.4·10 <sup>-3</sup>	< LOD	2.7·10 <sup>-3</sup> ± 3.6·10 <sup>-5</sup>	0.073 ± 3.4·10 <sup>-3</sup>	< LOD
17	Benzo[a]fluorene	6.1·10 <sup>-3</sup> ± 3.1·10 <sup>-4</sup>	9.7·10 <sup>-3</sup> ± 4.5·10 <sup>-4</sup>	8.3·10 <sup>-3</sup> ± 4.7·10 <sup>-4</sup>	8.4 ·10 <sup>-3</sup> ± 3.8·10 <sup>-4</sup>	7.2 ·10 <sup>-3</sup> ± 3.4·10 <sup>-4</sup>
18	Benzo[a]anthracene	7.3·10 <sup>-3</sup> ± 3.4·10 <sup>-4</sup>	< LOD	< LOD	< LOD	0.014 ± 6.6·10 <sup>-4</sup>

19	Chrysene	< LOD	$5.6 \cdot 10^{-3} \pm 2.6 \cdot 10^{-4}$	< LOD	< LOD	< LOD
20	3-Methylchrysene	$3.9 \cdot 10^{-3} \pm 1.9 \cdot 10^{-4}$	$4.8 \cdot 10^{-3} \pm 1.9 \cdot 10^{-4}$	< LOD	< LOD	$4.0 \cdot 10^{-3} \pm 1.8 \cdot 10^{-4}$
21	5-Methylchrysene	< LOD				
22	6-Methylchrysene	$7.6 \cdot 10^{-3} \pm 3.6 \cdot 10^{-4}$	$8.9 \cdot 10^{-3} \pm 4.1 \cdot 10^{-4}$	$0.015 \pm 8.0 \cdot 10^{-4}$	$6.3 \cdot 10^{-3} \pm 3.0 \cdot 10^{-4}$	$0.012 \pm 5.4 \cdot 10^{-4}$
23	Benzo[a]fluoranthene	$1.5 \cdot 10^{-3} \pm 9.8 \cdot 10^{-5}$	$6.8 \cdot 10^{-3} \pm 2.7 \cdot 10^{-4}$	$2.8 \cdot 10^{-3} \pm 1.3 \cdot 10^{-4}$	$5.5 \cdot 10^{-4} \pm 2.7 \cdot 10^{-5}$	$2.0 \cdot 10^{-3} \pm 9.4 \cdot 10^{-5}$
24	Benzo[b]fluoranthene	< LOD	$2.8 \cdot 10^{-3} \pm 9.9 \cdot 10^{-5}$	< LOD	$6.4 \cdot 10^{-3} \pm 2.9 \cdot 10^{-4}$	< LOD
25	Benzo[k]fluoranthene	< LOD				
26	Benzo[j]fluoranthene	< LOD				
27	Benzo[a]pyrene	< LOD	< LOD	$7.2 \cdot 10^{-4} \pm 3.1 \cdot 10^{-5}$	< LOD	$3.9 \cdot 10^{-3} \pm 1.8 \cdot 10^{-4}$
28	Indeno[1,2,3-cd]pyrene	$2.2 \cdot 10^{-3} \pm 1.0 \cdot 10^{-4}$	$2.2 \cdot 10^{-4} \pm 1.2 \cdot 10^{-5}$	$2.4 \cdot 10^{-4} \pm 1.3 \cdot 10^{-5}$	$1.3 \cdot 10^{-4} \pm 4.7 \cdot 10^{-6}$	$9.4 \cdot 10^{-4} \pm 5.0 \cdot 10^{-5}$
29	Benzo[ghi]perylene	$1.1 \cdot 10^{-3} \pm 8.2 \cdot 10^{-5}$	$2.3 \cdot 10^{-3} \pm 8.0 \cdot 10^{-5}$	< LOD	$1.6 \cdot 10^{-4} \pm 7.0 \cdot 10^{-6}$	$6.4 \cdot 10^{-4} \pm 3.2 \cdot 10^{-5}$
30	Dibenzo[a,h]anthracene	< LOD	$2.0 \cdot 10^{-3} \pm 9.1 \cdot 10^{-5}$	< LOD	< LOD	$3.3 \cdot 10^{-3} \pm 1.5 \cdot 10^{-4}$
31	Dibenz[a,e]pyrene	< LOD				
32	Dibenz[a,h]pyrene	< LOD				
33	Dibenz[a,i]pyrene	< LOD				
34	Dibenz[a,l]pyrene	< LOD				
N- and O-PAHs						
35	Nitronaphthalene	< LOD	< LOD	< LOD	$0.26 \pm 0.01$	< LOD
36	1-Methyl-5-nitronaphthalene	$0.13 \pm 4.0 \cdot 10^{-3}$	< LOD	< LOD	< LOD	< LOD
37	1-Methyl-6-nitronaphthalene	$0.12 \pm 5.4 \cdot 10^{-3}$	< LOD	< LOD	< LOD	< LOD
38	9,10-Anthracenedione	< LOD	< LOD	< LOD	< LOD	$0.057 \pm 5.7 \cdot 10^{-3}$
39	4H-cyclopenta(def)phenanthrene	$0.58 \pm 0.02$	$0.47 \pm 0.022$	< LOD	$0.25 \pm 0.01$	$0.27 \pm 0.01$
40	Nitropyrene	< LOD	$0.013 \pm 6.9 \cdot 10^{-3}$	< LOD	< LOD	< LOD

SD-standard deviation, <LOD- below the limit of detection

Table S5. The content of bioavailable PAHs and their derivatives in RBP-BC.

No.	Compound	Sample description		
		RBP-UH	RBP-KO	RBP-PI
		Analyte concentration [ng L <sup>-1</sup> ]		
1	Naphthalene	32.88 ± 1.20	2.73 ± 0.10	1.22 ± 0.045
2	1,3-di-iso-propylnaphthalene	7.6·10 <sup>-3</sup> ± 7.6·10 <sup>-4</sup>	0.23 ± 8.3·10 <sup>-3</sup>	0.70 ± 0.025
3	2-Phenylnaphthalene	< LOD	0.66 ± 0.024	0.60 ± 0.022
4	Acenaphthylene	2.71 ± 0.10	1.05 ± 0.039	0.72 ± 0.026
5	Acenaphthene	3.83 ± 0.14	1.04 ± 0.038	0.39 ± 0.014
6	Fluorene	1.06 ± 0.04	2.79 ± 0.10	4.23 ± 0.15
7	Anthracene	0.47 ± 0.02	1.50 ± 0.055	1.55 ± 0.057
8	Phenanthrene	< LOD	< LOD	< LOD
9	3-Methylphenanthrene	0.093 ± 3.4·10 <sup>-3</sup>	< LOD	0.024 ± 8.3·10 <sup>-4</sup>
10	2-Methylphenanthrene	0.065 ± 2.3·10 <sup>-3</sup>	< LOD	0.026 ± 9.3·10 <sup>-4</sup>
11	9-Methylphenanthrene	< LOD	0.054 ± 1.9·10 <sup>-3</sup>	< LOD
12	3,6-dimethylphenanthrene	0.013 ± 4.4·10 <sup>-4</sup>	< LOD	0.027 ± 9.9·10 <sup>-4</sup>
13	Fluoranthene	0.13 ± 4.9·10 <sup>-3</sup>	0.089 ± 3.2·10 <sup>-3</sup>	0.87 ± 0.032
14	Pyrene	0.16 ± 5.9·10 <sup>-3</sup>	0.20 ± 7.4·10 <sup>-3</sup>	< LOD
15	2-Methylpyrene	< LOD	< LOD	< LOD
16	4-Methylpyrene	< LOD	< LOD	7.0·10 <sup>-4</sup> ± 3.5·10 <sup>-5</sup>
17	Benzo[a]fluorene	0.014 ± 5.0·10 <sup>-4</sup>	< LOD	7.0·10 <sup>-4</sup> ± 2.3·10 <sup>-5</sup>
18	Benzo[a]anthracene	0.027 ± 9.8·10 <sup>-4</sup>	< LOD	< LOD
19	Chrysene	0.048 ± 1.8·10 <sup>-3</sup>	5.4·10 <sup>-3</sup> ± 2.0·10 <sup>-4</sup>	4.6·10 <sup>-3</sup> ± 1.7·10 <sup>-4</sup>

20	3-Methylchrysene	$6.2 \cdot 10^{-3} \pm 2.3 \cdot 10^{-4}$	< LOD	$4.4 \cdot 10^{-3} \pm 1.6 \cdot 10^{-4}$
21	5-Methylchrysene	$7.3 \cdot 10^{-3} \pm 2.7 \cdot 10^{-4}$	< LOD	$3.8 \cdot 10^{-3} \pm 1.4 \cdot 10^{-4}$
22	6-Methylchrysene	$3.5 \cdot 10^{-3} \pm 1.3 \cdot 10^{-4}$	< LOD	< LOD
23	Benzo[a]fluoranthene	$4.7 \cdot 10^{-5} \pm 4.7 \cdot 10^{-6}$	$2.9 \cdot 10^{-3} \pm 1.1 \cdot 10^{-4}$	$0.011 \pm 4.1 \cdot 10^{-4}$
24	Benzo[b]fluoranthene	$1.4 \cdot 10^{-4} \pm 4.7 \cdot 10^{-6}$	$1.6 \cdot 10^{-3} \pm 5.6 \cdot 10^{-5}$	$6.5 \cdot 10^{-3} \pm 2.4 \cdot 10^{-4}$
25	Benzo[k]fluoranthene	< LOD	$1.7 \cdot 10^{-3} \pm 6.3 \cdot 10^{-5}$	$3.6 \cdot 10^{-4} \pm 1.2 \cdot 10^{-5}$
26	Benzo[j]fluoranthene	< LOD	$3.5 \cdot 10^{-4} \pm 1.3 \cdot 10^{-5}$	< LOD
27	Benzo[a]pyrene	$4.7 \cdot 10^{-3} \pm 1.7 \cdot 10^{-4}$	$2.2 \cdot 10^{-3} \pm 7.7 \cdot 10^{-5}$	< LOD
28	Indeno[1,2,3-cd]pyrene	$3.4 \cdot 10^{-4} \pm 1.3 \cdot 10^{-5}$	< LOD	$1.2 \cdot 10^{-3} \pm 4.3 \cdot 10^{-5}$
29	Benzo[ghi]perylene	$1.6 \cdot 10^{-3} \pm 7.3 \cdot 10^{-5}$	$2.9 \cdot 10^{-4} \pm 9.6 \cdot 10^{-6}$	< LOD
30	Dibenzo[a,h]anthracene	< LOD	< LOD	< LOD
31	Dibenz[a,e]pyrene	< LOD	$5.1 \cdot 10^{-5} \pm 1.9 \cdot 10^{-6}$	$3.1 \cdot 10^{-5} \pm 1.2 \cdot 10^{-6}$
32	Dibenz[a,h]pyrene	< LOD	$3.2 \cdot 10^{-5} \pm 1.2 \cdot 10^{-6}$	$4.0 \cdot 10^{-5} \pm 1.5 \cdot 10^{-6}$
33	Dibenz[a,i]pyrene	< LOD	$2.3 \cdot 10^{-5} \pm 7.7 \cdot 10^{-7}$	$1.6 \cdot 10^{-5} \pm 5.9 \cdot 10^{-7}$
34	Dibenz[a,l]pyrene	< LOD	$2.5 \cdot 10^{-5} \pm 9.3 \cdot 10^{-7}$	$1.5 \cdot 10^{-5} \pm 5.9 \cdot 10^{-7}$
N- and O-PAHs				
35	Nitronaphthalene	$0.34 \pm 0.014$	< LOD	$1.65 \pm 0.060$
36	1-Methyl-5-nitronaphthalene	< LOD	< LOD	$1.54 \pm 0.056$
37	1-Methyl-6-nitronaphthalene	< LOD	< LOD	$1.42 \pm 0.052$
38	9,10-Anthracedione	$0.54 \pm 0.019$	$0.17 \pm 6.0 \cdot 10^{-3}$	< LOD
39	4H-cyclopenta(def)phenanthrene	$4.3 \cdot 10^{-3} \pm 2.1 \cdot 10^{-4}$	< LOD	< LOD
40	Nitropyrene	< LOD	$0.049 \pm 1.8 \cdot 10^{-3}$	$0.035 \pm 1.3 \cdot 10^{-3}$

SD-standard deviation, <LOD- below the limit of detection

Table S6. The content of bioavailable PAHs and their derivatives in SSL-BC.

No.	Compound	Sample description			
		SSL-CH	SSL-KZ	SSL-SI	SSL-Z
		Analyte concentration ± SD [ng L <sup>-1</sup> ]			
1	Naphthalene	4.69 ± 0.22	5.05 ± 0.23	< LOD	35.65 ± 1.30
2	1,3-di-iso-propylnaphthalene	< LOD	< LOD	< LOD	< LOD
3	2-Phenylnaphthalene	< LOD	2.37 ± 0.11	< LOD	0.16 ± 5.4·10 <sup>-3</sup>
4	Acenaphthylene	1.54 ± 0.10	< LOD	0.74 ± 0.03	1.81 ± 0.07
5	Acenaphthene	2.34 ± 0.18	1.21 ± 0.06	1.72 ± 0.08	1.46 ± 0.05
6	Fluorene	< LOD	1.31 ± 0.05	0.63 ± 0.03	0.59 ± 0.02
7	Anthracene	0.35 ± 0.03	< LOD	< LOD	0.015 ± 6.0·10 <sup>-4</sup>
8	Phenanthrene	< LOD	< LOD	< LOD	< LOD
9	3-Methylphenanthrene	< LOD	0.11 ± 5.2·10 <sup>-3</sup>	0.11 ± 4.9·10 <sup>-3</sup>	3.0·10 <sup>-3</sup> ± 9.9·10 <sup>-5</sup>
10	2-Methylphenanthrene	< LOD	< LOD	< LOD	2.0·10 <sup>-3</sup> ± 9.9·10 <sup>-4</sup>
11	9-Methylphenanthrene	< LOD	< LOD	< LOD	0.014 ± 4.9·10 <sup>-4</sup>
12	3,6-dimethylphenanthrene	< LOD	< LOD	< LOD	0.016 ± 5.6·10 <sup>-4</sup>
13	Fluoranthene	< LOD	< LOD	< LOD	< LOD
14	Pyrene	< LOD	< LOD	< LOD	0.16 ± 6.0·10 <sup>-3</sup>
15	2-Methylpyrene	0.028 ± 1.2·10 <sup>-3</sup>	0.029 ± 1.3·10 <sup>-3</sup>	0.051 ± 2.2·10 <sup>-3</sup>	0.025 ± 9.0·10 <sup>-4</sup>
16	4-Methylpyrene	0.071 ± 3.2·10 <sup>-3</sup>	< LOD	< LOD	0.036 ± 1.3·10 <sup>-3</sup>
17	Benzo[a]fluorene	8.1·10 <sup>-3</sup> ± 3.8·10 <sup>-4</sup>	9.7·10 <sup>-3</sup> ± 4.5·10 <sup>-5</sup>	6.9·10 <sup>-3</sup> ± 3.2·10 <sup>-4</sup>	2.1·10 <sup>-3</sup> ± 7.5·10 <sup>-5</sup>
18	Benzo[a]anthracene	< LOD	0.011 ± 5.1·10 <sup>-4</sup>	0.037 ± 2.4·10 <sup>-3</sup>	0.012 ± 4.2·10 <sup>-4</sup>
19	Chrysene	< LOD	9.6·10 <sup>-3</sup> ± 4.4·10 <sup>-4</sup>	0.021 ± 1.0·10 <sup>-3</sup>	1.5·10 <sup>-3</sup> ± 5.5·10 <sup>-5</sup>
20	3-Methylchrysene	< LOD	< LOD	< LOD	< LOD
21	5-Methylchrysene	< LOD	< LOD	< LOD	3.1·10 <sup>-3</sup> ± 1.1·10 <sup>-4</sup>

22	6-Methylchrysene	$0.013 \pm 5.0 \cdot 10^{-4}$	$7.9 \cdot 10^{-3} \pm 3.7 \cdot 10^{-4}$	$7.0 \cdot 10^{-3} \pm 3.3 \cdot 10^{-4}$	$4.6 \cdot 10^{-3} \pm 1.7 \cdot 10^{-4}$
23	Benzo[a]fluoranthene	< LOD	$4.7 \cdot 10^{-3} \pm 2.5 \cdot 10^{-4}$	$3.2 \cdot 10^{-3} \pm 1.5 \cdot 10^{-4}$	$7.0 \cdot 10^{-3} \pm 2.6 \cdot 10^{-4}$
24	Benzo[b]fluoranthene	< LOD	$5.6 \cdot 10^{-3} \pm 2.6 \cdot 10^{-4}$	$0.013 \pm 9.1 \cdot 10^{-4}$	$9.7 \cdot 10^{-3} \pm 3.5 \cdot 10^{-4}$
25	Benzo[k]fluoranthene	< LOD	< LOD	< LOD	$3.2 \cdot 10^{-3} \pm 1.2 \cdot 10^{-4}$
26	Benzo[j]fluoranthene	< LOD	< LOD	< LOD	$3.8 \cdot 10^{-4} \pm 1.3 \cdot 10^{-5}$
27	Benzo[a]pyrene	$6.0 \cdot 10^{-3} \pm 2.0 \cdot 10^{-4}$	< LOD	< LOD	$2.1 \cdot 10^{-3} \pm 7.5 \cdot 10^{-5}$
28	Indeno[1,2,3-cd]pyrene	$1.9 \cdot 10^{-4} \pm 8.0 \cdot 10^{-6}$	$6.5 \cdot 10^{-4} \pm 3.3 \cdot 10^{-5}$	$9.1 \cdot 10^{-4} \pm 4.2 \cdot 10^{-6}$	< LOD
29	Benzo[ghi]perylene	$6.1 \cdot 10^{-4} \pm 2.4 \cdot 10^{-5}$	$1.6 \cdot 10^{-3} \pm 7.3 \cdot 10^{-5}$	< LOD	< LOD
30	Dibenzo[a,h]anthracene	< LOD	$1.7 \cdot 10^{-3} \pm 7.8 \cdot 10^{-5}$	< LOD	$6.6 \cdot 10^{-4} \pm 2.4 \cdot 10^{-5}$
31	Dibenz[a,e]pyrene	< LOD	< LOD	< LOD	$3.3 \cdot 10^{-5} \pm 1.2 \cdot 10^{-6}$
32	Dibenz[a,h]pyrene	< LOD	< LOD	< LOD	< LOD
33	Dibenz[a,i]pyrene	< LOD	< LOD	< LOD	< LOD
34	Dibenz[a,l]pyrene	< LOD	< LOD	< LOD	< LOD
N- and O-PAHs					
35	Nitronaphthalene	< LOD	$0.34 \pm 0.015$	< LOD	< LOD
36	1-Methyl-5-nitronaphthalene	$0.083 \pm 2.8 \cdot 10^{-3}$	< LOD	< LOD	$0.94 \pm 0.03$
37	1-Methyl-6-nitronaphthalene	$0.070 \pm 4.2 \cdot 10^{-3}$	< LOD	< LOD	$0.77 \pm 0.03$
38	9,10-Anthracenedione	< LOD	$0.20 \pm 9.4 \cdot 10^{-3}$	$0.10 \pm 4.6 \cdot 10^{-3}$	$0.19 \pm 7.3 \cdot 10^{-3}$
39	4H-cyclopenta(def)phenanthrene	$0.78 \pm 0.04$	< LOD	$0.32 \pm 0.015$	< LOD
40	Nitropyrene	< LOD	< LOD	$3.1 \cdot 10^{-3} \pm 7.7 \cdot 10^{-5}$	< LOD

SD-standard deviation, <LOD- below the limit of detection

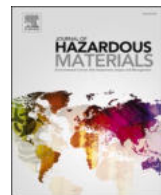
## References

- Hale, S.E., Lehmann, J., Rutherford, D., Zimmerman, A.R., Bachmann, R.T., Shitumbanuma, V., O'Toole, A., Sundqvist, K.L., Arp, H.P.H., Cornelissen, G., 2012. Quantifying the Total and Bioavailable Polycyclic Aromatic Hydrocarbons and Dioxins in Biochars. *Environ. Sci. Technol.* 46, 2830–2838. <https://doi.org/10.1021/es203984k>
- Hans-Peter Schmidt, 2015. European Biochar Certificate (EBC) - guidelines version 6.1. <https://doi.org/10.13140/RG.2.1.4658.7043>
- Hawthorne, S.B., Jonker, M.T.O., van der Heijden, S.A., Grabanski, C.B., Azzolina, N.A., Miller, D.J., 2011. Measuring Picogram per Liter Concentrations of Freely Dissolved Parent and Alkyl PAHs (PAH-34), Using Passive Sampling with Polyoxymethylene. *Anal. Chem.* 83, 6754–6761. <https://doi.org/10.1021/ac201411v>
- Josefsson, S., Arp, H.P.H., Kleja, D.B., Enell, A., Lundstedt, S., 2015. Determination of polyoxymethylene (POM) – water partition coefficients for oxy-PAHs and PAHs. *Chemosphere* 119, 1268–1274. <https://doi.org/10.1016/j.chemosphere.2014.09.102>
- Oleszczuk, P., Kuśmierz, M., Godlewska, P., Kraska, P., Pałys, E., 2016. The concentration and changes in freely dissolved polycyclic aromatic hydrocarbons in biochar-amended soil. *Environmental Pollution* 214, 748–755. <https://doi.org/10.1016/j.envpol.2016.04.064>

## **Publikacja D4**

**A. Krzyszczak, M. P. Dybowski, R. Zarzycki, R. Kobyłecki, P. Oleszczuk, B. Czech**  
*Long-term physical and chemical aging of biochar affected the amount and bioavailability of  
PAHs and their derivatives*

Journal of Hazardous Materials, 2022, 440, 129795



## Long-term physical and chemical aging of biochar affected the amount and bioavailability of PAHs and their derivatives

Agnieszka Krzyszczak <sup>a</sup>, Michał P. Dybowski <sup>b</sup>, Robert Zarzycki <sup>c</sup>, Rafał Kobyłecki <sup>c</sup>, Patryk Oleszczuk <sup>a</sup>, Bożena Czech <sup>a,\*</sup>

<sup>a</sup> Department of Radiochemistry and Environmental Chemistry, Institute of Chemical Sciences, Faculty of Chemistry, Maria Curie-Sklodowska University in Lublin, Pl. M. Curie-Sklodowskiej 3, 20-031 Lublin, Poland

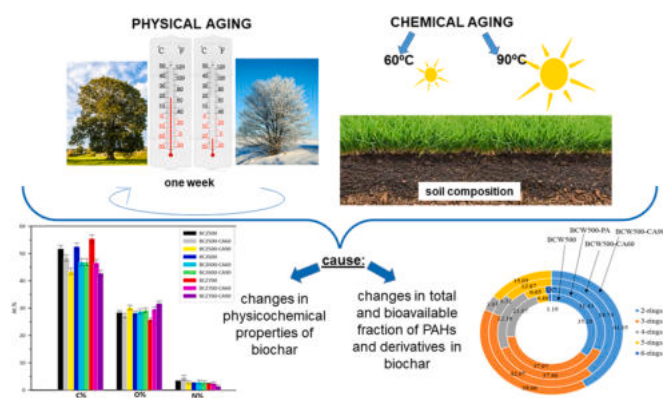
<sup>b</sup> Department of Chromatography, Institute of Chemical Sciences, Faculty of Chemistry, Maria Curie-Sklodowska University in Lublin, Pl. M. Curie-Sklodowskiej 3, 20-031 Lublin, Poland

<sup>c</sup> Department of Advanced Energy Technologies, Częstochowa University of Technology, Dąbrowskiego 73, 42-201 Częstochowa, Poland

### HIGHLIGHTS

- biochar can contain some potentially toxic PAHs and more toxic PAHs derivatives.
- There is a lack of information on their bioavailability during long-term experiment.
- physical and chemical aging affected total and bioavailable PAHs and derivatives.
- long-term (6 months) aging affected the physicochemical characteristic of biochar.
- aging promoted the increased in the bioavailability of PAHs and their derivatives.

### GRAPHICAL ABSTRACT



### ARTICLE INFO

Editor: Feng Xiao

**Keywords:**  
Biochar  
PAHs  
PAHs derivatives  
Physical aging  
Chemical aging

### ABSTRACT

Biochar applied into the soil is recommended as an effective tool for increasing its properties and crop productivity. However, biochar can contain some potentially toxic compounds such as polycyclic aromatic hydrocarbons (PAHs). Moreover, during biochar production or environmental application (e.g. as soil fertilizer), more toxic PAHs derivatives containing nitrogen, oxygen or sulfur can be formed. There is a lack of information on how the environmental factors affect the bioavailability of such compounds during the long-term application of BC into the soil. In the presented studies the effects of physical (freeze-thaw cycles) and chemical aging (temperatures 60 °C and 90 °C) on the total and bioavailable content of PAHs and their derivatives were estimated. The results indicate that long-term (6 months) aging affected the physicochemical characteristic of biochars promoting the formation of new C and O-containing species on the BC surface increasing their polarity and hydrophilicity. Physical and chemical aging promoted the formation of compounds with higher molecular weight and a significant (up to 550 %) increase in the bioavailability of PAHs and their derivatives. The results of this

\* Corresponding author.

E-mail address: [bczech@hektor.umcs.lublin.pl](mailto:bczech@hektor.umcs.lublin.pl) (B. Czech).

study highlight the importance of the bioavailable fraction of PAHs and their derivatives for evaluation of the toxicity of aged biochar.

## 1. Introduction

Polycyclic aromatic hydrocarbons (PAHs) (Oleszczuk et al., 2016), as well as their derivatives containing nitrogen, oxygen, or sulfur (Nowakowski et al., 2022), are considered as the soil (Krzyszczak and Czech, 2021; Tang et al., 2005) and air (Alves et al., 2016) contaminants. PAHs have been listed as priority pollutants by the US Environmental Protection Agency (USEPA) and European Union (Bandowe and Nkansah, 2016). They possess two or more fused aromatic rings in linear, angular, or cluster arrangement. PAHs may originate from incomplete combustion of organic substances (coal, oil, gas, wood, garbage, and petrochemical/oil refining industries), traffic emission (Yunker et al., 2002; Gope et al., 2018), and geochemical formation of fossil fuels (Abbas and Brack, 2006). They are toxic, carcinogenic, and mutagenic to living organisms (Gope et al., 2018). The content of PAHs in soils varied depending on soil properties and industrialization (Sushkova et al., 2019). The soil from the fallow lands of the 20 km around the power station contained  $\Sigma$ 16PAHs up to  $383.3\text{--}863.5 \mu\text{g kg}^{-1}$  in 2016 and  $600.3\text{--}2168.0 \mu\text{g kg}^{-1}$  in 2017 indicating that the level of pollution increased and PAHs accumulated in soils. Moreover, at monitoring sites located in direction of predominant winds from the plant, high-molecular-weight (HMW) PAHs concentrations were higher than the low-molecular-weight (LMW) PAHs content. The opposite relation was observed at sites situated around the power station (Sushkova et al., 2019). PAHs derivatives are considered to accompany PAHs (Krzyszczak et al., 2021). Although their presence was noted in airborne particles at a rather low concentration ( $\text{ng m}^{-3}$ ) (Cao et al., 2020), PAHs derivatives revealed higher toxicity than parent compounds (Nowakowski et al., 2022) and their hazardous properties should be considered when applied to soil (Pranagal and Kraska, 2020).

In the last years, there is a great need to develop agents to improve soil quality (Kamarudin et al., 2021; Chen et al., 2022; He et al., 2022). Nowadays, many papers showed the great potential of biochar (BC) application in soil remediation (Yi et al., 2020; Lin et al., 2023). BC is a porous, carbon-enrich material obtained via thermal decomposition of biomass under an oxygen-limited atmosphere (Lehmann and Joseph, 2009). Among various wastes, plants (Ahmed and Hameed, 2020) and sewage sludge (Agrafioti et al., 2013) are getting attention as the feedstocks for biochar production. BC addition improves soil properties and soil quality, increases crop productivity (Tang et al., 2013; Yang et al., 2019), and enhances moisture, and nutrient retention (Lehmann et al., 2006). The vast majority of papers have presented the effects of short-term BC agricultural usage. After field application, plenty of environmental factors affect biochar properties. The temperature differences, microbial activities, and precipitation events triggered the changes in BC physicochemical properties and structure (Wang et al., 2020). For example, rainfall or freeze–thaw events can cause mechanical fragmentation, surface oxidation, the release of dissolved organic matter, and the dissolution of minerals. On the other hand, biological and photochemical effects lead to oxidation and a decrease in labile carbon content in BC (Wang et al., 2020). All these changes in BC structure/composition can be accelerated experimentally by wet–dry cycling, freeze–thaw cycling, chemical oxidation, microbial inoculation, and UV irradiation (Wang et al., 2020).

The biochar-based papers are getting more numerous but very few of them are focused on long-term environmental behavior and consequences of BC application into the soil (Wang et al., 2020). The presented study aimed to i) estimate the effect of long-term, conducted for 6 months, chemical and physical aging of willow- and sewage sludge-derived biochar on their physicochemical properties; ii) to evaluate the aging effect on the content of total and bioavailable

(extractable by polyoxymethylene passive samplers) fraction of PAHs, and their more toxic derivatives.

## 2. Material and methods

### 2.1. Feedstock and biochar preparation

The two widely tested feedstocks were chosen for the preparation of the biochar: willow and sewage sludge. Willow (*Salix viminalis*) was harvested in the south-eastern part of Poland and air-dried for a couple of weeks. Before the pyrolysis process, the willow stems were cut into small parts (<5 cm) and grounded with a mill (TESTCHEM, Poland). Sewage sludge (SSL) was obtained from a municipal wastewater treatment plant located in Zamość ( $50^{\circ}43'14''\text{N}$   $23^{\circ}15'31''\text{E}$ , Poland). The SSL was also dried, crushed, sieved (<2 mm), and homogenized before the BC preparation.

Pyrolyses of prepared materials were carried out in a furnace (Czyłok, Poland). Biochars were obtained via slow pyrolysis at  $500^{\circ}\text{C}$ ,  $600^{\circ}\text{C}$ , and  $700^{\circ}\text{C}$ , and the following parameters were applied: the heating rate at the first step was  $10^{\circ}\text{C min}^{-1}$ , and the second step -  $3^{\circ}\text{C min}^{-1}$ , the resident time: 3 h. The atmosphere of the pyrolysis process was oxygen-free with the constant flow of nitrogen ( $630 \text{ cm}^3 \text{ min}^{-1}$ ) which was monitored by the mass flow controller (BETA-ERG, Poland). The biochars used in the experiment were named as follows: willow-derived BC produced at  $500^{\circ}\text{C}$  – BCW500, at  $600^{\circ}\text{C}$  – BCW600, at  $700^{\circ}\text{C}$  – BCW700, and sewage sludge-derived BC obtained at  $500^{\circ}\text{C}$  – BCZ500, at  $600^{\circ}\text{C}$  – BCZ600, at  $700^{\circ}\text{C}$  – BCZ700. BC was grounded to particles of about 2 mm, homogenized, washed out using distilled water (1:10, biochar: water) for 24 h, and dried at  $40^{\circ}\text{C}$  for 6 h. Before all experiments, BC was stored at room temperature in the absence of light.

### 2.2. The physical and chemical aging of biochars

Before aging, the water holding capacity of all studied biochars was determined to maintain their 40 % value during the experiments. Moreover, BC were sterilized with sodium azide solution (1 %) which was diluted from the stock solution (200 mg/L) (Sigma-Aldrich, Poland) and added to biochar to inhibit native microorganisms and remove the influence of biotic factors. Physical aging (PA) was carried out by exposure of the biochars to freeze-thaw cycles between  $+20^{\circ}\text{C}$  (7 days) and  $-20^{\circ}\text{C}$  (7 days) during all physical aging processes (6 months). Chemical aging was performed by the exposure of biochar to  $60^{\circ}\text{C}$  (CA60) and  $90^{\circ}\text{C}$  (CA90) in airtight stainless steel containers during the chemical aging process (6 months). The willow- and SSL- derived BC after aging were labeled as follows: after physical aging: BCW500-PA, BCW600-PA, BCW700-PA, BCZ500-PA, BCZ600-PA, BCZ700-PA, after chemical aging at  $60^{\circ}\text{C}$ : BCW500-CA60, BCW600-CA60, BCW700-CA60, BCZ500-CA60, BCZ600-CA60, BCZ700-CA60, and at  $90^{\circ}\text{C}$ : BCW500-CA90, BCW600-CA90, BCW700-CA90, BCZ500-CA90, BCZ600-CA90, BCZ700-CA90. Following previous studies (Siatecka et al., 2021), 6 months of aging were used as the first 6 months are the most significant considering BC oxidation and losses of volatile compounds, affecting physicochemical parameters of biochar.

### 2.3. The physicochemical characterization of BC before and after aging processes

The physicochemical analysis of the obtained BC (pH, ash, C, H, N content, X-ray photoelectron spectroscopy, SEM imaging, and EDS mapping) was performed according to the standard procedures described in the Supplementary Material.

#### 2.4. Freely dissolved ( $C_{\text{free}}$ ) PAHs and their derivatives determination in biochars

The content of freely dissolved PAHs and their derivatives (Table S1, Table S2) was performed using polyoxymethylene (POM) passive samplers according to the procedure described in the Supporting Material. The amount of total PAHs and their derivatives was determined using pressurized liquid extraction (PLE) and GC-MS/MS analysis (Supplementary material).

#### 2.5. The statistical analysis

The statistical analysis was carried out to determine the statistical significance of each parameter among the treatments by one-way analysis of variance (one-way ANOVA) followed by a Duncan multiple comparison test ( $p < 0.05$ ). The results were presented as the mean value of three replicates  $\pm$  standard deviation (SD). Pearson test was applied for the estimation of linear correlations.

### 3. Results

#### 3.1. The effect of physical and chemical aging on the physicochemical properties of biochars

The aging affected some properties of tested biochars (Figs. 1–3).

Considering the porosity of tested biochars before and after aging (Table 1), it can be observed that chemical (BCZ as the example presented in Fig. 1) and physical aging (Table 1) affected both surface area (Fig. 1A), pore volume (Fig. 1B) and pore diameter (Fig. 1C), and the highest changes were noted for CA at 90 °C. The increase of  $S_{\text{BET}}$  reached 24 %. This indicated the oxidation of the biochar and removal of the most labile components from the surface of BCZ that was cracked and fragmented (Wang et al., 2020), and new narrow pores were formed (Siatecka et al., 2021). On the other side, the lowered  $S_{\text{BET}}$  changes after aging (as observed for BCZ500-CA60) indicated the collapsing of inner pores (thus lowered pore volume (Fig. 1B) but not reduced mean pore diameter (Fig. 1C)). PA revealed also the impact on the porosity of tested BC (Table 1): increased surface area of BCZ but lowered BCW. Simultaneously, the other parameters such as pH or ash content were lowered for BCZ but increased for BCW (Table 1). Physically-aged sewage sludged-derived biochars were more hydrophilic and polar than before aging (increased O % and polarity and hydrophilicity related parameters, (O+N/C) and O/C, respectively), in contrast to willow-derived BC, where the observations were in contrary. These observations were confirmed when SEM images were collected (Fig. 2). It can be seen that the surface of BC was rougher than non-aged and full of pores, voids, etc. have arisen after aging. The results implied that the surface of SSL-derived BC was more sensitive to aging than willow-derived BC. In general, the effect of aging was connected both with pyrolysis

temperature and applied feedstock.

EDS mapping revealed that the surface of BCZ was composed mainly of carbon, oxygen, and calcium, however, the presence of N, Si, P, Fe, K, Mg, Al, and Zn was confirmed. Interestingly, the amount of carbon on the BCZ500 and BCZ600 surface after CA aging at 60°C was reduced, in contrast to BCZ700, where the amount of surface carbon increased after aging, confirming that CA60 influenced surface functional groups. The amount of O was similar after chemical aging, however, BCZ600-CA60 revealed higher O surface content than BCZ600 which may indicate the increased oxidation of surface species (Wang et al., 2020). The amount of N was also reduced due to aging. To verify the species formed on the BC surface, X-ray photoelectron spectroscopic (XPS) studies were performed (Fig. 3). XPS survey (Fig. 3A) of BCZ before and after physical and chemical aging looked similar, however, some peaks were having increased intensity confirming that aging did induce some changes on the surface of BC. Firstly, the number of observed oxygen- and carbon-containing species was increased (Fig. 3B, C).

For closer analysis, due to the highest effect of chemical aging on the content of PAHs and their derivatives (Sections 3.2–3.5), XPS spectra of BCZ before and after chemical aging were presented in Fig. 3B-D as the example. The intensity of XPS peaks of BCZ-CA aged at 60 °C was correlated with pyrolysis temperature and increased from 500 °C to 700 °C: the higher the pyrolysis temperature was applied the higher intensity of the carbon peak was observed. After CA the shape of the carbon peak was changed (Fig. 3B) and the deconvolution revealed the presence of eight peaks in comparison to four peaks present in pristine BCZ.

In general, the presence of carbon was evidenced by the presence of the peak at 284.7 eV. Before CA aging, C was present mainly (up to 16 at. %) as aliphatic carbon (C-C, C-H) which was confirmed by the presence of the peak at 285.25 eV and 284.7 eV (0.55 at. % and 1.58 at. %, respectively). The other carbon species included hydroxyl (C-OH at 286 eV up to 15 %at.) and carboxyl (O-C=O at 288.2 eV up to 2 %at.) groups (Rabchinskii et al., 2020). After aging, despite aliphatic carbon (up to 39.5 %at.), the surface of BC exposed more aromatic C=C sp<sup>2</sup> carbonic structures (peak at 284.14 eV, 31.5 %at.), increased content of carboxyl groups (up to 5 %at.) and some defective carbon structures (C-C, C=C peak at 283.57 eV) (Chiang et al., 2017). Aging was connected with oxidation of the BC surface (Fig. 3C). Oxygen before aging was detected in the form of O-(C=O\*)-C (532.4 eV 31.87 %at.), O=C-N (531.11 eV 22 at. %), and organic oxygen (533.97 eV), however some amount (4.83 at. %) of water/adsorbed oxygen was also noted (535.8 eV) (Wagstaffe et al., 2016). The process of aging increased the amount and number of O-containing functional groups. Carbonyl oxygen content increased above 40 %at., whereas aromatic hydroxyl and carboxyl groups were noted at the level of above 7.4 %at. Nitrogen was present mainly in the form of amines (peak at 398.14 eV) and O=C-N structures (peak at 400 eV) (He et al., 2017).

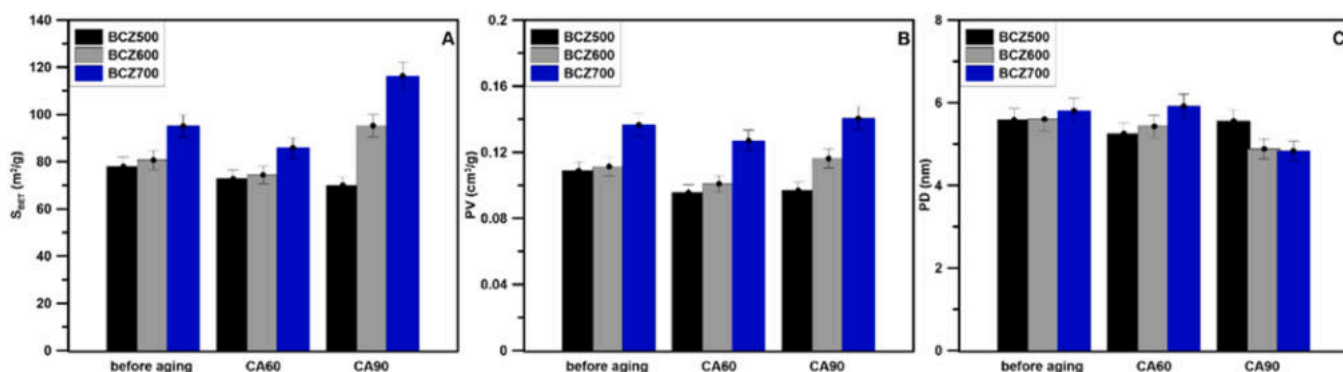


**Fig. 1.** Physicochemical properties of tested biochars A)  $S_{\text{BET}}$  (specific surface area), B) pore volume (PV), C) pore diameter (PD).

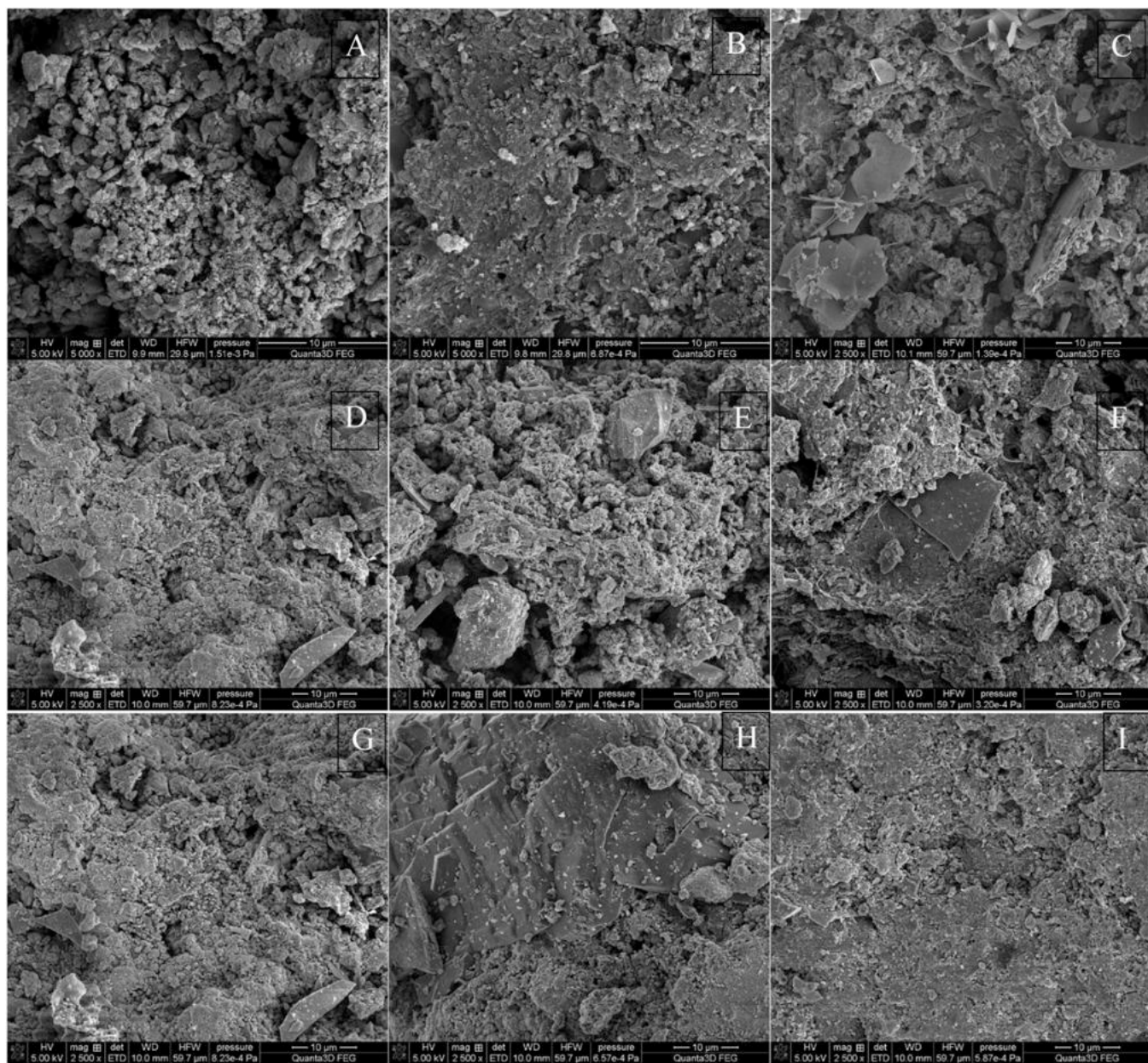


**Fig. 2.** SEM images of BC before (A (BCZ500), B (BCZ600), C (BCZ700)) and after chemical aging (D (BCZ500-CA60), E (BCZ600-CA60), F (BCZ700-CA60)) or physical aging G (BCZ500-PA), H (BCZ600-PA), I (BCZ700-PA).

The results clearly indicate that the aging was affecting the number of both carbon and oxygen species on the BC surface. This was confirmed when the bulk content of C and O was considered (Table 1). C % in BCZ and BCW was generally lowered after aging, whereas the content of O % increased. These changes were connected with aromaticity, hydrophilicity, and polarity of BC (expressed as the parameters H/C, O/C, and (O+N)/C, respectively). The polarity of BCZ increased (up to 30 %), and the hydrophilicity of BCZ and BCW after aging was also enhanced. Among other parameters of BC that were affected by aging it can be observed that the pH of BCZ and BCW was increased after CA, whereas PA has induced pH lowering in BCZ. An increase in pH suggests biochar lowers the environmental risk (Feng et al., 2022). The high stability of biochars (the physicochemical characteristic of materials before and after aging did not change significantly) is considered after aging (Sigmund et al., 2017; Cao et al., 2019). Cao et al (Cao et al., 2019) reported that due to the physical aging (freeze-thawed cycling and dry-wet cycling), the contents of acidic groups in BC increased, while the

contents of aromatic functional groups decreased with the consequence that the pH values of pyrolyzed material also dropped (Cao et al., 2019). Similar results were obtained in the study of Siatecka and Oleszczuk (Siatecka and Oleszczuk, 2022), where the stability of SSL-derived biochars lowered in the long term. Moreover, the stability of aged BC depended on the contents and character of carbon (Siatecka and Oleszczuk, 2022). SSL-derived materials with higher content of C and aliphatic matter/carbon substances located in surface pores but lower aromaticity were less stable than SSL-derived BC with lower content of carbon/aliphatic matter/carbon substance and higher aromaticity (Siatecka and Oleszczuk, 2022). Aging via oxidation also led to the division of BC into less stable (BC obtained at low temperature with lower aromaticity) and more stable ones (obtained at high temperature with higher aromaticity) (Siatecka et al., 2021; Siatecka and Oleszczuk, 2022). The intensity of the biochar oxidation and removal of the most labile components from the pyrolyzed material increased with the increasing aging temperature. Based on our study and the conclusions

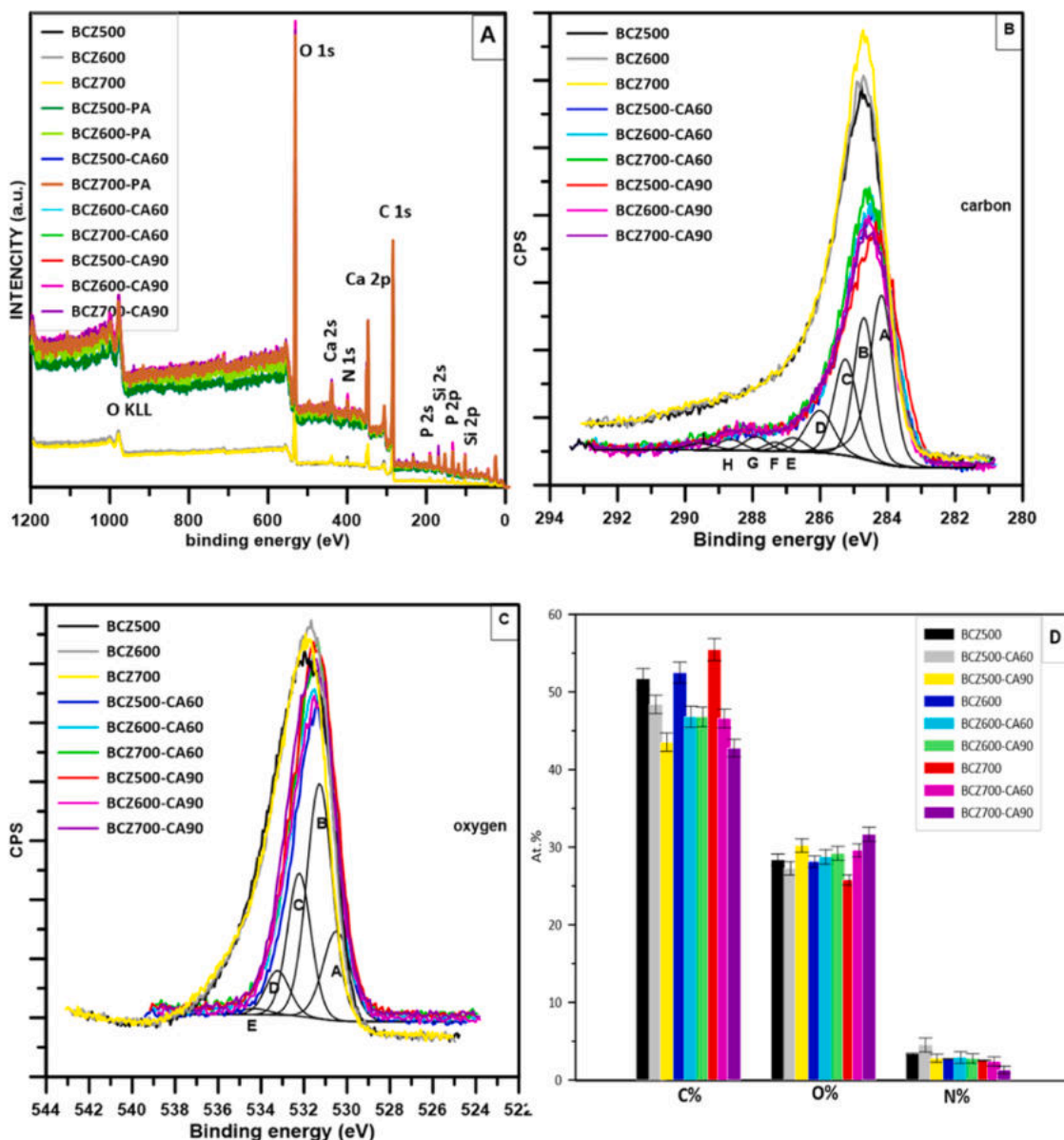


Fig. 3. XPS spectrum of tested BC, A) survey, B) carbon peaks, C) oxygen peaks, D) the content of C, O, and N on BCZ surface.

included in previous papers (Siatecka et al., 2021), the changes induced by aging depend on both the type of feedstock and pyrolysis temperature. Furthermore, due to the biochar oxidation, the number of surface oxygen functional groups, as well as the degree of hydrophilicity and polarity of BC will increase but pH will decrease. Wang et al (Wang et al., 2020) presented the mechanisms involved in BC aging and among them are dissolution of mineral components (divided into two stages), fragmentation, interactions with soil minerals, biological degradation, and abiotic oxidation.

### 3.2. The effect of the physical aging process on the total fraction of PAHs and their derivatives in biochar

#### 3.2.1. Pristine PAHs

The highest contents of pristine PAHs (as well as  $\Sigma$ 16US-EPA PAHs) before and after the physical aging, were found in BCW600 and BCW600-PA, respectively (Table 2, Table S3 and S4). Moreover, the content of the sum of quantified PAHs in aged biochar was higher than in non-aged materials by up to 26.64 % (BCW500 vs. BCW500-PA) and 32.13 % (BCW600 vs. BCW600-PA). 3-ring PAHs were the most

abundant (except BCW700) and constituted from 35.20 % to 37.97 % (34.08 % in BCW700). But 2-ring PAHs represented an almost equal percentage (31.43 %–36.83 %) with naphthalene as the most prevalent (constituted over 30 % of all BCW samples). Among 3-ring species, acenaphthene and acenaphthylene constituted the majority. 4-ring PAHs were in the range of 20.68 %–22.60 % with pyrene as the most widespread. 5- and 6-ring species amounted to 4.49 %–6.65 % and 1.19 %–2.64 %, respectively. Despite the similar percentage distribution of particular groups of PAHs, the concentration of 2-ring species increased up to 25.73 % (BCW600-PA) (Table S4). It is worth stressing that the content of 6-ring PAHs increased by at least 90%; up to even 130 % after aging. PAHs content increased disproportionately, and this led to the conclusion that PA promoted the formation of compounds with higher molecular weight. By comparing the changes in the concentration of individual PAHs in BCW samples before and after aging, the noted concentrations were usually less than two times higher. But in the case of BCW500-PA, the concentration of 2-methylpyrene, indeno[1,2,3-cd]pyrene, dibenz[a,h]pyrene, and dibenz[a,i]pyrene was even 4.5 times higher than in BCW500.

Before aging, the highest content of pristine PAHs in SSL-derived

**Table 1**

Physicochemical properties of pristine and aged biochars.

BC	$S_{BET}$ [ $m^2 g^{-1}$ ]	pH	Ash content [%]	C [%]	H [%]	N [%]	O [%]	H/C	(O + N)/C	O/C
BCZ500	78.04	7.84	61.53	24.96	1.35	3.38	8.78	0.054	0.487	0.352
BCZ600	79.56	7.79	63.58	24.45	0.86	2.24	8.84	0.035	0.453	0.362
BCZ700	94.00	7.73	67.76	24.14	0.76	1.39	5.95	0.031	0.304	0.246
BCZ500-CA60	72.81	8.21	60.87	23.15	1.29	2.79	11.90	0.056	0.634	0.514
BCZ600-CA60	74.36	7.99	63.98	24.06	0.92	2.22	8.82	0.038	0.459	0.367
BCZ700-CA60	85.91	8.34	68.12	23.29	0.77	1.39	6.44	0.033	0.336	0.276
BCZ500-CA90	69.95	8.13	61.48	22.98	1.35	2.85	11.35	0.059	0.618	0.494
BCZ600-CA90	95.32	8.22	65.07	23.25	1.03	2.32	8.33	0.044	0.458	0.358
BCZ700-CA90	116.36	7.89	69.20	21.77	0.67	1.32	7.04	0.031	0.384	0.324
BCZ500-PA	84.65	7.45	60.46	23.85	1.33	2.85	11.51	0.056	0.602	0.483
BCZ600-PA	86.59	7.34	62.25	23.84	0.95	1.74	11.22	0.040	0.544	0.471
BCZ700-PA	104.65	7.23	65.43	23.80	0.78	1.24	8.75	0.033	0.420	0.368
BCW500	119.50	10.18	8.18	75.18	2.52	2.47	11.65	0.034	0.188	0.155
BCW600	145.00	10.45	7.09	82.77	2.24	1.68	6.22	0.027	0.095	0.075
BCW700	13.23	11.39	5.64	82.38	1.46	1.67	8.85	0.018	0.128	0.107
BCW500-CA60	89.65	10.56	5.09	71.14	1.99	2.213	19.57	0.028	0.306	0.275
BCW600-CA60	76.56	10.4	6.82	81.77	1.46	1.05	8.90	0.018	0.122	0.109
BCW700-CA60	25.64	10.2	5.12	69.85	1.23	0.89	22.91	0.018	0.341	0.328
BCW500-CA90	75.55	11.19	6.23	84.40	2.53	1.10	5.73	0.030	0.081	0.068
BCW600-CA90	56.55	10.56	6.68	86.74	1.41	0.84	4.33	0.016	0.060	0.050
BCW700-CA90	12.44	9.57	6.21	82.43	0.93	1.18	9.25	0.011	0.126	0.112
BCW500-PA	110.49	10.35	7.79	74.53	1.76	1.98	13.94	0.024	0.214	0.187
BCW600-PA	134.58	10.42	6.69	53.56	0.88	1.65	37.22	0.016	0.726	0.695
BCW700-PA	16.89	9.89	7.86	83.33	0.46	1.54	6.81	0.006	0.100	0.082

**Table 2**

The content of total and bioavailable PAHs and their derivatives in tested BC.

Sample description	The concentration of total PAHs $\pm$ SD [ng g $^{-1}$ ]	The concentration of total $\Sigma 16$ PAHs $\pm$ SD [ng g $^{-1}$ ]	The concentration of total PAHs derivatives $\pm$ SD [ng g $^{-1}$ ]	The concentration of bioavailable $\Sigma$ PAHs <sub>free</sub> $\pm$ SD [ng L $^{-1}$ ]	The concentration of bioavailable $\Sigma 16$ PAHs $\pm$ SD [ng L $^{-1}$ ]	The concentration of bioavailable PAHs derivatives $\pm$ SD [ng L $^{-1}$ ]
BCW500	151.55 $\pm$ 6.94	144.00 $\pm$ 6.59	1.48 $\pm$ 0.07	3.51 $\pm$ 0.20	3.34 $\pm$ 0.20	0.25 $\pm$ 0.01
BCW600	181.08 $\pm$ 8.29	171.36 $\pm$ 7.85	1.92 $\pm$ 0.09	3.17 $\pm$ 0.15	2.92 $\pm$ 0.14	0.48 $\pm$ 0.02
BCW700	158.02 $\pm$ 7.23	148.27 $\pm$ 6.79	4.31 $\pm$ 0.20	3.53 $\pm$ 0.17	3.31 $\pm$ 0.16	0.48 $\pm$ 0.02
BCW500-PA	191.92 $\pm$ 8.35	180.66 $\pm$ 7.86	2.42 $\pm$ 0.11	11.66 $\pm$ 0.61	11.66 $\pm$ 0.61	0.62 $\pm$ 0.03
BCW600-PA	239.25 $\pm$ 11.44	223.27 $\pm$ 10.67	2.23 $\pm$ 0.11	14.16 $\pm$ 0.73	14.15 $\pm$ 0.73	0.40 $\pm$ 0.02
BCW700-PA	205.83 $\pm$ 8.96	190.42 $\pm$ 8.29	6.79 $\pm$ 0.30	12.38 $\pm$ 0.65	12.38 $\pm$ 0.65	0.55 $\pm$ 0.03
BCW500-CA60	17.38 $\pm$ 0.80	17.30 $\pm$ 0.79	0.42 $\pm$ 0.02	10.11 $\pm$ 0.50	10.11 $\pm$ 0.50	0.56 $\pm$ 0.03
BCW600-CA60	18.69 $\pm$ 0.86	18.57 $\pm$ 0.85	0.52 $\pm$ 0.02	15.22 $\pm$ 0.70	15.21 $\pm$ 0.70	0.27 $\pm$ 0.01
BCW700-CA60	15.87 $\pm$ 0.73	15.87 $\pm$ 0.73	0.62 $\pm$ 0.03	13.07 $\pm$ 0.69	13.06 $\pm$ 0.69	0.31 $\pm$ 0.02
BCW500-CA90	13.14 $\pm$ 0.60	13.14 $\pm$ 0.60	<LOD	11.68 $\pm$ 0.60	11.67 $\pm$ 0.60	0.97 $\pm$ 0.05
BCW600-CA90	14.71 $\pm$ 0.67	14.71 $\pm$ 0.67	<LOD	17.34 $\pm$ 0.85	17.33 $\pm$ 0.85	1.18 $\pm$ 0.06
BCW700-CA90	12.79 $\pm$ 0.59	12.75 $\pm$ 0.58	<LOD	15.58 $\pm$ 0.80	15.56 $\pm$ 0.80	1.32 $\pm$ 0.07
BCZ500	90.16 $\pm$ 4.13	80.05 $\pm$ 3.64	2.72 $\pm$ 0.12	33.50 $\pm$ 1.22	33.45 $\pm$ 1.22	0.81 $\pm$ 0.03
BCZ600	125.83 $\pm$ 5.76	103.74 $\pm$ 4.96	5.30 $\pm$ 0.25	39.98 $\pm$ 1.46	39.71 $\pm$ 1.45	1.90 $\pm$ 0.07
BCZ700	110.04 $\pm$ 5.04	93.41 $\pm$ 4.42	4.01 $\pm$ 0.18	38.33 $\pm$ 1.40	38.22 $\pm$ 1.40	0.93 $\pm$ 0.03
BCZ500-PA	133.49 $\pm$ 5.53	115.78 $\pm$ 5.53	4.18 $\pm$ 0.20	11.03 $\pm$ 0.51	11.01 $\pm$ 0.51	0.45 $\pm$ 0.02
BCZ600-PA	203.08 $\pm$ 8.51	157.10 $\pm$ 6.95	5.71 $\pm$ 0.24	13.43 $\pm$ 0.69	13.36 $\pm$ 0.69	0.87 $\pm$ 0.04
BCZ700-PA	209.17 $\pm$ 10.00	168.81 $\pm$ 8.33	9.27 $\pm$ 0.44	14.76 $\pm$ 0.76	14.71 $\pm$ 0.75	0.99 $\pm$ 0.05
BCZ500-CA60	109.78 $\pm$ 4.58	97.12 $\pm$ 4.06	2.84 $\pm$ 0.12	8.03 $\pm$ 0.41	8.03 $\pm$ 0.41	<LOD
BCZ600-CA60	174.25 $\pm$ 7.58	135.60 $\pm$ 6.18	5.47 $\pm$ 0.24	9.17 $\pm$ 0.42	9.13 $\pm$ 0.42	0.16 $\pm$ 0.01
BCZ700-CA60	176.17 $\pm$ 8.02	141.79 $\pm$ 6.69	6.38 $\pm$ 0.29	10.84 $\pm$ 0.57	10.80 $\pm$ 0.57	0.64 $\pm$ 0.03
BCZ500-CA90	126.35 $\pm$ 5.27	111.65 $\pm$ 4.68	3.12 $\pm$ 0.13	6.63 $\pm$ 0.30	6.61 $\pm$ 0.30	0.04 $\pm$ 2.0 $\cdot$ 10 $^{-3}$
BCZ600-CA90	198.13 $\pm$ 8.62	152.39 $\pm$ 6.97	5.85 $\pm$ 0.25	9.66 $\pm$ 0.50	9.45 $\pm$ 0.48	0.52 $\pm$ 0.03
BCZ700-CA90	193.91 $\pm$ 8.83	152.95 $\pm$ 7.23	7.70 $\pm$ 0.35	10.67 $\pm$ 0.55	10.63 $\pm$ 0.55	0.71 $\pm$ 0.04

SD- standard deviation; LOD- limit of detection.

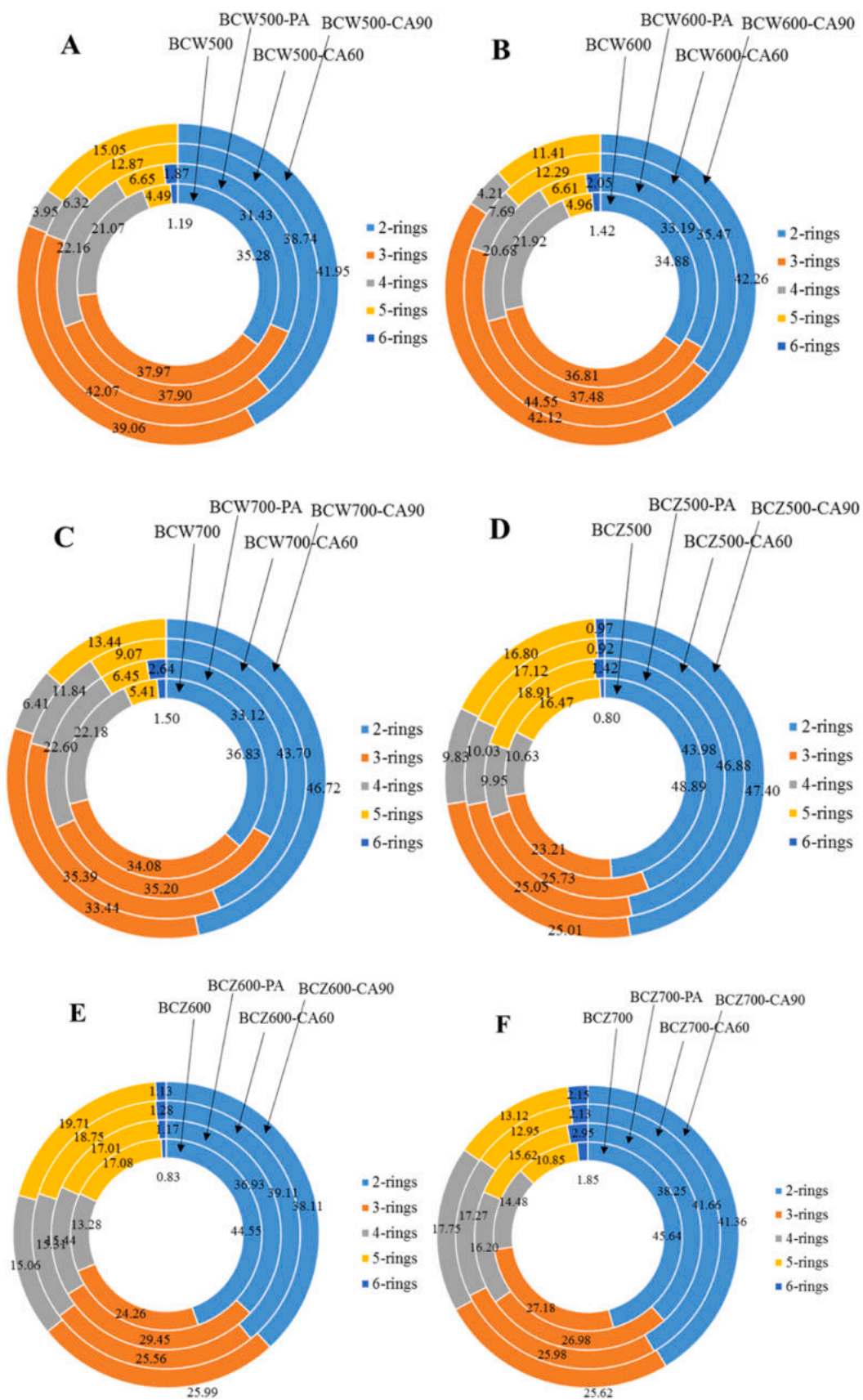


Fig. 4. The percentage of the PAHs and their derivatives in pristine and aged BC, A) BCW500, B) BCW600, C) BCW700, D) BCZ500, E) BCZ600, F) BCZ700.

biochar was found in BCZ600 (Table 2, Fig. 4). After physical aging, the content of PAHs increased 48–90 % up to  $209.17 \pm 10.00 \mu\text{g g}^{-1}$  (BCZ700-PA). 2-ring PAHs (predominantly naphthalene) were the most abundant and constituted 45 %–49 % in BCZ, and 36 %–44 % in BCZ-PA. Among 3-ring species (23 %–27 % in BCZ and 26–29 % in BCZ-PA), acenaphthylene and pyrene were the most noted. 4- and 5-ring PAHs constituted from 9.95 % to 16.20 % and from 10.95 % to 18.91 % of all quantified PAHs, before and after PA, respectively. PAHs possessing 6 aromatic rings constituted the minority (0.80 %–2.95 %). Despite the similar percentage of individual groups of PAHs, some of them increased more than others. For example, the concentration of 2-ring species increased by 32 %–59 %, whereas the content of 6-ring species increased 2.3–3.3 times after PA. Artificial aging caused the reduction of the relative content of LMW PAHs (compounds with  $\leq$ three aromatic rings) (Sigmund et al., 2017). LMW PAHs are more susceptible to desorption from biochar than HMW PAHs (with  $\geq$ four aromatic rings) because of their lower lipophilicity and higher solubility (Sigmund et al., 2017).

### 3.2.2. PAHs derivatives

Among all studied PAHs derivatives, in BCW samples only nitronaphthalene was quantified up to  $4.31 \pm 0.20 \mu\text{g g}^{-1}$  in BCW700, and  $6.79 \pm 0.30 \mu\text{g g}^{-1}$  in BCW700-PA, respectively, indicating up to 64 % increase. In BCZ samples only 2-ring N-PAHs (1-methyl-5-nitronaphthalene and 1-methyl-6-nitronaphthalene) were quantified. The lowest increase in the total fraction of PAHs derivatives concentration was observed in BCZ600 vs. BCZ600-PA (7.82 %). The highest increase in the content of total PAHs derivatives was observed in BCZ700-PA - 130.97 %.

### 3.3. The effect of the chemical aging process on the total fraction of PAHs and their derivatives in biochar

#### 3.3.1. Pristine PAHs

The chemical aging affected the total fraction of PAHs in willow-derived biochars (Table 2, Fig. 4). Considering the experiment at 60 °C (Table S5), the total concentration has dropped about 89–90 % (simultaneously the  $\Sigma$ 16PAHs decreased by 88–89 %). Similar results were obtained in biochar aged chemically at 90 °C (PAHs content was lower by approximately 90 %). In non-aged BC, 2- and 3-ring PAHs accounted for comparable levels, e.g. 34.88 %–36.83 % and 34.08 %–37.97 % in BCW samples, whereas 35.47–43.70 % and 35.39 %–44.55 % in BCW-CA60, and 41.95 %–46.72 % and 33.44 %–42.12 % in BCW-CA90. But the contribution of 4-ring species decreased significantly from 21.73 % to 8.62 % in BCW-CA60, and 4.86 % in BCW-CA90. On the other hand, the percentage of 5-ring PAHs increased from 4.95 % to 11.41 % and 13.30 %, respectively. The exposure of biochars at selected temperatures (60 °C and 90 °C) caused a reduction in the content of 6-ring species to the level below LOD. Considering the changes (in percentage) in individual groups of PAHs (regardless of the total values), the decrease amounted to 70.96 %–100 % in BCW-CA60 and 67.15 %–100 % in BCW-CA90. There was no significant difference in terms of the reduction of the content of high/low molecular weight PAHs.

Considering SSL-derived biochar, the total fraction of PAHs increased as a consequence of the chemical aging process. These materials have undergone some different transformations than willow-derived BC. Probably, some changes in physicochemical parameters of BCZ500, BCZ600, and BCZ700 resulted in PAHs formation. During chemical aging at 60 °C and 90 °C (Table S5, Table S6), the total PAHs content increased by 21.77 % and 40.15 % in BCZ500, 38.48 % and 57.46 % in BCZ600, 60.09 %, and 76.21 % in BCZ700. Chemical aging did not affect the percentage share of individual groups of PAHs diversified in terms of the number of aromatic rings. The BCZ500 and BCZ600 (as well as BCZ500-CA60, BCZ500-CA90, BCZ600-CA60, and BCZ600-CA90) contained 38.11–48.98 % of 2-ring PAHs. Then, in descending order were 3-, 5-, 4-, and 6-ring PAHs. Only in BCZ700 (and in BCZ700-

CA60 and BCZ700-CA90), 4-ring species constituted a higher percentage than 5-ring PAHs.

#### 3.3.2. PAHs derivatives

In BCW samples the content of nitronaphthalene (as the only representative of PAHs derivatives) decreased by 71.62 %, 72.95 %, and 85.61 % in BCW500-CA60, BCW600-CA60, and BCW700-CA60 during CA process at 60 °C (Table S5). The application of a higher temperature (90 °C) (Table S6) resulted in the total decomposition and elimination of nitronaphthalene. In BCZ500 and BCZ600, the content of 1-methyl-5-nitronaphthalene and 1-methyl-6-nitronaphthalene (which constituted all quantified PAHs derivatives) increased by 4.27 % and 3.18 % during CA at 60 °C, and 14.80 % and 10.37 % during CA at 90 °C. However, in BCZ700 the content of derivatives increased by 58.94 % and 91.96 % in BCZ700-CA60 and BCZ700-CA90, respectively.

Statistically, important correlations ( $p < 0.05$ ) were noted between feedstock type and total content of PAHs and content of PAHs after CA. CA affected also the content of PAHs derivatives.

### 3.4. The bioavailable fraction of PAHs and their derivatives in biochar before and after the physical aging process

#### 3.4.1. Pristine PAHs

The PA affected the bioavailable fraction of pristine PAHs (Table 2, Table S8). Considering willow-derived biochars, the concentration of bioavailable PAHs increased up to 4.5 times. Although the total fraction of PAHs in BCW samples increased by 26.64–32.13 % after 6 months of physical aging, the bioavailability of analytes increased disproportionately. The PA caused an increase in the bioavailability of studied contaminants. The processes occurring during PA facilitated the release of higher amounts of PAHs into the environment. Moreover, physical aging changed the percentage distribution of individual groups of PAHs differing in the number of aromatic rings. Before aging, 3-ring PAHs were the most abundant (and were in the range of 97.78 %–98.50 %), while 4-, 5-, and 6- ring PAHs constituted 1.14 %–1.78 %, 0.18 %–0.36 %, and 0.03 %–0.08 %, respectively. The concentration of 2-ring species was below the limit of detection. However, after PA, PAHs with two aromatic rings were the most prevalent (67.79 %–72.30 % of all quantified PAHs). Then, in descending order were 3-ring (26.11 %–30.25 %), 4-ring (<2 %), 5-ring (<0.04 %) and 6-ring species (<0.004 %). The temperature of pyrolysis affected the bioavailable fraction of analytes. Before PA, willow-derived biochars obtained at 600 °C contained the lowest amount of PAHsfree. However, after aging, the increase in the concentration was the largest. Without long-term experiments, biochar produced at 600 °C appeared to be the safest (considering PAHs contamination), but the results obtained after PA showed that the release of studied contaminants was enhanced.

In BCZ samples, physical aging caused a decrease in the bioavailable fraction of PAHs by 67.08 %, 66.42 %, and 61.48 % in BCZ500-PA, BCZ600-PA, and BCZ700-PA in comparison with biochar before aging (the specific values were included in Table 2, Fig. 5B). Despite PA causing an increase in the total fraction of PAHs by 48.06–90.08 %, the bioavailability of pristine compounds decreased significantly which is a great advantage in terms of the environmental application of biochar. 2-ring species were the most abundant in both BC (before and after PA) ranging from 89.56 % to 90.64 % in BCZ, and from 77.29 % to 84.35 % in BCZ-PA. 3-ring species constituted 8.97 %–9.77 % and 14.77 %–21.16 %, respectively. The other pristine compounds together accounted for less than 2 % in BC before and after PA.

#### 3.4.2. PAHs derivatives

The changes in the concentration of PAHs derivatives in willow-derived biochar did not show a clear trend. In BCW500-PA the sum of quantified derivatives increased by almost 2.5 times (compared to non-aged BC), while in BCW600-PA decreased by 15.56 %, but in BCW700-PA increased by 15.61 %. Before PA, only 4-ring derivatives were

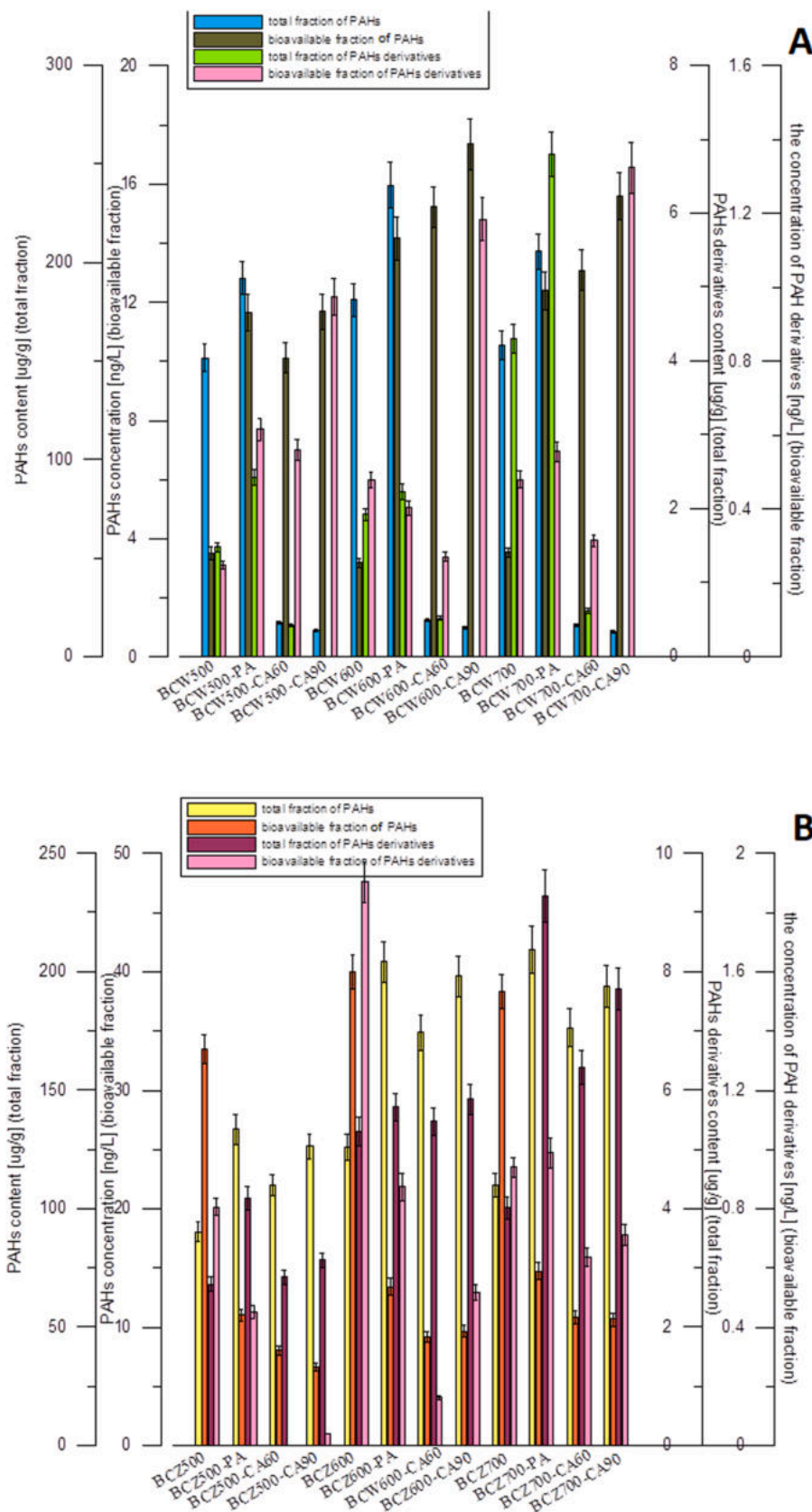


**Fig. 5.** The concentration of total and bioavailable PAHs and their derivatives in pristine and aged BC derived from willow (A) and sewage sludge (B).

quantified (4H-cyclopenta(def)phenanthrene and nitropyrene), while after PA only the concentration of 2–ring compound (nitronaphthalene) was quantified. In BCZ500-PA and BCZ600-PA the contents of analytes have halved, while in BCZ700-PA increased slightly (by 5.10%). Before aging, both N- and O-PAHs were quantified, but after aging, only N-PAHs were determined. Generally aging affected ( $p < 0.05$ ) total PAHs and bioavailable PAHs derivatives.

### 3.5. The bioavailable fraction of PAHs and their derivatives in biochar before and after the chemical aging process

#### 3.5.1. Pristine PAHs

The chemical aging caused changes in the bioavailable content of PAHs in biochars (Table S9, Table S10). After CA at 60 °C, the concentration of bioavailable PAHs increased about 2.9, 4.8, and 3.7 times in BCW500-CA60, BCW600-CA60, and BCW700-CA60. Application of higher temperature (90 °C) caused even greater enhancement of bioavailable PAHs content (3.3, 5.5, and 4.4 in BCW500-CA90, BCW600-CA90, and BCW700-CA90, respectively). Before CA, the smallest concentration of analytes was quantified in biochars obtained at 600 °C, which was environmentally beneficial. However, the largest increase in bioavailable PAHs concentration after CA was recorded also in these materials. Biochar obtained at 600 °C revealed initially the lowest environmental hazard, but after the long-term experiment, these materials contained the highest amount of PAHs which may be released into the environment. Another interesting finding is that CA caused a huge drop in the content of the total fraction of PAHs. But on the other hand, a major increase in the bioavailable fraction of analytes was observed. This situation showed why the quantification of the bioavailable fraction of PAHs and their derivatives (not only the total fraction) is so important. CA (at both temperatures) led to changes in the percentage distribution of individual groups of PAHs differing in the number of aromatic rings (Fig. 4). Before CA, 3-ring PAHs were predominant; 4-, 5-, and 6-ring species constituted less or about 2, and the concentration of 2-ring PAHs was below the limit of detection. But after CA, PAHs with 2 aromatic rings were the most abundant (67.56–74.64%). Then, in descending order were 3-ring species (23.66–30.34%), 4-, 5-, and 6-ring PAHs (less than 3%).

CA caused a decrease in the bioavailable fraction of PAHs in SSL-derived biochars. The decrease was in the range of 71.71–77.06% during CA60 and 72.16–80.22% during CA90. But the percentage distribution of PAHs with a different number of aromatic rings remained unchanged. 2-ring PAHs were the most prevalent (84.66–89.28% CA at 60 °C and 82.17–91.28% CA at 90 °C). 3-ring PAHs were in the range of 7.72–16.12%, and the rest of PAHs constituted less than 2% of all quantified PAHs.

#### 3.5.2. PAHs derivatives

The changes in the concentration of PAHs derivatives in willow-derived biochar resulting from CA60 and CA90 did not show a clear trend. In BCW500-CA60, BCW500-CA90, BCW600-CA90, and BCW700-CA90 the sum of quantified derivatives increased by almost 2.3, 4.0, 2.5, 2.8 times (compared to non-aged BC), while in BCW600-CA60 and BCW700-CA60 decreased by 43.31%, and 34.38%. CA60 and CA90 caused a drop in the concentration of bioavailable fraction of analytes (by 91.49% and 32.22% in BCZ600-CA60 and BCZ700-CA60; in BCZ500-CA60 the content of PAHs derivatives was below the limit of detection), 24.14% in BCZ700. As it was noted before, in the case of bioavailable fraction of PAHs derivatives changed by PA, in non-aged BC only 4-ring PAHs were quantified while in BC after CA60 and CA90 only nitronaphthalene was determined.

## 4. Conclusions

Field natural aging is affected by various factors and can be very slow. Artificial aging (physical and chemical) was selected for

shortening the aging duration from years to days. Biochar applied in the soil is subjected to many processes. These follow from some natural phenomena, such as rainfall, and freeze-thaw events, as well as from the interaction of BC and rich soil matrix. In our study, we focused on some changes caused by abiotic factors (PA and CA at both temperatures (60 °C and 90 °C)). It can be observed that chemical and physical aging affected the porosity and chemical composition (C and O content) of tested BC as the consequences of the oxidation of the biochar and removal of the most labile components from the surface that was cracked and fragmented. In general, the effect of aging was connected both with pyrolysis temperature and feedstock. PA promoted the formation of PAHs with higher molecular weight and increased total PAHs concentration (up to 27% in BCW and 90% in BCZ) with increased 2-ring (25–59%) and 6-ring PAHs (130–330%), simultaneously, the concentration of PAHs derivatives was higher (130%). It is worth stressing that PA increased the bioavailability of PAHs (450%) and PAHs derivatives (64%) in BCW and BCZ (7%) to a lesser extent. On the other hand, chemical aging was responsible for reduced total PAHs content (90%) in BCW but up to 76% increased total PAHs content in BCZ. Similar results were noted when PAHs derivatives were considered: 86% reduction in BCW but 92% increase in BCZ.

## CRediT authorship contribution statement

**Agnieszka Krzyszczak:** Investigation, Writing – review & editing; **Michał P. Dybowski:** Investigation, Methodology, Formal analysis, Validation; **Investigation;** **Robert Zarzycki:** Investigation; **Rafał Kobyłecki:** Investigation; **Patryk Oleszczuk:** Validation, Supervision **Bożena Czech:** Investigation, Methodology, Visualization, Writing – review & editing, Conceptualization, Validation, Supervision.

## Declaration of Competing Interest

The authors declare the following financial interests/personal relationships which may be considered as potential competing interests: Bozena Czech reports financial support was provided by National Science Centre Poland.

## Data availability

Data will be made available on request.

## Acknowledgments

The studies were supported by project No. 2018/31/B/NZ9/00317 funded by the National Science Centre, Poland. The research was partially funded by the statute subvention of the Częstochowa University of Technology, Faculty of Infrastructure and Environment.

## Environmental implication

In biochar, the toxic polycyclic aromatic hydrocarbons (PAHs) are noted. However, in the environment or during pyrolysis, more toxic PAHs derivatives are formed. Their environmental behavior was not studied yet. Aged biochar may contain a lower amount of PAHs, but their bioavailability may be enhanced. There is no data on the presence of PAHs derivatives in the aged BC, both in the context of their total content and most preferentially, on their bioavailability. The results indicated that despite the lowered total concentration of PAHs their bioavailability was significantly enhanced. The observed effect was connected with applied feedstock and pyrolysis temperature.

## Appendix A. Supporting information

Supplementary data associated with this article can be found in the online version at doi:10.1016/j.jhazmat.2022.129795.

## References

- Abbas, A.O., Brack, W., 2006. Polycyclic aromatic hydrocarbons in Niger Delta soil: contamination sources and profiles. *Int. J. Environ. Sci. Technol.* 2, 343–352. <https://doi.org/10.1007/BF03325895>.
- Agrafioti, E., Bouras, G., Kalderis, D., Diamadopoulos, E., 2013. Biochar production by sewage sludge pyrolysis. *J. Anal. Appl. Pyrolysis* 101, 72–78. <https://doi.org/10.1016/j.jaap.2013.02.010>.
- Ahmed, M.J., Hameed, B.H., 2020. Insight into the co-pyrolysis of different blended feedstocks to biochar for the adsorption of organic and inorganic pollutants: a review. *J. Clean. Prod.* 265, 121762 <https://doi.org/10.1016/j.jclepro.2020.121762>.
- Alves, C.A., Vicente, A.M.P., Gomes, J., Nunes, T., Duarte, M., Bandowe, B.A.M., 2016. Polycyclic aromatic hydrocarbons (PAHs) and their derivatives (oxygenated-PAHs, nitrated-PAHs and azaarenes) in size-fractionated particles emitted in an urban road tunnel. *Atmos. Res.* 180, 128–137. <https://doi.org/10.1016/j.atmosres.2016.05.013>.
- Bandowe, B.A.M., Nkansah, M.A., 2016. Occurrence, distribution and health risk from polycyclic aromatic compounds (PAHs, oxygenated-PAHs and azaarenes) in street dust from a major West African Metropolis. *Sci. Total Environ.* 553, 439–449. <https://doi.org/10.1016/j.scitotenv.2016.02.142>.
- Cao, Y., Jing, Y., Hao, H., Wang, X., 2019. Changes in the physicochemical characteristics of peanut straw biochar after freeze-thaw and dry-wet aging treatments of the biomass. *BioResources*. (<https://doi.org/10.15376/BIORES.14.2.4329-4343>).
- Cao, Z., Wang, M., Shi, S., Zhao, Y., Chen, X., Li, C., Li, Y., Wang, H., Bao, L., Cui, X., 2020. Size-distribution-based assessment of human inhalation and dermal exposure to airborne parent, oxygenated and chlorinated PAHs during a regional heavy haze episode. *Environ. Pollut.* 263, 114661 <https://doi.org/10.1016/j.envpol.2020.114661>.
- Chen, K., Li, N., Zhang, S., Liu, N., Yang, J., Zhan, X., Han, X., 2022. Biochar-induced changes in the soil diazotroph community abundance and structure in a peanut field trial. *Biochar* 4, 26. <https://doi.org/10.1007/s42773-022-00133-6>.
- Chiang, Y.-C., Chen, Y.-J., Wu, C.-Y., 2017. Effect of relative humidity on adsorption breakthrough of CO<sub>2</sub> on activated carbon fibers. *Materials* 10, 1296. <https://doi.org/10.3390/ma10111296>.
- Feng, Y., Feng, Y., Liu, Q., Chen, S., Hou, P., Poinern, G., Jiang, Z., Fawcett, D., Xue, L., Lam, S.S., Xia, C., 2022. How does biochar aging affect NH<sub>3</sub> volatilization and GHGs emissions from agricultural soils. *Environ. Pollut.* 294, 118598 <https://doi.org/10.1016/j.envpol.2021.118598>.
- Gope, M., Masto, R.E., George, J., Balachandran, S., 2018. Exposure and cancer risk assessment of polycyclic aromatic hydrocarbons (PAHs) in the street dust of Asansol city, India. *Sustain. Cities Soc.* 38, 616–626. <https://doi.org/10.1016/j.scs.2018.01.006>.
- He, H., Hu, Y., Chen, S., Zhuang, L., Ma, B., Wu, Q., 2017. Preparation and properties of A hyperbranched-polyamine adsorbent for carbon dioxide capture. *Sci. Rep.* 7, 3913. <https://doi.org/10.1038/s41598-017-04329-w>.
- He, Q., Li, X., Ren, Y., 2022. Analysis of the simultaneous adsorption mechanism of ammonium and phosphate on magnesium-modified biochar and the slow release effect of fertiliser. *Biochar* 4, 25. <https://doi.org/10.1007/s42773-022-00150-5>.
- Kamarudin, N.S., Dahalan, F.A., Hasan, M., An, O.S., Parmin, N.A., Ibrahim, N., Hamdzah, M., Zain, N.A.M., Muda, K., Wikurendra, E.A., 2021. Biochar: a review of its history, characteristics, factors that influence its yield, methods of production, application in wastewater treatment and recent development. *Biointerface Res Appl. Chem.* 12, 7914–7926. <https://doi.org/10.33263/BRIAC126.79147926>.
- Krzyszczak, A., Czech, B., 2021. Occurrence and toxicity of polycyclic aromatic hydrocarbons derivatives in environmental matrices. *Sci. Total Environ.* 147738 <https://doi.org/10.1016/j.scitotenv.2021.147738>.
- Krzyszczak, A., Dybowski, M.P., Czech, B., 2021. Formation of polycyclic aromatic hydrocarbons and their derivatives in biochars: The effect of feedstock and pyrolysis conditions. *J. Anal. Appl. Pyrolysis* 160, 105339. <https://doi.org/10.1016/j.jaap.2021.105339>.
- Lehmann, J., Joseph, S., 2009. Biochar for environmental management: an introduction. *Biochar for environmental management. Science and Technology*. Earthscan Publishers Ltd.
- Lehmann, J., Gaunt, J., Rondon, M., 2006. Bio-char sequestration in terrestrial ecosystems – a review. *Mitig. Adapt Strat Glob. Change* 11, 403–427. <https://doi.org/10.1007/s11027-005-9006-5>.
- Lin, P., Liu, H., Yin, H., Zhu, M., Luo, H., Dang, Z., 2023. Remediation performance and mechanisms of Cu and Cd contaminated water and soil using Mn/Al-layered double oxide-loaded biochar. *J. Environ. Sci.* 125, 593–602. <https://doi.org/10.1016/j.jes.2022.03.023>.
- Nowakowski, M., Rykowska, I., Wolski, R., Andrzejewski, P., 2022. Polycyclic aromatic hydrocarbons (PAHs) and their Derivatives (O-PAHs, N-PAHs, OH-PAHs): determination in suspended particulate matter (SPM) – a review. *Environ. Process.* 9, 2. <https://doi.org/10.1007/s40710-021-00555-7>.
- Oleszczuk, P., Kuśmierz, M., Godlewska, P., Kraska, P., Palys, E., 2016. The concentration and changes in freely dissolved polycyclic aromatic hydrocarbons in biochar-amended soil. *Environ. Pollut.* 214, 748–755. <https://doi.org/10.1016/j.envpol.2016.04.064>.
- Pranagal, J., Kraska, P., 2020. 10-years studies of the soil physical condition after one-time biochar application. *Agronomy* 10, 1589. <https://doi.org/10.3390/agronomy10101589>.
- Rabchinskii, M.K., Ryzhkov, S.A., Kirilenko, D.A., Ulin, N.V., Baidakova, M.V., Shnitov, V.V., Pavlov, S.I., Chumakov, R.G., Stolyarova, D.Yu., Besedina, N.A., Shvidchenko, A.V., Potorochin, D.V., Roth, F., Smirnov, D.A., Gudkov, M.V., Brzhezinskaya, M., Lebedev, O.I., Melnikov, V.P., Brunkov, P.N., 2020. From graphene oxide towards aminated graphene: facile synthesis, its structure and electronic properties. *Sci. Rep.* 10, 6902. <https://doi.org/10.1038/s41598-020-63935-3>.
- Siatecka, A., Oleszczuk, P., 2022. Mechanism of aging of biochars obtained at different temperatures from sewage sludges with different composition and character. *Chemosphere* 287, 132258. <https://doi.org/10.1016/j.chemosphere.2021.132258>.
- Siatecka, A., Rózylo, K., Ok, Y.S., Oleszczuk, P., 2021. Biochars ages differently depending on the feedstock used for their production: Willow- versus sewage sludge-derived biochars. *Sci. Total Environ.* 789, 147458 <https://doi.org/10.1016/j.scitotenv.2021.147458>.
- Sigmund, G., Bucheli, T.D., Hilber, I., Micić, V., Kah, M., Hofmann, T., 2017. Effect of ageing on the properties and polycyclic aromatic hydrocarbon composition of biochar. *Environ. Sci.: Process. Impacts* 19, 768–774. <https://doi.org/10.1039/C7EM00116A>.
- Sushkova, S., Minkina, T., Deryabkina, I., Rajput, V., Antonenko, E., Nazarenko, O., Yadav, B.K., Hakki, E., Mohan, D., 2019. Environmental pollution of soil with PAHs in energy producing plants zone. *Sci. Total Environ.* 655, 232–241. <https://doi.org/10.1016/j.scitotenv.2018.11.080>.
- Tang, J., Zhu, W., Kookana, R., Katayama, A., 2013. Characteristics of biochar and its application in remediation of contaminated soil. *J. Biosci. Bioeng.* 116, 653–659. <https://doi.org/10.1016/j.jbiotec.2013.05.035>.
- Tang, L., Tang, X.-Y., Zhu, Y.-G., Zheng, M.-H., Miao, Q.-L., 2005. Contamination of polycyclic aromatic hydrocarbons (PAHs) in urban soils in Beijing, China. *Environ. Int.* 31, 822–828. <https://doi.org/10.1016/j.envint.2005.05.031>.
- Wagstaffe, M., Thomas, A.G., Mark.J. Jackman, M., Torres-Molina, K.L., Syres, K., Handrup, 2016. An experimental investigation of the adsorption of a phosphonic acid on the anatase TiO<sub>2</sub> (101) surface. *J. Phys. Chem. C* 120, 1693–1700. <https://doi.org/10.1021/acs.jpcc.5b11258>.
- Wang, L., O'Connor, D., Rinklebe, J., Ok, Y.S., Tsang, D.C.W., Shen, Z., Hou, D., 2020. Biochar aging: mechanisms, physicochemical changes, assessment, and implications for field applications. *Environ. Sci. Technol.* 54, 14797–14814. <https://doi.org/10.1021/acs.est.0c04033>.
- Yang, X., Zhang, S., Ju, M., Liu, L., 2019. Preparation and modification of biochar materials and their application in soil remediation. *Appl. Sci.* 9, 1365. <https://doi.org/10.3390/app9071365>.
- Yi, Y., Huang, Z., Lu, B., Xian, J., Tsang, E.P., Cheng, W., Fang, J., Fang, Z., 2020. Magnetic biochar for environmental remediation: a review. *Bioreour. Technol.* 298, 122468 <https://doi.org/10.1016/j.biortech.2019.122468>.
- Yunker, M.B., Macdonald, R.W., Vingarzan, R., Mitchell, R.H., Goyette, D., Sylvestre, S., 2002. PAHs in the Fraser River basin: a critical appraisal of PAH ratios as indicators of PAH source and composition. *Org. Geochem.* 33, 489–515. [https://doi.org/10.1016/S0146-6380\(02\)00002-5](https://doi.org/10.1016/S0146-6380(02)00002-5).

**Long-term physical and chemical aging of biochar affected the amount and  
bioavailability of PAHs and their derivatives**

Agnieszka Krzyszczak<sup>1</sup>, Michał P. Dybowski<sup>2</sup>, Robert Zarzycki<sup>3</sup>, Rafał Kobyłecki<sup>3</sup>, Patryk Oleszczuk<sup>1</sup>, Bożena Czech<sup>1\*</sup>

<sup>1</sup>Department of Radiochemistry and Environmental Chemistry, Institute of Chemical Sciences, Faculty of Chemistry, Maria Curie-Sklodowska University in Lublin, Pl. M. Curie-Sklodowskiej 3, 20-031 Lublin, Poland

<sup>2</sup>Department of Chromatography, Institute of Chemical Sciences, Faculty of Chemistry, Maria Curie-Sklodowska University in Lublin, Pl. M. Curie-Sklodowskiej 3, 20-031 Lublin, Poland

<sup>3</sup>Department of Advanced Energy Technologies, Częstochowa University of Technology, Dąbrowskiego 73, 42-201 Częstochowa, Poland

\*corresponding author: Tel.: +48 81 537 55 54; fax: +48 81 537 55 65; E-mail address: bczech@hektor.umcs.lublin.pl (B. Czech)

**Journal:** Journal of Hazardous Materials

**No. pages:** 25

**No. of figures:** 0

**No. of tables:** 10

## **2. Material and methods**

### **2.3. The physico-chemical characterization of BC before and after aging processes**

The physicochemical analysis of the obtained BC (pH, ash, C, H, N content, XPS X-ray photoelectron spectroscopy, FT-IR spectroscopy, SEM imaging, and EDS mapping) was performed according to the standard procedures. The pH of 1g of biochar mixed with 10mL of distilled water was appointed by a digital pH meter HQ430d Benchtop Single Input (HACH, USA). The ash content was determined by exposure of 1g of biochar to 760°C in a furnace (MagmaTherm) for 6h. The difference in BC mass before and after heating was calculated and expressed in percentage. The content of elemental carbon, hydrogen, and nitrogen in milled biochar was specified by CHN/CHNS EuroEA3000 Elemental Analyser (EuroVector). The surface functional groups were determined via X-ray photoelectron spectroscope UHV (Prevac), whilst the surface morphology was investigated by Scanning Electron Microscopy Quanta 3D FEG (FEI). The surface area and porosity were determined via ASAP 2420 Analyzer (Micromeritics, USA). The technique required the biochar outgassing at 200°C for 12 h under vacuum. To complement the BC characteristic, the FT-IR technique was applied. FT-IR/PAS spectra were recorded via Bio-Rad Excalibur 3000 MX spectrometer equipped with photoacoustic detector MTEC300 (operating in a helium atmosphere). The 4000-400 cm<sup>-1</sup> range (with a resolution of 4 cm<sup>-1</sup>) and maximum source aperture were utilized during measurements.

### **2.4. Freely dissolved (Cfree) PAHs and their derivatives determination in biochars**

The bioavailability of PAHs and their derivatives was appointed by the protocol presented in [1] and in our previous work [2]. Briefly, the bioavailable fraction of analytes was extracted via 76-mm thick polyoxymethylene (POM) passive samplers (4cm x 4cm, about 0.35 g). After appropriate preparation (cleaning in methanol, n-heptane, and Millipore water) POMs were placed in Erlenmeyer flasks together with 1g of biochar and 40mL of sodium azide (200

mg/L) dissolved in water. Flasks were rolled on a rotary shaker ROTAX 6.8 VELP Scientifica (Italy) for 1 month at 10 RCF. Subsequently, POMs were extracted via a mixture of acetone/heptane (20:80, v/v) with the addition of 20 µL of deuterated PAHs for 48 hours on a horizontal shaking machine ELPIN 358A (Poland). The obtained extract (with the addition of 1 mL of iso-octane) was concentrated to about 1 mL via rotary vacuum concentrator RVC 2-25 CD plus (Martin Christ, Germany). Finally, GC-MS/MS analysis was carried out. The concentration of the bioavailable fraction of PAHs and their derivatives was calculated according to the equation presented in [2].

## **2.5. The total content of PAHs and their derivatives determination in biochars and soils**

The total fraction of PAHs and their derivatives was extracted via pressurized liquid extraction by applying the Dionex 350 system (Thermo Fisher Scientific). 22mL stainless steel cells were packed as follows: silica gel (activated at 300°C for 5h) and copper, 0.5g of biochar mixed with 0.1g ethylenediaminetetraacetic acid, the internal standard glass beads as a fulfillment. The extraction was performed using hexane (at 150°C using 2 extraction cycles with a flush volume at 60%). The static time was adjusted at 5 min and the purge time was - 60s 1 MPa with N<sub>2</sub>. The obtained extract (with the addition of iso-octane) was concentrated as it was described in the previous subsection. The GC-MS/MS analysis was carried out.

## **2.6. GC–MS/MS measurement**

Qualitative and quantitative measurements of PAHs and their derivatives were performed using a gas chromatograph hyphenated with a triple quadruple tandem mass spectrometer detector (GCMS-TQ8040; Shimadzu, Kyoto, Japan) equipped with a ZB5-MSi fused-silica capillary column (30 m × 0.25 mm i.d., 0.25 µm film thickness; Phenomenex, Torrance, CA, USA) and an AOC-20i+s type autosampler (Shimadzu). The helium (grade 5.0) and argon (grade 5.0) were applied as a carrier and collision gas, respectively. The chromatographic conditions were adjusted as follows: column flow -1.56 mL/min, the volume of injection - 1

$\mu\text{L}$ . The injector was working in high-pressure mode (250.0 kPa for 1.5 min; column flow at initial temperature was 4.90 mL/min) at the temperature of 310°C; the ion source temperature was 225°C. The qualitative and quantitative analyses were conducted with full scan mode (range 40-550 m/z) and SIM (Single Ion Monitoring) mode, respectively.

Table S1. Chemical characteristics of analyzed compounds.

No.	Compound	CAS <sup>(1)</sup>	MW <sup>(2)</sup>	Formula
1	Naphthalene*	91-20-3	128.17	C <sub>10</sub> H <sub>8</sub>
2	1,3-di-iso-propylnaphthalene	57122-16-4	212.33	C <sub>16</sub> H <sub>20</sub>
3	2-Phenylnaphthalene	612-94-2	204.26	C <sub>16</sub> H <sub>12</sub>
4	Acenaphthylene*	208-96-8	152.20	C <sub>12</sub> H <sub>8</sub>
5	Acenaphthene*	83-32-9	154.20	C <sub>12</sub> H <sub>10</sub>
6	Fluorene*	86-73-7	166.22	C <sub>13</sub> H <sub>10</sub>
7	Anthracene*	120-12-7	178.23	C <sub>14</sub> H <sub>10</sub>
8	Phenanthrene*	85-01-8	178.23	C <sub>14</sub> H <sub>10</sub>
9	3-Methylphenanthrene	832-71-3	192.25	C <sub>15</sub> H <sub>12</sub>
10	2-Methylphenanthrene	2531-84-2	192.25	C <sub>15</sub> H <sub>12</sub>
11	9-Methylphenanthrene	883-20-5	192.25	C <sub>15</sub> H <sub>12</sub>
12	3,6-dimethylphenanthrene	1576-67-6	206.28	C <sub>16</sub> H <sub>14</sub>
13	Fluoranthene*	206-44-0	202.25	C <sub>16</sub> H <sub>10</sub>
14	Pyrene*	129-00-0	202.25	C <sub>16</sub> H <sub>10</sub>
15	2-Methylpyrene	3442-78-2	216.28	C <sub>17</sub> H <sub>12</sub>
16	4-Methylpyrene	3353-12-6	216.28	C <sub>17</sub> H <sub>12</sub>
17	Benzo[a]fluorene	238-84-6	216.27	C <sub>17</sub> H <sub>12</sub>
18	Benzo[a]anthracene*	56-55-3	228.29	C <sub>18</sub> H <sub>12</sub>
19	Chryzene*	218-01-9	228.29	C <sub>18</sub> H <sub>12</sub>
20	3-Methylchrysene	3351-31-3	242.30	C <sub>19</sub> H <sub>14</sub>

21	5-Methylchrysene	3697-24-3	242.30	C <sub>19</sub> H <sub>14</sub>
22	6-Methylchrysene	1705-85-7	242.30	C <sub>19</sub> H <sub>14</sub>
23	Benzo[a]fluoranthene	203-33-8	252.31	C <sub>20</sub> H <sub>12</sub>
24	Benzo[b]fluoranthene*	205-99-2	252.31	C <sub>20</sub> H <sub>12</sub>
25	Benzo[k]fluoranthene*	207-08-9	252.32	C <sub>20</sub> H <sub>12</sub>
26	Benzo[j]fluoranthene*	205-82-3	252.31	C <sub>20</sub> H <sub>12</sub>
27	Benzo[a]pyrene*	50-32-8	252.31	C <sub>20</sub> H <sub>12</sub>
28	Indeno[1,2,3-cd]pyrene*	193-39-5	276.33	C <sub>22</sub> H <sub>12</sub>
29	Benzo[ghi]perylene*	191-24-2	276.33	C <sub>22</sub> H <sub>12</sub>
30	Dibenzo[a,h]anthracene*	53-70-3	278.10	C <sub>22</sub> H <sub>14</sub>
31	Dibenz[a,e]pyrene	192-65-4	302.37	C <sub>24</sub> H <sub>14</sub>
32	Dibenz[a,h]pyrene	189-64-0	302.37	C <sub>24</sub> H <sub>14</sub>
33	Dibenz[a,i]pyrene	189-55-9	302.37	C <sub>24</sub> H <sub>14</sub>
34	Dibenz[a,l]pyrene	192-65-4	302.37	C <sub>24</sub> H <sub>14</sub>
N- and O-PAHs				
35	Nitronaphthalene	86-57-7	173.16	C <sub>10</sub> H <sub>7</sub> NO <sub>2</sub>
36	1-Methyl-5-nitronaphthalene	91137-27-8	187.19	C <sub>11</sub> H <sub>9</sub> NO <sub>2</sub>
37	1-Methyl-6-nitronaphthalene	105752-67-8	187.19	C <sub>11</sub> H <sub>9</sub> NO <sub>2</sub>
38	9,10-Anthracenedione	84-65-1	208.21	C <sub>14</sub> H <sub>8</sub> O <sub>2</sub>
39	4H-cyclopenta(def)phenanthrene	203-64-5	190.24	C <sub>15</sub> H <sub>10</sub>
40	Nitropyrene	5522-43-0	247.25	C <sub>16</sub> H <sub>9</sub> NO <sub>2</sub>

<sup>(1)</sup>numerical identifier assigned by the Chemical Abstracts Service (CAS)

<sup>(2)</sup>MW-molecular weight

\* PAHs belonging to 16PAHs which have been classified by the United States Environmental Protection Agency (USEPA) as priority pollutants [3]

Table S2. The qualitative and quantitative parameters of PAHs and O/N-PAHs analysis.

No.	Compound	Quantification ion ( <i>m/z</i> )	Confirmation ion ( <i>m/z</i> )	LOD* [ $\mu\text{g L}^{-1}$ ]	LOQ** [ $\mu\text{g L}^{-1}$ ]
1	Naphthalene	128	102	1.01	3.36
2	1,3-di-iso-propylnaphthalene	197	212	1.41	4.69
3	2-Phenylnaphthalene	204	101	1.90	6.33
4	Acenaphthylene	152	76	2.10	6.99
5	Acenaphthene	153	76	2.30	7.66
6	Fluorene	166	82	1.10	3.66
7	Anthracene	178	89	1.30	4.33
8	Phenanthrene	178	89	1.34	4.36
9	3-Methylphenanthrene	192	165	2.42	8.06
10	2-Methylphenanthrene	192	165	2.42	8.06
11	9-Methylphenanthrene	192	96	3.23	10.76
12	3,6-dimethylphenanthrene	206	191	2.20	7.33
13	Fluoranthene	202	101	1.87	6.22
14	Pyrene	202	101	1.91	6.36
15	2-Methylpyrene	216	108	1.92	6.39
16	4-Methylpyrene	216	108	1.92	6.39
17	Benzo[a]fluorene	216	107	1.30	4.33
18	Benzo[a]anthracene	228	114	1.30	4.33
19	Chryzene	228	113	2.20	7.33

20	3-Methylchrysene	242	121	1.02	3.40
21	5-Methylchrysene	242	120	1.55	5.16
22	6-Methylchrysene	242	119	1.02	3.40
23	Benzo[a]fluoranthene	252	126	2.10	6.99
24	Benzo[b]fluoranthene	252	126	2.10	6.99
25	Benzo[k]fluoranthene	252	126	2.10	6.99
26	Benzo[j]fluoranthene	252	126	1.39	4.63
27	Benzo[a]pyrene	252	126	2.11	7.03
28	Indeno[1,2,3-cd]pyrene	276	138	1.30	4.33
29	Benzo[ghi]perylene	276	138	1.33	4.43
30	Dibenz[a,h]anthracene	278	139	2.21	7.36
31	Dibenz[a,e]pyrene	302	151	1.89	6.29
32	Dibenz[a,h]pyrene	302	151	1.89	6.29
33	Dibenz[a,i]pyrene	302	151	1.89	6.29
34	Dibenz[a,l]pyrene	302	151	1.89	6.29
<hr/>					
	N- and O-PAHs				
35	Nitronaphthalene	173	127	2.41	8.03
36	1-Methyl-5-nitronaphthalene	187	115	1.21	4.03
37	1-Methyl-6-nitronaphthalene	187	115	1.21	4.03
38	9,10-Anthracenedione	208	180	1.44	4.80
39	4H-cyclopenta(def)phenanthrene	190	94	3.01	10.02
40	Nitropyrene	247	201	1.66	5.53

\*-LOD – limit of detection; \*\*-LOQ – limit of quantitation; LOD and LOQ were not calculated via  $K_{POM}$ ; LOD and LOQ were considered to be signal-to-noise ratios equal to 3 and 10, respectively.

Table S3. PAHs and PAHs derivatives total content in non-aged biochars.

No.	Compound	Sample description					
		BCZ500	BCZ600	BCZ700	BCW500	BCW600	BCW700
1	Naphthalene	44.08 ± 2.02	54.80 ± 2.51	50.22 ± 2.30	52.75 ± 2.42	62.28 ± 2.85	56.96 ± 2.61
2	1,3-di-iso-propynaphthalene	< LOD	< LOD	< LOD	0.72 ± 0.03	0.88 ± 0.04	1.24 ± 0.06
3	2-Phenylnaphthalene	< LOD	1.26 ± 0.06	< LOD	< LOD	< LOD	< LOD
4	Acenaphthylene	12.47 ± 0.57	15.09 ± 0.69	16.01 ± 0.73	22.17 ± 1.02	25.12 ± 1.15	20.13 ± 0.92
5	Acenaphthene	2.14 ± 0.10	3.10 ± 0.14	2.68 ± 0.12	32.30 ± 1.48	37.34 ± 1.71	31.12 ± 1.43
6	Fluorene	4.44 ± 0.20	8.30 ± 0.38	10.00 ± 0.46	< LOD	0.42 ± 0.02	0.66 ± 0.03
7	Anthracene	< LOD	0.42 ± 0.02	< LOD	3.08 ± 0.14	3.32 ± 0.15	1.94 ± 0.09
8	Phenanthrene	< LOD	< LOD	< LOD	< LOD	< LOD	< LOD
9	3-Methylphenanthrene	0.080 ± 0.004	0.060 ± 0.003	0.080 ± 0.004	< LOD	0.24 ± 0.01	< LOD
10	2-Methylphenanthrene	< LOD	0.12 ± 0.01	< LOD	< LOD	0.22 ± 0.01	< LOD
11	9-Methylphenanthrene	0.52 ± 0.02	1.02 ± 0.05	0.28 ± 0.01	< LOD	< LOD	< LOD
12	3,6-dimethylphenanthrene	1.28 ± 0.06	2.42 ± 0.11	0.86 ± 0.04	< LOD	< LOD	< LOD
13	Fluoranthene	< LOD	< LOD	0.24 ± 0.01	1.48 ± 0.07	1.98 ± 0.09	1.70 ± 0.08
14	Pyrene	5.92 ± 0.27	8.30 ± 0.38	8.09 ± 0.37	20.79 ± 0.95	25.10 ± 1.15	22.11 ± 1.01
15	2-Methylpyrene	0.82 ± 0.04	1.10 ± 0.05	1.48 ± 0.07	0.20 ± 0.01	0.24 ± 0.01	0.32 ± 0.02
16	4-Methylpyrene	0.28 ± 0.01	1.96 ± 0.09	4.07 ± 0.19	0.24 ± 0.01	0.30 ± 0.01	0.42 ± 0.02
17	Benzo[a]fluorene	0.24 ± 0.01	0.56 ± 0.03	0.22 ± 0.01	5.47 ± 0.25	6.02 ± 0.28	5.93 ± 0.27
18	Benzo[a]anthracene	1.24 ± 0.06	1.98 ± 0.09	0.62 ± 0.03	3.32 ± 0.15	5.14 ± 0.24	3.08 ± 0.14
19	Chrysene	< LOD	0.24 ± 0.01	< LOD	0.44 ± 0.02	0.92 ± 0.04	1.48 ± 0.07

20	3-Methylchrysene	< LOD	< LOD	< LOD	< LOD	< LOD	< LOD
21	5-Methylchrysene	1.08 ± 0.05	1.92 ± 0.09	1.22 ± 0.06	< LOD	< LOD	< LOD
22	6-Methylchrysene	< LOD	0.66 ± 0.03	< LOD	< LOD	< LOD	< LOD
23	Benzo[a]fluoranthene	4.98 ± 0.23	9.72 ± 0.45	6.21 ± 0.28	< LOD	0.28 ± 0.01	< LOD
24	Benzo[b]fluoranthene	5.56 ± 0.26	6.30 ± 0.29	2.98 ± 0.14	< LOD	0.22 ± 0.01	< LOD
25	Benzo[k]fluoranthene	2.22 ± 0.10	2.28 ± 0.10	1.52 ± 0.07	< LOD	0.34 ± 0.02	< LOD
26	Benzo[j]fluoranthene	0.100 ± 0.005	0.26 ± 0.01	0.180 ± 0.008	< LOD	0.12 ± 0.01	< LOD
27	Benzo[a]pyrene	< LOD	0.52 ± 0.02	< LOD	6.29 ± 0.29	7.34 ± 0.34	8.25 ± 0.38
28	Indeno[1,2,3-cd]pyrene	< LOD	< LOD	< LOD	0.88 ± 0.04	1.10 ± 0.05	0.52 ± 0.02
29	Benzo[ghi]perylene	< LOD	< LOD	< LOD	< LOD	< LOD	< LOD
30	Dibenzo[a,h]anthracene	1.98 ± 0.09	2.42 ± 0.11	1.06 ± 0.05	0.52 ± 0.02	0.68 ± 0.03	0.30 ± 0.01
31	Dibenz[a,e]pyrene	0.72 ± 0.03	1.04 ± 0.05	2.04 ± 0.09	0.82 ± 0.04	1.16 ± 0.05	1.22 ± 0.06
32	Dibenz[a,h]pyrene	< LOD	< LOD	< LOD	0.060 ± 3·10 <sup>-3</sup>	0.18 ± 0.01	0.24 ± 0.01
33	Dibenz[a,i]pyrene	< LOD	< LOD	< LOD	0.040 ± 0.002	0.14 ± 0.01	0.38 ± 0.02
34	Dibenz[a,l]pyrene	< LOD	< LOD	< LOD	< LOD	< LOD	< LOD
N- and O-PAHs							
35	Nitronaphthalene	< LOD	< LOD	< LOD	1.48 ± 0.07	1.92 ± 0.09	4.31 ± 0.20
26	1-Methyl-5-nitronaphthalene	1.28 ± 0.06	2.42 ± 0.11	2.10 ± 0.10	< LOD	< LOD	< LOD
30	1-Methyl-6-nitronaphthalene	1.44 ± 0.07	2.88 ± 0.13	1.92 ± 0.09	< LOD	< LOD	< LOD
31	9,10-Anthracenedione	< LOD	< LOD	< LOD	< LOD	< LOD	< LOD
32	4H-cyclopenta(def)phenanthrene	40.21 ± 1.84	< LOD	10.91 ± 0.50	< LOD	< LOD	< LOD
33	Nitropyrene	< LOD	< LOD	0.68 ± 0.03	< LOD	< LOD	< LOD

Table S4. PAHs and PAHs derivatives total content in physically aged biochars.

No.	Compound	Sample description					
		BCW500-PA	BCW600-PA	BCW700-PA	BCZ500-PA	BCZ600-PA	BCZ700-PA
1	Naphthalene	59.28 ± 2.58	77.52 ± 3.71	66.91 ± 2.91	58.59 ± 2.80	72.27 ± 3.06	79.97 ± 3.82
2	1,3-di-iso-propylnaphthalene	1.04 ± 0.05	1.89 ± 0.09	1.26 ± 0.06	0.121 ± 0.006	0.040 ± 0.002	0.040 ± 0.002
3	2-Phenylnaphthalene	< LOD	< LOD	< LOD	< LOD	1.95 ± 0.08	< LOD
4	Acenaphthylene	28.28 ± 1.23	33.40 ± 1.60	28.00 ± 1.22	19.12 ± 0.91	24.36 ± 1.02	23.23 ± 1.11
5	Acenaphthene	39.36 ± 1.71	51.16 ± 2.45	42.61 ± 1.85	5.31 ± 0.25	9.07 ± 0.38	6.17 ± 0.30
6	Fluorene	< LOD	0.72 ± 0.04	0.56 ± 0.02	5.97 ± 0.29	12.45 ± 0.52	17.84 ± 0.85
7	Anthracene	5.10 ± 0.22	3.18 ± 0.15	1.28 ± 0.06	< LOD	2.23 ± 0.09	2.05 ± 0.10
8	Phenanthrene	< LOD	< LOD	< LOD	< LOD	< LOD	< LOD
9	3-Methylphenanthrene	< LOD	0.68 ± 0.03	< LOD	0.62 ± 0.03	2.53 ± 0.11	2.11 ± 0.10
10	2-Methylphenanthrene	< LOD	0.52 ± 0.03	< LOD	< LOD	0.42 ± 0.02	0.24 ± 0.01
11	9-Methylphenanthrene	< LOD	< LOD	< LOD	1.39 ± 0.07	3.06 ± 0.13	0.78 ± 0.04
12	3,6-dimethylphenanthrene	< LOD	< LOD	< LOD	1.95 ± 0.09	5.97 ± 0.25	4.00 ± 0.19
13	Fluoranthene	1.94 ± 0.08	2.25 ± 0.11	2.33 ± 0.10	< LOD	< LOD	0.89 ± 0.04
14	Pyrene	26.72 ± 1.16	29.14 ± 1.40	27.40 ± 1.19	8.26 ± 0.40	13.38 ± 0.56	16.21 ± 0.78
15	2-Methylpyrene	1.10 ± 0.05	0.89 ± 0.04	0.70 ± 0.03	0.24 ± 0.01	3.00 ± 0.13	1.95 ± 0.09
16	4-Methylpyrene	0.26 ± 0.01	0.52 ± 0.03	0.62 ± 0.03	0.121 ± 0.006	1.95 ± 0.08	2.33 ± 0.11
17	Benzo[a]fluorene	7.10 ± 0.31	8.14 ± 0.39	8.10 ± 0.35	0.86 ± 0.04	1.35 ± 0.06	0.42 ± 0.02
18	Benzo[a]anthracene	4.58 ± 0.20	6.82 ± 0.33	5.39 ± 0.24	1.55 ± 0.07	2.92 ± 0.12	3.10 ± 0.15
19	Chrysene	0.82 ± 0.04	1.71 ± 0.08	1.98 ± 0.09	< LOD	0.74 ± 0.03	0.97 ± 0.05
20	3-Methylchrysene	< LOD	< LOD	< LOD	< LOD	< LOD	0.76 ± 0.04
21	5-Methylchrysene	< LOD	< LOD	< LOD	2.25 ± 0.11	6.20 ± 0.26	3.60 ± 0.17

22	6-Methylchrysene	< LOD	< LOD	< LOD	< LOD	$1.99 \pm 0.08$	$3.66 \pm 0.18$
23	Benzo[a]fluoranthene	$0.060 \pm 0.003$	$0.52 \pm 0.03$	$0.020 \pm 0.001$	$7.98 \pm 0.38$	$14.96 \pm 0.62$	$13.45 \pm 0.64$
24	Benzo[b]fluoranthene	$0.180 \pm 0.008$	$0.68 \pm 0.203$	$0.040 \pm 0.002$	$8.06 \pm 0.39$	$7.42 \pm 0.31$	$8.14 \pm 0.39$
25	Benzo[k]fluoranthene	$0.120 \pm 0.005$	$0.89 \pm 0.04$	$0.120 \pm 0.005$	$4.24 \pm 0.20$	$3.78 \pm 0.16$	$5.57 \pm 0.27$
26	Benzo[j]fluoranthene	< LOD	$0.161 \pm 0.008$	$0.020 \pm 0.001$	$0.28 \pm 0.01$	$1.17 \pm 0.05$	$0.82 \pm 0.04$
27	Benzo[a]pyrene	$11.58 \pm 0.50$	$12.19 \pm 0.58$	$12.41 \pm 0.54$	< LOD	$1.29 \pm 0.05$	$0.22 \pm 0.01$
28	Indeno[1,2,3-cd]pyrene	$1.88 \pm 0.08$	$2.25 \pm 0.11$	$0.74 \pm 0.03$	< LOD	< LOD	< LOD
29	Benzo[ghi]perylene	< LOD	< LOD	< LOD	< LOD	< LOD	< LOD
30	Dibenzo[a,h]anthracene	$0.82 \pm 0.04$	$1.37 \pm 0.07$	$0.66 \pm 0.03$	$4.68 \pm 0.22$	$6.09 \pm 0.25$	$4.46 \pm 0.21$
31	Dibenz[a,e]pyrene	$1.38 \pm 0.06$	$1.89 \pm 0.09$	$2.16 \pm 0.09$	$1.89 \pm 0.09$	$2.39 \pm 0.10$	$6.17 \pm 0.30$
32	Dibenz[a,h]pyrene	$0.180 \pm 0.008$	$0.44 \pm 0.02$	$0.88 \pm 0.04$	< LOD	< LOD	< LOD
33	Dibenz[a,i]pyrene	$0.140 \pm 0.006$	$0.32 \pm 0.02$	$1.64 \pm 0.07$	< LOD	< LOD	< LOD
34	Dibenz[a,l]pyrene	< LOD	< LOD	< LOD	< LOD	< LOD	< LOD
N- and O-PAHs							
35	Nitronaphthalene	$2.42 \pm 0.11$	$2.23 \pm 0.11$	$6.79 \pm 0.30$	< LOD	< LOD	< LOD
26	1-Methyl-5-nitronaphthalene	< LOD	< LOD	< LOD	$2.23 \pm 0.11$	$2.60 \pm 0.11$	$5.27 \pm 0.25$
30	1-Methyl-6-nitronaphthalene	< LOD	< LOD	< LOD	$1.95 \pm 0.09$	$3.12 \pm 0.13$	$4.00 \pm 0.19$
31	9,10-Anthracenedione	< LOD	< LOD	< LOD	< LOD	< LOD	< LOD
32	4H-cyclopenta(def)phenanthrene	< LOD	< LOD	< LOD	< LOD	< LOD	< LOD
33	Nitropyrene	< LOD	< LOD	< LOD	< LOD	< LOD	< LOD

Table S5. The total content of PAHs and their derivatives in BC after chemical aging at 60°C.

No.	Compound	Sample description					
		BCW500-CA60	BCW600- CA60	BCW700- CA60	BCZ500- CA60	BCZ600- CA60	BCZ700- CA60
1	Naphthalene	6.65 ± 0.31	6.51 ± 0.30	6.94 ± 0.32	51.41 ± 2.14	66.70 ± 2.90	73.30 ± 3.34
2	1,3-di-iso-propynaphthalene	0.080 ± 0.004	0.120 ± 0.005	< LOD	0.060 ± 0.002	0.120 ± 0.005	0.100 ± 0.005
3	2-Phenylnaphthalene	< LOD	< LOD	< LOD	< LOD	1.32 ± 0.06	< LOD
4	Acenaphthylene	4.02 ± 0.18	3.92 ± 0.18	2.72 ± 0.12	16.15 ± 0.67	19.06 ± 0.83	20.30 ± 0.92
5	Acenaphthene	3.02 ± 0.14	4.03 ± 0.19	2.68 ± 0.12	4.41 ± 0.18	6.43 ± 0.28	4.59 ± 0.21
6	Fluorene	< LOD	< LOD	< LOD	4.68 ± 0.20	10.31 ± 0.45	15.01 ± 0.68
7	Anthracene	0.28 ± 0.01	0.38 ± 0.02	0.22 ± 0.01	< LOD	0.84 ± 0.04	0.72 ± 0.03
8	Phenanthrene	< LOD	< LOD	< LOD	< LOD	< LOD	< LOD
9	3-Methylphenanthrene	< LOD	< LOD	< LOD	0.24 ± 0.01	1.82 ± 0.08	1.71 ± 0.08
10	2-Methylphenanthrene	< LOD	< LOD	< LOD	< LOD	0.160 ± 0.007	0.181 ± 0.008
11	9-Methylphenanthrene	< LOD	< LOD	< LOD	0.71 ± 0.03	1.88 ± 0.08	0.28 ± 0.01
12	3,6-dimethylphenanthrene	< LOD	< LOD	< LOD	1.31 ± 0.06	4.03 ± 0.18	2.99 ± 0.14
13	Fluoranthene	< LOD	< LOD	< LOD	< LOD	< LOD	0.56 ± 0.03
14	Pyrene	1.10 ± 0.05	1.44 ± 0.07	1.82 ± 0.08	7.22 ± 0.30	11.55 ± 0.50	12.92 ± 0.59
15	2-Methylpyrene	< LOD	< LOD	< LOD	0.77 ± 0.04	2.34 ± 0.10	2.45 ± 0.11
16	4-Methylpyrene	< LOD	< LOD	< LOD	0.30 ± 0.01	4.45 ± 0.19	6.08 ± 0.28
17	Benzo[a]fluorene	< LOD	< LOD	< LOD	0.30 ± 0.01	0.88 ± 0.04	0.140 ± 0.006
18	Benzo[a]anthracene	< LOD	< LOD	0.060 ± 0.003	1.21 ± 0.05	1.78 ± 0.08	2.35 ± 0.11
19	Chrysene	< LOD	< LOD	< LOD	< LOD	0.32 ± 0.01	0.66 ± 0.03
20	3-Methylchrysene	< LOD	< LOD	< LOD	< LOD	< LOD	0.24 ± 0.01

21	5-Methylchrysene	< LOD	< LOD	< LOD	$1.21 \pm 0.05$	$4.13 \pm 0.18$	$2.25 \pm 0.010$
22	6-Methylchrysene	< LOD	< LOD	< LOD	< LOD	$1.22 \pm 0.05$	$2.79 \pm 0.13$
23	Benzo[a]fluoranthene	< LOD	< LOD	< LOD	$6.61 \pm 0.28$	$13.40 \pm 0.58$	$11.17 \pm 0.51$
24	Benzo[b]fluoranthene	< LOD	< LOD	< LOD	$6.27 \pm 0.26$	$8.23 \pm 0.36$	$5.94 \pm 0.27$
25	Benzo[k]fluoranthene	< LOD	< LOD	< LOD	$3.06 \pm 0.13$	$4.17 \pm 0.18$	$4.11 \pm 0.19$
26	Benzo[j]fluoranthene	< LOD	< LOD	< LOD	$0.139 \pm 0.006$	$0.68 \pm 0.03$	$0.26 \pm 0.01$
27	Benzo[a]pyrene	$2.24 \pm 0.10$	$2.30 \pm 0.11$	$1.44 \pm 0.07$	< LOD	$0.88 \pm 0.04$	< LOD
28	Indeno[1,2,3-cd]pyrene	< LOD	< LOD	< LOD	< LOD	< LOD	< LOD
29	Benzo[ghi]perylene	< LOD	< LOD	< LOD	< LOD	< LOD	< LOD
30	Dibenzo[a,h]anthracene	< LOD	< LOD	< LOD	$2.72 \pm 0.11$	$5.33 \pm 0.23$	$1.32 \pm 0.06$
31	Dibenz[a,e]pyrene	< LOD	< LOD	< LOD	$1.01 \pm 0.04$	$2.22 \pm 0.10$	$3.75 \pm 0.17$
32	Dibenz[a,h]pyrene	< LOD	< LOD	< LOD	< LOD	< LOD	< LOD
33	Dibenz[a,i]pyrene	< LOD	< LOD	< LOD	< LOD	< LOD	< LOD
34	Dibenz[a,l]pyrene	< LOD	< LOD	< LOD	< LOD	< LOD	< LOD
N- and O-PAHs							
35	Nitronaphthalene	$0.42 \pm 0.02$	$0.52 \pm 0.02$	$0.62 \pm 0.03$	< LOD	< LOD	< LOD
26	1-Methyl-5-nitronaphthalene	< LOD	< LOD	< LOD	$1.53 \pm 0.06$	$2.18 \pm 0.10$	$4.05 \pm 0.18$
30	1-Methyl-6-nitronaphthalene	< LOD	< LOD	< LOD	$1.31 \pm 0.06$	$3.28 \pm 0.14$	$2.33 \pm 0.11$
31	9,10-Anthracenedione	< LOD	< LOD	< LOD	< LOD	< LOD	< LOD
32	4H-cyclopenta(def)phenanthrene	< LOD	< LOD	< LOD	< LOD	< LOD	< LOD
33	Nitropyrene	< LOD	< LOD	< LOD	< LOD	< LOD	< LOD

Table S6. The total content of PAHs and their derivatives in BC after chemical aging at 90°C.

No.	Compound	Sample description					
		BCW500-CA90	BCW600- CA90	BCW700- CA90	BCZ500- CA90	BCZ600- CA90	BCZ700- CA90
Analyte concentration ± SD [µg g <sup>-1</sup> ]							
1	Naphthalene	5.51 ± 0.25	6.22 ± 0.29	5.93 ± 0.27	59.81 ± 2.49	73.41 ± 3.19	80.06 ± 3.64
2	1,3-di-iso-propynaphthalene	< LOD	< LOD	0.040 ± 0.002	0.080 ± 0.003	0.160 ± 0.007	0.140 ± 0.006
3	2-Phenylnaphthalene	< LOD	< LOD	< LOD	< LOD	1.94 ± 0.09	< LOD
4	Acenaphthylene	3.08 ± 0.14	3.24 ± 0.15	2.42 ± 0.11	18.66 ± 0.78	20.26 ± 0.88	22.38 ± 1.02
5	Acenaphthene	1.98 ± 0.09	2.82 ± 0.13	1.74 ± 0.08	4.99 ± 0.21	8.06 ± 0.35	4.61 ± 0.21
6	Fluorene	< LOD	< LOD	< LOD	5.33 ± 0.22	11.91 ± 0.52	13.91 ± 0.63
7	Anthracene	0.080 ± 0.004	0.140 ± 0.006	0.120 ± 0.005	< LOD	1.02 ± 0.04	0.82 ± 0.04
8	Phenanthrene	< LOD	< LOD	< LOD	< LOD	< LOD	< LOD
9	3-Methylphenanthrene	< LOD	< LOD	< LOD	0.26 ± 0.01	1.98 ± 0.09	2.22 ± 0.10
10	2-Methylphenanthrene	< LOD	< LOD	< LOD	< LOD	0.24 ± 0.01	0.24 ± 0.01
11	9-Methylphenanthrene	< LOD	< LOD	< LOD	0.88 ± 0.04	2.64 ± 0.12	1.96 ± 0.09
12	3,6-dimethylphenanthrene	< LOD	< LOD	< LOD	1.48 ± 0.06	5.37 ± 0.23	3.55 ± 0.16
13	Fluoranthene	< LOD	< LOD	< LOD	< LOD	< LOD	0.66 ± 0.03
14	Pyrene	0.52 ± 0.02	0.62 ± 0.03	0.82 ± 0.04	8.03 ± 0.34	13.32 ± 0.58	14.63 ± 0.67
15	2-Methylpyrene	< LOD	< LOD	< LOD	0.88 ± 0.04	2.44 ± 0.11	3.23 ± 0.15
16	4-Methylpyrene	< LOD	< LOD	< LOD	0.44 ± 0.02	4.19 ± 0.18	6.17 ± 0.28
17	Benzo[a]fluorene	< LOD	< LOD	< LOD	0.32 ± 0.01	1.26 ± 0.06	0.180 ± 0.008
18	Benzo[a]anthracene	< LOD	< LOD	< LOD	1.42 ± 0.06	1.88 ± 0.08	2.70 ± 0.12
19	Chrysene	< LOD	< LOD	< LOD	< LOD	0.38 ± 0.02	0.76 ± 0.04
20	3-Methylchrysene	< LOD	< LOD	< LOD	< LOD	< LOD	0.28 ± 0.01

21	5-Methylchrysene	< LOD	< LOD	< LOD	$1.32 \pm 0.06$	$4.89 \pm 0.21$	$2.60 \pm 0.12$
22	6-Methylchrysene	< LOD	< LOD	< LOD	< LOD	$1.48 \pm 0.06$	$3.21 \pm 0.15$
23	Benzo[a]fluoranthene	< LOD	< LOD	< LOD	$7.69 \pm 0.32$	$16.06 \pm 0.70$	$12.79 \pm 0.58$
24	Benzo[b]fluoranthene	< LOD	< LOD	< LOD	$7.13 \pm 0.30$	$10.19 \pm 0.44$	$6.85 \pm 0.31$
25	Benzo[k]fluoranthene	< LOD	< LOD	< LOD	$3.54 \pm 0.15$	$4.77 \pm 0.21$	$4.07 \pm 0.19$
26	Benzo[j]fluoranthene	< LOD	< LOD	< LOD	$0.120 \pm 0.005$	$0.84 \pm 0.04$	$0.22 \pm 0.01$
27	Benzo[a]pyrene	$1.98 \pm 0.09$	$1.68 \pm 0.08$	$1.72 \pm 0.08$	< LOD	$1.12 \pm 0.05$	< LOD
28	Indeno[1,2,3-cd]pyrene	< LOD	< LOD	< LOD	< LOD	< LOD	< LOD
29	Benzo[ghi]perylene	< LOD	< LOD	< LOD	< LOD	< LOD	< LOD
30	Dibenzo[a,h]anthracene	< LOD	< LOD	< LOD	$2.74 \pm 0.11$	$6.07 \pm 0.26$	$1.52 \pm 0.07$
31	Dibenz[a,e]pyrene	< LOD	< LOD	< LOD	$1.22 \pm 0.05$	$2.24 \pm 0.10$	$4.17 \pm 0.19$
32	Dibenz[a,h]pyrene	< LOD	< LOD	< LOD	< LOD	< LOD	< LOD
33	Dibenz[a,i]pyrene	< LOD	< LOD	< LOD	< LOD	< LOD	< LOD
34	Dibenz[a,l]pyrene	< LOD	< LOD	< LOD	< LOD	< LOD	< LOD
N- and O-PAHs							
35	Nitronaphthalene	< LOD	< LOD	< LOD	< LOD	< LOD	< LOD
26	1-Methyl-5-nitronaphthalene	< LOD	< LOD	< LOD	$1.56 \pm 0.07$	$2.48 \pm 0.11$	$4.43 \pm 0.20$
30	1-Methyl-6-nitronaphthalene	< LOD	< LOD	< LOD	$1.56 \pm 0.07$	$3.36 \pm 0.15$	$3.27 \pm 0.15$
31	9,10-Anthracenedione	< LOD	< LOD	< LOD	< LOD	< LOD	< LOD
32	4H-cyclopenta(def)phenanthrene	< LOD	< LOD	< LOD	< LOD	< LOD	< LOD
33	Nitropyrene	< LOD	< LOD	< LOD	< LOD	< LOD	< LOD

Table S7. PAHs and PAHs derivatives bioavailable content in non-aged biochars.

No.	Compound	Sample description					
		BCZ500	BCZ600	BCZ700	BCW500	BCW600	BCW700
Analyte concentration ± SD [ng L <sup>-1</sup> ]							
1	Naphthalene	30.36 ± 1.11	35.65 ± 1.30	34.51 ± 1.26	< LOD	< LOD	< LOD
2	1,3-di-iso-propynaphthalene	< LOD	< LOD	7.7·10 <sup>-3</sup> ± 9.9·10 <sup>-5</sup>	< LOD	< LOD	< LOD
3	2-Phenylnaphthalene	< LOD	0.16 ± 5.4·10 <sup>-3</sup>	< LOD	< LOD	< LOD	< LOD
4	Acenaphthylene	1.55 ± 0.06	1.81 ± 0.07	1.91 ± 0.07	1.64 ± 0.12	0.77 ± 0.04	0.38 ± 0.02
5	Acenaphthene	1.02 ± 0.04	1.46 ± 0.05	0.97 ± 0.04	1.06 ± 0.05	1.16 ± 0.05	1.72 ± 0.08
6	Fluorene	0.41 ± 0.02	0.59 ± 0.02	0.67 ± 0.02	0.62 ± 0.03	0.97 ± 0.05	1.19 ± 0.06
7	Anthracene	< LOD	0.015 ± 6.0·10 <sup>-4</sup>	< LOD	< LOD	< LOD	< LOD
8	Phenanthrene	< LOD					
9	3-Methylphenanthrene	2.8·10 <sup>-3</sup> ± 9.4·10 <sup>-5</sup>	3.0·10 <sup>-3</sup> ± 9.9·10 <sup>-5</sup>	3.9·10 <sup>-3</sup> ± 9.9·10 <sup>-5</sup>	0.12 ± 5.0·10 <sup>-3</sup>	0.17 ± 7.4·10 <sup>-3</sup>	9.9·10 <sup>-2</sup> ± 4.5·10 <sup>-3</sup>
10	2-Methylphenanthrene	2.8·10 <sup>-3</sup> ± 9.4·10 <sup>-5</sup>	2.0·10 <sup>-3</sup> ± 9.9·10 <sup>-4</sup>	< LOD	< LOD	0.03 ± 1.2·10 <sup>-3</sup>	< LOD
11	9-Methylphenanthrene	5.6·10 <sup>-3</sup> ± 1.9·10 <sup>-4</sup>	0.014 ± 4.9·10 <sup>-4</sup>	3.0·10 <sup>-3</sup> ± 9.9·10 <sup>-5</sup>	< LOD	< LOD	< LOD
12	3,6-dimethylphenanthrene	4.3·10 <sup>-3</sup> ± 1.4·10 <sup>-4</sup>	0.016 ± 5.6·10 <sup>-4</sup>	6.0·10 <sup>-3</sup> ± 2.2·10 <sup>-4</sup>	< LOD	< LOD	0.086 ± 4.0·10 <sup>-3</sup>
13	Fluoranthene	< LOD					
14	Pyrene	0.085 ± 3.1·10 <sup>-3</sup>	0.16 ± 6.0·10 <sup>-3</sup>	0.16 ± 5.8·10 <sup>-3</sup>	< LOD	< LOD	< LOD
15	2-Methylpyrene	0.016 ± 5.7·10 <sup>-4</sup>	0.025 ± 9.0·10 <sup>-4</sup>	0.034 ± 1.3·10 <sup>-3</sup>	0.024 ± 7.6·10 <sup>-4</sup>	0.027 ± 1.3·10 <sup>-3</sup>	0.023 ± 7.3·10 <sup>-4</sup>
16	4-Methylpyrene	0.010 ± 3.9·10 <sup>-4</sup>	0.036 ± 1.3·10 <sup>-3</sup>	0.045 ± 1.7·10 <sup>-3</sup>	< LOD	< LOD	< LOD
17	Benzo[a]fluorene	5.3·10 <sup>-4</sup> ± 1.8·10 <sup>-5</sup>	2.1·10 <sup>-3</sup> ± 7.5·10 <sup>-5</sup>	1.6·10 <sup>-3</sup> ± 5.6·10 <sup>-5</sup>	6.2·10 <sup>-3</sup> ± 2.1·10 <sup>-4</sup>	9.7·10 <sup>-3</sup> ± 4.6·10 <sup>-4</sup>	7.6·10 <sup>-3</sup> ± 2.5·10 <sup>-4</sup>
18	Benzo[a]anthracene	4.5·10 <sup>-3</sup> ± 1.7·10 <sup>-4</sup>	0.012 ± 4.2·10 <sup>-4</sup>	4.0·10 <sup>-3</sup> ± 1.4·10 <sup>-5</sup>	< LOD	< LOD	< LOD
19	Chrysene	< LOD	1.6·10 <sup>-3</sup> ± 5.5·10 <sup>-5</sup>	6.6·10 <sup>-4</sup> ± 2.2·10 <sup>-5</sup>	6.5·10 <sup>-3</sup> ± 3.0·10 <sup>-4</sup>	5.6·10 <sup>-3</sup> ± 2.6·10 <sup>-4</sup>	< LOD
20	3-Methylchrysene	< LOD	< LOD	< LOD	4.3·10 <sup>-3</sup> ± 1.9·10 <sup>-4</sup>	4.8·10 <sup>-3</sup> ± 1.9·10 <sup>-4</sup>	5.2·10 <sup>-3</sup> ± 2.5·10 <sup>-4</sup>
21	5-Methylchrysene	7.1·10 <sup>-4</sup> ± 2.8·10 <sup>-5</sup>	3.1·10 <sup>-3</sup> ± 1.1·10 <sup>-4</sup>	9.0·10 <sup>-4</sup> ± 3.0·10 <sup>-5</sup>	< LOD	< LOD	< LOD

22	6-Methylchrysene	$1.4 \cdot 10^{-4} \pm 7.1 \cdot 10^{-6}$	$4.6 \cdot 10^{-3} \pm 1.7 \cdot 10^{-4}$	$4.5 \cdot 10^{-4} \pm 1.5 \cdot 10^{-5}$	$7.6 \cdot 10^{-3} \pm 2.8 \cdot 10^{-4}$	$8.9 \cdot 10^{-3} \pm 4.1 \cdot 10^{-4}$	$4.3 \cdot 10^{-3} \pm 1.9 \cdot 10^{-4}$
23	Benzo[a]fluoranthene	$4.6 \cdot 10^{-3} \pm 1.7 \cdot 10^{-4}$	$7.0 \cdot 10^{-3} \pm 2.6 \cdot 10^{-4}$	$1.2 \cdot 10^{-3} \pm 4.2 \cdot 10^{-5}$	$3.9 \cdot 10^{-3} \pm 1.8 \cdot 10^{-4}$	$6.8 \cdot 10^{-3} \pm 2.7 \cdot 10^{-4}$	$5.0 \cdot 10^{-3} \pm 2.4 \cdot 10^{-4}$
24	Benzo[b]fluoranthene	$6.6 \cdot 10^{-3} \pm 2.4 \cdot 10^{-4}$	$9.7 \cdot 10^{-3} \pm 3.5 \cdot 10^{-4}$	$5.2 \cdot 10^{-3} \pm 1.9 \cdot 10^{-4}$	$2.4 \cdot 10^{-3} \pm 7.0 \cdot 10^{-5}$	$2.8 \cdot 10^{-3} \pm 9.9 \cdot 10^{-5}$	$3.9 \cdot 10^{-3} \pm 1.8 \cdot 10^{-4}$
25	Benzo[k]fluoranthene	$2.8 \cdot 10^{-3} \pm 1.0 \cdot 10^{-4}$	$3.2 \cdot 10^{-3} \pm 1.2 \cdot 10^{-4}$	$2.0 \cdot 10^{-3} \pm 7.0 \cdot 10^{-5}$	< LOD	< LOD	< LOD
26	Benzo[j]fluoranthene	$1.2 \cdot 10^{-4} \pm 3.0 \cdot 10^{-6}$	$3.8 \cdot 10^{-4} \pm 1.3 \cdot 10^{-5}$	$4.8 \cdot 10^{-4} \pm 1.6 \cdot 10^{-5}$	< LOD	< LOD	< LOD
27	Benzo[a]pyrene	$3.7 \cdot 10^{-4} \pm 1.2 \cdot 10^{-5}$	$2.1 \cdot 10^{-3} \pm 7.5 \cdot 10^{-5}$	$6.5 \cdot 10^{-5} \pm 3.3 \cdot 10^{-6}$	< LOD	< LOD	< LOD
28	Indeno[1,2,3-cd]pyrene	< LOD	< LOD	< LOD	< LOD	$2.2 \cdot 10^{-4} \pm 1.2 \cdot 10^{-5}$	< LOD
29	Benzo[ghi]perylene	< LOD	< LOD	< LOD	$1.0 \cdot 10^{-3} \pm 2.9 \cdot 10^{-5}$	$2.3 \cdot 10^{-3} \pm 8.0 \cdot 10^{-5}$	$1.9 \cdot 10^{-3} \pm 5.2 \cdot 10^{-5}$
30	Dibenzo[a,h]anthracene	$6.0 \cdot 10^{-4} \pm 2.1 \cdot 10^{-5}$	$6.6 \cdot 10^{-4} \pm 2.4 \cdot 10^{-5}$	< LOD	< LOD	$2.0 \cdot 10^{-3} \pm 9.1 \cdot 10^{-5}$	$1.8 \cdot 10^{-3} \pm 5.0 \cdot 10^{-5}$
31	Dibenz[a,e]pyrene	$2.4 \cdot 10^{-5} \pm 8.9 \cdot 10^{-7}$	$3.3 \cdot 10^{-5} \pm 1.2 \cdot 10^{-6}$	$5.2 \cdot 10^{-5} \pm 1.9 \cdot 10^{-6}$	< LOD	< LOD	< LOD
32	Dibenz[a,h]pyrene	$4.5 \cdot 10^{-6} \pm 1.5 \cdot 10^{-7}$	< LOD				
33	Dibenz[a,i]pyrene	< LOD					
34	Dibenz[a,l]pyrene	< LOD					
N- and O-PAHs							
35	Nitronaphthalene	< LOD					
26	1-Methyl-5-nitronaphthalene	$0.35 \pm 0.01$	$0.94 \pm 0.03$	$0.33 \pm 0.01$	< LOD	< LOD	< LOD
30	1-Methyl-6-nitronaphthalene	$0.42 \pm 0.01$	$0.77 \pm 0.03$	$0.36 \pm 0.01$	< LOD	< LOD	< LOD
31	9,10-Anthracenedione	$0.035 \pm 1.2 \cdot 10^{-3}$	$0.19 \pm 7.3 \cdot 10^{-3}$	$0.25 \pm 9.7 \cdot 10^{-3}$	< LOD	< LOD	< LOD
32	4H-cyclopenta(def)phenanthrene	< LOD	< LOD	< LOD	$0.24 \pm 0.01$	$0.47 \pm 0.02$	$0.47 \pm 0.02$
33	Nitropyrene	< LOD	< LOD	< LOD	$8.2 \cdot 10^{-3} \pm 2.2 \cdot 10^{-4}$	$0.013 \pm 6.9 \cdot 10^{-4}$	$0.012 \pm 5.9 \cdot 10^{-4}$

Table S8. The bioavailable content of PAHs and their derivatives in BCW and BCZ after physical aging.

No.	Compound	Sample description					
		BCW500-PA	BCW600-PA	BCW700-PA	BCZ500-PA	BCZ600-PA	BCZ700-PA
Analyte concentration ± SD [ng L <sup>-1</sup> ]							
1	Naphthalene	7.91 ± 0.42	10.12 ± 0.52	8.95 ± 0.47	9.30 ± 0.43	10.65 ± 0.55	11.41 ± 0.59
2	1,3-di-iso-propynaphthalene	< LOD					
3	2-Phenylnaphthalene	< LOD					
4	Acenaphthylene	0.81 ± 0.04	0.98 ± 0.05	0.86 ± 0.05	0.75 ± 0.03	0.87 ± 0.04	0.91 ± 0.05
5	Acenaphthene	2.63 ± 0.14	2.74 ± 0.14	2.36 ± 0.12	0.44 ± 0.02	0.76 ± 0.04	0.60 ± 0.03
6	Fluorene	< LOD	< LOD	< LOD	0.42 ± 0.02	0.88 ± 0.05	1.50 ± 0.08
7	Anthracene	0.088 ± 4.6·10 <sup>-3</sup>	0.045 ± 2.3·10 <sup>-3</sup>	7.1·10 <sup>-3</sup> ± 3.7·10 <sup>-4</sup>	< LOD	0.023 ± 1.2·10 <sup>-3</sup>	0.072 ± 3.7·10 <sup>-3</sup>
8	Phenanthrene	< LOD					
9	3-Methylphenanthrene	< LOD	< LOD	< LOD	< LOD	0.018 ± 9.2·10 <sup>-4</sup>	0.014 ± 7.0·10 <sup>-4</sup>
10	2-Methylphenanthrene	< LOD					
11	9-Methylphenanthrene	< LOD	< LOD	< LOD	7.5·10 <sup>-3</sup> ± 3.5·10 <sup>-4</sup>	0.023 ± 1.2·10 <sup>-3</sup>	6.4·10 <sup>-3</sup> ± 3.3·10 <sup>-4</sup>
12	3,6-dimethylphenanthrene	< LOD	< LOD	< LOD	5.7·10 <sup>-3</sup> ± 2.6·10 <sup>-4</sup>	0.017 ± 8.7·10 <sup>-4</sup>	0.019 ± 9.8·10 <sup>-4</sup>
13	Fluoranthene	0.015 ± 7.9·10 <sup>-4</sup>	0.027 ± 1.4·10 <sup>-3</sup>	0.025 ± 1.3·10 <sup>-3</sup>	< LOD	< LOD	< LOD
14	Pyrene	0.20 ± 0.01	0.23 ± 0.01	0.16 ± 8.2·10 <sup>-3</sup>	0.081 ± 3.7·10 <sup>-3</sup>	0.16 ± 8.2·10 <sup>-3</sup>	0.20 ± 0.01
15	2-Methylpyrene	2.9·10 <sup>-3</sup> ± 1.4·10 <sup>-4</sup>	2.1·10 <sup>-3</sup> ± 1.1·10 <sup>-4</sup>	1.8·10 <sup>-3</sup> ± 8.8·10 <sup>-5</sup>	< LOD	4.0·10 <sup>-3</sup> ± 2.0·10 <sup>-4</sup>	2.8·10 <sup>-3</sup> ± 1.4·10 <sup>-4</sup>
16	4-Methylpyrene	< LOD	4.2·10 <sup>-3</sup> ± 2.1·10 <sup>-4</sup>				
17	Benzo[a]fluorene	4.2·10 <sup>-3</sup> ± 2.2·10 <sup>-4</sup>	5.0·10 <sup>-3</sup> ± 2.6·10 <sup>-4</sup>	5.2·10 <sup>-3</sup> ± 2.7·10 <sup>-4</sup>	< LOD	< LOD	< LOD
18	Benzo[a]anthracene	4.4·10 <sup>-3</sup> ± 2.3·10 <sup>-4</sup>	8.1·10 <sup>-3</sup> ± 4.1·10 <sup>-4</sup>	3.8·10 <sup>-3</sup> ± 2.0·10 <sup>-4</sup>	5.3·10 <sup>-3</sup> ± 2.4·10 <sup>-4</sup>	6.8·10 <sup>-3</sup> ± 3.5·10 <sup>-4</sup>	7.1·10 <sup>-3</sup> ± 3.6·10 <sup>-4</sup>
19	Chrysene	2.1·10 <sup>-4</sup> ± 1.1·10 <sup>-5</sup>	4.2·10 <sup>-4</sup> ± 2.2·10 <sup>-5</sup>	8.4·10 <sup>-4</sup> ± 4.4·10 <sup>-5</sup>	< LOD	< LOD	< LOD
20	3-Methylchrysene	< LOD					
21	5-Methylchrysene	< LOD	< LOD	< LOD	1.5·10 <sup>-3</sup> ± 6.9·10 <sup>-5</sup>	3.9·10 <sup>-3</sup> ± 2.0·10 <sup>-4</sup>	2.3·10 <sup>-3</sup> ± 1.2·10 <sup>-4</sup>
22	6-Methylchrysene	< LOD	4.5·10 <sup>-3</sup> ± 2.3·10 <sup>-4</sup>				

23	Benzo[a]fluoranthene	< LOD	< LOD	< LOD	$4.1 \cdot 10^{-3} \pm 1.9 \cdot 10^{-4}$	$6.2 \cdot 10^{-3} \pm 3.2 \cdot 10^{-4}$	$4.3 \cdot 10^{-3} \pm 2.2 \cdot 10^{-4}$
24	Benzo[b]fluoranthene	< LOD	< LOD	< LOD	$2.6 \cdot 10^{-3} \pm 1.2 \cdot 10^{-4}$	$2.4 \cdot 10^{-3} \pm 1.3 \cdot 10^{-4}$	$2.7 \cdot 10^{-3} \pm 1.4 \cdot 10^{-4}$
25	Benzo[k]fluoranthene	< LOD	< LOD	< LOD	$1.1 \cdot 10^{-3} \pm 5.0 \cdot 10^{-5}$	$9.8 \cdot 10^{-4} \pm 5.0 \cdot 10^{-5}$	$9.7 \cdot 10^{-4} \pm 5.0 \cdot 10^{-5}$
26	Benzo[j]fluoranthene	< LOD					
27	Benzo[a]pyrene	$3.2 \cdot 10^{-3} \pm 1.7 \cdot 10^{-4}$	$4.7 \cdot 10^{-3} \pm 2.4 \cdot 10^{-4}$	$4.6 \cdot 10^{-3} \pm 2.4 \cdot 10^{-4}$	< LOD	< LOD	< LOD
28	Indeno[1,2,3-cd]pyrene	$2.4 \cdot 10^{-4} \pm 1.3 \cdot 10^{-5}$	$3.9 \cdot 10^{-4} \pm 2.0 \cdot 10^{-5}$	$4.0 \cdot 10^{-4} \pm 2.1 \cdot 10^{-5}$	< LOD	< LOD	< LOD
29	Benzo[ghi]perylene	< LOD					
30	Dibenzo[a,h]anthracene	$8.7 \cdot 10^{-5} \pm 4.6 \cdot 10^{-6}$	$1.1 \cdot 10^{-4} \pm 5.8 \cdot 10^{-6}$	$4.3 \cdot 10^{-5} \pm 2.2 \cdot 10^{-6}$	$6.4 \cdot 10^{-4} \pm 2.9 \cdot 10^{-5}$	$8.7 \cdot 10^{-4} \pm 4.5 \cdot 10^{-5}$	$7.6 \cdot 10^{-4} \pm 3.9 \cdot 10^{-5}$
31	Dibenz[a,e]pyrene	$3.0 \cdot 10^{-6} \pm 1.6 \cdot 10^{-7}$	$4.5 \cdot 10^{-6} \pm 2.3 \cdot 10^{-7}$	$1.3 \cdot 10^{-5} \pm 7.0 \cdot 10^{-7}$	$1.3 \cdot 10^{-5} \pm 6.2 \cdot 10^{-7}$	$2.2 \cdot 10^{-5} \pm 1.2 \cdot 10^{-6}$	$6.6 \cdot 10^{-5} \pm 3.4 \cdot 10^{-6}$
32	Dibenz[a,h]pyrene	< LOD					
33	Dibenz[a,i]pyrene	< LOD	< LOD	$5.9 \cdot 10^{-6} \pm 3.1 \cdot 10^{-7}$	< LOD	< LOD	< LOD
34	Dibenz[a,l]pyrene	< LOD					
N- and O-PAHs							
35	Nitronaphthalene	$0.62 \pm 0.03$	$0.40 \pm 0.02$	$0.55 \pm 0.03$	< LOD	< LOD	< LOD
26	1-Methyl-5-nitronaphthalene	< LOD	< LOD	< LOD	$0.29 \pm 0.01$	$0.40 \pm 0.02$	$0.45 \pm 0.02$
30	1-Methyl-6-nitronaphthalene	< LOD	< LOD	< LOD	$0.16 \pm 8.1 \cdot 10^{-3}$	$0.48 \pm 0.02$	$0.54 \pm 0.03$
31	9,10-Anthracenedione	< LOD					
32	4H-cyclopenta(def)phenanthrene	< LOD					
33	Nitropyrene	< LOD					

Table S9. The bioavailable content of PAHs and their derivatives in BC after chemical aging at 60°C.

No.	Compound	Sample description					
		BCW500-CA60	BCW600-CA60	BCW700-CA60	BCZ500-CA60	BCZ600-CA60	BCZ700-CA60
Analyte concentration ± SD [ng L <sup>-1</sup> ]							
1	Naphthalene	6.93 ± 0.34	11.36 ± 0.52	9.30 ± 0.49	7.17 ± 0.37	7.77 ± 0.36	9.24 ± 0.49
2	1,3-di-iso-propynaphthalene	< LOD					
3	2-Phenylnaphthalene	< LOD					
4	Acenaphthylene	0.71 ± 0.04	1.08 ± 0.05	0.91 ± 0.05	0.47 ± 0.02	0.62 ± 0.03	0.79 ± 0.04
5	Acenaphthene	2.21 ± 0.11	2.46 ± 0.11	2.53 ± 0.13	0.20 ± 0.01	0.40 ± 0.02	0.28 ± 0.01
6	Fluorene	< LOD	< LOD	< LOD	0.15 ± 7.7·10 <sup>-3</sup>	0.28 ± 0.01	0.41 ± 0.02
7	Anthracene	0.071 ± 3.5·10 <sup>-3</sup>	0.061 ± 2.8·10 <sup>-3</sup>	0.046 ± 2.4·10 <sup>-3</sup>	< LOD	< LOD	< LOD
8	Phenanthrene	< LOD					
9	3-Methylphenanthrene	< LOD					
10	2-Methylphenanthrene	< LOD					
11	9-Methylphenanthrene	< LOD					
12	3,6-dimethylphenanthrene	< LOD	< LOD	< LOD	1.1·10 <sup>-3</sup> ± 5.4·10 <sup>-5</sup>	0.011 ± 5.1·10 <sup>-4</sup>	7.9·10 <sup>-3</sup> ± 4.1·10 <sup>-4</sup>
13	Fluoranthene	0.012 ± 6.0·10 <sup>-4</sup>	0.020 ± 9.1·10 <sup>-4</sup>	0.016 ± 8.9·10 <sup>-4</sup>	< LOD	< LOD	< LOD
14	Pyrene	0.16 ± 8.1·10 <sup>-3</sup>	0.22 ± 0.01	0.24 ± 0.01	0.034 ± 1.7·10 <sup>-3</sup>	0.52 ± 2.4·10 <sup>-3</sup>	0.67 ± 3.5·10 <sup>-3</sup>
15	2-Methylpyrene	4.1·10 <sup>-3</sup> ± 2.1·10 <sup>-4</sup>	3.1·10 <sup>-3</sup> ± 1.6·10 <sup>-4</sup>	5.5·10 <sup>-3</sup> ± 2.7·10 <sup>-4</sup>	7.1·10 <sup>-4</sup> ± 3.5·10 <sup>-5</sup>	0.013 ± 6.5·10 <sup>-4</sup>	9.6·10 <sup>-3</sup> ± 4.8·10 <sup>-4</sup>
16	4-Methylpyrene	< LOD	< LOD	< LOD	< LOD	0.014 ± 6.9·10 <sup>-4</sup>	0.021 ± 1.0·10 <sup>-3</sup>
17	Benzo[a]fluorene	3.3·10 <sup>-3</sup> ± 1.7·10 <sup>-4</sup>	5.4·10 <sup>-3</sup> ± 2.5·10 <sup>-4</sup>	6.4·10 <sup>-3</sup> ± 3.3·10 <sup>-4</sup>	< LOD	3.5·10 <sup>-4</sup> ± 1.6·10 <sup>-5</sup>	< LOD
18	Benzo[a]anthracene	3.7·10 <sup>-3</sup> ± 1.8·10 <sup>-4</sup>	4.2·10 <sup>-3</sup> ± 1.9·10 <sup>-4</sup>	6.5·10 <sup>-3</sup> ± 3.4·10 <sup>-4</sup>	< LOD	6.8·10 <sup>-4</sup> ± 3.1·10 <sup>-5</sup>	8.8·10 <sup>-4</sup> ± 4.6·10 <sup>-5</sup>
19	Chrysene	3.1·10 <sup>-4</sup> ± 1.5·10 <sup>-5</sup>	5.1·10 <sup>-4</sup> ± 2.4·10 <sup>-5</sup>	6.1·10 <sup>-4</sup> ± 3.2·10 <sup>-5</sup>	< LOD	< LOD	< LOD
20	3-Methylchrysene	< LOD					
21	5-Methylchrysene	< LOD	< LOD	< LOD	3.5·10 <sup>-4</sup> ± 1.8·10 <sup>-5</sup>	2.2·10 <sup>-3</sup> ± 1.0·10 <sup>-4</sup>	1.6·10 <sup>-3</sup> ± 8.2·10 <sup>-5</sup>

22	6-Methylchrysene	< LOD	$0.001 \pm 5.2 \cdot 10^{-4}$				
23	Benzo[a]fluoranthene	< LOD	< LOD	< LOD	$2.4 \cdot 10^{-3} \pm 1.3 \cdot 10^{-4}$	$4.2 \cdot 10^{-3} \pm 1.9 \cdot 10^{-4}$	$4.0 \cdot 10^{-3} \pm 2.1 \cdot 10^{-4}$
24	Benzo[b]fluoranthene	< LOD	< LOD	< LOD	$2.0 \cdot 10^{-3} \pm 1.0 \cdot 10^{-4}$	$3.1 \cdot 10^{-3} \pm 1.4 \cdot 10^{-4}$	$1.7 \cdot 10^{-3} \pm 8.7 \cdot 10^{-5}$
25	Benzo[k]fluoranthene	< LOD	< LOD	< LOD	$1.7 \cdot 10^{-3} \pm 8.5 \cdot 10^{-5}$	$2.0 \cdot 10^{-3} \pm 9.3 \cdot 10^{-5}$	$3.0 \cdot 10^{-3} \pm 1.6 \cdot 10^{-4}$
26	Benzo[j]fluoranthene	< LOD					
27	Benzo[a]pyrene	$3.6 \cdot 10^{-3} \pm 1.8 \cdot 10^{-4}$	$3.3 \cdot 10^{-3} \pm 1.5 \cdot 10^{-4}$	$6.1 \cdot 10^{-3} \pm 3.2 \cdot 10^{-4}$	< LOD	< LOD	< LOD
28	Indeno[1,2,3-cd]pyrene	$2.7 \cdot 10^{-4} \pm 1.3 \cdot 10^{-5}$	$3.3 \cdot 10^{-4} \pm 1.5 \cdot 10^{-5}$	$5.8 \cdot 10^{-4} \pm 3.1 \cdot 10^{-5}$	< LOD	< LOD	< LOD
29	Benzo[ghi]perylene	< LOD					
30	Dibenz[a,h]anthracene	$6.9 \cdot 10^{-5} \pm 3.4 \cdot 10^{-6}$	$1.2 \cdot 10^{-4} \pm 1.0 \cdot 10^{-5}$	$3.4 \cdot 10^{-4} \pm 1.8 \cdot 10^{-5}$	$3.1 \cdot 10^{-4} \pm 1.6 \cdot 10^{-5}$	$9.5 \cdot 10^{-4} \pm 4.3 \cdot 10^{-5}$	$1.8 \cdot 10^{-4} \pm 9.7 \cdot 10^{-6}$
31	Dibenz[a,e]pyrene	$8.6 \cdot 10^{-6} \pm 4.7 \cdot 10^{-7}$	$5.8 \cdot 10^{-6} \pm 2.7 \cdot 10^{-7}$	$4.3 \cdot 10^{-6} \pm 2.2 \cdot 10^{-7}$	< LOD	$1.8 \cdot 10^{-5} \pm 8.2 \cdot 10^{-7}$	$2.4 \cdot 10^{-5} \pm 1.3 \cdot 10^{-6}$
32	Dibenz[a,h]pyrene	< LOD					
33	Dibenz[a,i]pyrene	< LOD	< LOD	$1.3 \cdot 10^{-5} \pm 6.7 \cdot 10^{-7}$	< LOD	< LOD	< LOD
34	Dibenz[a,l]pyrene	< LOD					
N- and O-PAHs							
35	Nitronaphthalene	$0.56 \pm 0.03$	$0.27 \pm 0.01$	$0.31 \pm 0.02$	< LOD	< LOD	< LOD
26	1-Methyl-5-nitronaphthalene	< LOD	< LOD	< LOD	< LOD	$0.12 \pm 0.01$	$0.45 \pm 0.02$
30	1-Methyl-6-nitronaphthalene	< LOD	< LOD	< LOD	< LOD	$0.04 \pm 2.0 \cdot 10^{-3}$	$0.19 \pm 9.4 \cdot 10^{-3}$
31	9,10-Anthracenedione	< LOD					
32	4H-cyclopenta(def)phenanthrene	< LOD					
33	Nitropyrene	< LOD					

Table S10. The bioavailable content of PAHs and their derivatives in BC after chemical aging at 90°C.

No.	Compound	Sample description					
		BCW500-CA90	BCW600-CA90	BCW700-CA90	BCZ500-CA90	BCZ600-CA90	BCZ700-CA90
Analyte concentration ± SD [ng L <sup>-1</sup> ]							
1	Naphthalene	7.89 ± 0.40	12.91 ± 0.64	10.95 ± 0.56	5.61 ± 0.26	7.79 ± 0.40	9.74 ± 0.50
2	1,3-di-iso-propynaphthalene	< LOD	< LOD	< LOD	< LOD	7.3·10 <sup>-3</sup> ± 3.8·10 <sup>-4</sup>	< LOD
3	2-Phenylnaphthalene	< LOD	< LOD	< LOD	< LOD	0.14 ± 7.4·10 <sup>-3</sup>	< LOD
4	Acenaphthylene	0.92 ± 0.05	1.35 ± 0.07	1.09 ± 0.06	0.55 ± 0.03	0.66 ± 0.03	0.31 ± 0.02
5	Acenaphthene	2.50 ± 0.13	2.67 ± 0.13	3.05 ± 0.16	0.31 ± 0.01	0.58 ± 0.03	0.27 ± 0.01
6	Fluorene	8.3·10 <sup>-3</sup> ± 4.3·10 <sup>-4</sup>	0.021 ± 1.0·10 <sup>-3</sup>	0.048 ± 2.5·10 <sup>-3</sup>	0.067 ± 3.1·10 <sup>-3</sup>	0.29 ± 0.01	0.22 ± 0.01
7	Anthracene	0.12 ± 6.2·10 <sup>-3</sup>	0.082 ± 4.1·10 <sup>-3</sup>	0.084 ± 4.3·10 <sup>-3</sup>	< LOD	7.2·10 <sup>-3</sup> ± 3.7·10 <sup>-4</sup>	2.8·10 <sup>-3</sup> ± 1.4·10 <sup>-4</sup>
8	Phenanthrene	< LOD					
9	3-Methylphenanthrene	< LOD	< LOD	< LOD	9.4·10 <sup>-4</sup> ± 4.3·10 <sup>-5</sup>	7.6·10 <sup>-3</sup> ± 3.9·10 <sup>-4</sup>	8.2·10 <sup>-3</sup> ± 4.2·10 <sup>-4</sup>
10	2-Methylphenanthrene	< LOD	< LOD	< LOD	< LOD	9.5·10 <sup>-4</sup> ± 4.9·10 <sup>-5</sup>	< LOD
11	9-Methylphenanthrene	< LOD	< LOD	< LOD	2.8·10 <sup>-3</sup> ± 1.3·10 <sup>-4</sup>	1.9·10 <sup>-3</sup> ± 9.7·10 <sup>-5</sup>	< LOD
12	3,6-dimethylphenanthrene	< LOD	< LOD	< LOD	5.0·10 <sup>-3</sup> ± 2.3·10 <sup>-4</sup>	0.012 ± 6.1·10 <sup>-4</sup>	7.6·10 <sup>-3</sup> ± 3.9·10 <sup>-4</sup>
13	Fluoranthene	0.019 ± 9.9·10 <sup>-4</sup>	0.026 ± 1.3·10 <sup>-3</sup>	0.036 ± 1.9·10 <sup>-3</sup>	< LOD	< LOD	4.6·10 <sup>-3</sup> ± 2.3·10 <sup>-4</sup>
14	Pyrene	0.20 ± 0.01	0.25 ± 0.01	0.27 ± 0.01	0.074 ± 3.4·10 <sup>-3</sup>	0.12 ± 6.0·10 <sup>-3</sup>	0.68 ± 3.5·10 <sup>-3</sup>
15	2-Methylpyrene	8.8·10 <sup>-3</sup> ± 4.5·10 <sup>-4</sup>	0.012 ± 6.1·10 <sup>-4</sup>	0.017 ± 8.5·10 <sup>-4</sup>	< LOD	0.015 ± 7.6·10 <sup>-4</sup>	8.7·10 <sup>-3</sup> ± 4.3·10 <sup>-4</sup>
16	4-Methylpyrene	< LOD	< LOD	< LOD	< LOD	0.013 ± 6.5·10 <sup>-4</sup>	0.014 ± 7.1·10 <sup>-4</sup>
17	Benzo[a]fluorene	3.8·10 <sup>-3</sup> ± 1.9·10 <sup>-4</sup>	7.0·10 <sup>-3</sup> ± 3.4·10 <sup>-4</sup>	8.6·10 <sup>-3</sup> ± 4.4·10 <sup>-4</sup>	< LOD	1.8·10 <sup>-4</sup> ± 9.2·10 <sup>-6</sup>	< LOD
18	Benzo[a]anthracene	4.6·10 <sup>-3</sup> ± 2.3·10 <sup>-4</sup>	5.8·10 <sup>-3</sup> ± 2.8·10 <sup>-4</sup>	9.1·10 <sup>-3</sup> ± 4.7·10 <sup>-4</sup>	1.7·10 <sup>-3</sup> ± 7.7·10 <sup>-5</sup>	2.6·10 <sup>-3</sup> ± 1.3·10 <sup>-4</sup>	1.3·10 <sup>-3</sup> ± 6.9·10 <sup>-5</sup>
19	Chrysene	1.3·10 <sup>-3</sup> ± 6.4·10 <sup>-5</sup>	1.2·10 <sup>-3</sup> ± 5.7·10 <sup>-5</sup>	3.8·10 <sup>-3</sup> ± 2.0·10 <sup>-4</sup>	< LOD	2.1·10 <sup>-4</sup> ± 1.1·10 <sup>-5</sup>	8.2·10 <sup>-4</sup> ± 4.2·10 <sup>-5</sup>
20	3-Methylchrysene	< LOD					
21	5-Methylchrysene	< LOD	< LOD	< LOD	1.1·10 <sup>-3</sup> ± 4.9·10 <sup>-5</sup>	3.2·10 <sup>-3</sup> ± 1.6·10 <sup>-4</sup>	1.5·10 <sup>-3</sup> ± 7.5·10 <sup>-5</sup>

22	6-Methylchrysene	< LOD	< LOD	< LOD	< LOD	$5.0 \cdot 10^{-4} \pm 2.6 \cdot 10^{-5}$	$4.2 \cdot 10^{-4} \pm 2.1 \cdot 10^{-5}$
23	Benzo[a]fluoranthene	< LOD	< LOD	< LOD	$3.5 \cdot 10^{-3} \pm 1.6 \cdot 10^{-4}$	$8.9 \cdot 10^{-3} \pm 4.6 \cdot 10^{-4}$	$4.4 \cdot 10^{-3} \pm 2.3 \cdot 10^{-4}$
24	Benzo[b]fluoranthene	< LOD	< LOD	< LOD	$3.7 \cdot 10^{-3} \pm 1.7 \cdot 10^{-4}$	$4.5 \cdot 10^{-3} \pm 2.3 \cdot 10^{-4}$	$1.7 \cdot 10^{-3} \pm 8.8 \cdot 10^{-5}$
25	Benzo[k]fluoranthene	< LOD	< LOD	< LOD	$1.5 \cdot 10^{-3} \pm 6.8 \cdot 10^{-5}$	$1.1 \cdot 10^{-3} \pm 5.7 \cdot 10^{-5}$	< LOD
26	Benzo[j]fluoranthene	< LOD	< LOD	< LOD	< LOD	$1.2 \cdot 10^{-4} \pm 6.3 \cdot 10^{-6}$	< LOD
27	Benzo[a]pyrene	$4.6 \cdot 10^{-3} \pm 2.4 \cdot 10^{-4}$	$3.9 \cdot 10^{-3} \pm 1.9 \cdot 10^{-4}$	$8.6 \cdot 10^{-3} \pm 4.4 \cdot 10^{-4}$	< LOD	$2.2 \cdot 10^{-4} \pm 1.1 \cdot 10^{-5}$	< LOD
28	Indeno[1,2,3-cd]pyrene	$5.5 \cdot 10^{-4} \pm 2.8 \cdot 10^{-5}$	$5.8 \cdot 10^{-4} \pm 2.8 \cdot 10^{-5}$	$7.6 \cdot 10^{-4} \pm 3.9 \cdot 10^{-5}$	< LOD	< LOD	< LOD
29	Benzo[ghi]perylene	< LOD					
30	Dibenz[a,h]anthracene	$1.7 \cdot 10^{-4} \pm 8.7 \cdot 10^{-6}$	$4.4 \cdot 10^{-4} \pm 2.2 \cdot 10^{-5}$	$5.3 \cdot 10^{-4} \pm 2.7 \cdot 10^{-5}$	$3.1 \cdot 10^{-4} \pm 1.4 \cdot 10^{-5}$	$6.6 \cdot 10^{-4} \pm 3.4 \cdot 10^{-5}$	$1.2 \cdot 10^{-4} \pm 6.4 \cdot 10^{-6}$
31	Dibenz[a,e]pyrene	$4.6 \cdot 10^{-5} \pm 2.3 \cdot 10^{-6}$	$7.0 \cdot 10^{-5} \pm 3.4 \cdot 10^{-6}$	$4.5 \cdot 10^{-5} \pm 2.3 \cdot 10^{-6}$	$1.3 \cdot 10^{-5} \pm 6.1 \cdot 10^{-7}$	$3.1 \cdot 10^{-5} \pm 1.6 \cdot 10^{-6}$	$4.5 \cdot 10^{-5} \pm 2.3 \cdot 10^{-6}$
32	Dibenz[a,h]pyrene	< LOD					
33	Dibenz[a,i]pyrene	< LOD	< LOD	$2.7 \cdot 10^{-5} \pm 1.4 \cdot 10^{-6}$	< LOD	< LOD	< LOD
34	Dibenz[a,l]pyrene	< LOD					
N- and O-PAHs							
35	Nitronaphthalene	$0.97 \pm 0.05$	$1.18 \pm 0.06$	$1.32 \pm 0.07$	< LOD	< LOD	< LOD
26	1-Methyl-5-nitronaphthalene	< LOD	< LOD	< LOD	$0.027 \pm 1.4 \cdot 10^{-3}$	$0.22 \pm 0.01$	$0.46 \pm 0.02$
30	1-Methyl-6-nitronaphthalene	< LOD	< LOD	< LOD	$0.014 \pm 6.7 \cdot 10^{-4}$	$0.30 \pm 0.02$	$0.25 \pm 0.01$
31	9,10-Anthracenedione	< LOD					
32	4H-cyclopenta(def)phenanthrene	< LOD					
33	Nitropyrene	< LOD					

## **References:**

- [1] S.E. Hale, J. Lehmann, D. Rutherford, A.R. Zimmerman, R.T. Bachmann, V. Shitumbanuma, A. O'Toole, K.L. Sundqvist, H.P.H. Arp, G. Cornelissen, Quantifying the Total and Bioavailable Polycyclic Aromatic Hydrocarbons and Dioxins in Biochars, *Environ. Sci. Technol.* 46 (2012) 2830–2838. <https://doi.org/10.1021/es203984k>.
- [2] A. Krzyszczak, M.P. Dybowski, B. Czech, Formation of polycyclic aromatic hydrocarbons and their derivatives in biochars: The effect of feedstock and pyrolysis conditions, *Journal of Analytical and Applied Pyrolysis.* 160 (2021) 105339. <https://doi.org/10.1016/j.jaap.2021.105339>.
- [3] D. Fabbri, A.G. Rombolà, C. Torri, K.A. Spokas, Determination of polycyclic aromatic hydrocarbons in biochar and biochar amended soil, *Journal of Analytical and Applied Pyrolysis.* 103 (2013) 60–67. <https://doi.org/10.1016/j.jaap.2012.10.003>.

## **Publikacja D5**

**A. Krzyszczak, M. P. Dybowski, B. Czech**

*Microorganisms and their metabolites affect the content of polycyclic aromatic hydrocarbons  
and their derivatives in pyrolyzed material*

Science of the Total Environment, 2023, 886, 163966



## Microorganisms and their metabolites affect the content of polycyclic aromatic hydrocarbons and their derivatives in pyrolyzed material



Agnieszka Krzyszczak <sup>a</sup>, Michał P. Dybowski <sup>b</sup>, Bożena Czech <sup>a,\*</sup>

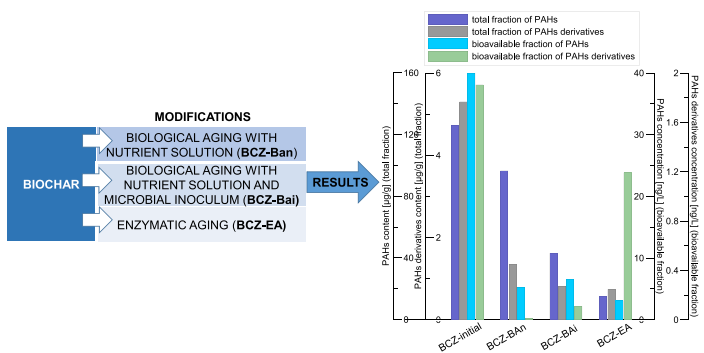
<sup>a</sup> Department of Radiochemistry and Environmental Chemistry, Institute of Chemical Sciences, Faculty of Chemistry, Maria Curie-Skłodowska University in Lublin, Pl. M. Curie-Skłodowskiej 3, 20-031 Lublin, Poland

<sup>b</sup> Department of Chromatography, Institute of Chemical Sciences, Faculty of Chemistry, Maria Curie-Skłodowska University in Lublin, Pl. M. Curie-Skłodowskiej 3, 20-031 Lublin, Poland

### HIGHLIGHTS

- During pyrolysis or under the environmental pressure in biochar toxic PAHs and derivatives can be formed.
- The experiments differentiate the effect of soil microorganisms and their activity, and the enzymes alone.
- The enzymatic aging usually lowered the content of PAHs and their derivatives in biochar.
- The biological aging reduced the bioavailability of tested compounds.
- There was no correlation between the PAHs bioavailability and the type of feedstock.

### GRAPHICAL ABSTRACT



### ARTICLE INFO

Editor: Paromita Chakraborty

#### Keywords:

Biochar  
PAHs  
PAHs derivatives  
Biological aging  
Enzymatic aging, feedstock

### ABSTRACT

Toxic polycyclic aromatic hydrocarbons (PAHs) and more toxic N- and O-containing derivatives can be determined in biochar. However, their fate in the environment and bioavailability depends on many parameters and was not studied yet. In the presented studies a set of biochars obtained from various feedstock at the same pyrolysis temperature (600 °C) subjected to environmental pressure e.g. soil microorganisms and enzymes was described. Presented study aimed to determine the effect of biological agents on the physicochemical characteristic and the content of PAHs and their derivatives in biochars after long-term treatment (6 months). The results indicated that enzymatic aging usually lowered (up to 94 %) the content of PAHs and their derivatives in biochar. Simultaneously, biological aging reduced the bioavailability of tested compounds. Considering the total fraction of PAHs and their derivatives, biochars treated with nutrients and microbial inoculum were characterized by the lowest content of analytes (even in comparison to biochars treated with nutrients alone). To complement the obtained results, the content of C, H, N, O, and ash as well as specific surface area, aromaticity, polarity, and hydrophilicity in biochar before and after modifications were determined. In general, enzymatic aging increased, and biological aging decreased the content of C% and H% in biochar. Both aging processes lowered the H/C ratio which indicated the decrease of the aromatization degree for artificially altered biochar.

### 1. Introduction

Biochar (BC) is a charred material obtained via pyrolysis, e.g. thermochemical decomposition of biomass at elevated temperatures in the absence or reduced content of oxygen (Bolan et al., 2022). The application potential

\* Corresponding author.

E-mail address: [bozena.czech@mail.umcs.pl](mailto:bozena.czech@mail.umcs.pl) (B. Czech).

of biochar is very broad. One of the most important from the environmental point of view is BC's addition to the soil which results in the improvement of soil properties (structure, increased pH, water and nutrient retention, reduced N<sub>2</sub>O and CH<sub>4</sub> emissions as well as lowered leaching of inorganic nitrogen, adsorption of organic and inorganic contaminants) and quality (improved soil fertility, vegetation yield, stimulated bacteria growth) (Atkinson et al., 2010; Beesley et al., 2011; Cao et al., 2009; Inyang and Dickenson, 2015; Lipczynska-Kochany, 2018; Spokas et al., 2009).

Soil microorganisms play an essential role in soil nutrient cycling, fertility maintenance, carbon sequestration, and crop production (Dai et al., 2021). Relatively little work has focused on understanding how biochar application to soil affects bacterial community structure and biogeochemical function (Anderson et al., 2011; Yao et al., 2017) and the topic is not fully understood yet. But published studies presented for example that the bacterial abundance in soil increased significantly with biochar enrichment, especially when the BC dosage was sufficiently high (Yao et al., 2017). The biochar addition changed the composition and alpha diversity of the bacterial community (Fan et al., 2020; Yao et al., 2017). Among all dominant bacterial phyla and bacterial communities found in the black soil of northeast China, after the BC addition, the relative abundances of *Acidobacteria* and *Bradyrhizobium* decreased, whereas abundances of *Chloroflexi*, *Bacillus*, and *Pedomicrobium* increased (Yao et al., 2017). Anderson et al. (2011) found that the biochar addition into soil had a positive effect (which means higher than 5 % changes in bacterial family abundances) on *Bradyrhizobiaceae*, *Hyphomicrobiaceae*, *Streptosporangineae*, and *Thermomonosporaceae*. In this case, the addition leads to an increase in the abundance or reduces losses. On the other hand, the biochar addition resulted in a negative effect on the bacterial family abundance of *Streptomycetaceae* and *Micromonosporacea* (Anderson et al., 2011). In BC-amended soil, an increased relative abundance of *Nitrospirae* and *Verrucomicrobia phylum* was noted in the studies of Fan et al. (Fan et al., 2020). On the other hand, a significant decrease in the *Acidobacteria phylum* was observed. The addition of BC also enhanced soil with some bacterial genera (uncultured *Nitrosomonadace*, uncultured *Nitrospiraceae*, uncultured *Gemmamimonadac*, and *Magnetovibrio*) (Fan et al., 2020). The presence of biochar in soil affects nitrogen cycling due to the enhancement of the abundance of bacteria that participated in this process (for example above-mentioned *Bradyrhizobiaceae* and *Hyphomicrobiaceae*) and promotes phosphate-solubilizing bacteria (Anderson et al., 2011). BC addition also increased the abundance of bacterial families that can modify more recalcitrant C compounds (Anderson et al., 2011). The effect of long-term biochar addition on the soil bacterial community is connected with the changes in soil physicochemical properties (Fan et al., 2020; Yao et al., 2017), such as pH, total N, C, and K content (Yao et al., 2017). BC affects soil microbial growth, diversity, and community compositions by delivering growth promoters for soil biota or shifting soil basic properties (Dai et al., 2021).

Biochar addition into soil modifies the quantitative and qualitative composition of biotic factors, and the changes are highly related to the modification of the physicochemical properties of soil. In biochar-amended soil, both soil and pyrolyzed material are affected by environmental factors. Several parameters of biochars (e.g. large surface area, pore volume, surface charge, density, and pore size distribution) provide indirectly suitable habitats and environmental conditions for microbes. In a 3 yr lasted experiment proceed by Quilliam et al. (2013), due to the stability, unavailability, recalcitrant properties of biochar, and lack of labile carbon, it was noted that changes in soil physicochemical characteristics and the implementation of metabolically available labile compounds into the soil by BC may stimulate and modify soil microbial structure and activity. But on the other hand, how does the soil microbial community affect biochar composition, structure, and properties? Soil microorganisms participate in biochar surface oxidation which leads to an increase in the oxygen-containing functional groups (Quan et al., 2020). Microbes decreased the content of labile carbon and dissolved organic matter (Quan et al., 2020). Moreover, they are involved in biochar solubilization (Quan et al., 2020).

During biochar production, PAHs and their derivatives may be formed. PAHs belong to a group of persistent organic pollutants sourced from natural phenomena (forest fires, volcanic eruptions) and anthropogenic activities (Zheng et al., 2019). Furthermore, they are also produced through the incomplete combustion of biomass (Buss et al., 2016). Together with PAHs, their O-, N-, and S-containing derivatives may be formed during biochar production (namely pyrolysis) (Krzyszczak et al., 2021). PAHs belong to a group of toxic and mutagenic compounds. Thus, International Biochar Initiative and the European Biochar Certificate established a range of permitted levels for the sum of the 16 US Environmental Protection Agency's (EPA) PAHs in BC (6–300 mg kg<sup>-1</sup> d.w. and 4–12 mg kg<sup>-1</sup> d.w., respectively) (Schmidt, 2015). Several papers reveal the bioavailability of PAHs (Oleszczuk and Koltowski, 2018). Thus, the information about the extent of PAHs derivatives' bioavailability is very limited.

Due to the literature data and research gaps, our study aimed to establish how biological and enzymatic aging affect the content of total and bioavailable fractions of polycyclic aromatic hydrocarbons (PAHs) and their N- and O-containing derivatives in biochars. We have assumed that biotic factors had significantly influenced the content, and mostly, the bioavailability of studied analytes. The selected analytes are toxic mutagenic and carcinogenic, and they can be formed during pyrolysis but also under environmental conditions. The physicochemical characterization of pristine and modified materials was also performed to associate the obtained data with the changes in analyte content. It is worth mentioning that only a few articles deal with the topic of biochar aging and its effect on the physicochemical parameters of pyrolyzed material. Some of them presented the changes in the content of PAHs. But none of them introduced the effect of aging processes on the content of total, and the most important, bioavailable fraction of PAHs derivatives. Moreover, most of the results available in the literature consider short-term experiments. Thus, our study aimed to determine the effect of biological agents on the physicochemical characteristic and the content of PAHs and their derivatives in biochars after long-term treatment (6 months). Previous research revealed that during this period the most significant changes in biochar characteristics took place (Siatecka et al., 2021) and continued aging did not affect the physicochemical parameters of BC significantly. Due to the nature of enzymes, enzymatic aging lasted only 11 days. Moreover, the experiments were led in two tracks to differentiate the effect of soil microorganisms and their activity, and the enzymes alone. It has been proven that the biochar physicochemical characteristics and the effect of aging depend on the type of feedstock and the pyrolysis temperature (Krzyszczak et al., 2022b; Siatecka et al., 2021). It was also demonstrated in our previous research that biochar obtained at 600 °C stand out from other (produced at 500 °C and 700 °C), and both the measured physicochemical parameters and the content of bioavailable and total fraction of PAHs and their derivatives often did not change linear but the biochar (obtained at 600 °C) was characterized by the highest/lowest values (boundary values) (Krzyszczak et al., 2021, 2022a, 2022b), e.g. the highest content of total fraction and the lowest content of bioavailable fraction of PAHs in willow-derived BC; the lowest surface area in biochars obtained from residues from biogas production and the highest in willow-derived materials. Thus, we presented the results considering biochar obtained from various feedstocks at the same pyrolysis temperature of 600 °C.

## 2. Material and methods

### 2.1. Feedstock and biochar preparation

For the BC preparation, several feedstocks were used (Table 1). Among all feedstocks, ash-rich materials (A-rich) (e.g. sewage sludge), lignin-rich (L-rich) (e.g. hardwood/softwood), cellulose-rich (C-rich) (e.g. wheat straw, willow), and residues from biogas production-derived BC (RBP) can be distinguished (Table 1). Wheat straw-derived biochar (BCS-initial) was collected from Mostostal Sp. z o.o. (Wrocław, Poland). The other biochars (from willow (BCW-initial), sewage sludge (BCZ-initial), softwood (BCD-initial) and hardwood residues (BCF-initial), and RBP (BCUHS-initial,

**Table 1**

Applied feedstock and the labeling of studied biochars.

Feedstock		Location/supplier	Initial biochar name
Type	Detail		
C-rich	Wheat straw ( <i>Triticum L.</i> )	Mostostal Sp. z o.o. (Wrocław, Poland)	BCS-initial
	Willow ( <i>Salix viminalis</i> )	The southeastern part of Poland	BCW-initial
L-rich	Residues from hardwood	Fluid S.A. (Sędziszów, Poland)	BCD-initial
	Residues from softwood	Fluid S.A. (Sędziszów, Poland)	BCF-initial
RBP	Residues from biogas production (RBP)		BCUHS-initial
	Uhnin (51°58'33"N, 23°03'33"E, Poland)		BCKOS-initial
	Kocergi (51°63'33"N, 22°58'33"E, Poland)		BCKOS-initial
A-rich	Piaski (51°61'07"N, 22°55'00"E, Poland)		BCPIL-initial
	Zamość (50°43'14"N 23°15'31"E, Poland)		BCZ-initial
	Zamość (50°43'14"N 23°15'31"E, Poland)		BCZ-initial

BCKOS-initial, BCPII-initial)) were produced according to the protocol described in our previous papers (Krzyszczak et al., 2021, 2022a). The feedstocks were carefully maintained (air-dried, fragmented, grounded with a mill (TESTCHEM, Poland), and homogenized) before pyrolysis.

Detailed information on pyrolysis conditions is presented in Supplementary Information (SI). Before all experiments, BC was stored at room temperature in the absence of light.

## 2.2. The biological aging of biochars

Biological aging (BA) was designed to expose the biochar to a microbial inoculum and nutrient solution (BAi samples) or only nutrient solution (BAn) following the protocol described by Oleszczuk and Kołtowski (2018). The microbial inoculum was extracted from soil acquired from farmland in Podborze, Poland (50°42'21"N 22°50'58"E). The soil was incubated for 18 days at 30 °C. Then, the deionized water was added and the system was rolled on a rotary shaker ROTAX 6.8 VELP Scientifica (Italy) for 2 days at 10 RCF. Subsequently, the mixture was filtered via 2.7 µm paper. The composition of the nutrient solution (NS) was as follows: 6.38 g L<sup>-1</sup> glucose, 40.66 g L<sup>-1</sup> NH<sub>4</sub>Cl, 4.67 g L<sup>-1</sup> KH<sub>2</sub>PO<sub>4</sub>, 10.00 mg L<sup>-1</sup> peptone, 24.00 mg L<sup>-1</sup> CaCl<sub>2</sub>, 4.00 mg L<sup>-1</sup> MnSO<sub>4</sub>, 4.00 mg L<sup>-1</sup> ZnCl<sub>2</sub>, 4.00 mg L<sup>-1</sup> CuSO<sub>4</sub>, 16.00 mg L<sup>-1</sup> MgCl<sub>2</sub> and a glucose supplement 40 mg mg<sup>-1</sup> BC. The volume of added microbial inoculum and nutrient solution (BAi samples) or only nutrient solution (BAn) amounted to 40 % of BC water holding capacity (WHC) and this level of WHC was maintained during 6 months of the experiment. The period was selected because, as it was presented in previous studies (Siatecka et al., 2021), the extension of the aging process (e.g. to 12 months) did not significantly affect the physicochemical characteristics of BC. Biologically-aged biochars were named by substitution the word "initial" from biochars names (Table 1) with "BAi" (biochars aged with microbial inoculum and nutrient solution) or "BAn" (BC aged with nutrient solution), for example before aging: BCW-initial, BCD-initial, after aging with inoculum and NS: BCW-BAi, BCD-BAi, after aging with NS: BCW-BAn, BCD-BAn.

**Table 2**  
Methods applied for BC characterization.

Technique	Measured parameter	Apparatus	Selected parameters
pH measurement	pH of studied biochars	digital pH meter HQ430d Benchtop Single Input (HACH, USA)	1 g of biochar/10 mL of distilled water
ash content	ash content [%]	furnace (MagmaTherm)	exposure of 1 g of biochar to 760 °C for 6 h
The content of basic elements	C, H, N content [%]	CHN/CHNS EuroEA3000 Elemental Analyzer (EuroVector)	milled biochar
X-ray photoelectron spectroscope	surface composition and functional groups	UHV (Prevac)	milled biochar
Scanning Electron Microscopy	surface morphology	Quanta 3D FEG (FEI)	milled biochar
N <sub>2</sub> adsorption	surface area and porosity	ASAP 2420 Analyzer (Micromeritics, USA)	outgassing at 200 °C for 12 h under vacuum
FT-IR technique	Surface characterization functional groups	Bio-Rad Excalibur 3000 MX spectrometer equipped with photoacoustic detector MTEC300	Milled biochar

## 2.3. The enzymatic aging of biochars

Biochars were aged by enzymatic oxidation using horseradish peroxidase, according to a protocol described by Sigmund et al. (2017). Biochar (1 g) was suspended in an aqueous solution consisting of 0.01 mol L<sup>-1</sup> phosphate-buffered saline adjusted to a pH = 6 and 600 enzyme units of horseradish peroxidase (Sigma Aldrich, Poland). The system was incubated for 24 h. Then, the enzyme was activated with 500 µmol L<sup>-1</sup> H<sub>2</sub>O<sub>2</sub>. The slurry was mixed on a magnetic stirrer (IKA, Poland) (300 rpm) for 10 days. The suspension was filtered and aged BC was dried at 105 °C for 2 h. Enzymatically-aged biochars were named by substitution the word "initial" from biochars names (Table 1) to "EA", for example before aging: BCW-initial, BCZ-initial, after aging with horseradish peroxidase: BCW-EA, BCZ-EA.

## 2.4. The physicochemical characterization of BC before and after aging processes

The physicochemical characteristics of biochars involved several methods presented and described in Table 2.

## 2.5. The determination of the total and bioavailable fraction of PAHs and their derivatives in biochar

The total fraction of PAHs and their derivatives were extracted and determined via the protocol described in our previous paper (Krzyszczak et al., 2022b). Briefly, analytes were isolated using pressurized liquid extraction (Dionex 350 system, Thermo Fisher Scientific). The obtained extract (enriched with isoctane) was concentrated (to 1.0 mL) and gas chromatography with tandem mass spectrometry (GC-MS/MS) analysis was performed. The details of GC-MS/MS are specified in SI.

The bioavailable fraction of PAHs and their derivatives was determined via the protocol described in our previous studies (Krzyszczak et al., 2021, 2022a, 2022b) using polyoxymethylene (POM) passive samplers and 30 days-interaction. The second step included the extraction of analytes with a mixture of acetone/heptane (20:80, v/v) with the addition of

**Table 3**

Physicochemical properties of pristine and aged biochar.

BC	$S_{BET}$ [ $\text{m}^2 \text{ g}^{-1}$ ]	Ash content [%]	C [%]	H [%]	N [%]	O [%]	H/C	(O + N)/C	O/C
BCS-initial	2.47	19.59	66.14	1.66	1.26	11.36	0.300	0.145	0.129
BCS-EA	34.89	11.11	70.58	1.66	1.53	15.12	0.024	0.236	0.214
BCW-initial	145.02	7.09	82.77	2.24	1.68	9.53	0.027	0.135	0.115
BCW-BAn	2.96	3.58	81.40	1.43	1.11	12.47	0.018	0.167	0.153
BCW-BAi	<LOD	3.74	82.41	0.98	1.16	11.71	0.012	0.156	0.142
BCW-EA	<LOD	2.84	82.65	1.61	1.17	11.73	0.020	0.156	0.142
BCD-initial	1.15	10.77	61.50	3.11	1.18	23.41	0.051	0.400	0.381
BCD-BAn	1.65	11.85	59.89	2.61	1.07	24.57	0.044	0.428	0.410
BCD-BAi	1.65	11.96	56.95	2.41	1.23	27.45	0.042	0.504	0.482
BCF-initial	0.75	3.90	77.54	3.93	0.24	22.18	0.051	0.289	0.286
BCF-BAn	14.03	0.87	74.66	3.22	0.64	20.62	0.043	0.285	0.276
BCF-BAi	<LOD	0.78	75.30	2.31	<LOD	21.62	0.031	0.287	0.287
BCUHS-initial	6.80	35.40	51.25	1.27	1.97	10.11	0.300	0.180	0.150
BCUHS-EA	13.36	20.84	63.01	1.81	1.86	12.48	0.029	0.228	0.198
BCKOS-initial	1.20	15.00	66.86	1.67	2.09	14.37	0.300	0.190	0.160
BCKOS-EA	0.43	9.90	72.21	1.76	2.01	14.12	0.024	0.223	0.196
BCPIL-initial	1.80	44.30	34.95	1.06	2.10	17.57	0.360	0.430	0.380
BCPIL-EA	199.50	26.71	52.12	1.84	3.19	16.14	0.035	0.371	0.310
BCZ-initial	79.56	63.58	24.45	0.86	2.24	8.84	0.035	0.453	0.362
BCZ-BAn	56.25	64.74	23.75	0.52	2.52	8.48	0.022	0.463	0.357
BCZ-BAi	47.08	64.10	25.42	0.88	2.43	7.18	0.035	0.378	0.282
BCZ-EA	66.92	58.75	29.09	1.03	2.21	8.92	0.035	0.383	0.307

 $S_{BET}$  – the specific surface area of adsorbents;

O-oxygen, C-carbon, N-nitrogen, H-hydrogen;

O content is calculated by subtracting ash, C, H, and N content from the total mass of the sample;

O/C, (N + O)/C, H/C = molar ratios;

&lt;LOD - below the limit of detection.

20  $\mu\text{L}$  of deuterated PAHs for 48 h on a horizontal shaking machine ELPIN 358A (Poland). The obtained extract (enriched with isoctane) was concentrated and the GC-MS/MS analysis was carried out.

## 2.6. Statistical analysis

The statistical analysis was carried out to determine the statistical significance of each parameter (both physicochemical parameters of biochars and the total and bioavailable fraction of PAHs and their derivatives in pyrolyzed materials) affected by aging processes by one-way analysis of variance (one-way ANOVA). The level of statistical significance was considered at  $p < 0.05$ . The Statgraphics Plus 3.0 software was used for these calculations. The results were presented as the mean value of three replicates  $\pm$  standard deviation (SD). Pearson test was applied for the estimation of linear correlations.

## 3. Results and discussion

### 3.1. The effect of the biological and enzymatic aging on the physicochemical properties of biochar

The physicochemical properties of biochar derived from several feedstocks at 600 °C are shown in Table 3.

The type of feedstock as well as the aging processes did not affect significantly the  $S_{BET}$  ( $p > 0.05$ ) as no clear correlations were noted. However, in almost all cases EA increased and BA decreased the content of C% and H% in BC. There was no clear trend considering the content of N% and O%. Cellulose-rich biochars were characterized by the highest content of C whereas the ash-rich ones had the lowest C%. EA decreased the content of ash in all cases, whereas BA caused a drop only in 50 % of samples. In the other ones, biological aging increased the percentage of ash content. Both aging processes lowered the H/C ratio which indicated the decrease of the aromatization degree for artificially altered biochar. Moreover, the correlation between the H/C ratio and the aging processes was found to be statistically significant ( $p < 0.05$ ). It means that both enzymatic and biological aging affects significantly the H/C ratio. Considering lignin- and cellulose-rich biochar, and RBP-derived BC, EA caused an increase in their polarity ((O + N)/C) and hydrophilicity (O/C). Only in BCZ and BCPIL samples, these parameters were reduced. In the case of biochars aged biologically, the trend was not so obvious. It is worth mentioning, that the content of ash, C%, H%, N%, and O% were affected by the type of feedstock ( $p < 0.05$ ). H/C ratio and polarity were also significantly influenced by the type of raw material. This observation is consistent with the literature data. It was evidenced that biochar obtained at a lower temperature (350 °C) was more susceptible to biological degradation by soil microbes (*Streptomyces* isolate) than that obtained at 550 °C (Zeba et al.,

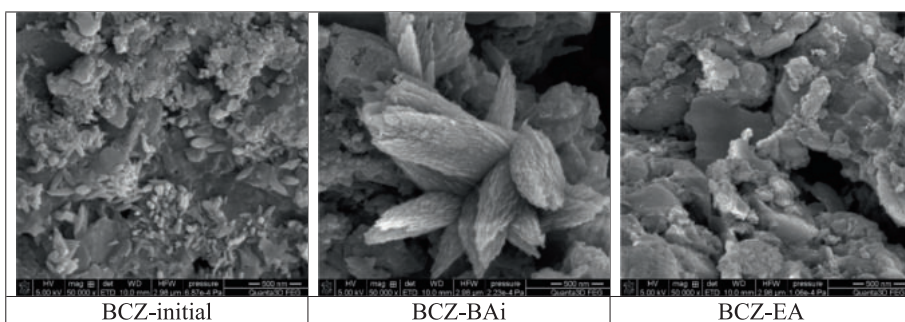


Fig. 1. SEM images of BCZ samples before and after biological and enzymatic aging.

2022). The lower total C and higher total O content than initial materials (Zeba et al., 2022), and thus an increase in O/C ratios (Cheng et al., 2006; Quan et al., 2020; Zeba et al., 2022) in aged biochar may indicate that formation and transformation of PAHs and derivatives in BC in the environment may be altered.

The morphology of the BC after aging was changed (with BCZ as the example presented in Fig. 1), however, the changes in the morphology were subtle. In general, before aging the structure was more compact, and after aging several heterostructures were observed. After contact with microbial inoculum, the structure was disordered and resembles seeds and flowers. Due to the action of the enzyme, horseradish peroxidase, the structure of BC was crushed and more powdered.

Aging affected the BC structure and surface composition. In the XPS spectrum, it was noted that although the general survey was not changed (Fig. 2a.) the closer analysis revealed that the amount of C and O changed whereas the character of the surface groups also was altered (Fig. 2 b, c, d). The surface of BCZ600 before aging was composed mostly of C in the form of carbonyl, hydroxyl, and carboxylic groups, and aliphatic carbons (Koinuma et al., 2013; Rabchinskii et al., 2020); O in the form of bonds: O-(C=O)-C, O=C-N, and organic C—O (Oh et al., 2014), with the addition of N, Ca, P, Si, Fe, S (below 5 at.%). In the case of BCZ600 samples, the content of C% (from initial 52.5 at.%) increased to 55.9 at.% of C after BA and lowered to 55.2 at.% after EA. At the same time, the content

of O% (starting from 28.15 at.%) was lowered to 25.5 at.% after BA and to 25.1 at.% after EA. It is worth mentioning that the character of the functional groups was changed. In general, the XPS peak of C in aged BC (Fig. 2b) after deconvolution revealed the presence of different species such as aliphatic carbon (C—H sp<sup>3</sup>, C—C sp<sup>3</sup>), aromatic carbon (C=C sp<sup>2</sup>), hydroxyl, epoxy, carbonyl and carboxyl groups, and defective carbon structures (C—C C=—C) (Koinuma et al., 2013).

### 3.2. The effect of the biological aging process on the total content and characteristics of PAHs and their derivatives in biochar

The aging of biochar, occurring naturally in the environment, can be accelerated with the aid of microorganisms. The microbial activity can be amplified through the addition of labile organic compounds (in our case glucose and several different components) or fresh biomass (Hamer et al., 2004; Mia et al., 2017; Pietikäinen et al., 2000). After the biological aging of BCW (BCW-initial, BCW-BAn, BCW-BAi) and BCZ (BCZ-initial, BCZ-BAn, BCZ-BAi), the identical trend is observed: the highest content of the total fraction of PAHs, Σ16PAHs, and PAHs derivatives was in the sample before aging (initial BC). Then, in descending order were samples with nutrient solution (BAn), and the lowest content was quantified for biochar aged with nutrient solution and microbial inoculum (BAi) (Table 4). Biological aging with NS and microorganisms extracted from soil resulted in the

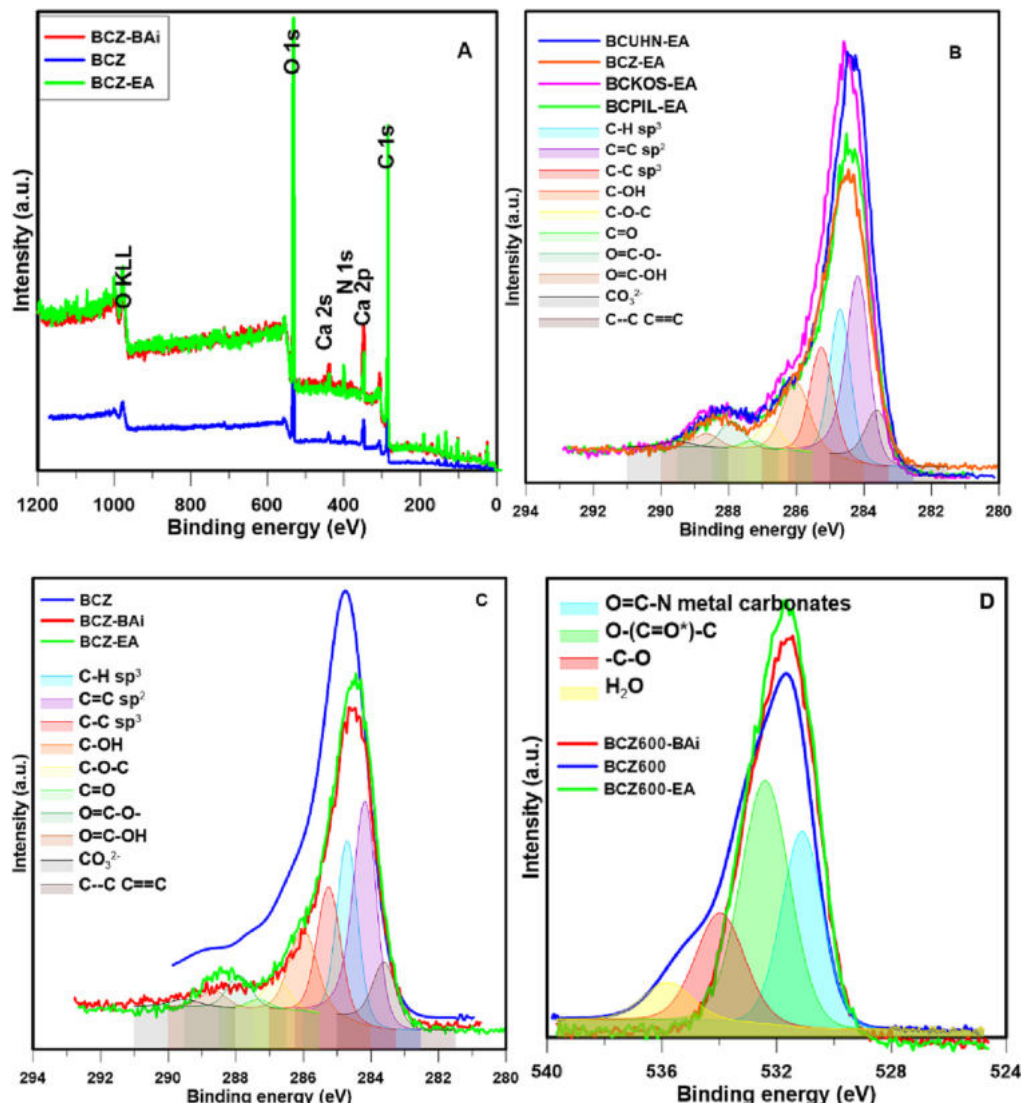


Fig. 2. XPS studies of the BC samples, A) survey, B) Carbon peak after enzymatic aging, C) Carbon peaks in aged BCZ, D) Oxygen peaks.

**Table 4**

The content of total and bioavailable PAHs and their derivatives in tested BC.

Sample description	The concentration of total PAHs ± SD [µg g⁻¹]	The concentration of total Σ16PAHs ± SD [µg g⁻¹]	The concentration of total PAHs derivatives ± SD [µg g⁻¹]	The concentration of bioavailable PAHs ± SD [ng L⁻¹]	The concentration of bioavailable Σ16PAHs ± SD [ng L⁻¹]	The concentration of bioavailable PAHs derivatives ± SD [ng L⁻¹]
BCW-initial	181.08 ± 8.29	171.30 ± 7.85	1.92 ± 0.09	3.17 ± 0.15	2.92 ± 0.14	0.48 ± 0.02
BCW-BAn	140.25 ± 6.59	134.55 ± 6.32	1.76 ± 0.08	4.02 ± 0.21	4.02 ± 0.21	<LOD
BCW-BAi	99.18 ± 4.14	96.14 ± 4.01	1.38 ± 0.06	7.35 ± 0.39	7.33 ± 0.39	0.18 ± 0.01
BCW-EA	10.14 ± 0.46	9.86 ± 0.45	0.120 ± 0.005	2.00 ± 0.07	1.99 ± 0.07	1.21 ± 0.04
BCD-initial	57.36 ± 2.63	20.54 ± 0.95	<LOD	2.21 ± 0.11	2.12 ± 0.11	<LOD
BCD-BAn	66.47 ± 3.12	24.75 ± 1.20	<LOD	0.28 ± 0.01	0.124 ± 0.006	<LOD
BCD-BAi	57.61 ± 2.56	21.13 ± 0.96	<LOD	1.12 ± 0.06	0.81 ± 0.04	<LOD
BCF-initial	134.01 ± 6.14	75.24 ± 3.46	11.89 ± 0.54	3.67 ± 0.17	3.53 ± 0.17	0.32 ± 0.02
BCF-BAn	165.93 ± 7.93	94.20 ± 4.59	12.70 ± 0.61	2.87 ± 0.15	2.77 ± 0.15	0.127 ± 0.007
BCF-BAi	140.80 ± 6.26	81.35 ± 3.67	11.58 ± 0.52	4.40 ± 0.23	4.24 ± 0.22	0.24 ± 0.01
BCZ-initial	125.83 ± 5.76	103.74 ± 4.96	5.30 ± 0.24	39.98 ± 1.46	39.71 ± 1.45	1.90 ± 0.07
BCZ-BAn	96.42 ± 4.53	81.17 ± 3.94	1.35 ± 0.06	5.28 ± 0.27	5.28 ± 0.27	0.013 ± 0.001
BCZ-BAi	43.05 ± 2.02	36.72 ± 1.76	0.82 ± 0.04	6.59 ± 0.35	6.49 ± 0.34	0.109 ± 0.005
BCZ-EA	15.03 ± 0.69	12.65 ± 0.59	0.74 ± 0.03	3.08 ± 0.11	3.04 ± 0.11	1.19 ± 0.04
BCS-initial	145.21 ± 6.65	56.63 ± 2.59	28.39 ± 1.30	2.56 ± 0.11	2.36 ± 0.10	0.83 ± 0.03
BCS-EA	30.40 ± 1.39	8.35 ± 0.38	4.62 ± 0.21	0.35 ± 0.01	0.29 ± 0.01	0.35 ± 0.01
BCUHS-initial	201.64 ± 9.23	184.93 ± 8.47	5.62 ± 0.26	41.53 ± 1.52	41.32 ± 1.51	0.88 ± 0.03
BCUHS-EA	39.85 ± 1.82	35.01 ± 1.60	1.14 ± 0.05	4.00 ± 0.15	3.97 ± 0.15	0.195 ± 0.006
BCKOS-initial	180.18 ± 8.25	163.16 ± 7.70	3.42 ± 0.16	10.36 ± 0.38	9.41 ± 0.34	0.217 ± 0.008
BCKOS-EA	14.98 ± 0.69	14.98 ± 0.69	0.68 ± 0.03	1.87 ± 0.07	1.87 ± 0.07	0.038 ± 0.001
BCPIL-initial	187.31 ± 8.58	159.81 ± 7.55	16.19 ± 0.74	10.38 ± 0.38	8.99 ± 0.33	4.64 ± 0.17
BCPIL-EA	25.63 ± 1.17	20.50 ± 1.03	4.87 ± 0.22	1.07 ± 0.04	0.91 ± 0.03	2.40 ± 0.09

LOD- limit of detection.

highest ratio between LMW (low-molecular-weight compounds with  $\leq 3$  aromatic rings) and HMW (high-molecular-weight compounds with  $\geq 4$  aromatic rings) PAHs.

The total fraction of PAHs derivatives dropped by 8 % and 28 % in BCW, as well as 74 % and 85 % for BCZ after BA with NS alone and both NS and microbial inoculum, respectively. In all cases (BCW-initial, BCW-BAn, BCW-BAi, BCZ-initial, BCZ-BAn, BCZ-BAi) only two-ring derivatives: 1-methyl-5-nitronaphthalene, 1-methyl-6-nitronaphthalene, and nitroacenaphthalene were identified. In BCW samples, the content of 2- and 3-ring PAHs were in majority (~75 %) with naphthalene, acenaphthylene, and acenaphthene as the most widespread (Fig. 3a). In BCZ samples, compounds with two rings (mostly naphthalene) accounted for nearly two times higher values than those with 3 rings (mostly acenaphthylene, fluorene, and acenaphthene) (45 %–49 % for 2-rings, and 24 %–25 % for 3-rings). Moreover, 5-ring species constituted a majority in comparison to 4-ring ones (15 %–17 %, and 11 %–13 %, respectively) (Fig. 3b). The first group was mainly represented by benzo[a]fluoranthene and benzo[b]fluoranthene, while the second one was by pyrene. As the presence of microbial inoculum in biochar caused the highest drop in the content of analytes, thus the organisms acquired from the soil play a significant role in PAHs and their derivatives' degradation and modification.

In softwood and hardwood-derived biochar, the highest content of total PAHs (and Σ16PAHs) was quantified in the sample subjected to the effect of the nutrient solution alone (Table 4). In hardwood-derived biochar (BCD), 4-ring species constituted >50 % of all quantified PAHs, and benzo[a]fluorene and 6-methylchryzene were predominant. Among 3-, 2-, 5- and 6-ring compounds (Fig. 3c), acenaphthene, 1,3-di-isopropylnaphthalene, benzo[a]pyrene, and both dibenz[a,e]pyrene and dibenz[a,h]pyrene were determined. In BCF, fluorene, 3,6-dimethylphenanthrene, benzo[a]fluorene, and benzo[a]anthracene were representing 3- and 4-ring PAHs, whereas, 2- (only naphthalene) and 5-ring (mostly dibenz[a,h]anthracene and benzo[a]pyrene) compounds were in minority (6 %–7 % and 19 %–22 %, respectively). There were no 6-ring species quantified. It is worth mentioning that the content of the total fraction of PAHs derivatives in hardwood-derived biochar was below the limit of detection. In BCD and BCF, the highest percentages of LMW PAHs were detected in initial samples (41.76 % and 43.75 %, respectively), and aging lowered the content of LMW PAHs. In softwood-derived BC both 3- and 4-ring species were quantified (9,10-anthracenedione and 4H-cyclopenta(def)phenanthrene), and PAHs derivatives constituted up to 8 % of all quantified compounds. The

highest content of derivatives (considering all BCF samples) was found in BCF-BAn and the lowest in BCF-BAi.

The changes in the content of bioavailable and total fraction of PAHs and their derivatives before and after biological aging, however, were not statistically significant considering the type of feedstocks applied in the experiment. Biological aging (conducted on two tracks: biochar with NS and biochar with NS and microbial inoculum) also did not affect significantly the sum of bioavailable and total PAHs and derivatives ( $p > 0.05$ ). As was presented in Siatecka et al. (2021), biochar with a higher mineral content (for example obtained from SSL) was less stable during abiotic aging than the other BC (willow-derived BC). In the case of our results, the conclusions were not evident. The range of changes in the content of bioavailable and total fraction of PAHs and their derivatives depended on the type of biochar and aging conditions. They also concluded that this type of aging-triggered modification was governed by the type of feedstock and the pyrolysis temperature (Siatecka et al., 2021). But it is worth pointing out that abiotic factors caused biochar oxidation, an increase in the amount of surface oxygen functional groups, degree of hydrophilicity, polarity, and pH decrease. According to the literature (Oleszczuk and Kołtowski, 2018), biological aging (with microbial inoculum and nutrient solution as well as with nutrients alone) caused the greatest reduction in the content of bioavailable and total fraction of PAHs (12 % - 100 % and 30 % - 100 %, respectively) in comparison to chemical and physical aging. The addition of nutrients and/or providing a suitable amount of water to achieve saturated conditions constitute an important factor influencing PAHs degradation (Oleszczuk and Kołtowski, 2018; White et al., 1999; White and Alexander, 1996).

### 3.3. The effect of the enzymatic aging process on the total content and characteristics of PAHs and their derivatives in biochar

Enzymatic aging decreased the content of the total fraction of PAHs (Σ16PAHs) and their derivatives (Table 4). The decrease in the PAHs concentration amounted to 79 %–94 %, whereas the content of PAHs derivatives dropped by 67 %–94 %. EA changed also the content of individual groups of PAHs differing in the number of aromatic rings. In almost all cases (except BCPIL), EA reduced the percentage of 2-ring species and increased 4-ring PAHs, for example, the contribution of the first-mentioned group in BCW decreased from 35 % to 23 %, and the second-mentioned increase from 22 % to 31 % (Fig. 3a). Naphthalene was the most abundant 2-

ring PAHs (except BCS and BCPII - 1,3-di-isopropylnaphthalene) in biochar before enzymatic aging and the only representative of 2-ring species in biochar after EA. Among 4-ring compounds, the highest content was determined for pyrene (in BCW-initial, BCW-EA, BCZ-initial, and BCZ-EA), benzo[a]fluorene, and benzo[a]antracene (in BCS-initial and BCS-EA), chrysene, pyrene, and fluoranthene (in BCUHS, BCKOS, and BCPII samples, respectively). In half of the samples, EA increased the content of 3-(in BCW, BCZ, and BCPII) and 5-ring compounds (in BCW, BCUHS, and BCPII) (Fig. 3 a, b, and c). Among 3-ring PAHs, the most abundant were acenaphthylene and/or acenaphthene (in BCW, BCUHS, and BCZ samples), 3-methylphenanthrene (in BCS-initial and 2-methylphenanthrene in BCS-EA), and anthracene (in BCKOS, and BCPII samples). In the other biochars, the effect of EA was the opposite. In most cases, enzymatic aging decreased the percentage of the 6-ring compounds, even to a level below the limit of detection. EA caused a decrease in the percentage share of LMW PAHs in comparison to HMW PAHs (except BCPII-initial and BCPII-EA). The decline was between 7 % (for BCZ-initial vs. BCZ-EA) and 25 % (for BCUHS-initial vs. BCUHS-EA).

EA did not change the qualitative analysis of PAHs derivatives in studied biochars. Only their concentration declined (Table 4). 2-, 3-, and 4-ring PAHs derivatives were determined. In BCW-initial and BCZ-EA only nitronaphthalene was determined, whereas, in other plant-derived BC (BCS-initial and BCS-EA), 1-methyl-5-nitronaphthalene, 1-methyl-6-nitronaphthalene, and 4H-cyclopenta(*def*)phenanthrene were identified. In BCZ-initial and BCZ-EA only 2-ring N-PAHs were measured (1-methyl-5-nitronaphthalene, 1-methyl-6-nitronaphthalene). The findings concerning RBP-derived BC were also not tendentious and both N- and O-PAHs were quantified. Thus, the type of feedstock does not affect the qualitative and quantitative analysis of PAHs derivatives in BC. The changes in the content of the total fraction of PAHs and their derivatives before and after enzymatic aging are not statistically significant considering the type of feedstocks applied in the experiment. But EA affects significantly the total fraction of PAHs ( $p < 0.05$ ) and their derivatives ( $p \sim 0.05$ ). Sigmund et al. (2017) found that the properties of biochar such as surface areas, pore volumes, and elemental compositions were resilient to  $H_2O_2$  thermal oxidation or horseradish peroxidase enzymatic oxidation of biochar. This indicated the high biochar stability. The concentrations of total and bioavailable  $\Sigma 16$ PAHs ranged from 4.4 to 22.6 mg kg<sup>-1</sup> and 0.0 to 9.7 mg kg<sup>-1</sup>, respectively (Sigmund et al., 2017). Their results considering the effect of enzymatic aging on the content of the total fraction of PAHs showed the same trend as it can be found in our data: EA significantly decreased the content of PAHs. Artificial aging ( $H_2O_2$  thermal oxidation or horseradish peroxidase enzymatic oxidation) resulted in a decrease in the relative content of LMW PAHs (with  $\leq 3$  aromatic rings). It can be caused by lower lipophilicity and higher solubility of LMW PAHs which lead to their facilitated desorption from biochar (in comparison to HMW PAHs (with  $\geq$  four aromatic rings)) (Sigmund et al., 2017). In general, agricultural application of biochar with low initial PAHs concentration (with amounts that meet the requirements of European Biochar Certificate (EBC) and International Biochar Initiative (IBI) quality thresholds for total PAHs concentrations) can be assumed to be safe. Otherwise, pyrolyzed materials require more critical evaluation because their addition to soil may be associated with the risk (especially in high doses) (Sigmund et al., 2017).

### 3.4. The bioavailable fraction of PAHs and their derivatives in biochar before and after the biological aging process

The most important from an environmental point of view is the bioavailability of PAHs and their derivatives. In each plant-derived BC subjected to biological aging, the trend was different. Particularly, in BCW samples the lowest amount of bioavailable PAHs were found in the initial material ( $3.17 \pm 0.15$  ng L<sup>-1</sup>), while the highest was in BCW-BAi ( $7.35 \pm 0.39$  ng L<sup>-1</sup>) (Table 4). In this case, biological aging caused a significant increase in PAHs bioavailability. In all other cases, BCD, BCF, BCZ, the lowest amount was quantified in the BAn sample (biochar with NS: BCD-BAn, BCF-BAn, BCZ-BAn) (Fig. 4a). In BCD and BCZ, the higher

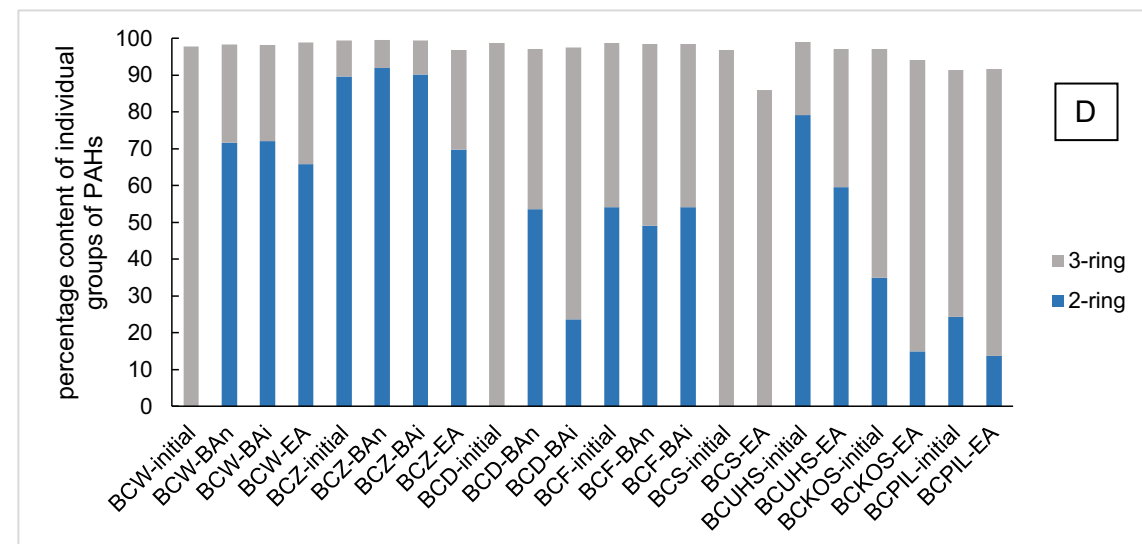
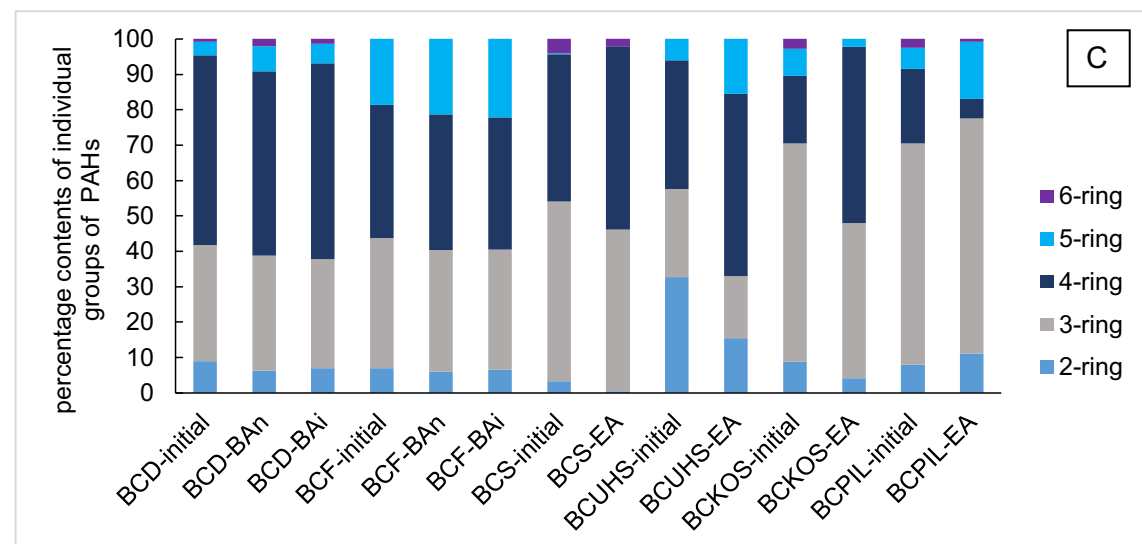
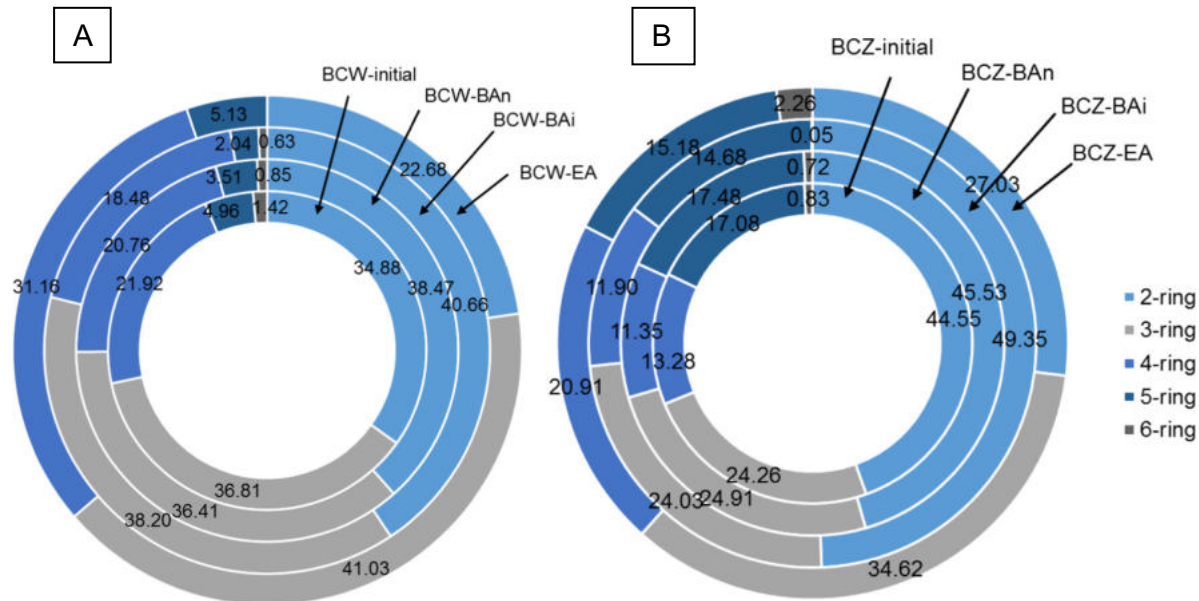
content was found in BAi samples (BCD-BAi:  $1.12 \pm 0.06$  ng L<sup>-1</sup> and BCZ-BAi:  $6.59 \pm 0.35$  ng L<sup>-1</sup>) and the highest in initial BC (Table 4), which indicated that the presence of inoculum inhibits the decomposition/transformation of PAHs compared to blank samples. In BCF the content of the bioavailable fraction of analytes increased in the following order: BCF-BAn < BCF-initial < BCF-BAi, which indicated that biological aging without inoculum caused the decrease in analyte bioavailability and the presence of inoculum increased the content of studied fraction of PAHs. In the case of the content of  $\Sigma 16$ PAHs, the trends were identical. The biological aging slightly affected the percentage of 2- and 3-ring PAHs in BCZ (2-ring: 90 % (BCZ-initial) - 92 % (in BCZ-BAn), 3-ring: 8 % (BCZ-BAn)- 10 % (BCZ-initial) and BCF samples (2-ring: 49 % (BCF-BAn) - 54 % (BCF-BAi), 3-ring: 44 % (BCF-BAi)-49 % (BCF-BAn)) (Fig. 3d), where the most dominant were naphthalene, acenaphthylene, and fluorene. In the other biochar (BCD and BCW), the content of 2-ring species in biochar before aging was below the limit of detection (Fig. 3d) and after BA, their level increased to 72 % in BCW-BAi, BCW-BAn, 24 % in BCD-BAi, and 54 % in BCD-BAn. The highest percentages of 3-ring compounds (mostly acenaphthene) were found in initial samples: BCD-initial – 99 % and BCW-initial 98 %, then in biologically aged BC. In the case of 4-, 5- and 6-ring species, the changes in the percentage were not tendentious and significant. In certain cases, biological aging caused a decrease in the percentage of the 6-ring group, even to a level below the limit of detection. In all biochars (aged and non-aged) the percentage share of LMW PAHs was in the range of 97 %–9 %, respectively, while HMW constituted <3 % of all quantified PAHs. Biological aging did not significantly affect the ratio between LMW and HMW PAHs.

The content of the bioavailable fraction of PAHs derivatives in residues from hardwood-derived biochar before and after biological aging was below the limit of detection. In the other biochars (BCF, BCW, and BCZ) the content of PAHs derivatives decreased in the following order: initial biochars, biochar treated with microbial inoculum and NS (a decline of 26 % in BCF-BAi, 62 % in BCW-BAi, and 94 % in BCZ-BAi), and biochar contacted only with NS (a drop of 61 % in BCF-BAn, 99 % in BCZ-BAn and below the limit of detection in BCW-BAn) (Fig. 4a). Biological aging also caused the changes in the PAHs derivatives profile in the case of BCW samples. In BCW-initial there were 4H-cyclopenta(*def*)phenanthrene and nitropyrene quantified, whereas in BCW-BAi only nitronaphthalene was determined. In BCZ-initial, both 3- and 4-ring PAHs derivatives were noted (1-methyl-5-nitronaphthalene, 1-methyl-6-nitronaphthalene, and 9,10-anthracenedione), whereas, in BCZ-BAi and BCZ-BAn, only the 4-ring PAHs derivatives were represented. In BCF samples, only O-PAHs were determined (9,10-anthracenedione and 4H-cyclopenta(*def*)phenanthrene in BCF-initial and BCF-BAi).

The changes in the content of both fractions of PAHs and their derivatives before and after BA are not statistically significant considering the type of feedstocks. Biological aging also did not affect significantly the sum of bioavailable and total PAHs and derivatives ( $p > 0.05$ ). However, some positive correlations (Pearson test,  $p < 0.05$ ) considering PAHs and their derivatives were observed, e.g. i) between the total fraction of PAHs derivatives in biochar after treatment with NS and both NS and microbial inoculum; ii) the bioavailable fraction of PAHs derivatives in biochar treated with microbial inoculum and the total fraction of PAHs in biochar treated with NS; bioavailable fraction of PAHs derivatives in biochar after treatment with NS and total fraction of PAHs derivatives after treatment with NS and both NS and microbial inoculum; iii) total fraction of PAHs (initial samples) and the bioavailable fraction of PAHs derivatives (initial samples).

### 3.5. The bioavailable fraction of PAHs and their derivatives in biochar before and after the enzymatic aging process

In almost all studied BC, enzymatic aging caused a significant decrease in the content of the bioavailable fraction of PAHs ( $\Sigma 16$ PAHs) and their derivatives (Table 4 and Fig. 4b) except for the content of the derivatives in BCW (Table 4). The smallest decrease was recorded for BCW-initial vs.



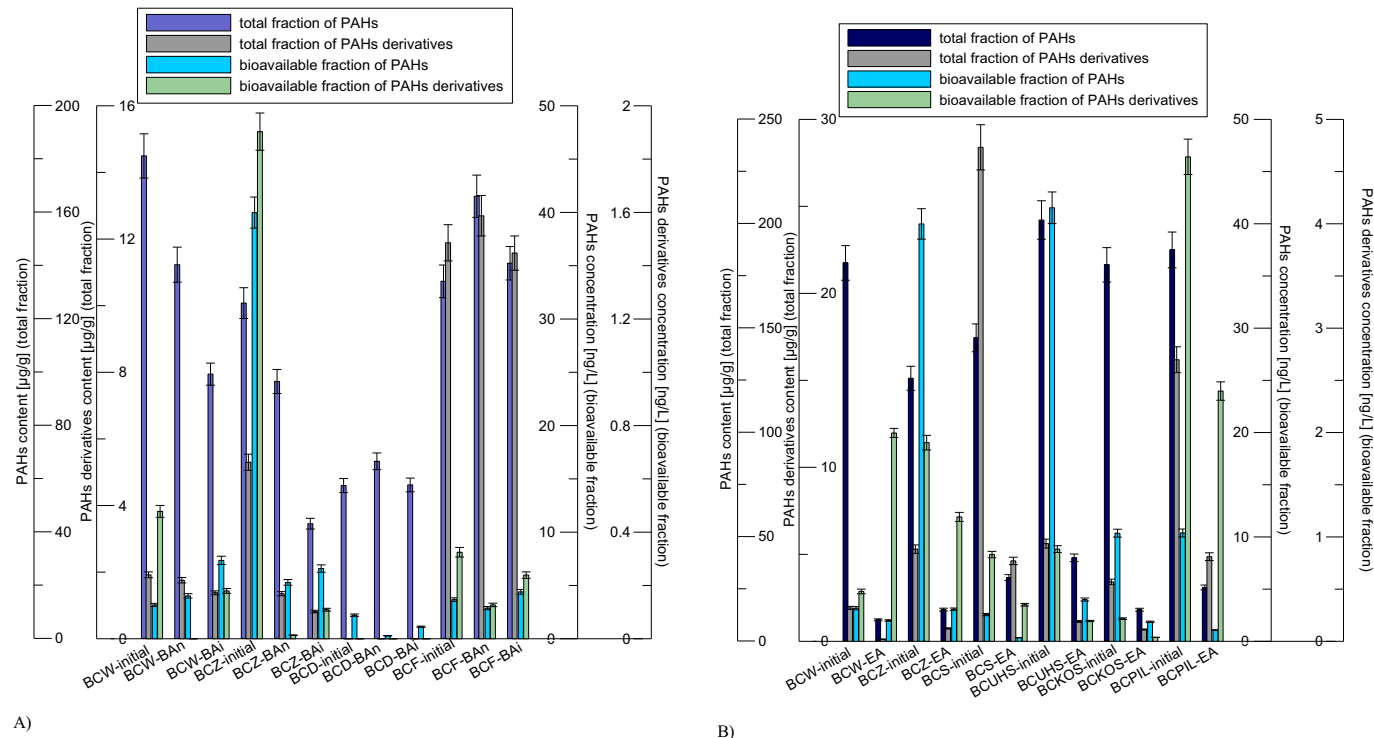


**Fig. 4.** The bioavailable and total PAHs and their derivatives in biochar before and after: A) biological aging; B) after enzymatic aging. The error bars mean the standard deviation of obtained results (number of replicates,  $n = 3$ ).

BCW-EA (37 %). In the other biochars, the decline amounted from 82 % (BCKOS-initial vs. BCKOS-EA) to 92 % (BCZ-initial vs. BCZ-EA). Enzymatic aging resulted in changes in the ratios between particular groups of PAHs differing in the number of aromatic rings. In BCW-EA (compared to initial biochars), the percentage of 2-ring species increased from <LOD to 66 % (naphthalene as the only representative) (Fig. 3d). In BCS-initial (as well as in BCS-EA) the content of 2-ring PAHs was below the limit of detection. In the other biochars, EA reduced the content of 2-ring compounds (from 90 % to 70 % in BCZ, from 79 % to 60 % in BCUHS, from 35 % to 15 % in BCKOS, and from 24 % to 14 % in BCPII) (Fig. 3d) with naphthalene as the most abundant compound in almost all BC. The content of 3-ring PAHs decreased from 98 % in BCW-initial even up to 33 % in BCW-EA and from 97 % to 86 % in BCS (initial vs. after EA) (with the highest quantified content mostly for acenaphthylene and acenaphthene) (Fig. 3d). EA caused an increase of 3-ring PAHs in other BC. In almost all biochars (except BCW and BCPII samples), enzymatic aging increased the percentage of 4-ring compounds from 2 to almost 5 times. In the case of willow-derived biochars, SSL-derived BC, and BCUHS, EA caused the total decomposition of 6-ring species. In BCZ, BCUHS, BCPII, and BCKOS EA lowered significantly the content of 2-ring species and increased 3- and 4-ring PAHs. There was no clear trend proving the correlation between the content of the bioavailable fraction of PAHs and its changes influenced by EA and the type of feedstock. In two-thirds of all samples, enzymatic aging caused a decrease in the percentage share of LMW PAHs in comparison to HMW PAHs (except BCW and BCPII samples where an increase was negligible). The drop was in the range of 2 % (for BCKOS samples) - 11 % (for BCS samples). The highest percentage share of HMW PAHs in biochar before EA was in the BCPII-initial (9 %), while after EA in BCS-EA (14 %).

Enzymatic aging caused a significant decrease (except BCW-EA) in the content of the bioavailable PAHs derivatives (from 37 % in BCZ-initial vs. BCZ-EA to 83 % in BCKOS-initial vs. BCKOS-EA) (Fig. 4b). 4H-cyclopenta(*def*)phenanthrene and nitropyrene were quantified in BCW-initial, whereas in BCW-EA there was only nitronaphthalene. Enzymatic aging did not affect the qualitative analysis of a bioavailable fraction of PAHs derivatives in BCS samples (1-methyl-5-nitronaphthalene, 1-methyl-6-nitronaphthalene, and 4H-cyclopenta(*def*)phenanthrene), BCZ samples (1-methyl-5-nitronaphthalene, 1-methyl-6-nitronaphthalene, and 9,10-anthracenedione), and BCPII-initial and BCPII-EA (2- and 4-ring O and N-PAHs).

The changes in the content of bioavailable fraction of PAHs and their derivatives before and after enzymatic aging are not statistically significant considering the type of feedstocks applied in the experiment. However, EA affects significantly the bioavailable fraction of PAHs ( $p \sim 0.05$ ). Moreover, considering the Pearson test, there is a statistically significant (positive) correlation between the total fraction of PAHs derivatives in biochar before and after EA as well as between the bioavailable fraction of PAHs before and after EA ( $p < 0.05$ ).

#### 4. Conclusions

Aging processes (both biological and enzymatic) affected the physicochemical characteristic of biochars, especially considering the content of C, H, and ash as well as aromatization, polarity, and hydrophilicity. Biological aging reduced the content of the total fraction of PAHs and PAHs derivatives in ash-rich and willow-derived biochar, however, PAHs bioavailability in willow-derived BC increased, whereas, in most other biochars, significantly decreased. Thus the organisms acquired from the

**Fig. 3.** The percentage of the PAHs (total fraction) differing in the number of aromatic rings in pristine and enzymatically aged BC, A) BCW, B) BCZ; C) BCD, BCF, BCS, BCUHS, BCKOS, and BCPII; D). The percentage of bioavailable fraction of the PAHs differing in the number of aromatic rings (only 2- and 3-ring species) in pristine and aged BC.

soil play a significant role in PAHs and their derivatives' degradation and modification. Enzymatic aging decreased the total and bioavailable PAHs and derivatives in almost all cases (except the bioavailability of PAHs derivatives in biochar obtained from willow).

## CRediT authorship contribution statement

**Agnieszka Krzyszczak:** Investigation, Visualization, Writing – review & editing. **Michał P. Dybowski:** Methodology, Validation. **Bożena Czech:** Investigation, Methodology, Visualization, Writing – review & editing, Conceptualization, Validation, Supervision.

## Data availability

Data will be made available on request.

## Declaration of competing interest

The authors declare the following financial interests/personal relationships which may be considered as potential competing interests: Bozena Czech reports financial support was provided by National Science Centre Poland.

## Acknowledgments

The studies were supported by project No. 2018/31/B/NZ9/00317 funded by the National Science Centre, Poland.

## Appendix A. Supplementary data

Supplementary data to this article can be found online at <https://doi.org/10.1016/j.scitotenv.2023.163966>.

## References

- Anderson, C.R., Condron, L.M., Clough, T.J., Fiers, M., Stewart, A., Hill, R.A., Sherlock, R.R., 2011. Biochar induced soil microbial community change: implications for biogeochemical cycling of carbon, nitrogen and phosphorus. *Pedobiologia* 54, 309–320. <https://doi.org/10.1016/j.pedobi.2011.07.005>.
- Atkinson, C.J., Fitzgerald, J.D., Hippis, N.A., 2010. Potential mechanisms for achieving agricultural benefits from biochar application to temperate soils: a review. *Plant Soil* 337, 1–18. <https://doi.org/10.1007/s11104-010-0464-5>.
- Beesley, L., Moreno-Jiménez, E., Gomez-Eyles, J.L., Harris, E., Robinson, B., Sizmur, T., 2011. A review of biochars' potential role in the remediation, revegetation and restoration of contaminated soils. *Environ. Pollut.* 159, 3269–3282. <https://doi.org/10.1016/j.envpol.2011.07.023>.
- Bolan, N., Hoang, S.A., Beiyuan, J., Gupta, S., Hou, D., Karakoti, A., Joseph, S., Jung, S., Kim, K.-H., Kirkham, M.B., WeiKua, H., Kumar, M., Kwon, E.E., Ok, Y.S., Perera, V., Rinklebe, J., Shaheen, S.B., Sarkar, B., Sarmah, A.K., Singh, B.P., Singh, G., Tsang, D.C.W., Vikrant, K., Vithanage, M., Vinu, A., Wang, H., Wijesekara, H., Yan, Y., Younis, S.A., Van Zwieten, L., 2022. Multifunctional applications of biochar beyond carbon storage. *Int. Mater. Rev.* 67, 150–200. <https://doi.org/10.1080/09506608.2021.1922047>.
- Buss, W., Graham, M.C., MacKinnon, G., Mašek, O., 2016. Strategies for producing biochars with minimum PAH contamination. *J. Anal. Appl. Pyrolysis* 119, 24–30. <https://doi.org/10.1016/j.jaap.2016.04.001>.
- Cao, X., Ma, L., Gao, B., Harris, W., 2009. Dairy-manure derived biochar effectively sorbs lead and atrazine. *Environ. Sci. Technol.* 43, 3285–3291. <https://doi.org/10.1021/es803092k>.
- Cheng, C.-H., Lehmann, J., Thies, J.E., Burton, S.D., Engelhard, M.H., 2006. Oxidation of black carbon by biotic and abiotic processes. *Org. Geochem.* 37, 1477–1488. <https://doi.org/10.1016/j.orggeochem.2006.06.022>.
- Dai, Z., Xiong, X., Zhu, H., Xu, H., Leng, P., Li, J., Tang, C., Xu, J., 2021. Association of biochar properties with changes in soil bacterial, fungal and fauna communities and nutrient cycling processes. *Biochar* 3, 239–254. <https://doi.org/10.1007/s42773-021-00099-x>.
- Fan, S., Zuo, J., Dong, H., 2020. Changes in soil properties and bacterial community composition with biochar amendment after six years. *Agronomy* 10, 746. <https://doi.org/10.3390/agronomy10050746>.
- Hamer, U., Marschner, B., Brodowski, S., Amelung, W., 2004. Interactive priming of black carbon and glucose mineralisation. *Org. Geochem.* 35, 823–830. <https://doi.org/10.1016/j.orggeochem.2004.03.003>.
- Inyang, M., Dickenson, E., 2015. The potential role of biochar in the removal of organic and microbial contaminants from potable and reuse water: a review. *Chemosphere* 134, 232–240. <https://doi.org/10.1016/j.chemosphere.2015.03.072>.
- Koinuma, M., Tateishi, H., Hatakeyama, K., Miyamoto, S., Ogata, C., Funatsu, A., Taniguchi, T., Matsumoto, Y., 2013. Analysis of reduced graphene oxides by X-ray photoelectron spectroscopy and electrochemical capacitance. *Chem. Lett.* 42, 924–926. <https://doi.org/10.1246/cl.130152>.
- Krzyszczak, A., Dybowski, M.P., Czech, B., 2021. Formation of polycyclic aromatic hydrocarbons and their derivatives in biochars: the effect of feedstock and pyrolysis conditions. *J. Anal. Appl. Pyrolysis* 160, 105339. <https://doi.org/10.1016/j.jaap.2021.105339>.
- Krzyszczak, A., Dybowski, M.P., Kończak, M., Czech, B., 2022a. Low bioavailability of derivatives of polycyclic aromatic hydrocarbons in biochar obtained from different feedstock. *Environ. Res.* 214, 113787. <https://doi.org/10.1016/j.envres.2022.113787>.
- Krzyszczak, A., Dybowski, M.P., Zarzycki, R., Kobylecki, R., Oleszczuk, P., Czech, B., 2022b. Long-term physical and chemical aging of biochar affected the amount and bioavailability of PAHs and their derivatives. *J. Hazard. Mater.* 440, 129795. <https://doi.org/10.1016/j.jhazmat.2022.129795>.
- Lipczynska-Kochany, E., 2018. Humic substances, their microbial interactions and effects on biological transformations of organic pollutants in water and soil: a review. *Chemosphere* 202, 420–437. <https://doi.org/10.1016/j.chemosphere.2018.03.104>.
- Mia, S., Dijkstra, F.A., Singh, B., 2017. Long-Term Aging of Biochar, in: *Advances in Agronomy*. Elsevier, pp. 1–51. <https://doi.org/10.1016/bs.agron.2016.10.001>.
- Oh, Y.J., Yoo, J.J., Kim, Y.I., Yoon, J.K., Yoon, H.N., Kim, J.-H., Park, S.B., 2014. Oxygen functional groups and electrochemical capacitive behavior of incompletely reduced graphene oxides as a thin-film electrode of supercapacitor. *Electrochim. Acta* 116, 118–128. <https://doi.org/10.1016/j.electacta.2013.11.040>.
- Oleszczuk, P., Koltowski, M., 2018. Changes of total and freely dissolved polycyclic aromatic hydrocarbons and toxicity of biochar treated with various aging processes. *Environ. Pollut.* 237, 65–73. <https://doi.org/10.1016/j.envpol.2018.01.073>.
- Pietikäinen, J., Kiikkilä, O., Fritze, H., 2000. Charcoal as a habitat for microbes and its effect on the microbial community of the underlying humus. *Oikos* 89, 231–242. <https://doi.org/10.1034/j.1600-0706.2000.890203.x>.
- Quan, G., Fan, Q., Zimmerman, A.R., Sun, J., Cui, L., Wang, H., Gao, B., Yan, J., 2020. Effects of laboratory biotic aging on the characteristics of biochar and its water-soluble organic products. *J. Hazard. Mater.* 382, 121071. <https://doi.org/10.1016/j.jhazmat.2019.121071>.
- Quilliam, R.S., Glanville, H.C., Wade, S.C., Jones, D.L., 2013. Life in the 'charosphere' – does biochar in agricultural soil provide a significant habitat for microorganisms? *Soil Biol. Biochem.* 65, 287–293. <https://doi.org/10.1016/j.soilbio.2013.06.004>.
- Rabchinski, M.K., Ryzhkov, S.A., Kirilenko, D.A., Ulin, N.V., Baidakova, M.V., Shnitov, V.V., Pavlov, S.I., Chumakov, R.G., Stolyarova, D.Yu., Besedina, N.A., Shvidchenko, A.V., Potorochin, D.V., Roth, F., Smirnov, D.A., Gudkov, M.V., Brzhezinskaya, M., Lebedev, O.I., Melnikov, V.P., Brunkov, P.N., 2020. From graphene oxide towards aminated graphene: facile synthesis, its structure and electronic properties. *Sci. Rep.* 10, 6902. <https://doi.org/10.1038/s41598-020-63935-3>.
- Schmidt, H.-P., 2015. European Biochar Certificate (EBC) - Guidelines Version 6.1. <https://doi.org/10.13140/RG.2.1.4658.7043>.
- Siatecka, A., Różyło, K., Ok, Y.S., Oleszczuk, P., 2021. Biochars ages differently depending on the feedstock used for their production: willow- versus sewage sludge-derived biochars. *Sci. Total Environ.* 789, 147458. <https://doi.org/10.1016/j.scitotenv.2021.147458>.
- Sigmund, G., Bucheli, T.D., Hilber, I., Mićić, V., Kah, M., Hofmann, T., 2017. Effect of ageing on the properties and polycyclic aromatic hydrocarbon composition of biochar. *Environ. Sci. Process Impacts* 19, 768–774. <https://doi.org/10.1039/C7EM00116A>.
- Spokas, K.A., Koskinen, W.C., Baker, J.M., Reicosky, D.C., 2009. Impacts of woodchip biochar additions on greenhouse gas production and sorption/degradation of two herbicides in a Minnesota soil. *Chemosphere* 77, 574–581. <https://doi.org/10.1016/j.chemosphere.2009.06.053>.
- White, J.C., Alexander, M., 1996. Reduced biodegradability of desorption-resistant fractions of polycyclic aromatic hydrocarbons in soil and aquifer solids. *Environ. Toxicol. Chem.* 15, 1973–1978. <https://doi.org/10.1002/etc.5620151116>.
- White, J.C., Alexander, M., Pignatello, J.J., 1999. Enhancing the bioavailability of organic compounds sequestered in soil and aquifer solids. *Environ. Toxicol. Chem.* 18, 182–187. <https://doi.org/10.1002/etc.5620180212>.
- Yao, Q., Liu, J., Yu, Z., Li, Y., Jin, J., Liu, X., Wang, G., 2017. Changes of bacterial community compositions after three years of biochar application in a black soil of Northeast China. *Appl. Soil Ecol.* 113, 11–21. <https://doi.org/10.1016/j.apsoil.2017.01.007>.
- Zeba, N., Berry, T.D., Panke-Buisse, K., Whitman, T., 2022. Effects of physical, chemical, and biological ageing on the mineralization of pine wood biochar by a *Streptomyces* isolate. *PLoS One* 17, e0265663. <https://doi.org/10.1371/journal.pone.0265663>.
- Zheng, H., Qu, C., Zhang, J., Talpur, S.A., Ding, Y., Xing, X., Qi, S., 2019. Polycyclic aromatic hydrocarbons (PAHs) in agricultural soils from Ningde, China: levels, sources, and human health risk assessment. *Environ. Geochem. Health* 41, 907–919. <https://doi.org/10.1007/s10653-018-0188-7>.

**Microorganisms and their metabolites affect the content of polycyclic aromatic hydrocarbons and their derivatives in pyrolyzed material**

Agnieszka Krzyszczak<sup>1</sup>, Michał P. Dybowski<sup>2</sup>, Bożena Czech<sup>1\*</sup>

<sup>1</sup>Department of Radiochemistry and Environmental Chemistry, Institute of Chemical Sciences, Faculty of Chemistry, Maria Curie-Sklodowska University in Lublin, Pl. M. Curie-Sklodowskiej 3, 20-031 Lublin, Poland

<sup>2</sup>Department of Chromatography, Institute of Chemical Sciences, Faculty of Chemistry, Maria Curie-Sklodowska University in Lublin, Pl. M. Curie-Sklodowskiej 3, 20-031 Lublin, Poland

\*corresponding author: Tel.: +48 81 537 55 54; fax: +48 81 537 55 65; E-mail address: bozena.czech@mail.umcs.pl (B. Czech)

Agnieszka Krzyszczak ORCID: 0000-0002-0143-0489

Michał P. Dybowski ORCID: 0000-0002-1028-759X

Bożena Czech ORCID: 0000-0002-4895-5186

**Journal: Science of the Total Environment**

**No. pages: 28**

**No. of figures: 0**

**No. of tables: 10**

## **2.1. Feedstock and biochar preparation**

The slow pyrolysis of raw materials was carried out in a furnace (Czylok, Poland) under the following conditions: the heating rate at the first step was  $10^{\circ}\text{C min}^{-1}$ , and the second step -  $3^{\circ}\text{C min}^{-1}$ , the resident time: 3h, and the constant flow of nitrogen ( $630 \text{ cm}^3 \text{ min}^{-1}$ ) monitored by the mass flow controller (BETA-ERG, Poland). All studied biochars were obtained at  $600^{\circ}\text{C}$ . Collected biochars were grounded (<2 mm), homogenized, washed out using distilled water (1:10, biochar: water) continuously for 24 h, and dried at  $40^{\circ}\text{C}$  for 6 h. Before all experiments, BC was stored at room temperature in the absence of light.

## **2.7. GC–MS/MS measurement**

Qualitative and quantitative measurements of PAHs and their derivatives were performed using a gas chromatograph hyphenated with a triple quadruple tandem mass spectrometer detector (GCMS-TQ8040; Shimadzu, Kyoto, Japan) equipped with a ZB5-MSi fused-silica capillary column ( $30 \text{ m} \times 0.25 \text{ mm i.d.}, 0.25 \mu\text{m}$  film thickness; Phenomenex, Torrance, CA, USA) and an AOC-20i+s type autosampler (Shimadzu). The helium (grade 5.0) and argon (grade 5.0) were applied as a carrier and collision gas, respectively. The chromatographic conditions were adjusted as follows: column flow - $1.56 \text{ mL/min}$ , the volume of injection -  $1 \mu\text{L}$ . The injector was working in high-pressure mode (250.0 kPa for 1.5 min; column flow at initial temperature was  $4.90 \text{ mL/min}$ ) at the temperature of  $310^{\circ}\text{C}$ ; the ion source temperature was  $225^{\circ}\text{C}$ . The qualitative and quantitative analyses were conducted with full scan mode (range 40-550 m/z) and SIM (Single Ion Monitoring) mode, respectively.

Table S1. Chemical characteristics of analyzed compounds.

No.	Compound	CAS <sup>(1)</sup>	MW <sup>(2)</sup>	Formula
1	Naphthalene*	91-20-3	128.17	C <sub>10</sub> H <sub>8</sub>
2	1,3-di-iso-propylnaphthalene	57122-16-4	212.33	C <sub>16</sub> H <sub>20</sub>
3	2-Phenylnaphtalene	612-94-2	204.26	C <sub>16</sub> H <sub>12</sub>
4	Acenaphthylene*	208-96-8	152.20	C <sub>12</sub> H <sub>8</sub>
5	Acenaphthene*	83-32-9	154.20	C <sub>12</sub> H <sub>10</sub>
6	Fluorene*	86-73-7	166.22	C <sub>13</sub> H <sub>10</sub>
7	Anthracene*	120-12-7	178.23	C <sub>14</sub> H <sub>10</sub>
8	Phenanthrene*	85-01-8	178.23	C <sub>14</sub> H <sub>10</sub>
9	3-Methylphenantrene	832-71-3	192.25	C <sub>15</sub> H <sub>12</sub>
10	2-Methylphenantrene	2531-84-2	192.25	C <sub>15</sub> H <sub>12</sub>
11	9-Methylphenantrene	883-20-5	192.25	C <sub>15</sub> H <sub>12</sub>
12	3,6-dimethylphenantrene	1576-67-6	206.28	C <sub>16</sub> H <sub>14</sub>
13	Fluoranthene*	206-44-0	202.25	C <sub>16</sub> H <sub>10</sub>
14	Pyrene*	129-00-0	202.25	C <sub>16</sub> H <sub>10</sub>
15	2-Methylpyrene	3442-78-2	216.28	C <sub>17</sub> H <sub>12</sub>
16	4-Methylpyrene	3353-12-6	216.28	C <sub>17</sub> H <sub>12</sub>
17	Benzo[a]fluorene	238-84-6	216.27	C <sub>17</sub> H <sub>12</sub>

18	Benzo[a]anthracene*	56-55-3	228.29	C <sub>18</sub> H <sub>12</sub>
19	Chryzene*	218-01-9	228.29	C <sub>18</sub> H <sub>12</sub>
20	3-Methylchrysene	3351-31-3	242.30	C <sub>19</sub> H <sub>14</sub>
21	5-Methylchrysene	3697-24-3	242.30	C <sub>19</sub> H <sub>14</sub>
22	6-Methylchrysene	1705-85-7	242.30	C <sub>19</sub> H <sub>14</sub>
23	Benzo[a]fluoranthene	203-33-8	252.31	C <sub>20</sub> H <sub>12</sub>
24	Benzo[b]fluoranthene*	205-99-2	252.31	C <sub>20</sub> H <sub>12</sub>
25	Benzo[k]fluoranthene*	207-08-9	252.32	C <sub>20</sub> H <sub>12</sub>
26	Benzo[j]fluoranthene	205-82-3	252.31	C <sub>20</sub> H <sub>12</sub>
27	Benzo[a]pyrene*	50-32-8	252.31	C <sub>20</sub> H <sub>12</sub>
28	Indeno[1,2,3-cd]pyrene*	193-39-5	276.33	C <sub>22</sub> H <sub>12</sub>
29	Benzo[ghi]perylene*	191-24-2	276.33	C <sub>22</sub> H <sub>12</sub>
30	Dibenzo[a,h]anthracene*	53-70-3	278.10	C <sub>22</sub> H <sub>14</sub>
31	Dibenz[a,e]pyrene	192-65-4	302.37	C <sub>24</sub> H <sub>14</sub>
32	Dibenz[a,h]pyrene	189-64-0	302.37	C <sub>24</sub> H <sub>14</sub>
33	Dibenz[a,i]pyrene	189-55-9	302.37	C <sub>24</sub> H <sub>14</sub>
34	Dibenz[a,l]pyrene	192-65-4	302.37	C <sub>24</sub> H <sub>14</sub>

N- and O-PAHs				
35	Nitronaphthalene	86-57-7	173.16	C <sub>10</sub> H <sub>7</sub> NO <sub>2</sub>
36	1-Methyl-5-nitronaphthalene	91137-27-8	187.19	C <sub>11</sub> H <sub>9</sub> NO <sub>2</sub>

37	1-Methyl-6-nitronaphthalene	105752-67-8	187.19	C <sub>11</sub> H <sub>9</sub> NO <sub>2</sub>
38	9,10-Anthracenedione	84-65-1	208.21	C <sub>14</sub> H <sub>8</sub> O <sub>2</sub>
39	4H-cyclopenta(def)phenanthrene	203-64-5	190.24	C <sub>15</sub> H <sub>10</sub>
40	Nitropyrene	5522-43-0	247.25	C <sub>16</sub> H <sub>9</sub> NO <sub>2</sub>

<sup>(1)</sup>numerical identifier assigned by the Chemical Abstracts Service (CAS)

<sup>(2)</sup>MW-molecular weight

\* PAHs belonging to 16PAHs which have been classified by the United States Environmental Protection Agency (USEPA) as priority pollutants [1].

Table S2. The qualitative and quantitative parameters of PAHs and O/N-PAHs analysis.

No.	Compound	Quantification ion ( <i>m/z</i> )	Confirmation ion ( <i>m/z</i> )	LOD*	LOQ**
1	Naphthalene	128	102	1.01	3.36
2	1,3-di-iso-propynaphthalene	197	212	1.41	4.69
3	2-Phenylnaphthalene	204	101	1.90	6.33
4	Acenaphthylene	152	76	2.10	6.99
5	Acenaphthene	153	76	2.30	7.66
6	Fluorene	166	82	1.10	3.66
7	Anthracene	178	89	1.30	4.33
8	Phenanthrene	178	89	1.34	4.36

9	3-Methylphenanthrene	192	165	2.42	8.06
10	2-Methylphenanthrene	192	165	2.42	8.06
11	9-Methylphenanthrene	192	96	3.23	10.76
12	3,6-dimethylphenanthrene	206	191	2.20	7.33
13	Fluoranthene	202	101	1.87	6.22
14	Pyrene	202	101	1.91	6.36
15	2-Methylpyrene	216	108	1.92	6.39
16	4-Methylpyrene	216	108	1.92	6.39
17	Benzo[a]fluorene	216	107	1.30	4.33
18	Benzo[a]anthracene	228	114	1.30	4.33
19	Chryzene	228	113	2.20	7.33
20	3-Methylchrysene	242	121	1.02	3.40
21	5-Methylchrysene	242	120	1.55	5.16
22	6-Methylchrysene	242	119	1.02	3.40
23	Benzo[a]fluoranthene	252	126	2.10	6.99
24	Benzo[b]fluoranthene	252	126	2.10	6.99
25	Benzo[k]fluoranthene	252	126	2.10	6.99
26	Benzo[j]fluoranthene	252	126	1.39	4.63
27	Benzo[a]pyrene	252	126	2.11	7.03

28	Indeno[1,2,3-cd]pyrene	276	138	1.30	4.33
29	Benzo[ghi]perylene	276	138	1.33	4.43
30	Dibenzo[a,h]anthracene	278	139	2.21	7.36
31	Dibenz[a,e]pyrene	302	151	1.89	6.29
32	Dibenz[a,h]pyrene	302	151	1.89	6.29
33	Dibenz[a,i]pyrene	302	151	1.89	6.29
34	Dibenz[a,l]pyrene	302	151	1.89	6.29
<b>N- and O-PAHs</b>					
35	Nitronaphthalene	173	127	2.41	8.03
36	1-Methyl-5-nitronaphthalene	187	115	1.21	4.03
37	1-Methyl-6-nitronaphthalene	187	115	1.21	4.03
38	9,10-Anthracenedione	208	180	1.44	4.80
39	4H-cyclopenta(def)phenanthrene	190	94	3.01	10.02
40	Nitropyrene	247	201	1.66	5.53

\*-LOD – limit of detection; \*\*-LOQ – limit of quantitation; LOD and LOQ were not calculated via K<sub>POM</sub>; LOD and LOQ were considered to be signal-to-noise ratios equal to 3 and 10, respectively.

Table S3. PAHs and PAHs derivatives total content in non-aged PT-derived biochars.

No.	Compound	Sample description			
		BCS-initial	BCW-initial	BCD-initial	BCF-initial

		Analyte concentration [ $\mu\text{g g}^{-1}$ ]			
1	Naphthalene	$0.24 \pm 0.01$	$62.28 \pm 2.85$	< LOD	$9.37 \pm 0.43$
2	1,3-di-iso-propylnaphthalene	$4.43 \pm 0.20$	$0.88 \pm 0.04$	$5.11 \pm 0.23$	< LOD
3	2-Phenylnaphthalene	< LOD	< LOD	< LOD	< LOD
4	Acenaphthylene	$15.62 \pm 0.72$	$25.12 \pm 1.15$	$4.87 \pm 0.22$	$2.34 \pm 0.11$
5	Acenaphthene	$18.27 \pm 0.84$	$37.34 \pm 1.71$	$9.31 \pm 0.43$	$6.73 \pm 0.31$
6	Fluorene	< LOD	$0.42 \pm 0.02$	$4.43 \pm 0.20$	$19.46 \pm 0.89$
7	Anthracene	$1.48 \pm 0.07$	$3.32 \pm 0.15$	< LOD	< LOD
8	Phenanthrene	< LOD	< LOD	< LOD	< LOD
9	3-Methylphenanthrene	$27.28 \pm 1.25$	$0.24 \pm 0.01$	< LOD	$4.88 \pm 0.22$
10	2-Methylphenanthrene	$10.96 \pm 0.50$	$0.22 \pm 0.01$	$0.24 \pm 0.01$	$0.72 \pm 0.03$
11	9-Methylphenanthrene	< LOD	< LOD	< LOD	$0.22 \pm 0.01$
12	3,6-dimethylphenanthrene	$0.32 \pm 0.02$	< LOD	< LOD	$14.91 \pm 0.68$
13	Fluoranthene	$0.46 \pm 0.02$	$1.98 \pm 0.09$	< LOD	< LOD
14	Pyrene	< LOD	$25.10 \pm 1.15$	< LOD	$1.24 \pm 0.06$
15	2-Methylpyrene	$6.33 \pm 0.29$	$0.24 \pm 0.01$	$0.32 \pm 0.02$	< LOD
16	4-Methylpyrene	$2.30 \pm 0.11$	$0.30 \pm 0.01$	$0.82 \pm 0.04$	< LOD
17	Benzo[a]fluorene	$16.27 \pm 0.75$	$6.02 \pm 0.28$	$12.21 \pm 0.56$	$16.28 \pm 0.75$
18	Benzo[a]anthracene	$12.04 \pm 0.55$	$5.14 \pm 0.24$	< LOD	$11.47 \pm 0.53$
19	Chrysene	$2.24 \pm 0.10$	$0.92 \pm 0.04$	< LOD	< LOD
20	3-Methylchrysene	$10.02 \pm 0.46$	< LOD	$0.82 \pm 0.04$	$6.21 \pm 0.28$
21	5-Methylchrysene	$8.85 \pm 0.41$	< LOD	$6.28 \pm 0.29$	$4.98 \pm 0.23$
22	6-Methylchrysene	$1.82 \pm 0.08$	< LOD	$10.35 \pm 0.47$	$10.33 \pm 0.47$
23	Benzo[a]fluoranthene	< LOD	$0.28 \pm 0.01$	$0.22 \pm 0.01$	$0.24 \pm 0.01$
24	Benzo[b]fluoranthene	< LOD	$0.22 \pm 0.01$	< LOD	< LOD

25	Benzo[k]fluoranthene	< LOD	$0.34 \pm 0.02$	< LOD	< LOD
26	Benzo[j]fluoranthene	< LOD	$0.12 \pm 0.01$	< LOD	< LOD
27	Benzo[a]pyrene	$0.38 \pm 0.02$	$7.34 \pm 0.34$	$1.94 \pm 0.09$	$10.23 \pm 0.47$
28	Indeno[1,2,3-cd]pyrene	$4.03 \pm 0.19$	$1.10 \pm 0.05$	< LOD	< LOD
29	Benzo[ghi]perylene	$1.88 \pm 0.09$	< LOD	< LOD	< LOD
30	Dibenzo[a,h]anthracene	< LOD	$0.68 \pm 0.03$	< LOD	$14.41 \pm 0.66$
31	Dibenz[a,e]pyrene	< LOD	$1.16 \pm 0.05$	$0.22 \pm 0.01$	< LOD
32	Dibenz[a,h]pyrene	< LOD	$0.18 \pm 0.01$	$0.24 \pm 0.01$	< LOD
33	Dibenz[a,i]pyrene	< LOD	$0.14 \pm 0.01$	< LOD	< LOD
34	Dibenz[a,l]pyrene	< LOD	< LOD	< LOD	< LOD
N- and O-PAHs					
35	Nitronaphthalene	< LOD	$1.92 \pm 0.09$	< LOD	< LOD
36	1-Methyl-5-nitronaphthalene	$1.88 \pm 0.09$	< LOD	< LOD	< LOD
37	1-Methyl-6-nitronaphthalene	$2.32 \pm 0.11$	< LOD	< LOD	< LOD
38	9,10-Anthracenedione	< LOD	< LOD	< LOD	$0.82 \pm 0.04$
39	4H-cyclopenta(def)phenanthrene	$24.20 \pm 1.11$	< LOD	< LOD	$11.07 \pm 0.51$
40	Nitropyrene	< LOD	< LOD	< LOD	< LOD

SD-standard deviation, <LOD- below the limit of detection

Table S4. The concentration of total PAHs and their derivatives in RBP-BC and SSL-BC.

No.	Compound	Sample description			
		BCUHS-initial	BCKOS-initial	BCPIL-initial	BCZ-initial
		Analyte concentration [ $\mu\text{g g}^{-1}$ ]			
1	Naphthalene	$66.05 \pm 3.02$	$8.83 \pm 0.40$	$6.24 \pm 0.29$	$54.80 \pm 2.51$
2	1,3-di-iso-propynaphthalene	< LOD	$2.88 \pm 0.13$	$6.44 \pm 0.30$	< LOD

3	2-Phenylnaphthalene	< LOD	$4.02 \pm 0.18$	$2.30 \pm 0.11$	$1.26 \pm 0.06$
4	Acenaphthylene	$16.21 \pm 0.74$	$16.84 \pm 0.77$	$7.93 \pm 0.36$	$15.09 \pm 0.69$
5	Acenaphthene	$14.89 \pm 0.68$	$6.31 \pm 0.29$	$2.30 \pm 0.11$	$3.10 \pm 0.14$
6	Fluorene	$3.92 \pm 0.18$	$3.12 \pm 0.14$	$48.84 \pm 2.24$	$8.30 \pm 0.38$
7	Anthracene	$12.21 \pm 0.56$	$82.80 \pm 3.79$	$53.42 \pm 02.45$	$0.42 \pm 0.02$
8	Phenanthrene	< LOD	< LOD	< LOD	< LOD
9	3-Methylphenanthrene	$1.34 \pm 0.06$	< LOD	$0.72 \pm 0.03$	$0.060 \pm 0.003$
10	2-Methylphenanthrene	$0.68 \pm 0.03$	< LOD	$0.88 \pm 0.04$	$0.12 \pm 0.01$
11	9-Methylphenanthrene	< LOD	$2.24 \pm 0.10$	< LOD	$1.02 \pm 0.05$
12	3,6-dimethylphenanthrene	$0.84 \pm 0.04$	< LOD	$2.94 \pm 0.13$	$2.42 \pm 0.11$
13	Fluoranthene	$6.38 \pm 0.29$	$10.09 \pm 0.46$	$32.79 \pm 1.15$	< LOD
14	Pyrene	$14.89 \pm 0.68$	$21.90 \pm 0.10$	< LOD	$8.30 \pm 0.38$
15	2-Methylpyrene	< LOD	< LOD	< LOD	$1.10 \pm 0.05$
16	4-Methylpyrene	< LOD	< LOD	$0.88 \pm 0.04$	$1.96 \pm 0.09$
17	Benzo[a]fluorene	$8.61 \pm 0.39$	< LOD	< LOD	$0.56 \pm 0.03$
18	Benzo[a]anthracene	$11.07 \pm 0.51$	< LOD	< LOD	$1.98 \pm 0.09$
19	Chrysene	$27.30 \pm 1.25$	$2.30 \pm 0.11$	$1.94 \pm 0.09$	$0.24 \pm 0.01$
20	3-Methylchrysene	$2.44 \pm 0.11$	< LOD	$2.04 \pm 0.09$	< LOD
21	5-Methylchrysene	$2.06 \pm 0.09$	< LOD	$1.96 \pm 0.09$	$1.92 \pm 0.09$
22	6-Methylchrysene	$0.74 \pm 0.03$	< LOD	< LOD	$0.66 \pm 0.03$
23	Benzo[a]fluoranthene	< LOD	$2.88 \pm 0.13$	$6.88 \pm 0.32$	$9.72 \pm 0.45$
24	Benzo[b]fluoranthene	< LOD	$1.98 \pm 0.09$	$4.04 \pm 0.19$	$6.30 \pm 0.29$
25	Benzo[k]fluoranthene	< LOD	$1.44 \pm 0.07$	< LOD	$2.28 \pm 0.10$
26	Benzo[j]fluoranthene	< LOD	$1.22 \pm 0.06$	< LOD	$0.26 \pm 0.01$
27	Benzo[a]pyrene	$12.03 \pm 0.55$	$6.27 \pm 0.29$	< LOD	$0.52 \pm 0.02$

28	Indeno[1,2,3-cd]pyrene	< LOD	< LOD	$2.32 \pm 0.11$	< LOD
29	Benzo[ghi]perylene	< LOD	$1.28 \pm 0.06$	< LOD	< LOD
30	Dibenzo[a,h]anthracene	< LOD	< LOD	< LOD	$2.42 \pm 0.11$
31	Dibenz[a,e]pyrene	< LOD	$1.44 \pm 0.07$	$1.34 \pm 0.06$	$1.04 \pm 0.05$
32	Dibenz[a,h]pyrene	< LOD	$0.88 \pm 0.04$	$0.62 \pm 0.03$	< LOD
33	Dibenz[a,i]pyrene	< LOD	$0.76 \pm 0.04$	$0.24 \pm 0.01$	< LOD
34	Dibenz[a,l]pyrene	< LOD	$0.72 \pm 0.03$	$0.28 \pm 0.01$	< LOD
N- and O-PAHs					
35	Nitronaphthalene	$1.60 \pm 0.07$	< LOD	$3.24 \pm 0.15$	< LOD
36	1-Methyl-5-nitronaphthalene	< LOD	< LOD	$6.88 \pm 0.32$	$2.42 \pm 0.11$
37	1-Methyl-6-nitronaphthalene	< LOD	< LOD	$4.16 \pm 0.19$	$2.88 \pm 0.13$
38	9,10-Anthracenedione	$4.02 \pm 0.18$	$1.48 \pm 0.07$	< LOD	< LOD
39	4H-cyclopenta(def)phenanthrene	< LOD	< LOD	< LOD	< LOD
40	Nitropyrene	< LOD	$1.94 \pm 0.09$	$1.92 \pm 0.09$	< LOD

SD-standard deviation, <LOD- below the limit of detection

Table S5. PAHs and PAHs derivatives total content in biologically aged biochars (samples with nutrient solution).

No.	Compound	Sample description			
		BCW-BAn	BCD-BAn	BCF-BAn	BCZ-BAn
		Analyte concentration [ $\mu\text{g g}^{-1}$ ]			
1	Naphthalene	$53.24 \pm 2.50$	< LOD	$9.91 \pm 0.47$	$42.89 \pm 2.02$
2	1,3-di-iso-propylnaphthalene	$0.72 \pm 0.03$	$4.16 \pm 0.20$	< LOD	< LOD
3	2-Phenylnaphthalene	< LOD	< LOD	< LOD	$1.02 \pm 0.05$
4	Acenaphthylene	$20.22 \pm 0.95$	$4.00 \pm 0.19$	$3.01 \pm 0.14$	$11.88 \pm 0.56$

5	Acenaphthene	28.80 ± 1.35	8.78 ± 0.41	6.00 ± 0.29	2.63 ± 0.12
6	Fluorene	0.22 ± 0.01	5.74 ± 0.27	24.16 ± 1.16	6.41 ± 0.30
7	Anthracene	1.82 ± 0.09	< LOD	< LOD	0.32 ± 0.02
8	Phenanthrene	< LOD	< LOD	< LOD	< LOD
9	3-Methylphenanthrene	< LOD	0.42 ± 0.02	6.00 ± 0.29	0.040 ± 0.002
10	2-Methylphenanthrene	< LOD	0.72 ± 0.03	1.34 ± 0.06	0.080 ± 0.004
11	9-Methylphenanthrene	< LOD	0.88 ± 0.04	0.98 ± 0.05	0.82 ± 0.04
12	3,6-dimethylphenanthrene	< LOD	1.10 ± 0.05	15.59 ± 0.75	1.85 ± 0.09
13	Fluoranthene	1.10 ± 0.05	< LOD	< LOD	< LOD
14	Pyrene	19.92 ± 0.94	< LOD	2.01 ± 0.10	6.01 ± 0.28
15	2-Methylpyrene	< LOD	0.32 ± 0.02	< LOD	0.90 ± 0.04
16	4-Methylpyrene	< LOD	0.82 ± 0.63	< LOD	1.19 ± 0.06
17	Benzo[a]fluorene	4.10 ± 0.19	13.32 ± 0.63	26.58 ± 1.27	0.26 ± 0.01
18	Benzo[a]anthracene	3.34 ± 0.16	2.21 ± 0.10	15.57 ± 0.75	1.47 ± 0.07
19	Chrysene	0.66 ± 0.03	< LOD	< LOD	0.12 ± 0.01
20	3-Methylchrysene	< LOD	1.25 ± 0.06	6.44 ± 0.31	< LOD
21	5-Methylchrysene	< LOD	6.75 ± 0.32	3.93 ± 0.19	0.70 ± 0.03
22	6-Methylchrysene	< LOD	9.94 ± 0.47	9.07 ± 0.43	0.30 ± 0.01
23	Benzo[a]fluoranthene	< LOD	0.72 ± 0.02	1.81 ± 0.09	7.22 ± 0.34
24	Benzo[b]fluoranthene	< LOD	< LOD	< LOD	5.59 ± 0.26
25	Benzo[k]fluoranthene	0.100 ± 0.005	< LOD	< LOD	2.01 ± 0.09
26	Benzo[j]fluoranthene	< LOD	< LOD	< LOD	0.18 ± 0.01
27	Benzo[a]pyrene	4.44 ± 0.21	4.02 ± 0.19	14.27 ± 0.68	0.32 ± 0.02
28	Indeno[1,2,3-cd]pyrene	0.32 ± 0.02	< LOD	< LOD	< LOD
29	Benzo[ghi]perylene	< LOD	< LOD	< LOD	< LOD

30	Dibenzo[a,h]anthracene	$0.38 \pm 0.02$	< LOD	$19.26 \pm 0.92$	$1.53 \pm 0.07$
31	Dibenz[a,e]pyrene	$0.88 \pm 0.04$	$0.46 \pm 0.02$	< LOD	$0.70 \pm 0.03$
32	Dibenz[a,h]pyrene	< LOD	$0.88 \pm 0.04$	< LOD	< LOD
33	Dibenz[a,i]pyrene	< LOD	< LOD	< LOD	< LOD
34	Dibenz[a,l]pyrene	< LOD	< LOD	< LOD	< LOD
N- and O-PAHs					
35	Nitronaphthalene	$1.76 \pm 0.08$	< LOD	< LOD	< LOD
36	1-Methyl-5-nitronaphthalene	< LOD	< LOD	< LOD	< LOD
37	1-Methyl-6-nitronaphthalene	< LOD	< LOD	< LOD	$1.35 \pm 0.06$
38	9,10-Anthracenedione	< LOD	< LOD	$1.10 \pm 0.05$	< LOD
39	4H-cyclopenta(def)phenanthrene	< LOD	< LOD	$11.60 \pm 0.56$	< LOD
40	Nitropyrene	< LOD	< LOD	< LOD	< LOD

SD-standard deviation, <LOD- below the limit of detection

Table S6. PAHs and PAHs derivatives total content in biologically aged biochars (with microbial inoculum and nutrient solution).

No.	Compound	Sample description			
		BCW-BAi	BCD-BAi	BCF-BAi	BCZ-BAi
		Analyte concentration [ $\mu\text{g g}^{-1}$ ]			
1	Naphthalene	$40.06 \pm 1.67$	< LOD	$9.15 \pm 0.41$	$21.03 \pm 0.99$
2	1,3-di-iso-propynaphthalene	$0.26 \pm 0.01$	$4.00 \pm 0.18$	< LOD	< LOD
3	2-Phenylnaphthalene	< LOD	< LOD	< LOD	$0.22 \pm 0.01$
4	Acenaphthylene	$16.67 \pm 0.70$	$3.60 \pm 0.16$	$1.99 \pm 0.09$	$5.26 \pm 0.25$
5	Acenaphthene	$19.35 \pm 0.81$	$7.38 \pm 0.33$	$5.13 \pm 0.23$	$1.34 \pm 0.06$
6	Fluorene	$0.040 \pm 0.002$	$5.21 \pm 0.23$	$20.32 \pm 0.90$	$2.01 \pm 0.10$
7	Anthracene	$1.82 \pm 0.08$	< LOD	< LOD	< LOD

8	Phenanthrene	< LOD	< LOD	< LOD	< LOD
9	3-Methylphenanthrene	< LOD	0.020 ± 0.001	5.21 ± 0.23	< LOD
10	2-Methylphenanthrene	< LOD	0.28 ± 0.01	0.93 ± 0.04	< LOD
11	9-Methylphenanthrene	< LOD	0.24 ± 0.01	0.26 ± 0.01	0.50 ± 0.02
12	3,6-dimethylphenanthrene	< LOD	1.03 ± 0.05	14.05 ± 0.62	1.24 ± 0.06
13	Fluoranthene	0.74 ± 0.03	< LOD	< LOD	< LOD
14	Pyrene	13.31 ± 0.56	< LOD	1.59 ± 0.07	2.29 ± 0.11
15	2-Methylpyrene	< LOD	0.62 ± 0.03	0.24 ± 0.01	0.50 ± 0.02
16	4-Methylpyrene	< LOD	1.11 ± 0.05	0.22 ± 0.01	0.66 ± 0.03
17	Benzo[a]fluorene	2.28 ± 0.10	11.16 ± 0.50	22.05 ± 0.98	0.060 ± 0.003
18	Benzo[a]anthracene	1.94 ± 0.08	2.05 ± 0.09	13.17 ± 0.59	1.16 ± 0.05
19	Chrysene	0.060 ± 0.003	< LOD	< LOD	0.020 ± 0.001
20	3-Methylchrysene	< LOD	0.72 ± 0.03	5.41 ± 0.24	< LOD
21	5-Methylchrysene	< LOD	6.29 ± 0.28	2.89 ± 0.13	0.38 ± 0.02
22	6-Methylchrysene	< LOD	9.93 ± 0.44	6.98 ± 0.31	0.060 ± 0.003
23	Benzo[a]fluoranthene	< LOD	0.32 ± 0.01	1.23 ± 0.05	2.71 ± 0.13
24	Benzo[b]fluoranthene	< LOD	< LOD	< LOD	2.17 ± 0.10
25	Benzo[k]fluoranthene	< LOD	< LOD	< LOD	1.16 ± 0.05
26	Benzo[j]fluoranthene	< LOD	< LOD	< LOD	< LOD
27	Benzo[a]pyrene	1.98 ± 0.08	2.89 ± 0.13	13.05 ± 0.58	< LOD
28	Indeno[1,2,3-cd]pyrene	0.12 ± 0.01	< LOD	< LOD	< LOD
29	Benzo[ghi]perylene	< LOD	< LOD	< LOD	< LOD
30	Dibenzo[a,h]anthracene	0.040 ± 0.002	< LOD	16.97 ± 0.75	0.28 ± 0.01
31	Dibenz[a,e]pyrene	0.50 ± 0.02	0.32 ± 0.01	< LOD	0.020 ± 0.001
32	Dibenz[a,h]pyrene	< LOD	0.44 ± 0.02	< LOD	< LOD

33	Dibenz[a,i]pyrene	< LOD	< LOD	< LOD	< LOD
34	Dibenz[a,l]pyrene	< LOD	< LOD	< LOD	< LOD
N- and O-PAHs					
35	Nitronaphthalene	1.38 ± 0.06	< LOD	< LOD	< LOD
36	1-Methyl-5-nitronaphthalene	< LOD	< LOD	< LOD	< LOD
37	1-Methyl-6-nitronaphthalene	< LOD	< LOD	< LOD	0.82 ± 0.04
38	9,10-Anthracenedione	< LOD	< LOD	1.39 ± 0.06	< LOD
39	4H-cyclopenta(def)phenanthrene	< LOD	< LOD	10.19 ± 0.45	< LOD
40	Nitropyrene	< LOD	< LOD	< LOD	< LOD

SD-standard deviation, <LOD- below the limit of detection

Table S7. PAHs and PAHs derivatives total content in enzymatically-aged biochars.

No.	Compound	Sample description					
		BCS-EA	BCW-EA	BCUHS-EA	BCKOS-EA	BCPIL-EA	BCZ-EA
		Analyte concentration [ $\mu\text{g g}^{-1}$ ]					
1	Naphthalene	< LOD	2.30 ± 0.11	6.17 ± 0.28	0.62 ± 0.03	1.48 ± 0.07	4.06 ± 0.19
2	1,3-di-iso-propynaphthalene	0.12 ± 0.01	< LOD	< LOD	< LOD	1.32 ± 0.06	< LOD
3	2-Phenylnaphthalene	< LOD	< LOD	< LOD	< LOD	0.040 ± 0.002	< LOD
4	Acenaphthylene	2.82 ± 0.13	1.70 ± 0.08	2.42 ± 0.11	2.10 ± 0.10	1.64 ± 0.08	2.42 ± 0.11
5	Acenaphthene	1.92 ± 0.09	2.30 ± 0.11	2.10 ± 0.10	0.24 ± 0.01	< LOD	1.24 ± 0.06
6	Fluorene	< LOD	< LOD	0.44 ± 0.02	1.92 ± 0.09	6.83 ± 0.31	0.88 ± 0.04
7	Anthracene	0.040 ± 0.002	0.120 ± 0.005	2.04 ± 0.09	2.30 ± 0.11	8.31 ± 0.38	< LOD
8	Phenanthrene	< LOD	< LOD	< LOD	< LOD	< LOD	< LOD
9	3-Methylphenanthrene	4.30 ± 0.20	< LOD	< LOD	< LOD	< LOD	< LOD
10	2-Methylphenanthrene	4.82 ± 0.22	< LOD	< LOD	< LOD	< LOD	< LOD



35	Nitronaphthalene	< LOD	0.12 ± 0.01	0.060 ± 0.003	< LOD	0.88 ± 0.04	< LOD
36	1-Methyl-5-nitronaphthalene	0.26 ± 0.01	< LOD	< LOD	< LOD	2.30 ± 0.11	0.62 ± 0.03
37	1-Methyl-6-nitronaphthalene	0.30 ± 0.01	< LOD	< LOD	< LOD	1.38 ± 0.06	0.12 ± 0.01
38	9,10-Anthracenedione	< LOD	< LOD	1.08 ± 0.05	0.22 ± 0.01	< LOD	< LOD
39	4H-cyclopenta(def)phenanthrene	4.06 ± 0.19	< LOD	< LOD	< LOD	< LOD	< LOD
40	Nitropyrene	< LOD	< LOD	< LOD	0.46 ± 0.02	0.30 ± 0.01	< LOD

SD-standard deviation, <LOD- below the limit of detection

Table S8. The content of bioavailable PAHs and their derivatives in PT-BC.

No.	Compound	Sample description			
		BCS-initial	BCW-initial	BCD-initial	BCF-initial
		Analyte concentration [ng L <sup>-1</sup> ]			
1	Naphthalene	< LOD	< LOD	< LOD	1.98 ± 0.09
2	1,3-di-iso-propylnaphthalene	< LOD	< LOD	< LOD	< LOD
3	2-Phenylnaphthalene	< LOD	< LOD	< LOD	< LOD
4	Acenaphthylene	0.86 ± 0.04	0.77 ± 0.04	0.24 ± 0.01	0.15 ± 0.01
5	Acenaphthene	1.49 ± 0.07	1.16 ± 0.05	1.45 ± 0.08	0.58 ± 0.03
6	Fluorene	< LOD	0.97 ± 0.05	0.33 ± 0.02	0.79 ± 0.04
7	Anthracene	< LOD	< LOD	(10.0 ± 0.5)·10 <sup>-2</sup>	< LOD
8	Phenanthrene	< LOD	< LOD	< LOD	< LOD
9	3-Methylphenanthrene	0.130 ± 6.2·10 <sup>-3</sup>	0.170 ± 7.4·10 <sup>-3</sup>	< LOD	0.045 ± 2.1·10 <sup>-3</sup>
10	2-Methylphenanthrene	< LOD	0.030 ± 1.2·10 <sup>-3</sup>	< LOD	< LOD
11	9-Methylphenanthrene	< LOD	< LOD	< LOD	< LOD
12	3,6-dimethylphenanthrene	< LOD	< LOD	0.640 ± 3.4·10 <sup>-3</sup>	0.072 ± 3.3·10 <sup>-3</sup>

13	Fluoranthene	< LOD	< LOD	< LOD	< LOD
14	Pyrene	< LOD	< LOD	< LOD	< LOD
15	2-Methylpyrene	$0.023 \pm 1.1 \cdot 10^{-3}$	$0.027 \pm 1.3 \cdot 10^{-3}$	< LOD	< LOD
16	4-Methylpyrene	$0.030 \pm 1.4 \cdot 10^{-3}$	< LOD	$2.7 \cdot 10^{-3} \pm 3.6 \cdot 10^{-5}$	< LOD
17	Benzo[a]fluorene	$6.1 \cdot 10^{-3} \pm 3.1 \cdot 10^{-4}$	$9.7 \cdot 10^{-3} \pm 4.5 \cdot 10^{-4}$	$8.3 \cdot 10^{-3} \pm 4.7 \cdot 10^{-4}$	$7.2 \cdot 10^{-3} \pm 3.4 \cdot 10^{-4}$
18	Benzo[a]anthracene	$7.3 \cdot 10^{-3} \pm 3.4 \cdot 10^{-4}$	< LOD	< LOD	$0.014 \pm 6.6 \cdot 10^{-4}$
19	Chrysene	< LOD	$5.6 \cdot 10^{-3} \pm 2.6 \cdot 10^{-4}$	< LOD	< LOD
20	3-Methylchrysene	$3.9 \cdot 10^{-3} \pm 1.9 \cdot 10^{-4}$	$4.8 \cdot 10^{-3} \pm 1.9 \cdot 10^{-4}$	< LOD	$4.0 \cdot 10^{-3} \pm 1.8 \cdot 10^{-4}$
21	5-Methylchrysene	< LOD	< LOD	< LOD	< LOD
22	6-Methylchrysene	$7.6 \cdot 10^{-3} \pm 3.6 \cdot 10^{-4}$	$8.9 \cdot 10^{-3} \pm 4.1 \cdot 10^{-4}$	$0.015 \pm 8.0 \cdot 10^{-4}$	$0.012 \pm 5.4 \cdot 10^{-4}$
23	Benzo[a]fluoranthene	$1.5 \cdot 10^{-3} \pm 9.8 \cdot 10^{-5}$	$6.8 \cdot 10^{-3} \pm 2.7 \cdot 10^{-4}$	$2.8 \cdot 10^{-3} \pm 1.3 \cdot 10^{-4}$	$2.0 \cdot 10^{-3} \pm 9.4 \cdot 10^{-5}$
24	Benzo[b]fluoranthene	< LOD	$2.8 \cdot 10^{-3} \pm 9.9 \cdot 10^{-5}$	< LOD	< LOD
25	Benzo[k]fluoranthene	< LOD	< LOD	< LOD	< LOD
26	Benzo[j]fluoranthene	< LOD	< LOD	< LOD	< LOD
27	Benzo[a]pyrene	< LOD	< LOD	$7.2 \cdot 10^{-4} \pm 3.1 \cdot 10^{-5}$	$3.9 \cdot 10^{-3} \pm 1.8 \cdot 10^{-4}$
28	Indeno[1,2,3-cd]pyrene	$2.2 \cdot 10^{-3} \pm 1.0 \cdot 10^{-4}$	$2.2 \cdot 10^{-4} \pm 1.2 \cdot 10^{-5}$	$2.4 \cdot 10^{-4} \pm 1.3 \cdot 10^{-5}$	$9.4 \cdot 10^{-4} \pm 5.0 \cdot 10^{-5}$
29	Benzo[ghi]perylene	$1.1 \cdot 10^{-3} \pm 8.2 \cdot 10^{-5}$	$2.3 \cdot 10^{-3} \pm 8.0 \cdot 10^{-5}$	< LOD	$6.4 \cdot 10^{-4} \pm 3.2 \cdot 10^{-5}$
30	Dibenzo[a,h]anthracene	< LOD	$2.0 \cdot 10^{-3} \pm 9.1 \cdot 10^{-5}$	< LOD	$3.3 \cdot 10^{-3} \pm 1.5 \cdot 10^{-4}$
31	Dibenz[a,e]pyrene	< LOD	< LOD	< LOD	< LOD
32	Dibenz[a,h]pyrene	< LOD	< LOD	< LOD	< LOD
33	Dibenz[a,i]pyrene	< LOD	< LOD	< LOD	< LOD
34	Dibenz[a,l]pyrene	< LOD	< LOD	< LOD	< LOD
N- and O-PAHs					
35	Nitronaphthalene	< LOD	< LOD	< LOD	< LOD
36	1-Methyl-5-nitronaphthalene	$0.13 \pm 4.0 \cdot 10^{-3}$	< LOD	< LOD	< LOD

37	1-Methyl-6-nitronaphthalene	$0.12 \pm 5.4 \cdot 10^{-3}$	< LOD	< LOD	< LOD
38	9,10-Anthracenedione	< LOD	< LOD	< LOD	$0.057 \pm 5.7 \cdot 10^{-3}$
39	4H-cyclopenta(def)phenanthrene	$0.58 \pm 0.02$	$0.47 \pm 0.022$	< LOD	$0.27 \pm 0.01$
40	Nitropyrene	< LOD	$0.013 \pm 6.9 \cdot 10^{-3}$	< LOD	< LOD

SD-standard deviation, <LOD- below the limit of detection

Table S9. The content of bioavailable PAHs and their derivatives in RBP-BC.

No.	Compound	Sample description			
		BCUHS-initial	BCKOS-initial	BCPIL-initial	BCZ-initial
		Analyte concentration [ng L <sup>-1</sup> ]			
1	Naphthalene	32.88 ± 1.20	2.73 ± 0.10	1.22 ± 0.045	35.65 ± 1.30
2	1,3-di-iso-propylnaphthalene	7.6·10 <sup>-3</sup> ± 7.6·10 <sup>-4</sup>	0.23 ± 8.3·10 <sup>-3</sup>	0.70 ± 0.025	< LOD
3	2-Phenylnaphthalene	< LOD	0.66 ± 0.024	0.60 ± 0.022	0.16 ± 5.4·10 <sup>-3</sup>
4	Acenaphthylene	2.71 ± 0.10	1.05 ± 0.039	0.72 ± 0.026	1.81 ± 0.07
5	Acenaphthene	3.83 ± 0.14	1.04 ± 0.038	0.39 ± 0.014	1.46 ± 0.05
6	Fluorene	1.06 ± 0.04	2.79 ± 0.10	4.23 ± 0.15	0.59 ± 0.02
7	Anthracene	0.47 ± 0.02	1.50 ± 0.055	1.55 ± 0.057	0.015 ± 6.0·10 <sup>-4</sup>
8	Phenanthrene	< LOD	< LOD	< LOD	< LOD
9	3-Methylphenanthrene	0.093 ± 3.4·10 <sup>-3</sup>	< LOD	0.024 ± 8.3·10 <sup>-4</sup>	3.0·10 <sup>-3</sup> ± 9.9·10 <sup>-5</sup>
10	2-Methylphenanthrene	0.065 ± 2.3·10 <sup>-3</sup>	< LOD	0.026 ± 9.3·10 <sup>-4</sup>	2.0·10 <sup>-3</sup> ± 9.9·10 <sup>-4</sup>
11	9-Methylphenanthrene	< LOD	0.054 ± 1.9·10 <sup>-3</sup>	< LOD	0.014 ± 4.9·10 <sup>-4</sup>
12	3,6-dimethylphenanthrene	0.013 ± 4.4·10 <sup>-4</sup>	< LOD	0.027 ± 9.9·10 <sup>-4</sup>	0.016 ± 5.6·10 <sup>-4</sup>
13	Fluoranthene	0.13 ± 4.9·10 <sup>-3</sup>	0.089 ± 3.2·10 <sup>-3</sup>	0.87 ± 0.032	< LOD
14	Pyrene	0.16 ± 5.9·10 <sup>-3</sup>	0.20 ± 7.4·10 <sup>-3</sup>	< LOD	0.16 ± 6.0·10 <sup>-3</sup>
15	2-Methylpyrene	< LOD	< LOD	< LOD	0.025 ± 9.0·10 <sup>-4</sup>
16	4-Methylpyrene	< LOD	< LOD	7.0·10 <sup>-4</sup> ± 3.5·10 <sup>-5</sup>	0.036 ± 1.3·10 <sup>-3</sup>
17	Benzo[a]fluorene	0.014 ± 5.0·10 <sup>-4</sup>	< LOD	7.0·10 <sup>-4</sup> ± 2.3·10 <sup>-5</sup>	2.1·10 <sup>-3</sup> ± 7.5·10 <sup>-5</sup>
18	Benzo[a]anthracene	0.027 ± 9.8·10 <sup>-4</sup>	< LOD	< LOD	0.012 ± 4.2·10 <sup>-4</sup>
19	Chrysene	0.048 ± 1.8·10 <sup>-3</sup>	5.4·10 <sup>-3</sup> ± 2.0·10 <sup>-4</sup>	4.6·10 <sup>-3</sup> ± 1.7·10 <sup>-4</sup>	1.5·10 <sup>-3</sup> ± 5.5·10 <sup>-5</sup>

20	3-Methylchrysene	$6.2 \cdot 10^{-3} \pm 2.3 \cdot 10^{-4}$	< LOD	$4.4 \cdot 10^{-3} \pm 1.6 \cdot 10^{-4}$	< LOD
21	5-Methylchrysene	$7.3 \cdot 10^{-3} \pm 2.7 \cdot 10^{-4}$	< LOD	$3.8 \cdot 10^{-3} \pm 1.4 \cdot 10^{-4}$	$3.1 \cdot 10^{-3} \pm 1.1 \cdot 10^{-4}$
22	6-Methylchrysene	$3.5 \cdot 10^{-3} \pm 1.3 \cdot 10^{-4}$	< LOD	< LOD	$4.6 \cdot 10^{-3} \pm 1.7 \cdot 10^{-4}$
23	Benzo[a]fluoranthene	$4.7 \cdot 10^{-5} \pm 4.7 \cdot 10^{-6}$	$2.9 \cdot 10^{-3} \pm 1.1 \cdot 10^{-4}$	$0.011 \pm 4.1 \cdot 10^{-4}$	$7.0 \cdot 10^{-3} \pm 2.6 \cdot 10^{-4}$
24	Benzo[b]fluoranthene	$1.4 \cdot 10^{-4} \pm 4.7 \cdot 10^{-6}$	$1.6 \cdot 10^{-3} \pm 5.6 \cdot 10^{-5}$	$6.5 \cdot 10^{-3} \pm 2.4 \cdot 10^{-4}$	$9.7 \cdot 10^{-3} \pm 3.5 \cdot 10^{-4}$
25	Benzo[k]fluoranthene	< LOD	$1.7 \cdot 10^{-3} \pm 6.3 \cdot 10^{-5}$	$3.6 \cdot 10^{-4} \pm 1.2 \cdot 10^{-5}$	$3.2 \cdot 10^{-3} \pm 1.2 \cdot 10^{-4}$
26	Benzo[j]fluoranthene	< LOD	$3.5 \cdot 10^{-4} \pm 1.3 \cdot 10^{-5}$	< LOD	$3.8 \cdot 10^{-4} \pm 1.3 \cdot 10^{-5}$
27	Benzo[a]pyrene	$4.7 \cdot 10^{-3} \pm 1.7 \cdot 10^{-4}$	$2.2 \cdot 10^{-3} \pm 7.7 \cdot 10^{-5}$	< LOD	$2.1 \cdot 10^{-3} \pm 7.5 \cdot 10^{-5}$
28	Indeno[1,2,3-cd]pyrene	$3.4 \cdot 10^{-4} \pm 1.3 \cdot 10^{-5}$	< LOD	$1.2 \cdot 10^{-3} \pm 4.3 \cdot 10^{-5}$	< LOD
29	Benzo[ghi]perylene	$1.6 \cdot 10^{-3} \pm 7.3 \cdot 10^{-5}$	$2.9 \cdot 10^{-4} \pm 9.6 \cdot 10^{-6}$	< LOD	< LOD
30	Dibenzo[a,h]anthracene	< LOD	< LOD	< LOD	$6.6 \cdot 10^{-4} \pm 2.4 \cdot 10^{-5}$
31	Dibenz[a,e]pyrene	< LOD	$5.1 \cdot 10^{-5} \pm 1.9 \cdot 10^{-6}$	$3.1 \cdot 10^{-5} \pm 1.2 \cdot 10^{-6}$	$3.3 \cdot 10^{-5} \pm 1.2 \cdot 10^{-6}$
32	Dibenz[a,h]pyrene	< LOD	$3.2 \cdot 10^{-5} \pm 1.2 \cdot 10^{-6}$	$4.0 \cdot 10^{-5} \pm 1.5 \cdot 10^{-6}$	< LOD
33	Dibenz[a,i]pyrene	< LOD	$2.3 \cdot 10^{-5} \pm 7.7 \cdot 10^{-7}$	$1.6 \cdot 10^{-5} \pm 5.9 \cdot 10^{-7}$	< LOD
34	Dibenz[a,l]pyrene	< LOD	$2.5 \cdot 10^{-5} \pm 9.3 \cdot 10^{-7}$	$1.5 \cdot 10^{-5} \pm 5.9 \cdot 10^{-7}$	< LOD
N- and O-PAHs					
35	Nitronaphthalene	$0.34 \pm 0.014$	< LOD	$1.65 \pm 0.060$	< LOD
36	1-Methyl-5-nitronaphthalene	< LOD	< LOD	$1.54 \pm 0.056$	$0.94 \pm 0.03$
37	1-Methyl-6-nitronaphthalene	< LOD	< LOD	$1.42 \pm 0.052$	$0.77 \pm 0.03$
38	9,10-Anthracenedione	$0.54 \pm 0.019$	$0.17 \pm 6.0 \cdot 10^{-3}$	< LOD	$0.19 \pm 7.3 \cdot 10^{-3}$
39	4H-cyclopenta(def)phenanthrene	$4.3 \cdot 10^{-3} \pm 2.1 \cdot 10^{-4}$	< LOD	< LOD	< LOD
40	Nitropyrene	< LOD	$0.049 \pm 1.8 \cdot 10^{-3}$	$0.035 \pm 1.3 \cdot 10^{-3}$	< LOD

SD-standard deviation, <LOD- below the limit of detection

Table S10. The content of bioavailable PAHs and their derivatives in biologically aged biochars (samples with nutrient solution).

No.	Compound	Sample description			
		BCW-BAn	BCD-BAn	BCF-BAn	BCZ-BAn
		Analyte concentration [ng L <sup>-1</sup> ]			
1	Naphthalene	2.88 ± 0.15	< LOD	1.41 ± 0.07	4.86 ± 0.25
2	1,3-di-iso-propylnaphthalene	< LOD	0.15 ± 7.8·10 <sup>-3</sup>	< LOD	< LOD
3	2-Phenylnaphthalene	< LOD	< LOD	< LOD	< LOD
4	Acenaphthylene	0.38 ± 0.02	< LOD	0.103 ± 0.005	0.188 ± 0.010
5	Acenaphthene	0.69 ± 0.04	0.045 ± 2.3·10 <sup>-3</sup>	0.39 ± 0.02	0.079 ± 0.004
6	Fluorene	< LOD	0.079 ± 4.1·10 <sup>-3</sup>	0.84 ± 0.04	0.13 ± 0.01
7	Anthracene	< LOD	< LOD	< LOD	< LOD
8	Phenanthrene	< LOD	< LOD	< LOD	< LOD
9	3-Methylphenanthrene	< LOD	< LOD	0.037 ± 1.9·10 <sup>-3</sup>	< LOD
10	2-Methylphenanthrene	< LOD	< LOD	4.7·10 <sup>-3</sup> ± 2.5·10 <sup>-4</sup>	< LOD
11	9-Methylphenanthrene	< LOD	< LOD	7.5·10 <sup>-3</sup> ± 3.9·10 <sup>-4</sup>	9.2·10 <sup>-4</sup> ± 4.7·10 <sup>-5</sup>
12	3,6-dimethylphenanthrene	< LOD	< LOD	0.030 ± 1.5·10 <sup>-3</sup>	3.8·10 <sup>-3</sup> ± 2.0·10 <sup>-4</sup>
13	Fluoranthene	< LOD	< LOD	< LOD	< LOD
14	Pyrene	0.067 ± 3.5·10 <sup>-3</sup>	< LOD	0.011 ± 5.6·10 <sup>-4</sup>	0.024 ± 1.2·10 <sup>-3</sup>
15	2-Methylpyrene	< LOD	3.5·10 <sup>-4</sup> ± 1.8·10 <sup>-5</sup>	< LOD	7.0·10 <sup>-4</sup> ± 3.6·10 <sup>-5</sup>
16	4-Methylpyrene	< LOD	2.8·10 <sup>-3</sup> ± 1.5·10 <sup>-4</sup>	< LOD	< LOD
17	Benzo[a]fluorene	9.4·10 <sup>-4</sup> ± 4.8·10 <sup>-5</sup>	2.4·10 <sup>-4</sup> ± 1.2·10 <sup>-5</sup>	0.012 ± 6.4·10 <sup>-4</sup>	< LOD
18	Benzo[a]anthracene	1.1·10 <sup>-3</sup> ± 5.5·10 <sup>-5</sup>	< LOD	9.5·10 <sup>-3</sup> ± 5.0·10 <sup>-4</sup>	2.9·10 <sup>-4</sup> ± 1.5·10 <sup>-5</sup>
19	Chrysene	< LOD	< LOD	< LOD	< LOD

20	3-Methylchrysene	< LOD	< LOD	$2.6 \cdot 10^{-3} \pm 1.3 \cdot 10^{-4}$	< LOD
21	5-Methylchrysene	< LOD	$2.8 \cdot 10^{-3} \pm 1.4 \cdot 10^{-4}$	$1.6 \cdot 10^{-3} \pm 8.2 \cdot 10^{-5}$	< LOD
22	6-Methylchrysene	< LOD	$1.5 \cdot 10^{-3} \pm 7.6 \cdot 10^{-5}$	$4.1 \cdot 10^{-3} \pm 2.1 \cdot 10^{-4}$	< LOD
23	Benzo[a]fluoranthene	< LOD	< LOD	$5.8 \cdot 10^{-4} \pm 3.1 \cdot 10^{-5}$	$5.3 \cdot 10^{-4} \pm 2.7 \cdot 10^{-5}$
24	Benzo[b]fluoranthene	< LOD	< LOD	< LOD	$1.3 \cdot 10^{-3} \pm 6.8 \cdot 10^{-5}$
25	Benzo[k]fluoranthene	< LOD	< LOD	< LOD	$2.4 \cdot 10^{-4} \pm 1.2 \cdot 10^{-5}$
26	Benzo[j]fluoranthene	< LOD	< LOD	< LOD	< LOD
27	Benzo[a]pyrene	< LOD	$5.9 \cdot 10^{-4} \pm 3.0 \cdot 10^{-5}$	$3.2 \cdot 10^{-3} \pm 1.7 \cdot 10^{-4}$	$3.0 \cdot 10^{-5} \pm 1.6 \cdot 10^{-6}$
28	Indeno[1,2,3-cd]pyrene	$4.3 \cdot 10^{-4} \pm 2.2 \cdot 10^{-5}$	< LOD	< LOD	< LOD
29	Benzo[ghi]perylene	< LOD	< LOD	< LOD	< LOD
30	Dibenzo[a,h]anthracene	< LOD	< LOD	$2.3 \cdot 10^{-3} \pm 1.2 \cdot 10^{-4}$	$6.9 \cdot 10^{-5} \pm 3.6 \cdot 10^{-6}$
31	Dibenz[a,e]pyrene	< LOD	< LOD	< LOD	< LOD
32	Dibenz[a,h]pyrene	< LOD	$3.0 \cdot 10^{-6} \pm 1.5 \cdot 10^{-7}$	< LOD	< LOD
33	Dibenz[a,i]pyrene	< LOD	< LOD	< LOD	< LOD
34	Dibenz[a,l]pyrene	< LOD	< LOD	< LOD	< LOD
N- and O-PAHs					
35	Nitronaphthalene	< LOD	< LOD	< LOD	< LOD
36	1-Methyl-5-nitronaphthalene	< LOD	< LOD	< LOD	< LOD
37	1-Methyl-6-nitronaphthalene	< LOD	< LOD	< LOD	$0.013 \pm 6.8 \cdot 10^{-4}$
38	9,10-Anthracenedione	< LOD	< LOD	< LOD	< LOD
39	4H-cyclopenta(def)phenanthrene	< LOD	< LOD	$0.127 \pm 0.007$	< LOD
40	Nitropyrene	< LOD	< LOD	< LOD	< LOD

SD-standard deviation, <LOD- below the limit of detection

Table S11. The content of bioavailable PAHs and their derivatives in biologically aged biochars (with microbial inoculum and nutrient solution).

No.	Compound	Sample description			
		BCW-BAi	BCD-BAi	BCF-BAi	BCZ-BAi
		Analyte concentration [ng L <sup>-1</sup> ]			
1	Naphthalene	5.28 ± 0.28	< LOD	2.38 ± 0.12	5.86 ± 0.31
2	1,3-di-iso-propylnaphthalene	0.015 ± 7.8·10 <sup>-4</sup>	0.265 ± 0.014	< LOD	< LOD
3	2-Phenylnaphthalene	< LOD	< LOD	< LOD	0.078 ± 0.004
4	Acenaphthylene	0.47 ± 0.02	0.090 ± 0.005	0.16 ± 0.01	0.29 ± 0.02
5	Acenaphthene	1.44 ± 0.08	0.53 ± 0.03	0.59 ± 0.03	0.135 ± 0.007
6	Fluorene	4.3·10 <sup>-3</sup> ± 2.2·10 <sup>-4</sup>	0.19 ± 0.01	1.07 ± 0.05	0.173 ± 0.009
7	Anthracene	0.010 ± 5.3·10 <sup>-4</sup>	< LOD	< LOD	2.9·10 <sup>-3</sup> ± 1.5·10 <sup>-4</sup>
8	Phenanthrene	< LOD	< LOD	< LOD	< LOD
9	3-Methylphenanthrene	< LOD	3.8·10 <sup>-3</sup> ± 1.9·10 <sup>-4</sup>	0.062 ± 0.003	< LOD
10	2-Methylphenanthrene	< LOD	5.7·10 <sup>-3</sup> ± 2.9·10 <sup>-4</sup>	8.5·10 <sup>-3</sup> ± 4.3·10 <sup>-4</sup>	< LOD
11	9-Methylphenanthrene	< LOD	7.6·10 <sup>-3</sup> ± 3.9·10 <sup>-4</sup>	0.0122 ± 6.3·10 <sup>-4</sup>	4.7·10 <sup>-3</sup> ± 2.5·10 <sup>-4</sup>
12	3,6-dimethylphenanthrene	< LOD	3.2·10 <sup>-3</sup> ± 1.7·10 <sup>-4</sup>	0.0415 ± 2.1·10 <sup>-4</sup>	3.9·10 <sup>-3</sup> ± 2.1·10 <sup>-4</sup>
13	Fluoranthene	7.1·10 <sup>-3</sup> ± 3.7·10 <sup>-4</sup>	< LOD	< LOD	< LOD
14	Pyrene	0.122 ± 6.4·10 <sup>-3</sup>	< LOD	0.0168 ± 8.6·10 <sup>-4</sup>	0.027 ± 0.001
15	2-Methylpyrene	< LOD	1.4·10 <sup>-3</sup> ± 7.4·10 <sup>-5</sup>	< LOD	2.2·10 <sup>-3</sup> ± 1.1·10 <sup>-4</sup>
16	4-Methylpyrene	< LOD	3.2·10 <sup>-3</sup> ± 1.7·10 <sup>-4</sup>	< LOD	3.9·10 <sup>-3</sup> ± 2.0·10 <sup>-4</sup>
17	Benzo[a]fluorene	2.3·10 <sup>-3</sup> ± 1.2·10 <sup>-4</sup>	5.0·10 <sup>-3</sup> ± 2.6·10 <sup>-4</sup>	0.0149 ± 7.6·10 <sup>-4</sup>	1.2·10 <sup>-4</sup> ± 6.2·10 <sup>-6</sup>
18	Benzo[a]anthracene	2.8·10 <sup>-3</sup> ± 1.5·10 <sup>-4</sup>	3.2·10 <sup>-3</sup> ± 1.6·10 <sup>-4</sup>	0.0159 ± 8.1·10 <sup>-4</sup>	7.9·10 <sup>-4</sup> ± 4.1·10 <sup>-5</sup>
19	Chrysene	1.1·10 <sup>-4</sup> ± 5.6·10 <sup>-6</sup>	< LOD	< LOD	< LOD
20	3-Methylchrysene	< LOD	6.5·10 <sup>-4</sup> ± 3.3·10 <sup>-5</sup>	5.3·10 <sup>-3</sup> ± 2.7·10 <sup>-4</sup>	< LOD

21	5-Methylchrysene	< LOD	$7.1 \cdot 10^{-3} \pm 3.6 \cdot 10^{-4}$	$2.8 \cdot 10^{-3} \pm 1.4 \cdot 10^{-4}$	$3.6 \cdot 10^{-4} \pm 1.9 \cdot 10^{-5}$
22	6-Methylchrysene	< LOD	$5.7 \cdot 10^{-3} \pm 2.9 \cdot 10^{-4}$	$6.1 \cdot 10^{-3} \pm 3.1 \cdot 10^{-4}$	< LOD
23	Benzo[a]fluoranthene	< LOD	$2.3 \cdot 10^{-4} \pm 1.2 \cdot 10^{-5}$	$9.9 \cdot 10^{-4} \pm 5.1 \cdot 10^{-5}$	$2.0 \cdot 10^{-3} \pm 1.0 \cdot 10^{-4}$
24	Benzo[b]fluoranthene	< LOD	< LOD	< LOD	$1.7 \cdot 10^{-3} \pm 9.0 \cdot 10^{-5}$
25	Benzo[k]fluoranthene	< LOD	< LOD	< LOD	$4.6 \cdot 10^{-4} \pm 2.4 \cdot 10^{-5}$
26	Benzo[j]fluoranthene	< LOD	< LOD	< LOD	< LOD
27	Benzo[a]pyrene	$1.1 \cdot 10^{-3} \pm 5.8 \cdot 10^{-5}$	$1.2 \cdot 10^{-3} \pm 6.3 \cdot 10^{-5}$	$4.3 \cdot 10^{-3} \pm 2.2 \cdot 10^{-5}$	$9.4 \cdot 10^{-5} \pm 4.9 \cdot 10^{-6}$
28	Indeno[1,2,3-cd]pyrene	< LOD	< LOD	< LOD	< LOD
29	Benzo[ghi]perylene	< LOD	< LOD	< LOD	< LOD
30	Dibenzo[a,h]anthracene	$1.4 \cdot 10^{-5} \pm 7.6 \cdot 10^{-7}$	< LOD	$3.0 \cdot 10^{-3} \pm 1.5 \cdot 10^{-4}$	$1.1 \cdot 10^{-4} \pm 6.0 \cdot 10^{-6}$
31	Dibenz[a,e]pyrene	$4.5 \cdot 10^{-6} \pm 2.4 \cdot 10^{-7}$	$4.5 \cdot 10^{-6} \pm 2.3 \cdot 10^{-7}$	< LOD	$6.0 \cdot 10^{-6} \pm 3.1 \cdot 10^{-7}$
32	Dibenz[a,h]pyrene	< LOD	$7.5 \cdot 10^{-6} \pm 3.9 \cdot 10^{-7}$	< LOD	< LOD
33	Dibenz[a,i]pyrene	< LOD	< LOD	< LOD	< LOD
34	Dibenz[a,l]pyrene	< LOD	< LOD	< LOD	< LOD
N- and O-PAHs					
35	Nitronaphthalene	$0.179 \pm 0.009$	< LOD	< LOD	< LOD
36	1-Methyl-5-nitronaphthalene	< LOD	< LOD	< LOD	< LOD
37	1-Methyl-6-nitronaphthalene	< LOD	< LOD	< LOD	$0.109 \pm 0.005$
38	9,10-Anthracenedione	< LOD	< LOD	$0.0578 \pm 2.9 \cdot 10^{-3}$	< LOD
39	4H-cyclopenta(def)phenanthrene	< LOD	< LOD	$0.181 \pm 0.009$	< LOD
40	Nitropyrene	< LOD	< LOD	< LOD	< LOD

SD-standard deviation, <LOD- below the limit of detection

Table S12. The content of bioavailable PAHs and their derivatives in enzymatically-aged biochars.

No.	Compound	Sample description					
		BCS-EA	BCZ-EA	BCKOS-EA	BCPIL-EA	BCUHS-EA	BCW-EA
		Analyte concentration [ng L <sup>-1</sup> ]					
1	Naphthalene	< LOD	2.15 ± 0.08	0.28 ± 0.01	< LOD	2.38 ± 0.09	1.31 ± 0.05
2	1,3-di-iso-propylnaphthalene	< LOD	< LOD	< LOD	0.122 ± 0.004	< LOD	< LOD
3	2-Phenylnaphthalene	< LOD	< LOD	< LOD	0.025 ± 1.3·10 <sup>-3</sup>	< LOD	< LOD
4	Acenaphthylene	0.119 ± 0.004	0.47 ± 0.02	0.55 ± 0.02	0.056 ± 1.9·10 <sup>-3</sup>	0.39 ± 0.01	0.235 ± 0.009
5	Acenaphthene	0.165 ± 0.006	0.29 ± 0.01	0.56 ± 0.02	8.8·10 <sup>-3</sup> ± 1.2·10 <sup>-4</sup>	0.71 ± 0.03	0.41 ± 0.01
6	Fluorene	< LOD	0.074 ± 0.003	0.228 ± 0.008	0.46 ± 0.02	0.29 ± 0.01	< LOD
7	Anthracene	< LOD	< LOD	0.145 ± 0.005	0.30 ± 0.01	0.078 ± 0.003	0.0145 ± 5.8·10 <sup>-4</sup>
8	Phenanthrene	< LOD	< LOD	< LOD	< LOD	< LOD	< LOD
9	3-Methylphenanthrene	0.019 ± 7.3·10 <sup>-4</sup>	< LOD	< LOD	< LOD	0.010 ± 4.0·10 <sup>-4</sup>	< LOD
10	2-Methylphenanthrene	< LOD	< LOD	< LOD	< LOD	0.0194 ± 7.0·10 <sup>-4</sup>	< LOD
11	9-Methylphenanthrene	< LOD	< LOD	< LOD	< LOD	< LOD	< LOD
12	3,6-dimethylphenanthrene	< LOD	< LOD	< LOD	9.5·10 <sup>-3</sup> ± 4.0·10 <sup>-4</sup>	< LOD	< LOD
13	Fluoranthene	< LOD	< LOD	0.0173 ± 6.0·10 <sup>-4</sup>	0.075 ± 0.003	0.0253 ± 9.0·10 <sup>-4</sup>	< LOD
14	Pyrene	< LOD	0.052 ± 0.002	0.091 ± 0.003	< LOD	0.0689 ± 2.5·10 <sup>-3</sup>	0.0202 ± 7.0·10 <sup>-4</sup>
15	2-Methylpyrene	0.016 ± 5.9·10 <sup>-4</sup>	9.6·10 <sup>-3</sup> ± 3.3·10 <sup>-4</sup>	< LOD	< LOD	< LOD	< LOD
16	4-Methylpyrene	0.027 ± 1.0·10 <sup>-3</sup>	0.0229 ± 8.5·10 <sup>-4</sup>	< LOD	< LOD	< LOD	< LOD
17	Benzo[a]fluorene	1.3·10 <sup>-3</sup> ± 4.6·10 <sup>-5</sup>	< LOD	< LOD	< LOD	3.1·10 <sup>-3</sup> ± 1.0·10 <sup>-4</sup>	1.9·10 <sup>-3</sup> ± 6.6·10 <sup>-5</sup>
18	Benzo[a]anthracene	1.1·10 <sup>-3</sup> ± 3.8·10 <sup>-5</sup>	4.3·10 <sup>-3</sup> ± 1.5·10 <sup>-4</sup>	< LOD	< LOD	4.5·10 <sup>-3</sup> ± 2.0·10 <sup>-4</sup>	3.0·10 <sup>-4</sup> ± 1.0·10 <sup>-5</sup>
19	Chrysene	< LOD	< LOD	< LOD	2.0·10 <sup>-4</sup> ± 1.0·10 <sup>-5</sup>	0.0104 ± 4.0·10 <sup>-4</sup>	< LOD
20	3-Methylchrysene	< LOD	< LOD	< LOD	2.9·10 <sup>-3</sup> ± 1.0·10 <sup>-4</sup>	1.5·10 <sup>-3</sup> ± 6.0·10 <sup>-5</sup>	< LOD

21	5-Methylchrysene	< LOD	$2.2 \cdot 10^{-4} \pm 7.4 \cdot 10^{-6}$	< LOD	$2.6 \cdot 10^{-3} \pm 1.0 \cdot 10^{-4}$	$8.0 \cdot 10^{-4} \pm 3.0 \cdot 10^{-5}$	< LOD
22	6-Methylchrysene	$1.6 \cdot 10^{-3} \pm 5.5 \cdot 10^{-5}$	$8.1 \cdot 10^{-4} \pm 3.0 \cdot 10^{-5}$	< LOD	< LOD	$4.0 \cdot 10^{-4} \pm 1.0 \cdot 10^{-5}$	< LOD
23	Benzo[a]fluoranthene	$1.3 \cdot 10^{-4} \pm 4.4 \cdot 10^{-6}$	$4.4 \cdot 10^{-3} \pm 1.6 \cdot 10^{-4}$	< LOD	$5.1 \cdot 10^{-3} \pm 2.0 \cdot 10^{-4}$	< LOD	< LOD
24	Benzo[b]fluoranthene	< LOD	$4.9 \cdot 10^{-3} \pm 1.8 \cdot 10^{-4}$	< LOD	$4.1 \cdot 10^{-3} \pm 2.0 \cdot 10^{-4}$	< LOD	< LOD
25	Benzo[k]fluoranthene	< LOD	$5.4 \cdot 10^{-3} \pm 1.9 \cdot 10^{-5}$	< LOD	< LOD	< LOD	< LOD
26	Benzo[j]fluoranthene	< LOD					
27	Benzo[a]pyrene	< LOD	$4.5 \cdot 10^{-4} \pm 1.6 \cdot 10^{-5}$	$3.0 \cdot 10^{-4} \pm 1.0 \cdot 10^{-5}$	< LOD	$2.9 \cdot 10^{-3} \pm 1.0 \cdot 10^{-4}$	$3.8 \cdot 10^{-4} \pm 1.3 \cdot 10^{-5}$
28	Indeno[1,2,3-cd]pyrene	$1.5 \cdot 10^{-3} \pm 5.6 \cdot 10^{-5}$	< LOD				
29	Benzo[ghi]perylene	$1.6 \cdot 10^{-4} \pm 6.7 \cdot 10^{-6}$	< LOD	$7.0 \cdot 10^{-5} \pm 2.0 \cdot 10^{-6}$	< LOD	< LOD	< LOD
30	Dibenzo[a,h]anthracene	< LOD	$2.9 \cdot 10^{-5} \pm 1.5 \cdot 10^{-6}$	< LOD	< LOD	< LOD	< LOD
31	Dibenz[a,e]pyrene	< LOD	< LOD	$4.0 \cdot 10^{-6} \pm 1.0 \cdot 10^{-7}$	$1.0 \cdot 10^{-6} \pm 1.2 \cdot 10^{-7}$	< LOD	< LOD
32	Dibenz[a,h]pyrene	< LOD	< LOD	< LOD	$4.0 \cdot 10^{-6} \pm 1.0 \cdot 10^{-7}$	< LOD	< LOD
33	Dibenz[a,i]pyrene	< LOD	< LOD	$3.0 \cdot 10^{-6} \pm 1.0 \cdot 10^{-7}$	$3.0 \cdot 10^{-6} \pm 1.0 \cdot 10^{-7}$	< LOD	< LOD
34	Dibenz[a,l]pyrene	< LOD	< LOD	$4.0 \cdot 10^{-6} \pm 1.0 \cdot 10^{-7}$	< LOD	< LOD	< LOD
N- and O-PAHs							
35	Nitronaphthalene	< LOD	< LOD	< LOD	$0.52 \pm 0.02$	$0.025 \pm 0.001$	$1.21 \pm 0.04$
36	1-Methyl-5-nitronaphthalene	$0.118 \pm 0.004$	$0.58 \pm 0.02$	< LOD	$1.24 \pm 0.05$	< LOD	< LOD
37	1-Methyl-6-nitronaphthalene	$0.105 \pm 0.004$	$0.59 \pm 0.02$	< LOD	$0.63 \pm 0.02$	< LOD	< LOD
38	9,10-Anthracenedione	< LOD	$0.024 \pm 0.001$	< LOD	< LOD	$0.170 \pm 0.001$	< LOD
39	4H-cyclopenta(def)phenanthrene	$0.127 \pm 0.005$	< LOD				
40	Nitropyrene	< LOD	< LOD	$0.038 \pm 0.001$	$4.5 \cdot 10^{-3} \pm 2.0 \cdot 10^{-4}$	< LOD	< LOD

SD-standard deviation, <LOD- below the limit of detection

## References

- [1] D. Fabbri, A.G. Rombolà, C. Torri, K.A. Spokas, Determination of polycyclic aromatic hydrocarbons in biochar and biochar amended soil, *Journal of Analytical and Applied Pyrolysis.* 103 (2013) 60–67. <https://doi.org/10.1016/j.jaat.2012.10.003>.

## **Publikacja D6**

**A. Krzyszczak, M. Dybowski, I. Jośko, M. Kusiak, M. Sikora, B. Czech**

*The antioxidant defense responses of Hordeum vulgare L. to polycyclic aromatic hydrocarbons and their derivatives in biochar-amended soil*

Environmental Pollution, 2022, 294, 118664



## The antioxidant defense responses of *Hordeum vulgare* L. to polycyclic aromatic hydrocarbons and their derivatives in biochar-amended soil<sup>☆</sup>

Agnieszka Krzyszczak<sup>a</sup>, Michał Dybowski<sup>b</sup>, Izabela Jośko<sup>c</sup>, Magdalena Kusiak<sup>d</sup>, Małgorzata Sikora<sup>d</sup>, Bożena Czech<sup>a,\*</sup>

<sup>a</sup> Department of Radiochemistry and Environmental Chemistry, Institute of Chemical Sciences, Faculty of Chemistry, Maria Curie-Skłodowska University in Lublin, Pl. M. Curie-Skłodowskiej 3, 20-031, Lublin, Poland

<sup>b</sup> Department of Chromatography, Institute of Chemical Sciences, Faculty of Chemistry, Maria Curie Skłodowska University in Lublin, Pl. M. Curie-Skłodowskiej 3, 20-031, Lublin, Poland

<sup>c</sup> Institute of Plant Genetics, Breeding and Biotechnology, Faculty of Agrobioengineering, University of Life Sciences, Akademicka 15 St., 20-950, Lublin, Poland

<sup>d</sup> Department of Biochemistry and Food Chemistry, Faculty of Food Science and Biotechnology, University of Life Sciences, Skromna 8 St., 20-704, Lublin, Poland



### ARTICLE INFO

#### Keywords:

Oxidative stress

N-PAHs

O-PAHs

Antioxidative enzymes

MDA

### ABSTRACT

The recent studies indicated that the biochar (BC) may be a source of polycyclic aromatic hydrocarbons (PAHs) as well as their oxygen, nitrogen, or sulfur-containing derivatives that are considered as more toxic pollutants than their parent compounds. Here, the assessment of the impact of various biochars addition (1% wt.) to soil on barley *Hordeum vulgare* L. growth was presented. The concentrations of bioavailable PAHs and their derivatives in biochar were determined. PAHs increased reactive oxygen species generation resulting in oxidative stress in organisms. In this study, the response of soil-grown plants was examined in terms of the activity of the antioxidative enzymes (superoxide dismutase, catalase, peroxidase), lipid peroxidation, and the expression of genes related to oxidative stress. The results indicate that despite low content of a bioavailable fraction of parent compounds and their derivatives (up to  $4.45 \pm 0.24 \text{ ng g}^{-1}$  and  $0.83 \pm 0.03 \text{ ng L}^{-1}$ , respectively) the biochemical response of plant was present, the activity of superoxide dismutase increased up to 2 times, but the activity of the other enzymes was lowered. The transcript level values support the studies on enzymatic activity. The presence of PAHs and their derivatives induced oxidative stress slightly but the plant was able to mitigate it.

### 1. Introduction

Polycyclic aromatic hydrocarbons (PAHs) derivatives belong to a large group of organic contaminants. PAHs consist of two or more aromatic rings, whereas their derivatives possess carbonyl-, nitro-, hydroxyl-functional groups (in a place of hydrogen), or sulfur, oxygen, and nitrogen atom (in a place of carbon in the aromatic ring) (Wei et al., 2015). Therefore, O-PAHs, N-PAHs, OH-PAHs, PASHs, and AZAs (azaarenes) can be distinguished. PAHs derivatives are widespread and occur in various matrices, e.g. air (Alves et al., 2017; Souza et al., 2014), soil (Lundstedt et al., 2014; Musa Bandowe et al., 2019, 2010; Wilcke et al., 2014), sediments (Han et al., 2019) or rivers (Qiao et al., 2014). Weidemann et al. (2018) reported the formation of selected PAHs derivatives in biochar-carbon material obtained from the pyrolysis of biomass. The content of PAHs derivatives was governed by the applied

feedstock and pyrolysis conditions (mainly temperature): total O-PAHs and N-PAHs concentrations amounted to  $34\text{--}3100 \text{ ng g}^{-1}$  and  $0.4\text{--}477 \text{ ng g}^{-1}$ , respectively. Our studies indicated that these values may be lower (Table 1). Lower content, however, does not exclude the higher hazard. It was noted that N-PAHs exhibit higher polarity and water solubility than parental PAHs, thereby their bioavailability and toxicity are expected to be also increased (Pašková et al., 2006).

PAHs are considered as abiotic stressors that induce oxidative stress by excessive generation of reactive oxygen species (ROS) (Demidchik, 2015). Further, oxidative stress may entail cell damage and death (Kordrostami et al., 2019). A few studies confirmed the overproduction of ROS under the presence of PAHs derivatives. 1-nitropyrene (1-NP, at a concentration of  $\leq 10 \mu\text{M}$ ) caused DNA damage and induced the formation of ROS in human umbilical vein endothelial cells (Andersson

<sup>☆</sup> This paper has been recommended for acceptance by Dr. Da Chen.

\* Corresponding author.

E-mail address: [bczech@hektor.umcs.lublin.pl](mailto:bczech@hektor.umcs.lublin.pl) (B. Czech).

et al., 2009) and a cultured human lung epithelial cell line (Kim et al., 2005). Sklorz et al. (2007) found that some O-PAHs can participate in the formation of ROS and oxygen-free radicals. Biochar can stimulate soil microflora and increase the accumulation of carbon in soil. Yun et al. suggested that the radicals  $O_2^-$  and  $H_2O_2$  formed upon N-PAHs (especially 1-nitropyrene) exposure caused the genotoxicity in barley (Yun et al., 2019). Some studies have already proved that derivatives are much more toxic than parent PAHs inducing lipid peroxidation, DNA damage (Chatel et al., 2014). The study by Burýšková et al. (2006) revealed higher embryonic mortality in *Xenopus laevis* preceded by oxidative stress under N-heterocyclic derivatives of PAHs exposure than parent PAHs. Little is known about the toxicity of O-PAHs (Abbas et al., 2018). In response to the imbalance of ROS content, the defense system involving enzymatic and non-enzymatic systems is activated (Racchi, 2013). So far, only the effect of parental PAHs on antioxidant defense responses was investigated (Ahamed et al., 2012; Li et al., 2008; Liu et al., 2009a). Phenanthrene increased peroxidase (POD) and ascorbate peroxidase (APX) activity in *Arabidopsis thaliana* at 0.25 mM and declined at higher concentrations (Liu et al., 2009a). Superoxide dismutase (SOD) activity in *Oryza sativa* L. was the most sensitive to the presence of phenanthrene and pyrene (Li et al., 2008). There is a knowledge gap in the antioxidant effects induced by PAHs derivatives.

The addition of biochar into soil results in an increase in crop growth and yield (Rawat et al., 2019). It also improves soil quality, retains nutrients (Bonanomi et al., 2017). BC amendment to the soil affects the physicochemical properties of modified soil: increased pH, moisture-holding capacity, electric conductivity, organic carbon, total nitrogen, available phosphorus, potassium, zinc, calcium, copper, and the cation-exchange capacity (Dume et al., 2016; Lehmann et al., 2003; Mensah and Frimpong, 2018). Biochar can stimulate soil microflora and caused an increase in the accumulation of carbon in soil (Rawat et al., 2019). The BC addition into soil increased maize yield (Major et al., 2010), the higher grain yield of upland rice (*Oryza sativa*) (Asai et al., 2009), increased proportion of the nitrogen fixed by bean plants (*Phaseolus vulgaris*), production of biomass and bean yield (Rondon et al., 2007). From practical point of view a 1% addition of BC is often applied that corresponds to 30 t per ha in the field (Oleszczuk et al., 2016). In the context of the application of biochar to soil, there is a pressing need to evaluate the antioxidant response of plants, crucial components of the agroecosystem, in biochar-amended soil.

To narrow the above-mentioned knowledge gaps, here we determined the bioavailability of PAHs and their derivatives in biochars applied to the soil with different properties as well as their phytotoxicity. The antioxidant enzymes activity, lipid peroxidation, and the

expression of genes (Zn/Cu SOD, CAT (catalase), APX, GPX (glutathione peroxidase)) related to oxidative stress in barley, *Hordeum vulgare* L were investigated. Due to its importance for food, feed, and brewing (Mayer et al., 2011), it is crucial to test the impact of PAHs derivatives introduced with biochar on barley. The study provides new insights into the fate of PAHs derivatives in the BC-soil-plant system.

## 2. Materials and methods

### 2.1. Biochar preparation and characterization

Slow pyrolysis of biomass in an oxygen-poor atmosphere (<2%  $O_2$ ) was applied using feedstock or temperatures presented in Table 1. The abbreviations of studied biochars mean as follows: BCS500, BCS600, and BCS700 – straw-derived biochars obtained at 500 °C, 600 °C, and 700 °C, respectively; BCA600, BCD600, and BCF600 – biochars obtained at 600 °C from sunflower, hardwood, and softwood wastes, respectively. The chemical properties of biochar were determined by standard methods (Hale et al., 2012; Oleszczuk et al., 2016). The characteristic of biomass included elemental analysis (C, H, N analysis in CHN analyzer 2400 PerkinElmer), surface area estimation (nitrogen adsorption-desorption in ASAP 2420, Micromeritics Inc. USA), surface characterization (FT-IR spectra collected in FTIR iN10 MX, Thermo Scientific). The content of total and bioavailable PAHs and PAHs derivatives was performed using GCMS-TQ8040 (Shimadzu) according to the procedure described in SI. The main physicochemical parameters of tested biochar were presented in Table 1.

### 2.2. Soil experiment

Three soils characterized at different properties (Table S1) were used in the experiment. Air-dried soils (65 g) were placed in the polyethylene probes, then the different biochars at 1% wt. were added. Next, the samples were homogenized. 5 g of soil samples were taken for the chemical extraction of PAHs bioavailable fraction content. The rest of the soil samples (60 g) were watered with MQ-water to reach 40% of water holding capacity and used for plant growth. As a blank sample e.g. soil without BC was applied.

### 2.3. Plant growth conditions and response to the presence of PAHs and their derivatives

The procedure of *H. vulgare* (cultivar Ella) cultivation was described in the Supporting Information. The studies on the antioxidant enzyme

**Table 1**

The characteristics of the applied materials (n = 3; n-number of replicates).

Biochar label	Feedstock	T <sub>P</sub> [°C]	S <sub>BET</sub>	TOC [%]	C [%]	H [%]	N [%]	O [%]	H/C	(O + N)/C	O/C	T-PAHs ± SD [ng g <sup>-1</sup> ]	DT-PAHs ± SD [ng g <sup>-1</sup> ]	TB-PAHs ± SD [ng L <sup>-1</sup> ]	DTB-PAHs ± SD [ng L <sup>-1</sup> ]
BCS500	Wheat straw ( <i>Triticum L.</i> )	500	24.32	21.85	65.79	2.20	1.43	8.73	0.033	0.154	0.133	124.53 ± 5.70	22.81 ± 1.04	3.53 ± 0.18	0.177 ± 6.8 × 10 <sup>-3</sup>
BCS600		600	2.47	19.59	66.14	1.66	1.26	11.36	0.025	0.191	0.172	145.21 ± 6.65	28.40 ± 1.30	2.56 ± 0.11	0.83 ± 0.03
BCS700		700	0.37	14.73	68.39	1.20	1.22	14.48	0.018	0.230	0.212	65.37 ± 2.99	19.16 ± 0.88	1.67 ± 0.07	0.62 ± 0.03
BCA600	Sunflower ( <i>Helianthus L.</i> )	600–650 °C	0.494	4.42	81.29	1.58	1.03	11.61	0.019	0.155	0.143	151.47 ± 6.94	7.64 ± 0.35	4.45 ± 0.24	0.51 ± 0.02
BCD600	Hardwood wastes	600–650 °C	1.149	10.77	61.50	3.11	1.18	23.41	0.051	0.400	0.381	57.36 ± 2.63	< LOD	2.22 ± 0.11	< LOD
BCF600	Softwood wastes	600–650 °C	0.749	3.90	77.54	3.93	0.24	22.18	0.051	0.289	0.286	134.01 ± 6.14	11.89 ± 0.54	3.67 ± 0.17	0.32 ± 0.02

T<sup>P</sup> - Pyrolysis temperature, S<sub>BET</sub> - BET specific surface area [ $m^2 g^{-1}$ ], TOC – total organic content [%], C, H, N, O – content [%], T-PAHs - the total PAHs content [ $ng g^{-1}$ ], SD - standard deviation, DT-PAHs - The total PAHs derivatives content [ $ng g^{-1}$ ], TB-PAHs - The total bioavailable PAHs concentration [ $ng L^{-1}$ ], DTB-PAHs - The total bioavailable PAHs derivatives concentration [ $ng L^{-1}$ ].

activity were conducted using plant tissues extract. The activities of superoxide dismutase and catalase were measured using SOD Assay Kit® and Catalase Assay Kit® (Merck, Germany), whereas the activity of peroxidase was determined by the procedure described in (Złotek et al., 2019), measuring the absorbance at 470 nm. The protein content in samples was determined according to Bradford (1976). The tissue malondialdehyde (MDA) levels were analyzed according to the protocol described in (Wessely-Szponder et al., 2015). The mean values were obtained from three different plants.

For the expression of genes (Zn/Cu SOD, CAT, APX, GPX) related with oxidative stress isolation of the total RNA from leaves modified TRIzol™ reagent (Thermo Fisher Scientific Inc.) was applied (Wang et al., 2012). RNA concentration and purity were determined spectrophotometrically (NanoDrop 2000, Thermo Fisher Scientific Inc.). Electrophoresis in 2% agarose gel stained with ethidium bromide was applied for the determination of the integrity of RNA samples. Genomic DNA was removed by DNase I (Thermo Fisher Scientific Inc.) treatment. The reaction of reverse transcription was performed on 1 µg RNA with NG dART RT kit (EURx Sp. z o.o.). Obtained cDNA was used as a template in the qPCR analysis. Seven commonly used candidate reference genes (ADP, ACT, GAPDH, RNABP, TUB, UBI, EF) were tested in three replicates per treatment. geNorm algorithm was used to analyze the stability of the candidate reference genes under test conditions. The two most stable genes (ACT, ADP) were selected as reference genes sufficient to normalize gene expression data. The transcript levels of Cu/Zn-SOD, CAT, APX, GPX genes were determined by real-time PCR analysis. The ACT (GenBank Accession No. GQ339780.1) and ADP (GenBank Accession No. EF405961.1) genes were used for data normalization (an internal control). The used primers are provided in Table 2. Real time-PCR was carried out according to the cycling program described in Supplementary Information. Each sample was analyzed in two technical replicates. The results were analyzed using the dedicated relative quantification software module from ThermoFisher Cloud (Thermo-Fisher Scientific).

#### 2.4. Statistical analysis

Significant differences between treatments were tested by one-way analysis of variance (ANOVA) followed by the least significant difference (LSD) test (for the chemical and biochemical results) and Dunnett's post hoc test (for the gene expression analysis) at a significance level of 0.05. Two-tailed Pearson correlation analysis was performed to test variables. The significance of the correlation factors was evaluated at a significance level of 0.01 and 0.05.

### 3. Results

#### 3.1. Physicochemical properties of tested biochar

The composition of biochars varied greatly with the feedstock and pyrolysis temperature (Table 1). The tested biochar was characterized

by low specific surface area ( $S_{BET}$ ) and it can be seen that when straw was used as a feedstock, the increase of the pyrolysis temperature lowered the  $S_{BET}$  significantly. Among BC obtained at 600 °C, the highest  $S_{BET}$  revealed BCS600 and the other biochars possessed a significantly lower surface area. The chemical composition of tested materials indicated the predominance of carbon and the highest percentage of C was noted in sunflower-derived biochars - 81.29% and the lowest – in BC obtained from hardwood 61.50%. At the same time, the content of H was the highest in wood-derived BC (3.11% and 3.93%, for hard- and soft-wood as the feedstock, respectively). The presence of N in biochars was related to the presence of lignins in the feedstock.

The ratios of H/C, (O + N)/C, and O/C were calculated to characterize the aromaticity, hydrophilicity, and polarity of biochar, respectively. The H/C ratio is used for predicting the sorption of hydrophobic organic contaminants (HOCs) such as PAHs onto biochars (Xiao et al., 2016): an increase in the H/C ratio will lower the adsorption of HOCs. The highest hydrophilicity revealed BCD600 and BCF600 being at the same time the most polar biochar. It may result from the presence of many surface functional groups (presented in Fig. S1A) e.g. -OH in polymeric compounds representing dehydration of cellulose and ligneous compounds (3465 cm<sup>-1</sup> O-H stretching) (Rafiq et al., 2016), C-O in alcohols, esters, or ethers (1100 cm<sup>-1</sup> C-O stretching). Biochar surface is enriched in alkanes (1397 cm<sup>-1</sup> C-H deformation) and alkenes (1635 cm<sup>-1</sup> C=C stretching). Van Krevelen diagram presented in Fig. S1B showed that an increase of the pyrolysis temperature reduced the aromaticity of BCS biochars. Overall, the hydrogen content decreased whereas the content of oxygen increased with increasing temperature suggesting greater hydrophilicity of the biochars (Rafiq et al., 2016).

To verify the effect of the presence of PAHs and their derivatives on the grown *Hordeum vulgare* L. the amount of total (T-) and bioavailable (B-) PAHs and their derivatives (D-PAHs) (Table 1; Table S2; Table S3; Fig. S1) was estimated. Firstly, the amount of PAHs determined in all BC samples was in the range of 57.36–151.47 ng g<sup>-1</sup> (for BCD600 and BCA600, respectively). The low content of O-, N-PAHs derivatives was noted in biochars but their amounts varied from 5.04% (BCA600) to 29.31% (BCS700). The environmental hazard of PAHs, however, may be excluded if their bioaccessibility is low. Therefore, the concentrations fraction of bioavailable PAHs and their derivatives were estimated. The concentrations of bioavailable PAHs did not differ significantly (1.67–4.45 ng L<sup>-1</sup>, for BCS700 and BCA600, respectively), and the percentage of bioavailable PAHs in the total PAHs content reached 1.46–3.87%, for BCS600 and BCD600, respectively. It may indicate that only a small fraction of PAHs is mobile and can affect the cultivated plant (Oleszczuk et al., 2016). BCS600 was characterized by the highest concentration of bioavailable PAHs derivatives 0.83 ± 0.03 ng L<sup>-1</sup>. In the case of BCD600 biochar, there were no quantified derivatives. The highest percentage of PAHs derivatives compared to the total concentration of bioavailable parent PAHs and derivatives was determined for BCS700 and BCS600 (27.22% and 24.49%, respectively) (Fig. S2).

The effect of physicochemical parameters on the amount of PAHs

**Table 2**

Sequences of primers and internal reference used for RT-PCR.

Gene	Primer	Primer (5' → 3') sequence	NCBI/Phytozome Acc. number
Cu/Zn SOD	SODCuZn-F	CTGGAAATGCTGGTGGAA	U69536.1
	SODCuZn-R	GAGAATGGCGTCGTTACA	
CAT	Cat-F	TCACCAACAACCATCAT	X94352.1
	Cat-R	GGCAGGCCAGATAGAACAC	
APX	APX-F	AAGATGCCACAAGGAGAG	Traes_2AS_007D8F7BD.1
	APX-R	GCTCAGTGAAGTAAGAGTTG	
GPX	GPX-F	CTTATACAAGTCCCTGAAGTCT	KP844737.1
	GPX-R	GGCATAGCGGTCTACAAAC	
ADP	ADP-F	AGGTTCTTGATGCTGATGTG	EF405961.1
	ADP-R	CGGAGTCAACTACTGAATG	
ACT	ACT-F	GGACGCACACAGGTATC	GQ339780.1
	ACT-R	CGAGGTCAAGACGAAGGA	

and their derivatives both in the total and bioavailable forms was noted. The Pearson correlation between physicochemical parameters of biochars revealed that with increased C content in BC the amount of total PAHs was statistically significant ( $R = 0.92$ ,  $p < 0.01$ ). The fraction of the bioavailable PAHs and bioavailable PAHs derivatives was negatively correlated ( $p < 0.05$ ) with the extension of the surface area. As it can be expected, the increased surface area will sorb PAHs more efficiently, and lower bioavailable PAHs and their derivatives can be observed. Considering BCS, it can be noted that an increase of the H content and related to its aromaticity, increases the amount of free PAHs ( $p < 0.01$ ). An increase of O content lowered the amount of bioaccessible PAHs.

### 3.2. Oxidative stress response

#### 3.2.1. Antioxidant enzymes activity

The addition of BC affected the plant growth (Fig S3). It can be noted that BC obtained from pyrolysis of straw at highest temperature was the most efficient. However, all noted increases in the barley dry mass were above 300% (Fig S3A). Considering the type of the BC applied, it also was seen that independently from applied feedstock a fertilizing effect was noted (Fig S3B). The dry mass of obtained plants were enhanced up to 160% (BCF600) and 304% (BCS600). Only when soil from Chwałowice (Model Organic Farm) was used for barley cultivation (Fig. S3C), no statistically important changes in plant dry mass were noted. The data confirm that BC addition to soil increase plant growth.

The levels of enzymes activity were presented in Fig. 1 and grouped considering the effect of pyrolysis temperature (Fig. 1A), feedstock (Fig. 1B), and the effect of the soil matrix (Fig. 1C).

Several studies indicated the phytotoxicity of PAHs and their derivatives towards different plant species (Pašková et al., 2006; Sverdrup et al., 2003; Yun et al., 2019). PAHs induced oxidative stress in plants, presented damages on wheat leaf organelle and subcellular structure, furthermore plasmolized and distorted these structures under the influence of phenanthrene (Shen et al., 2018).

The oxidative stress response occurs the overproduction of ROS and antioxidants leading to the destruction of redox homeostasis in the plant (Ahmad, 2014). The high reactivity of ROS with proteins, lipids, carbohydrates, or nucleic acids is responsible for the changes in the morphological system of plants: reduced growth of the root and shoot, the decreased leaves number and size, chlorosis, deformed trichomes, reduced root hairs, late flowering, necrosis and cell death caused by produced  $H_2O_2$  (Alkio et al., 2005). The most important enzymatic ROS scavengers in plant cells are SOD, CAT, and APX (Liu et al., 2009b), and their activity was strictly connected with the presence of bioavailable PAHs. SOD is the first line against ROS catalyzing the dismutation of  $O_2^{•-}$  to  $O_2$  and  $H_2O_2$  (Alscher, 2002; Sharma et al., 2012). After this reaction, at a high concentration of substrate, CAT destroys the peroxide product: two molecules of  $H_2O_2$  combine resulting in the formation of water and molecular oxygen, therefore CAT and SOD act in tandem (Racchi, 2013). CAT differs from the other  $H_2O_2$  degrading enzymes because it conducts this reaction without consuming cellular reducing equivalents, thus in an energy-efficient manner (Scandalios, 2005). POD also degrades hydrogen peroxide to the water molecule but with the help of a reducing substrate (Willekens et al., 1995). This system is very effective in the removal of ROS from cell organelles. To determine and evaluate lipid peroxidation, a low-molecular-weight aldehyde, malondialdehyde (MDA) was assigned to be the most suitable product for this purpose and the best biomarker (Grotto et al., 2009). The presence of a double bond between two carbons in polyunsaturated fatty acids results in a decrease in the strength of the carbon-hydrogen bond. Then in sequence, hydrogen as a free radical, lipid-free radical, peroxy radical, and lipid peroxide can be formed (Grotto et al., 2009).

As Fig. 1A shows, the addition of BCS to soil increased the activity of SOD in plants compared to the control sample. No effect of the pyrolysis temperature was observed. The amount of MDA in barley growing in BCS-amended soil was lower than in untreated soil (without BC)

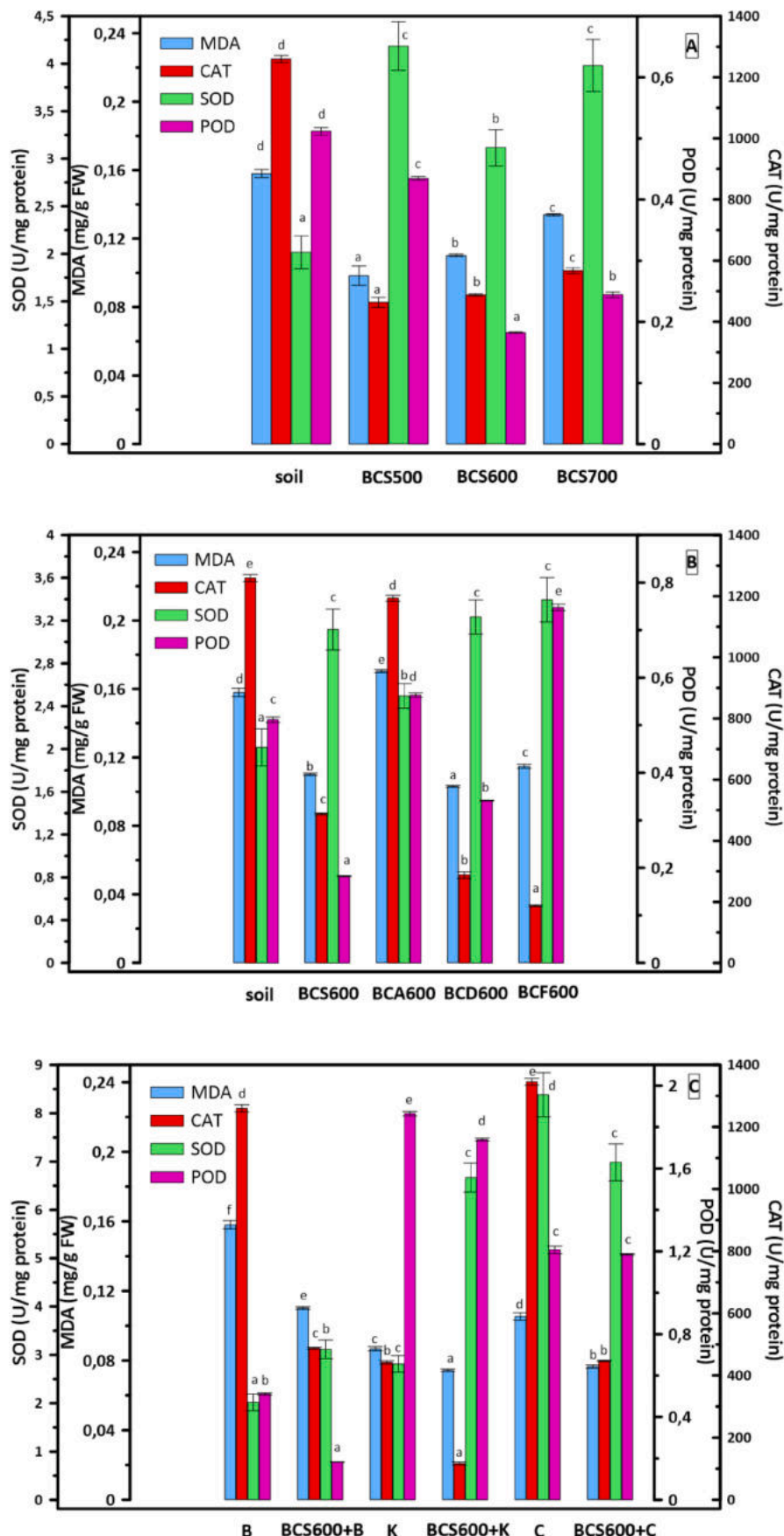
preserving membrane integrity. 1.5–2 times higher SOD activity may imply that the introduction of biochar to soil may improve the mitigation of oxidative stressors. The activity of CAT and POD decreased in barley exposed to BCS in comparison to control. The reduction of CAT activity was inversely correlated with temperature pyrolysis – from 63.21 to 54.99% for BCS500 and BCS700, respectively. Among obtained POD values, the highest reduction (64.3%) was observed after amendment BCS6000. CAT and POD detoxify  $H_2O_2$  to  $H_2O$  (Ma et al., 2015). A drop of activity of CAT and POD in plants treated with BCS may indicate that another antioxidant path was involved in the  $H_2O_2$  detoxification.

Regardless of feedstock (Fig. 1B), the SOD activity was increased 1.2–1.7 times after BC addition in comparison to control. BC-amendment resulted in the reduction of CAT activity in a wide range – from 5% for BCA600 to 85% for BCF600. The dual effect of BC application on POD activity was observed: BCD600, BCS600 reduced the enzyme activity (up to 64%), while BCF600 and BCA600 increased (up to 46%) the level of POD activity. MDA content was increased only in the case of BCA600 (7.85%), whereas the addition of another BC resulted in a drop in MDA content (30–35%). PAH-induced lipid peroxidation can be considered only to a small extend.

The antioxidant enzyme activity and lipid peroxidation were evaluated in plants growing in the different soil amended with BCS600 (Fig. 1C). The SOD activity was prompted in treated B and K soils, whereas it was unaffected in C soil. Regardless of soil type, BCS600 decreased CAT accumulation (61.29%) as well as POD (64.32%) activity. The percentages of decrease in the activities of individual enzymes and the concentrations of MDA amounted: for BCS600-amended Bezek soil 30.27% (MDA), 61.29% (CAT), and 64.32% (POD), for BCS600-amended Konstantynów soil 14.23%, 73.63%, and 6.74%; for BCS600-amended Chwałowice soil: 27.29%, 66.77%, and 1.70%, respectively.

Previous studies have revealed that the presence of PAHs and their derivatives in soil and biochar amended soil might exert a negative effect on plants. Zhan et al. (2012) reported damage of wheat (*Triticum aestivum* L.) growing in the soil amended with biochar containing PAHs. Some PAHs and the N-, S-, O-substituted analogs of fluorene (fluoranthene, fluorene, phenanthrene, and pyrene) were toxic to terrestrial plants (*Sinapis alba*, *Trifolium pratense*, and *Lolium perenne*) (Sverdrup et al., 2003). The mechanisms of wheat root uptake of PAHs involve active (mediated by phenanthrene (PAH)/ $H^+$  symporter) and passive processes (glycerol mediated) (Zhan et al., 2012).

Generally, the molecular mechanisms leading to the expression of SOD genes exposed to the presence of PAHs and their derivatives are poorly understood but the expression is independently regulated and concentrated in the place of ROS concentration in the cell (Scandalios, 2005). APX metabolizes  $H_2O_2$  and catalyzes the initial stage of the ASC-GSH (ascorbate-reduced glutathione) cycle (Grene, 2002). Glutathione peroxidase (GPX) can also detoxify  $H_2O_2$  but via directly GSH and catalyzed the degradation of hydrogen peroxide or organic and lipid peroxides into water or alcohols (Margis et al., 2008). As GPX synthesis occurs in response to the stress factor, the noted presence of GPX may imply oxidative stress after the application of biochars with a bioavailable fraction of PAHs and their derivatives. The statistically important correlation was noted for POD activity and the amount of total determined PAHs, however, the amount of the bioavailable fraction of PAHs derivatives lowered the level of POD using BCS-amendment. The fraction of bioavailable PAHs affected positively the transcription of genes encoding APX, CAT, and SOD enzymes. It was established that phytotoxicity induced by N-PAHs was generally higher than the effects of parent PAHs. Furthermore, the influence of PAHs with nitrogen in the aromatic ring significantly differed concerning the structure of the individual compound. PAHs and N-PAHs affected the germination and growth of *Sinapis alba*, *Triticum aestivum*, and *Phaseolus vulgaris* plants. They also induced activities of detoxification and antioxidant enzymes (GR, GPX, and glutathione-S-transferase) and caused an increase in lipid peroxidation (Pašková et al., 2006). The data indicate that the production of ROS due to biochar-amendment soil was noted. The increased



activity of SOD indicated the overproduction of  $O_2^{\bullet-}$  decomposed to  $H_2O_2$ , that was however not requiring the other enzymes for its decomposition. This may imply that the presence of bioavailable fraction of PAHs and their derivatives in biochar during cultivation of barley was slightly inducing oxidative stress but the plant was able to mitigate it probably due to low amount of produced  $H_2O_2$  or application of other detoxifying mechanisms. Increased SOD activity was generally considered as the positive response of the plant to the stressor (PAHs and their derivatives) actuating the effective detoxification.

In the study of the effect of phenanthrene on the mechanism of oxidative stress on *Arabidopsis thaliana* (Liu et al., 2009b), like in our studies, SOD enzyme activity increased under the influence of selected in our studies PAHs and derivatives. CAT activity did not change significantly (Liu et al., 2009b), whilst in our experiments, the content of CAT was affected by the addition of biochar into soils. POD and APX content increased initially but at the higher concentrations of phenanthrene, the enzyme activities decreased. Phenanthrene inhibited the germination rates and root lengths, and the roots were deformed (Liu et al., 2009b). Also, MDA levels increased significantly (Liu et al., 2009b). It implied lipid peroxidation, but this effect in our studies was noted only in one sample: MDA content increased only for BCA600-amended soil Bezek. One of the representatives of AZAs (PAH derivative with a nitrogen atom embedded in the aromatic ring) is acridine. The phytotoxicity of acridine was also confirmed in the previous studies (Gissel-nielsen and Nielsen, 1996; Pašková et al., 2006). Acridine affected the seed production of navew (*Brassica campestris* L.) at a lower concentration by the inhibition of seed germination and led to death at a higher content (Gissel-nielsen and Nielsen, 1996). The rate of growth of Italian ryegrass (*Lolium multiflorum* L.) was reduced and the condition of the germinated barley seeds (*Hordeum vulgare* L.) was affected but these effects were overcome over the growth period. The authors suggested that acridine was degraded by microorganisms during the experiment (Gissel-nielsen and Nielsen, 1996).

### 3.2.2. The gene expression

The gene expression pattern in barley differed regarding biochar properties and soil type. The influence of temperature on biochar production was noted. The transcript level values of APX, CAT, and SOD decreased with the increased pyrolysis temperature of BCS biochars (Fig. 2A).

The results are supported by the studies on enzymatic activity. The lowest levels of genes expression were obtained for soil-BCS700 (13.89% reduced APX, 32.06% CAT, and 16.99% SOD). Only in the case of GPX, the trend was reversed. Moreover, the obtained values in some cases were below the transcript level of the soil. The highest results obtained for SOD were nearly 14.5 times higher than for soil (and the lowest almost 2.5 times higher). The relative expression level of SOD was significantly increased after the addition of biochar (Fig. 2A) indicating that the plant was affected by oxidative stress and the over-production of  $O_2^{\bullet-}$  was noted. Increased expression of APX confirmed that  $H_2O_2$  produced by SOD after  $O_2^{\bullet-}$  dismutation are needed to be also removed from barley tissues. APX requires additional ascorbate for  $H_2O_2$  decomposition (Jóško et al., 2021). The transcripts of SOD and APX were lowered with increased pyrolysis temperature.

The effect of biochar feedstock on gene expression was also observed (Fig. 2B). The transcript level of APX was higher for BC-amended soil with the highest vale noted for BCS600-amended soil (35.5% increase). BCF600 significantly (81.4%) caused down-regulation of APX in relation to control. The transcripts of CAT and GPX were lower than noted in the untreated sample. The distribution of SOD Cu Zn values was depended on the applied feedstock.

The effects of different soils and soils with the addition of BCS600 on the on gene expression in *Hordeum vulgare* L. were determined (Fig. 2C). The transcript levels of APX for the samples with straw-derived biochars were over 4 times higher for Konstantynów soil, nearly 1.4 times higher for Bezek, and almost identical to soil alone for Chwałowice. In the case

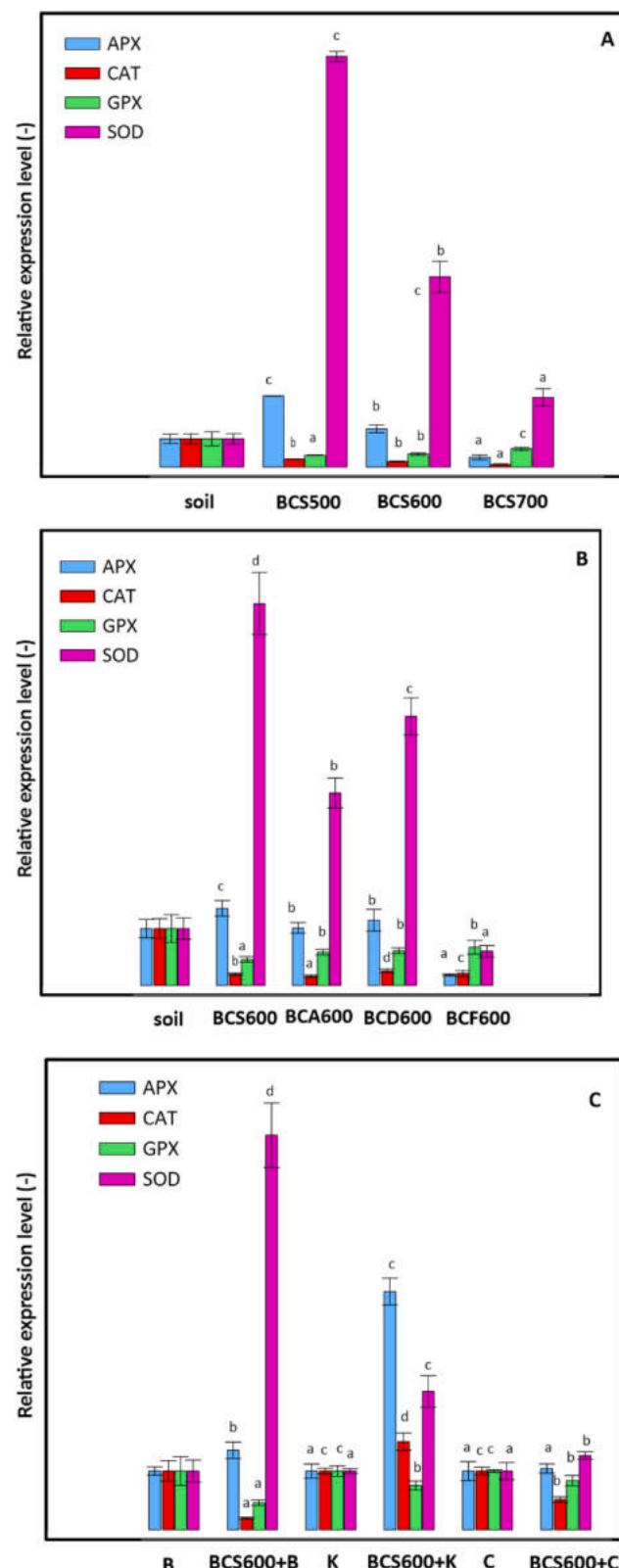


**Fig. 2.** The effect of BC addition on gene expression in *Hordeum vulgare* L., A) effect of pyrolysis temperature, B) effect of feedstock, C) effect of soil; APX-ascorbate peroxidase, CAT - catalase, GPX-glutathione peroxidase, SOD - superoxide dismutase, B- Bezek soil, K- Konstantynów soil, C- Chwałowice soil. 500, 600, 700 corresponds to the BC pyrolysis temperature [°C]. Values of each enzyme level were means of three replicates with standard deviations ( $n = 3$ ). Different alphabetical letters on the bars indicate significant differences among the treatments considering individual measured parameters ( $p < 0.05$ ).

of CAT values, the highest value was also received for Konstantynów soil-BCS600 (1.503). The remaining data constituted 34.13% of the above for Chwałowice and 13.24% for Bezek. The highest GPX content was obtained for BCS600-soil Chwałowice and the lowest for BCS600-soil Bezek. The distribution of the SOD results was the opposite of the above. Moreover, the R<sub>f</sub> value for biochar-amended Chwałowice soil was almost 1.3 times higher than for soil alone, for BCS600 Konstantynów soil-2.4, and straw-derived BC-Bezek soil- 6.7.

#### 4. Conclusions

The results indicate that the addition of biochar to the soil was connected with the increment of oxidative stress in the barley leaves. Increased levels of SOD activities confirmed that the ROS-induced stress occurred in plants growing in biochar-amended soil. The influence of pyrolysis temperature of biochar on the transcriptional response of barley was observed. One of the most important enzymatic ROS scavengers in plant cells are CAT and APX and their transcripts were strictly connected with the presence of bioavailable PAHs indicating that the presence of a bioavailable fraction of PAHs and their derivatives (but to a lower extend) may induce the overproduction of O<sub>2</sub><sup>-</sup> and H<sub>2</sub>O<sub>2</sub> and the oxidative stress. The transcript levels of SOD were lowered with increased pyrolysis temperature and depended on applied feedstock. However, lower MDA concentration and lower activity of other enzymes involved in ROS detoxification imply that the addition of biochar containing the bioavailable fraction of PAHs and their derivatives is an environmentally safe solution.

#### Credit author statement

A. Krzyszczak: Investigation, Visualization, Writing – original draft Reviewing and Editing. M. Dybowski: Investigation, Methodology, Visualization. I. Jośko: Investigation, Methodology, Visualization, Writing- Reviewing and Editing. M. Kusiak: Investigation, Methodology. M. Sikora: Investigation, Methodology. B. Czech: Investigation, Methodology, Visualization, Writing- Reviewing and Editing Conceptualization, Validation, Supervision.

#### Declaration of competing interest

The authors declare that they have no known competing financial interests or personal relationships that could have appeared to influence the work reported in this paper.

#### Acknowledgments

The studies were supported by project No. 2018/31/B/NZ9/00317 funded by the National Science Centre, Poland.

#### Appendix A. Supplementary data

Supplementary data to this article can be found online at <https://doi.org/10.1016/j.envpol.2021.118664>.

#### References

- Abbas, I., Badran, G., Verdin, A., Ledoux, F., Roumié, M., Courcot, D., Garçon, G., 2018. Polycyclic aromatic hydrocarbon derivatives in airborne particulate matter: sources, analysis and toxicity. *Environ. Chem. Lett.* <https://doi.org/10.1007/s10311-017-0697-0>.
- Ahammed, G.J., Wang, M.-M., Zhou, Y.-H., Xia, X.-J., Mao, W.-H., Shi, K., Yu, J.-Q., 2012. The growth, photosynthesis and antioxidant defense responses of five vegetable crops to phenanthrene stress. *Ecotoxicol. Environ. Saf.* **80**, 132–139. <https://doi.org/10.1016/j.ecoenv.2012.02.015>.
- Ahmad, P., 2014. Oxidative Damage to Plants: Antioxidant Networks and Signaling. Academic Press, Amsterdam.
- Alkio, M., Tabuchi, T.M., Wang, X., Colón-Carmona, A., 2005. Stress responses to polycyclic aromatic hydrocarbons in *Arabidopsis* include growth inhibition and hypersensitive response-like symptoms. *J. Exp. Bot.* **56**, 2983–2994. <https://doi.org/10.1093/jxb/eri295>.
- Alischer, R.G., 2002. Role of superoxide dismutases (SODs) in controlling oxidative stress in plants. *J. Exp. Bot.* **53**, 1331–1341. <https://doi.org/10.1093/jexbot/53.372.1331>.
- Alves, C.A., Vicente, A.M., Custódio, D., Cerqueira, M., Nunes, T., Pio, C., Lucarelli, F., Calzolai, G., Nava, S., Diapouli, E., Eleftheriadis, K., Querol, X., Musa Bandowe, B.A., 2017. Polycyclic aromatic hydrocarbons and their derivatives (nitro-PAHs, oxygenated PAHs, and azaarenes) in PM 2.5 from Southern European cities. *Sci. Total Environ.* **595**, 494–504. <https://doi.org/10.1016/j.scitotenv.2017.03.256>.
- Andersson, H., Piras, E., Demma, J., Hellman, B., Brittebo, E., 2009. Low levels of the air pollutant 1-nitropyrene induce DNA damage, increased levels of reactive oxygen species and endoplasmic reticulum stress in human endothelial cells. *Toxicology* **262**, 57–64. <https://doi.org/10.1016/j.tox.2009.05.008>.
- Asai, H., Samson, B.K., Stephan, H.M., Songyikhangsuthor, K., Homma, K., Kiyono, Y., Inoue, Y., Shiraiwa, T., Horie, T., 2009. Biochar amendment techniques for upland rice production in Northern Laos: 1. Soil physical properties, leaf SPAD and grain yield. *Field Crop. Res.* **111**, 81–84. <https://doi.org/10.1016/j.fcr.2008.10.008>.
- Bonanomi, G., Ippolito, F., Cesaroni, G., Nanni, B., Lombardi, N., Rita, A., Saracino, A., Scala, F., 2017. Biochar as plant growth promoter better off alone or mixed with organic amendments? *Front. Plant Sci.* **8**, 1570 <https://doi.org/10.3389/fpls.2017.01570>.
- Bradford, M.M., 1976. A rapid and sensitive method for the quantitation of microgram quantities of protein utilizing the principle of protein-dye binding. *Anal. Biochem.* **72**, 248–254. [https://doi.org/10.1016/0003-2697\(76\)90527-3](https://doi.org/10.1016/0003-2697(76)90527-3).
- Buryšková, B., Hilscherová, K., Bláha, L., Maršílek, B., Holoubek, I., 2006. Toxicity and modulations of biomarkers in *Xenopus laevis* embryos exposed to polycyclic aromatic hydrocarbons and their N-heterocyclic derivatives. *Environ. Toxicol.* **21**, 590–598. <https://doi.org/10.1002/tox.20222>.
- Chatel, A., Faucet-Marquis, V., Pfohl-Leszkowicz, A., Gourlay-France, C., Vincent-Hubert, F., 2014. DNA adduct formation and induction of detoxification mechanisms in *Dreissena polymorpha* exposed to nitro-PAHs. *Mutagenesis* **29**, 457–465. <https://doi.org/10.1093/mutage/geu040>.
- Demidchik, V., 2015. Mechanisms of oxidative stress in plants: from classical chemistry to cell biology. *Environ. Exp. Bot.* **109**, 212–228. <https://doi.org/10.1016/j.enexpbot.2014.06.021>.
- Dume, B., Mosissa, T., Nebiyu, A., 2016. Effect of biochar on soil properties and lead (Pb) availability in a military camp in South West Ethiopia. *Afr. J. Environ. Sci. Technol.* **10**, 77–85. <https://doi.org/10.4314/ajest.v10i1>.
- Gissel-nielsen, G., Nielsen, T., 1996. Phytotoxicity of acridine, an important representative of a group of tar and creosote contaminants, N-pac compounds. *Polycycl. Aromat. Comp.* **8**, 243–249. <https://doi.org/10.1080/10406639608048351>.
- Grene, R., 2002. Oxidative stress and acclimation mechanisms in plants. *Arabidopsis Book* **1**. <https://doi.org/10.1199/tabc.0036.1>.
- Grotto, D., Maria, L.S., Valentini, J., Paniz, C., Schmitt, G., Garcia, S.C., Pomblum, V.J., Rocha, J.B.T., Farina, M., 2009. Importance of the lipid peroxidation biomarkers and methodological aspects FOR malondialdehyde quantification. *Quím. Nova* **32**, 169–174. <https://doi.org/10.1590/S0100-40422009000100032>.
- Hale, S.E., Lehmann, J., Rutherford, D., Zimmerman, A.R., Bachmann, R.T., Shitumbanuma, V., O'Toole, A., Sundqvist, K.L., Arp, H.P.H., Cornelissen, G., 2012. Quantifying the total and bioavailable polycyclic aromatic hydrocarbons and dioxins in biochars. *Environ. Sci. Technol.* **46**, 2830–2838. <https://doi.org/10.1021/es203984k>.
- Han, M., Kong, J., Yuan, J., He, H., Hu, J., Yang, S., Li, S., Zhang, L., Sun, C., 2019. Method development for simultaneous analyses of polycyclic aromatic hydrocarbons and their nitro-, oxy-, hydroxy- derivatives in sediments. *Talanta* **205**, 120128. <https://doi.org/10.1016/j.talanta.2019.120128>.
- Jośko, I., Kusiak, M., Oleszczuk, P., Świeca, M., Kończak, M., Sikora, M., 2021. Transcriptional and biochemical response of barley to co-exposure of metal-based nanoparticles. *Sci. Total Environ.* **782**, 146883. <https://doi.org/10.1016/j.scitotenv.2021.146883>.
- Kim, Y.-D., Ko, Y.-J., Kawamoto, T., Kim, H., 2005. The effects of 1-nitropyrene on oxidative DNA damage and expression of DNA repair enzymes. *J. Occup. Health* **47**, 261–266. <https://doi.org/10.1539/joh.47.261>.
- Kordrostami, M., Rabiei, B., Ebadi, A., 2019. Oxidative Stress in Plants: Production, Metabolism, and Biological Roles of Reactive Oxygen Species, 974. <https://doi.org/10.1201/9781351104609-6>.
- Lehmann, J., Pereira da Silva, J., Steiner, C., Nehls, T., Zech, W., Glaser, B., 2003. Nutrient availability and leaching in an archaeological Anthrosol and a Ferralsol of the Central Amazon basin: fertilizer, manure and charcoal amendments. *Plant Soil* **249**, 343–357. <https://doi.org/10.1023/A:1022833116184>.
- Li, J.H., Gao, Y., Wu, S.C., Cheung, K.C., Wang, X.R., Wong, M.H., 2008. Physiological and biochemical responses of rice (*Oryza sativa* L.) to phenanthrene and pyrene. *Int. J. Phytoremediation* **10**, 106–118. <https://doi.org/10.1080/15226510801913587>.
- Liu, H., Weisman, D., Ye, Y., Cui, B., Huang, Y., Colón-Carmona, A., Wang, Z., 2009a. An oxidative stress response to polycyclic aromatic hydrocarbon exposure is rapid and complex in *Arabidopsis thaliana*. *Plant Sci.* **176**, 375–382. <https://doi.org/10.1016/j.plantsci.2008.12.002>.
- Liu, H., Weisman, D., Ye, Y., Cui, B., Huang, Y., Colón-Carmona, A., Wang, Z., 2009b. An oxidative stress response to polycyclic aromatic hydrocarbon exposure is rapid and complex in *Arabidopsis thaliana*. *Plant Sci.* **176**, 375–382. <https://doi.org/10.1016/j.plantsci.2008.12.002>.
- Lundstedt, S., Bandow, B.A.M., Wilcke, W., Boll, E., Christensen, J.H., Vila, J., Griffol, M., Faure, P., Biache, C., Lorgeoux, C., Larsson, M., Frech Igum, K., Ivarsson, P., Ricci, M., 2014. First intercomparison study on the analysis of oxygenated polycyclic aromatic hydrocarbons (oxy-PAHs) and nitrogen heterocyclic

- polycyclic aromatic compounds (N-PACs) in contaminated soil. *Trac. Trends Anal. Chem.* 57, 83–92. <https://doi.org/10.1016/j.trac.2014.01.007>.
- Ma, C., White, J.C., Dhankher, O.P., Xing, B., 2015. Metal-Based nanotoxicity and detoxification pathways in higher plants. *Environ. Sci. Technol.* 49, 7109–7122. <https://doi.org/10.1021/acs.est.5b00685>.
- Major, J., Rondon, M., Molina, D., Riha, S.J., Lehmann, J., 2010. Maize yield and nutrition during 4 years after biochar application to a Colombian savanna oxisol. *Plant Soil* 333, 117–128. <https://doi.org/10.1007/s11104-010-0327-0>.
- Margis, R., Dunand, C., Teixeira, F.K., Margis-Pinheiro, M., 2008. Glutathione peroxidase family – an evolutionary overview. *FEBS J.* 275, 3959–3970. <https://doi.org/10.1111/j.1742-4658.2008.06542.x>.
- Mayer, K.F.X., Martis, M., Hedley, P.E., Šimková, H., Liu, H., Morris, J.A., Steuernagel, B., Taudien, S., Roessner, S., Gundlach, H., Kubaláková, M., Suchánková, P., Murat, F., Felder, M., Nussbaumer, T., Graner, A., Salse, J., Endo, T., Sakai, H., Tanaka, T., Itoh, T., Sato, K., Platzer, M., Matsumoto, T., Scholz, U., Doležel, J., Waugh, R., Stein, N., 2011. Unlocking the barley genome by chromosomal and comparative genomics. *Plant Cell* 23, 1249–1263. <https://doi.org/10.1105/tpc.110.082537>.
- Mensah, A.K., Frimpong, K.A., 2018. Biochar and/or compost applications improve soil properties, growth, and yield of maize grown in acidic rainforest and coastal Savannah soils in Ghana. *Int. J. Agron.*, e6837404 <https://doi.org/10.1155/2018/6837404>.
- Musa Bandowe, B.A., Shukurov, N., Kersten, M., Wilcke, W., 2010. Polycyclic aromatic hydrocarbons (PAHs) and their oxygen-containing derivatives (OPAHs) in soils from the Angren industrial area, Uzbekistan. *Environ. Pollut.* 158, 2888–2899. <https://doi.org/10.1016/j.envpol.2010.06.012>.
- Musa Bandowe, B.A., Wei, C., Han, Y., Cao, J., Zhan, C., Wilcke, W., 2019. Polycyclic aromatic compounds (PAHs, oxygenated PAHs, nitrated PAHs and azaarenes) in soils from China and their relationship with geographic location, land use and soil carbon fractions. *Sci. Total Environ.* 690, 1268–1276. <https://doi.org/10.1016/j.scitotenv.2019.07.022>.
- Oleszczuk, P., Kuśmierz, M., Godlewska, P., Kraska, P., Palys, E., 2016. The concentration and changes in freely dissolved polycyclic aromatic hydrocarbons in biochar-amended soil. *Environ. Pollut.* 214, 748–755. <https://doi.org/10.1016/j.envpol.2016.04.064>.
- Pásková, V., Hilscherová, K., Feldmannová, M., Bláha, L., 2006. Toxic effects and oxidative stress in higher plants exposed to polycyclic aromatic hydrocarbons and their N-heterocyclic derivatives. *Environ. Toxicol. Chem.* 25, 3238–3245. <https://doi.org/10.1897/06-162R.1>.
- Qiao, M., Qi, W., Liu, H., Qu, J., 2014. Oxygenated, nitrated, methyl and parent polycyclic aromatic hydrocarbons in rivers of Haihe River System, China: occurrence, possible formation, and source and fate in a water-shortage area. *Sci. Total Environ.* 481, 178–185. <https://doi.org/10.1016/j.scitotenv.2014.02.050>.
- Racchi, M.L., 2013. Antioxidant defenses in plants with attention to prunus and citrus spp. *Antioxidants* 2, 340–369. <https://doi.org/10.3390/antiox2040340>.
- Rafiq, M.K., Bachmann, R.T., Rafiq, M.T., Shang, Z., Joseph, S., Long, R., 2016. Influence of pyrolysis temperature on physico-chemical properties of corn Stover (*Zea mays L.*) biochar and feasibility for carbon capture and energy balance. *PLoS One* 11, e0156894. <https://doi.org/10.1371/journal.pone.0156894>.
- Rawat, J., Saxena, J., Sanwal, P., 2019. Biochar: A Sustainable Approach for Improving Plant Growth and Soil Properties, Biochar - an Imperative Amendment for Soil and the Environment. <https://doi.org/10.5772/intechopen.82151>. IntechOpen.
- Rondon, M.A., Lehmann, J., Ramírez, J., Hurtado, M., 2007. Biological nitrogen fixation by common beans (*Phaseolus vulgaris L.*) increases with bio-char additions. *Biol. Fertil. Soils* 43, 699–708. <https://doi.org/10.1007/s00374-006-0152-z>.
- Scandalios, J.G., 2005. Oxidative stress: molecular perception and transduction of signals triggering antioxidant gene defenses. *Braz. J. Med. Biol. Res.* 38, 995–1014. <https://doi.org/10.1590/S0100-879X2005000700003>.
- Sharma, P., Jha, A.B., Dubey, R.S., Pessarakli, M., 2012. Reactive oxygen species, oxidative damage, and antioxidative defense mechanism in plants under stressful conditions. *J. Bot.*, e217037 <https://doi.org/10.1155/2012/217037>.
- Shen, Y., Li, J., Gu, R., Yue, L., Wang, H., Zhan, X., Xing, B., 2018. Carotenoid and superoxide dismutase are the most effective antioxidants participating in ROS scavenging in phenanthrene accumulated wheat leaf. *Chemosphere* 197, 513–525. <https://doi.org/10.1016/j.chemosphere.2018.01.036>.
- Sklorz, M., Briedé, J.-J., Schnelle-Kreis, J., Liu, Y., Cyrys, J., de Kok, T.M., Zimmermann, R., 2007. Concentration of oxygenated polycyclic aromatic hydrocarbons and oxygen free radical formation from urban particulate matter. *J. Toxicol. Environ. Health, Part A* 70, 1866–1869. <https://doi.org/10.1080/15287390701457654>.
- Souza, K.F., Carvalho, L.R.F., Allen, A.G., Cardoso, A.A., 2014. Diurnal and nocturnal measurements of PAH, nitro-PAH, and oxy-PAH compounds in atmospheric particulate matter of a sugar cane burning region. *Atmos. Environ.* 83, 193–201. <https://doi.org/10.1016/j.atmosenv.2013.11.007>.
- Sverdrup, L.E., Krogh, P.H., Nielsen, T., Kjær, C., Stenersen, J., 2003. Toxicity of eight polycyclic aromatic compounds to red clover (*Trifolium pratense*), ryegrass (*Lolium perenne*), and mustard (*Sinapis alba*). *Chemosphere* 53, 993–1003. [https://doi.org/10.1016/S0045-6535\(03\)00584-8](https://doi.org/10.1016/S0045-6535(03)00584-8).
- Wang, Guifeng, Wang, Gang, Zhang, X., Wang, F., Song, R., 2012. Isolation of high quality RNA from cereal seeds containing high levels of starch. *Phytochem. Anal.* 23, 159–163. <https://doi.org/10.1002/pca.1337>.
- Wei, C., Bandowe, B.A.M., Han, Y., Cao, J., Zhan, C., Wilcke, W., 2015. Polycyclic aromatic hydrocarbons (PAHs) and their derivatives (alkyl-PAHs, oxygenated-PAHs, nitrated-PAHs and azaarenes) in urban road dusts from Xi'an, Central China. *Chemosphere* 134, 512–520. <https://doi.org/10.1016/j.chemosphere.2014.11.052>.
- Weidemann, E., Buss, W., Edo, M., Mašek, O., Jansson, S., 2018. Influence of pyrolysis temperature and production unit on formation of selected PAHs, oxy-PAHs, N-PACs, PCDDs, and PCDFs in biochar—a screening study. *Environ. Sci. Pollut. Control Ser.* 25, 3933–3940. <https://doi.org/10.1007/s11356-017-0612-z>.
- Wessely-Szponder, J., Belköt, Z., Bobowiec, R., Kosior-Korzecka, U., Wójcik, M., 2015. Transport induced inflammatory responses in horses. *Pol. J. Vet. Sci.* 18, 407–413. <https://doi.org/10.1515/pjvs-2015-0052>.
- Wilcke, W., Kiesewetter, M., Musa Bandowe, B.A., 2014. Microbial formation and degradation of oxygen-containing polycyclic aromatic hydrocarbons (OPAHs) in soil during short-term incubation. *Environ. Pollut.* 184, 385–390. <https://doi.org/10.1016/j.envpol.2013.09.020>.
- Willekens, H., Inzé, D., Van Montagu, M., van Camp, W., 1995. Catalases in plants. *Mol. Breed.* 1, 207–228. <https://doi.org/10.1007/BF02277422>.
- Xiao, X., Chen, Z., Chen, B., 2016. H/C atomic ratio as a smart linkage between pyrolytic temperatures, aromatic clusters and sorption properties of biochars derived from diverse precursory materials. *Sci. Rep.* 6, 22644 <https://doi.org/10.1038/srep22644>.
- Yun, Y., Liang, L., Wei, Y., Luo, Z., Yuan, F., Li, G., Sang, N., 2019. Exposure to Nitro-PAHs interfere with germination and early growth of *Hordeum vulgare* via oxidative stress. *Ecotoxicol. Environ. Saf.* 180, 756–761. <https://doi.org/10.1016/j.ecoenv.2019.05.032>.
- Zhan, X., Zhang, X., Yin, X., Ma, H., Liang, J., Zhou, L., Jiang, T., Xu, G., 2012. H<sup>+</sup>/phenanthrene symporter and aquaglyceroporin are implicated in phenanthrene uptake by wheat (*Triticum aestivum L.*) roots. *J. Environ. Qual.* 41, 188–196. <https://doi.org/10.2134/jeq2011.0275>.
- Złotek, U., Świeca, M., Regula, J., Jakubczyk, A., Sikora, M., Gawlik-Dziki, U., Kapusta, I., 2019. Effects of probiotic *L. plantarum* 299v on consumer quality, accumulation of phenolics, antioxidant capacity and biochemical changes in legume sprouts. *Int. J. Food Sci. Technol.* 54, 2437–2446. <https://doi.org/10.1111/ijfs.14158>.

**The antioxidant defense responses of *Hordeum vulgare* L. to polycyclic aromatic hydrocarbons and their derivatives in biochar-amended soil**

Agnieszka Krzyszczak<sup>1</sup>, Michał Dybowski<sup>2</sup>, Izabela Jośko<sup>3</sup>, Magdalena Kusiak<sup>4</sup>, Małgorzata Sikora<sup>4</sup>, Bożena Czech<sup>1\*</sup>,

<sup>1</sup>Department of Radiochemistry and Environmental Chemistry, Institute of Chemical Sciences, Faculty of Chemistry, Maria Curie-Sklodowska University in Lublin, Pl. M. Curie-Sklodowskiej 3, 20-031 Lublin, Poland

<sup>2</sup>Department of Chromatography, Institute of Chemical Sciences, Faculty of Chemistry, Maria Curie Skłodowska University in Lublin, Pl. M. Curie-Sklodowskiej 3, 20-031 Lublin, Poland

<sup>3</sup>Institute of Plant Genetics, Breeding and Biotechnology, Faculty of Agrobioengineering, University of Life Sciences, Akademicka 15 St., 20-950 Lublin, Poland

<sup>4</sup>Department of Biochemistry and Food Chemistry, Faculty of Food Science and Biotechnology, University of Life Sciences, Skromna 8 St., 20-704 Lublin, Poland

\*corresponding author: Tel.: +48 81 537 55 54; fax: +48 81 537 55 65; E-mail address:  
[bczech@hektor.umcs.lublin.pl](mailto:bczech@hektor.umcs.lublin.pl) (B. Czech)

Journal: Environmental Pollution

No. of Pages: 14

No. of Tables: 3

No. of Figures: 2

## **2. Materials and methods**

### **2.1. The physico-chemical properties of biochar**

The pH of 1g of biochar mixed with 10 mL of deionized water was determined by a digital pH meter HQ430d Benchtop Single Input (HACH, USA). To quantified the elemental carbon (C), hydrogen (H), and nitrogen (N), biochar was milled and EuroEA Elemental Analyser was applied. ASAP 2420 (Micromeritics, USA) surface area and porosity analyzer were used for adsorption measurements and biochars were outgassed at 200°C for 12 h under vacuum. Total organic carbon (TOC) and dissolved organic carbon (DOC) were quantified via TOC-VCSH (SHIMADZU). FT-IR/PAS spectra of the samples were recorded by Bio-Rad Excalibur 3000 MX spectrometer provided with photoacoustic detector MTEC300 (in the helium atmosphere in a detector) at RT over the 4000-400 cm<sup>-1</sup> range at the resolution of 4 cm<sup>-1</sup> and maximum source aperture. X-ray photoelectron spectroscopy (UHV Prevac) was used for the determination of surface functional groups of BC, whereas surface morphology was examined by scanning electron microscopy (Quanta 3D FEG, FEI).

### **2.2. The total content of PAHs and their derivatives determination in biochar**

PAHs and their derivatives were extracted via pressurized liquid extraction (PLE) using Dionex 350 system (Thermo Fisher Scientific) equipped with a 22 mL stainless steel cell. The first layer with silica gel (activated in 300°C, 5h) and copper, and the second, i.e. 0.5g of each biochar mixed with 0.1g ethylenediaminetetraacetic acid, were loaded into the cell. The internal standard (IS) e.g. deuterated mix of US EPA-Σ16 PAHs, were added and the cells were completed by glass beads. Then, PLE was performed with hexane at 150°C using 2 extraction cycles and a flush volume at 60%. The static time was set at 5 min and the purge time was 60 s 1 MPa with N<sub>2</sub>. After extraction 1 mL of iso-octane was added into an extract and obtained solvent was concentrated to about 1 mL using rotary vacuum concentrator RVC 2-25 CD plus (Martin Christ, Germany). Then, GC-MS/MS analysis was carried out.

### **2.3. Freely dissolved (C<sub>free</sub>) PAHs and their derivatives determination in biochars**

The determination of bioaccessibility of PAHs and their derivatives was carried out by the protocol described in Oleszczuk et al. (Oleszczuk et al., 2016) and Hale et al. (Hale et al., 2012). Before the sample preparation procedure, 76-mm thick polyoxymethylene (POM) passive samplers (4cm x 4cm and about 0.35 g each) were cleaned and submerged in methanol, shaken for 24 hours on a shaking machine (ELPIN 358A, Poland). Subsequently, methanol was substituted with n-heptane and Millipore water (in each solvent POM samplers were shaken for 24). Next, sheets were rinsed with Millipore water, placed in a glass bottle with water, and stored at 4°C. Biochar (1 g) dried at 40°C for 24 hours were placed in 50 mL Erlenmeyer flasks with glass lids. 40 mL of sodium azide (200 mg/L) dissolved in water was added for the elimination of any possible effect of residual microorganisms. POM samplers were added to Erlenmeyer flasks (all carried out in triplicates) and vials were tightly sealed to prevent leakage. Flasks were rolled on a rotary shaker ROTAX 6.8 VELP Scientifica (Italy) for 1 month at 10 RCF. After this period, POM samplers were cleaned with distilled water. The remaining visible impurities were removed using a tissue. Treated POM samplers were placed in a 50 mL dry Erlenmeyer flask. Then, they were extracted in 20 mL of 20/80 acetone/heptane (v/v) with the addition of 20 µL of deuterated PAHs (naphthalene, pyrene, and phenanthrene with a concentration of 10 ng µL<sup>-1</sup>) and shaken in horizontal shaking machine ELPIN 358A (Poland) for 48 hours. After this time 1 mL of iso-octane was added and obtained solvent was concentrated to about 1 mL using rotary vacuum concentrator RVC 2-25 CD plus (Martin Christ, Germany). Then, GC-MS/MS analysis was carried out. The concentration of PAHs and their derivatives on POM passive samplers (C<sub>POM</sub>) was calculated according to the equation (1):

$$C_{POM}(\text{ng kg}^{-1}) = \frac{m_{PAH}(\text{ng})}{m_{2POM}(\text{kg})}$$

where  $m_{PAH}$  (ng) (or  $m_{PAH}$  derivatives) is the mass of PAHs (or PAHs derivatives) determined by GC-MS/MS and  $m_{2POM}$  (kg) is the mass of two used POM passive samplers.

$C_{free}$  concentrations were calculated using POM-water partitioning coefficients ( $K_{POM}$ ) known from previous studies (Josefsson et al., 2015). In the case of some PAHs derivatives,  $K_{POM}$  was adopted considering parent PAHs due to the lack of the available data in literature: nitronaphthalene, 1-methyl-5-nitronaphthalene, 1-methyl-6-nitronaphthalene, nitropyrene, 2-phenylnaphthalene (Hawthorne et al., 2011), benzo[a]fluorene, and benzo[a]fluoranthene (Hans-Peter Schmidt, 2015).  $K_{POM}$  constitutes an individual value to each compound. Freely dissolved ( $C_{free}$ ) PAHs and derivatives were measured according to equation (2):

$$C_{free}(\text{ng L}^{-1}) = \frac{K_{POM-w}(\text{L kg}^{-1})}{C_{POM}(\text{ng kg}^{-1})}$$

where  $C_{free}$  (ng L<sup>-1</sup>) is the bioavailable pollutant concentration,  $K_{POM-w}$  (L kg<sup>-1</sup>) is the POM-water partitioning coefficient and  $C_{POM}$  (ng kg<sup>-1</sup>) is the measured POM concentration.

The physicochemical analysis of biochar, detailed information on GC-MS/MS measurements, chemical characteristics of analyzed compounds (Table S2), and the qualitative and quantitative parameters of PAHs and O/N-PAHs analysis (Table S3) were presented in Supporting Information.

#### 2.4. Freely dissolved ( $C_{free}$ ) PAH and their derivatives determination in biochars

The qualitative and quantitative determinations of bioaccessibility of PAHs and their derivatives were carried out by the protocol described in Oleszczuk et al. (Oleszczuk et al., 2016) and Hale et al. (Hale et al., 2012).

#### 2.5. GC-MS/MS measurement

Qualitative and quantitative analyses of PAHs were conducted using a gas chromatograph hyphenated with a triple quadruple tandem mass spectrometer detector (GCMS-TQ8040; Shimadzu, Kyoto, Japan) equipped with a ZB5-MSi fused-silica capillary column (30 m × 0.25 mm i.d., 0.25 μm film thickness; Phenomenex, Torrance, CA, USA). Helium (grade 5.0) as carrier gas and argon (grade 5.0) as collision gas were used. Column flow was 1.56 mL min<sup>-1</sup>, and 1 μL of the sample was injected by an AOC-20i+s type autosampler (Shimadzu). The injector was working in high-pressure mode (250.0 kPa for 1.5 min; column flow at initial temperature was 4.90 mL min<sup>-1</sup>) at the temperature of 310°C; the ion source temperature was 225°C. For qualitative purposes, the full scan mode with range 40-550 m/z was employed and for quantitative analyses, the SIM mode was used.

Table S1. Properties of tested soils.

soil	location	type	Total organic carbon content [g kg <sup>-1</sup> ]	pH <sub>KCl</sub>	N <sub>total</sub> [g kg <sup>-1</sup> ]	P [mg kg <sup>-1</sup> ]	K [mg kg <sup>-1</sup> ]	Ref.
Bezek	51°12' N; 23°17' E Agricultural Experimental Farm in Bezek—	Podzol originating from glaciofluvial fine-grained loamy sand brown soil (CAMBISOLS according to the World Reference Base for Soil Resources 2014)	5.3	4.9	3.05	18.84	78.92	(Pranagal and Kraska, 2020)
Chwałowice	50°45'57"N 21°53'10"E Model Organic Farm in Chwałowice		14.11	6.15	-	73.9	1430	(Kraska et al., 2019)
Konstantynów	52°12'21" N, 23°05'02" E farm	on Luvisol (loamy sand)	-	5.14	-	52.80	152.76	(Kraska et al., 2019)

## 2.6. Plant growth conditions

*H. vulgare* (cultivar Ella) seeds were soaked in Mili-Q® water for 2 h. The seeds were surface sterilized with 2% calcium hypochlorite for 15 min and then 70% ethanol for 1 min. The seeds were then rinsed 3 times with Mili-Q® water. The sterilized seeds were transferred to Petri dishes containing filter paper soaked with Mili-Q® water. The Petri dishes were placed in a growth chamber in darkness at 23°C. The 4-day seedlings were transplanted into tubes filled with soil samples. The plants were placed in a growth chamber (Conviron GEN1000) with a relative humidity of 60% and a 16h light/8h dark cycle at 23°C (day time) and 18°C (night time). Every day 1 mL of Mili-Q® water was added to each tube to maintain the moisture content. After 12 days of exposure, plants were harvested and part of the leaves (around 500 mg) was immediately ground in liquid nitrogen for RNA isolation, and the remaining leaves were frozen at -80°C for biochemical analysis.

## 2.7. Antioxidant enzyme activity

The plant tissues (around 250 mg of frozen leaves) were homogenized in 5 mL of 0.1M phosphate buffer (pH 7.5) and shaken for 15 min at 4°C. The plant extract was further centrifuged at 17,000g for 15 min at 4°C. The supernatant was used to measure the activities of SOD (superoxide dismutase), POD (peroxidase), CAT (catalase) in 96-well microplates. The POD activity was determined at 25°C in a reaction mixture (270 µL of 100 mM phosphate buffer pH 7.5 with 1mM EDTA, 10µL of 0.15% H<sub>2</sub>O<sub>2</sub>, 10 µL of 0.73% guaiacol with 10 µL of plant extracts). The absorbance was recorded at 470 nm using a BioTek Microplate Reader. The activity of POD was expressed as U, where 1U is defined as activity oxidizing µmol guaiacol per minute in the assay conditions (Złotek et al., 2019). The SOD and CAT activities were determined using SOD Assay Kit® (Cat. No. 19160-1KT-F, Merck, Germany) and Catalase Assay Kit® (Cat. No. 219265-1KIT, Merck, Germany) according to the protocols provided by the manufacturer. One unit of SOD activity inhibits the rate of reduction of cytochrome c by 50% in a coupled system, using xanthine and xanthine oxidase. One unit of CAT activity is defined as activity converting µmol H<sub>2</sub>O<sub>2</sub> per min. in the assay conditions. The protein content in samples was determined according to Bradford using bovine serum albumin as the standard (Bradford, 1976). Results were expressed a specific activity in U per mg of protein.

## **2.8. Lipid peroxidation**

The tissue malondialdehyde (MDA) level was analyzed to monitor oxidative damage of lipid membranes. Frozen leaf tissue was homogenized in 80% cold ethanol and centrifuged to pellet debris. The aliquots of supernatants were mixed with tri-chloroacetic acid (TCA) and thiobarbituric acid and thereafter heated for 20 min in a boiling water bath. After cooling to room temperature, 2 mL of n-butanol was added and the mixture was shaken vigorously for 3 min and centrifuged for 10 min at 1500×g. After the transfer of the upper n-butanol layer to a glass cuvette, its absorbance was measured at 532 nm. Concentrations of MDA were estimated based on the standard curve obtained by using malondialdehyde bis-dimethylacetal (Wessely-Szponder et al., 2015).

## **2.9. Gene expression**

500 mg fresh leaves were ground into a fine powder in liquid nitrogen using mortar and pestle. Total RNA from seeds was isolated using TRIzolTM reagent (Thermo Fisher Scientific Inc.) following Wang et al. (Wang et al., 2012) with two modifications: (i) phenol:chloroform: isoamyl alcohol (25:24:1) mixture saturated with 100 mM TRIS pH 8.0 was used instead of citrate buffer saturated phenol (pH 4.3): chloroform (1:1); (ii) pH of used 3M sodium acetate was adjusted to the level of 5.3. Isolation of RNA was performed for 3 biological replicates. The concentration and purity of RNA were determined spectrophotometrically with NanoDrop 2000 (Thermo Fisher Scientific Inc.). The integrity of RNA samples was analyzed using electrophoresis in 2% agarose gel stained with ethidium bromide. Genomic DNA was removed by DNase I (Thermo Fisher Scientific Inc.) treatment. The reaction of reverse transcription was performed on 1 µg RNA with NG dART RT kit (EURx Sp. z o.o.) following the manufacturer's instructions. Obtained cDNA was used as a template in the qPCR analysis.

The transcript levels of Cu/Zn-SOD, CAT, APX, GPX genes were determined by real-time PCR analysis. The ACT (GenBank Accession No. GQ339780.1) and ADP (GenBank Accession No. EF405961.1) genes were used as an internal control to normalize the data. Standard curves were generated from five dilution points for each primer pair. The primers were provided in Table 2. Real time-PCR was carried out according to the following cycling program: initial denaturation with UNG pre-treatment for 2 min at 50 °C, 10 min at 95 °C followed by 40 cycles of 15 s at 94 °C, 30 s at 60 °C and 30 s at 72°C in the total reaction volume of 25 µL containing 1x SG/ROX qPCR Master Mix (EURx Sp. z o.o.), 500nM of each primer and 10 ng of cDNA. For qPCR analyses, the Quant Studio3 system (Thermo Fisher Scientific Inc.) was used. Relative gene expression was assessed using the 2– $\Delta\Delta Ct$  method. Each sample was analyzed in two technical replicates. The melting curves of the PCR products were analyzed to confirm the uniqueness of the product. To determine the specificity of qPCR reaction NTC (No Template Control) was applied for each reaction. The results were analyzed using the dedicated relative quantification software module from ThermoFisher Cloud (ThermoFisher Scientific).

### 3. Results and discussion

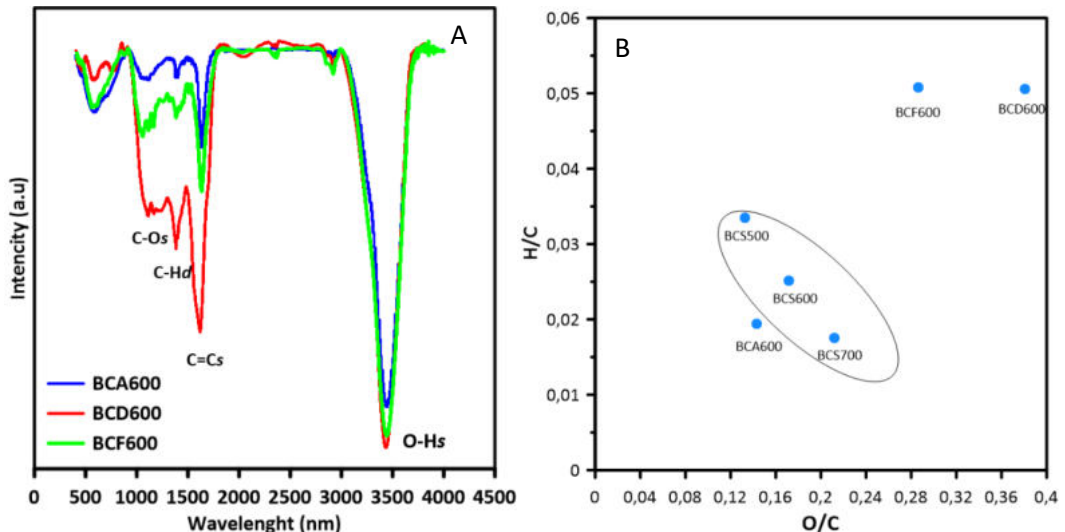
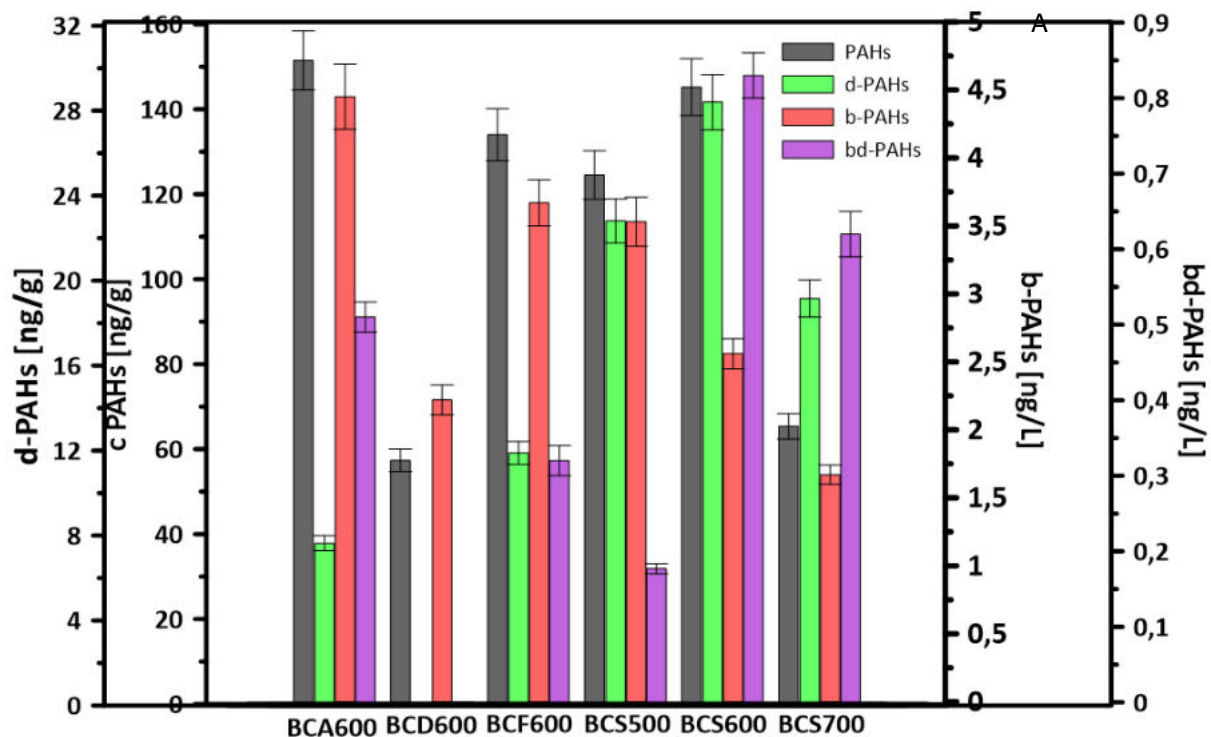


Fig. S1. A) FT-IR spectra of BCA, BCD, BCF. B) Van Krevelen plot of tested BC.



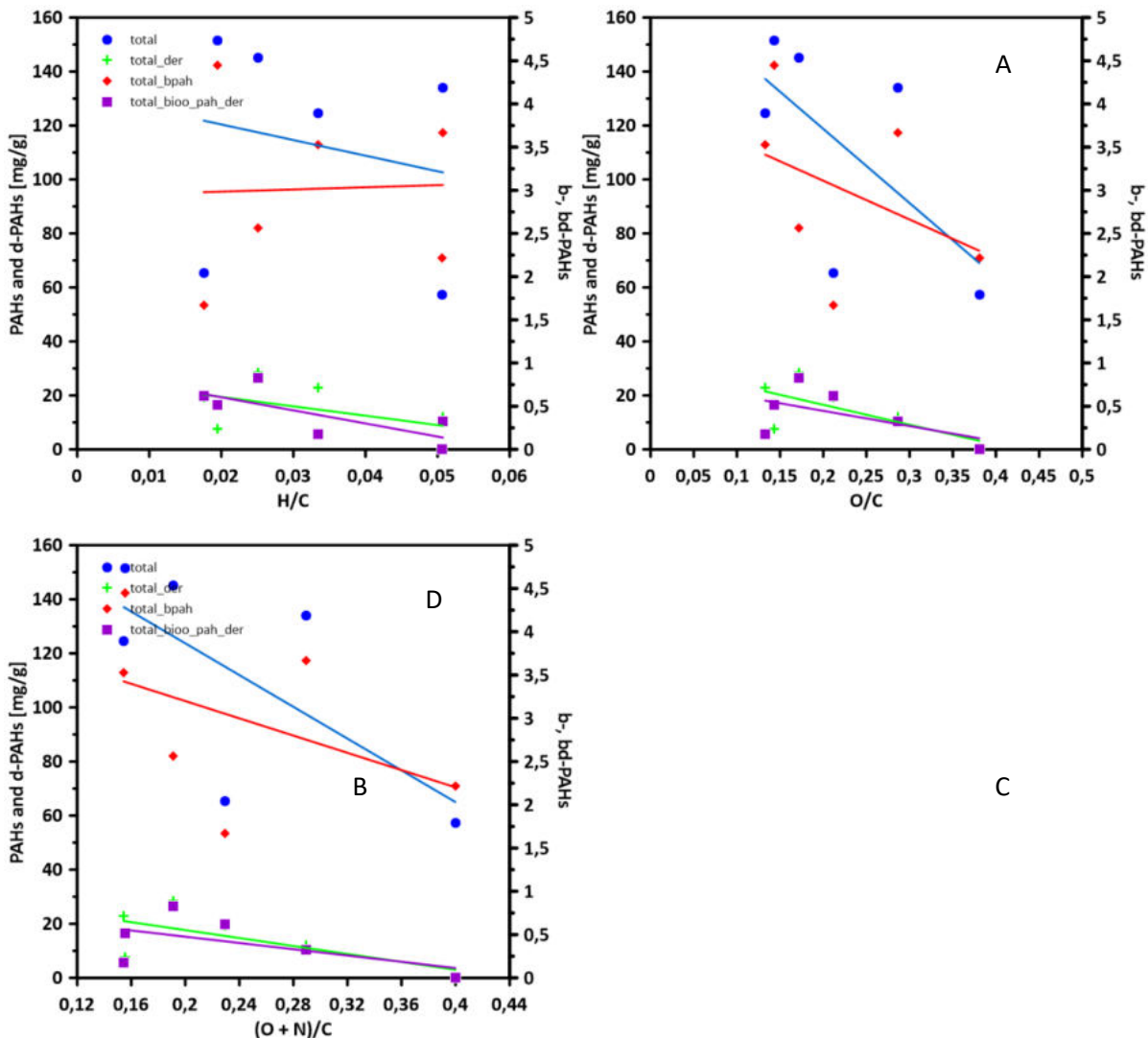


Fig. S2. A) concentration of PAHs and their derivatives in tested biochars. The dependence of the amount of determined PAHs and their derivatives on biochar characteristics: B) aromaticity, C) hydrophilicity, D) polarity index.

D

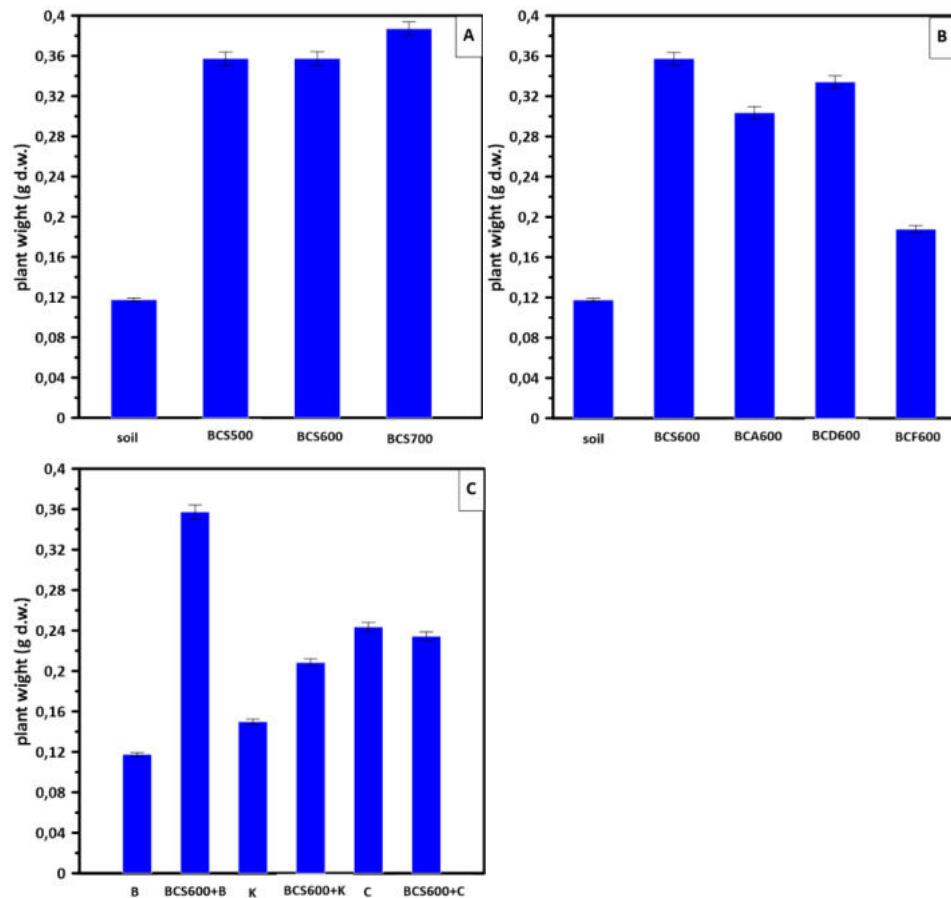


Fig. S3. Weight of barley cultivated on soil and BC-amended soil, A) effect of pyrolysis temperature, (d. w. - dry weight).

Table S2. The concentrations of PAHs and their derivatives in BC samples (n=3; n-number of replicates).

No	Compound	Sample description					
		BCS500	BCS600	BCS700	BCD600	BCF600	BCA600
		Analyte concentration ± SD* [ng L <sup>-1</sup> ]					
1	Naphthalene	< LOD	< LOD	< LOD	< LOD	1.98 ± 0.093	0.49 ± 0.023
2	1,3-di-iso-propylnaphthalene	< LOD	< LOD	< LOD	< LOD	< LOD	< LOD
3	2-Phenylnaphthalene	< LOD	< LOD	< LOD	< LOD	< LOD	< LOD
4	Acenaphthylene	1.36 ± 0.07	0.86 ± 0.04	0.49 ± 0.02	0.24 ± 0.012	0.15 ± 8.4·10 <sup>-3</sup>	1.60 ± 0.11
5	Acenaphthene	1.82 ± 0.09	1.49 ± 0.07	0.94 ± 0.04	1.45 ± 0.076	0.58 ± 0.028	1.89 ± 0.086
6	Fluorene	< LOD	< LOD	< LOD	0.33 ± 0.015	0.79 ± 0.037	< LOD
7	Anthracene	< LOD	< LOD	< LOD	1.10 ± 5·10 <sup>-3</sup>	< LOD	0.25 ± 0.012
8	Phenanthrene	< LOD	< LOD	< LOD	< LOD	< LOD	< LOD
9	3-Methylphenanthrene	0.31 ± 0.02	0.13 ± 6.2·10 <sup>-3</sup>	0.136 ± 6.0·10 <sup>-3</sup>	< LOD	0.045 ± 2.1·10 <sup>-3</sup>	0.059 ± 2.7·10 <sup>-3</sup>
10	2-Methylphenanthrene	< LOD	< LOD	< LOD	< LOD	< LOD	< LOD
11	9-Methylphenanthrene	< LOD	< LOD	< LOD	< LOD	< LOD	< LOD
12	3,6-dimethylphenanthrene	< LOD	< LOD	< LOD	0.064 ± 3.4·10 <sup>-3</sup>	0.072 ± 3.3·10 <sup>-3</sup>	0.059 ± 2.7·10 <sup>-3</sup>
13	Fluoranthene	< LOD	< LOD	< LOD	< LOD	< LOD	< LOD
14	Pyrene	< LOD	< LOD	< LOD	< LOD	< LOD	< LOD
15	2-Methylpyrene	0.024 ± 1.0·10 <sup>-3</sup>	0.023 ± 1.1·10 <sup>-3</sup>	< LOD	< LOD	< LOD	< LOD
16	4-Methylpyrene	< LOD	0.030 ± 1.4·10 <sup>-3</sup>	0.078 ± 3.4·10 <sup>-3</sup>	2.9·10 <sup>-3</sup> ± 3.6·10 <sup>-5</sup>	< LOD	0.073 ± 3.4·10 <sup>-3</sup>
17	Benzo[a]fluorene	5.2·10 <sup>-3</sup> ± 2.4·10 <sup>-4</sup>	6.1·10 <sup>-3</sup> ± 3.1·10 <sup>-4</sup>	0.012 ± 5.6·10 <sup>-4</sup>	8.3·10 <sup>-3</sup> ± 4.7·10 <sup>-4</sup>	7.2 ·10 <sup>-3</sup> ± 3.4·10 <sup>-4</sup>	8.4·10 <sup>-3</sup> ± 3.8·10 <sup>-4</sup>

18	Benzo[a]anthracene	$6.2 \cdot 10^{-3} \pm 2.9 \cdot 10^{-4}$	$7.3 \cdot 10^{-3} \pm 3.4 \cdot 10^{-4}$	$9.9 \cdot 10^{-3} \pm 4.6 \cdot 10^{-4}$	< LOD	$0.014 \pm 6.6 \cdot 10^{-4}$	< LOD
19	Chryzene	< LOD					
20	3-Methylchrysene	< LOD	$3.9 \cdot 10^{-3} \pm 1.9 \cdot 10^{-4}$	$1.7 \cdot 10^{-3} \pm 8.1 \cdot 10^{-5}$	< LOD	$4.0 \cdot 10^{-3} \pm 1.8 \cdot 10^{-4}$	< LOD
21	5-Methylchrysene	< LOD					
22	6-Methylchrysene	$3.6 \cdot 10^{-3} \pm 1.6 \cdot 10^{-4}$	$7.6 \cdot 10^{-3} \pm 3.6 \cdot 10^{-4}$	$3.2 \cdot 10^{-3} \pm 2.1 \cdot 10^{-4}$	$0.015 \pm 8.0 \cdot 10^{-4}$	$0.012 \pm 5.4 \cdot 10^{-4}$	$6.4 \cdot 10^{-3} \pm 3.0 \cdot 10^{-4}$
23	Benzo[a]fluoranthene	$4.9 \cdot 10^{-4} \pm 1.3 \cdot 10^{-5}$	$1.5 \cdot 10^{-3} \pm 9.8 \cdot 10^{-5}$	$8.4 \cdot 10^{-4} \pm 4.6 \cdot 10^{-5}$	$2.8 \cdot 10^{-3} \pm 1.3 \cdot 10^{-4}$	$2.0 \cdot 10^{-3} \pm 9.4 \cdot 10^{-5}$	$5.5 \cdot 10^{-4} \pm 2.7 \cdot 10^{-5}$
24	Benzo[b]fluoranthene	< LOD	$6.4 \cdot 10^{-3} \pm 2.9 \cdot 10^{-4}$				
25	Benzo[k]fluoranthene	< LOD					
26	Benzo[j]fluoranthene	< LOD					
27	Benzo[a]pyrene	< LOD	< LOD	< LOD	$7.2 \cdot 10^{-4} \pm 3.1 \cdot 10^{-5}$	$3.9 \cdot 10^{-3} \pm 1.8 \cdot 10^{-4}$	< LOD
28	Indeno[1,2,3-cd]pyrene	$1.5 \cdot 10^{-3} \pm 6.9 \cdot 10^{-4}$	$2.2 \cdot 10^{-3} \pm 1.0 \cdot 10^{-4}$	$6.3 \cdot 10^{-4} \pm 5.0 \cdot 10^{-5}$	$2.4 \cdot 10^{-4} \pm 1.3 \cdot 10^{-5}$	$9.4 \cdot 10^{-4} \pm 5.0 \cdot 10^{-5}$	$1.3 \cdot 10^{-4} \pm 4.7 \cdot 10^{-6}$
29	Benzo[ghi]perylene	< LOD	$1.1 \cdot 10^{-3} \pm 8.2 \cdot 10^{-5}$	$3.1 \cdot 10^{-4} \pm 2.2 \cdot 10^{-5}$	< LOD	$6.4 \cdot 10^{-4} \pm 3.2 \cdot 10^{-5}$	$1.6 \cdot 10^{-4} \pm 7.0 \cdot 10^{-6}$
30	Dibenzo[a,h]anthracene	< LOD	< LOD	< LOD	< LOD	$3.3 \cdot 10^{-3} \pm 1.5 \cdot 10^{-4}$	< LOD
31	Dibenz[a,e]pyrene	< LOD					
32	Dibenz[a,h]pyrene	< LOD					
33	Dibenz[a,i]pyrene	< LOD					
34	Dibenz[a,l]pyrene	< LOD					

#### N- and O-PAHs

35	Nitronaphthalene	< LOD	< LOD	< LOD	< LOD	< LOD	$0.26 \pm 0.013$
j26	1-Methyl-5-nitronaphthalene	$0.095 \pm 4.1 \cdot 10^{-3}$	$0.13 \pm 4.0 \cdot 10^{-3}$	$0.098 \pm 2.8 \cdot 10^{-3}$	< LOD	< LOD	< LOD
30	1-Methyl-6-nitronaphthalene	$0.081 \pm 2.7 \cdot 10^{-3}$	$0.12 \pm 5.4 \cdot 10^{-3}$	$0.12 \pm 4.2 \cdot 10^{-3}$	< LOD	< LOD	< LOD
31	9,10-Anthracenedione	< LOD	< LOD	< LOD	< LOD	$0.057 \pm 5.7 \cdot 10^{-3}$	< LOD
32	4H-cyclopenta(def)phenanthrene	< LOD	$0.58 \pm 0.02$	$0.41 \pm 0.02$	< LOD	$0.27 \pm 0.012$	$0.25 \pm 0.011$

33

Nitropyrene

&lt; LOD

&lt; LOD

&lt; LOD

&lt; LOD

&lt; LOD

&lt; LOD

\*SD – standard deviation

Table S3. The concentrations of PAHs and their derivatives in BC samples (n=3; n-number of replicates).

No	Compound	Sample description					
		BCS500	BCS600	BCS700	BCD600	BCF600	BCA600
1	Naphthalene	< LOD	0.24 ± 0.01	< LOD	< LOD	9.47 ± 0.43	2.88 ± 0.13
2	1,3-di-iso-propynaphthalene	3.22 ± 0.15	4.43 ± 0.20	0.92 ± 0.04	5.11 ± 0.23	< LOD	0.22 ± 0.01
3	2-Phenylnaphthalene	< LOD	< LOD	< LOD	< LOD	< LOD	< LOD
4	Acenaphthylene	13.48 ± 0.62	15.62 ± 0.72	7.09 ± 0.33	4.87 ± 0.22	2.34 ± 0.11	29.27 ± 1.34
5	Acenaphthene	14.01 ± 0.64	18.27 ± 0.84	7.99 ± 0.37	9.31 ± 0.43	6.73 ± 0.31	20.28 ± 0.93
6	Fluorene	< LOD	< LOD	< LOD	4.43 ± 0.20	19.46 ± 0.89	12.30 ± 0.56
7	Anthracene	1.04 ± 0.05	1.48 ± 0.07	0.44 ± 0.02	< LOD	< LOD	0.86 ± 0.04
8	Phenanthrene	< LOD	< LOD	< LOD	< LOD	< LOD	< LOD
9	3-Methylphenanthrene	24.29 ± 1.11	27.28 ± 1.25	10.99 ± 0.50	< LOD	4.88 ± 0.22	2.94 ± 0.14
10	2-Methylphenanthrene	12.04 ± 0.55	10.96 ± 0.50	2.05 ± 0.09	0.24 ± 0.01	0.72 ± 0.03	0.92 ± 0.04
11	9-Methylphenanthrene	< LOD	< LOD	< LOD	< LOD	0.22 ± 0.01	0.22 ± 0.01
12	3,6-dimethylphenanthrene	0.34 ± 0.02	0.32 ± 0.02	0.24 ± 0.01	< LOD	14.91 ± 0.68	12.34 ± 0.57
13	Fluoranthene	0.28 ± 0.01	0.46 ± 0.02	0.22 ± 0.01	< LOD	< LOD	1.38 ± 0.06
14	Pyrene	< LOD	< LOD	< LOD	< LOD	1.24 ± 0.06	2.28 ± 0.10
15	2-Methylpyrene	9.10 ± 0.42	6.33 ± 0.29	4.46 ± 0.20	0.32 ± 0.02	< LOD	2.22 ± 0.10

16	4-Methylpyrene	$3.02 \pm 0.14$	$2.30 \pm 0.11$	< LOD	$0.82 \pm 0.04$	< LOD	$13.98 \pm 0.64$
17	Benzo[a]fluorene	$12.88 \pm 0.59$	$16.27 \pm 0.75$	$10.26 \pm 0.47$	$12.21 \pm 40.56$	$16.28 \pm 0.75$	$8.88 \pm 0.41$
18	Benzo[a]anthracene	$9.06 \pm 0.42$	$12.04 \pm 0.55$	$6.73 \pm 0.31$	< LOD	$11.47 \pm 0.53$	< LOD
19	Chryzene	$1.94 \pm 0.09$	$2.24 \pm 0.10$	$1.27 \pm 0.06$	< LOD	< LOD	< LOD
20	3-Methylchrysene	$6.04 \pm 0.28$	$10.02 \pm 0.46$	$3.27 \pm 0.15$	$0.82 \pm 0.04$	$6.21 \pm 0.28$	$5.48 \pm 0.25$
21	5-Methylchrysene	$6.84 \pm 0.31$	$8.85 \pm 0.41$	$4.28 \pm 0.20$	$6.28 \pm 0.29$	$4.98 \pm 0.23$	$8.32 \pm 0.38$
22	6-Methylchrysene	$1.26 \pm 0.06$	$1.82 \pm 0.08$	$0.82 \pm 0.04$	$10.35 \pm 0.47$	$10.33 \pm 0.47$	$14.52 \pm 0.67$
23	Benzo[a]fluoranthene	< LOD	< LOD	< LOD	$0.22 \pm 0.01$	$0.24 \pm 0.01$	$4.30 \pm 0.20$
24	Benzo[b]fluoranthene	< LOD	< LOD	< LOD	< LOD	< LOD	$6.28 \pm 0.29$
25	Benzo[k]fluoranthene	< LOD	< LOD	< LOD	< LOD	< LOD	$1.22 \pm 0.06$
26	Benzo[j]fluoranthene	< LOD	< LOD	< LOD	< LOD	< LOD	$0.120 \pm 5.0 \cdot 10^{-3}$
27	Benzo[a]pyrene	$0.32 \pm 0.02$	$0.38 \pm 0.02$	$0.24 \pm 0.01$	$1.94 \pm 0.09$	$10.23 \pm 0.47$	< LOD
28	Indeno[1,2,3-cd]pyrene	$3.86 \pm 0.18$	$4.03 \pm 0.19$	$2.87 \pm 0.13$	< LOD	< LOD	< LOD
29	Benzo[ghi]perylene	$1.54 \pm 0.07$	$1.88 \pm 0.09$	$1.25 \pm 0.06$	< LOD	< LOD	< LOD
30	Dibenz[a,h]anthracene	< LOD	< LOD	< LOD	< LOD	$14.41 \pm 0.66$	$0.24 \pm 0.01$
31	Dibenz[a,e]pyrene	< LOD	< LOD	< LOD	$0.22 \pm 0.01$	< LOD	$0.040 \pm 2.0 \cdot 10^{-3}$
32	Dibenz[a,h]pyrene	< LOD	< LOD	< LOD	$0.24 \pm 0.01$	< LOD	< LOD
33	Dibenz[a,i]pyrene	< LOD	< LOD	< LOD	< LOD	< LOD	< LOD
34	Dibenz[a,l]pyrene	< LOD	< LOD	< LOD	< LOD	< LOD	< LOD

#### N- and O-PAHs

35	Nitronaphthalene	< LOD	< LOD	< LOD	< LOD	< LOD	$1.32 \pm 0.06$
j26	1-Methyl-5-nitronaphthalene	$1.70 \pm 0.08$	$1.88 \pm 0.09$	$1.31 \pm 0.06$	< LOD	< LOD	< LOD
30	1-Methyl-6-nitronaphthalene	$2.24 \pm 0.10$	$2.32 \pm 0.11$	$1.67 \pm 0.08$	< LOD	< LOD	< LOD

31	9,10-Anthracenedione	< LOD	< LOD	< LOD	< LOD	0.82 ± 0.04	< LOD
32	4H-cyclopenta(def)phenanthrene	18.87 ± 0.86	24.20 ± 1.11	16.17 ± 0.74	< LOD	11.07 ± 0.51	6.32 ± 0.29
33	Nitropyrene	< LOD	< LOD	< LOD	< LOD	< LOD	< LOD

\*SD – standard deviation

## References

- Bradford, M.M., 1976. A rapid and sensitive method for the quantitation of microgram quantities of protein utilizing the principle of protein-dye binding. *Analytical Biochemistry* 72, 248–254. [https://doi.org/10.1016/0003-2697\(76\)90527-3](https://doi.org/10.1016/0003-2697(76)90527-3)
- Hale, S.E., Lehmann, J., Rutherford, D., Zimmerman, A.R., Bachmann, R.T., Shitumbanuma, V., O'Toole, A., Sundqvist, K.L., Arp, H.P.H., Cornelissen, G., 2012. Quantifying the Total and Bioavailable Polycyclic Aromatic Hydrocarbons and Dioxins in Biochars. *Environ. Sci. Technol.* 46, 2830–2838. <https://doi.org/10.1021/es203984k>
- Hans-Peter Schmidt, 2015. European Biochar Certificate (EBC) - guidelines version 6.1. <https://doi.org/10.13140/RG.2.1.4658.7043>
- Hawthorne, S.B., Jonker, M.T.O., van der Heijden, S.A., Grabanski, C.B., Azzolina, N.A., Miller, D.J., 2011. Measuring Picogram per Liter Concentrations of Freely Dissolved Parent and Alkyl PAHs (PAH-34), Using Passive Sampling with Polyoxymethylene. *Anal. Chem.* 83, 6754–6761. <https://doi.org/10.1021/ac201411v>
- Josefsson, S., Arp, H.P.H., Kleja, D.B., Enell, A., Lundstedt, S., 2015. Determination of polyoxymethylene (POM) – water partition coefficients for oxy-PAHs and PAHs. *Chemosphere* 119, 1268–1274. <https://doi.org/10.1016/j.chemosphere.2014.09.102>
- Kraska, P., Andruszczak, S., Kwiecińska-Poppe, E., Staniak, M., Różyło, K., Rusecki, H., 2019. Supporting Crop and Different Row Spacing as Factors Influencing Weed Infestation in Lentil Crop and Seed Yield under Organic Farming Conditions. *Agronomy* 10, 9. <https://doi.org/10.3390/agronomy10010009>
- Oleszczuk, P., Kuśmierz, M., Godlewska, P., Kraska, P., Pałys, E., 2016. The concentration and changes in freely dissolved polycyclic aromatic hydrocarbons in biochar-amended soil. *Environmental Pollution* 214, 748–755. <https://doi.org/10.1016/j.envpol.2016.04.064>

Pranagal, J., Kraska, P., 2020. 10-Years Studies of the Soil Physical Condition after One-Time Biochar Application. *Agronomy* 10, 1589.

<https://doi.org/10.3390/agronomy10101589>

Wang, Guifeng, Wang, Gang, Zhang, X., Wang, F., Song, R., 2012. Isolation of High Quality RNA from Cereal Seeds Containing High Levels of Starch. *Phytochemical Analysis* 23, 159–163. <https://doi.org/10.1002/pca.1337>

Wessely-Szponder, J., Bełkot, Z., Bobowiec, R., Kosior-Korzecka, U., Wójcik, M., 2015. Transport induced inflammatory responses in horses. *Pol J Vet Sci* 18, 407–413.

<https://doi.org/10.1515/pjvs-2015-0052>

Złotek, U., Świeca, M., Reguła, J., Jakubczyk, A., Sikora, M., Gawlik-Dziki, U., Kapusta, I., 2019. Effects of probiotic L. plantarum 299v on consumer quality, accumulation of phenolics, antioxidant capacity and biochemical changes in legume sprouts. *International Journal of Food Science & Technology* 54, 2437–2446.

<https://doi.org/10.1111/ijfs.14158>

## **Publikacja D7**

**A. Krzyszczak-Turczyn, M. P. Dybowski, M. Kończak, P. Oleszczuk, B. Czech**  
*Increased concentration of PAHs derivatives in biochar-amended soil observed in a long-term experiment, artykuł w trakcie recenzji*  
Journal of Hazardous Materials

**Journal of Hazardous Materials**  
**Increased concentration of PAHs derivatives in biochar-amended soil observed in a long-term experiment**  
--Manuscript Draft--

<b>Manuscript Number:</b>	HAZMAT-D-23-06519
<b>Article Type:</b>	Research Paper
<b>Keywords:</b>	soil; biochar-amended soil; PAHs; PAHs derivatives; bioavailability
<b>Corresponding Author:</b>	Bozena Czech, Ph.D. Maria Curie-Sklodowska University in Lublin Faculty of Chemistry Lublin, POLAND
<b>First Author:</b>	Agnieszka Krzyszczak-Turczyn
<b>Order of Authors:</b>	Agnieszka Krzyszczak-Turczyn Michał Dybowski Magdalena Kończak Patryk Oleszczuk Bozena Czech, Ph.D.
<b>Abstract:</b>	During biochar preparation or application some toxic substances may be formed. The established limitations of the content of polycyclic aromatic hydrocarbons (PAHs) aim to monitor the fate of PAHs in the life cycle of biochar. The latest studies have revealed that besides PAHs, some of their derivatives with confirmed toxicity are formed. There has been no policy regards PAHs derivatives in biochar yet. The aim of the presented studies was the estimation the changes in the content of PAHs and their derivatives during the agricultural application of biochar. A pot experiment with grass revealed that in a short time, both the content of PAHs and their derivatives was reduced. Similarly, when biochar was added to soil in a long-term experiment, the content of determined derivatives was below the limit of detection, whereas interestingly, the content of pristine PAHs increased with time. Co-addition of biochar and sewage sludge increased the content of PAHs and their derivatives indicating potential environmental hazard due to their presence. However, the key point is the estimation of the bioavailability of PAHs and their derivatives as only the bioavailable fraction is revealing the environmental hazard.
<b>Suggested Reviewers:</b>	Yanzheng Gao gaoyanzheng@njau.edu.cn  Zisis Vryzas zvryzas@agro.duth.gr

*Journal of Hazardous Materials*

June 9, 2023

Dear Editor,

On behalf of all the authors, I am submitting a manuscript titled "Increased concentration of PAHs derivatives in biochar-amended soil observed in the long-term experiment" prepared by Agnieszka Krzyszczak-Turczyn, Michał P. Dybowski, Magdalena Kończak, Patryk Oleszczuk, and Bożena Czech to your kind consideration for possible publication in the *Journal of Hazardous Materials*.

The present manuscript has not been published previously and it is not being considered for publication elsewhere, and will not be published in part or entirety, in English or any other language, without the written consent of the Publisher. All the named authors have materially participated in this research work and equally contributed to the preparation of the manuscript and fully approved its final publication in your esteemed journal. There are no conflicts of interest to declare. The presented study does not involve human subjects.

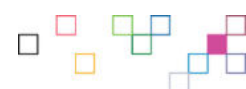
The formation of PAHs derivatives in biochar was confirmed. Although there are established limitations considering PAHs content on biochar, there is no policy on PAHs derivatives. The objective of the studies was the estimation of the fate of PAHs derivatives and pristine PAHs in biochar-amended soil in pot and field experiments. The results indicate that during biochar production besides PAHs, their more toxic derivatives are formed. The problem is that the application of biochar into the soil may be connected with the introduction of PAHs and their derivatives. It was established that initial biochar was characterized by low (up to  $28.4 \pm 1.3 \mu\text{g g}^{-1}$ ) content of derivatives and the amount of determined PAHs derivatives cannot be directly connected with the content of pristine PAHs in biochar. The increase in the pyrolysis temperature did not result in increased bioavailability of PAHs and their derivatives in biochar. During soil amendment, the concentration of PAHs (originating from biochars) decreased during the short-term agricultural application of pyrolyzed material, however, increased in long-term field experiments. Moreover, the amount of PAHs depends on the type of feedstock and the temperature of pyrolysis. Thus, the agricultural and environmental safety of biochars depends mostly on these two parameters. A significant increase in the content of PAHs and their derivatives (N-and O-PAHs) was noted when biochar was applied simultaneously with sewage sludge as fertilizer up to  $0.092 \mu\text{g g}^{-1}$ .

We believe that the research findings demonstrated in this work are relevant to the Aim and Scope of the *Journal of Hazardous Materials* e.g. identification and the fate of pollutants in real environmental studies and will be of interest to its broad readership. We would be very much grateful if the manuscript could be carefully reviewed and considered for publication. The manuscript was prepared according to the Guide for Authors and the references are in the correct format. References were managed by Zotero. The manuscript counts 8842 words (with references), 5 Figures, 1 Table, and 44 references. All color figures should appear in color only in the web version but in black in print. Supporting material is also added.

Thank you very much for your kind consideration.

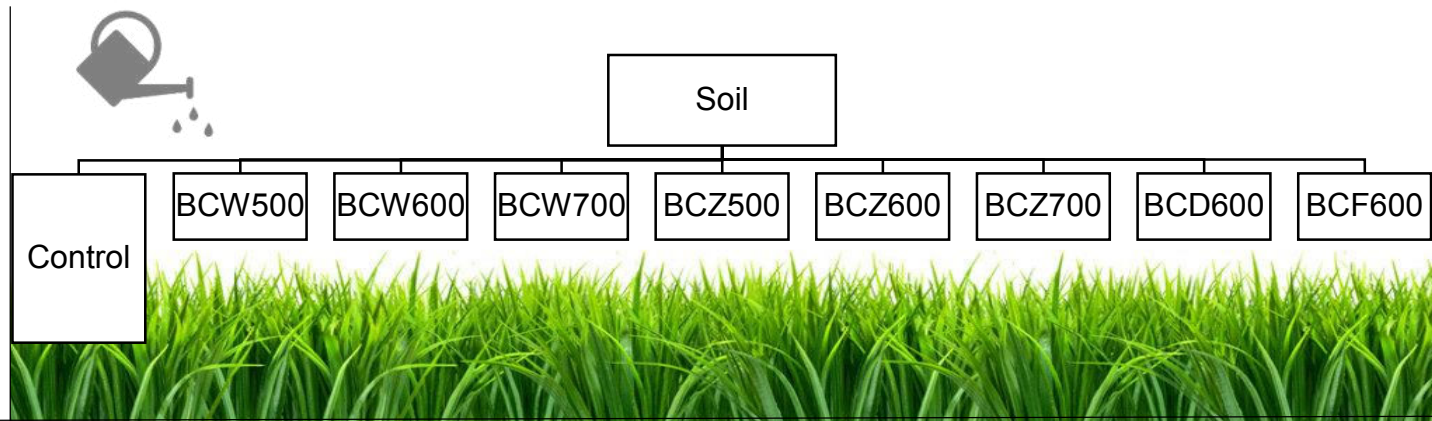
Sincerely,

Bożena Czech



During preparation or application of biochar polycyclic aromatic hydrocarbons (PAHs) and more toxic derivatives are formed. The limitations of the PAHs content aim to monitor their fate but there is no information on the derivatives in biochar. Pot experiment revealed that in a short time content of PAHs and their derivatives was reduced. Similarly, in biochar-amended soil in long-term experiments, the amount of derivatives was below the LOD but the total amount of PAHs increased with time. When a natural organic fertilizer was added, both contents of PAHs and their derivatives increased indicating potential environmental hazards due to their presence.

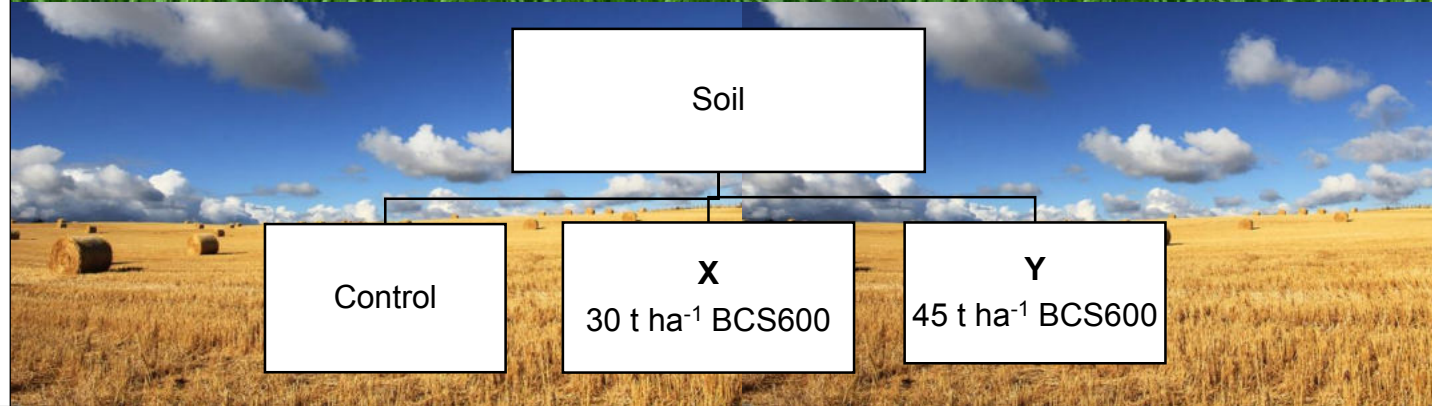
### Experiment 1 pot experiment



Content of  
PAHs  
decreases  
(lower than  
expected)



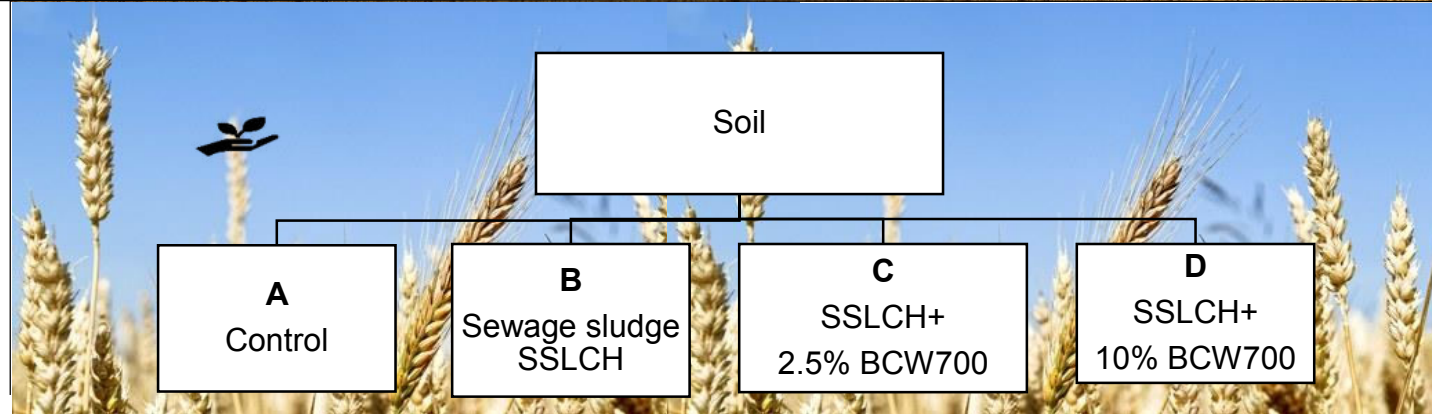
### Experiment 2 field experiment



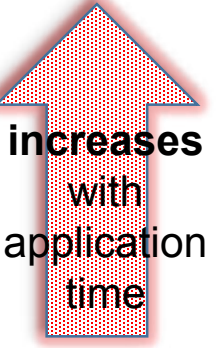
increases  
with  
application  
time



### Experiment 3 field experiment



increases  
with  
application  
time



1. The fate of PAHs derivatives in biochar-amended soil was monitored.
2. In pot experiment the content of PAHs and their derivatives was reduced.
3. In long-term field experiment PAHs persistence was confirmed.
4. In biochar-amended soil the content of PAHs derivatives was lowered.
5. Co-addition of sewage sludge and biochar increased PAHs and their derivatives in soil.

# 1 Increased concentration of PAHs derivatives in biochar-amended soil observed in a

## 2 long-term experiment

3

4 Agnieszka Krzyszczak-Turczyn<sup>1</sup>, Michał P. Dybowski<sup>2</sup>, Magdalena Kończak<sup>3</sup>, Patryk  
5 Oleszczuk<sup>1</sup>, Bożena Czech<sup>1\*</sup>

6

7     <sup>1</sup>Department of Radiochemistry and Environmental Chemistry, Institute of Chemical Sciences,  
8     Faculty of Chemistry, Maria Curie-Sklodowska University in Lublin, Pl. M. Curie-  
9     Sklodowskiej 3, 20-031 Lublin, Poland

<sup>10</sup> <sup>2</sup>Department of Chromatography, Institute of Chemical Sciences, Faculty of Chemistry, Maria  
<sup>11</sup> Curie Skłodowska University in Lublin, Pl. M. Curie-Skłodowskiej 3, 20-031 Lublin, Poland

12 <sup>3</sup>Institute of Earth and Environmental Sciences, Faculty of Earth Sciences and Spatial  
13 Management, Maria Curie-Sklodowska University, ul. Kraśnicka 2cd, 20-718, Lublin, Poland

14

15 \*corresponding author: Tel.: +48 81 537 55 54; fax: +48 81 537 55 65; E-mail address:  
16 bozena.czech@mail.umcs.pl (B. Czech)

17

18 Abstract

19 During biochar preparation or application some toxic substances may be formed. The  
20 established limitations of the content of polycyclic aromatic hydrocarbons (PAHs) aim to  
21 monitor the fate of PAHs in the life cycle of biochar. The latest studies have revealed that  
22 besides PAHs, some of their derivatives with confirmed toxicity are formed. There has been no  
23 policy regards PAHs derivatives in biochar yet. The aim of the presented studies was the  
24 estimation the changes in the content of PAHs and their derivatives during the agricultural  
25 application of biochar. A pot experiment with grass revealed that in a short time, both the

26 content of PAHs and their derivatives was reduced. Similarly, when biochar was added to soil  
27 in a long-term experiment, the content of determined derivatives was below the limit of  
28 detection, whereas interestingly, the content of pristine PAHs increased with time. Co-addition  
29 of biochar and sewage sludge increased the content of PAHs and their derivatives indicating  
30 potential environmental hazard due to their presence. However, the key point is the estimation  
31 of the bioavailability of PAHs and their derivatives as only the bioavailable fraction is revealing  
32 the environmental hazard.

33 **Environmental Implication**

34 During preparation or application of biochar polycyclic aromatic hydrocarbons (PAHs) and  
35 more toxic derivatives are formed. The limitations of the PAHs content aim to monitor their  
36 fate but there is no information on the derivatives in biochar. Pot experiment revealed that in a  
37 short time content of PAHs and their derivatives was reduced. Similarly, in biochar-amended  
38 soil in long-term experiments, the amount of derivatives was below the LOD but the total  
39 amount of PAHs increased with time. When a natural organic fertilizer was added, both contents  
40 of PAHs and their derivatives increased indicating potential environmental hazards due to their  
41 presence.

42

43 **Keywords:** soil, biochar-amended soil, PAHs, PAHs derivatives; bioavailability

44

45 **1. Introduction**

46 An environmentally friendly attitude should be accompanied by all people in the world  
47 in their personal and business life. Nowadays, sustainable techniques and methods for waste  
48 treatment and disposal are searching. Biochar (BC) is a carbon material that can be obtained

49 during for example pyrolysis (fast and slow), gasification, and hydrothermal carbonization of  
50 various feedstock [1,2]. In recent years the number of studies on biochar, its physicochemical  
51 characteristics, composition, and application have increased. Despite the material was known  
52 for centuries [3], the areas in which it can be applied are constantly expanding. Depending on  
53 chosen precursor material, the properties and composition of obtained BC vary [4]. Biochars  
54 can be produced from various types of feedstock, e.g. biomass (rice husk, cacao shell [5],  
55 willow, wheat straw [6], amur silver grass residue, paddy straw, umbrella tree [7]), sewage  
56 sludge [6], animal manure [8,9]. Thus, biochar has gained increased interest, recently. Biochar  
57 production from wastes and utilization in agriculture and environmental protection are the  
58 examples of implementation of a circular economy and sustainable development and enable the  
59 realization of several SDGoals [sdgs.un.org].

60 There are some advantages and disadvantages of biochar's addition to soil. The  
61 indisputable benefits of applying biochar in soil include mitigation of greenhouse gas emissions  
62 by carbon storage in the ground, remediation of soils, and enhanced fertility [1,10]. The further  
63 consequences of BC addition are stimulation of plant growth (which also reduces carbon  
64 dioxide in the atmosphere), increase in crop productivity, and soil sustainability [1,11]. Adekiya  
65 et al. [11] found that biochar addition improved the porosity of the soil, moisture content, mean  
66 weight diameter, and infiltration rate. On the other hand, the enrichment reduced bulk density  
67 and soil loss. The addition of biochar into soil affects also the chemical characteristics of the  
68 soil. The enrichment increased in organic matter, N, P, K, Ca, Mg contents, and soil cation  
69 exchange capacity (CEC) [11]. Similar results were obtained by another Researcher. Many of  
70 them confirm that BC addition into soil improves soil porosity [12,13], pH [2,12,14], plant-  
71 available phosphorus [12,14], soil water-holding capacity [12,13], CEC [2,14,15], electrical  
72 conductivity, organic carbon, total nitrogen contents [14], soil microbial activity, nutrient  
73 retention [16] and reduces soil bulk density [15]. Moreover, Herath et al. [17] suggested that

74 BC application significantly enhanced aggregate stability, volumetric water content,  
75 macroporosity, mesoporosity, and saturated hydraulic conductivity. The beneficial effect of  
76 biochar addition to soil improves with time [18,19]. Another benefit of BC application in the  
77 soil is the high stability of pyrolyzed material in the soil (compared to other organic matter  
78 components) which results in an accumulation of soil organic carbon [20]. Moreover, the effect  
79 of adding biochar to soil persisted over 10 years [12].

80 Despite all of the benefits associated with the use of biochar in agriculture, pyrolyzed  
81 material (being obtained during a high-temperature process) can be a source of toxins  
82 introduced to the environment or BC application can cause unintended consequences [2].  
83 Toxicants may originate from feedstock - waste materials that may contain some contaminants  
84 or their precursors, or they can also be derived during biochar production [2]: polycyclic  
85 aromatic hydrocarbons (PAHs), PAHs derivatives, volatile organic compounds (VOCs),  
86 chlorinated hydrocarbons, dioxins, furans, metals [9,21–26]. Toxins entering the environment  
87 can cause adverse effects on plant growth and microbial community in soil [21]. VOCs (mostly  
88 ethylene) can induce ‘soil volatilomics’ - plant and microbial responses which cause mimicking  
89 plant hormones [27]. PAHs are mutagenic, toxic, and carcinogenic for living organisms [28,29].  
90 The content of the total fraction of PAHs in biochar varied widely and the values depend mainly  
91 on types of feedstock, pyrolysis temperature, and the resident time [6,23,25]. The total and  
92 bioavailable fraction of contaminants (PAHs and their derivatives) can be determined. The total  
93 fraction of toxins does not show the real threat to living organisms and does not fully  
94 demonstrate an actual environmental quality but the bioavailable fraction does [25,30].  
95 Bioavailable compounds can be defined as compounds that are freely available to go through  
96 an organism’s cellular membrane from a medium (in which it is currently located) [31].  
97 Moreover they are more labile as well as able to leach to the ambience [25]. Oleszczuk et al.  
98 [23] found that the content of the sum of PAHs in biochars derived from elephant grass

99 (miscanthus), coconut shell, wicker, and wheat straw amounted in the range from 1124 to  
100 28,339 µg/kg [23]. Hale et al. [25] presented the range of the total fraction of PAHs (in BC  
101 obtained via slow pyrolysis) from 70 µg kg<sup>-1</sup> to 3270 µg kg<sup>-1</sup> and the range of the bioavailable  
102 fraction of PAHs from 0.17 ng L<sup>-1</sup> to 10.0 ng L<sup>-1</sup>.

103 Our previous studies have proven that in BC besides PAHs, their toxic derivatives  
104 containing O- or N- in the PAHs molecule are noted [32]. As was described in the case of PAHs  
105 amount and bioavailability are dependent on the feedstock type and pyrolysis conditions [6].  
106 According to our knowledge, this is the first study describing the formation and bioavailability  
107 of PAHs derivatives in biochar-amended soil. What is worth stressing, the results from the pot  
108 and field experiment are presented, and the conclusions for future perspective and BC  
109 application in the context of PAHs derivatives safety and persistence and bioavailability. Thus,  
110 the study aimed to investigate how the concentration of the bioavailable and total fraction of  
111 PAHs and their derivatives changes during the agricultural application of biochar, both in pot  
112 and field experiments. The content of individual PAHs and derivatives was quantified in initial  
113 biochars, biochar-amended and biochar-amended soil fertilized with sewage sludge.

## 114 **2. Material and methods**

### 115 **2.1. Feedstock and biochar preparation**

116 For the biochar preparation, several feedstocks were used: willow (*Salix viminalis*), two sewage  
117 sludges (from municipal wastewater treatment plants in Zamość (50°43'14"N 23°15'31"E,  
118 Poland, labeled as SSLZ, and Chełm, labeled as SSLCH). Slow pyrolysis was applied for the  
119 preparation of biochar (Czylok, Poland, applied temperatures: 500°C, 600°C, and 700°C at  
120 heating rates at the first step 10°C min<sup>-1</sup>, and the second step 3°C min<sup>-1</sup>, the resident time: 3h  
121 with the constant flow of nitrogen at 630 cm<sup>3</sup> min<sup>-1</sup>). The other biochars were pyrolyzed at  
122 600°C using hardwood, softwood wastes or wheat straw. Thus, biochars used in the experiment  
123 were named as follows: willow-derived BC produced at 500°C – BCW500, at 600°C –

124 BCW600, at 700°C – BCW700, sewage sludge-derived BC produced at 500°C – BCZ500, at  
125 600°C – BCZ600, at 700°C – BCZ700, BC obtained from residues from hardwood at 600°C –  
126 BCD600, from residues from softwood at 600°C – BCF600, and BC obtained from wheat straw-  
127 BCS600. The biochar samples were grounded to particles of about 2 mm. All BC were  
128 homogenized, washed out using distilled water (1:10, biochar: water) for 24 h, and dried at  
129 40°C for 6 h. Before the experiment BCs were stored at room temperature, in the absence of  
130 light.

131 **2.2. Soil experiments (preparation, enrichment with biochars)**

132 **Experiment 1 – pot experiment**

133 The soil was collected from the Polish village of Podborcze, Poland (50°41'47.5"N 22°50'41.3"  
134 E). The top soil samples (0-20 cm, classified as acidic brown soil developed from deep loess)  
135 were air-dried, sieved (<2 mm), homogenized, and divided into several groups. Almost every  
136 portion (except the control one) was enriched with specified biochar (0.5%) (Fig. 1), and  
137 thoroughly mixed. Then, soil alone (control) and biochar-amended soils were transferred to  
138 special propylene containers (size 19/12/7cm) and tap water was added to reach 40% of the  
139 water-holding capacity of the soil. The 30 grass seeds (*Lolium multiflorum*) were placed in  
140 each container. The samples were exposed to a regular light/dark cycle resulting from day/night  
141 changes. After harvest, the soil alone as well as biochar-amended soils were air-dried, sieved  
142 (<2 mm), homogenized, and analyzed as described in captions 2.3 and 2.4.

143 **Experiment 2 – a field experiment 1**

144 In experiment 2, the effect of BC doses was established by considering the amount and quality  
145 of PAHs in BC-amended soil in a long-term experiment. Field experiment 1 was conducted in  
146 the growing season at the Experimental Station located in Bezek village in the South-East part  
147 of Poland (50°20'04"N 23°29'49"E). Simultaneously, it was an agricultural area with limited  
148 anthropogenic pressure. In this case, the experiment was carried out in triplicate in a randomized

149 block design with an area of 15 m<sup>2</sup> each. The biochar obtained from wheat straw (BCS) was  
150 applied into the soil in the following doses: 30 t ha<sup>-1</sup> (30BCS - X) and 45 t ha<sup>-1</sup> (45BCS - Y)  
151 (Fig. 1). The soil without fertilization (as a control sample) was also prepared. Biochar was  
152 distributed by hand on the field and mixed with soil through a cultivator and plow (10 cm deep).  
153 Soil without amendment was proceeded the same way. Thereafter, barley (*Hordeum sativum*  
154 L.) in the first year and oat (*Avena sativa* L.) in the second year of Experiment 2 were sown.  
155 The representative samples for analyses were collected immediately after the experiment was  
156 started and then, after 21, 105, and 474 days. The samples were transported to the laboratory,  
157 air-dried in an air-conditioned room (20–23°C) in the absence of light, manually crushed, sieved  
158 (<2mm), and analyzed as described in captions 2.3 and 2.4.

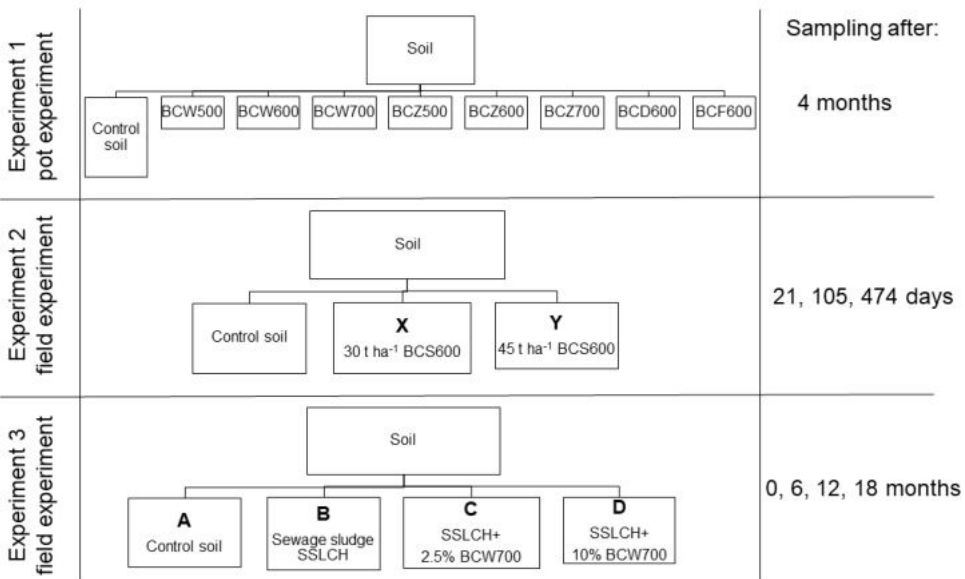
159 **Experiment 3 – a field experiment 1**

160 Experiment 3 was performed to verify the effect of fertilizing effect of SSL and SSL-  
161 derived BC on PAHs behavior in a long-term study. Field experiment 3 was carried out also at  
162 the Bezek Experimental Station (Poland) (as described above). The experiment was carried out  
163 in triplicate in a randomized block design with an area of 18.5 m<sup>2</sup> each. The soil was enriched  
164 with BCW700 and/or SSLCH which act as fertilizers (Fig. 1). The spring wheat (*Triticum*  
165 *aestivum* L.) was selected as the tested crop. The details considering technical issues about the  
166 amendment and sowing were presented in Supporting Information. The following variants were  
167 used in this field experiment: (A) control soil (without amendments) (S); (B) soil with the  
168 addition of SSLCH (10 t<sub>dw</sub> ha<sup>-1</sup>) (S + SSLCH); (C) soil with the addition of SSLCH and a 2.5%  
169 of BCW700 (S + SSLCH + 2.5% BCW700); (D) soil with the addition of SSLCH and a 10.0%  
170 of BCW700 (S + SSLCH + 10.0% BCW700). Thus in Figure 4 the following descriptors: B, C,  
171 and D were used. The representative soil samples were collected at the beginning of the  
172 experiment (labeled as 0), as well as 6, 12, and 18 months after the application of amendments

173 to the soil. The samples were transported to the laboratory, air-dried in an air-conditioned room  
174 (25°C), manually crushed, sieved (<2mm), and analyzed as described in captions 2.3 and 2.4.

175 **Experiment 3 – a field experiment 2**

176 In experiment 3 the effect of BC doses was established considering the amount and quality of  
177 PAHs in BC-amended soil in the long-term experiment. Field experiment 3 was carried out also  
178 at the Bezek Experimental Station (Poland) (as described above). In this case, the experiment  
179 was carried out in triplicate in a randomized block design with an area of 15 m<sup>2</sup> each. The  
180 biochar obtained from wheat straw (BCS600) was applied into the soil in the following doses:  
181 30 t ha<sup>-1</sup> (30BCS600 – labeled as X in Figure 1) and 45 t ha<sup>-1</sup> (45BCS600 – labeled as Y) (Fig.  
182 1). The soil without fertilization (as a control sample) was also prepared. Biochar was  
183 distributed by hand on the field and mixed with soil through a cultivator and plow (10 cm deep).  
184 Soil without amendment was proceeded the same way. Thereafter, barley (*Hordeum sativum*  
185 L.) in the first year and oat (*Avena sativa* L.) in the second year of Experiment 3 were sown.  
186 The representative samples for analyses were collected immediately after the experiment was  
187 started and then, after 21, 105, and 474 days. The samples were transported to the laboratory,  
188 air-dried in an air-conditioned room (20–23°C) in the absence of light, manually crushed, sieved  
189 (<2mm), and analyzed as described in captions 2.3 and 2.4.



190

191 Fig. 1. Scheme of conducted research.

192 **2.3. The total fraction of PAHs and their derivatives determination in biochar and  
193 soil**

194 The total fraction of PAHs and their derivatives in biochar was determined via protocols  
195 described in our previous studies [32,33]. The same group of compounds was also extracted  
196 from soil samples using a similar procedure with slight modifications. PAHs and their  
197 derivatives were extracted via pressurized liquid extraction (PLE) using Dionex 350 system  
198 (Thermo Fisher Scientific, USA). 22 mL stainless steel cells were packed as follows: activated  
199 silica gel mixed with copper, biochar (or soil sample) with ethylenediaminetetraacetic acid, the  
200 internal standard, and glass beads as a fulfillment. PLE was carried out with hexane at 150°C  
201 (2 extraction cycles; flush volume - 60%, the static time - 5 min, purge time - 60s, 1 MPa with  
202 N<sub>2</sub>). After extraction, iso-octane was added to the extract. The obtained solvent was  
203 concentrated and analyzed via GC-MS/MS (Supporting Information: caption 2.5, Table S1,  
204 Table S2).

205 **2.4. The bioavailable fraction of PAHs and their derivatives determination in biochar**

206 The bioavailable fraction of PAHs and their derivatives in biochar was determined via protocols  
207 described in our previous studies [6,32–34]. Briefly, the experiment required the application of  
208 polyoxymethylene (POM) passive samplers (4 cm x 4cm, ~0.35 g) which were cleaned,  
209 submerged, and shaken (shaking machine (ELPIN 358A, Poland)) for 24 h in methanol, then  
210 in n-heptane, and Millipore water. Prepared POMs were rinsed with Millipore water and stored  
211 in a glass bottle at 4°C. Biochar, the aqueous solution of sodium azide, and POMs were placed  
212 in Erlenmeyer flasks. Flasks were rolled on a rotary shaker (ROTAX 6.8 VELP Scientifica  
213 (Italy)) for 30 days at 10 RCF. Then, POM samplers were cleaned with distilled water and  
214 extracted via 1/4 acetone/heptane (v/v) with the addition of deuterated 16 USEPA PAHs for 48  
215 hours. After this period, iso-octane was added, and the extract was concentrated using a rotary  
216 vacuum concentrator (RVC 2-25 CD plus (Martin Christ, Germany)). Then, GC-MS/MS  
217 analysis was conducted (Supporting Information, caption 2.5). The concentration of the  
218 bioavailable fraction of PAHs and their derivatives was calculated according to the calculation  
219 described in [6].

220 **3. Results and discussion**

221 **3.1. The content of total fraction and bioavailable of PAHs and their derivatives in  
222 biochar**

223 **3.1.1. The total fraction of PAHs and their derivatives in biochar**

224 The obtained biochars were characterized by a very diverse content of PAHs (Table 1); but the  
225 presence of PAHs derivatives in BC was confirmed (Table 1, Table S3). In BCZ samples the  
226 total content of PAHs varied between  $90.16 \pm 4.13 \mu\text{g g}^{-1}$  (BCZ500) and  $125.83 \pm 5.76 \mu\text{g g}^{-1}$   
227 (BCZ600). The percentage distribution of compounds differing in the number of aromatic rings  
228 is very similar in BCZ samples. 2-ring species constituted 44.36%-49.47% (for BCZ500 and  
229 BCZ700) with the west majority of naphthalene (form  $44.08 \pm 2.02 \mu\text{g g}^{-1}$  to  $54.80 \pm 2.51 \mu\text{g}$

230  $\text{g}^{-1}$  for BCZ500 and BCZ600, respectively). 3-ring species accounted for 22.64% (BCZ500) –  
 231 26.93% (BCZ700), and the most abundant were acenaphthylene, acenaphthene, and fluorene.  
 232 4-, 5-, 6-ring PAHs were in the range 10.63%- 14.48%, 10.85%-17.08%, and 0.80%-1.85%.  
 233 Pyrene and benzo[a]fluoranthene were the most prevalent. In all SSLZ-derived BCs, only 2-  
 234 rings N-PAHs were quantified (1-methyl-5-nitronaphthalene and 1-methyl-6-nitronaphthalene)  
 235 and they were in the range of  $2.72 \pm 0.13 \mu\text{g g}^{-1}$  (BCZ500) and  $5.30 \pm 0.24 \mu\text{g g}^{-1}$  (BCZ600)  
 236 (Supporting Information, Table S3). It is worth stressing that PAHs derivatives were determined  
 237 at a significantly lower (generally 2 orders of magnitude lower (Table 1)) concentration range.

238

239 Table 1. The concentration of the total and bioavailable fraction of PAHs and their derivatives  
 240 in biochar used during the experiments.

Sample description	The concentration of total PAHs $\pm$ SD [ $\mu\text{g g}^{-1}$ ]	The concentration of total $\Sigma 16\text{PAHs}$ $\pm$ SD [ $\mu\text{g g}^{-1}$ ]	The concentration of total PAHs derivatives $\pm$ SD [ $\mu\text{g g}^{-1}$ ]	The concentration of bioavailable $\Sigma\text{PAHs}$ $\pm$ SD [ $\text{ng L}^{-1}$ ]	The concentration of bioavailable $\Sigma 16\text{PAHs}$ $\pm$ SD [ $\text{ng L}^{-1}$ ]	The concentration of bioavailable PAHs derivatives $\pm$ SD [ $\text{ng L}^{-1}$ ]
BCZ500	$90.16 \pm 4.13$	$79.47 \pm 3.64$	$2.72 \pm 0.13$	$33.50 \pm 1.22$	$33.45 \pm 1.22$	$0.81 \pm 0.03$
BCZ600	$125.83 \pm 5.76$	$107.16 \pm 4.91$	$5.30 \pm 0.24$	$39.98 \pm 1.46$	$39.71 \pm 1.45$	$1.90 \pm 0.07$
BCZ700	$110.04 \pm 5.04$	$96.65 \pm 4.43$	$4.01 \pm 0.18$	$38.33 \pm 1.40$	$38.22 \pm 1.40$	$0.94 \pm 0.03$
BCW500	$151.55 \pm 6.94$	$144.00 \pm 6.59$	$1.48 \pm 0.07$	$3.51 \pm 0.20$	$3.34 \pm 0.20$	$0.25 \pm 0.01$
BCW600	$181.08 \pm 8.29$	$171.36 \pm 7.85$	$1.92 \pm 0.09$	$3.17 \pm 0.15$	$2.92 \pm 0.14$	$0.48 \pm 0.02$
BCW700	$158.02 \pm 7.24$	$148.27 \pm 6.79$	$4.31 \pm 0.20$	$3.53 \pm 0.17$	$3.30 \pm 0.16$	$0.48 \pm 0.02$
BCD600	$57.36 \pm 2.63$	$57.36 \pm 2.63$	<LOD	$2.21 \pm 0.11$	$2.12 \pm 0.11$	<LOD
BCF600	$134.01 \pm 6.14$	$75.49 \pm 3.46$	$11.89 \pm 0.54$	$3.67 \pm 0.17$	$3.53 \pm 0.17$	$0.32 \pm 0.02$
BCS600	$145.21 \pm 6.65$	$56.63 \pm 2.59$	$28.40 \pm 1.30$	$2.56 \pm 0.11$	$2.36 \pm 0.10$	$0.83 \pm 0.03$

241 <LOD- below the limit of detection; red highlight– the highest level, blue highlight – the lowest level

242

243 In willow-derived BC the total fraction of PAHs was higher than in SSLZ-derived BC  
 244 (and amounted to  $181.08 \pm 8.29 \mu\text{g g}^{-1}$  (BCW600) (Table 1). The biochar obtained at 600°C  
 245 was distinguished by the highest content of PAHs, thus it was chosen in Experiment 2.  
 246 Generally, 2- and 3-ring PAHs accounted for 34.08% - 37.97% with naphthalene,  
 247 acenaphthylene, and acenaphthene as the most abundant. 4-ring PAHs constituted 21.07%-

248 22.18% of all PAHs with the west majority of pyrene (13.72% - 13.99% of all PAHs). The rest  
249 of the PAHs accounted for 5.68%-6.91% of all quantified PAHs. Among PAHs derivatives,  
250 only nitroacenaphthalene was quantified and amounted to  $1.48 \pm 0.07 \mu\text{g g}^{-1}$ ,  $1.92 \pm 0.09 \mu\text{g g}^{-1}$   
251 and  $4.31 \pm 0.20 \mu\text{g g}^{-1}$  for BCW500, BCW600, and BCW700 (Supporting Information, Table  
252 S3). Although the BCW contained a higher amount of total PAHs than BCZ, the content of  
253 their derivatives was lower, thus the amount of determined PAHs derivatives cannot be directly  
254 connected with the content of pristine PAHs.

255 In the BCD600 sample (as well as in BCF600) 4-ring PAHs were the most abundant,  
256 then in descending order were 3-rings (32.86%), 2-rings (8.90%), 5-rings (3.76%), and 6-ring  
257 PAHs (0.80%) (Table 1). Among determined PAHs, benzo[a]fluorene (4 rings), 6-  
258 methylchrysene (4 rings), acenaphthene (3 rings), and 5-methylchrysene (4 rings) were noted  
259 at the highest level. The concentration of PAHs derivatives was below the limit of detection. In  
260 BCF600 there were no 6-ring PAHs quantified. 2-, 3-, 4-, and 5-ring compounds constituted  
261 7.16%, 36.59%, 37.69%, and 18.56%. Among them, the most abundant were (in descending  
262 order) fluorene, benzo[a]fluorene, 3,6-dimethylphenanthrene, dibenz[a,h]anthracene, and  
263 benzo[a]antracene. In the case of PAHs derivatives, only O-PAHs were quantified (4H-  
264 cyclopenta(def)phenanthrene – 93.11% and 9,10-anthracenedione – 6.89%) (Supporting  
265 Information, Table S3). It is worth stressing that N-PAHs were not noted in wood-derived  
266 material.

267 In BCS600 (Table 1), the content of the total fraction of PAHs amounted to  $145.21 \pm$   
268  $6.65 \mu\text{g g}^{-1}$ . The value was rather in the middle of all plant-derived BC, but the content of  
269  $\Sigma 16\text{PAHs}$  was the lowest. Thus, the majority constituted the compounds outside the USEPA-  
270 listed PAHs. It indicated that the determination of only 16 PAHs is insufficient in some cases.  
271 2- and 3-ring PAHs accounted for 50.91% and 41.54%, whereas other PAHs constituted the  
272 minority. As it was in the case of the bioavailable fraction, among all plant-derived biochars,

273 the highest content of PAHs derivatives was detected in BCS600 – being the same compounds  
274 as quantified in the bioavailable fraction (Supporting Information, Table S3).

275 **3.1.2. The bioavailable fraction of PAHs and their derivatives in biochars**

276 Biochars were obtained from two types of feedstock: sewage sludge (BCZ500, BCZ600,  
277 and BCZ700) and plants (willow (BCW500, BCW600, and BCW700), residues from hardwood  
278 (BCD600) and softwood (BCF600)). Moreover, in the case of SSLZ-derived and willow-  
279 derived BC, three pyrolysis temperatures were applied. Therefore, both the effects of feedstock  
280 and the temperature of pyrolysis on the total and bioavailable fraction of PAHs and their  
281 derivatives in soil enriched with biochar can be investigated.

282 SSL-derived BC was characterized by the highest content of bioavailable PAHs and  
283 their derivatives (Table 1). The concentration of bioavailable PAHs in sewage sludge-derived  
284 BC amounted to  $33.50 \pm 1.22 \text{ ng L}^{-1}$ ,  $39.98 \pm 1.46 \text{ ng L}^{-1}$ , and  $38.33 \pm 1.40 \text{ ng L}^{-1}$  for BCZ500,  
285 BCZ600, and BCZ700, respectively (Table 1, Table S3). No obvious effect of pyrolysis  
286 temperature on the bioavailability of PAHs and their derivatives was noted. In described  
287 samples, 2-ring PAHs were the most abundant and accounted for about 90% of all PAHs with  
288 the vast majority of naphthalene (90.64%, 89.15%, and 90.02% of all PAHs). The 3-ring species  
289 constituted  $\approx 9\%$  of all PAHs with such representatives as acenaphthylene, acenaphthene, and  
290 fluorene (8.92%, 9.64%, and 9.26% of all PAHs). The sum of 4-, 5-, and 6-ring analytes  
291 constituted a minority (0.39%, 0.68%, and 0.66%, respectively). It should be highlighted that  
292 the content of pyrene was higher than other 4-, 5-, and 6-ring species. In all samples (BCZ500,  
293 BCZ600, BCZ700), two and three-rings PAHs derivatives were quantified (1-methyl-5-  
294 nitronaphthalene, 1-methyl-6-nitronaphthalene, 9,10-anthracenedione (in BCZ700 additionally  
295 4H-cyclopenta(def)phenanthrene-as the only representative of 4-ring species)). The total  
296 content of derivatives amounted to  $0.81 \pm 0.03 \text{ ng L}^{-1}$ ,  $1.90 \pm 0.07 \text{ ng L}^{-1}$ , and  $0.94 \pm 0.03 \text{ ng L}^{-1}$   
297 <sup>1</sup> for BCZ500, BCZ600, and BCZ700, respectively, and derivatives with 2 aromatic rings were

298 prevalent (95.71%, 89.81%, and 72.70% of all derivatives) (Supporting Information Table S3).  
299 It can be seen that the increase in the pyrolysis temperature did not result in increased  
300 bioavailability of PAHs and their derivatives in biochar. However, the derivatives concentration  
301 was as low as 2.4% - 4.75% of the content of bioavailable pristine PAHs in BCZ.

302 In willow-derived biochar, the bioavailable fraction of PAHs amounted to  $3.51 \pm 0.20$   
303 ng L<sup>-1</sup>,  $3.17 \pm 0.15$  ng L<sup>-1</sup>, and  $3.53 \pm 0.17$  ng L<sup>-1</sup> for BCW500, BCW600, and BCW700,  
304 respectively (Table 1). The contents of the 2-ring species were below the limit of detection.  
305 However, 3-ring PAHs were the most prevalent (almost 98% of all PAHs), and the majority of  
306 them were acenaphthylene, acenaphthene, and fluorene (94.90%, 91.44%, and 93.29% of all  
307 PAHs in BCW500, BCW600, and BCW700, respectively). The rest of the PAHs constituted  
308 1.58%, 2.22%, and 1.50%. The total contents of derivatives are presented in Table 1. Only 4-  
309 ring derivatives (nitropyrene and 4H-cyclopenta(def)phenanthrene) were quantified with the  
310 vast majority (approximately 97% of all derivatives) constituting O-PAHs derivatives  
311 (Supporting Information, Table S3).

312 Although the BCD600 and BCF600 samples were obtained from wood (softwood-  
313 BCD600 and hardwood-BCF600), the concentration of PAHs and their derivatives as well as  
314 the distribution of analytes varies (Table 1, Table S3). The bioavailable fraction of PAHs  
315 amounted to  $2.21 \pm 0.11$  ng L<sup>-1</sup> (BCD600) and  $3.67 \pm 0.17$  ng L<sup>-1</sup> (BCF600). The concentration  
316 of 2-ring PAHs was below the limit of detection in BCD600, while in BCF600 naphthalene (as  
317 the only representative of 2-ring PAHs) constituted the majority (54.07% of all PAHs).  
318 BCD600 was characterized by the highest concentration of 3-ring species (98.64% of all  
319 quantified PAHs), while in BCF600 they constituted 44.63% (with the highest contents for  
320 acenaphthylene, acenaphthene, and fluorene for both biochars). The rest of the PAHs accounted  
321 for less than 1.5%. In BCD600 any of the PAHs derivatives were quantified. While in BCF600

322 only O-PAHs were (9,10-anthracenedione and 4H-cyclopenta(def)phenanthrene) (Supporting  
323 Information Table S3).

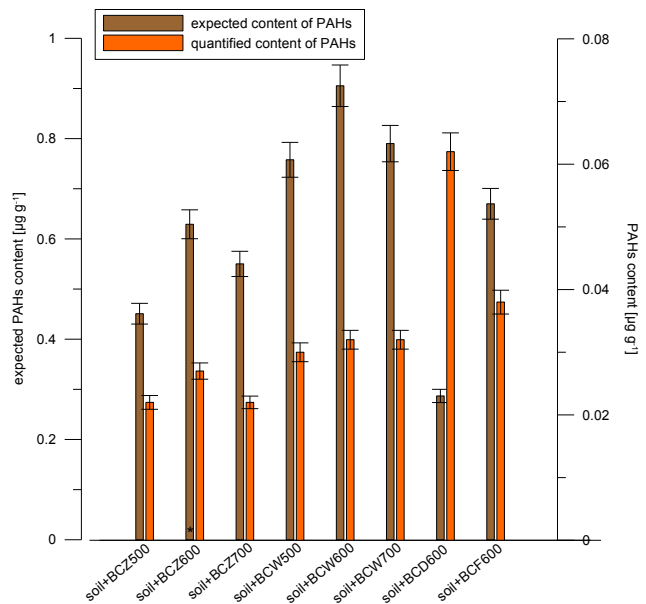
324 In Experiment 3, wheat straw-derived biochar was also applied. Among all plant-  
325 derived biochars, BCS600 was distinguished by the highest content of PAHs derivatives  
326 (bioavailable fraction -  $0.83 \pm 0.03 \text{ ng L}^{-1}$ ). Whereas the content of pristine PAHs was rather  
327 low, but the ratio determined PAHs derivatives to pristine PAHs was 0.32 indicating high  
328 content of PAHs derivatives. Among parent PAHs, 3-ring species constituted the majority  
329 (96.78% of all PAHs). Then in descending order were 4-, 6-, and 5-ring compounds (3.03%,  
330 0.13%, and 0.06%, respectively). There were no 2-ring PAHs detected. Considering PAHs  
331 derivatives, both N- and O-PAHs were detected, namely 1-methyl-5-nitronaphthalene, 1-  
332 methyl-6-nitronaphthalene, and 4H-cyclopenta(def)phenanthrene. Among them, 4-ring species  
333 constituted 69.20%, and 2-ring derivatives 30.80% (Supporting Information Table S3). It can  
334 be concluded that the presence and bioavailability of PAHs derivatives in biochar cannot be  
335 directly related to the pyrolysis temperature or content of pristine PAHs.

### 336 **3.2. The content of PAHs and their derivatives in biochar-amended soil**

#### 337 **3.2.1. Experiment 1 – a pot experiment**

338 Applied soil (without amendment) as well as soil alone after grass cultivation did not  
339 contain any of PAHs and their derivatives e.g. the concentrations were below the limit of  
340 detection (Figure 2, Table S4). The soil enriched with biochar contained a small amount of  
341 PAHs ( $0.022 - 0.062 \mu\text{g g}^{-1}$ ) but did not contain any PAHs derivatives. In biochar-amended  
342 soil, 2-, 3-, and 4-ring PAHs were quantified and in all enriched samples the concentration of  
343 naphthalene was above the limit detection with the highest content in soil+BCD600 sample  
344 ( $0.015 \pm 7.2 \cdot 10^{-4} \mu\text{g g}^{-1}$ ), and the lowest in soil+BCW500 sample and soil+BCF600 sample  
345 ( $7.5 \cdot 10^{-3} \pm 3.5 \cdot 10^{-4} \mu\text{g g}^{-1}$ ). In soils enriched with SSL-derived and willow-derived biochar also  
346 acenaphthylene, acenaphthene (except soil+BCZ700), and pyrene were determined. The

347 qualitative analysis of the other two samples (soil+BCD600 and soil+BCF600) differs from  
 348 described above. In soil mixed with BCD600 acenaphthylene, anthracene, benzo[a]anthracene  
 349 and 6-methylchrysene were quantified, while in soil with BCF600, the concentration of 2-  
 350 phenylnaphthalene, acenaphthene, fluorene, and pyrene were determined (Supporting  
 351 Information Table S5).



352 Fig. 2. The expected content of the total fraction of PAHs in BC-amended soils (model system  
 353 calculated as 0.5% of the content of particular PAHs in initial biochars) vs. the quantified  
 354 content of the total fraction of PAHs in samples.

355 The concentration of the total fraction of PAHs in biochar amounted to 90.16-125.83  
 356  $\mu\text{g g}^{-1}$  for BCZ samples and 57.46 – 181.08  $\mu\text{g g}^{-1}$  for plant-derived biochars (BCW500,  
 357 BCW600, BCW700, BCD600, BCF600). Considering the total concentrations of PAHs and  
 358 their derivatives in studied biochars and the fact that soils were enriched with 0.5% biochar  
 359 (w/w), the concentration of total PAHs should bring down to 0.45-0.63  $\mu\text{g g}^{-1}$  and 0.29-0.91  $\mu\text{g}$   
 360  $\text{g}^{-1}$ , respectively. However, the obtained concentration of PAHs in soils with additions  
 361 constitutes only 4.00%-4.88%, 3.53%-4.05%, 21.62%, and 5.67% of model/expected value (i.e.  
 362 0.5% of initial contents in biochars) for BCZ, BCW, BCD600, and BCF600 samples. The  
 363 results obtained in Experiment 1 indicate clearly that the BC addition to soil may lead to an  
 364 increase in the content of PAHs. But the content of PAHs derivatives was below LOD.

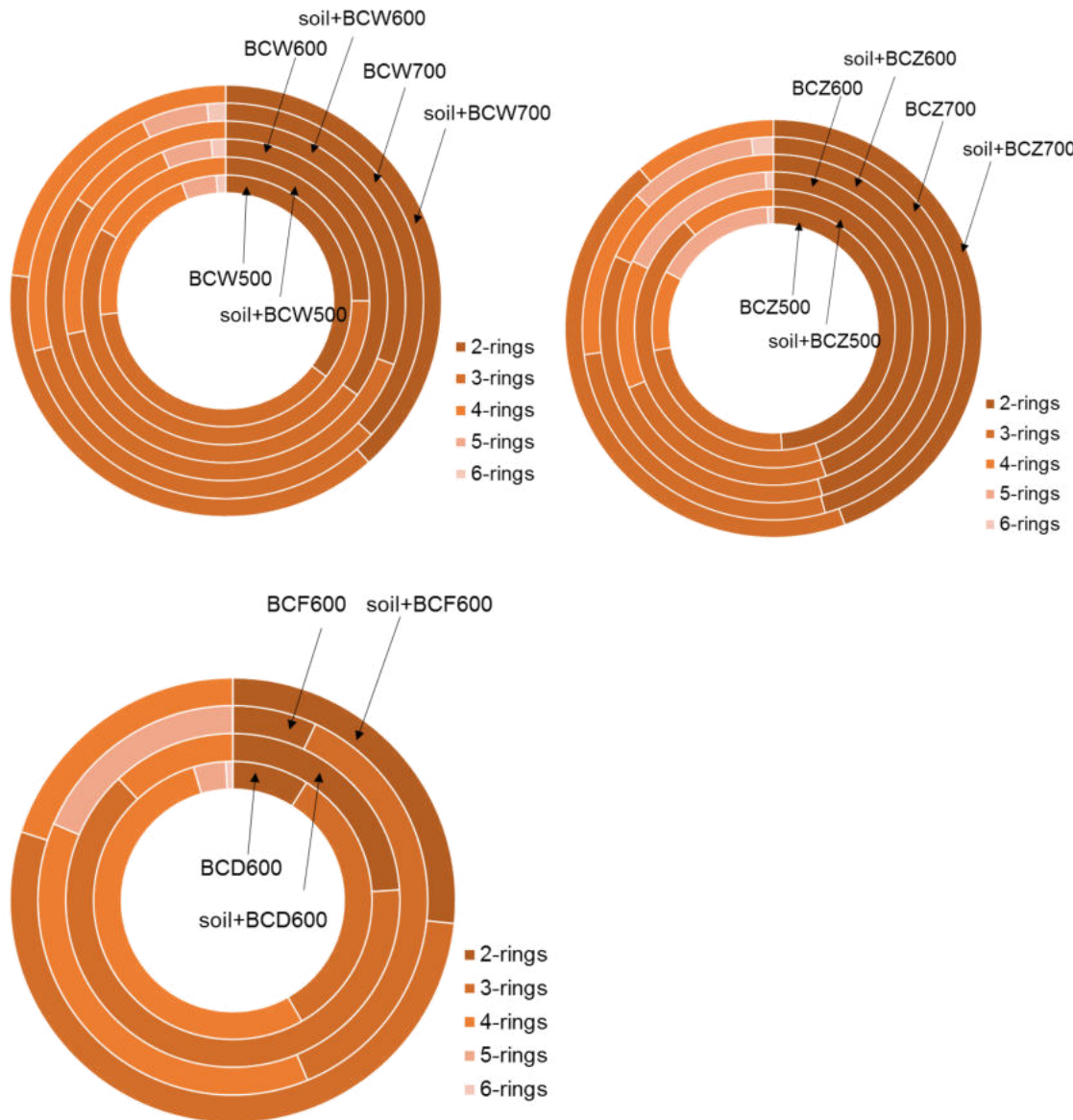
365 The studies on PAHs and derivatives content in the soil indicated that besides pristine  
 366 PAHs, N-PAHs, O-PAHs, and N/S/O-heterocyclic PAHs in soil samples from residential,

recreational, smoking, and industrial areas of Newcastle (Australia) were noted [35]. In the recreational soils, the total concentrations of  $\Sigma 9$  heterocyclic-PAHs ranged from 37 ng g<sup>-1</sup> – 216 ng g<sup>-1</sup>,  $\Sigma 7$ O-PAHs: from 357 – 2790 ng g<sup>-1</sup>,  $\Sigma 3$ NPAHs: from 60– 890 ng g<sup>-1</sup> and PAHs: 5567 – 100931 ng g<sup>-1</sup>. However, soil collected from industrial areas was characterized by a higher concentration of  $\Sigma 9$  heterocyclic-PAHs: 52.9 ng g<sup>-1</sup> – 6240 ng g<sup>-1</sup>,  $\Sigma 7$ O-PAHs: 377 – 11536 ng g<sup>-1</sup>,  $\Sigma 3$ NPAHs: max. value 3795 ng g<sup>-1</sup> and PAHs: 2509 – 392932 ng g<sup>-1</sup>. Considering all results (total and individual concentrations) they also presented the most likely sources of contamination, e.g. road coal tar abrasions, vehicular emission, coal contamination, and gaswork activities [35]. In surface soil samples collected from the Yangtze River Delta region, the total concentration of PAHs, N-PAHs, and O-PAHs ranged from 21.0-3563.2 ng g<sup>-1</sup>, 0.4-4.6 ng g<sup>-1</sup>, and 2.1-834.1 ng g<sup>-1</sup>, respectively [36]. Moreover, the most abundant derivatives were 9-fluorenone, anthraquinone, and 1-nitronaphthalene [36]. Wilcke et al. [37] studied the concentration of PAHs and their derivatives (oxygenated PAHs, azaarenes) in soils along a 2100-km north–south transect in Argentina. They found that the concentrations of  $\Sigma 29$ PAHs,  $\Sigma 15$ OPAHs, and  $\Sigma 4$ AZAs ranged from 2.4–38 ng g<sup>-1</sup>, 0.05–124 ng g<sup>-1</sup>, and <LOD to 0.97 ng g<sup>-1</sup>, respectively [37]. On the other hand, Bandowe et al. [38] found that along a 20-km transect from a metal mining and metallurgical industrial complex in Uzbekistan, the contents of  $\Sigma 29$  PAHs and  $\Sigma 16$  US-EPA PAHs were in the range 41–2670 ng g<sup>-1</sup> and 29–1940 ng g<sup>-1</sup>, respectively. The highest content was noted in the location close to the copper smelting factory. They compared their results with the limit values set in the regulations of Switzerland and Germany, and the content of PAHs in only one soil exceeded these guidelines [38]. Nevertheless, the obtained results were generally low even though they originated from locations affected by several decades-long heavy industrial activities [38].

Considering our previous work (corresponding to the biological (BA) and enzymatic (EA) aging of biochar – the model experiments) [39], microorganisms present in the soil as well as the enzymatic processes affect the content of the total fraction of PAHs and their derivatives. In most cases, the content of the total fraction of analytes in biochars aged with microbial inoculum or model enzyme (horseradish peroxidase) decreased significantly (approx. 2-5 times considering PAHs and even 16 times considering PAHs derivatives in BCW600) (except in biochars obtained from residues from softwood and hardwood). The results obtained from Experiment 1 can be compiled with those obtained after biological and enzymatic aging, and it could be an explanation for the low content of analytes. The results from the model experiments proceeded earlier [39] closely correspond with those obtained during short-term biochar application into the soil. Moreover, enzymatic and biological aging affects the

402 physicochemical characteristic of biochar. The EA increased whereas the BA decreased the  
403 content of C% and H% in BC. And both of the artificial agings decrease the H/C ratio, which  
404 means a drop in the aromatization of pyrolyzed materials [39]. The changes were statistically  
405 significant. Both agings affect the morphology, structure, and surface composition of biochars.

406



407

408

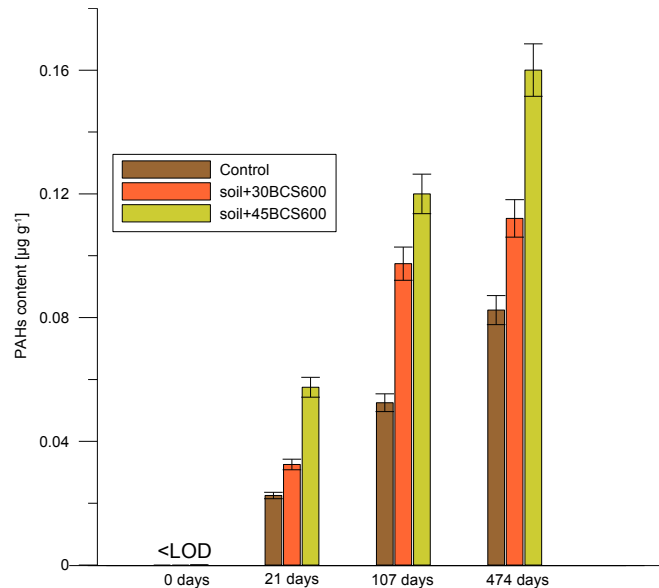
409 Fig. 3. The percentage distribution of PAHs (differing in the number of aromatic rings) in initial  
410 biochars vs. in biochar-amended soils in Experiment 1.

411 Moreover, the percentage distribution of PAHs in biochar and biochar-amended soils  
412 changed. In initial biochars, all groups of PAHs (2-, 3-, 4-, 5-, and 6-rings species) were  
413 detected. Whereas, after the pot experiment, only 2-, 3, and 4-ring PAHs were quantified. In

414 the case of soils enriched with BCW500, BCW600, BCZ500, and BCZ700, the content of 2-  
 415 ring compounds decreased (Fig. 3). While in other examples, the content increased. The soil  
 416 fertilization with biochar increased the content of 3-ring PAHs in all cases. In the case of 4-ring  
 417 species, an increase was observed in soil enriched with BCW700, BCZ500, and BCZ600. The  
 418 results indicated that biochar addition into soil increased the content of PAHs in biochar-  
 419 amended soils. Moreover, the amount of PAHs depends on the type of feedstock and the  
 420 temperature of pyrolysis. Thus, the agricultural and environmental safety of biochars depends  
 421 mostly on these two parameters.

### 422 3.2.3. Experiment 2 – a field experiment

423 The content of BC in soil may affect the concentration of PAHs and their derivatives.  
 424 Thus, during Experiment 2 various levels ( $30 \text{ t ha}^{-1}$  and  $45 \text{ t ha}^{-1}$ ) of BCS into the soil were  
 425 added. At the beginning of the Experiment, PAHs content was below LOD in all samples. But  
 426 during the Experiment, the content of analytes increased in both control and enriched soils  
 427 (Figure 4, Table S6).



428 Fig. 4. The changes in PAHs content in soil and biochar-amended soil during Experiment 2.

429 In the case of control samples, the content of PAHs increased from <LOD to  
 430  $0.082 \pm 0.005 \mu\text{g g}^{-1}$  (474 days) (Table S5). The majority constituted 3-ring species (66.67%,  
 431 76.19%, and 57.58% after 21, 107, and 474 days). Then, in descending order were 2-ring PAHs  
 432 (from 19.05% to 27.27%), and 4-ring PAHs. The concentration of 5- and 6-ring compounds  
 433 was below LOD. The addition of BCS600 increased the content of PAHs. The lower level of  
 434 enrichment increased the concentration from  $0.033 \pm 0.002 \mu\text{g g}^{-1}$  to  $0.112 \pm 0.006 \mu\text{g g}^{-1}$ , and the  
 435

higher from  $0.057 \pm 0.003 \mu\text{g g}^{-1}$  to  $0.160 \pm 0.008 \mu\text{g g}^{-1}$ . But the distribution of the particular groups of PAHs differing in the number of aromatic rings remained similar (as in the case of the control samples). Among two-ring species, only naphthalene and 1,3-di-iso-propylnaphthalene were detected, thus, among 3-ring PAHs only acenaphthene, anthracene, and 9-methylphenanthrene were quantified. The greatest increase was observed during the initial stages of the Experiment. The total fraction of PAHs increased significantly from the level <LOD to  $0.022 \pm 0.001 \mu\text{g g}^{-1}$ ,  $0.033 \pm 0.002 \mu\text{g g}^{-1}$ , and  $0.057 \pm 0.003 \mu\text{g g}^{-1}$  in control, X, and Y. Then, after 104 days the contents increased by 133.40%, 199.63%, and 180.56% for control, X, and Y samples. The continuation of Experiment 2 increased the content of PAHs by 57.06%, 15.04%, and 63.39%, respectively.

#### 3.2.3. Experiment 3– a field experiment

The content of the total fraction of PAHs and their derivatives in control samples (without amendment) (A-see Fig.1)) was below the LOD. In all cases, the extension of the time of the experiment increases the content of studied groups of compounds (Figure 5, Table S7).

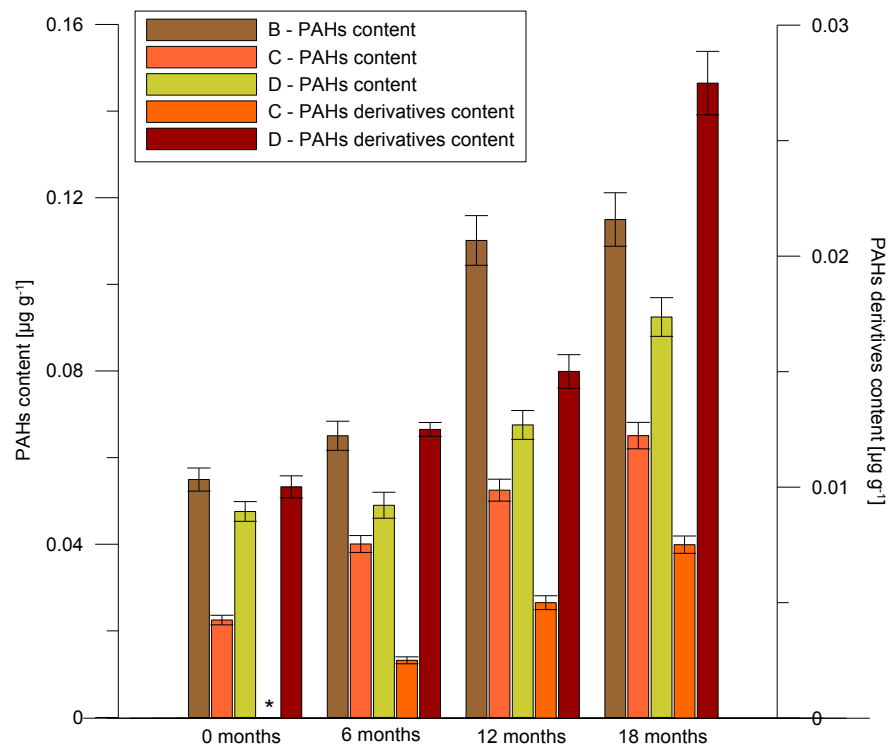


Fig. 5. The changes in the PAHs and their derivatives content during a field experiment (Experiment 3). \* below the limit of detection (LOD). B, C, D – as in Fig. 1.

The total fraction of PAHs in sewage sludge-enriched soils (B) amounted to  $0.055 \mu\text{g g}^{-1}$  (0 months) to  $0.115 \mu\text{g g}^{-1}$  (18 months). Only 2- and 3-ring PAHs were quantified. The

percentage content of 2-ring species decreases whereas, the content of 3-ring PAHs increases during the experiment. There were no quantified PAHs derivatives. The soil fortified with SSLCH and biochar (2.5%) contained from  $0.023 \mu\text{g g}^{-1}$  (0 months) to  $0.065 \mu\text{g g}^{-1}$  (18 months) of PAHs. The changes in the percentage content of 2-, 3, and 4-ring PAHs were not tendentious and correlated (5- and 6-ring species did not quantified). They constituted from <LOD to 11.54%, from 30.77% to 50.00%, and from 43.75% to 57.69%, respectively. Among the two-ring species, only naphthalene was quantified. The experiment did not affect straight the percentage distribution of PAHs. Some additional mechanisms (e.g. including the microorganism's activity, enzymatic processes, or physical and chemical factors [33,39]) must be considered. The biochemical processes occurring in soil may change the physicochemical properties of biochar which consequently may lead to the release of blocked PAHs. On the other hand, the content of PAHs derivatives in initial sample C (soil with SSLCH and 2.5% BCW700-0 months) was below the limit of detection. Whereas after 6, 12, and 18 months, it increased from  $0.0025 \mu\text{g g}^{-1}$  (6 mths) to  $0.0075 \mu\text{g g}^{-1}$  (18 mths). Among them, both N-and O-PAHs were quantified (namely nitroacenaphthalene and 9,10-anthracenedione). The higher dose of biochar (soil + SSLCH and 10% biochar) caused an increase in the content of the total fraction of PAHs from  $0.048 \mu\text{g g}^{-1}$  (0 mths) to  $0.092 \mu\text{g g}^{-1}$  (18 mths). Naphthalene (as the only representative of 2-ring PAHs) constituted from <LOD to 3.70% of all PAHs, whereas 3- and 4-ring accounted for 15.79-22.22% and 74.07-84.21%, respectively. There were no 5- and 6-ring species quantified. The content of PAHs derivatives also increased through Experiment 2 from  $0.010 \mu\text{g g}^{-1}$  (0 mths) to  $0.027 \mu\text{g g}^{-1}$  (18 mths). In initial samples (0 months) only nitroacenaphthalene, 9,10-anthracenedione, 2-methylpyrene were quantified. Whereas in the last samples (18 months) nitroacenaphthalene, 1-methyl-5-nitronaphthalene, 1-methyl-6-nitronaphthalene, 9,10-anthracenedione, 2-methylpyrene, and 4-methylpyrene were determined with the first one as the most abundant. The increase in the mass of added biochar as well as the time of biochar application increased the content of PAHs and their derivatives. Moreover, the increase of PAHs was directly proportional to the amount of added biochar.

Several papers presented the effect of biochar addition into soils. The addition affects the physical, chemical, and biological parameters of enriched soils. But significantly fewer Researchers focus on the contaminants which may be introduced into soils when biochar is added. Rombola et al. [40] studied the changes in PAHs contents in soil alone and soil enriched with biochar obtained from orchard pruning biomass (*Pirus communis*, *Malus domestica*, *Persica vulgaris*, *Vitis vinifera*) via slow pyrolysis process at  $500^\circ\text{C}$ . The content of analyte in

488 the control sample has remained stable ( $24 \pm 3 \text{ ng g}^{-1}$  at the beginning and  $23 \pm 3 \text{ ng g}^{-1}$  after  
489 35 months), whereas in biochar-amended soil the concentration of PAHs decreased ( $153 \pm 38$   
490  $\text{ng g}^{-1}$  initially and  $78 \pm 20 \text{ ng g}^{-1}$  after almost 3 years) [40]. Kuśmierz et al. [41] also studied  
491 the effect of biochar addition into the soil on PAHs contents. The straw-derived biochar was  
492 introduced in the following doses: soil without fertilization, soil with  $30 \text{ t ha}^{-1}$ , and soil with  $45$   
493  $\text{t ha}^{-1}$  of biochar. Control soil contained  $0.239 \mu\text{g g}^{-1}$  PAHs when the biochar addition resulted  
494 in an increase in the analyte contents to  $0.526 \mu\text{g g}^{-1}$  and  $1.310 \mu\text{g g}^{-1}$  in  $30$  and  $45 \text{ t ha}^{-1}$  biochar-  
495 amended soil. Moreover, during a 2.5-year experiment, PAHs contents decreased significantly  
496 even to the level of control soil. In BC-amended samples, a significant increase in the contents  
497 of the PAHs (fluorene, phenanthrene, and pyrene) was observed, and these PAHs  
498 concentrations in the biochar were also high [41].

499 Researchers found that in soil systems the concentration of 2- or 3-ring PAHs decreases  
500 faster than the concentration of PAHs with four to six rings [42]. In our case, the content of 5-  
501 and 6-ring species, decreased to the level below LOD. Moreover, some plant root exudates  
502 facilitate the release of PAHs from BC [43,44]. The changes in PAHs and their derivatives  
503 content in biochar-amended soils can be closely related to the changes in physicochemical  
504 characteristics of biochars caused by microbial activity, enzymes [39], or physical and chemical  
505 factors [33].

506 During Experiment 1, various factors affected the biochar (its physicochemical  
507 composition and PAHs and derivatives content), such as soil matrices, day/night sun cycle, the  
508 constant water content, the grass cultivation. But the temperature remained constant (room  
509 temperature), thus obtained results were strictly related to the data obtained during the artificial  
510 biological and enzymatic aging. However, during Experiments 2 and 3, in addition to the above-  
511 mentioned, also the changes in the temperature (large temperature fluctuation), in the water  
512 content (drought/rainfall), freezing and thawing events, and unregular day/night cycles  
513 occurred. Moreover, live plant and animal organisms' activity and rich soil matrix affect the soil  
514 as well as biochar. Thus, the results obtained during Experiments 2 and 3 can be related to the  
515 data obtained after the artificial physical aging [33]. The freeze-thaw cycles (which lasted 6  
516 months) increased the content of the total fraction of PAHs and derivatives in willow- and  
517 sewage sludge-derived biochar (whether the pyrolysis temperature was,  $500^\circ\text{C}$ ,  $600^\circ\text{C}$  or  
518  $700^\circ\text{C}$ ) [33]. The chemical aging increased the content of analytes in sewage-sludge-derived  
519 biochar and decreased it in willow-derived biochar. Both, physical and chemical aging affects  
520 the physicochemical characteristics of biochar (e.g. porosity, the content of some base elements

521 (C, O)). The changes led to the biochar oxidation and removal of the labile components from  
522 the crushed and fragmented surface [33].

523 **Conclusions**

524 The results indicate that during biochar production besides PAHs, their more toxic derivatives  
525 are formed. The problem is that the application of biochar into the soil may be connected with  
526 the introduction of PAHs and their derivatives. It was established that initial biochar was  
527 characterized by low (up to  $28.4 \pm 1.3 \mu\text{g g}^{-1}$ ) content of derivatives and the amount of  
528 determined PAHs derivatives cannot be directly connected with the content of pristine PAHs  
529 in biochar. The increase in the pyrolysis temperature did not result in increased bioavailability  
530 of PAHs and their derivatives in biochar. During soil amendment, the concentration of PAHs  
531 (originating from biochars) decreased during the short-term agricultural application of  
532 pyrolyzed material, however, increased in long-term field experiments. Moreover, the amount  
533 of PAHs depends on the type of feedstock and the temperature of pyrolysis. Thus, the  
534 agricultural and environmental safety of biochars depends mostly on these two parameters. A  
535 significant increase in the content of PAHs and their derivatives (N-and O-PAHs) was noted  
536 when biochar was applied simultaneously with sewage sludge as fertilizer up to  $0.092 \mu\text{g g}^{-1}$   
537 (18 mths).

538 **CRediT authorship contribution statement**

539 **Agnieszka Krzyszczak:** Investigation, Visualization, Writing – review & editing; **Michał P.**  
540 **Dybowski:** Methodology, Validation; **Magdalena Kończak:** Investigation, Validation; **Patryk**  
541 **Oleszczuk:** Methodology, Conceptualization, Supervision; **Bożena Czech:** Investigation,  
542 Methodology, Visualization, Writing – review & editing, Conceptualization, Validation,  
543 Supervision.

544 **Declaration of Competing Interest**

545 The authors declare the following financial interests/personal relationships which may be  
546 considered as potential competing interests: Bozena Czech reports financial support was  
547 provided by National Science Centre Poland.

548

549 **Data availability**

550 Data will be made available on request.

551 **Acknowledgments**

552 The studies were supported by project No. 2018/31/B/NZ9/00317 funded by the National  
553 Science Centre, Poland.

554

555 **References:**

- 556 [1] K. Qian, A. Kumar, H. Zhang, D. Bellmer, R. Huhnke, Recent advances in utilization of  
557 biochar, *Renewable and Sustainable Energy Reviews*. 42 (2015) 1055–1064.  
558 <https://doi.org/10.1016/j.rser.2014.10.074>.
- 559 [2] R.S. Kookana, A.K. Sarmah, L. Van Zwieten, E. Krull, B. Singh, Chapter three -  
560 Biochar Application to Soil: Agronomic and Environmental Benefits and Unintended  
561 Consequences, in: D.L. Sparks (Ed.), *Advances in Agronomy*, Academic Press, 2011:  
562 pp. 103–143. <https://doi.org/10.1016/B978-0-12-385538-1.00003-2>.
- 563 [3] B. O'Neill, J. Grossman, M.T. Tsai, J.E. Gomes, J. Lehmann, J. Peterson, E. Neves, J.E.  
564 Thies, Bacterial community composition in Brazilian Anthrosols and adjacent soils  
565 characterized using culturing and molecular identification, *Microb Ecol*. 58 (2009) 23–  
566 35. <https://doi.org/10.1007/s00248-009-9515-y>.
- 567 [4] S.K. Das, G.K. Ghosh, R. Avasthe, Application of biochar in agriculture and  
568 environment, and its safety issues, *Biomass Conv. Bioref.* (2020).  
569 <https://doi.org/10.1007/s13399-020-01013-4>.
- 570 [5] G. Cornelissen, Jubaedah, N.L. Nurida, S.E. Hale, V. Martinsen, L. Silvani, J. Mulder,  
571 Fading positive effect of biochar on crop yield and soil acidity during five growth  
572 seasons in an Indonesian Ultisol, *Science of The Total Environment*. 634 (2018) 561–  
573 568. <https://doi.org/10.1016/j.scitotenv.2018.03.380>.
- 574 [6] A. Krzyszczak, M.P. Dybowski, B. Czech, Formation of polycyclic aromatic  
575 hydrocarbons and their derivatives in biochars: The effect of feedstock and pyrolysis

- 576 conditions, Journal of Analytical and Applied Pyrolysis. 160 (2021) 105339.
- 577 <https://doi.org/10.1016/j.jaat.2021.105339>.
- 578 [7] A. El-Naggar, S.S. Lee, Y.M. Awad, X. Yang, C. Ryu, M. Rizwan, J. Rinklebe, D.C.W.  
579 Tsang, Y.S. Ok, Influence of soil properties and feedstocks on biochar potential for  
580 carbon mineralization and improvement of infertile soils, Geoderma. 332 (2018) 100–  
581 108. <https://doi.org/10.1016/j.geoderma.2018.06.017>.
- 582 [8] L. Zhao, X. Cao, O. Mašek, A. Zimmerman, Heterogeneity of biochar properties as a  
583 function of feedstock sources and production temperatures, Journal of Hazardous  
584 Materials. 256–257 (2013) 1–9. <https://doi.org/10.1016/j.jhazmat.2013.04.015>.
- 585 [9] B. Singh, B.P. Singh, A.L. Cowie, Characterisation and evaluation of biochars for their  
586 application as a soil amendment, Soil Res. 48 (2010) 516.  
587 <https://doi.org/10.1071/SR10058>.
- 588 [10] S. Meyer, B. Glaser, P. Quicker, Technical, Economical, and Climate-Related Aspects of  
589 Biochar Production Technologies: A Literature Review, Environ. Sci. Technol. 45  
590 (2011) 9473–9483. <https://doi.org/10.1021/es201792c>.
- 591 [11] A.O. Adekiya, T.M. Agbede, A. Olayanju, W.S. Ejue, T.A. Adekanye, T.T. Adenusi,  
592 J.F. Ayeni, Effect of Biochar on Soil Properties, Soil Loss, and Cocoyam Yield on a  
593 Tropical Sandy Loam Alfisol, The Scientific World Journal. 2020 (2020) e9391630.  
594 <https://doi.org/10.1155/2020/9391630>.
- 595 [12] T. Kätterer, D. Roobroeck, O. Andrén, G. Kimutai, E. Karlton, H. Kirchmann, G.  
596 Nyberg, B. Vanlauwe, K. Röing de Nowina, Biochar addition persistently increased soil  
597 fertility and yields in maize-soybean rotations over 10 years in sub-humid regions of  
598 Kenya, Field Crops Research. 235 (2019) 18–26.  
599 <https://doi.org/10.1016/j.fcr.2019.02.015>.

- 600 [13] E. Ndor, J.O. Jayeoba, C. Asadu, Effect of Biochar Soil Amendment on Soil Properties  
601 and Yield of Sesame Varieties in Lafia, Nigeria, American Journal of Experimental  
602 Agriculture. 9 (2015) 1–8. <https://doi.org/10.9734/AJEA/2015/19637>.
- 603 [14] A. Nigussie, E. Kissi, M. Misganaw, G. Ambaw, Effect of Biochar Application on Soil  
604 Properties and Nutrient Uptake of Lettuces (*Lactuca sativa*) Grown in Chromium  
605 Polluted Soils, Am.-Eurasian J. Agric. Environ. Sci. 12 (2012) 369–376.
- 606 [15] H.-X. Chen, Z.-L. Du, W. Guo, Q.-Z. Zhang, [Effects of biochar amendment on  
607 cropland soil bulk density, cation exchange capacity, and particulate organic matter  
608 content in the North China Plain], Ying Yong Sheng Tai Xue Bao. 22 (2011) 2930–  
609 2934.
- 610 [16] J. Lehmann, M.C. Rillig, J. Thies, C.A. Masiello, W.C. Hockaday, D. Crowley, Biochar  
611 effects on soil biota – A review, Soil Biology and Biochemistry. 43 (2011) 1812–1836.  
612 <https://doi.org/10.1016/j.soilbio.2011.04.022>.
- 613 [17] H.M.S.K. Herath, M. Camps-Arbestain, M. Hedley, Effect of biochar on soil physical  
614 properties in two contrasting soils: An Alfisol and an Andisol, Geoderma. 209–210  
615 (2013) 188–197. <https://doi.org/10.1016/j.geoderma.2013.06.016>.
- 616 [18] A.O. Adekiya, T.M. Agbede, C.M. Aboyeji, O. Dunsin, V.T. Simeon, Effects of biochar  
617 and poultry manure on soil characteristics and the yield of radish, Scientia Horticulturae.  
618 243 (2019) 457–463. <https://doi.org/10.1016/j.scienta.2018.08.048>.
- 619 [19] J. Major, J. Lehmann, M. Rondon, C. Goodale, Fate of soil-applied black carbon:  
620 downward migration, leaching and soil respiration, Global Change Biology. 16 (2010)  
621 1366–1379. <https://doi.org/10.1111/j.1365-2486.2009.02044.x>.
- 622 [20] J.M. Kimetu, J. Lehmann, Stability and stabilisation of biochar and green manure in soil  
623 with different organic carbon contents, Australian Journal of Soil Research. (2010).  
624 <http://dx.doi.org/10.1071/SR10036> (accessed November 28, 2021).

- 625 [21] T. Dutta, E. Kwon, S.S. Bhattacharya, B.H. Jeon, A. Deep, M. Uchimiya, K.-H. Kim,  
626 Polycyclic aromatic hydrocarbons and volatile organic compounds in biochar and  
627 biochar-amended soil: a review, GCB Bioenergy. 9 (2017) 990–1004.  
628 <https://doi.org/10.1111/gcbb.12363>.
- 629 [22] R.A. Brown, A.K. Kercher, T.H. Nguyen, D.C. Nagle, W.P. Ball, Production and  
630 characterization of synthetic wood chars for use as surrogates for natural sorbents,  
631 Organic Geochemistry. 37 (2006) 321–333.  
632 <https://doi.org/10.1016/j.orggeochem.2005.10.008>.
- 633 [23] P. Oleszczuk, I. Jośko, M. Kuśmierz, Biochar properties regarding to contaminants  
634 content and ecotoxicological assessment, Journal of Hazardous Materials. 260 (2013)  
635 375–382. <https://doi.org/10.1016/j.jhazmat.2013.05.044>.
- 636 [24] A. Freddo, C. Cai, B.J. Reid, Environmental contextualisation of potential toxic  
637 elements and polycyclic aromatic hydrocarbons in biochar, Environmental Pollution.  
638 171 (2012) 18–24. <https://doi.org/10.1016/j.envpol.2012.07.009>.
- 639 [25] S.E. Hale, J. Lehmann, D. Rutherford, A.R. Zimmerman, R.T. Bachmann, V.  
640 Shitumbanuma, A. O'Toole, K.L. Sundqvist, H.P.H. Arp, G. Cornelissen, Quantifying  
641 the Total and Bioavailable Polycyclic Aromatic Hydrocarbons and Dioxins in Biochars,  
642 Environ. Sci. Technol. 46 (2012) 2830–2838. <https://doi.org/10.1021/es203984k>.
- 643 [26] E. Weidemann, W. Buss, M. Edo, O. Mašek, S. Jansson, Correction to: Influence of  
644 pyrolysis temperature and production unit on formation of selected PAHs, oxy-PAHs, N-  
645 PACs, PCDDs, and PCDFs in biochar—a screening study, Environmental Science and  
646 Pollution Research. 25 (2018) 3941–3942. <https://doi.org/10.1007/s11356-017-0804-6>.
- 647 [27] H. Insam, M.S.A. Seewald, Volatile organic compounds (VOCs) in soils, Biol Fertil  
648 Soils. 46 (2010) 199–213. <https://doi.org/10.1007/s00374-010-0442-3>.

- 649 [28] A. Krzyszczak, B. Czech, Occurrence and toxicity of polycyclic aromatic hydrocarbons  
650 derivatives in environmental matrices, *Science of The Total Environment*. (2021)  
651 147738. <https://doi.org/10.1016/j.scitotenv.2021.147738>.
- 652 [29] R.K. Rajpara, D.R. Dudhagara, J.K. Bhatt, H.B. Gosai, B.P. Dave, Polycyclic aromatic  
653 hydrocarbons (PAHs) at the Gulf of Kutch, Gujarat, India: Occurrence, source  
654 apportionment, and toxicity of PAHs as an emerging issue, *Marine Pollution Bulletin*.  
655 119 (2017) 231–238. <https://doi.org/10.1016/j.marpolbul.2017.04.039>.
- 656 [30] S.B. Hawthorne, N.A. Azzolina, E.F. Neuhauser, J.P. Kreitinger, Predicting  
657 Bioavailability of Sediment Polycyclic Aromatic Hydrocarbons to *Hyalella azteca* using  
658 Equilibrium Partitioning, Supercritical Fluid Extraction, and Pore Water Concentrations,  
659 *Environ. Sci. Technol.* 41 (2007) 6297–6304. <https://doi.org/10.1021/es0702162>.
- 660 [31] K.T. Semple, K.J. Doick, K.C. Jones, P. Burauel, A. Craven, H. Harms, Defining  
661 bioavailability and bioaccessibility of contaminated soil and sediment is complicated,  
662 *Environ Sci Technol.* 38 (2004) 228A-231A. <https://doi.org/10.1021/es040548w>.
- 663 [32] A. Krzyszczak, M.P. Dybowski, M. Kończak, B. Czech, Low bioavailability of  
664 derivatives of polycyclic aromatic hydrocarbons in biochar obtained from different  
665 feedstock, *Environ Res.* 214 (2022) 113787.  
666 <https://doi.org/10.1016/j.envres.2022.113787>.
- 667 [33] A. Krzyszczak, M.P. Dybowski, R. Zarzycki, R. Kobyłecki, P. Oleszczuk, B. Czech,  
668 Long-term physical and chemical aging of biochar affected the amount and  
669 bioavailability of PAHs and their derivatives, *Journal of Hazardous Materials*. 440  
670 (2022) 129795. <https://doi.org/10.1016/j.jhazmat.2022.129795>.
- 671 [34] A. Krzyszczak, M. Dybowski, I. Jośko, M. Kusiak, M. Sikora, B. Czech, The antioxidant  
672 defense responses of *Hordeum vulgare* L. to polycyclic aromatic hydrocarbons and their

- 673 derivatives in biochar-amended soil, Environmental Pollution. 294 (2022) 118664.
- 674 <https://doi.org/10.1016/j.envpol.2021.118664>.
- 675 [35] O. Idowu, K.T. Semple, K. Ramadass, W. O'Connor, P. Hansbro, P. Thavamani,
- 676 Analysis of polycyclic aromatic hydrocarbons (PAHs) and their polar derivatives in soils
- 677 of an industrial heritage city of Australia, Science of The Total Environment. 699 (2020)
- 678 134303. <https://doi.org/10.1016/j.scitotenv.2019.134303>.
- 679 [36] C. Cai, J. Li, D. Wu, X. Wang, D.C.W. Tsang, X. Li, J. Sun, L. Zhu, H. Shen, S. Tao, W.
- 680 Liu, Spatial distribution, emission source and health risk of parent PAHs and derivatives
- 681 in surface soils from the Yangtze River Delta, eastern China, Chemosphere. 178 (2017)
- 682 301–308. <https://doi.org/10.1016/j.chemosphere.2017.03.057>.
- 683 [37] W. Wilcke, B.A.M. Bandowe, M.G. Lueso, M. Ruppenthal, H. del Valle, Y. Oelmann,
- 684 Polycyclic aromatic hydrocarbons (PAHs) and their polar derivatives (oxygenated
- 685 PAHs, azaarenes) in soils along a climosequence in Argentina, Science of The Total
- 686 Environment. 473–474 (2014) 317–325. <https://doi.org/10.1016/j.scitotenv.2013.12.037>.
- 687 [38] B.A.M. Bandowe, N. Shukurov, S. Leimer, M. Kersten, Y. Steinberger, W. Wilcke,
- 688 Polycyclic aromatic hydrocarbons (PAHs) in soils of an industrial area in semi-arid
- 689 Uzbekistan: spatial distribution, relationship with trace metals and risk assessment,
- 690 Environ Geochem Health. 43 (2021) 4847–4861. <https://doi.org/10.1007/s10653-021-00974-3>.
- 692 [39] A. Krzyszczak, M.P. Dybowski, B. Czech, Microorganisms and their metabolites affect
- 693 the content of polycyclic aromatic hydrocarbons and their derivatives in pyrolyzed
- 694 material, Sci Total Environ. 886 (2023) 163966.
- 695 <https://doi.org/10.1016/j.scitotenv.2023.163966>.
- 696 [40] A.G. Rombolà, W. Meredith, C.E. Snape, S. Baronti, L. Genesio, F.P. Vaccari, F.
- 697 Miglietta, D. Fabbri, Fate of Soil Organic Carbon and Polycyclic Aromatic

698        Hydrocarbons in a Vineyard Soil Treated with Biochar, Environ. Sci. Technol. 49 (2015)  
699        11037–11044. <https://doi.org/10.1021/acs.est.5b02562>.

700        [41] M. Kuśmierz, P. Oleszczuk, P. Kraska, E. Pałys, S. Andruszczak, Persistence of  
701        polycyclic aromatic hydrocarbons (PAHs) in biochar-amended soil, Chemosphere. 146  
702        (2016) 272–279. <https://doi.org/10.1016/j.chemosphere.2015.12.010>.

703        [42] C.E. Cerniglia, Biodegradation of polycyclic aromatic hydrocarbons, Current Opinion in  
704        Biotechnology. 4 (1993) 331–338. [https://doi.org/10.1016/0958-1669\(93\)90104-5](https://doi.org/10.1016/0958-1669(93)90104-5).

705        [43] L. Wang, D. O'Connor, J. Rinklebe, Y.S. Ok, D.C.W. Tsang, Z. Shen, D. Hou, Biochar  
706        Aging: Mechanisms, Physicochemical Changes, Assessment, And Implications for Field  
707        Applications, Environ. Sci. Technol. 54 (2020) 14797–14814.  
708        <https://doi.org/10.1021/acs.est.0c04033>.

709        [44] J. Wang, E.S. Odinga, W. Zhang, X. Zhou, B. Yang, M.G. Waigi, Y. Gao, Polyaromatic  
710        hydrocarbons in biochars and human health risks of food crops grown in biochar-  
711        amended soils: A synthesis study, Environment International. 130 (2019) 104899.  
712        <https://doi.org/10.1016/j.envint.2019.06.009>.

713

714



Click here to access/download  
**Supplementary Material**  
SI.docx



**Declaration of interests**

The authors declare that they have no known competing financial interests or personal relationships that could have appeared to influence the work reported in this paper.

The authors declare the following financial interests/personal relationships which may be considered as potential competing interests:

Bozena Czech reports financial support was provided by National Science Centre Poland.

## **Increased concentration of PAHs derivatives in biochar-amended soil observed in long-term experiment**

Agnieszka Krzyszczak-Turczyn<sup>1</sup>, Michał P. Dybowski<sup>2</sup>, Magdalena Kończak<sup>3</sup>, Patryk Oleszczuk<sup>1</sup>, Bożena Czech<sup>1\*</sup>

<sup>1</sup>Department of Radiochemistry and Environmental Chemistry, Institute of Chemical Sciences, Faculty of Chemistry, Maria Curie-Sklodowska University in Lublin, Pl. M. Curie-Sklodowskiej 3, 20-031 Lublin, Poland

<sup>2</sup>Department of Chromatography, Institute of Chemical Sciences, Faculty of Chemistry, Maria Curie Skłodowska University in Lublin, Pl. M. Curie-Sklodowskiej 3, 20-031 Lublin, Poland

<sup>3</sup>Institute of Earth and Environmental Sciences, Faculty of Earth Sciences and Spatial Management, Maria Curie-Sklodowska University, ul. Kraśnicka 2cd, 20-718, Lublin, Poland

\*corresponding author: Tel.: +48 81 537 55 54; fax: +48 81 537 55 65; E-mail address: bozena.czech@mail.umcs.pl (B. Czech)

**Journal:** Journal of Hazardous Materials

**No. pages:** 18

**No. of figures:** 0

**No. of tables:** 8

## **2.2. Soil experiments (preparation, enrichment with biochars)**

### **Experiment 2 – a field experiment**

SSLCH and BCW700F were mixed with soil with the usage of a rotatory tiller with an operating depth of  $22 \pm 2$  cm and a width - 185 cm. The prepared mixtures of SSLCH and BCW700F or SSLCH alone were applied to the soil during spring tillage operations before sowing. The spring wheat (*Triticum aestivum L.*) was planted from the third week of March to the first week of April, depending on the weather. The seeding rate was 450 seeds per m<sup>2</sup>, due to the low class of the soil. The certified seeds with a germination rate of 97.2% were used. Before the experiment, the soil was amended without using any pesticides, chemicals, or other mineral fertilizers.

After the experiment, all soil samples were taken according to the PN-ISO 10381-2:2007P (2002). From each plot, the 10 sub-samples were taken from the entire length of the arable layer of soil (25 - 30 cm) using a stainless steel corer (2 cm in diameter). Next, the 10 sub-samples from each plot were mixed to obtain a representative sample.

### **2.5. GC–MS/MS measurement**

Qualitative and quantitative measurements of PAHs and their derivatives were performed using a gas chromatograph hyphenated with a triple quadruple tandem mass spectrometer detector (GCMS-TQ8040; Shimadzu, Kyoto, Japan) equipped with a ZB5-MSi fused-silica capillary column (30 m × 0.25 mm i.d., 0.25 µm film thickness; Phenomenex, Torrance, CA, USA) and an AOC-20i+s type autosampler (Shimadzu). The helium (grade 5.0) and argon (grade 5.0) were applied as a carrier and collision gas, respectively. The chromatographic conditions were adjusted as follows: column flow - 1.56 mL/min, the volume of injection - 1 µL. The injector was working in high-pressure mode (250.0 kPa for 1.5 min; column flow at initial temperature was 4.90 mL/min) at the temperature of 310°C; the ion source temperature was 225°C. The qualitative and quantitative analyses were conducted with full scan mode (range 40-550 m/z) and SIM (Single Ion Monitoring) mode, respectively.

**Table S1. Chemical characteristics of analyzed compounds.**

No.	Compound	CAS <sup>(1)</sup>	MW <sup>(2)</sup>	Formula
1	Naphthalene*	91-20-3	128.17	C <sub>10</sub> H <sub>8</sub>
2	1,3-di-iso-propynaphthalene	57122-16-4	212.33	C <sub>16</sub> H <sub>20</sub>

3	2-Phenylnaphthalene	612-94-2	204.26	C <sub>16</sub> H <sub>12</sub>
4	Acenaphthylene*	208-96-8	152.20	C <sub>12</sub> H <sub>8</sub>
5	Acenaphthene*	83-32-9	154.20	C <sub>12</sub> H <sub>10</sub>
6	Fluorene*	86-73-7	166.22	C <sub>13</sub> H <sub>10</sub>
7	Anthracene*	120-12-7	178.23	C <sub>14</sub> H <sub>10</sub>
8	Phenanthrene*	85-01-8	178.23	C <sub>14</sub> H <sub>10</sub>
9	3-Methylphenanthrene	832-71-3	192.25	C <sub>15</sub> H <sub>12</sub>
10	2-Methylphenanthrene	2531-84-2	192.25	C <sub>15</sub> H <sub>12</sub>
11	9-Methylphenanthrene	883-20-5	192.25	C <sub>15</sub> H <sub>12</sub>
12	3,6-dimethylphenanthrene	1576-67-6	206.28	C <sub>16</sub> H <sub>14</sub>
13	Fluoranthene*	206-44-0	202.25	C <sub>16</sub> H <sub>10</sub>
14	Pyrene*	129-00-0	202.25	C <sub>16</sub> H <sub>10</sub>
15	2-Methylpyrene	3442-78-2	216.28	C <sub>17</sub> H <sub>12</sub>
16	4-Methylpyrene	3353-12-6	216.28	C <sub>17</sub> H <sub>12</sub>
17	Benzo[a]fluorene	238-84-6	216.27	C <sub>17</sub> H <sub>12</sub>
18	Benzo[a]anthracene*	56-55-3	228.29	C <sub>18</sub> H <sub>12</sub>
19	Chryzene*	218-01-9	228.29	C <sub>18</sub> H <sub>12</sub>
20	3-Methylchrysene	3351-31-3	242.30	C <sub>19</sub> H <sub>14</sub>
21	5-Methylchrysene	3697-24-3	242.30	C <sub>19</sub> H <sub>14</sub>
22	6-Methylchrysene	1705-85-7	242.30	C <sub>19</sub> H <sub>14</sub>
23	Benzo[a]fluoranthene	203-33-8	252.31	C <sub>20</sub> H <sub>12</sub>
24	Benzo[b]fluoranthene*	205-99-2	252.31	C <sub>20</sub> H <sub>12</sub>
25	Benzo[k]fluoranthene*	207-08-9	252.32	C <sub>20</sub> H <sub>12</sub>
26	Benzo[j]fluoranthene	205-82-3	252.31	C <sub>20</sub> H <sub>12</sub>
27	Benzo[a]pyrene*	50-32-8	252.31	C <sub>20</sub> H <sub>12</sub>

28	Indeno[1,2,3-cd]pyrene*	193-39-5	276.33	C <sub>22</sub> H <sub>12</sub>
29	Benzo[ghi]perylene*	191-24-2	276.33	C <sub>22</sub> H <sub>12</sub>
30	Dibenzo[a,h]anthracene*	53-70-3	278.10	C <sub>22</sub> H <sub>14</sub>
31	Dibenz[a,e]pyrene	192-65-4	302.37	C <sub>24</sub> H <sub>14</sub>
32	Dibenz[a,h]pyrene	189-64-0	302.37	C <sub>24</sub> H <sub>14</sub>
33	Dibenz[a,i]pyrene	189-55-9	302.37	C <sub>24</sub> H <sub>14</sub>
34	Dibenz[a,l]pyrene	192-65-4	302.37	C <sub>24</sub> H <sub>14</sub>
<b>N- and O-PAHs</b>				
35	Nitronaphthalene	86-57-7	173.16	C <sub>10</sub> H <sub>7</sub> NO <sub>2</sub>
36	1-Methyl-5-nitronaphthalene	91137-27-8	187.19	C <sub>11</sub> H <sub>9</sub> NO <sub>2</sub>
37	1-Methyl-6-nitronaphthalene	105752-67-8	187.19	C <sub>11</sub> H <sub>9</sub> NO <sub>2</sub>
38	9,10-Anthracenedione	84-65-1	208.21	C <sub>14</sub> H <sub>8</sub> O <sub>2</sub>
39	4H-cyclopenta(def)phenanthrene	203-64-5	190.24	C <sub>15</sub> H <sub>10</sub>
40	Nitropyrene	5522-43-0	247.25	C <sub>16</sub> H <sub>9</sub> NO <sub>2</sub>

<sup>(1)</sup>numerical identifier assigned by the Chemical Abstracts Service (CAS)

<sup>(2)</sup>MW-molecular weight

\* PAHs belonging to 16PAHs which have been classified by the United States Environmental Protection Agency (USEPA) as priority pollutants [1].

**Table S2. The qualitative and quantitative parameters of PAHs and O/N-PAHs analysis.**

No.	Compound	Quantification ion ( <i>m/z</i> )	Confirmati on ion ( <i>m/z</i> )	LOD*	LOQ**
1	Naphthalene	128	102	1.01	3.36

2	1,3-di-iso-propynaphthalene	197	212	1.41	4.69
3	2-Phenylnaphthalene	204	101	1.90	6.33
4	Acenaphthylene	152	76	2.10	6.99
5	Acenaphthene	153	76	2.30	7.66
6	Fluorene	166	82	1.10	3.66
7	Anthracene	178	89	1.30	4.33
8	Phenanthrene	178	89	1.34	4.36
9	3-Methylphenanthrene	192	165	2.42	8.06
10	2-Methylphenanthrene	192	165	2.42	8.06
11	9-Methylphenanthrene	192	96	3.23	10.76
12	3,6-dimethylphenanthrene	206	191	2.20	7.33
13	Fluoranthene	202	101	1.87	6.22
14	Pyrene	202	101	1.91	6.36
15	2-Methylpyrene	216	108	1.92	6.39
16	4-Methylpyrene	216	108	1.92	6.39
17	Benzo[a]fluorene	216	107	1.30	4.33
18	Benzo[a]anthracene	228	114	1.30	4.33
19	Chryzene	228	113	2.20	7.33
20	3-Methylchrysene	242	121	1.02	3.40
21	5-Methylchrysene	242	120	1.55	5.16
22	6-Methylchrysene	242	119	1.02	3.40
23	Benzo[a]fluoranthene	252	126	2.10	6.99
24	Benzo[b]fluoranthene	252	126	2.10	6.99
25	Benzo[k]fluoranthene	252	126	2.10	6.99
26	Benzo[j]fluoranthene	252	126	1.39	4.63
27	Benzo[a]pyrene	252	126	2.11	7.03
28	Indeno[1,2,3-cd]pyrene	276	138	1.30	4.33

29	Benzo[ghi]perylene	276	138	1.33	4.43
30	Dibenzo[a,h]anthracene	278	139	2.21	7.36
31	Dibenz[a,e]pyrene	302	151	1.89	6.29
32	Dibenz[a,h]pyrene	302	151	1.89	6.29
33	Dibenz[a,i]pyrene	302	151	1.89	6.29
34	Dibenz[a,l]pyrene	302	151	1.89	6.29

---

#### N- and O-PAHs

35	Nitronaphthalene	173	127	2.41	8.03
36	1-Methyl-5-nitronaphthalene	187	115	1.21	4.03
37	1-Methyl-6-nitronaphthalene	187	115	1.21	4.03
38	9,10-Anthracenedione	208	180	1.44	4.80
39	4H-cyclopenta(def)phenanthrene	190	94	3.01	10.02
40	Nitropyrene	247	201	1.66	5.53

---

\*-LOD – limit of detection; \*\*-LOQ – limit of quantitation; LOD and LOQ were not calculated via K<sub>POM</sub>; LOD and LOQ were considered to be signal-to-noise ratios equal to 3 and 10, respectively.

**Table S3. The total fraction of PAHs and their derivatives in biochars (n=3; n-number of replicates).**

No.	Compound	Sample description								
		BCZ500	BCZ600	BCZ700	BCW500	BCW600	BCW700	BCD600	BCF600	BCS600
		Analyte concentration [ $\mu\text{g g}^{-1}$ ]								
1	Naphthalene	44.08 ± 2.02	54.80 ± 2.51	50.22 ± 2.30	52.75 ± 2.42	62.28 ± 2.85	56.96 ± 2.61	< LOD	9.37 ± 0.43	0.24 ± 0.01
2	1,3-di-iso-propynaphthalene	< LOD	< LOD	< LOD	0.72 ± 0.03	0.88 ± 0.04	1.24 ± 0.06	5.11 ± 0.23	< LOD	4.43 ± 0.20
3	2-Phenylnaphthalene	< LOD	1.26 ± 0.06	< LOD	< LOD	< LOD	< LOD	< LOD	< LOD	< LOD
4	Acenaphthylene	12.47 ± 0.57	15.09 ± 0.69	16.01 ± 0.73	22.17 ± 1.02	25.12 ± 1.15	20.13 ± 0.92	4.87 ± 0.22	2.34 ± 0.11	15.62 ± 0.72
5	Acenaphthene	2.14 ± 0.10	3.10 ± 0.14	2.68 ± 0.12	32.30 ± 1.48	37.34 ± 1.71	31.12 ± 1.43	9.31 ± 0.43	6.73 ± 0.31	18.27 ± 0.84
6	Fluorene	4.44 ± 0.20	8.30 ± 0.38	10.00 ± 0.46	< LOD	0.42 ± 0.02	0.66 ± 0.03	4.43 ± 0.20	19.46 ± 0.89	< LOD
7	Anthracene	< LOD	0.42 ± 0.02	< LOD	3.08 ± 0.14	3.32 ± 0.15	1.94 ± 0.09	< LOD	< LOD	1.48 ± 0.07
8	Phenanthrene	< LOD	< LOD	< LOD	< LOD	< LOD	< LOD	< LOD	< LOD	< LOD
9	3-Methylphenanthrene	0.080 ± 0.004	0.060 ± 0.003	0.080 ± 0.004	< LOD	0.24 ± 0.01	< LOD	< LOD	4.88 ± 0.22	27.28 ± 1.25
10	2-Methylphenanthrene	< LOD	0.12 ± 0.01	< LOD	< LOD	0.22 ± 0.01	< LOD	0.24 ± 0.01	0.72 ± 0.03	10.96 ± 0.50
11	9-Methylphenanthrene	0.52 ± 0.02	1.02 ± 0.05	0.28 ± 0.01	< LOD	< LOD	< LOD	< LOD	0.22 ± 0.01	< LOD
12	3,6-dimethylphenanthrene	1.28 ± 0.06	2.42 ± 0.11	0.86 ± 0.04	< LOD	< LOD	< LOD	< LOD	14.91 ± 0.68	0.32 ± 0.02
13	Fluoranthene	< LOD	< LOD	0.24 ± 0.01	1.48 ± 0.07	1.98 ± 0.09	1.70 ± 0.08	< LOD	< LOD	0.46 ± 0.02
14	Pyrene	5.92 ± 0.27	8.30 ± 0.38	8.09 ± 0.37	20.79 ± 0.95	25.10 ± 1.15	22.11 ± 1.01	< LOD	1.24 ± 0.06	< LOD
15	2-Methylpyrene	0.82 ± 0.04	1.10 ± 0.05	1.48 ± 0.07	0.20 ± 0.01	0.24 ± 0.01	0.32 ± 0.02	0.32 ± 0.02	< LOD	6.33 ± 0.29
16	4-Methylpyrene	0.28 ± 0.01	1.96 ± 0.09	4.07 ± 0.19	0.24 ± 0.01	0.30 ± 0.01	0.42 ± 0.02	0.82 ± 0.04	< LOD	2.30 ± 0.11
17	Benzo[a]fluorene	0.24 ± 0.01	0.56 ± 0.03	0.22 ± 0.01	5.47 ± 0.25	6.02 ± 0.28	5.93 ± 0.27	12.21 ± 0.56	16.28 ± 0.75	16.27 ± 0.75
18	Benzo[a]anthracene	1.24 ± 0.06	1.98 ± 0.09	0.62 ± 0.03	3.32 ± 0.15	5.14 ± 0.24	3.08 ± 0.14	< LOD	11.47 ± 0.53	12.04 ± 0.55
19	Chrysene	< LOD	0.24 ± 0.01	< LOD	0.44 ± 0.02	0.92 ± 0.04	1.48 ± 0.07	< LOD	< LOD	2.24 ± 0.10

20	3-Methylchrysene	< LOD	< LOD	< LOD	< LOD	< LOD	< LOD	0.82 ± 0.04	6.21 ± 0.28	10.02 ± 0.46
21	5-Methylchrysene	1.08 ± 0.05	1.92 ± 0.09	1.22 ± 0.06	< LOD	< LOD	< LOD	6.28 ± 0.29	4.98 ± 0.23	8.85 ± 0.41
22	6-Methylchrysene	< LOD	0.66 ± 0.03	< LOD	< LOD	< LOD	< LOD	10.35 ± 0.47	10.33 ± 0.47	1.82 ± 0.08
23	Benzo[a]fluoranthene	4.98 ± 0.23	9.72 ± 0.45	6.21 ± 0.28	< LOD	0.28 ± 0.01	< LOD	0.22 ± 0.01	0.24 ± 0.01	< LOD
24	Benzo[b]fluoranthene	5.56 ± 0.26	6.30 ± 0.29	2.98 ± 0.14	< LOD	0.22 ± 0.01	< LOD	< LOD	< LOD	< LOD
25	Benzo[k]fluoranthene	2.22 ± 0.10	2.28 ± 0.10	1.52 ± 0.07	< LOD	0.34 ± 0.02	< LOD	< LOD	< LOD	< LOD
26	Benzo[j]fluoranthene	0.10 ± 0.01	0.26 ± 0.01	0.18 ± 0.01	< LOD	0.12 ± 0.01	< LOD	< LOD	< LOD	< LOD
27	Benzo[a]pyrene	< LOD	0.52 ± 0.02	< LOD	6.29 ± 0.29	7.34 ± 0.34	8.25 ± 0.38	1.94 ± 0.09	10.23 ± 0.47	0.38 ± 0.02
28	Indeno[1,2,3-cd]pyrene	< LOD	< LOD	< LOD	0.88 ± 0.04	1.10 ± 0.05	0.52 ± 0.02	< LOD	< LOD	4.03 ± 0.19
29	Benzo[ghi]perylene	< LOD	< LOD	< LOD	< LOD	< LOD	< LOD	< LOD	< LOD	1.88 ± 0.09
30	Dibenzo[a,h]anthracene	1.98 ± 0.109	2.42 ± 0.11	1.06 ± 0.05	0.52 ± 0.02	0.68 ± 0.03	0.308 ± 0.01	< LOD	14.41 ± 0.66	< LOD
31	Dibenz[a,e]pyrene	0.72 ± 0.03	1.04 ± 0.05	2.04 ± 0.09	0.82 ± 0.04	1.16 ± 0.05	1.22 ± 0.06	0.22 ± 0.01	< LOD	< LOD
32	Dibenz[a,h]pyrene	< LOD	< LOD	< LOD	0.060 ± 0.003	0.18 ± 0.01	0.24 ± 0.01	0.24 ± 0.01	< LOD	< LOD
33	Dibenz[a,i]pyrene	< LOD	< LOD	< LOD	0.040 ± 0.002	0.14 ± 0.01	0.38 ± 0.02	< LOD	< LOD	< LOD
34	Dibenz[a,l]pyrene	< LOD	< LOD	< LOD	< LOD	< LOD	< LOD	< LOD	< LOD	< LOD
N- and O-PAHs										
35	Nitronaphthalene	< LOD	< LOD	< LOD	1.48 ± 0.07	1.92 ± 0.09	4.31 ± 0.20	< LOD	< LOD	< LOD
36	1-Methyl-5-nitronaphthalene	1.28 ± 0.06	2.42 ± 0.11	2.10 ± 0.10	< LOD	< LOD	< LOD	< LOD	< LOD	1.88 ± 0.09
37	1-Methyl-6-nitronaphthalene	1.44 ± 0.07	2.88 ± 0.13	1.92 ± 0.09	< LOD	< LOD	< LOD	< LOD	< LOD	2.32 ± 0.11
38	9,10-Anthracenedione	< LOD	< LOD	< LOD	< LOD	< LOD	< LOD	< LOD	0.82 ± 0.04	< LOD
39	4H-cyclopenta(def)phenanthrene	< LOD	< LOD	< LOD	< LOD	< LOD	< LOD	< LOD	11.07 ± 0.51	24.20 ± 1.11
40	Nitropyrene	< LOD	< LOD	< LOD	< LOD	< LOD	< LOD	< LOD	< LOD	< LOD

<LOD-below the limit of detection

**Table S4. The bioavailable fraction of PAHs and their derivatives in biochars (n=3; n-number of replicates)**

No.	Compound	Sample description								
		BCZ500	BCZ600	BCZ700	BCW500	BCW600	BCW700	BCD600	BCF600	BCS600
		Analyte concentration [ng L <sup>-1</sup> ]								
1	Naphthalene	30.36 ± 1.11	35.65 ± 1.30	34.51 ± 1.26	< LOD	< LOD	< LOD	< LOD	1.98 ± 0.09	< LOD
2	1,3-di-iso-propynaphthalene	< LOD	< LOD							
3	2-Phenylnaphthalene	< LOD	0.16 ± 5.4·10 <sup>-3</sup>	< LOD	< LOD					
4	Acenaphthylene	1.55 ± 0.06	1.81 ± 0.07	1.91 ± 0.07	1.64 ± 0.12	0.77 ± 0.04	0.38 ± 0.02	0.24 ± 0.01	0.15 ± 0.01	0.86 ± 0.04
5	Acenaphthene	1.02 ± 0.04	1.46 ± 0.05	0.97 ± 0.04	1.06 ± 0.05	1.16 ± 0.05	1.72 ± 0.09	1.45 ± 0.08	0.58 ± 0.03	1.49 ± 0.07
6	Fluorene	0.41 ± 0.02	0.59 ± 0.02	0.67 ± 0.02	0.62 ± 0.03	0.97 ± 0.05	1.19 ± 0.06	0.33 ± 0.02	0.79 ± 0.04	< LOD
7	Anthracene	< LOD	0.015 ± 6.0·10 <sup>-4</sup>	< LOD	< LOD	< LOD	< LOD	0.10 ± 5.0·10 <sup>-3</sup>	< LOD	< LOD
8	Phenanthrene	< LOD	< LOD							
9	3-Methylphenanthrene	2.8·10 <sup>-3</sup> ± 9.4·10 <sup>-5</sup>	3.0·10 <sup>-3</sup> ± 9.9·10 <sup>-5</sup>	3.9·10 <sup>-3</sup> ± 9.9·10 <sup>-5</sup>	0.12 ± 5.0·10 <sup>-3</sup>	0.17 ± 7.4·10 <sup>-3</sup>	9.9·10 <sup>-2</sup> ± 4.5·10 <sup>-3</sup>	< LOD	0.045 ± 2.1·10 <sup>-3</sup>	0.130 ± 6.2·10 <sup>-3</sup>
10	2-Methylphenanthrene	2.8·10 <sup>-3</sup> ± 9.4·10 <sup>-5</sup>	2.0·10 <sup>-3</sup> ± 9.9·10 <sup>-4</sup>	< LOD	< LOD	0.030 ± 1.2·10 <sup>-3</sup>	< LOD	< LOD	< LOD	< LOD
11	9-Methylphenanthrene	5.6·10 <sup>-3</sup> ± 1.9·10 <sup>-4</sup>	0.014 ± 4.9·10 <sup>-4</sup>	3.0·10 <sup>-3</sup> ± 9.9·10 <sup>-5</sup>	< LOD	< LOD				
12	3,6-dimethylphenanthrene	4.3·10 <sup>-3</sup> ± 1.4·10 <sup>-4</sup>	0.016 ± 5.6·10 <sup>-4</sup>	6.0·10 <sup>-3</sup> ± 2.2·10 <sup>-4</sup>	< LOD	< LOD	0.086 ± 4.0·10 <sup>-3</sup>	0.64 ± 3.4·10 <sup>-3</sup>	0.072 ± 3.3·10 <sup>-3</sup>	< LOD
13	Fluoranthene	< LOD	< LOD							
14	Pyrene	0.85 ± 3.1·10 <sup>-3</sup>	0.16 ± 6.0·10 <sup>-3</sup>	0.16 ± 5.8·10 <sup>-3</sup>	< LOD	< LOD				
15	2-Methylpyrene	0.016 ± 5.7·10 <sup>-4</sup>	0.025 ± 9.0·10 <sup>-4</sup>	0.034 ± 1.3·10 <sup>-3</sup>	0.024 ± 7.6·10 <sup>-4</sup>	0.027 ± 1.3·10 <sup>-3</sup>	0.023 ± 7.3·10 <sup>-4</sup>	< LOD	< LOD	0.023 ± 1.1·10 <sup>-3</sup>
16	4-Methylpyrene	0.010 ± 3.9·10 <sup>-4</sup>	0.036 ± 1.3·10 <sup>-3</sup>	0.045 ± 1.6·10 <sup>-3</sup>	< LOD	< LOD	< LOD	2.7·10 <sup>-3</sup> ± 3.6·10 <sup>-5</sup>	< LOD	0.030 ± 1.4·10 <sup>-3</sup>
17	Benzo[a]fluorene	5.3·10 <sup>-4</sup> ± 1.8·10 <sup>-5</sup>	2.1·10 <sup>-3</sup> ± 7.5·10 <sup>-5</sup>	1.6·10 <sup>-3</sup> ± 5.6·10 <sup>-5</sup>	6.2·10 <sup>-3</sup> ± 2.1·10 <sup>-4</sup>	9.7·10 <sup>-3</sup> ± 4.5·10 <sup>-4</sup>	7.6·10 <sup>-3</sup> ± 2.5·10 <sup>-4</sup>	8.3·10 <sup>-3</sup> ± 4.7·10 <sup>-4</sup>	7.2 ·10 <sup>-3</sup> ± 3.4·10 <sup>-4</sup>	6.1·10 <sup>-3</sup> ± 3.1·10 <sup>-4</sup>
18	Benzo[a]anthracene	4.5·10 <sup>-3</sup> ± 1.7·10 <sup>-4</sup>	0.012 ± 4.2·10 <sup>-4</sup>	4.0·10 <sup>-3</sup> ± 1.4·10 <sup>-4</sup>	< LOD	< LOD	< LOD	< LOD	0.014 ± 6.6·10 <sup>-4</sup>	7.3·10 <sup>-3</sup> ± 3.4·10 <sup>-4</sup>

											<sup>4</sup>
19	Chrysene	< LOD	$1.5 \cdot 10^{-3} \pm 5.5 \cdot 10^{-5}$	$6.6 \cdot 10^{-4} \pm 2.2 \cdot 10^{-5}$	$6.5 \cdot 10^{-3} \pm 3.0 \cdot 10^{-4}$	$5.6 \cdot 10^{-3} \pm 2.6 \cdot 10^{-4}$	< LOD	< LOD	< LOD	< LOD	< LOD
20	3-Methylchrysene	< LOD	< LOD	< LOD	$4.3 \cdot 10^{-3} \pm 1.9 \cdot 10^{-4}$	$4.8 \cdot 10^{-3} \pm 1.9 \cdot 10^{-4}$	$5.2 \cdot 10^{-3} \pm 2.5 \cdot 10^{-4}$	< LOD	$4.0 \cdot 10^{-3} \pm 1.8 \cdot 10^{-4}$	$3.9 \cdot 10^{-3} \pm 1.9 \cdot 10^{-4}$	
21	5-Methylchrysene	$7.1 \cdot 10^{-3} \pm 2.8 \cdot 10^{-5}$	$3.1 \cdot 10^{-3} \pm 1.1 \cdot 10^{-4}$	$9.0 \cdot 10^{-4} \pm 3.0 \cdot 10^{-5}$	< LOD	< LOD					
22	6-Methylchrysene	$1.4 \cdot 10^{-4} \pm 7.1 \cdot 10^{-6}$	$4.6 \cdot 10^{-3} \pm 1.7 \cdot 10^{-4}$	$4.5 \cdot 10^{-4} \pm 1.5 \cdot 10^{-5}$	$7.6 \cdot 10^{-3} \pm 2.8 \cdot 10^{-4}$	$8.9 \cdot 10^{-3} \pm 4.1 \cdot 10^{-4}$	$4.3 \cdot 10^{-3} \pm 1.9 \cdot 10^{-4}$	$0.015 \pm 8.0 \cdot 10^{-4}$	$0.012 \pm 5.4 \cdot 10^{-4}$	$7.6 \cdot 10^{-3} \pm 3.6 \cdot 10^{-4}$	
23	Benzo[a]fluoranthene	$4.6 \cdot 10^{-3} \pm 1.7 \cdot 10^{-4}$	$7.0 \cdot 10^{-3} \pm 2.6 \cdot 10^{-4}$	$1.2 \cdot 10^{-3} \pm 4.2 \cdot 10^{-5}$	$3.9 \cdot 10^{-3} \pm 1.8 \cdot 10^{-4}$	$6.8 \cdot 10^{-3} \pm 2.7 \cdot 10^{-4}$	$5.0 \cdot 10^{-3} \pm 2.4 \cdot 10^{-4}$	$2.8 \cdot 10^{-3} \pm 1.3 \cdot 10^{-4}$	$2.0 \cdot 10^{-3} \pm 9.4 \cdot 10^{-5}$	$1.5 \cdot 10^{-3} \pm 9.8 \cdot 10^{-5}$	
24	Benzo[b]fluoranthene	$6.5 \cdot 10^{-3} \pm 2.4 \cdot 10^{-4}$	$9.7 \cdot 10^{-3} \pm 3.5 \cdot 10^{-4}$	$5.2 \cdot 10^{-3} \pm 1.9 \cdot 10^{-4}$	$2.4 \cdot 10^{-3} \pm 7.0 \cdot 10^{-5}$	$2.8 \cdot 10^{-3} \pm 9.9 \cdot 10^{-5}$	$3.9 \cdot 10^{-3} \pm 1.8 \cdot 10^{-4}$	< LOD	< LOD	< LOD	
25	Benzo[k]fluoranthene	$2.8 \cdot 10^{-3} \pm 1.0 \cdot 10^{-4}$	$3.2 \cdot 10^{-3} \pm 1.2 \cdot 10^{-4}$	$1.9 \cdot 10^{-3} \pm 7.0 \cdot 10^{-5}$	< LOD						
26	Benzo[j]fluoranthene	$1.2 \cdot 10^{-4} \pm 3.0 \cdot 10^{-6}$	$3.8 \cdot 10^{-4} \pm 1.3 \cdot 10^{-5}$	$4.8 \cdot 10^{-4} \pm 1.6 \cdot 10^{-5}$	< LOD						
27	Benzo[a]pyrene	$3.7 \cdot 10^{-4} \pm 1.2 \cdot 10^{-5}$	$2.1 \cdot 10^{-3} \pm 7.5 \cdot 10^{-5}$	$6.5 \cdot 10^{-5} \pm 3.3 \cdot 10^{-6}$	< LOD	< LOD	< LOD	$7.2 \cdot 10^{-4} \pm 3.1 \cdot 10^{-5}$	$3.9 \cdot 10^{-3} \pm 1.8 \cdot 10^{-4}$	< LOD	
28	Indeno[1,2,3-cd]pyrene	< LOD	< LOD	< LOD	< LOD	$2.2 \cdot 10^{-4} \pm 1.2 \cdot 10^{-5}$	< LOD	$2.4 \cdot 10^{-4} \pm 1.3 \cdot 10^{-5}$	$9.4 \cdot 10^{-4} \pm 5.0 \cdot 10^{-5}$	$2.2 \cdot 10^{-3} \pm 1.0 \cdot 10^{-4}$	
29	Benzo[ghi]perylene	< LOD	< LOD	< LOD	$1.0 \cdot 10^{-3} \pm 2.9 \cdot 10^{-5}$	$2.3 \cdot 10^{-3} \pm 8.0 \cdot 10^{-5}$	$1.9 \cdot 10^{-3} \pm 5.2 \cdot 10^{-5}$	< LOD	$6.4 \cdot 10^{-4} \pm 3.2 \cdot 10^{-5}$	$1.1 \cdot 10^{-3} \pm 8.2 \cdot 10^{-5}$	
30	Dibenzo[a,h]anthracene	$6.0 \cdot 10^{-4} \pm 2.1 \cdot 10^{-5}$	$6.6 \cdot 10^{-4} \pm 2.4 \cdot 10^{-5}$	< LOD	< LOD	$2.0 \cdot 10^{-3} \pm 9.1 \cdot 10^{-5}$	$1.8 \cdot 10^{-3} \pm 5.0 \cdot 10^{-5}$	< LOD	$3.3 \cdot 10^{-3} \pm 1.5 \cdot 10^{-4}$	< LOD	
31	Dibenz[a,e]pyrene	$2.4 \cdot 10^{-5} \pm 8.9 \cdot 10^{-7}$	$3.3 \cdot 10^{-5} \pm 1.2 \cdot 10^{-6}$	$5.2 \cdot 10^{-5} \pm 1.9 \cdot 10^{-6}$	< LOD						
32	Dibenz[a,h]pyrene	$4.5 \cdot 10^{-6} \pm 1.5 \cdot 10^{-7}$	< LOD								
33	Dibenz[a,i]pyrene	< LOD									
34	Dibenz[a,l]pyrene	< LOD									
N- and O-PAHs											
35	Nitronaphthalene	< LOD	< LOD								
36	1-Methyl-5-nitronaphthalene	$0.35 \pm 0.01$	$0.94 \pm 0.03$	$0.33 \pm 0.01$	< LOD	$0.13 \pm 4.0 \cdot 10^{-3}$					
37	1-Methyl-6-nitronaphthalene	$0.42 \pm 0.01$	$0.77 \pm 0.03$	$0.36 \pm 0.01$	< LOD	$0.12 \pm 5.4 \cdot 10^{-3}$					
38	9,10-Anthracenedione	$0.035 \pm 1.2 \cdot 10^{-3}$	$0.19 \pm 7.3 \cdot 10^{-3}$	$0.25 \pm 0.01$	< LOD	< LOD	< LOD	< LOD	$0.057 \pm 5.7 \cdot 10^{-3}$	< LOD	
39	4H-cyclopenta(def)phenanth	< LOD	< LOD	$2.2 \cdot 10^{-3} \pm 1.0 \cdot 10^{-4}$	$0.24 \pm 0.01$	$0.47 \pm 0.022$	$0.47 \pm 0.02$	< LOD	$0.27 \pm 0.01$	$0.58 \pm 0.02$	

	rene									
40	Nitropyrene	< LOD	< LOD	< LOD	$8.2 \cdot 10^{-3} \pm 2.2 \cdot 10^{-4}$	$0.013 \pm 6.9 \cdot 10^{-3}$	$0.012 \pm 5.9 \cdot 10^{-4}$	< LOD	< LOD	< LOD

<LOD-below the limit of detection

**Table S5. The total fraction of PAHs in biochar amended soils (n=3; n-number of replicates) – Experiment 1.**

No.	Compound	Sample									
		Soil <sup>0</sup>	Soil <sup>1</sup>	Soil+BCZ500 <sup>1</sup>	Soil+BCZ600 <sup>1</sup>	Soil+BCZ700 <sup>1</sup>	Soil+BCW500 <sup>1</sup>	Soil+BCW600 <sup>1</sup>	Soil+BCW700 <sup>1</sup>	Soil+BCD600 <sup>1</sup>	Soil+BCF600 <sup>1</sup>
		Concentration [ $\mu\text{g g}^{-1}$ ]									
1	Naphthalene	< LOD	< LOD	$0.010 \pm 4.5 \cdot 10^{-4}$	$0.012 \pm 5.8 \cdot 10^{-4}$	$0.010 \pm 4.8 \cdot 10^{-4}$	$7.5 \cdot 10^{-3} \pm 4.0 \cdot 10^{-4}$	$0.010 \pm 4.8 \cdot 10^{-4}$	$0.012 \pm 5.5 \cdot 10^{-4}$	$0.015 \pm 7.2 \cdot 10^{-4}$	$7.5 \cdot 10^{-3} \pm 3.5 \cdot 10^{-4}$
2	2-Phenylnaphthalene	< LOD	< LOD	< LOD	< LOD	< LOD	< LOD	< LOD	< LOD	< LOD	$2.5 \cdot 10^{-3} \pm 1.3 \cdot 10^{-4}$
3	Acenaphthylene	< LOD	< LOD	$7.5 \cdot 10^{-3} \pm 3.8 \cdot 10^{-4}$	$7.5 \cdot 10^{-3} \pm 4.0 \cdot 10^{-4}$	$0.010 \pm 4.5 \cdot 10^{-4}$	$0.010 \pm 4.5 \cdot 10^{-4}$	$7.5 \cdot 10^{-3} \pm 3.5 \cdot 10^{-4}$	$7.5 \cdot 10^{-3} \pm 3.5 \cdot 10^{-4}$	$0.012 \pm 5.7 \cdot 10^{-4}$	< LOD
4	Acenaphthene	< LOD	< LOD	$2.5 \cdot 10^{-3} \pm 1.0 \cdot 10^{-4}$	$2.5 \cdot 10^{-3} \pm 1.0 \cdot 10^{-4}$	< LOD	$7.5 \cdot 10^{-3} \pm 3.8 \cdot 10^{-4}$	$0.010 \pm 4.3 \cdot 10^{-4}$	$5.0 \cdot 10^{-3} \pm 2.3 \cdot 10^{-4}$	< LOD	$0.013 \pm 6.0 \cdot 10^{-4}$
5	Fluorene	< LOD	< LOD	< LOD	< LOD	< LOD	< LOD	< LOD	< LOD	< LOD	$7.5 \cdot 10^{-3} \pm 4.0 \cdot 10^{-4}$
6	Anthracene	< LOD	< LOD	< LOD	< LOD	< LOD	< LOD	< LOD	< LOD	$0.027 \pm 1.3 \cdot 10^{-3}$	< LOD
7	Pyrene	< LOD	< LOD	$2.5 \cdot 10^{-3} \pm 1.5 \cdot 10^{-4}$	$5.0 \cdot 10^{-3} \pm 2.5 \cdot 10^{-4}$	$2.5 \cdot 10^{-3} \pm 1.3 \cdot 10^{-4}$	$5.0 \cdot 10^{-3} \pm 2.8 \cdot 10^{-4}$	$5.0 \cdot 10^{-3} \pm 2.5 \cdot 10^{-4}$	$7.5 \cdot 10^{-3} \pm 4.0 \cdot 10^{-4}$	< LOD	$7.5 \cdot 10^{-3} \pm 3.8 \cdot 10^{-4}$
8	Benzo[a]anthracene	< LOD	< LOD	< LOD	< LOD	< LOD	< LOD	< LOD	< LOD	$5.0 \cdot 10^{-3} \pm 2.2 \cdot 10^{-4}$	< LOD
9	Chrysene	< LOD	< LOD	< LOD	< LOD	< LOD	< LOD	< LOD	< LOD	< LOD	< LOD
10	6-Methylchrysene	< LOD	< LOD	< LOD	< LOD	< LOD	< LOD	< LOD	< LOD	$2.5 \cdot 10^{-3} \pm 1.5 \cdot 10^{-4}$	< LOD
Total		< LOD	< LOD	$0.022 \pm 1.1 \cdot 10^{-3}$	$0.027 \pm 1.3 \cdot 10^{-3}$	$0.022 \pm 1.0 \cdot 10^{-3}$	$0.030 \pm 1.5 \cdot 10^{-3}$	$0.032 \pm 1.5 \cdot 10^{-3}$	$0.032 \pm 1.5 \cdot 10^{-3}$	$0.062 \pm 3.0 \cdot 10^{-3}$	$0.038 \pm 1.9 \cdot 10^{-3}$

<sup>0</sup> soil before grass cultivation; <sup>1</sup> soil/BC amended soil after grass cultivation; <LOD-below the limit of detection

**Table S6. The total fraction of PAHs in biochar amended soils (n=3; n-number of replicates) – Experiment 2 – part 1.**

No.	Compound	Sampling after:							
		0 months				6 months			
		A	B	C	D	A	B	C	D
		Concentration [ $\mu\text{g g}^{-1}$ ]							
1	Naphthalene	< LOD	$2.5 \cdot 10^{-3} \pm 1.0 \cdot 10^{-4}$	< LOD	< LOD	< LOD	$5.0 \cdot 10^{-3} \pm 2.3 \cdot 10^{-4}$	$2.5 \cdot 10^{-3} \pm 1.0 \cdot 10^{-4}$	< LOD
2	Acenaphthylene	< LOD	< LOD	< LOD	< LOD	< LOD	< LOD	< LOD	< LOD
3	Acenaphthene	< LOD	$5.0 \cdot 10^{-3} \pm 2.5 \cdot 10^{-4}$	< LOD	< LOD	< LOD	$7.5 \cdot 10^{-3} \pm 3.8 \cdot 10^{-4}$	$2.5 \cdot 10^{-3} \pm 1.3 \cdot 10^{-4}$	< LOD
4	1,3-di-iso-propynaphthalene	< LOD	$2.5 \cdot 10^{-3} \pm 1.5 \cdot 10^{-4}$	< LOD	< LOD	< LOD	$2.5 \cdot 10^{-3} \pm 1.5 \cdot 10^{-4}$	< LOD	< LOD
5	Fluorene	< LOD	< LOD	< LOD	$5.0 \cdot 10^{-3} \pm 2.3 \cdot 10^{-4}$	< LOD	< LOD	$2.5 \cdot 10^{-3} \pm 1.0 \cdot 10^{-4}$	$5.0 \cdot 10^{-3} \pm 2.3 \cdot 10^{-4}$
6	Anthracene	< LOD	$2.5 \cdot 10^{-3} \pm 1.5 \cdot 10^{-4}$	< LOD	$2.5 \cdot 10^{-3} \pm 1.3 \cdot 10^{-4}$	< LOD	$2.5 \cdot 10^{-3} \pm 1.5 \cdot 10^{-4}$	< LOD	$2.5 \cdot 10^{-3} \pm 1.3 \cdot 10^{-4}$
7	3-Methylphenanthrene	< LOD	$5.0 \cdot 10^{-3} \pm 2.5 \cdot 10^{-4}$	$7.5 \cdot 10^{-3} \pm 3.3 \cdot 10^{-4}$	< LOD	< LOD	$7.5 \cdot 10^{-3} \pm 3.5 \cdot 10^{-4}$	$0.010 \pm 5.3 \cdot 10^{-4}$	< LOD
8	2-Methylphenanthrene	< LOD	$2.5 \cdot 10^{-3} \pm 1.2 \cdot 10^{-4}$	$2.5 \cdot 10^{-3} \pm 1.5 \cdot 10^{-4}$	< LOD	< LOD	$2.5 \cdot 10^{-3} \pm 1.3 \cdot 10^{-4}$	$5.0 \cdot 10^{-3} \pm 2.8 \cdot 10^{-4}$	< LOD
9	2-Phenylnaphthalene	< LOD	$0.027 \pm 1.3 \cdot 10^{-3}$	< LOD	< LOD	< LOD	$0.028 \pm 1.3 \cdot 10^{-3}$	< LOD	< LOD
10	3,6-dimethylphenanthrene	< LOD	$7.5 \cdot 10^{-3} \pm 3.0 \cdot 10^{-4}$	< LOD	< LOD	< LOD	$0.010 \pm 6.0 \cdot 10^{-4}$	< LOD	< LOD
11	Fluoranthene	< LOD	< LOD	$5.05 \cdot 10^{-3} \pm 2.5 \cdot 10^{-4}$	$0.010 \pm 4.5 \cdot 10^{-4}$	< LOD	< LOD	$5.0 \cdot 10^{-3} \pm 2.8 \cdot 10^{-4}$	$0.010 \pm 4.5 \cdot 10^{-4}$
12	Pyrene	< LOD	< LOD	$1.5 \cdot 10^{-3} \pm 1.3 \cdot 10^{-4}$	$7.5 \cdot 10^{-3} \pm 3.8 \cdot 10^{-4}$	< LOD	< LOD	$2.5 \cdot 10^{-3} \pm 1.0 \cdot 10^{-4}$	$7.5 \cdot 10^{-3} \pm 3.8 \cdot 10^{-4}$
13	Chrysene	< LOD	< LOD	$1.5 \cdot 10^{-3} \pm 1.5 \cdot 10^{-4}$	< LOD	< LOD	< LOD	$2.5 \cdot 10^{-3} \pm 1.5 \cdot 10^{-4}$	< LOD
14	3-Methylchrysene	< LOD	< LOD	$1.5 \cdot 10^{-3} \pm 1.3 \cdot 10^{-4}$	$0.010 \pm 4.8 \cdot 10^{-4}$	< LOD	< LOD	$5.0 \cdot 10^{-3} \pm 2.0 \cdot 10^{-4}$	$0.010 \pm 4.8 \cdot 10^{-4}$
15	5-Methylchrysene	< LOD	< LOD	< LOD	$7.5 \cdot 10^{-3} \pm 3.8 \cdot 10^{-4}$	< LOD	< LOD	$2.5 \cdot 10^{-3} \pm 1.0 \cdot 10^{-4}$	$7.5 \cdot 10^{-3} \pm 3.8 \cdot 10^{-4}$
16	6-Methylchrysene	< LOD	< LOD	< LOD	$5.0 \cdot 10^{-3} \pm 2.5 \cdot 10^{-4}$	< LOD	< LOD	< LOD	$5.0 \cdot 10^{-3} \pm 2.5 \cdot 10^{-4}$

17	Nitroacenaphthalene	< LOD	< LOD	< LOD	$5.0 \cdot 10^{-3} \pm 2.3 \cdot 10^{-4}$	< LOD	< LOD	$2.5 \cdot 10^{-3} \pm 1.5 \cdot 10^{-4}$	$5.0 \cdot 10^{-3} \pm 2.3 \cdot 10^{-4}$
18	1-Methyl-5-nitronaphthalene	< LOD	< LOD	< LOD	< LOD	< LOD	< LOD	< LOD	< LOD
19	1-Methyl-6-nitronaphthalene	< LOD	< LOD	< LOD	< LOD	< LOD	< LOD	< LOD	< LOD
20	9,10-Anthracenedione	< LOD	< LOD	< LOD	$2.5 \cdot 10^{-3} \pm 1.3 \cdot 10^{-4}$	< LOD	< LOD	< LOD	$2.5 \cdot 10^{-3} \pm 1.3 \cdot 10^{-4}$
21	2-Methylpyrene	< LOD	< LOD	< LOD	$2.5 \cdot 10^{-3} \pm 1.3 \cdot 10^{-4}$	< LOD	< LOD	< LOD	$2.5 \cdot 10^{-3} \pm 1.3 \cdot 10^{-4}$
22	4-Methylpyrene	< LOD	< LOD	< LOD	< LOD	< LOD	< LOD	< LOD	< LOD

<LOD-below the limit of detection

**Table S7. The total fraction of PAHs in biochar amended soils (n=3; n-number of replicates) – Experiment 2 – part 2.**

No.	Compound	Sampling after:							
		12 months				18 months			
		A	B	C	D	A	B	C	D
		Concentration [ $\mu\text{g g}^{-1}$ ]							
1	Naphthalene	< LOD	$0.010 \pm 4.3 \cdot 10^{-4}$	$2.5 \cdot 10^{-3} \pm 1.0 \cdot 10^{-4}$	$2.5 \cdot 10^{-3} \pm 1.3 \cdot 10^{-4}$	< LOD	$0.015 \pm 9.0 \cdot 10^{-4}$	$7.5 \cdot 10^{-3} \pm 3.5 \cdot 10^{-4}$	$2.5 \cdot 10^{-3} \pm 1.3 \cdot 10^{-4}$
2	Acenaphthylene	< LOD	$2.5 \cdot 10^{-3} \pm 1.3 \cdot 10^{-4}$	< LOD	< LOD	< LOD	$2.5 \cdot 10^{-3} \pm 1.3 \cdot 10^{-4}$	< LOD	< LOD
3	Acenaphthene	< LOD	$0.010 \pm 5.8 \cdot 10^{-4}$	$5.0 \cdot 10^{-3} \pm 2.0 \cdot 10^{-4}$	$2.5 \cdot 10^{-3} \pm 1.3 \cdot 10^{-4}$	< LOD	$0.010 \pm 5.5 \cdot 10^{-4}$	$5.0 \cdot 10^{-3} \pm 2.3 \cdot 10^{-4}$	$5.0 \cdot 10^{-3} \pm 2.0 \cdot 10^{-4}$
4	1,3-di-iso-propylnaphthalene	< LOD	$2.5 \cdot 10^{-3} \pm 1.3 \cdot 10^{-4}$	< LOD	< LOD	< LOD	$2.5 \cdot 10^{-3} \pm 1.5 \cdot 10^{-4}$	< LOD	< LOD
5	Fluorene	< LOD	< LOD	$2.5 \cdot 10^{-3} \pm 1.2 \cdot 10^{-4}$	$7.5 \cdot 10^{-3} \pm 4.0 \cdot 10^{-4}$	< LOD	< LOD	$2.5 \cdot 10^{-3} \pm 1.3 \cdot 10^{-4}$	$7.5 \cdot 10^{-3} \pm 4.0 \cdot 10^{-4}$
6	Anthracene	< LOD	$0.030 \pm 1.6 \cdot 10^{-3}$	< LOD	$2.5 \cdot 10^{-3} \pm 1.3 \cdot 10^{-4}$	< LOD	$0.030 \pm 1.5 \cdot 10^{-3}$	< LOD	$2.5 \cdot 10^{-3} \pm 1.3 \cdot 10^{-4}$
7	3-Methylphenanthrene	< LOD	$0.010 \pm 5.3 \cdot 10^{-4}$	$0.010 \pm 5.5 \cdot 10^{-4}$	< LOD	$2.5 \cdot 10^{-3} \pm 1.3 \cdot 10^{-4}$	$7.5 \cdot 10^{-3} \pm 3.8 \cdot 10^{-4}$	$7.5 \cdot 10^{-3} \pm 3.5 \cdot 10^{-4}$	$5.0 \cdot 10^{-3} \pm 2.3 \cdot 10^{-4}$

8	2-Methylphenanthrene	< LOD	$5.0 \cdot 10^{-3} \pm 2.3 \cdot 10^{-4}$	$5.0 \cdot 10^{-3} \pm 2.7 \cdot 10^{-4}$	< LOD	< LOD	$5.0 \cdot 10^{-3} \pm 2.0 \cdot 10^{-4}$	$5.0 \cdot 10^{-3} \pm 2.3 \cdot 10^{-4}$	< LOD
9	2-Phenylnaphthalene	< LOD	$0.030 \pm 1.6 \cdot 10^{-3}$	< LOD	< LOD	< LOD	$0.030 \pm 1.6 \cdot 10^{-3}$	< LOD	< LOD
10	3,6-dimethylphenanthrene	< LOD	$0.010 \pm 6.3 \cdot 10^{-4}$	< LOD	< LOD	< LOD	$0.012 \pm 7.8 \cdot 10^{-4}$	< LOD	< LOD
11	Fluoranthene	< LOD	< LOD	$7.5 \cdot 10^{-3} \pm 3.7 \cdot 10^{-4}$	$0.010 \pm 5.0 \cdot 10^{-4}$	< LOD	< LOD	$7.5 \cdot 10^{-3} \pm 3.5 \cdot 10^{-4}$	$0.015 \pm 7.3 \cdot 10^{-4}$
12	Pyrene	< LOD	< LOD	$7.5 \cdot 10^{-3} \pm 3.5 \cdot 10^{-4}$	$0.018 \pm 8.3 \cdot 10^{-4}$	< LOD	< LOD	$7.5 \cdot 10^{-3} \pm 3.5 \cdot 10^{-4}$	$0.025 \pm 1.3 \cdot 10^{-3}$
13	Chrysene	< LOD	< LOD	$5.0 \cdot 10^{-3} \pm 2.5 \cdot 10^{-4}$	$2.5 \cdot 10^{-3} \pm 1.3 \cdot 10^{-4}$	< LOD	< LOD	$0.010 \pm 4.8 \cdot 10^{-4}$	$5.0 \cdot 10^{-3} \pm 2.3 \cdot 10^{-4}$
14	3-Methylchrysene	< LOD	< LOD	$5.0 \cdot 10^{-3} \pm 2.0 \cdot 10^{-4}$	$0.010 \pm 4.8 \cdot 10^{-4}$	< LOD	< LOD	$5.0 \cdot 10^{-3} \pm 2.5 \cdot 10^{-4}$	$0.012 \pm 5.8 \cdot 10^{-4}$
15	5-Methylchrysene	< LOD	< LOD	$2.5 \cdot 10^{-3} \pm 1.0 \cdot 10^{-4}$	$7.5 \cdot 10^{-3} \pm 4.0 \cdot 10^{-4}$	< LOD	< LOD	$7.5 \cdot 10^{-3} \pm 3.3 \cdot 10^{-4}$	$7.5 \cdot 10^{-3} \pm 3.8 \cdot 10^{-4}$
16	6-Methylchrysene	< LOD	< LOD	< LOD	$2.5 \cdot 10^{-3} \pm 1.3 \cdot 10^{-4}$	< LOD	< LOD	$5.0 \cdot 10^{-3} \pm 2.510^{-4}$	$5.0 \cdot 10^{-3} \pm 2.3 \cdot 10^{-4}$
17	Nitroacenaphthalene	< LOD	< LOD	$2.5 \cdot 10^{-3} \pm 1.5 \cdot 10^{-4}$	$5.0 \cdot 10^{-3} \pm 2.3 \cdot 10^{-4}$	< LOD	< LOD	$2.5 \cdot 10^{-3} \pm 1.3 \cdot 10^{-4}$	$0.010 \pm 5.3 \cdot 10^{-4}$
18	1-Methyl-5-nitronaphthalene	< LOD	< LOD	< LOD	< LOD	< LOD	< LOD	< LOD	$2.5 \cdot 10^{-3} \pm 1.3 \cdot 10^{-4}$
19	1-Methyl-6-nitronaphthalene	< LOD	< LOD	< LOD	< LOD	< LOD	< LOD	< LOD	$2.5 \cdot 10^{-3} \pm 1.3 \cdot 10^{-4}$
20	9,10-Anthracenedione	< LOD	< LOD	$2.5 \cdot 10^{-3} \pm 1.5 \cdot 10^{-4}$	$2.5 \cdot 10^{-3} \pm 1.3 \cdot 10^{-4}$	< LOD	< LOD	$2.5 \cdot 10^{-3} \pm 1.3 \cdot 10^{-4}$	$5.0 \cdot 10^{-3} \pm 2.3 \cdot 10^{-4}$
21	2-Methylpyrene	< LOD	< LOD	< LOD	$5.0 \cdot 10^{-3} \pm 2.3 \cdot 10^{-4}$	< LOD	< LOD	< LOD	$5.0 \cdot 10^{-3} \pm 2.3 \cdot 10^{-4}$
22	4-Methylpyrene	< LOD	< LOD	< LOD	$2.5 \cdot 10^{-3} \pm 1.3 \cdot 10^{-4}$	< LOD	< LOD	< LOD	$2.5 \cdot 10^{-3} \pm 1.3 \cdot 10^{-4}$

<LOD-below the limit of detection

**Table S8. The total fraction of PAHs in biochar amended soils (n=3; n-number of replicates) – Experiment 3 – part 1.**

No.	Compound	Sampling after:
-----	----------	-----------------

		0 days			21 days		
		control	X	Y	control	X	Y
		Concentration [ $\mu\text{g g}^{-1}$ ]					
1	Naphthalene	< LOD	< LOD	< LOD	$2.5 \cdot 10^{-3} \pm 1.0 \cdot 10^{-4}$	$5.0 \cdot 10^{-3} \pm 2.5 \cdot 10^{-4}$	$5.0 \cdot 10^{-3} \pm 2.2 \cdot 10^{-4}$
2	Acenaphthylene	< LOD	< LOD	< LOD	< LOD	< LOD	< LOD
3	Acenaphthene	< LOD	< LOD	< LOD	$5.0 \cdot 10^{-3} \pm 2.7 \cdot 10^{-4}$	< LOD	$0.012 \pm 6.7 \cdot 10^{-4}$
4	1,3-di-iso-propynaphthalene	< LOD	< LOD	< LOD	$2.5 \cdot 10^{-3} \pm 1.2 \cdot 10^{-4}$	$5.0 \cdot 10^{-3} \pm 2.0 \cdot 10^{-4}$	$2.5 \cdot 10^{-3} \pm 1.0 \cdot 10^{-4}$
5	Fluorene	< LOD	< LOD	< LOD	< LOD	< LOD	< LOD
6	Anthracene	< LOD	< LOD	< LOD	$7.5 \cdot 10^{-3} \pm 3.7 \cdot 10^{-4}$	$0.015 \pm 9.0 \cdot 10^{-4}$	$0.017 \pm 1.1 \cdot 10^{-4}$
7	3-Methylphenanthrene	< LOD	< LOD	< LOD	< LOD	< LOD	< LOD
8	2-Methylphenanthrene	< LOD	< LOD	< LOD	< LOD	< LOD	< LOD
9	9-Methylphenanthrene	< LOD	< LOD	< LOD	$2.5 \cdot 10^{-3} \pm 1.2 \cdot 10^{-4}$	$5.0 \cdot 10^{-3} \pm 2.5 \cdot 10^{-4}$	$7.5 \cdot 10^{-3} \pm 4.0 \cdot 10^{-4}$
10	2-Phenylnaphthalene	< LOD	< LOD	< LOD	< LOD	< LOD	< LOD
11	3,6-dimethylphenanthrene	< LOD	< LOD	< LOD	< LOD	< LOD	< LOD
12	Fluoranthene	< LOD	< LOD	< LOD	< LOD	< LOD	< LOD
13	Pyrene	< LOD	< LOD	< LOD	< LOD	< LOD	< LOD
14	Benzo[a]fluorene	< LOD	< LOD	< LOD	< LOD	< LOD	< LOD
15	Benzo[a]anthracene	< LOD	< LOD	< LOD	< LOD	< LOD	< LOD
16	Chrysene	< LOD	< LOD	< LOD	$2.5 \cdot 10^{-3} \pm 1.2 \cdot 10^{-4}$	$2.5 \cdot 10^{-3} \pm 1.0 \cdot 10^{-4}$	$5.0 \cdot 10^{-3} \pm 3.0 \cdot 10^{-4}$
17	3-Methylchrysene	< LOD	< LOD	< LOD	< LOD	< LOD	$2.5 \cdot 10^{-3} \pm 1.3 \cdot 10^{-4}$
18	5-Methylchrysene	< LOD	< LOD	< LOD	< LOD	< LOD	$2.5 \cdot 10^{-3} \pm 1.3 \cdot 10^{-4}$
19	6-Methylchrysene	< LOD	< LOD	< LOD	< LOD	< LOD	$2.5 \cdot 10^{-3} \pm 1.5 \cdot 10^{-4}$

<LOD-below the limit of detection

**Table S8. The total fraction of PAHs in biochar amended soils (n=3; n-number of replicates) – Experiment 3 – part 2.**

No.	Compound	Sampling after:					
		104 days			474 days		
		control	X	Y	control	X	Y
		Concentration [ $\mu\text{g g}^{-1}$ ]					
1	Naphthalene	$2.5 \cdot 10^{-3} \pm 1.3 \cdot 10^{-4}$	$7.5 \cdot 10^{-3} \pm 4.3 \cdot 10^{-4}$	$7.5 \cdot 10^{-3} \pm 4.0 \cdot 10^{-4}$	$7.5 \cdot 10^{-3} \pm 4.0 \cdot 10^{-4}$	$0.010 \pm 6.2 \cdot 10^{-4}$	$0.010 \pm 5.8 \cdot 10^{-4}$
2	Acenaphthylene	< LOD					
3	Acenaphthene	$5.0 \cdot 10^{-3} \pm 3.0 \cdot 10^{-4}$	$0.010 \pm 5.5 \cdot 10^{-4}$	$0.018 \pm 1.0 \cdot 10^{-3}$	$5.0 \cdot 10^{-3} \pm 2.8 \cdot 10^{-4}$	$0.013 \pm 6.5 \cdot 10^{-4}$	$0.023 \pm 1.2 \cdot 10^{-3}$
4	1,3-di-iso-propynaphthalene	$7.5 \cdot 10^{-3} \pm 4.0 \cdot 10^{-4}$	$0.020 \pm 1.2 \cdot 10^{-3}$	$0.015 \pm 9.3 \cdot 10^{-4}$	$0.015 \pm 9.5 \cdot 10^{-4}$	$0.017 \pm 9.2 \cdot 10^{-4}$	$0.028 \pm 1.4 \cdot 10^{-3}$
5	Fluorene	< LOD					
6	Anthracene	$0.022 \pm 1.2 \cdot 10^{-4}$	$0.025 \pm 1.3 \cdot 10^{-3}$	$0.030 \pm 1.5 \cdot 10^{-3}$	$0.025 \pm 1.3 \cdot 10^{-3}$	$0.027 \pm 1.4 \cdot 10^{-3}$	$0.035 \pm 2.0 \cdot 10^{-3}$
7	3-Methylphenanthrene	< LOD					
8	2-Methylphenanthrene	< LOD					
9	9-Methylphenanthrene	$0.012 \pm 7.3 \cdot 10^{-4}$	$0.017 \pm 1.1 \cdot 10^{-3}$	$0.023 \pm 1.2 \cdot 10^{-3}$	$0.017 \pm 1.1 \cdot 10^{-3}$	$0.022 \pm 1.3 \cdot 10^{-3}$	$0.030 \pm 1.6 \cdot 10^{-3}$
10	2-Phenylnaphthalene	< LOD					
11	3,6-dimethylphenanthrene	< LOD					
12	Fluoranthene	< LOD					
13	Pyrene	< LOD	$2.5 \cdot 10^{-3} \pm 1.3 \cdot 10^{-4}$	$2.5 \cdot 10^{-3} \pm 1.0 \cdot 10^{-4}$	$2.5 \cdot 10^{-3} \pm 1.5 \cdot 10^{-4}$	$2.5 \cdot 10^{-3} \pm 1.0 \cdot 10^{-4}$	$5.0 \cdot 10^{-3} \pm 2.5 \cdot 10^{-4}$

14	Benzo[a]fluorene	< LOD					
15	Benzo[a]anthracene	< LOD					
16	Chrysene	$2.5 \cdot 10^{-3} \pm 1.0 \cdot 10^{-4}$	$5.0 \cdot 10^{-3} \pm 2.5 \cdot 10^{-4}$	$7.5 \cdot 10^{-3} \pm 3.8 \cdot 10^{-4}$	$5.0 \cdot 10^{-3} \pm 2.8 \cdot 10^{-4}$	$5.0 \cdot 10^{-3} \pm 2.7 \cdot 10^{-4}$	$7.5 \cdot 10^{-3} \pm 4.0 \cdot 10^{-4}$
17	3-Methylchrysene	< LOD	$2.5 \cdot 10^{-3} \pm 1.3 \cdot 10^{-4}$	$5.0 \cdot 10^{-3} \pm 2.3 \cdot 10^{-4}$	$2.5 \cdot 10^{-3} \pm 1.0 \cdot 10^{-4}$	$5.0 \cdot 10^{-3} \pm 2.2 \cdot 10^{-4}$	$7.5 \cdot 10^{-3} \pm 3.8 \cdot 10^{-4}$
18	5-Methylchrysene	< LOD	$2.5 \cdot 10^{-3} \pm 1.3 \cdot 10^{-4}$	$7.5 \cdot 10^{-3} \pm 4.3 \cdot 10^{-4}$	< LOD	$5.0 \cdot 10^{-3} \pm 3.0 \cdot 10^{-4}$	$7.5 \cdot 10^{-3} \pm 4.0 \cdot 10^{-4}$
19	6-Methylchrysene	< LOD	$5.0 \cdot 10^{-3} \pm 2.0 \cdot 10^{-4}$	$5.0 \cdot 10^{-3} \pm 2.3 \cdot 10^{-4}$	$2.5 \cdot 10^{-3} \pm 1.3 \cdot 10^{-4}$	$5.0 \cdot 10^{-3} \pm 2.5 \cdot 10^{-4}$	$7.5 \cdot 10^{-3} \pm 4.0 \cdot 10^{-4}$

<LOD-below the limit of detection

## References

- [1] D. Fabbri, A.G. Rombolà, C. Torri, K.A. Spokas, Determination of polycyclic aromatic hydrocarbons in biochar and biochar amended soil, *Journal of Analytical and Applied Pyrolysis.* 103 (2013) 60–67. <https://doi.org/10.1016/j.jaap.2012.10.003>.

dr hab. Bożena Czech, prof. UMCS  
Katedra Radiochemii i Chemii Środowiskowej  
Instytut Nauk Chemicznych  
Wydział Chemii UMCS w Lublinie  
tel. 81 537 55 54  
e-mail: bozena.czech@mail.umcs.pl

Lublin, dn. 25.09.2023

## Oświadczenie

Niniejszym oświadczam, że w pracy:

A. Krzyszczak-Turczyn, **B. Czech**, *Occurrence and toxicity of polycyclic aromatic hydrocarbons derivatives in environmental matrices*, Science of the Total Environment, 2021, 788: 147738

mój udział polegał na współtworzeniu jej koncepcji, przeglądzie i edycji manuskryptu oraz odpowiedzi na uwagi recenzentów, pełnieniu roli autora korespondencyjnego.

A. Krzyszczak-Turczyn, M. Dybowski, **B. Czech**, *Formation of polycyclic aromatic hydrocarbons and their derivatives in biochars: The effect of feedstock and pyrolysis conditions*, Journal of Analytical and Applied Pyrolysis, 2021, 160, 105339

mój udział polegał na współtworzeniu jej koncepcji, przeglądzie i edycji manuskryptu oraz odpowiedzi na uwagi recenzentów, pełnieniu roli autora korespondencyjnego.

A. Krzyszczak-Turczyn, M. P. Dybowski, M. Kończak, **B. Czech**, *Low bioavailability of derivatives of polycyclic aromatic hydrocarbons in biochar obtained from different feedstock*, Environmental Research, 2022, 214(1), 113787

mój udział polegał na współtworzeniu jej koncepcji, przeglądzie i edycji manuskryptu oraz odpowiedzi na uwagi recenzentów, pełnieniu roli autora korespondencyjnego.

A. Krzyszczak-Turczyn, M. Dybowski, I. Jośko, M. Kusiak, M. Sikora, **B. Czech**, *The antioxidant defense responses of *Hordeum vulgare L.* to polycyclic aromatic hydrocarbons and their derivatives in biochar-amended soil*, Environmental Pollution, 2022, 294, 118664

mój udział polegał na współtworzeniu jej koncepcji, przeglądzie i edycji manuskryptu oraz odpowiedzi na uwagi recenzentów, pełnieniu roli autora korespondencyjnego.

A. Krzyszczak-Turczyn, M. P. Dybowski, R. Zarzycki, R. Kobyłecki, P. Oleszczuk, **B. Czech**, *Long-term physical and chemical aging of biochar affected the amount and bioavailability of PAHs and their derivatives*, Journal of Hazardous Materials, 2022, 440, 129795

mój udział polegał na współtworzeniu jej koncepcji, przeglądzie i edycji manuskryptu oraz odpowiedzi na uwagi recenzentów, pełnieniu roli autora korespondencyjnego.

A. Krzyszczak-Turczyn, M. P. Dybowski, **B. Czech**, *Microorganisms and their metabolites affect the content of polycyclic aromatic hydrocarbons and their derivatives in pyrolyzed material*, Science of the Total Environment, 2023, 886, 163966

mój udział polegał na współtworzeniu jej koncepcji, przeglądzie i edycji manuskryptu oraz odpowiedzi na uwagi recenzentów, pełnieniu roli autora korespondencyjnego.

A. Krzyszczak-Turczyn, M. P. Dybowski, M. Kończak, P. Oleszczuk, **B. Czech**, *Increased concentration of PAHs derivatives in biochar-amended soil observed in a long-term experiment*, artykuł w trakcie recenzji w czasopismie Journal of Hazardous Materials

mój udział polegał na współtworzeniu jej koncepcji, przeglądzie i edycji manuskryptu oraz odpowiedzi na uwagi recenzentów, pełnieniu roli autora korespondencyjnego.

Jednocześnie wyrażam zgodę na przedłożenie przez Panią Agnieszkę Krzyszczak-Turczyn wyżej wymienionych prac jako część rozprawy doktorskiej w formie spójnego tematycznie cyklu prac opublikowanych w czasopismach naukowych.

*Bożena Czech*

.....  
podpis

dr Michał Dybowski  
Katedra Chromatografii  
Instytut Nauk Chemicznych  
Wydział Chemii UMCS w Lublinie  
tel. 81 5375659  
e-mail: michal.dybowski@mail.umcs.pl

Lublin, dn. 25.09.2023

## Oświadczenie

Niniejszym oświadczam, że w pracy:

A. Krzyszczak, **M. P. Dybowski**, B. Czech, *Formation of polycyclic aromatic hydrocarbons and their derivatives in biochars: The effect of feedstock and pyrolysis conditions*, Journal of Analytical and Applied Pyrolysis, 2021, 160, 105339

mój udział polegał na wykonaniu analiz chromatograficznych.

A. Krzyszczak, **M. P. Dybowski**, M. Kończak, B. Czech, *Low bioavailability of derivatives of polycyclic aromatic hydrocarbons in biochar obtained from different feedstock*, Environmental Research, 2022, 214(1), 113787

mój udział polegał na wykonaniu analiz chromatograficznych.

A. Krzyszczak, **M. P. Dybowski**, I. Jośko, M. Kusiak, M. Sikora, B. Czech, *The antioxidant defense responses of Hordeum vulgare L. to polycyclic aromatic hydrocarbons and their derivatives in biochar-amended soil*, Environmental Pollution, 2022, 294, 118664

mój udział polegał na wykonaniu analiz chromatograficznych.

A. Krzyszczak, **M. P. Dybowski**, R. Zarzycki, R. Kobyłecki, P. Oleszczuk, B. Czech, *Long-term physical and chemical aging of biochar affected the amount and bioavailability of PAHs and their derivatives*, Journal of Hazardous Materials, 2022, 440, 129795

mój udział polegał na wykonaniu analiz chromatograficznych.

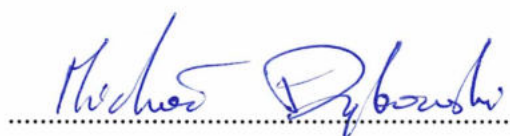
A. Krzyszczak, **M. P. Dybowski**, B. Czech, *Microorganisms and their metabolites affect the content of polycyclic aromatic hydrocarbons and their derivatives in pyrolyzed material*, Science of the Total Environment, 2023, 886, 163966

mój udział polegał na wykonaniu analiz chromatograficznych.

A. Krzyszczak-Turczyn, **M. P. Dybowski**, M. Kończak, P. Oleszczuk, B. Czech, *Increased concentration of PAHs derivatives in biochar-amended soil observed in a long-term experiment*, artykuł w trakcie recenzji w czasopismie Journal of Hazardous Materials

mój udział polegał na wykonaniu analiz chromatograficznych.

Jednocześnie wyrażam zgodę na przedłożenie przez Panią Agnieszkę Krzyszczak-Turczyn wyżej wymienionych prac jako część rozprawy doktorskiej w formie spójnego tematycznie cyklu prac opublikowanych w czasopismach naukowych.



podpis

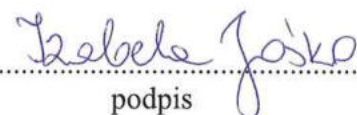
Dr hab. Izabela Jośko, prof. uczelni  
Instytut Genetyki, Hodowli i Biotechnologii Roślin  
Wydział Agrobioinżynierii  
Uniwersytet Przyrodniczy w Lublinie  
tel. 814456675  
e-mail: izabela.josko@up.lublin.pl

Tajpej, 24.08.2023 r.

### Oświadczenie

Niniejszym oświadczam, że w pracy:  
A. Krzyszczak, M. P. Dybowski, **I. Jośko**, M. Kusiak, M. Sikora, B. Czech, *The antioxidant defense responses of Hordeum vulgare L. to polycyclic aromatic hydrocarbons and their derivatives in biochar-amended soil*, Environmental Pollution, 2022, 294, 118664  
mój udział polegał na wykonaniu części eksperymentów dotyczących analizy ekspresji genów.

Jednocześnie wyrażam zgodę na przedłożenie przez Panią Agnieszkę Krzyszczak-Turczyn wyżej wymienionej pracy jako część rozprawy doktorskiej w formie spójnego tematycznie cyklu prac opublikowanych w czasopismach naukowych.



.....  
podpis



dr hab. inż. Rafał Kobyłecki, prof. PCz  
Katedra Zaawansowanych Technologii Energetycznych  
Wydział Infrastruktury i Środowiska  
Politechnika Częstochowska  
e-mail: rafal.kobylecki@pcz.pl

Lublin, dn. 23.08.2023

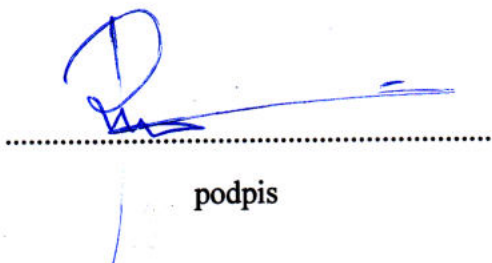
### Oświadczenie

Niniejszym oświadczam, że w pracy:

A. Krzyszczak, M. P. Dybowski, R. Zarzycki, **R. Kobyłecki**, P. Oleszczuk, B. Czech, *Long-term physical and chemical aging of biochar affected the amount and bioavailability of PAHs and their derivatives*, Journal of Hazardous Materials, 2022, 440, 129795

mój udział polegał na otrzymaniu części materiału badawczego.

Jednocześnie wyrażam zgodę na przedłożenie przez Panią Agnieszkę Krzyszczak-Turczyn wyżej wymienionej pracy jako część rozprawy doktorskiej w formie spójnego tematycznie cyklu prac opublikowanych w czasopismach naukowych.



.....

podpis

---

dr Magdalena Kończak

Lublin, 25.09.2023r.

## Oświadczenie

Niniejszym oświadczam, że w pracy:

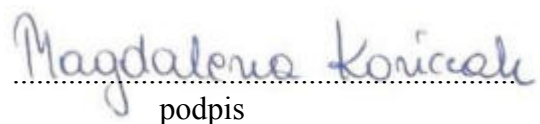
A. Krzyszczak, M. P. Dybowski, **M. Kończak**, B. Czech, *Low bioavailability of derivatives of polycyclic aromatic hydrocarbons in biochar obtained from different feedstock*, Environmental Research, 2022, 214(1), 113787

mój udział polegał na otrzymaniu części materiału badawczego.

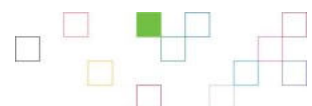
A. Krzyszczak-Turczyn, M. P. Dybowski, **M. Kończak**, P. Oleszczuk, B. Czech, *Increased concentration of PAHs derivatives in biochar-amended soil observed in a long-term experiment*, artykuł w trakcie recenzji w czasopismie Journal of Hazardous Materials

mój udział polegał na przeprowadzeniu części eksperymentów polowych.

Jednocześnie wyrażam zgodę na przedłożenie przez Panią Agnieszkę Krzyszczak-Turczyn wyżej wymienionej pracy jako część rozprawy doktorskiej w formie spójnego tematycznie cyklu prac opublikowanych w czasopismach naukowych.



Magdalena Kończak  
podpis



## Oświadczenie

Niniejszym oświadczam, że w pracy:

**A. Krzyszczak, B. Czech,** *Occurrence and toxicity of polycyclic aromatic hydrocarbons derivatives in environmental matrices*, Science of the Total Environment, 2021, 788: 147738

mój udział polegał na współtworzeniu ogólnej jej koncepcji i projektu, przygotowaniu i przeglądzie manuskryptu oraz jego oprawy graficznej, opracowaniu odpowiedzi na uwagi recenzentów.

**A. Krzyszczak, M. Dybowski, B. Czech,** *Formation of polycyclic aromatic hydrocarbons and their derivatives in biochars: The effect of feedstock and pyrolysis conditions*, Journal of Analytical and Applied Pyrolysis, 2021, 160, 105339

mój udział polegał na współtworzeniu ogólnej jej koncepcji i projektu, wykonaniu eksperymentów, opracowaniu wyników oraz ich interpretacji, wykonaniu analizy statystycznej, przygotowaniu i przeglądzie manuskryptu oraz jego oprawy graficznej, poprowadzeniu dyskusji, sporządzeniu odpowiedzi na uwagi recenzentów.

**A. Krzyszczak, M. P. Dybowski, M. Kończak, B. Czech,** *Low bioavailability of derivatives of polycyclic aromatic hydrocarbons in biochar obtained from different feedstock*, Environmental Research, 2022, 214(1), 113787

mój udział polegał na współtworzeniu ogólnej jej koncepcji i projektu, wykonaniu eksperymentów, opracowaniu wyników oraz ich interpretacji, wykonaniu analizy statystycznej, przygotowaniu i przeglądzie manuskryptu oraz jego oprawy graficznej, poprowadzeniu dyskusji, sporządzeniu odpowiedzi na uwagi recenzentów.

**A. Krzyszczak, M. Dybowski, I. Jośko, M. Kusiak, M. Sikora, B. Czech,** *The antioxidant defense responses of *Hordeum vulgare L.* to polycyclic aromatic hydrocarbons and their derivatives in biochar-amended soil*, Environmental Pollution, 2022, 294, 118664

mój udział polegał na współtworzeniu ogólnej jej koncepcji i projektu, wykonaniu części eksperymentów, opracowaniu wyników oraz ich interpretacji, wykonaniu analizy statystycznej, przygotowaniu i przeglądzie manuskryptu oraz jego oprawy graficznej, poprowadzeniu dyskusji, sporządzeniu odpowiedzi na uwagi recenzentów.

**A. Krzyszczak**, M. P. Dybowski, R. Zarzycki, R. Kobyłecki, P. Oleszczuk, B. Czech, *Long-term physical and chemical aging of biochar affected the amount and bioavailability of PAHs and their derivatives*, Journal of Hazardous Materials, 2022, 440, 129795

mój udział polegał na współtworzeniu ogólnej jej koncepcji i projektu, wykonaniu eksperymentów, opracowaniu wyników oraz ich interpretacji, wykonaniu analizy statystycznej, przygotowaniu i przeglądzie manuskryptu oraz jego oprawy graficznej, poprowadzeniu dyskusji, sporządzeniu odpowiedzi na uwagi recenzentów.

**A. Krzyszczak**, M. P. Dybowski, B. Czech, *Microorganisms and their metabolites affect the content of polycyclic aromatic hydrocarbons and their derivatives in pyrolyzed material*, Science of the Total Environment, 2023, 886, 163966

mój udział polegał na współtworzeniu ogólnej jej koncepcji i projektu, wykonaniu eksperymentów, opracowaniu wyników oraz ich interpretacji, wykonaniu analizy statystycznej, przygotowaniu i przeglądzie manuskryptu oraz jego oprawy graficznej, poprowadzeniu dyskusji, sporządzeniu odpowiedzi na uwagi recenzentów.

**A. Krzyszczak-Turczyn**, M. P. Dybowski, M. Kończak, P. Oleszczuk, B. Czech, *Increased concentration of PAHs derivatives in biochar-amended soil observed in a long-term experiment*, artykuł w trakcie recenzji w czasopismie Journal of Hazardous Materials

mój udział polegał na współtworzeniu ogólnej jej koncepcji i projektu, wykonaniu eksperymentów, opracowaniu wyników oraz ich interpretacji, przygotowaniu i przeglądzie manuskryptu oraz jego oprawy graficznej, poprowadzeniu dyskusji, sporządzeniu odpowiedzi na uwagi recenzentów.

  
podpis

mgr Magdalena Kusiak  
Instytut Genetyki, Hodowli i Biotechnologii Roślin  
Wydział Agrobioinżynierii  
Uniwersytet Przyrodniczy w Lublinie  
e-mail: magdalena.kusiak@up.lublin.pl

Lublin, dn. 23.08.2023

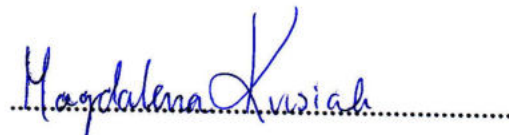
### Oświadczenie

Niniejszym oświadczam, że w pracy:

A. Krzyszczak, M. P. Dybowski, I. Jośko, **M. Kusiak**, M. Sikora, B. Czech, *The antioxidant defense responses of Hordeum vulgare L. to polycyclic aromatic hydrocarbons and their derivatives in biochar-amended soil*, Environmental Pollution, 2022, 294, 118664

mój udział polegał na wykonaniu części eksperymentów dotyczących analizy ekspresji genów.

Jednocześnie wyrażam zgodę na przedłożenie przez Panią Agnieszkę Krzyszczak-Turczyn wyżej wymienionej pracy jako część rozprawy doktorskiej w formie spójnego tematycznie cyklu prac opublikowanych w czasopismach naukowych.



podpis

prof. dr hab. Patryk Oleszczuk  
Katedra Radiochemii i Chemii Środowiskowej  
Instytut Nauk Chemicznych  
Wydział Chemii UMCS w Lublinie  
tel. 81 537 55 15  
e-mail: patryk.oleszczuk@mail.umcs.pl

Lublin, dn. 25.09.2023

### Oświadczenie

Niniejszym oświadczam, że w pracy:

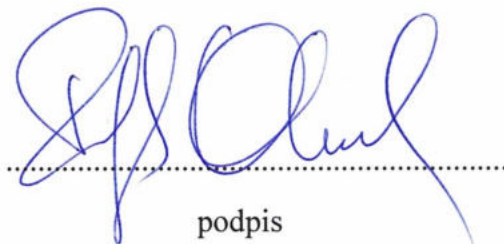
A. Krzyszczak, M. P. Dybowski, R. Zarzycki, R. Kobyłecki, **P. Oleszczuk**, B. Czech, *Long-term physical and chemical aging of biochar affected the amount and bioavailability of PAHs and their derivatives*, Journal of Hazardous Materials, 2022, 440, 129795

mój udział polegał na przeglądzie i edycji manuskryptu.

A. Krzyszczak-Turczyn, M. P. Dybowski, M. Kończak, **P. Oleszczuk**, B. Czech, *Increased concentration of PAHs derivatives in biochar-amended soil observed in a long-term experiment*, artykuł w trakcie recenzji w czasopismie Journal of Hazardous Materials

mój udział polegał na przeglądzie i edycji manuskryptu.

Jednocześnie wyrażam zgodę na przedłożenie przez Panią Agnieszkę Krzyszczak-Turczyn wyżej wymienionej pracy jako część rozprawy doktorskiej w formie spójnego tematycznie cyklu prac opublikowanych w czasopismach naukowych.



The image shows a handwritten signature in blue ink, consisting of stylized letters that appear to read "P. Oleszczuk". Below the signature, there is a horizontal dotted line and the word "podpis" written in a smaller, plain font.

Dr inż. Małgorzata Sierocka z d. Sikora  
Katedra Biochemii i Chemii Żywności  
Wydział Nauk o Żywności i Biotechnologii  
Uniwersytet Przyrodniczy w Lublinie  
tel. 814623328  
e-mail: malgorzata.sierocka@up.lublin.pl

Lublin, dn. 23.08.2023

## Oświadczenie

Niniejszym oświadczam, że w pracy:

A. Krzyszczak, M. P. Dybowski, I. Jośko, M. Kusiak, **M. Sikora**, B. Czech, *The antioxidant defense responses of Hordeum vulgare L. to polycyclic aromatic hydrocarbons and their derivatives in biochar-amended soil*, Environmental Pollution, 2022, 294, 118664

mój udział polegał na wykonaniu części eksperymentów dotyczących analizy aktywności enzymów antyoksydacyjnych.

Jednocześnie wyrażam zgodę na przedłożenie przez Panią Agnieszkę Krzyszczak-Turczyn wyżej wymienionej pracy jako część rozprawy doktorskiej w formie spójnego tematycznie cyklu prac opublikowanych w czasopismach naukowych.

Małgorzata Sierocka

.....  
Podpis

dr inż. Robert Zarzycki  
Katedra Zaawansowanych Technologii Energetycznych  
Wydział Infrastruktury i Środowiska  
Politechnika Częstochowska  
e-mail: robert.zarzycki@pcz.pl

Lublin, dn. 23.08.2023

### Oświadczenie

Niniejszym oświadczam, że w pracy:

A. Krzyszczak, M. P. Dybowski, **R. Zarzycki**, R. Kobyłecki, P. Oleszczuk, B. Czech, *Long-term physical and chemical aging of biochar affected the amount and bioavailability of PAHs and their derivatives*, Journal of Hazardous Materials, 2022, 440, 129795

mój udział polegał na otrzymaniu części materiału badawczego.

Jednocześnie wyrażam zgodę na przedłożenie przez Panią Agnieszkę Krzyszczak-Turczyn wyżej wymienionej pracy jako część rozprawy doktorskiej w formie spójnego tematycznie cyklu prac opublikowanych w czasopismach naukowych.



.....  
podpis